Sudan University of Science and Technology

College of Graduate Studies

Strategic design, quantitative structure activity relationship and selective synthesis of some pyrazoline derivatives

by:

Maysoon Mohammed Almahdi

MSc Chemistry , BSc Chemistry

A thesis submitted in fulfillment of the requirements of the degree of Doctor Philosophy in Chemistry

Supervisor:

Prof. Dr. Ahmed Elsadig Mohammed Saeed

October 2018

DEDICATION

This work is dedicated,

to my father Soul,

to my lovely mother, brother and sisters for their immortal support and encouragement

to my husband and our little angle **Ibrahim**.

To all I say, thank you will never be enough for inspiring me to follow my dreams and to never give up after failure, may god bless you all.

<div align="right">

MAYSOON

</div>

AKNOWLDEDGMENT

ABSTRACT

Numerous pyrazoline derivatives have been found to possess considerable biological activities; this fact had led us to model and design 120 trisubstituted 2-pyrazoline derivatives by linking pyrazoline ring system with different substituents in position 1, 3 and 5.

Quantitative structure–activity relationship (QSAR) studies were carried out in order to get models that can be used to predict the anti-cancer activity of designed compounds. Data set of compounds consisting of pyrazoline derivatives were collected and their anti-cancer activity were correlated with their physicochemical descriptors using multiple linear regression method. QSAR study revealed three good predictive and statistically significant descriptor models ($r^2 = 0.7603$; r= 0.8720 for training set, $Q^2 = 0.5348$ for cross validation and $r^2 = 0.8593$; r= 0.9270 for test set); all other statistical parameters were found in the acceptable range (RMSE= 0.33535, s= 0.56, F= 34.05 and P= 0.133). Obtained model showed that the biological activity was proportionally correlated with density and inversely correlated with log P(o/w) partition coefficient and ionization potential. This model was used to predict the biological activity of designed 120 pyrazoline derivatives, and the results were compared with Combretastin A-4.

Drug ability of designed compounds was evaluated using Lipinski's "rule of five" to select compounds for synthesis. Therefor, 33 out of 120 compounds were selected for synthesis. Although only eight of them were found to have less anti-cancer activity (2.64 - 6.45 M) than that of the standard Combretastin A-4 (6.51 M), all the others had much more anti-cancer activity (6.72-14.88 M). These promising results have lured similar investigation of anti-cancer activity of breast cancer of another group of α,β-unsaturated carbonyl derivatives.

New data set consist of α,β-unsaturated carbonyl derivatives were collected. Their anti-cancer activity and descriptors were correlated using multiple linear regression method. The best descriptor model was selected yielding a very high performance in terms of coefficient of determination (r^2) as 0.84684 for training set and 0.9430 for test set; other statistical parameters calculated to justify the statistical quality of model were in acceptable range, RMSE= 0.14550, s= 0.384, F= 101.43 and P= 0.010. Model equation showed that there is proportional correlation between the biological activity, density and log P(o/w) partition coefficient, and inverse correlation with potential energy.

Derived model was used to predict the activity of designed α-β unsaturated carbonyl derivatives against human breast cancer. All compounds gave biological activity ranging from 3.74 to 6.24 M less than that given by standard drug Tamoxifen (7.39 M). The drug ability of these compounds were also evaluated through Lipinski's parameters, and they conformed with them.

In synthetic work, different aromatic acetophenone derivatives were treated with some substituted aromatic benzaldehydes in the presence of ethanol as solvent and sodium hydroxide as basic medium to give substituted α,β-unsaturated carbonyl derivatives. These derivatives were further converted into pyrazolines by condensation of various synthesized α,β-unsaturated carbonyl derivatives with hydrazine hydrate. The structures of previous compounds were characterized by melting point, FT-IR and other physicochemical properties. New Chloroacetyl pyrazoline derivatives have been synthesised by the condensation of pyrazoline derivatives obtained from previous step with chloroacetyl chloride. These derivatives were tested as alkylating agents in the reaction with sulfanilamide and sulfadoxine in dry DMF and anhydrous K_2CO_3 with stirring under reflux. Thus the corresponding 1-[(aryl)aminoacetyl] -

3,5-diaryl-2-pyrazoline derivatives have been obtained. The structures of newly synthesized trisubstituted pyrazoline derivatives were established on the basis of melting point, FT-IR, UV, MS, ^{1}H- NMR spectroscopies analysis and other physicochemical properties. All the synthesized compounds were isolated in satisfactory yields.

Docking studies were performed for synthesized compounds in order to evaluate their affinity to cancer proteins. 1JD0 protein obtained from protein data bank was selected for docking study of pyrazoline derivatives and acetazolamide carbonic anhydrase inhibitor was used as the reference drug.

The docking scores were calculated, least energy indicated the easy binding character of ligand and receptor. Some compounds have shown excellent docking scores (-21.9174, -22.2056, -22.0545 and -21.2136 kcal/mol respectively) comparing with that standard drug AZA (-21.0578 kcal/mol).

3DKC protein was selected for docking study of α,β-unsaturated carbonyl derivatives. The result suggested that all compounds were capable of forming metal complex interaction and their docking score ranged from -22.9170 to -16.1714 kcal/mol. All *in silico* studies were achieved by ACD\Lab and MOE soft wares.

الخلاصة

تظهر العديد من مشتقات البيرازولين انشطه بيولوجيه مختلفة، قادت هذه الحقيقه لتصميم 120 من مشتقات 2- بيرازولين الثلاثية من خلال ربط حلقة البيرازولين بمستبدلات مختلفة في الموقع 1 و 2 و 3. تم إجراء دراسات كمية للعلاقة بين البنية والنشاط (QSAR) من أجل الحصول على نماذج يمكن استخدامها للتنبؤ بنشاط المركبات المصممة كمضادات لسرطان الثدي. تم جمع مجموعة بيانات من مشتقات البيرازولين وربط نشاطها المضاد للسرطان مع الواصفات الجزيئية لها باستخدام طريقة الارتداد الخطي المتعددة كما تم تقدير قدرة النموذج علي التنبؤ باستخدام طرق التنبؤ الداخلية والخارجية.

كشفت دراسة QSAR عن نموذج تنبؤي ذو ثلاث واصفات جزيئيه ودلالات إحصائية جيدة ($r^2 = 0.7603$ ، $r = 0.8720$ لمجموعة التدريب ، $Q^2 = 0.5348$ و $r^2 = 0.8593$ ، $r = 0.9270$ لمجموعة الاختبار). كما ان جميع الدلالات الإحصائية الأخرى كانت في المدى المقبول ($RMSE = 0.33535$ ، $s = 0.56$ ، $F = 34.05$ و $P = 0.133$). وضح النموذج المتحصل عليه أن النشاط البيولوجي يرتبط ارتباطًا إيجابيًا بالكثافة و عكسيا مع معامل التقسيم $P (o / w)$ وقوة التأين. تم استخدام هذا النموذج للتنبؤ بالنشاط الحيوي لحوالي 120 من مشتقات البيرازولين المصممة، وتمت مقارنة النتائج مع كمبرتاستسن أ-4.

تم تقييم امكانية المركبات المصممة كعقارات يمكن تعاطيها من خلال قاعدة الخمسه لليبينسكي من أجل اختيار مركبات للتخليق. لذلك ، تم اختيار 33 من أصل 120 مركبًا. اظهرت بعض المركبات المختارة نشاطا ضد السرطان (2.64 - 6.45 مولار) اقل من ذلك العقار المرجعي كمبرتاستسن أ-4 (6.51 مولار)، كما أظهرت بقية المجموعة المختارة نشاطًا كبيرًا ضد السرطان (6.72-14.88 مولار) مقارنة مع ذلك العقار المرجعي. وقد قادت هذه النتائج للتحقق من نشاط مجموعة أخرى من مشتقات الفا،بيتا-كربونيل غير المشبعة كمضادات لسرطان الثدي.

تم جمع مجموعة بيانات جديدة تتكون من مشتقات الفا،بيتا-كربونيل غير المشبعة وربط نشاطها كمضادات للسرطان مع واصفاتها الجزيئيه. وقد تم اختيار أفضل نموذج بناءا علي أعلى معامل ارتباط (r^2) حيث يساوي 0.84684 لمجموعة التدريب و 0.9430 لمجموعة الاختبار، كما كانت الدلالات الإحصائية الأخرى المحسوبة لتقدير الجودة الإحصائية للنموذج في المدى المقبول($RMSE = 0.14550$ ، $s = 0.384$ ، $F = 101.43$ و $P = 0.010$). أظهرت معادلة النموذج وجود علاقة طردية بين النشاط البيولوجي والكثافة ومعامل التقسيم $P (o / w)$ وارتباط عكسي مع الطاقة الكامنة. تم استخدام النموذج المشتق للتنبؤ بنشاط مشتقات الفا،بيتا-كربونيل

غير المشبعة ضد سرطان الثدي البشري.، حيث أعطت جميع المركبات نشاط بيولوجي يتراوح من 3.74 إلى 6.24 م أقل من عقار تاموكسيفين المرجعي (7.39 م). كما تم تقييم امكانية هذه المركبات للتعاطي من خلال معايير لليبينسكي وكلها كانت مناسبة لذلك.

عند التخليق، تم معالجة بعض مشتقات الاسيتوفينون العطريه مع بعض مشتقات البنزالدهيد العطرية في وجود الإيثانول كمذيب وهيدروكسيد الصوديوم كقاعدة لإعطاء مشتقات الفا،بيتا-كربونيل غير المشبعة. بعد ذلك تم تحويل هذه المشتقات إلى بيرازولينات عن طريق تكثيف مشتقات الفا،بيتا-كربونيل غير المشبعة مع الهيدرازين المائي. تم التحقق من بنية هذه المركبات طيفيا من خلال طيف الاشعة تحت الحمراء كما تم تحديد نقاط انصهارها وخواصها الفيزيوكيميائية. مشتقات البيرازولين الكلور أسيتيل الجديدة تم تخليقها عن طريق تكثيف مشتقات البيرازولين التي تم الحصول عليها من الخطوة السابقة مع كلورو اسيتيل كلورايد. تم اختبار هذه المشتقات كعوامل ألكلة في التفاعل مع السلفانيلاميد والسلفادوكسين في وجود ثنائي ميثيل الفورماميد الجاف وكربونات البوتسيوم اللامائيه مع التكثيف والتحريك المستمر، وبالتالي تم الحصول علي مشتقات 1-((اريل)امينو اسيتيل)-3،5-ثنائي اريل 2-بيرازولين. تم التأكد من بنية هذه المركبات طيفيا من خلال طيف الاشعه تحت الحمراء، فوق البنفسجيه، مطيافية الكتلة والرنين النووي المغنطيسي، كما تقدير نقاط انصهارها وخواصها الفيزيوكيميائيه.

أجريت دراسات الالتحام الجزيئي لجميع المركبات التي تم تخليقها من أجل تقدير انجزابها مع بروتينات السرطان. البروتين 1JD0الذي تم الحصول عليه من بنك بيانات البروتين، تم اخياره لدراسة الالتحام الجزيئي لمشتقات البيرازولين المخلقه واستُخدم مثبط الكربونيك انهيدريز الاسيتوزولاميد كعقار مرجعي. تم حساب نتيجة الالتحام وعرضها في جدول، قيم الطاقات الاقل اشارة الي سهولة الالتحام الجزيئي بين المعقد والمستقبل. وأشارت أقل الطاقة إلى الطابع الملزم السهل للرابطات والمستقبلات. أظهرت بعض المركبات قيم التحام ممتازه (-21.9174 ، -22.2056 ، -22.0545 و -21.2136 كيلو سعر/مول) مقارنة بالدواء القياسي AZA (-21.0578 كيلو سعر/مول).

تم اختيار بروتين 3DKC لدراسة الالتحام الجزيئي لمشتقات الفا،بيتا-كربونيل غير المشبعة واقترحت النتائج أن جميع هذه المركبات قادرة على تكوين ترابط معقد معدني وتتراوح قيم الالتحام بين -16.1714 الي -22.9170 كيلو سعر/مول. جميع الدراسات النظرية تمت من خلال برنامجي ACD\Lab و MOE.

LIST OF PUBLICATIONS

Published Papers:

- Maysoon Mohammed Almahdi [1,*], Ahmed Elsadig Mohamed Saeed [2] and Nadia Hanafy Metwally [3]. QSAR and docking studies of α,β-unsaturated carbonyl compounds against human breast adenocarcinoma cell line MCF-7. *European Journal of Chemistry*
- Maysoon Mohammed Almahdi [1,*], Ahmed Elsadig Mohamed Saeed [2] and Nadia Hanafy Metwally [3]. Synthesis and antimicrobial activity of some new pyrazoline derivatives bearing sulfanilamido moiety. European Journal of Chemistry.

LIST OF CONTENTS

Content	Page

Chapter One

Chapter Two

Chapter four

Chapter Five

LISTB OF FIGURES

LIST OF TABLES

LIST OF SCHEMES

LIST OF ABBREVIATIONS

Abbreviation	Meaning
IUPAC	International union of pure and applied chemistry
ICT	Intramolecular Charge Transfer
DABCO	bis-1,4-diazabicyclo[2.2.2]octane
TBPA	Tri (4-bromophenyl) aminium
CB1	Cannabinoid
DMSO	Dimethylsulfoxide
NCE	Novel Chemical Entities
QSAR	Quantitative structure-activity relationship
QSTR	Quantitative structure-toxicity relationship
QSPR	Quantitative structure-property relationship
LR	Linear regression
MLR	Multiple linear regression
PLS	Partial least-squares
PCA	Principal component analysis
PCR	Principal component regression
ANN	Artificial neural networks
kNN	k-nearest neighbors
GA	Genetic algorithms
F	Field component
R	Resonance component
LOO	leave-one-out
Q^2	Cross validation regression coefficient
CV	Cross validation
r	Correlation coefficient
r^2	Square of the correlation coefficient
PDB	Protein data bank
DNA	Deoxyribonucleic acid
MCF-7	Michigan cancer foundation-7
MF	Molecular formula
MW	Molecular weight
IR	Infra-red
FT-IR	Fourier infra-red
UV	Ultra Violet
VIS	Visible
^{1}HNMR	Proton Nuclear Magnetic Resonance
TMS	Tetramethyl silane
s	singlet
d	doublet

t	triplet
q	quartet
m	multiplet
dd	doublet of doublet
GC-MS	Gas Chromatography Mass Spectrometer
TLC	Thin Layer Chromatography
ACD	Advanced Chemistry Development
MOE	Molecular Operating Environment
SPSS	Statistical package for social sciences
h	Hour
DMF	Dimethylformamide
m.p.	Melting point
R_f	Retardation factor
sym	Symmetry
asym	Asymmetry
str.vib.	Stretching vibration
λmax	Maximum wavelength
J	Geminal coupling
pIC_{50}	anticancer potential
IC_{50}	Inhibitory concentration, 50%
MR	Molar Refractivity
MV	Molar volume
RI	Refractive index
D	Density
ST	Surface tension
Log P(o/w)	logarithm of octanol-water partition coefficient
HF	Heat of Formation
IP	Ionization Potential
dipole	Dipole Moment
E	Potential energy
RMSE	Root mean square error
s	Standard error of estimate
Thr	Thyrosine
His	Histamine
Asn	Asparagine
Lys	Lysine
Asp	Aspartic acid
CAI	Carbonic anhydrase inhibitor
hCAXII	Human carbonic anhydrase XII
HB	Hydrogen bond
MOE	Molecular Operating Environment
SPSS	Statistical Package for Social Sciences

AZA	Acetazolamide
FT	Fourier transform
c-Met	Tyrosine kinase human mesenchymal-epithelial transition factor
HGF	Hepatocyte growth factor
CA-4	Combretastatin A-4

1. Introduction

Synthetic chemistry is the science of constructing complex molecules from simple ones. It is possible to divide it into two great landscapes: the total synthesis, where the synthetic chemists study how step by step it is possible to build a structure usually with biological importance, and the methodologies which introduce new reactions. One might think that the synthetic chemistry is only focused on C-H bond making therefore a huge mistake because synthetic chemistry doesn't look only to molecules built by carbon and hydrogen but also to heterocyclic compounds (Marsili, 2013).

Structures of organic compounds can be acyclic or cyclic. The cyclic systems containing only carbon atoms are called carbocyclic and the cyclic systems containing carbons and at least one other element (heteroatom) are called heterocyclic (Nikitin & Andryukhova, 1954).

IUPAC gold book defined heterocyclic compounds as "cyclic compounds having as ring members atoms of at least two different elements". In short, heterocyclic chemistry is the branch of chemistry dealing with the synthesis, properties, and applications of heterocycles (Alvarez-Builla & Barluenga, 2011).

According to the heteroatom (s) present in the ring structures, heterocygles can be classified as oxygen, nitrogen or sulfur based and, within each class, compounds are organized based on the size of the ring structure size determined by the total number of atoms (Eicher *et al*, 2003). These make compounds with the most diverse physical, chemical and biological properties available, so is very easy to guess the huge diffusion and importance of heterocyclic compounds (Marsili, 2013).

Heterocyclic compounds also may be classified as aliphatic and aromatic heterocycles. The aliphatic heterocycles are the cyclic analogues of amines, ethers and thioethers and their properties are influenced by the ring strain. The common aliphatic heterocyclic compounds are aziridine, oxirane, thiirane, azetidine, oxetane, thietane, pyrrolidine, tetrahydrofuran, tetrahydrothiophene and piperidine fig (1.1) (Nikitin & Andryukhova, 1954)
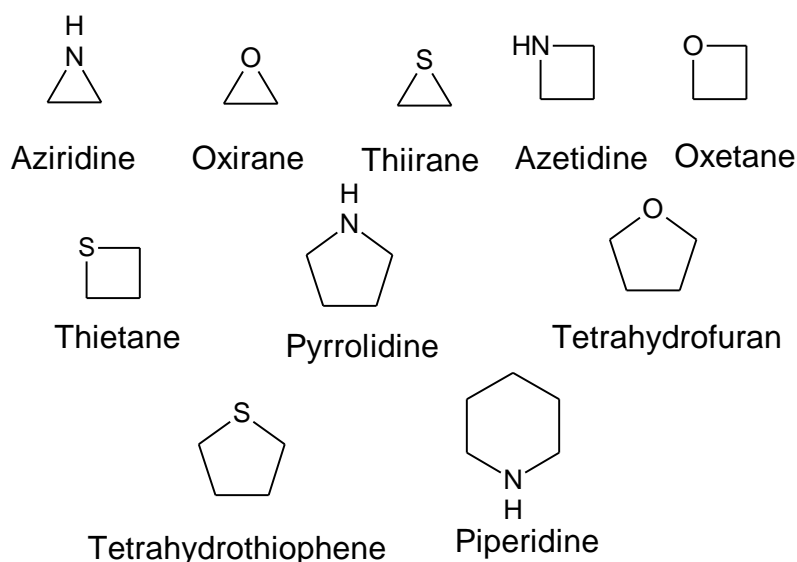
Figure (1.1): Examples of aliphatic heterocyclic compounds

The heterocycles which show aromatic behavior as in homocyclic benzene analogues are called the aromatic heterocyclic compounds. These compounds follow the Hückel's rule which states that cyclic conjugated and planar systems having (4n+2) π electrons are aromatic. Some simple aromatic heterocyclic compounds are pyrrole, furan, thiophene, imidazole, pyrazole, oxazole, thiazole and pyridine fig (1.2) (Nikitin & Andryukhova, 1954)
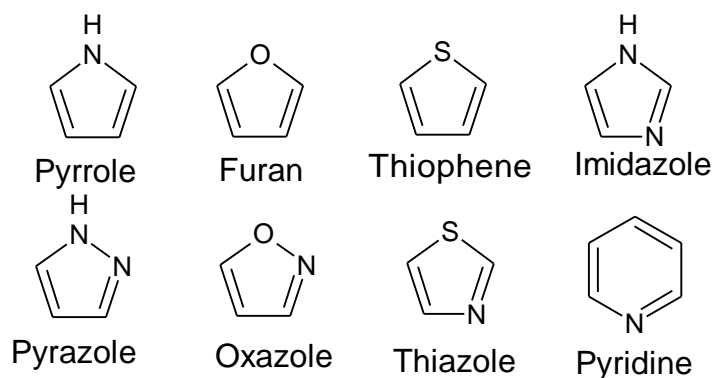
Figure (1.2): Examples of aromatic heterocyclic compounds

Among heterocyclic compounds five-membered heterocycles constitute a group with broad spectrum of biological activity (Pitucha *et al.*, 2013). Pyrazolines are one of the five-membered heterocyclic compounds with very important biological activities.

1.1.Pyrazoline

1.1.1. Definition of pyrazoline

Pyrazoline is an unsaturated compound containing three carbon atoms and two nitrogen atoms in adjacent positions. It consists of only one endocyclic double bond in the structure. It is a reduction product of pyrazole, which is further reduced to pyrazolidine fig (1.3) (Shinkar *et al.*, 2015).
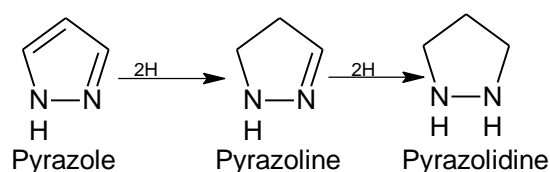
Figure (1.3): Hydrogenation of pyrazole

1-Pyrazoline, 2-pyrazoline and 3-pyrazoline are the three partially reduced forms of the pyrazole structure with different positions of the double bond and exists in equilibrium one with the other fig (1.4).
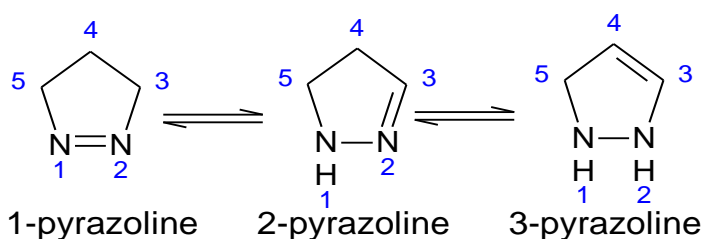
Figure (1.4): The three partially reduced forms of pyrazoline

It was in the late nineteenth century that Fischer and Knovenagel described the reaction of acrolein with phenylhydrazine to provide a 2-pyrazoline . Their experiment seems to be the first example of pyrazoline formation by the reaction of an α, β-enone with a hydrazine derivative. It was revealed that the product of this reaction was 1-phenyl 2-pyrazoline (Avupati & Yejella, 2014).

Pyrazoline is a tautomeric substance; the existence of tautomerism can be demonstrated by the consideration of pyrazoline derivatives. Unsubstituted pyrazoline can be represented in three tautomeric forms fig (1.5).
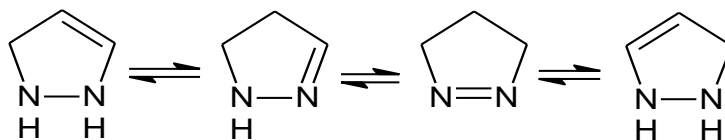
Figure (1.5): Tautomeric forms of unsubstituted pyrazoline

Pyrazoline derivatives in which two carbon atoms neighboring the nitrogen atoms on the ring have different substituents, five tautomeric structures are possible fig (1.6) (Kumar & Govindaraju, 2015).
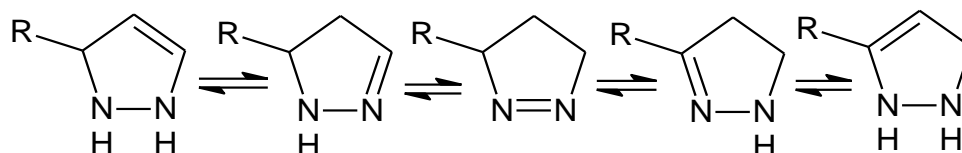
Figure (1.6): Tautomeric forms of substituted pyrazoline

Pyrazoline derivatives are the electron rich nitrogen heterocycles which play an important role in the diverse biological activities (Yusuf & Jain, 2014). Among its various derivatives, 2-pyrazolines seem to be the most frequently studied pyrazoline type compounds (Li *et al.*, 2007).

1.1.2. 2-Pyrazolines

2-Pyrazolines (4,5-dihydro-1H-pyrazole) fig (1.7) are an important class of five-membered heterocyclic compounds and were found to be vital building block in medicinal chemistry and led to the discovery of a number of bioactive derivatives (Aboul-Enein *et al.*, 2014).

2-Pyrazolines can be considered as a cyclic hydrazine moiety (Kelekci *et al.*, 2009). It exhibits the monoamino character and hence is more stable than the rest of the reduced forms. 2- Pyrazoline seems to be the most

frequently studied form of pyrazoline because it have a considerably easy route of synthesis and rich biological activity (Shinkar *et al.*, 2015).
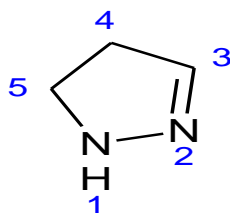
Figure (1.7): 2- Pyrazoline structure

1.2.2.1. Nomenclature

Application of present heterocyclic nomenclature to the pyrazolines requires that the nitrogen atoms be numbered one and two in each structure. Substituted 1-pyrazolines are numbered to produce the lower of two possible numbers for substituent group locants, or in the case of complicated structures to produce the simplest name consistent with clarity of meaning. Numbering of the 2-pyrazolines begins with the amino nitrogen (Jadhav *et al.*, 2016). The following pattern has been adopted by "Chemical Abstracts" published by American chemical society fig (1.8).
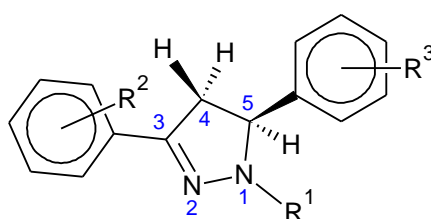
Figure (1.8): Numbering of pyrazoline ring

1.2.2.2. Properties of 2-pyrazoline

2-pyrazoline is insoluble in water but soluble in propylene glycol because of its lipophilic character (Eisinger *et al.*, 1981). It contains two types of nitrogen atom, pyrrole and pyridine at position 1 and 2 respectively.

Pyridine type nitrogen is susceptible to electrophilic attack, and the hydrogen atom attached to the nitrogen at position 1 is more acidic than pyrrolic N-H, so easily removed by nucleophiles (Alam *et al.*, 2015).

As follows from the X-ray analysis, it has the structure of the five-membered dihydropyrazole ring, has an envelope conformation, C5 atom is deviated from the almost planar system of the other four atoms of the heterocyclic ring (Hadi, 2012).

Pyrazolines are used extensively as useful synthons in organic synthesis (Gupta *et al.*, 2010). Pyrazoline derivatives, typical ICT (Intramolecular Charge Transfer) compounds (Li *et al.,* 2007), are known as a kind of fluorescent brightening agents because they have strong blue fluorescence in solution (Bai *et al.*, 2007) and they have a hole transport tendency (Lu *et al.*, 2000).

These compounds show stronger fluorescence because of the double bond hindering which occurred due to cyclization. Bulky groups in both the 4- and 5-positions improved both the fluorescence efficiency and the stability to light of the molecule. It has significance for the design of pyrazoline whitening agents (Evans *et al.*, 1974). Aryl group at position-5 is also responsible for spiroconjugated charge transfer quenching of pyrazoline fluorescence (Rahman & Siddiqui, 2010).

An intramolecular conjugated charge transfer process has been reported to exist in it in the excited state. In the conjugated part ($-N^1-N^2=C^3-$) of the ring, the nitrogen atom at the 1-position and the carbon atom at the 3-position are, respectively, electron donating and withdrawing moieties. The carbon atoms at 4- and 5-positions do not conjugate with the above conjugated part. Its fluorescence spectrum exhibits a large red shift with an increase in the polarity of solvents (Li *et al*, 2007).

1.1.3. Naturally Occurring pyrazoline derivatives

Pyrazoline derivatives are rarely found in nature probably due to difficulty in the formation of N-N bond by the living organisms (Suri *et al.*, 2012). In 1996, the violet pigment named nostocine **A** fig (1.9) was isolated from the freshwater cyanobacterium Nostoc spongiaeforme TISTR 8169 growing in a Thai paddy field (Hirata *et al.*, 1996). It has been proposed that the pigment is released from the cyanobacterium in response to oxidative stress (Blair & Sperry, 2013).
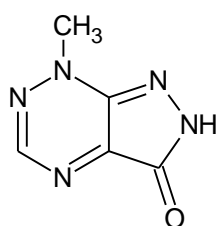
Figure (1.9): Structure of nostocine A

Nostocine **A** inhibits the growth of various human cancer cell lines at concentrations as low as 0.1 μg/mL and has a cytotoxicity comparable to 5-fluorouracil (Hirata *et al.*, 1996). Acute toxicity was observed following the administration of Nostocine **A** to mice (Blair & Sperry, 2013).

Fluviols **A−E** fig (1.10) were isolated from strains of *P. f luorescens var. pseudoiodinum*. Natural fluviol **E** inhibits the growth of various bacteria, with weaker activity against fungi, inhibited the growth of the ascetic form of Ehrlich carcinoma *in vivo*, and was also toxic to the mice used. Natural fluviol **C** proved to be an inferior antibacterial and was also less toxic to mice, with moderate antitumor activity. Fluviol **A** was the least toxic, yet possessed the strongest antitumor activity (Smirnov *et al.*, 1997).
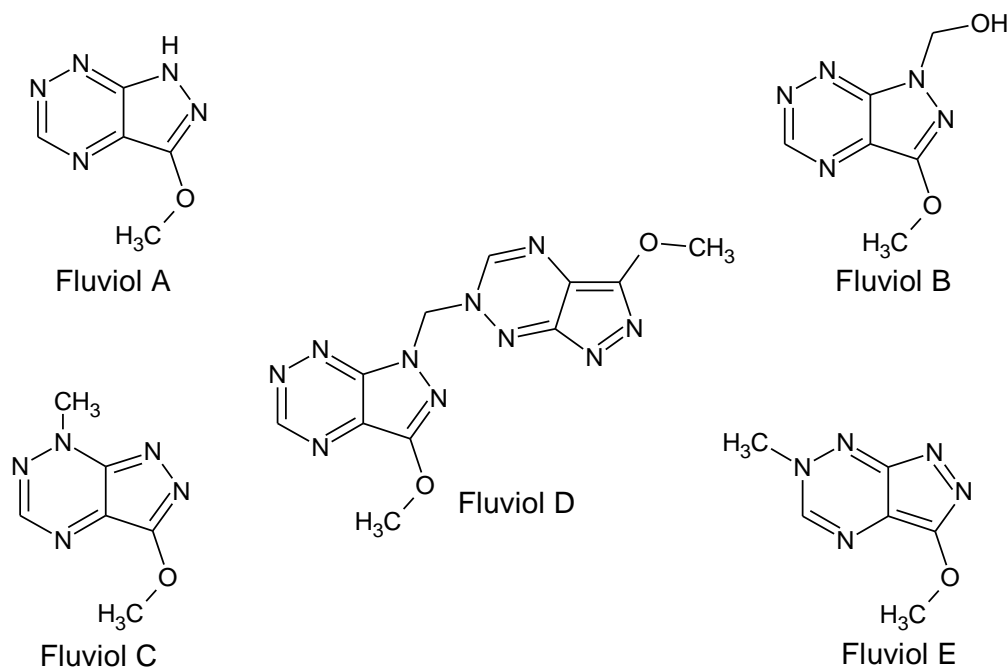
Figure (1.10): Structures of fluviol A-E

Boudiar *et al.*, 2010 was isolated a 2-pyrazoline derivative (1,5-diphenyl-3-[(*E*)-2-phenylethenyl]-4,5-dihydro-1*H*-pyrazole) fig (1.11) from the aerial parts of Euphorbia guyoniana.
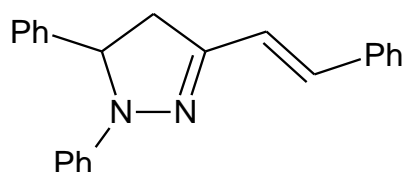
Figure (1.11): Structure of 1,5-diphenyl-3-[(*E*)-2-phenylethenyl]-4,5-dihydro-1*H*-pyrazole

1.1.4. Reactions of pyrazoline

An important reaction of pyrazoline is aromatization. It was achieved by heating 1,3,5-trisubstituted-2-pyrazoline with bis-1,4-diazabicyclo [2.2.2] octane complex, (DABCO-bromine), to get corresponding pyrazoles.

The method was found efficient and convenient for its easy isolation procedures and use of eco-friendly reagents fig (1.12) (Azarifar *et al.*, 2010).
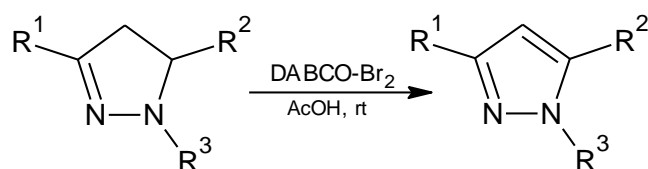
Figure (1.12): Aromatization of pyrazoline

Pyrazoline derivatives can be oxidized to corresponding pyrazoles with weak oxidizing agents like bromine water fig (1.13) (Basaif *et al.*, 1997).
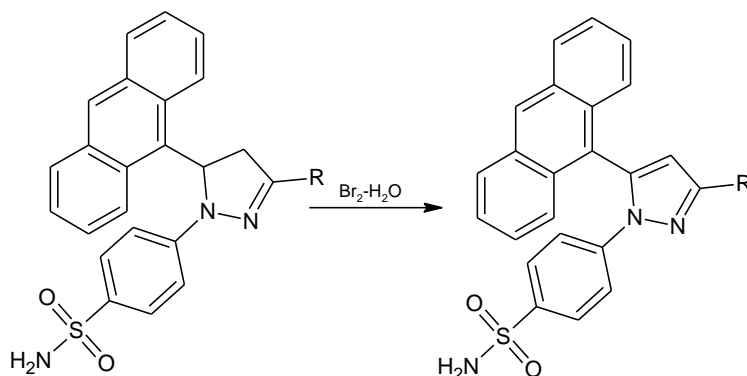
Figure (1.13): Oxidation of pyrazoline

1,3,5-Trisubstituted pyrazolines have been oxidized to the corresponding pyrazoles with tri (4-bromophenyl) aminium (TBPA) hexachloroantimo nate in chloroform at room temperature fig (1.14) (Yusuf & Jain, 2014).
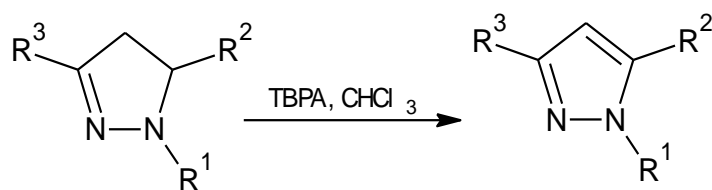
Figure (1.14): Oxidation of 1,3,5-trisubstituted pyrazolines

Oxidative dehydrogenation of 3-vinyl-4,5-dihydro-3H-pyrazoles with 20eq of MnO_2 in benzene at room temperature produce 3-alkenyl-1H-pyrazoles in good yield. While, oxidative dehydrogenation of 4,4′,5,5′-tetrahydro-3*H*,3′*H*- 3,3′-bipyrazole having two dihydropyrazole rings was accompanied by elimination of nitrogen molecule from one dihydro

pyrazole ring, leading to the formation of a mixture of bipyrazole and 3-cyclopropyl-1*H*-pyrazole fig (1.15) (Yakovlev *et al.*, 2009).
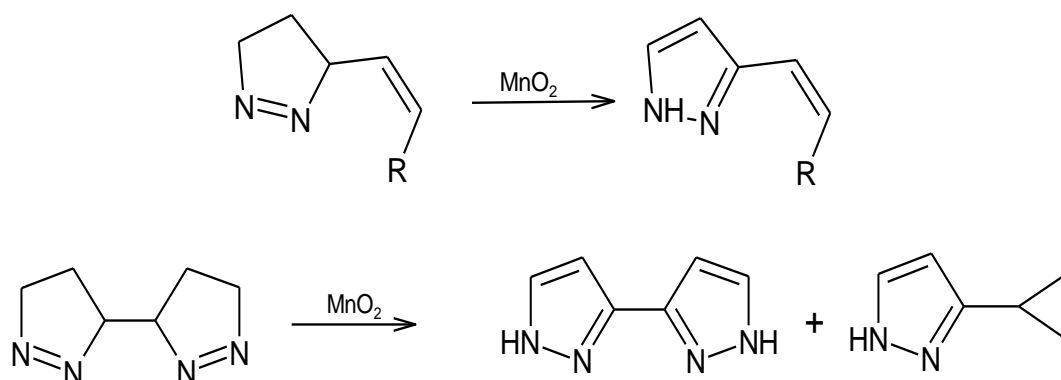
Figure (1.15): Oxidative dehydrogenation of 4,5-dihydro-3*H*-pyrazoles and 4,4′,5,5′-tetrahydro-3*H*,3′*H*- 3,3′-bipyrazole

Reaction of 3-methyl-5-oxo-1-phenyl-2 -pyrazoline-4-thiocarbohydrazide with phenyl isothiocyanate in absolute ethanol afforded N^1 -(4,5-dihydro-3- methyl-5-oxo-1-phenylpyrazol-4-yl) thiocarbonyl-N-phenylthiosemi carbazide.

Hydrolysis of N^1 -(4,5-dihydro-3- methyl-5-oxo-1-phenylpyrazol-4-yl) thiocarbonyl-N-phenylthiosemicarbazide with 10% sodium hydroxide solution followed by acidification with dilute hydrochloric acid gave 4-(4,5-dihydro-1-phenyl-5-thioxo-1,3,4-triazol-2- yl)-3-methyl-1-phenyl-2 -pyrazolin-5-one. Treatment of 3-methyl-5-oxo-1-phenyl-2 -pyrazoline-4-thiocarbohydrazide with sodium nitrite in acetic acid yielded 4-azidothiocarbonyl-3-methyl-1-phenyl-2 -pyrazolin-5- one (Kandeel *et al.*, 2002).

3-methyl-5-oxo-1-phenyl-2 -pyrazoline-4-thiocarbohydrazide was also subjected to the reaction with carbon disulphide. It was found that it is reacted with CS_2 in KOH to give 4-(4,5-dihydro-5-thioxo-1,3,4-thiadiazol-2-yl) - 3-methyl-1-phenyl-2 -pyrazolin-5-one and then reacted

with hydrazine hydrate to give 4-(1-amino-4,5-dihydro-5-thioxo-1,3,4-triazol- 2-yl)-3-methyl-1-phenyl-2 -pyrazolin-5-one fig (1.16) (Kandeel *et al.*, 2002).
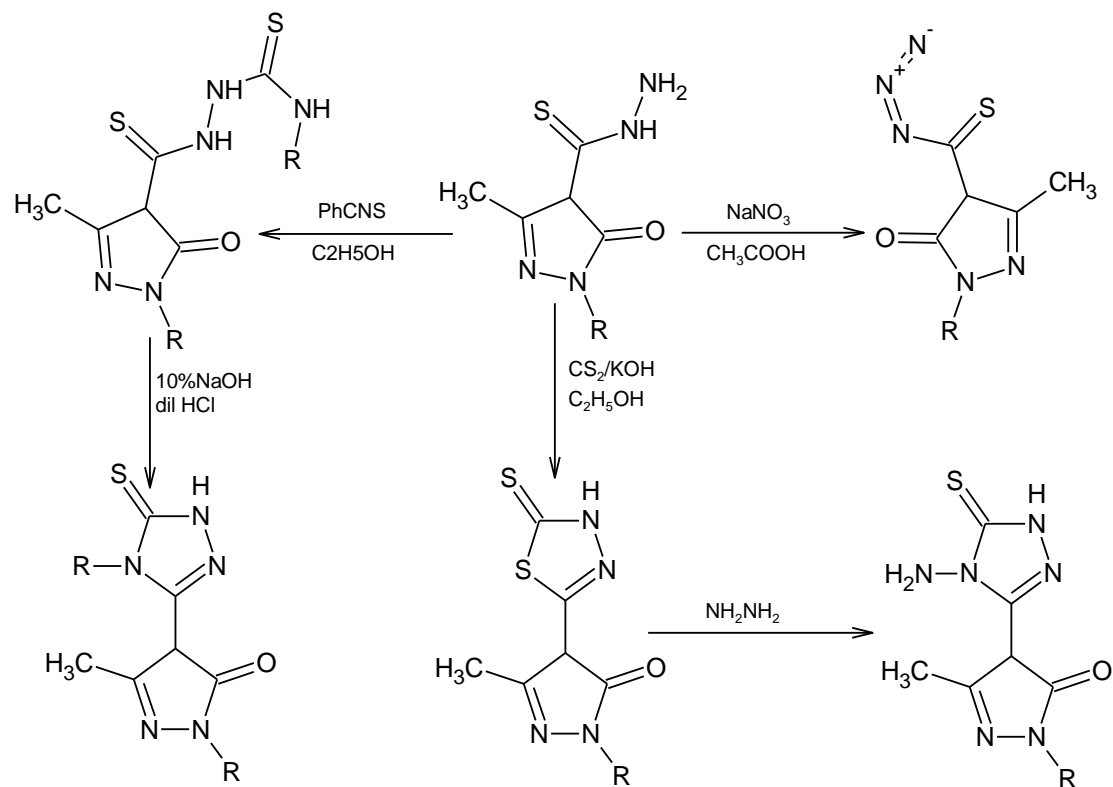
Figure (1.16): Reactions of 3-methyl-5-oxo-1-phenyl-2-pyrazoline-4-thiocarbohydrazide

1.1.5. Therapeutic potential of pyrazolines

2-Pyrazolines display a broad spectrum of potential pharmacological activities and are present in a number of pharmacologically active molecules such as phenazone/ amidopyrene/ methampyrone (analgesic and antipyretic), azolid/ tandearil (anti-inflammatory), indoxacarb (insecticidal), anturane (uricosuric), etc. Considerable interest has been focused on the pyrazoline structure. The discovery of this class of drugs provides an outstanding case history of modern drug development and also points out the unpredictability of pharmacological activity from structural modification of a prototype drug molecule. It is having a

variety of medicinal applications. Pyrazoline derivatives were found to have potential antipyretic-analgesic, tranquillizing, muscle relaxant, psycho analeptic, antiepileptic, antidepressant, anti-inflammatory, insecticidal, antimicrobial and antihypotensive activities. Their derivatives were also found to exhibit cytotoxic activity, inhibitory activity of platelet aggregation, herbicidal activity and cannabinoid receptor modulators. Pyrazoline interest extended to dyes and dye couplers too fig (1.17) (Rahman & Siddiqui, 2010).

Phenazone   Amidopyrene   Methampyrone

Azolid   Tandearil   Anturane
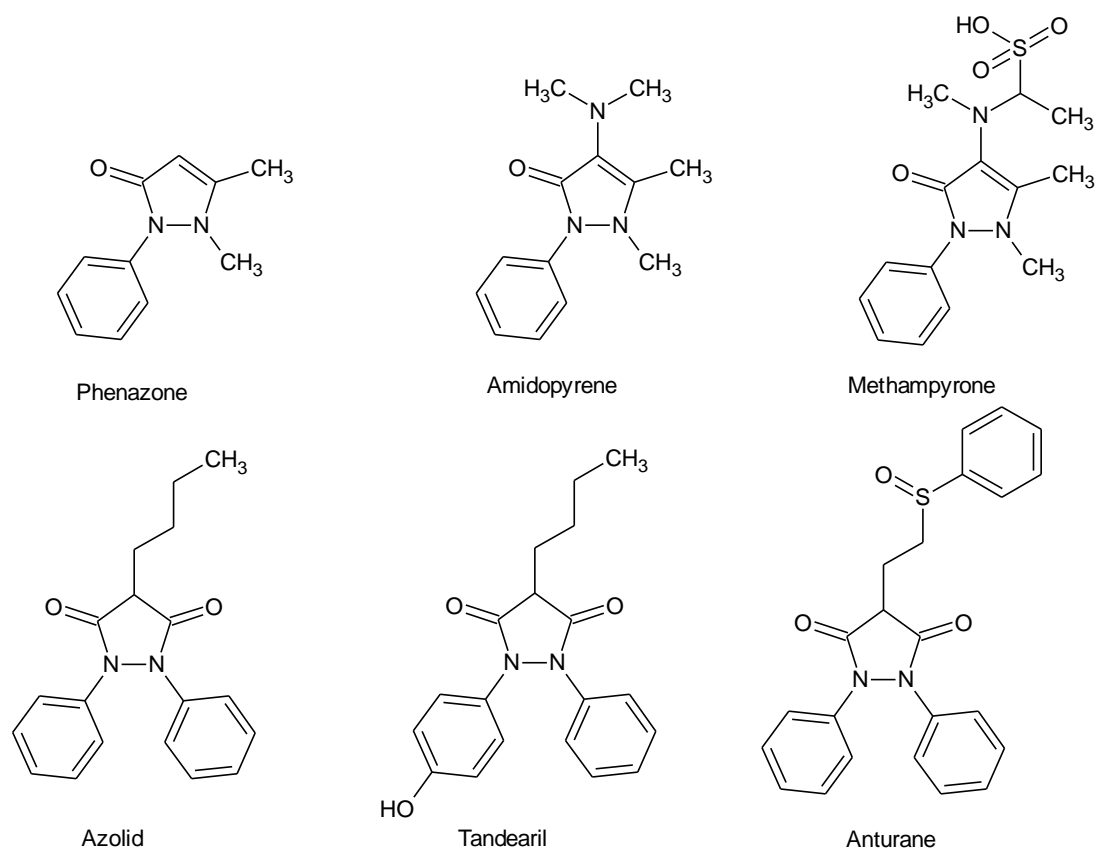
Figure (1.17): Structures of some pharmacologically active molecules containing pyrazloine moiety

1.1.6. Synthesis of 2-pyrazolines

Pyrazoline derivatives are considered as useful building blocks in organic synthesis for designing pharmaceutical and agrochemicals (Kumar & Govindaraju, 2015). It has variety of methods for their synthesis,

a) Cyclization, which proceeds stepwise through one or more intermediates involving the expulsion of a small molecule such as an alcohol or water.

b) Cycloaddition, which proceed via no distinct intermediate but the bond formation may be asynchronous (Krishna & Sekhar, 2008).

c) Fischer and Knoevenagel reaction *i.e.* the condensation of *α, β*-unsaturated compounds with hydrazines under refluxing condition (Sharma *et al.*, 2014).

[3+2] cycloaddition reaction strategy to form five membered ring systems is the most accessible route for formation pyrazolines. Loh *et al.*, 2013 were synthesized N-substituted pyrazolines by the reaction of respective chalcone with hydrazine hydrate in the presence of different aliphatic acids namely formic acid, acetic acid and propionic acid as shown fig (1.18).
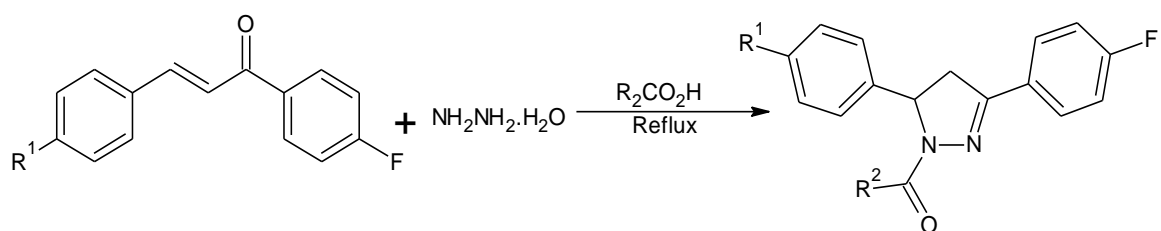
Figure (1.18): Synthesis of N-substituted pyrazoline derivatives

Also (Kumar & Jayaroopa, 2013), (Joshi *et al.,* 2012), (Sridhar & Rajendraprasad, 2012), (Pant *et al.,* 2011), (Sahoo *et al.,* 2011), (Sid *et al.*, 2011), (Acharya *et al.*, 2010), (Das *et al.*, 2010), (Karuppasamy *et al.*, 2010), (Venkataraman *et al.,* 2010), (Gowramma *et al.,* 2009), (Kaplancikli *et al.,* 2009), (Sauzem *et al*, 2008), (Shoman *et al.*, 2009), (Chimenti *et al.*, 2008), (Jayaprakash *et al.*,2008), (Krishna & Sekhar, 2008), (Ali *et al.*, 2007), (Li *et al.*, 2007), (Mishra *et al.,* 2007) and

(Shinde *et al.,* 2004) were followed the same strategy in synthesis of pyrazoline derivatives.

The intensity of diverse biological applications of pyrazolines made them popular drugs that created an interest among the scientists to work in this area (Kumar & Govindaraju, 2015), another important reason for the popularity of this scaffold is its ease of synthesis (Shinkar *et al.*, 2015).

1.2. Molecular modeling and drug design

Molecular modeling is a tool for doing chemistry. Models are central for understanding of chemistry. Molecular modeling allows to do and teach chemistry better by providing better tools for investigating, interpreting, explaining and discovering new phenomena. Molecular modeling is easy to perform with currently available software, but the difficulty lies in getting the right model and proper interpretation. Molecular modeling is the general term used to describe the use of computers to construct molecules and perform a variety of calculations on these molecules in order to predict their chemical characteristics and behaviour. The term molecular modeling is often used synonymously with the term computational chemistry. Computational chemistry is a broader term, referring to any use of computers to study chemical systems. Molecular modeling encompasses all theoretical methods and computational techniques used to model or mimic the behaviour of molecules. The techniques are used in the field of computational chemistry, computational biology and materials science for studying molecular systems ranging from small chemical systems to large biological molecules and material assemblies (Mukesh & Rakesh, 2011).

Drug design is a process which is driven by technological breakthroughs implying advanced experimental and computational methods. Nowadays,

the techniques or the drug design methods are of paramount importance for prediction of biological profile, identification of hits, generation of leads, and moreover to accelerate the optimization of leads into drug candidates (Patel *et al.*, 2014).

Drug discovery has often evolved from serendipitous and fortuitous findings, for example, the discovery of penicillin by Alexander Fleming in 1928 triggered the Antibiotic Revolution which contributed tremendously to humankind's quest of longevity. If not by chance, such discoveries may be achieved through random systematic experimentation or chemical intuition where combinatorial libraries are synthesized and screened for potent activities. Such approach is extremely time consuming, labor intensive, and impractical in terms of costs. A more lucrative solution to this problem is to rationally design drugs using computer-aided tools via molecular modeling, simulation, and virtual screening for the purpose of identifying promising candidates prior to synthesis (Nantasenamat *et al*., 2009).

Quantitative structure-activity relationship modeling is an important approach in drug discovery that correlates molecular structure with biological and pharmaceutical activities (Shahlaei, 2013).

1.3. Quantitative structure-activity relationships
1.3.1. Definition of QSAR
Differentiating between drug-like from non-drug-like molecules is essential to reduce the cost associated with failed drug development. Various *in silico* approaches have shown the potential for screening chemical databases against the desired biological targets for the development of new potential leads. Among them, ligand-based virtual screening has become popular because of its ability to screen millions of

molecules rapidly from available chemical databases (Danishuddin & Khan, 2016).

Quantitative structure-activity relationship (QSAR) is the name usually applied to methods which correlate molecular structure to some kind of *in vitro* or *in vivo* biological property. When this approach is applied to modelling of toxicological data, it is termed quantitative structure-toxicity relationships (QSTR). When applied to modelling physicochemical properties it is called quantitative structure-property relationships (QSPR) (Winkler, 2001).

Quantitative structure-activity relationship (QSAR) and quantitative structure- property relationship (QSPR) makes it possible to predict the activities/properties of a given compound as a function of its molecular substituent. Essentially, new and untested compounds possessing similar molecular features as compounds used in the development of QSAR/QSPR models are likewise assumed to also possess similar activities/properties (Nantasenamat *et al*., 2009).

In simplest terms, quantitative structure-activity relationship is a method for building computational or mathematical models which attempts to find a statistically significant correlation between structure and function using a chemometric technique. In terms of drug design, structure here refers to the properties or descriptors of the molecules, their substituents or interaction energy fields, function corresponds to an experimental biological/biochemical endpoint like binding affinity, activity, toxicity or rate constants, while chemometric method include multiple linear regression (MLR), partial least-squares (PLS), principal component analysis (PCA), principal component regression (PCR), artificial neural networks (ANN), genetic algorithms (GA) *etc*. Various QSAR

approaches have been developed gradually over a time span of more than a hundred years and served as a valuable predictive tool, particularly in the design of pharmaceuticals and agrochemicals (Verma *et al*., 2010). If we can understand how a molecular structure brings about a particular effect in a biological system, we have a key to unlocking the relationship and using that information to our advantage (Consonni & Todeschini, 2010).

1.3.2. Historical overview

It is generally accepted that Hansch was the first to use QSARs to explain the biological activity of series of structurally related molecules. Hansch pioneered the use of descriptors related to a molecule's electronic characteristics and to its hydrophobicity. This led him to propose that biological activity could be related to the molecular structure via equations of the following form:

$$\log (1/C) = k1 \log P + k2\sigma + k3 \qquad (eq.1.1)$$

Where *C* is the concentration of compound required to produce a standard response in a given time, log *P* is the logarithm of the molecule's partition coefficient between 1-octanol and water and σ is the appropriate Hammett substitution parameter. This formalism expresses both sides of the equation in terms of free energy. An alternative formulation of this equation uses the parameter π, which is the difference between the log *P* for the compound and the analogous hydrogen-substituted compound:

$$\log (1/C) = k1\pi + k2\sigma + k3; \quad \pi = \log PX - \log PH \qquad (eq.1.2)$$

Another important breakthrough was Hansch's proposal that the activity was parabolically dependent on log *P*:

$$\log (1/C) = -k1 (\log P)^2 + k2 (\log P) + k3\sigma + k4 \qquad (eq.1.3)$$

Hansch's rationale for suggesting the parabolic dependence on log *P* was that the drug's hydrophobicity should not be so low that the drug did not partition into the cell membrane nor so high that once in the membrane it simply remained there. An early example of such a non-linear relationship between a biological response and the partition coefficient is the following equation derived for the narcotic effect of thirteen barbiturates on mice:

$$\log (1/C) = -0.44 \, (\log P)^2 + 1.58 \, (\log P) + 1.93 \qquad \text{(eq.1.4)}$$

The electronic characteristics of a molecule are also important in determining its activity against the target; the Hammett parameters provided a concise and convenient way to quantify these. Hammett and others had shown that for related compounds reaction rates (e.g. for the hydrolysis of benzoate esters) and positions of equilibrium (e.g. the ionisation constants of substituted benzoic acids) could be quantified using equations of the following form:

$$\mathrm{Log} \, (k/k0) = \rho\sigma$$

$$\log (K/K0) = \rho\sigma \qquad \text{(eq.1.5)}$$

These equations express the rate *(k)* or equilibrium *(K)* constant for a particular substituent relative to that for a reference compound. The substituent parameter σ is determined by the nature of the substituent and whether it is *meta* or *para* to the carboxylic acid or ester group on the aromatic ring. The reaction constant ρ is fixed for a particular process with the standard reaction being the dissociation of benzoic acids *($\rho = 1$)*. There have been many extensions to Hammett's original formulation, such as the work of Taft who showed how to incorporate steric effects. Another key development of particular relevance to the QSAR community was the suggestion by Swain and Lupton that σ values could

be written as a weighted linear combination of two components: a field component *(F)* and a resonance component *(R)*. Many phenomena had been found to follow a Hammett-style equation but were not well correlated using Hammett's original substitution values (Winkler, 2001).

1.3.3. QSAR method

The QSAR method involves recognition that molecule (organic, peptide, protein, etc.) is really a three-dimensional distribution of properties. The most important of these properties are steric (e.g. Shape and volume), electronic (e.g. Electric charge and electrostatic potential), and what are termed "lipophilic" properties (how polar or non-polar the sections of the molecular are, usually exemplified by the log of the octanol-water partition coefficient, *log P*). Scientists are used to visualising mainly steric properties of molecules. However, molecules look different when viewed in electrostatic, or lipophilic space.

The QSAR method (and analogously QSTR and QSPR) involves a number of key steps. Firstly, converting molecular structures into mathematical descriptors that encapsulate the key properties of the molecules relevant to the activity or property being modelled. Secondly, selecting the best descriptors from a larger set of accessible, relevant descriptors. Thirdly, mapping the molecular descriptors into the properties, preferably using a "model-free" mapping system in which no assumptions are needed as to the functional form of the structure-activity relationship. These relationships are often complex, unknown and non-linear. Finally, validating the model to determine how predictive it is, and how well it will generalise to new molecules not in the data set used to generate the model (the training set) (Winkler, 2001).

Briefly, this method included data collection, molecular descriptor selection, correlation model development, and lastly model evaluation. QSAR studies have predictive ability and simultaneously provide deeper insight into mechanism of drug receptor interactions (Hansch *et al*., 1995)

1.3.4 Validation of quantitative structure–activity relationship model

To test the internal stability and predictive ability of the derived QSAR model, it was validated or cross-checked by the internal validation and external validation test procedure as follows:

a) *Internal validation by training set compounds:* Internal validation of the derived QSAR model was carried out by using leave-one-out (LOO) validation method. For calculating cross validation regression coefficient (Q^2), each molecule in the training set was eliminated once, and the activity of the eliminated molecule was predicted by using the QSAR model developed by the remaining molecules.

b) *External validation by test set compounds:* For external validation of QSAR model, the activity of each molecule in the test set was predicted by using the derived QSAR model developed by the training set compounds. The predictive accuracy of the derived QSAR model for external test set refers by correlation coefficient (r) and square of the correlation coefficient (r^2) (Yadav *et al*., 2014)

1.3.5. Molecular descriptors

Molecular descriptors can be defined as numerical values that characterise properties of molecules (Leach & Gillet, 2007). Also it can be defined as the essential information of a molecule in terms of its physicochemical properties such as constitutional, electronic, geometrical, hydrophobic, lipophilicity, solubility, steric, quantum

chemical, and topological descriptors. From a practical viewpoint, molecular descriptors are chemical information that is encoded within the molecular structures for which numerous sets of algorithms are available for such transformation (Nantasenamat *et al*., 2009). Molecular descriptors have now become some of the most important variables used in molecular modeling, and, consequently, managed by statistics, chemometrics, and chemoinformatics (Consonni & Todeschini, 2010).

1.3.5.1. Classification of molecular descriptors

Molecular descriptors are divided into two main classes:

a) *Experimental measurements*: such as log P, molar refractivity, dipole moment, polarizability, and, in general, physico-chemical properties.

b) *Theoretical molecular descriptors*: theoretical descriptors derived from physical and physico-chemical theories show some natural overlap with experimental measurements. Several quantumchemical descriptors, surface areas, and volume descriptors are examples of such descriptors also having an experimental counterpart. With respect to experimental measurements, the greatest recognized advantages of the theoretical descriptors are usually (but not always) in terms of cost, time, and availability.

The fundamental difference between theoretical descriptors and experimentally measured ones is that theoretical descriptors contain no statistical error due to experimental noise, as opposed to experimental measurements.

There are simple molecular descriptors derived by counting some atom types or structural fragments in the molecule, as well as physico-chemical

and bulk properties such as, for example, molecular weight, number of hydrogen bond donors/acceptors, number of OH-groups, and so on. Other molecular descriptors are derived from algorithms applied to a topological representation. These are usually termed topological, or 2D-descriptors. Other molecular descriptors are derived from the spatial (x, y, z) coordinates of the molecule, usually called geometrical, or 3D-descriptors; another class of molecular descriptors, called 4D-descriptors, is derived from the interaction energies between the molecule, imbedded into a grid, and some probe (Consonni & Todeschini, 2010).

1.3.5.2. Descriptor selection method

Descriptor selection is an important step for several reasons, because of using a few descriptors increases the interpretability and understanding of resulting models, it can reduce the risk of overfitting from noisy redundant molecular descriptors, it can provide faster and cost-effective models and it removes the activity cliff. However, noisy, redundant, or irrelevant descriptors should be removed in a way that the dimension of the input space is reduced without any loss of significant information.

To remove irrelevant descriptors, a selection criterion is required that can measure the relevance of each selected descriptor with the output of any classifier. Depicts the procedure that can be used for the selection of the descriptors. Such descriptor selection techniques have become an obvious requirement in development of the robust QSAR models. The interpretability and generality of the models obtained by these methods are highly dependent on the statistical relations among the descriptors and target properties. Thus, expert knowledge in the selection process is required to gain user confidence in the selected set of descriptors (Danishuddin & Khan, 2016).

1.3.6. Purpose of QSAR

QSAR should not be seen as an academic tool to allow for the post-rationalization of data. Relationships between molecular structure, chemistry and biology must be derived for good reason. From these relationship models can be developed, and with luck, good judgment and expertise these will be predictive. For many practical purposes including QSAR techniques are utilized widely in many situations in the following:

a) to quantitatively correlate and recapitulate the relationships between trends in chemical structure alterations and respective changes in biological endpoint for comprehending which chemical properties are most likely determinants for their biological activities

b) to optimize the existing leads so as to improve their biological activities

c) to predict the biological activities of untested and sometimes yet unavailable compounds fig (1.19) (Verma *et al.*, 2010).

d) to save in the cost of product development (e.g. in the pharmaceutical, pesticide, personal products, etc. areas).

e) to be able to reduce the requirement for lengthy and expensive animal tests in predictions.

f) to reduce (and even, in some cases, to replace) animal tests, thus reducing animal use and obviously pain and discomfort to animals.

g) to promote green and greener chemistry in other areas to increase efficiency and eliminate waste by not following leads unlikely to be successful (Consonni & Todeschini, 2010).
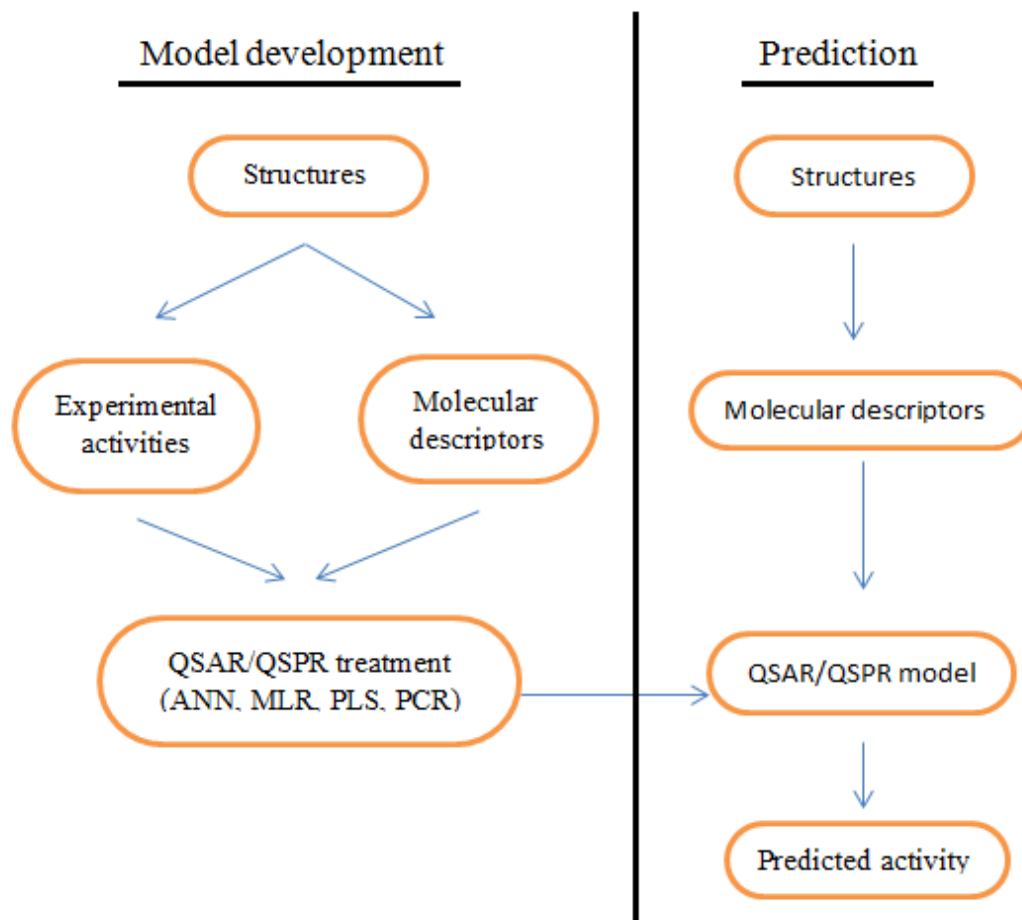
Figure (1.19): Overview of QSAR/QSPR modelling model

1.3.7. Applications of QSAR

Some of the major applications of QSAR are to: optimize of pharmacological, biocidal or pesticidal activity, identify rationally new leads with pharmacological, biocidal or pesticidal activity, design rationally numerous other products such as surface-active agents, perfumes, dyes, and fine chemicals, identify hazardous compounds at early stages of product development or the screening of inventories of existing compounds, designing out of toxicity and side-effects in new compounds, predict toxicity to humans through deliberate, occasional and occupational exposure, predict toxicity to environmental species, select compounds with optimal pharmacokinetic properties (whether it be

stability or availability in biological systems), predict a variety of physico-chemical properties of molecules (whether they be pharmaceuticals, pesticides, personal products, fine chemicals, etc.), rationalize and predict the combined effects of molecules (whether it be in mixtures or formulations) and predict the fate of molecules which are released into the environment (Consonni & Todeschini, 2010).

1.3.8. Classification of QSAR Methodologies

a) *Based on dimensionality*, most often the QSAR methods are categorized into following classes, based on the structural representation or the way by which the descriptor values are derived:

- 1D-QSAR correlating activity with global molecular properties like pKa, log P, etc.

- 2D-QSAR correlating activity with structural patterns like connectivity indices, 2D pharmacophores, without taking into account the 3D-representation of these properties.

- 3D-QSAR correlating activity with non-covalent interaction fields surrounding the molecules.

- 4D-QSAR additionally including ensemble of ligand configurations in 3D-QSAR.

- 5D-QSAR explicitly representing different induced-fit models in 4D-QSAR.

- 6D-QSAR further incorporating different solvation models in 5D-QSAR (Patel *et al*., 2014).

a) *Based on the type of chemometric methods used* , sometimes QSAR methods are also classified into following two categories, depending upon the type of correlation technique employed to

establish a relationship between structural properties and biological activity:

- Linear methods including linear regression (LR), multiple linear regression (MLR), partial least-squares (PLS), and principal component analysis/regression (PCA/ PCR).
- Non-linear methods consisting of artificial neural networks (ANN), *k*-nearest neighbors (*k*NN), and Bayesian neural nets (Verma *et al*., 2010).

1.4. Molecular docking

Molecular docking methodologies are of great importance in the planning and design of new drugs. These methods aim to predict the experimental binding mode and affinity of a small molecule within the binding site of the receptor target of interest (Guedes *et al.*, 2014).

The molecular docking approach can be used to model the interaction between a small molecule and a protein at the atomic level, which allows us to characterize the behaviour of small molecules in the binding site of target proteins as well as to elucidate fundamental biochemical processes. The docking process involves two basic steps: prediction of the ligand conformation as well as its position and orientation within these sites (usually referred to as *pose*) and assessment of the binding affinity. Knowing the location of the binding site before docking processes significantly increases the docking efficiency. In many cases, the binding site is indeed known before docking ligands into it. Also, one can obtain information about the sites by comparison of the target protein with a family of proteins sharing a similar function or with proteins co-crystallized with other ligands. In the absence of knowledge about the binding sites, cavity detection programs or online servers can be utilized to identify putative active sites within proteins. Docking without any

assumption about the binding site is called blind docking (Meng *et al*, 2011).

The interaction between ligand and target molecule involves many types of non-covalent interactions such as hydrogen bond, ionic bond, hydrophobic and van der Waals. Molecular docking study can be possible in between protein-protein, protein-ligand and protein-nucleotide (Tripathi & Misra, 2017).

Molecular docking can be divided into two separate sections:

a) *Search algorithm*: these algorithms determine all possible optimal conformations for a given complex (protein-protein, protein-ligand) in an environment, i.e., the position and orientation of both molecules relative to each other. They can also calculate the energy of the resulting complex and of each individual interaction.

b) *Scoring function* : these are mathematical methods used to predict the strength of the non-covalent interaction called as binding affinity, between two molecules after they have been docked. Scoring functions have also been developed to predict the strength of other types of intermolecular interactions, for example between two proteins or between protein and DNA or protein and drug. These configurations are evaluated using scoring functions to distinguish the experimental binding modes from all other modes explored through the searching algorithm (Mukesh & Rakesh, 2011).

1.4.1. Applications of molecular docking

1.4.1.1. Applications of molecular docking in drug development

Docking is most commonly used in the field of drug design, most drugs are small organic molecules and docking may be applied to:

a) *Hit identification*: Docking combined with a scoring function can be used to quickly screen large databases of potential drugs *in silico* to identify molecules that are likely to bind to protein target of interest

b) *Lead optimization:* Docking can be used to predict in where and in which relatives orientation a ligand binds to a protein. This information may in turn be used to design more potent and selective analogs.

c) *Bioremedation:* Protein ligand docking can also be used to predict pollutants that can be degraded by enzymes (Supriya *et al.*, 2016).

1.4.1.2. Application of molecular modelling in modern drug development

It is used in screening for the side effects that can be caused by the interactions with other proteins, like proteases and Cytochrome P450. It is also possible to check the specificity of the potential drug against homologous proteins through docking, and it is a widely used tool in predicting protein-protein interactions and knowledge of the molecular associations aids in understanding a variety of pathways taking place in the living and in revealing of the possible pharmacological targets. The technique is used in the field of computational chemistry, computerised biology material used for molecular system ranging from small molecules to large biological molecules and material assemblies.

Molecular docking is an inexpensive, safe and easy to use tool and helps in investigating, interpreting, explaining and identification of molecular properties using three-dimensional structures (Supriya *et al.*, 2016).

Aims and objectives

There has always been and will continue to be a need for new and novel chemical entities with diverse biological activities. The present work deals with the:

- ✓ Design of new trisubistituted pyrazoline derivatives expected to possess anticancer activity.
- ✓ Generation of QSAR models that can be used to predict anticancer activity against MCF-7 breast cancer cell line by using compounds collected from literature.
- ✓ Study of the usefulness of QSAR model in the prediction of the anticancer activity of designed trisubistituted pyrazoline derivatives against MCF-7 breast cancer cell line.
- ✓ Evaluation of the druggability of designed compounds by using Lipinski's rule.
- ✓ Selection of pyrazoline derivatives that fit in Lipinski's rule.
- ✓ Synthesis of selected trisubistituted pyrazoline derivatives.
- ✓ Calculation of the physicochemical properties of the synthesized compounds.
- ✓ Characterization of these compounds for structure elucidation using spectroscopic techniques like FT-IR, UV, GC-MS and ^{1}HNMR spectral studies.
- ✓ Prediction of the ligand-receptor complex structure through molecular docking studies of the synthesize compounds.

2. Materials and Methods

2.1. Materials, soft wares and instruments

2.1.1. Dataset

In QSAR studies, a total of **18** trisubstituted pyrazoline derivatives (group I) and **18** α,β-unsaturated carbonyl derivatives (group II) were gathered from Qin *et al*. (2015) and Syam *et al*. (2012), respectively. They reported the *in vitro* cytotoxicity of mentioned compounds against various human cell lines, including human breast adenocarcinoma cell line MCF-7. The biological activities in each group expressed as IC_{50} (concentration of the compounds exhibiting 50% inhibition of cell growth for human breast cancer MCF-7), and were compared with combretastatin A-4 (CA-4) in group (I) and with tamoxifen in group (II).

2.1.2. Chemicals

Acetic acid (99.9%) was obtained from Chemajet company (Egypt).

Acetone (99%), dioxane (99.5%) and n-hexane (99%) were obtained from ADWIC company (Egypt).

Acetophenone (99%), benzaldehyde (98.5%), chloroacetylchloride (98%), 4-dimethylaminobenzaldehyde (98%), furfural (98%), 4-nitroacetophenone (99%), sodium hydroxide (98%) and potassium carbonate unhydrous (99%) were obtained from Loba Chemie company (India).

4-Bromoacetophenone(98%), 4-chlorobenzaldehyde (98%), sulfanilamide (98%) and sulfadoxine (98%) were obtained from Alfa Aesar company (Germany).

Cinnamaldehyde (98%) and hydrazine hydrate (99%) were obtained from Scharlau company (Spain).

Dimethyl formmaide (99%) was obtained from Oxford company (India).

Ethanol (99.5%) was obtained from Alamia company (Egypt).

Ethylacetate (99%) was obtained from Alpha Chemicals company (Eygpt).

Hydrochloric acid (32%) was obtained from Piochem company (Egypt).

4-Methylacetophenone (95%), triethylamine (99%) and toluene (99%) were obtained from Honeywell Riedel-de Haen (Germany).

Sodium sulfate unhydrous (99%) was obtained from LABCO Chemical LTD.

2.1.3. Soft wares

2.1.3.1. ACD/Labs Software

 ACD/ChemSketch (Freeware) is a drawing package that allows to draw chemical structures including organics, organometallics, and polymers structures. It also includes features such as calculation of molecular properties (e.g., molecular weight, density molar refractivity etc.), 2D and 3D structure cleaning and viewing, functionality for naming structures (fewer than 50 atoms and 3 rings), and prediction of logP. The freeware version of ChemSketch does not include all of the functionality of the commercial version such as ACD/Dictinory and search of files on personal computer by structures. Copyright © 1994-2016, ACD/Labs 2016.2 (File Version C30E41, Build 90752, 20 Dec 2016).

2.1.3.2. ChemBioDraw Soft ware

ChemBioDraw (version 14.0) designed for scientists, students, and scientific authors, ChemBioDraw is a powerful, yet easy-to use, tool for producing chemical and biological drawings. Copyright 1998-2014 CambridgeSoft Corporation, a subsidiary of PerkinElmer, Inc.

2.1.3.3. Molecular Operating Environment (MOE) Soft ware

MOE, Chemical Computing Group's Molecular Operating Environment is an interactive, windows-based chemical computing and molecular modeling tool with a broad base of scientific applications: bioinformatics, cheminformatics, structure based design, protein modeling, high throughput discovery, molecular modeling and simulations, and methodology development and deployment.

Molecular Operating Environment (MOE), 2010.10; Chemical Computing Group Inc., 1010 Sherbooke St. West, Suite #910, Montreal, QC, Canada, H3A 2R7, 2010

2.1.3.4. Statistical package for social sciences (SPSS) Soft ware

SPSS for windows version 11.5.0 programme provides a powerful statistical analysis and data management system in a graphical environment, using descriptive menus and simple dialog boxes to do most of the work for you.

2.1.4. Spectroscopic Instruments

2.1.4.1. Infrared Spectrophotometer (IR)

The infrared spectra (cm^{-1}) were recorded using KBr disk by using infrared spectrophotometer, model FT-IR 4100 shimadzu – Japan.

2.1.4.2. Ultra Violet Spectrophotometer (UV)

Ultra violet spectral data were obtained using UV.3101PC. shimadzu – Japan.

2.1.4.3. Nuclear Magnetic Resonance Spectrophotometer (NMR)

^{1}HNMR spectra were recorded in Bruker (Germany) Avance III 400 spectrometer using DMSO as a solvent and TMS as an internal standard. Chemical shifts (δ) are reported in ppm. Splitting patterns are designed as follows: s- singlet, d- doublet, t- triplet, q- quartet and m- multiplet.

2.1.4.4. Gas Chromatography Mass Spectrometer (GC-MS)

The mass spectra were recorded on GC-MS Shimadzu Qp-2010 Plus Spectrometer.

2.1.4.5. General Instruments

 -Ultra violet lamp model UVGL-58 multiband UV.254-365 NM, Upland, CA91786 U.S.A.

 -Hot plate with magnetic stirrer VELP scientific – Europe.

 - Sensitive balance Sartorius-BI2105 model.

- Melting points were determined by using Fisher-Johns 6200 melting point apparatus and were uncorrected (Fisher scientific company made in U.S.A)

2.1.5. Thin Layer Chromatography (TLC)

The progress and purity of synthesized trisubstituted pyrazolines were carried out on pre-coated TLC silica gel 60 F254 plates and the spots were visualized in ultraviolet light with different eluting system.

2.2. Methods

2.2.1. QSAR modeling

The activity in terms of IC_{50} in group (I) and (II) (IC_{50} in microgram per milliliter) were converted to negative logarithmic concentration in moles (anticancer potential pIC_{50}), in order to obtain higher mathematical values when the structures are biologically very efficient (N'guessan *et al*., 2017).

The anticancer activity which is expressed by the anticancer potential (pIC_{50}) is defined in equation (2.1):

$1\mu M= 10^{-6}M$

$pIC_{50}= \log 1/IC_{50}$

$pIC_{50}= -\log_{10} (IC_{50} \; x \; 10^{-6})$ \qquad\qquad (eq.2.1)

ChemSketch/ACDlab software was used for drawing series of the studied compounds tables (2.1) and (2.2). Then, the data set of trisubstituted pyrazoline derivatives (group I) and α,β-unsaturated carbonyl derivatives (group II) were divided into a training set of **15** and a test set of **3** compounds by random selection.

Table (2.1): Structures, IC_{50} and pIC_{50} of 1,3,5-trisubstituted pyrazoline derivatives (Qin *et al*., 2015)
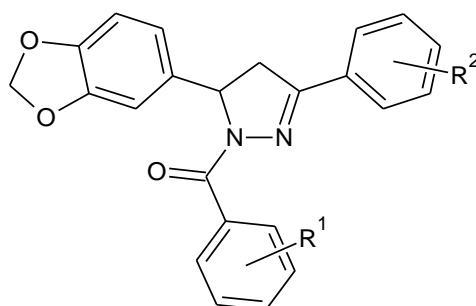
Compound No.	R^1	R^2	IC_{50}	pIC_{50}
1a	3,4,5-$(OCH_3)_3$	2-OCH_3	0.21	6.68
2a	3,4,5-$(OCH_3)_3$	3-OCH_3	0.06	7.22
3a	3,4,5-$(OCH_3)_3$	4-OCH_3	0.05	7.30
4a	3,4,5-$(OCH_3)_3$	4-Cl	4.26	5.37
5a	3,4,5-$(OCH_3)_3$	4-F	0.32	6.49
6a	3,4,5-$(OCH_3)_3$	3-Cl	9.23	5.03
7a	3,4,5-$(OCH_3)_3$	4-CH_3	2.35	5.63
8a	3,4,5-$(OCH_3)_3$	3-CH_3	7.34	5.13
9a	3,4,5-$(OCH_3)_3$	H	3.38	5.47
10a	4-Br	4-F	5.11	5.29
11a	4-F	4-OCH_3	1.77	5.75
12a	4-Cl	4-OCH_3	8.66	5.06
13a	3-OCH_3	4-OCH_3	8.22	5.09
14a	4-OCH_3	4-OCH_3	6.41	5.19
15a	3,4-$(OCH_3)_2$	4-OCH_3	3.56	5.45
16a	H	4-OCH_3	5.37	5.27
17a	4-F	3,4,5-$(OCH_3)_3$	0.22	6.66
18a	4-Cl	3,4,5-$(OCH_3)_3$	4.77	5.32
Combretastatin	-	-	0.31	6.51

Table (2.2): Structures, IC_{50} and pIC_{50} of α,β-unsaturated carbonyl derivatives (Syam *et al*., 2012)
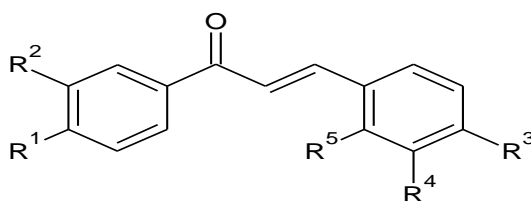
Compound No.	R^1	R^2	R^3	R^4	R^5	IC_{50}	pIC_{50}
1b	H	H	H	H	H	6.875	5.16
2b	CH_3	H	H	H	H	13.62	4.87
3b	OCH_3	H	H	H	H	19.15	4.72
4b	H	H	H	H	Cl	7.992	5.10
5b	OH	H	H	H	Cl	10.01	5.00
6b	H	H	H	CH_3	H	9.34	5.03
7b	OH	H	H	CH_3	H	8.343	5.08
8b	CH_3	H	H	CH_3	H	10.16	4.99
9b	OCH_3	H	H	CH_3	H	9.53	5.02
10b	H	H	OCH_3	H	H	11.62	4.93
11b	CH_3	H	OCH_3	H	H	32.37	4.49
12b	OCH_3	H	OCH_3	H	H	41.44	4.38
13b	H	H	$N(CH_3)_2$	H	H	99.29	4.00
14b	CH_3	H	$N(CH_3)_2$	H	H	57.28	4.24
15b	H	H	H	H	OH	9.353	5.03
16b	H	CH_3	H	H	OH	6.873	5.16
17b	H	OCH_3	H	H	OH	7.149	5.15
18b	H	H	H	Cl	H	5.251	5.28
Tamoxifen	-	-	-	-	-	0.04	7.39

2.2.2. Molecular modeling parameters

Total of **11** molecular descriptors listed in table (2.3) were initially calculated for each compound in training set of group (I) using MOE and ACD/lab. 2D descriptors (MW, MR, MV, RI and D) was calculated by ACD/lab programme, the rest of 3D descriptors and log P(o/w) descriptor were calculated by MOE programme. Table (2.4) illustrated values of descriptors that calculated by programmes for group (I).

Eight molecular descriptors namely, molecular weight (MW), molar volume (MV), surface tension (ST), molar reactivity (MR), potential energy (E), refractive index (RI), density(D) and logP (octanol/water) (logP(o/w)) were calculated for each compound in training set of group (II) using MOE and ACD/lab programmes and listed in table (2.5).

Table 2.3: List of chemical descriptors with details used in QSAR modeling

No.	Descriptor	Description
1	Molecular Weight (MW)	The molecular formula is determined from the atoms in the chemical sample at the time of evaluation (Yadav *et al.*, 2017).
2	Molar Refractivity (MR)	Reflects arrangements of the electron shells of ions in molecules and yields information about the electronic polarization of ions (Pacak, 1989).
3	Molar volume (MV)	Defined as the volume change of solution when the solute is immersed into the solution (Imai, 2007).
4	Refractive index (RI)	Is a measure of the change in velocity of a light wave as it goes from one medium to another (Samuels, 1981). It useful to assess purity of substances and to calculate the molecular electronic polarizibility (Shukla *et al.*, 2012).

5	Density (D)	Density is the mass per unit volume and is usually expressed in grams per cubic centimeter The values are then directly comparable, since(or per milliliter)' at some definite temperature (Hidnert & Peffer, 1950)
6	Surface tension (ST)	It is measure of energy loss per unit area of surface (Bush, 2011).
7	Logarithm of the Partition coefficient: $\log P = \log (C_{org}/C_{water})$ Log P(o/w)	Hydrophobicity/lipophilicity, expressed by the logarithm of octanol-water partition coefficient log P, logP>0 – greater solubility in the organic phase; logP<0 – greater solubility in the aqueous phase (Pallicer *et al*., 2014).
8	Heat of Formation (HF)	The energy released or used when a molecule is formed from elements in their standard states (Yadav *et al*., 2017).
9	Ionization Potential (IP)	The energy required to remove an electron from a molecule in its ground state (Yadav *et al*., 2017).
10	Dipole Moment (dipole)	The dipole moment indicates the stability of a molecule in water. Thus, a high dipole moment will result in poor solubility in organic solvents and high solubility in water (N'guessan *et al*., 2017).
11	Potential energy (E)	The Potential energy of a system of a particles s equal to negative of the work by the conservative force as a particle is brought from infinity to its position in the presence of the other particles of the system (Singh, 2009).

Table 2.4: Values of chemical descriptors with details used in QSAR modeling of group (I)

Compound No.	MW	MR	MV	RI	D	ST	logP(o/w)	HF	IP	dipole	E
1a	490.504	129.69	129.69	129.69	1.31	45.5	4.43548	-99.2623	8.73152	1.819013	149.3456
3a	490.504	129.69	372.3	1.613	1.31	45.5	4.43748	-101.624	8.65333	1.688911	144.9774
4a	494.923	128.48	360	1.632	1.37	47.6	5.07348	-47.8222	8.96887	1.215617	135.8836
5a	478.469	123.75	353.6	1.617	1.35	45.2	4.63448	-109.418	8.94147	1.227071	133.4252
6a	494.923	128.48	360	1.632	1.37	47.6	5.11048	-66.5089	8.95443	1.023524	133.596
7a	474.505	128.3	365.9	1.618	1.29	45	4.77948	-71.2613	8.7929	1.551001	138.316
9a	460.478	123.87	350.7	1.624	1.31	46.7	4.48148	-64.2462	8.91351	1.53525	134.8879
10a	467.287	113.86	301.2	1.68	1.55	52.2	5.991	3.47809	9.00173	1.046086	96.19308
11a	481.417	112.12	310.3	1.642	1.34	47.9	5.149	-39.8802	8.69181	1.579098	104.5233
12a	434.871	116.85	316.7	1.659	1.37	50.7	5.588	-1.75945	8.6971	1.611742	105.5788
13a	430.452	118.06	329.1	1.636	1.3	48.1	4.989	-32.2138	8.662	1.596563	113.0786
15a	460.478	123.87	350.7	1.624	1.31	16.7	4.69474	-55.6539	8.65394	1.744001	130.2732
16a	400.426	112.25	307.5	1.65	1.3	49.7	4.996	5.29364	8.61974	1.33213	106.1936
17a	478.469	123.75	353.6	1.617	1.35	45.2	4.63448	-109.192	8.79335	1.501933	136.1933
18a	494.923	128.48	360	1.632	1.37	47.6	5.07348	-69.2972	8.824781	1.57097	137.2353

Table 2.5: Values of chemical descriptors with details used in QSAR modeling of group (II)

Compound No.	MW	MV	ST	MR	E	RI	D	logP(o/w)
1b	208.255	189.8	44.7	67.1	53.88202	1.624	1.097	4.065
2b	222.281	206	43.2	71.93	56.0874	1.615	1.078	4.363
4b	242.7	201.7	46.4	72	61.17518	1.632	1.202	4.655
5b	238.281	204.5	49.9	73.81	55.46881	1.641	1.165	4.053
6b	222.281	206	43.2	71.93	56.1036	1.615	1.078	4.4
7b	238.281	204.5	49.9	73.81	53.3754	1.641	1.165	4.092
8b	236.308	222.3	42	76.75	58.28762	1.606	1.062	4.698
9b	252.307	230.1	41.8	78.61	65.41583	1.598	1.096	4.356
11b	252.307	230.1	41.8	78.61	68.13621	1.598	1.096	4.319
12b	268.307	237.8	41.6	80.46	72.26687	1.591	1.128	3.977
13b	251.322	227.8	45.9	81.42	72.06151	1.633	1.103	3.98
14b	265.349	244	44.5	86.24	71.59818	1.624	1.087	4.278
15b	224.254	188.2	52.1	68.99	56.14378	1.653	1.191	3.755
16b	238.281	204.5	49.9	73.81	58.24109	1.641	1.165	4.09
18b	242.7	201.7	46.4	72	55.27224	1.632	1.202	4.694

2.2.2.1. Selection of subset descriptors

The ratio of the number of compounds to the physicochemical descriptors used for the correlation is usually 5:1(Vaidya *et al.*, 2012). To select the best sub-set of physico-chemical properties in group (I) and (II), highly correlated chemical descriptors were excluded through co-variance analysis using correlation fig (2.1) and (2.2).

Figure (2.1): Details of correlation matrix for chemical descriptors in group (I)

	1	2	3	4	5	6	7	8	9	10	11
1. MW	100	-26	72	68	-47	-7	18	-69	56	-13	66
2. logP(o/w)	-26	100	-60	-74	94	37	76	79	18	-45	-79
3. MR	72	-60	100	98	-78	-23	-30	-77	34	10	95
4. MV	68	-74	98	100	-88	-28	-43	-85	24	19	99
5. RI	-47	94	-78	-88	100	36	71	89	4	-39	-90
6. ST	-7	37	-23	-28	36	100	29	23	24	-37	-28
7. D	18	76	-30	-43	71	29	100	36	55	-61	-45
8. HF	-69	79	-77	-85	89	23	36	100	-20	-21	-88
9. IP	56	18	34	24	4	24	55	-20	100	-74	22
10. dipole	-13	-45	10	19	-39	-37	-61	-21	-74	100	23
11. E	66	-79	95	99	-90	-28	-45	-88	22	23	100

Figure (2.2): Details of correlation matrix for chemical descriptors in group (II)

The correlation matrix in fig (2.1) showed that the MR and MV are correlated to each other and are highly correlated to E, also RI correlated to log P(o/w). So, MR, MV and RI are excluded from the study.

In fig (2.2) which showed the correlation matrix for descriptors in group (II) showed that the MV correlated to MR, and ST correlated to RI. So, MV and ST are excluded from the study.

About 46 regression equation was employed for MCF-7 cancer cell line in group (I) table (2.6), and 20 regression equation in group (II) table (2.7) using multiple linear regression method. Lastly, a QSAR model equation with high square of the correlation coefficient (r^2) was selected.

Table (2.6): The QSAR models between descriptors and biological activity of trisubisitiuted pyrazoline derivatives for MCF-7 cancer cell line (group I)

No.	Removed descriptors	QSAR Equations	r^2*	RMSE*
1	LogP(o/w), HF, IP, dipole, E	Pc = 4.86949+ 0.01214 x MW- 3.75986 x D+ 0.00472 x ST	0.27158	0.58462
2	ST, HF, IP, dipole, E	Pc = 4.63012+ 0.00056 x MW+ 7.73790 x D- 1.94430 x logP(o/w)	0.61690	0.42397
3	ST, LogP(o/w), IP, dipole, E	Pc = 5.37941- 0.01005 x MW+ 2.87081 x D- 0.02054 x HF	0.64726	0.40682
4	ST, LogP(o/w), HF, dipole, E	Pc = 17.99979+0.01588 x MW- 1.22742 x D- 2.05586 x IP	0.33955	0.55667
5	ST, LogP(o/w), HF, IP, E	Pc = 1.06646+ 0.01162 x MW- 1.51180 x D+ 0.83895 x dipole	0.31985	0.56491
6	ST, LogP(o/w), HF, IP, dipole	Pc = 1.97532+ 0.00195 x MW- 0.02904 x D+ 0.02259 x E	0.34248	0.55544
7	D, HF, IP, dipole, E	Pc = 7.02095+ 0.00699 x MW+ 0.01617 x ST- 1.07730 x logP(o/w)	0.52595	0.47162
8	D, LogP(o/w), IP, dipole, E	Pc = 6.81460- 0.00552 x MW+ 0.01106 x ST- 0.01716 x HF	0.62785	0.41787
9	D, LogP(o/w), HF, dipole, E	Pc = 21.00521+ 0.01700 x MW+ 0.00896 x ST- 2.69203 x IP	0.34156	0.55583
10	D, LogP(o/w), HF, IP, E	Pc = -1.82038+ 0.01135 x MW+ 0.00954 x ST+ 1.20923 x dipole	0.31925	0.56516
11	D, LogP(o/w), HF, IP, dipole	Pc = 1.63929+ 0.00143 x MW+ 0.00739 x ST+ 0.02420 x E	0.34905	0.55266

		Table (2.6): continued		
12	D, ST, IP, dipole, E	Pc = 6.86882- 0.00600 x MW+ 0.12683 x logP(o/w)- 0.01797 x HF	0.61383	0.42566
13	D, ST, HF, dipole, E	Pc = 15.04582+ 0.01037 x MW- 0.81942 x logP(o/w)- 1.15441 x IP	0.52465	0.47226
14	D, ST, HF, IP, E	Pc = 6.10138+ 0.00760 x MW- 0.87711x logP(o/w)+ 0.25782 x dipole	0.50147	0.48364
15	D, ST, HF, IP, dipole	Pc = 9.09529+ 0.01192 x MW- 1.39387 x logP(o/w)- 0.01649 x E	0.51917	0.47498
16	D, ST,LogP(o/w), dipole, E	Pc = 16.20079- 0.00034 x MW- 0.01467 x HF- 1.27014 x IP	0.65103	0.40464
17	D, ST, LogP(o/w) IP, E	Pc = 6.04160- 0.00360 x MW- 0.01515 x HF+ 0.33376 x dipole	0.62348	0.42032
18	D, ST, LogP(o/w) IP, dipole	Pc = 8.23919- 0.00417 x MW- 0.02125 x HF- 0.01412 x E	0.63892	0.41161
19	D, ST, LogP(o/w) HF, E	Pc = 14.03145+ 0.01501 x MW- 1.80934 x IP+ 0.37776 x dipole	0.33778	0.55742
20	D, ST, LogP(o/w) HF, dipole	Pc = 16.33772+ 0.00817 x MW- 1.90292 x IP+ 0.01797 x E	0.43159	0.51643
21	D, ST, LogP(o/w) HF, IP	Pc = 0.47529+ 0.00444 x MW+ 0.01702 x E+ 0.68097 x dipole	0.38663	0.53647
22	MW, HF, IP. dipole, E	Pc = 4.68881+ 7.85347 x D+ 0.01571 x ST- 2.07904 x logP(o/w)	0.64493	0.40816
23	MW, LogP(o/w), IP. dipole, E	Pc = 3.97425+ 0.38978 x D+ 0.00827 x ST- 0.01462 x HF	0.60378	0.43117
24	MW, LogP(o/w), HF, dipole, E	Pc = 9.44427- 2.58419 x D- 0.00007 x ST- 0.02833 x IP	0.05529	0.66578

Table (2.6): continued				
25	MW, LogP(o/w), HF, IP, E	Pc = 4.55017- 0.46096 x D+ 0.00648 x ST+ 1.01278 x dipole	0.12452	0.64092
26	MW, LogP(o/w), HF, IP, dipole	Pc = 1.72659+ 0.23982 x D+ 0.00767 x ST+ 0.02617 x E	0.34755	0.55329
27	MW, ST, IP, dipole, E	Pc = 5.95961+ 0.03688 x D- 0.20217 x logP(o/w)- 0 .01224 x HF	0.59784	0.43439
28	MW, ST, HF, dipole, E	Pc = 23.81540+ 14.28884 x D- 2.47851 x logP(o/w)- 2.85524 x IP	0.76032	0.33535
29	MW, ST, HF, IP, E	Pc = 1.01531+ 9.75596 x D- 1.95039 x logP(o/w)+ 0.80942 x dipole	0.66407	0.39701
30	MW, ST, HF, IP, dipole	Pc = 6.01618+ 8.68553 x D- 2.26218 x logP(o/w)- 0.00656 x E	0.62386	0.42010
31	MW, ST, LogP(o/w) dipole, E	Pc = 24.20153+ 5.59623 x D- 0.01866 x HF- 3.08125 x IP	0.75750	0.33732
32	MW, ST, LogP(o/w) IP, E	Pc = 0.17225+ 2.61133 x D- 0.01420 x HF+ 0.82302 x dipole	0.64475	0.40827
33	MW, ST, LogP(o/w) IP, dipole	Pc = 6.47510+ 0.03953 x D- 0.01974 x HF- 0.01538 x E	0.62455	0.41971
34	MW, ST, LogP(o/w) HF, E	Pc = -7.82801- 1.10728 x D+ 1.47270 x IP+ 1.41622 x dipole	0.15129	0.63104
35	MW, ST, LogP(o/w) HF, dipole	Pc = 20.45600+ 6.10469 x D- 3.16643 x IP+ 0.03852 x E	0.48772	0.49027
36	MW, ST, LogP(o/w) HF, IP	Pc = -2.34064+ 2.61597 x D+ 0.90225 x dipole+0.02530 x E	0.39972	0.53071
37	MW, D, IP, dipole, E	Pc = 5.98416+ 0.01244 x ST- 0.30750 x logP(o/w)- 0.01189 x HF	0.61468	0.42520

38	MW, D, HF, dipole, E	Pc = 11.62452+ 0.01755 x ST- 1.18037 x logP(o/w)- 0.10018 x IP	0.45524	0.50557
39	MW, D, HF, IP, E	Pc = 10.13340+ 0.01872 x ST- 1.13309 x logP(o/w)+ 0.22017x dipole	0.45890	0.50387
40	MW, D, HF, IP, dipole	Pc =8.77928+ 0.01679 x ST- 0.96129 x logP(o/w)+ 0.00724 x E	0.46572	0.50069
41	MW, D, ST, dipole, E	Pc = 17.72311+ 0.28977 x logP(o/w)- 0.01719 x HF- 1.64066 x IP	0.65883	0.40010
42	MW, D, ST, IP, E	Pc = 4.16518+ 0.02263 x logP(o/w)- 0.01343 x HF+ 0.45309 x dipole	0.61389	0.42563
43	MW, D, ST, IP, dipole	Pc = 9.20085- 0.40057 x logP(o/w)- 0.01796 x HF- 0.02006 x E	0.64442	0.40846
44	MW, D, ST, logP(o/w), E	Pc = 22.37216- 0.01549 x HF- 1.92346 x IP- 0.43140 x dipole	0.65806	0.40055
45	MW, D, ST, logP(o/w), dipole	Pc = 17.55650- 0.01999 x HF- 1.26551 x IP- 0.01470 x E	0.67993	0.38753
46	MW, D, ST, logP(o/w), HF	Pc = 13.45334- 1.24925 x IP- 0.04304 x dipole+ 0.02611 x E	0.38795	0.53589

*r^2: Squared correlation coefficient   **RMSE**: Root mean square error

The best QSAR model equation which showed a high square of the correlation coefficient (r^2= 0.76032) and low root mean square error (RMSE= 0.33535) was QSAR equation No. 28:

Pc =

23.81540

+14.28884 x D

-2.47851 x log P(o/w)

-2.85524 x IP   ………………................ (model I)

Table (2.7): The QSAR models between descriptors and biological activity of α,β-unsaturated carbonyl derivatives for MCF-7 cancer cell line (group II)

No.	Removed descriptors	QSAR Equations	r^2*	RMSE*
1	RI, D, LogP(o/w)	Pc = 8.02897+ 0.01426 x MW- 0.05759 x MR- 0.03740 x E	0.76217	0.16976
2	E, D, LogP(o/w)	Pc = 8.04777+ 0.01009 x MW- 0.08764 x MR+ 0.59657 x RI	0.65289	0.20508
3	E, RI, LogP(o/w)	Pc = 8.45117+ 0.00777 x MW- 0.08014 x MR+ 0.49546 x D	0.65340	0.20493
4	E, RI, D	Pc = 7.86782+ 0.01139 x MW- 0.09254 x MR+ 0.28628 x logP(o/w)	0.70543	0.18892
5	MR, D, LogP(o/w)	Pc = 7.01369+ 0.00528 x MW- 0.05619 x E+ 0.00006 x RI	0.65955	0.20311
6	MR, RI, LogP(o/w)	Pc = 5.38107+ 0.00023 x MW- 0.04233 x E+ 1.77534 x D	0.69441	0.19243
7	MR, RI, D	Pc =7.42878+ 0.00635 x MW- 0.05970 x E- 0.10943 x logP(o/w)	0.66611	0.20114
8	MR, E, LogP(o/w)	Pc = 3.49361- 0.01406 x MW+ 0.40613 x RI+ 3.63031 x D	0.56502	0.22958
9	MR, E, D	Pc = -1.07920 - 0.01137 x MW+ 4.63071 x RI+ 0.28014 x logP(o/w)	0.39128	0.27159
10	MR, E, RI	Pc = 1.97753- 0.01411 x MW+ 4.25481 x D+0.35259 x logP(o/w)	0.65133	0.20554
11	MW, D, LogP(o/w)	Pc = 10.82209- 0.02605 x MR- 0.03107 x E- 1.30124 x RI	0.67825	0.19745
12	MW, RI, LogP(o/w)	Pc = 6.42033- 0.02117 x MR-0.02889 x E+ 1.58659 x D	0.71456	0.18597

Table (2.7): continued				
13	MW, RI, D	Pc = 8.34131- 0.03261 x MR-0.02385 x E+ 0.10098 x logP(o/w)	0.67964	0.19702
14	MW, E, LogP(o/w)	Pc = 11.18250- 0.05599 x MR- 2.85107 x RI+ 2.22149 x D	0.65533	0.20436
15	MW, E, D	Pc = 4.58307- 0.05718 x MR+ 2.08874 x RI+ 0.28320 x logP(o/w)	0.65545	0.20433
16	MW, E, RI	Pc = 5.18834- 0.05301 x MR+ 2.04285 x D+ 0.32151 x logP(o/w)	0.70904	0.18776
17	MW, MR, LogP(o/w)	Pc = 16.63297- 0.04885 x E- 7.83019 x RI+ 3.45288 x D	0.76773	0.16776
18	MW, MR, D	Pc = 12.50550- 0.05064 x E- 2.53114 x RI- 0.10823 x logP(o/w)	0.65246	0.20521
19	MW, MR, RI	Pc = 4.37301 - 0.04322 x E + 1.59035 x D+ 0.31076 x log P (o/w)	0.84684	0.14550
20	MW, MR, E	Pc = -3.86561+ 0.38354 x logP(o/w) + 2.02825 x RI+ 3.39382 x D	0.29551	0.29217

*r^2: Squared correlation coefficient   **RMSE**: Root mean square error

The QSAR model equation with high square of the correlation coefficient (r^2= 0.84684) and low root mean square error (RMSE= 0.14550) was QSAR equation No. 19:

Pc =

   4.37301

   - 0.04322 x E

   + 1.59035 x D

   + 0.31076 x log P (o/w)   ……………………………. (model II)

2.2.2.2. Calculation of statistical parameters

The statistical quality of models were justified by statistical parameters such as the root mean square error (RMSE), correlation coefficient (r), squared correlation coefficient (r^2), standard error of estimate (s) and F-test value (ratio between the variances of observed and calculated activities, F). Calculation of statistical parameters was carried out by using statistical program SPSS version 15.5, table (2.8).

Table 2.8: Statistical parameters used for statistical quality of models

Model No.	r	r^2	RMSE	Q^2	s	F	*P* value
I	0.8720	0.7603	0.33535	0.5348	0.56	34.05	0.133
II	0.9202	0.84684	0.14550	0.7621	0.384	101.43	0.010

2.2.3. Validation of quantitative structure–activity relationship model

To test the internal stability and predictive ability of the derived QSAR models, they were validated or cross-checked by the internal validation and external validation test procedure as follows:

(a) Internal validation by training set compounds:

Internal validations of the derived QSAR models were carried out by using LOO validation method to calculate cross validation regression coefficient (Q^2) and the results were illustrated in table (2.9) and (2.11) for group (I) and (II) respectively.

(b) External validation by test set compounds:

For external validation of QSAR models, the activity of each compound in the test set was predicted by using the derived QSAR models developed by the training set compounds in each group table (2.10) and (2.12).

Table 2.9: Experimental and predicted activities of training data set compounds and cross validation against the MCF-7 breast cancer cell line (group I)
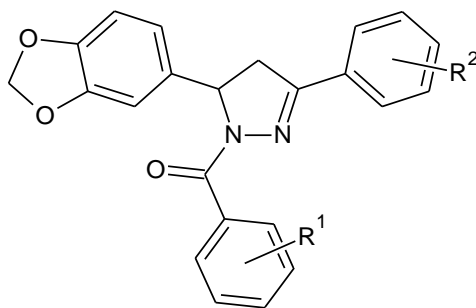
Compou-nd No.	R^1	R^2	Experimental pIC$_{50}$ (M)	Predicted pIC$_{50}$ (M)	Residuals	Predicted CV	Residuals
6a	3,4,5-(OCH$_3$)$_3$	3-Cl	5.03	5.157716	-0.12772	5.197089	-0.16709
12a	4-Cl	4-OCH$_3$	5.06	4.708918	0.351082	4.512287	0.547713
13a	3-OCH$_3$	4-OCH$_3$	5.09	5.293543	-0.20354	5.343726	-0.25373
16a	H	4-OCH$_3$	5.27	5.396856	-0.12686	5.434356	-0.16436
10a	4-Br	4-F	5.29	5.412277	-0.12228	5.992558	-0.70256
18a	4-Cl	3,4,5-(OCH$_3$)$_3$	5.32	5.6196	-0.2996	5.644421	-0.32442
4a	3,4,5-(OCH$_3$)$_3$	4-Cl	5.37	5.208189	0.161811	5.153699	0.216301

Table (2.9): continued

15a	3,4-(OCH$_3$)$_2$	4-OCH$_3$	5.45	6.188769	-0.73877	6.344928	-0.89493
9a	3,4,5-(OCH$_3$)$_3$	H	5.47	5.9762	-0.5062	6.169512	-0.69951
11a	4-F	4-OCH$_3$	5.57	5.383421	0.186579	5.351064	0.218936
7a	3,4,5-(OCH$_3$)$_3$	4-CH$_3$	5.63	5.296199	0.333801	5.201725	0.428275
5a	3,4,5-(OCH$_3$)$_3$	4-F	6.49	6.088712	0.401288	5.96823	0.52177
17a	4-F	3,4,5-(OCH$_3$)$_3$	6.66	6.51163	0.148371	6.474853	0.185147
1a	3,4,5-(OCH$_3$)$_3$	2-OCH$_3$	6.68	6.609838	0.070162	6.589902	0.090097
3a	3,4,5-(OCH$_3$)$_3$	4-OCH$_3$	7.30	6.828132	0.471868	6.568437	0.731563

Table 2.10: Predicted biological activity values of test set (group I)

Compound No.	R^1	R^2	Experimental pIC$_{50}$ (M)	Predicted pIC$_{50}$ (M)	Residuals
2a	3,4,5-(OCH$_3$)$_3$	3-OCH$_3$	7.22	6.111	1.109
8a	3,4,5-(OCH$_3$)$_3$	3-CH$_3$	5.13	5.042	0.088
14a	4-OCH$_3$	4-OCH$_3$	5.19	5.470	-0.28

Table 2.11: Experimental and predicted activities of training data set compounds and cross validation against the MCF-7

breast cancer cell line (group II)
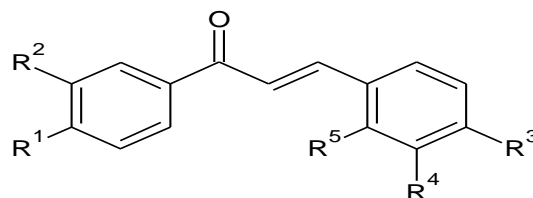
Compound No.	R^1	R^2	R^3	R^4	R^5	Experimental pIC_{50} (M)	Predicted pIC_{50} (M)	Residuals	Predicted CV	Residuals
13b	H	H	$N(CH_3)_2$	H	H	4	4.2493	-0.2493	4.351688	-0.35169
14b	CH_3	H	$N(CH_3)_2$	H	H	4.24	4.336486	-0.09649	4.367906	-0.12791
12b	OCH_3	H	OCH_3	H	H	4.38	4.279251	0.10075	4.234203	0.145797
11b	CH_3	H	OCH_3	H	H	4.49	4.513175	-0.02318	4.517511	-0.02751
2b	CH_3	H	H	H	H	4.87	5.019001	-0.149	5.060885	-0.19088
8b	CH_3	H	H	CH_3	CH_3	4.99	5.002559	-0.01256	5.009727	-0.01973
5b	OH	H	H	H	OH	5	5.087764	-0.08776	5.105386	-0.10539

Table (2.11): continued									
9b	OCH$_3$	H	H	CH$_3$	OCH$_3$	5.02	4.642254	0.377746	4.589873	0.430127
15b	H	H	H	H	OH	5.03	5.007334	0.022666	4.99276	0.03724
6b	H	H	H	CH$_3$	H	5.03	5.029799	0.000202	5.029741	0.000259
7b	OH	H	H	CH$_3$	OH	5.08	5.190366	-0.11037	5.216456	-0.13646
4b	H	H	H	H	H	5.1	5.087039	0.012961	5.075714	0.024286
1b	H	H	H	H	H	5.16	5.051935	0.108065	5.011246	0.148754
16b	H	CH$_3$	H	H	OH	5.16	4.979438	0.180562	4.952883	0.207117
18b	H	H	H	Cl	H	5.28	5.354298	-0.0743	5.415618	-0.13562

Table 2.12: Predicted biological activity values of test set (group II)

Compound No.	R^1	R^2	R^3	R^4	R^5	Experimental pIC$_{50}$ (M)	Predicted pIC$_{50}$ (M)	Residuals
3b	OCH$_3$	H	H	H	H	4.72	4.66	0.06
10b	H	H	OCH$_3$	H	H	4.93	4.67	0.26
17b	H	OCH$_3$	H	H	OH	5.15	4.69	0.46

2.2.4. Modeling of pyrazoline derivatives

Literature survey reveals that the 2-pyrazoline derivatives have engrossed substantial attention from medicinal chemists, it is an important scaffold since several 2-pyrazoline derivatives are found to be associated with wide range of biological activities. Furthermore, the use of the combinations of different pharmacological compounds in the design of new drugs may lead to finding novel drugs with interesting biological activity. In view of these points, about 120 trisubstituted 2-pyrazoline derivatives were modeled and designed as anticancer agent by using a hybrid pharmacophore approach. The new designed hybrid compounds were made by linking pyrazoline ring system with different substituents in position 1, 3 and 5 fig (2.3). All designed hybrid compounds were found in appendix A.
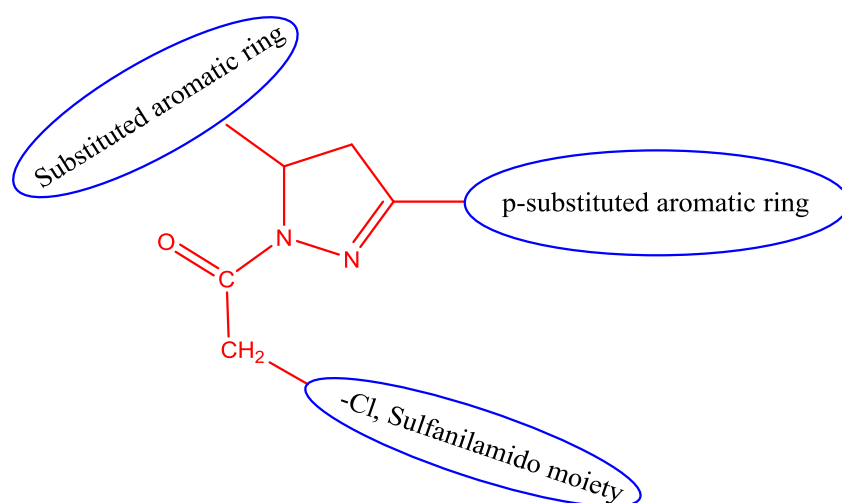
Figure (2.3): Designing of target compounds

α,β-unsaturated carbonyl derivatives are an interesting target class of compounds which are extensively investigated due to their broad spectrum of biological activities, including anti-inflammatory, anti-invasive, antitumour and antibacterial properties. They are regarded as promising anticancer agents against most human cancers (Syam *et al*.,

2012). Twenty of α,β-unsaturated carbonyl derivatives were modeled and designed as anticancer agent against human breast cancer cell line MCF-7 table (2.15).

2.2.4.1. Predicting the biological activity of designed compounds

The QSAR model (I) was selected to predict the biological activity of designed trisubstituted pyrazolines (1-120) against human breast cancer MCF-7, the results along with their predicted chemical descriptors were calculated and displayed as given in appendix A.

Druggability of designed trisubstituted pyrazolines was evaluated using Lipinski's "rule of five" in order to select compounds for synthesis. According to Lipinski rule of five, most "drug-like" molecules have logP≤5, number of hydrogen bond acceptors ≤10, molecular weight ≤500, and number of hydrogen bond donors ≤5. Molecules violating one or more of these rules may have problems with bioavailability (Jagadish *et al*, 2013). Therefor, 33 out of 120 compounds were selected for synthesis in the next step. Descriptors of selected compounds, predicted pIC_{50} and Lipinski's parameters were listed in table (2.13).

Table 2.13: Predicted descriptors, predicted activity against human breast cancer and Lipinski's parameters of selected trisubstituted pyrazolines

Compound No.	MW	D	logP (o/w)	IP	HB donors	HB acceptors	Predicted pIC_{50}
1	298.76	1.23	4.100	8.972	0	2	5.60
2	333.21	1.32	4.692	9.064	0	2	5.16
3	341.83	1.20	4.015	8.319	0	2	7.25
4	324.80	1.18	4.744	8.964	0	2	3.32
5	288.72	1.32	2.816	8.984	0	2	10.04
6	377.66	1.47	4.899	9.066	0	2	6.79

10	367.62	1.60	3.614	9.075	0	2	11.80
11	343.76	1.38	4.035	9.482	2	4	6.45
12	378.20	1.46	4.627	9.591	2	7	5.82
13	386.83	1.33	3.951	8.500	2	7	8.75
14	369.80	1.31	4.679	9.226	2	7	4.58
15	333.72	1.49	2.750	9.497	2	7	11.17
16	312.79	1.21	4.399	8.841	2	7	4.95
17	347.23	1.29	4.991	8.937	2	7	4.35
18	355.86	1.18	4.314	8.311	2	7	6.25
19	338.83	1.16	5.023	8.842	2	7	2.64
20	302.75	1.30	3.114	8.909	2	7	9.23
21	434.51	1.34	3.237	9.022	0	2	9.17
22	468.95	1.41	3.829	9.073	2	7	8.56
23	477.57	1.31	3.153	8.405	2	7	10.71
24	460.54	1.29	3.882	9.070	2	7	6.72
25	424.47	1.42	1.952	9.056	2	7	13.40
31	479.50	1.46	4.664	8.613	2	7	8.38
35	469.47	1.55	1.888	9.246	0	2	14.88
36	448.53	1.32	3.536	9.032	0	2	8.12
37	482.98	1.38	4.127	9.084	0	2	7.36
38	491.60	1.29	3.451	8.439	0	2	9.59
39	474.57	1.28	4.314	8.309	0	2	7.48
40	438.49	1.40	2.250	9.052	0	2	12.39
62	607.07	1.41	4.244	9.083	2	5	7.50
63	615.70	1.33	3.567	8.394	2	5	10.00
76	586.66	1.35	3.950	8.948	2	5	7.76
78	629.72	1.32	3.865	8.413	2	5	9.07
Combretastatin	-	-	-	-	-	-	6.51

QSAR model (II) was used to predict the biological activity of designed α,β-unsaturated carbonyl derivatives against human breast cancer MCF-7 (16 out of 20 compounds), druggability of these compounds was also evaluated using Lipinski's "rule of five", the results along with their predicted chemical descriptors were displayed in table (2.14).

Table 2.14: Predicted descriptors, predicted activity against human breast cancer and Lipinski's parameters of designed α,β-unsaturated carbonyl derivatives

Compound No.	MW	E	logP(o/w)	D	HB donors	HB acceptors	Predicted pIC$_{50}$
II	242.70	53.405	4.657	1.202	0	1	5.42
IV	234.29	56.242	4.709	1.082	0	1	5.13
V	198.21	45.018	2.78	1.148	0	1	5.12
VI	287.15	54.397	4.863	1.393	0	1	5.75
VII	321.59	53.933	5.455	1.475	0	1	6.08
VIII	330.21	69.933	4.778	1.353	0	1	4.99
IX	313.18	56.813	5.507	1.346	0	1	5.77
X	277.11	36.410	3.578	1.467	0	1	6.24
XI	253.25	72.698	4.000	1.255	0	1	4.47
XII	287.69	72.231	4.592	1.346	0	1	4.82
XIII	296.32	88.256	3.915	1.236	0	1	3.74
XIV	279.29	75.030	4.644	1.223	0	1	4.52
XV	243.21	54.943	2.715	1.318	0	1	4.94
XVII	256.72	55.604	4.955	1.177	0	1	5.38
XIX	248.31	58.428	5.007	1.066	0	1	5.09
XX	212.24	38.118	3.078	1.123	0	1	5.47
Tamoxifen		-	-	-	0	1	7.39

2.3. Synthesis

2.3.1. General procedure for the synthesis of compounds

2.3.1.1. Synthesis of α,β-unsaturated carbonyl derivatives (I-XX)

A mixture of the substituted aromatic aldehyde (0.05 mol), substituted aromatic acetophenone (0.05 mol) and sodium hydroxide (10%) in ethanol (30 mL) was stirred at room temperature until the mixture was so thick that stirring was no longer effective (3-5 h); reaction mixture was removed and kept in refrigerator overnight. The resulting solid was filtered, washed with cold water until the washings were neutral to litmus. The crude α,β-unsaturated carbonyl derivative, was air-dried and recrystallized from ethanol (see scheme (2.1), (2.2), (2.3) and (2.4)). Chemical names and physiochemical properties are tabulated in table (2.15) and (2.19), respectively.
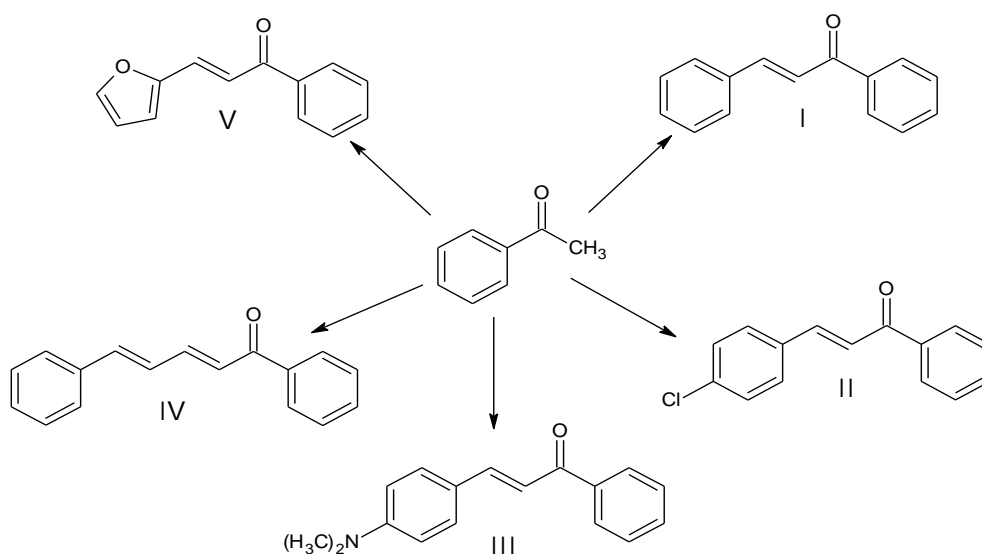
Scheme (2.1): Chemical structures of α,β-unsaturated carbonyl derivatives (I-V) (Acetophenone derivatives)
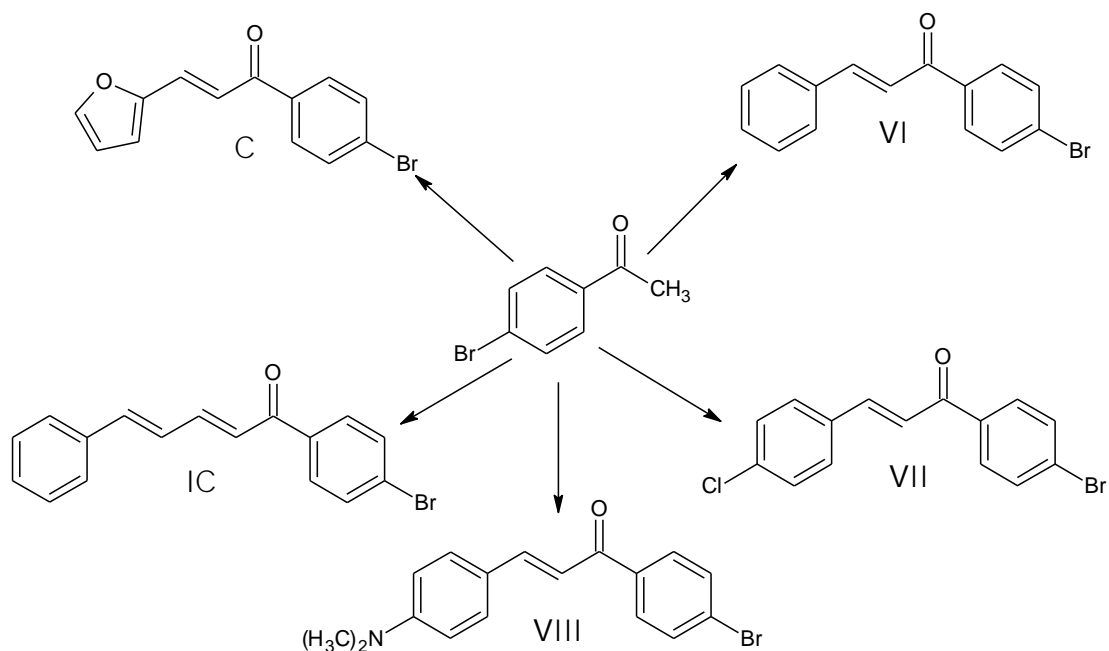
Scheme (2.2): Chemical structures of α,β-unsaturated carbonyl derivatives (VI-X) (*p*-bromoacetophenone derivatives)
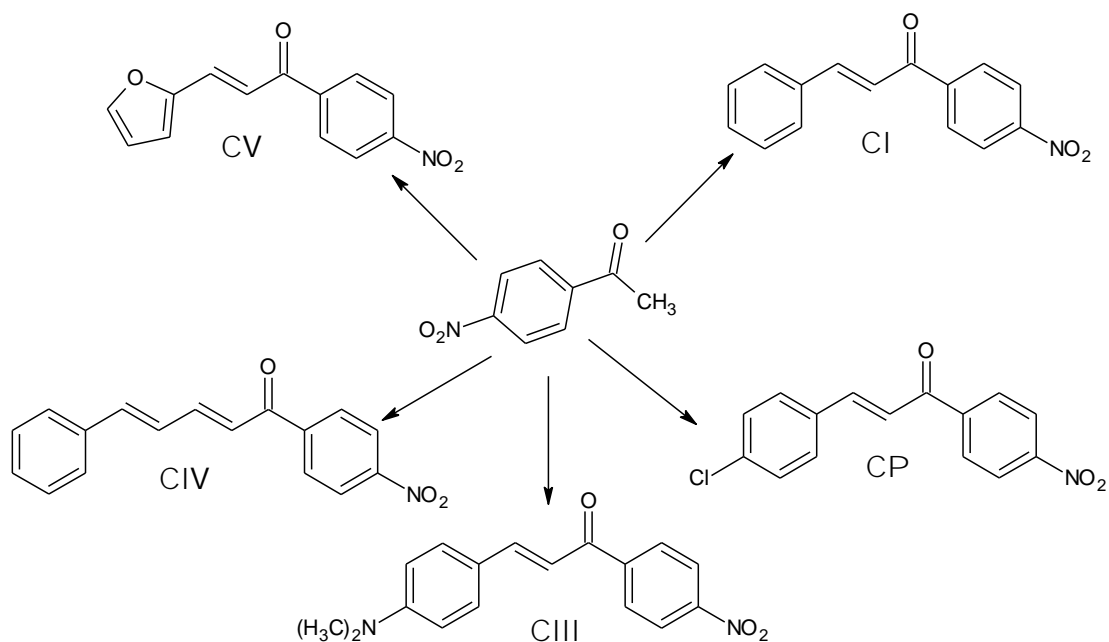
Scheme (2.3): Chemical structures of α,β-unsaturated carbonyl derivatives (XI-XV) (*p*-nitroacetophenone derivatives)
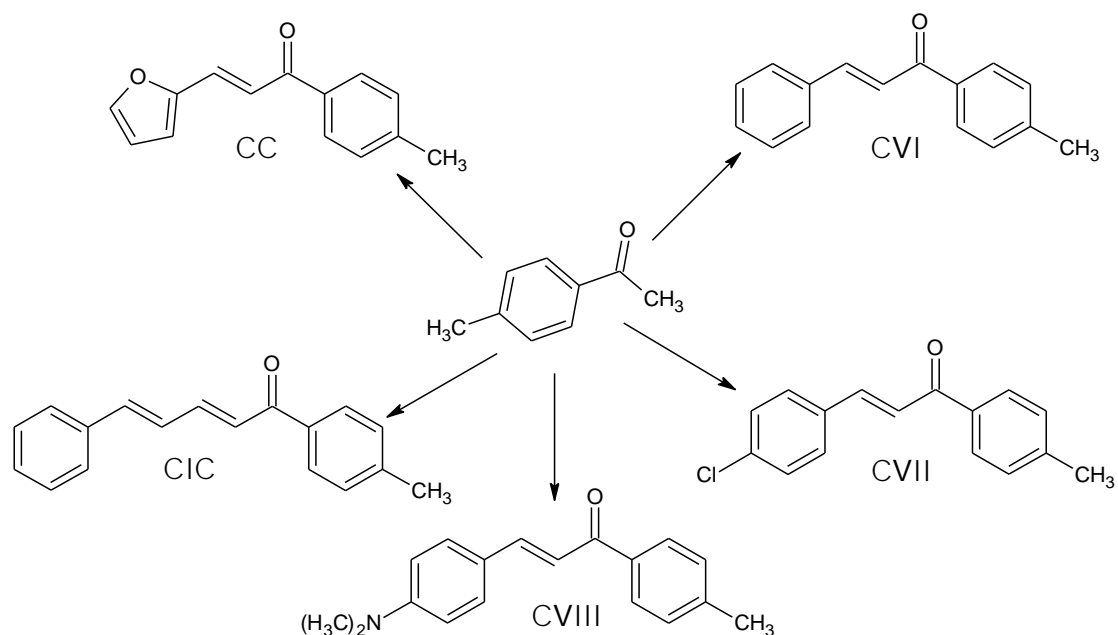
Scheme (2.4): Chemical structures of α,β-unsaturated carbonyl derivatives (XVI-XX) (*p*-methylacetophenone derivatives)

2.3.1.2. Synthesis of 3,5-Diaryl-2-pyrazoline derivatives (XXI-XL)

A mixture of appropriate α,β-unsaturated carbonyl derivative (0.03 mol) and hydrazine hydrate (2.9 ml, 3 g, 0.06 mol) in ethanol (30 ml) were refluxed for 6 h. The reaction mixture was cooled and kept in refrigerator overnight. The resulting solid was filtered, and the crude pyrazoline, after drying and recrystallization from ethanol, was taken for the next step (see scheme (2.5)). Chemical names and physiochemical properties are tabulated in table (2.16) and (2.20).
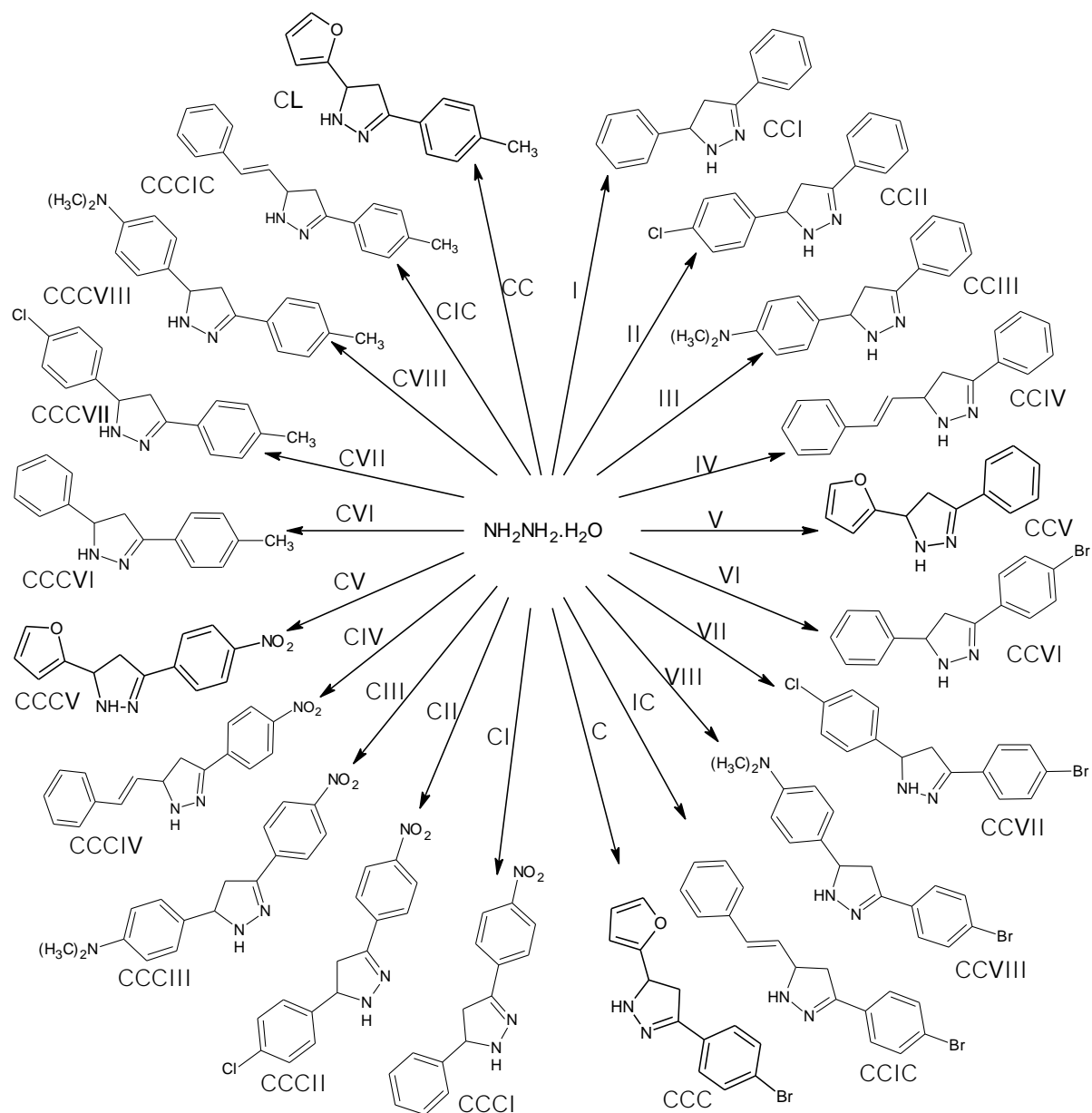
Scheme (2.5): Chemical structures of 3,5-Diaryl-2-pyrazoline derivatives (XXI-XL)

2.3.1.3. Synthesis of 1-(Chloroacetyl)-3,5-diaryl-2-pyrazoline derivatives (XLI-LVII)

3,5-Diaryl-2-pyrazoline derivative (0.025 mol) and triethylamine (3.48 ml, 2.52 g, 0.025 mol) were dissolved in dry toluene (30 ml) with constant stirring. The mixture was cooled in an ice bath, and chloroacetylchloride (1.99 ml, 2.82 g, 0.025 mol) was added drop wise

with stirring. The reaction mixture thus obtained was further agitated for 3 h at room temperature and followed by TLC. The precipitate (triethylamine hydrochloride) was filtered; the solvent was evaporated to dryness under reduced pressure. The products were recrystallized from ethanol and were taken for the next step (see scheme (2.6)). Chemical names and physiochemical properties are tabulated in table (2.17) and (2.21).

2.3.1.4. Synthesis of 1-[(aryl)aminoacetyl]-3,5-diaryl-2-pyrazoline derivatives (LVIII-LXXI)

A mixture of 0.5 mmol sulfanilamide (0.086 g) or sulfadoxine (0.155 g), 0.5 mmol of 1-(Chloroacetyl)-3,5-diaryl-2-pyrazoline derivative, and 0.069 g of potassium carbonate anhydrous was stirred under reflux in 10 mL of dry DMF. Reaction was followed by TLC. The reaction mixture was poured in crushed ice, the products were separated by filtration, washed with water, ethanol, and dried. Recrystallization from ethanol/dioxane rendered desired products in pure form (see schemes (2.7) and (2.8)). Chemical names and physiochemical properties are tabulated in table (2.18) and (2.22).
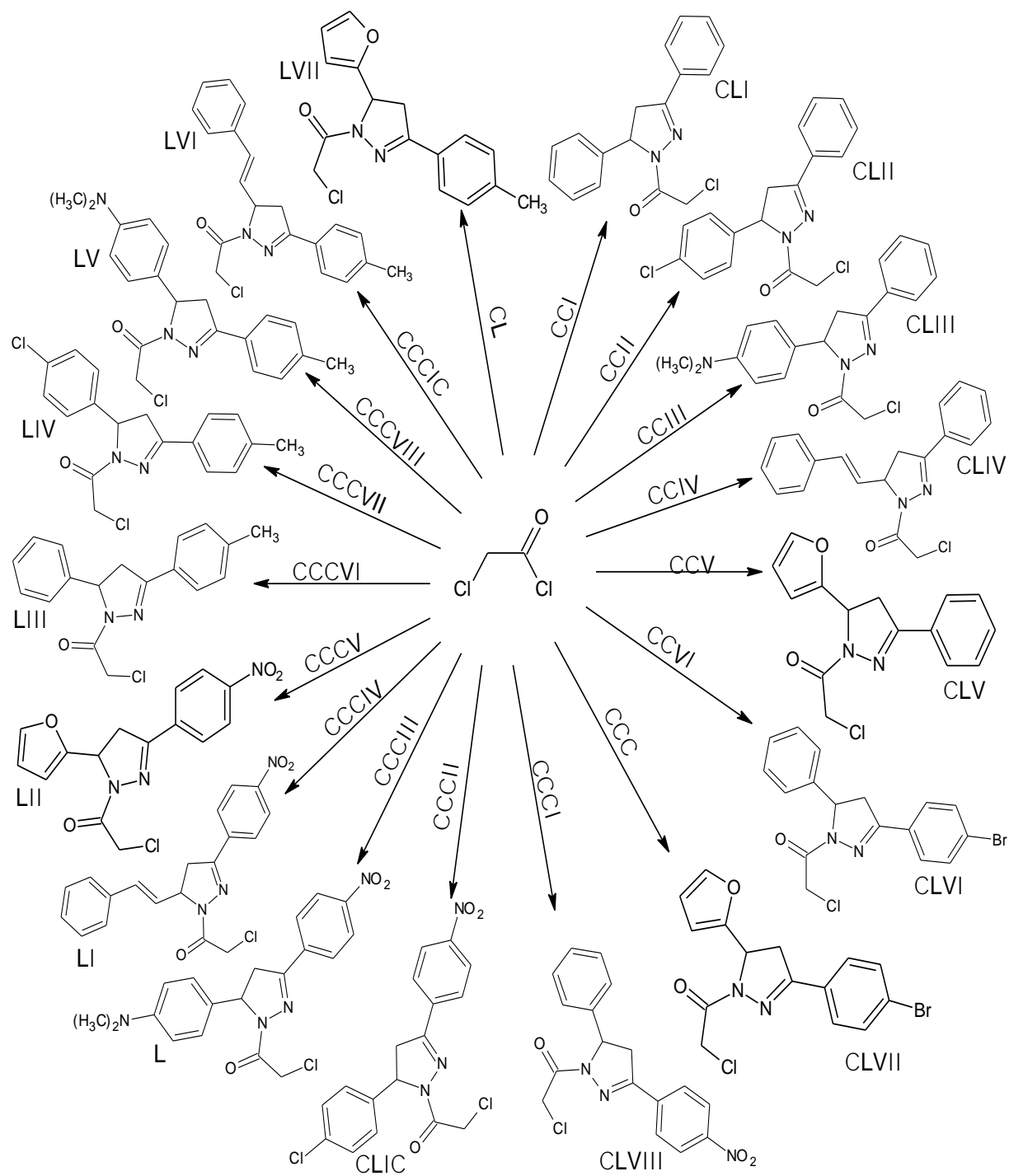
Scheme (2.6): Chemical structures of 1-(Chloroacetyl)-3,5-diaryl-2-pyrazoline derivatives (XLI-LVII)
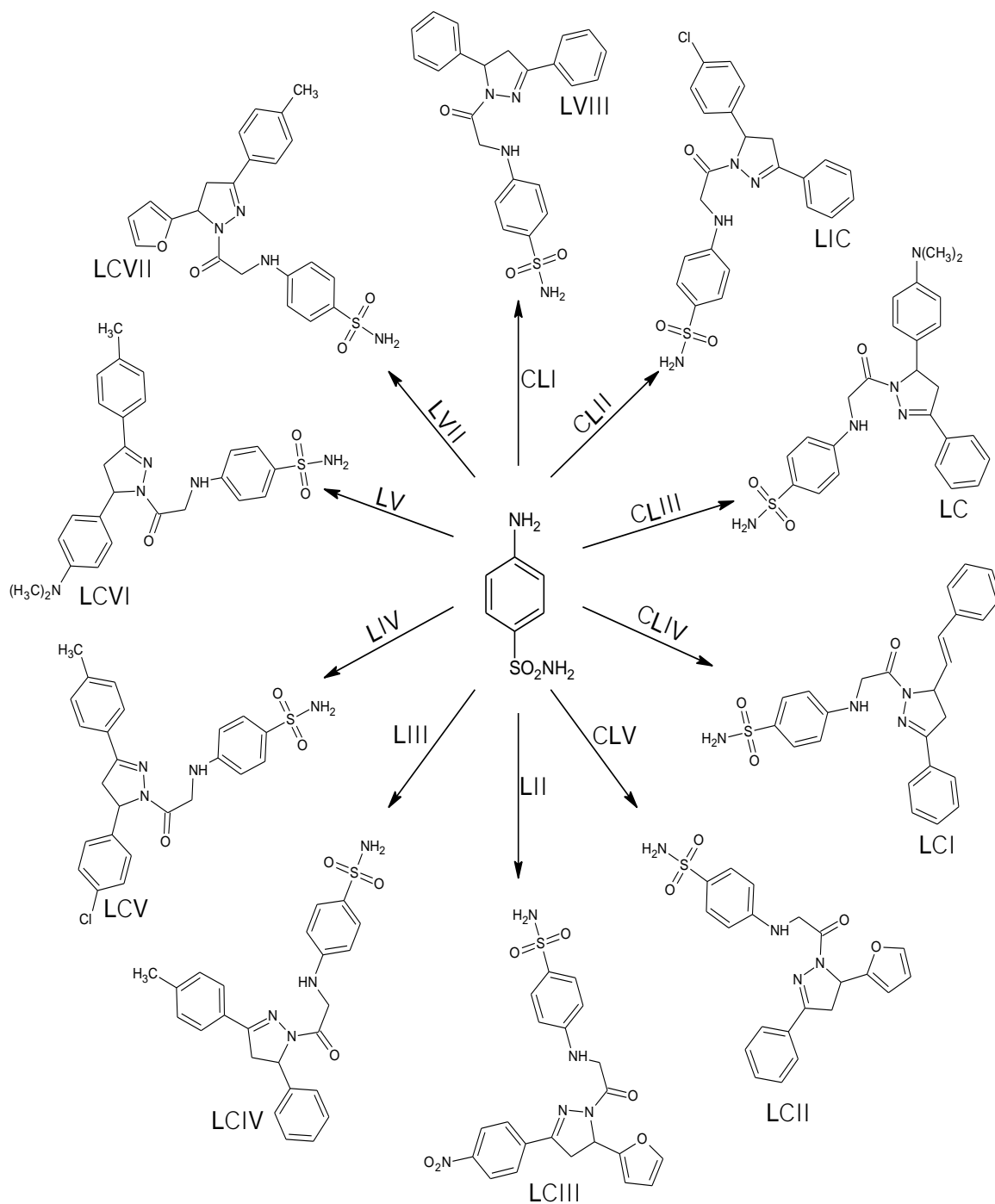
Scheme (2.7): Chemical structures of 1-[(aryl) amino acetyl] -3,5-diaryl-
2-pyrazoline derivatives (LVIII-LXVII)
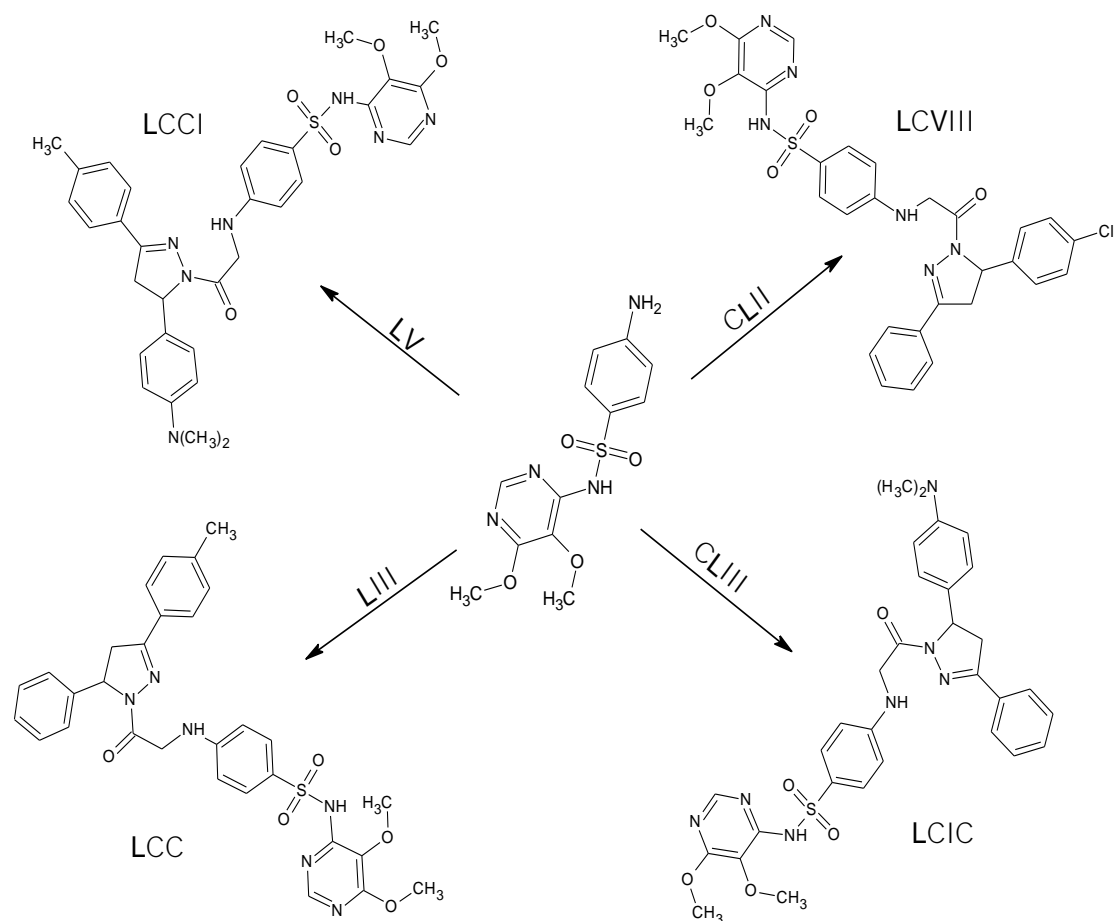
Scheme (2.8): Chemical structures of 1-[(aryl) amino acetyl] -3,5-diaryl-
2-pyrazoline derivatives (LXVIII-LXXI)

Table (2.15): Chemical names of synthesized α,β-unsaturated carbonyl derivatives（I-XX）
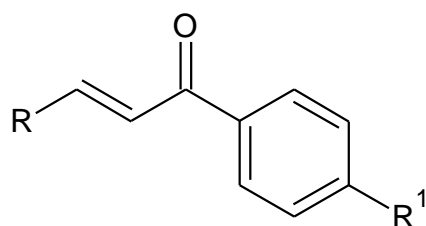
Compound No.	R	R^1	Chemical name
I		-H	(2E)-1,3-diphen ylprop-2-en-1-one
II		-H	(2E)-3-(4-chloro phenyl)-1-phenyl prop-2-en-1-one
III		-H	(2E)-3-[4-(dimethy lamino)phenyl]-1-phenylprop-2-en-1-one
IV		-H	(2E,4E)-1,5-diphenylpenta-2,4-dien-1-one
V		-H	(2Z)-3-(furan-2-yl)-1-phenylprop-2-en-1-one
VI		-Br	(2E)-1-(4-bromo phenyl)-3-phenyl prop-2-en-1-one
VII		-Br	(2E)-1-(4-bromo phenyl -3-(4-chlorophenyl) prop -2-en-1-one
VIII		-Br	(2E)-1-(4-bromophenyl)-3-[4-(dimethylamino) phenyl]prop-2-en-1-one
IX		-Br	(2E,4E)-1-(4-bromo phenyl)-5-phenylpenta-2,4-dien-1-one
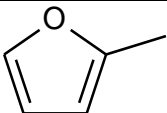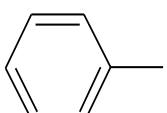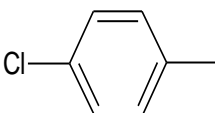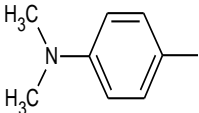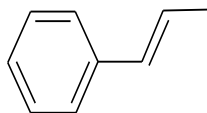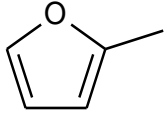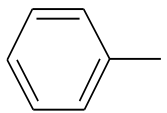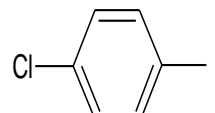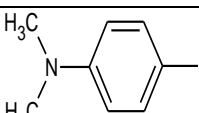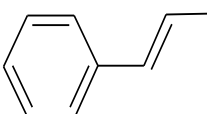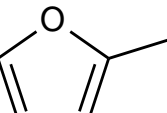
Table (2.15): continued			
X		-Br	(2Z)-1-(4-bromo phenyl)-3-(furan-2-yl)propen-1-one
XI		-NO$_2$	(2E)-1-(4-nitro phenyl)-3-phenyl prop-2-en-1-one
XII		-NO$_2$	(2E)-3-(4-chloro phe nyl)-1-(4-nitr ophenyl) prop-2-en-1-one
XIII		-NO$_2$	(2E)-3-[4-(dimethylami- no)phenyl]-1-(4-nitro phenyl) prop-2-en-1-one
XIV		-NO$_2$	(2E,4E)-1-(4-nitro phe nyl)-5-phenylpenta-2,4-dien-1-one
XV		-NO$_2$	(2Z)-3-(furan-2-yl)-1-(4-nitrophenyl)prop-2-en-1-one
XVI		-CH$_3$	(2E)-1-(4-methyl phenyl)-3-phenyl prop-2-en-1-one
XVII		-CH$_3$	(2E)-3-(4-chloro phenyl)-1-(4-methyl phenyl) prop-2-en-1-one
XVIII		-CH$_3$	(2E)-3-[4-(dimethylami- no)phenyl]-1-(4-methyl phenyl)prop-2-en-1-one
XIX		-CH$_3$	(2E,4E)-1-(4-methyl phenyl)-5-phenyl penta-2,4-dien-1-one
XX		-CH$_3$	(2Z)-3-(furan-2-yl)-1-(4-methyl phenyl) prop-2-en-1-one

67

Table (2.16): Chemical names of synthesized 3,5-Diaryl-2-pyrazoline derivatives (XXI-XL)
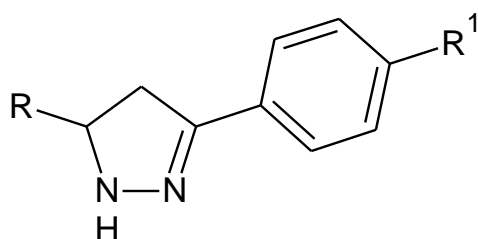
Compo-und No.	R	R¹	Chemical name
XXI		-H	3,5-diphenyl-4,5-dihydro-1H-pyrazole
XXII		-H	5-(4-chlorophenyl)-3-phenyl-4,5-dihydro-1H-pyrazole
XXIII		-H	N,N-dimethyl-4-(3-phenyl-4,5-di hydro-1H-pyrazol-5-yl)aniline
XXIV		-H	3-phenyl-5-[(E)-2-phenyl ethenyl]-4,5-dihydro-1H-pyrazole
XXV		-H	5-(furan-2-yl)-3-phenyl-4,5-dihydro-1H-pyrazole
XXVI		-Br	3-(4-bromophenyl)-5-phenyl-4,5-dihydro-1H-pyrazole
XXVII		-Br	3-(4-bromophenyl)-5 -(4-chlorophenyl)-4, 5-dihydro-1H-pyrazole
XXVIII		-Br	4-[3-(4-bromophenyl)-4,5-dihyd ro-1H-pyrazol-5-yl]-N,N-dimethyl aniline
XXIX		-Br	3-(4-bromophenyl)-5-[(E)-2-phenylethenyl]-4,5-dihydro-1H-pyrazole
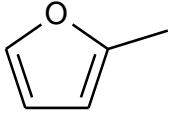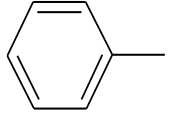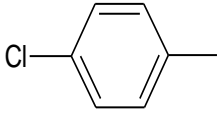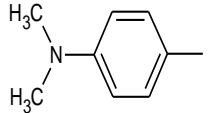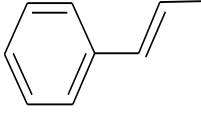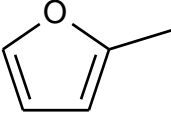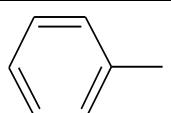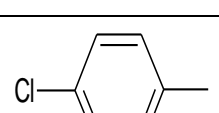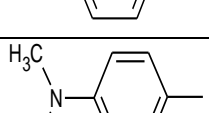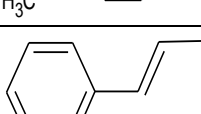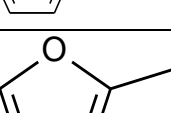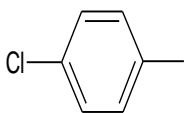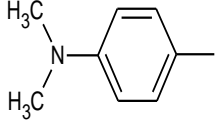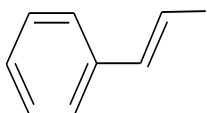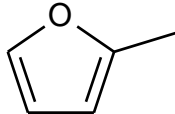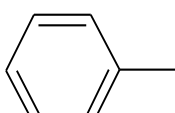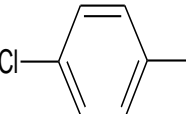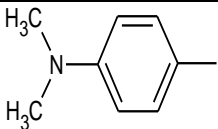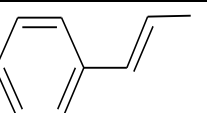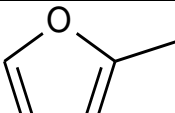
			Table (2.16): continued
XXX		-Br	3-(4-bromophenyl)-5-(furan-2-yl)-4,5-dihydro-1H-pyrazole
XXXI		-NO₂	3-(4-nitrophenyl)-5-phenyl-4,5-dihydro-1H-pyrazole
XXXII		-NO₂	5-(4-chlorophenyl)-3-(4-nitrophenyl)-4,5-dihydro-1H-pyrazole
XXXIII		-NO₂	N,N-dimethyl-4-[3-(4-nitrophenyl)-4,5-dihydro-1H-pyrazol-5-yl]aniline
XXXIV		-NO₂	3-(4-nitrophenyl)-5-[(E)-2-phenylethenyl]-4,5-dihydro-1H-pyrazole
XXXV		-NO₂	5-(furan-2-yl)-3-(4-nitrophenyl)-4,5-dihydro-1H-pyrazole
XXXVI		-CH₃	3-(4-methylphenyl)-5-phenyl-4,5-dihydro-1H-pyrazole
XXXVII		-CH₃	5-(4-chlorophenyl)-3-(4-methyl phenyl)-4,5-dihydro-1H-pyrazole
XXXVIII		-CH₃	N,N-dimethyl-4-[3-(4-methylphenyl)-4,5-dihydro -1H-pyrazol-5-yl]aniline
XXXIX		-CH₃	3-(4-methylphenyl)-5-[(E)-2-phenylethenyl]-4,5-dihydro-1H-pyrazole
XL		-CH₃	5-(furan-2-yl)-3-(4-methylphenyl)-4,5-dihydro-1H-pyrazole

Table (2.17): Chemical names of synthesized 1-(Chloroacetyl)-3,5-diaryl-2-pyrazoline derivatives (XLI-LVII)
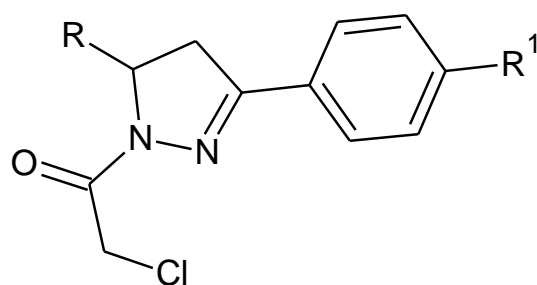
Compou-nd No*	R	R^1	Chemical name
XLI		-H	2-chloro-1-(3,5-diphe nyl-4,5-dih ydro-1*H*-pyrazol-1-yl) ethan-1-one
XLII		-H	2-chloro-1-[5-(4-chlorophenyl)-3-phenyl-4,5-dihyd-ro-1*H*-pyra zol-1-yl] ethan-1-one
XLIII		-H	2-chloro-1-{5-[4-(dimethylamino) phenyl]-3-phenyl-4,5-dihydro-1*H*-pyrazol-1-yl} ethan-1-one
XLIV		-H	2-chloro-1-{3-phenyl-5-[(*E*)-2-phenylethenyl]-4,5-dihydro-1*H*-pyrazol-1-yl}ethan-1-one
XLV		-H	2-chloro-1-[5-(fura n-2-yl)-3-phenyl-4,5-dihydro-1H-pyrazol-1-yl]ethan-1-one
XLVI		-Br	1-[3-(4-bromophenyl)-5-phenyl-4,5-dihydro-1*H*-pyrazol-1-yl]-2-chloroethan-1-one
XLVII		-Br	1-[3-(4-bromophenyl)-5-(furan-2-yl)-4,5-dihydro-1*H*-pyrazol-1-yl]-2-chloroethan-1-one
XLVIII		-NO$_2$	2-chloro-1-[3- (4 –nitrophenyl)-5-phenyl-4,5-dihy dro-1*H*-pyr azol-1-yl] ethan-1-one

Table (2.17): continued			
XLIX	Cl— (4-chlorophenyl)	-NO$_2$	2-chloro-1-[5-(4-chlorophenyl)-3-(4-nitrophenyl) - 4,5-dihydro-1H-pyrazol-1-yl]ethan-1-one
L	H$_3$C–N(CH$_3$)– (4-(dimethylamino)phenyl)	-NO$_2$	2-chloro-1-{5-[4-(dimethylamino)phenyl]-3-(4-nitro phenyl)-4,5-dihydro-1 H-pyrazol-1-yl} ethan-1-one
LI	(E)-styryl	-NO$_2$	2-chloro-1-{3-(4-nitrophenyl)-5-[(E) -2-phenyl ethenyl]-4,5-dihydro-1H-pyrazol-1-yl}ethan-1-one
LII	furan-2-yl	-NO$_2$	2-chloro-1-[5-(furan-2-yl)-3-(4-nitrophenyl)-4,5- dihydro-1H-pyrazol-1-yl]ethan-1-one
LIII	phenyl	-CH$_3$	2-chloro-1-[3-(4-methy l phenyl)-5-ph enyl-4,5-dihy dro-1H-pyr azol-1-yl] ethan-1-one
LIV	Cl— (4-chlorophenyl)	-CH$_3$	2-chloro-1-[5- (4-chlorophenyl)-3-(4-methylphenyl)- 4,5-dihydro-1H-pyrazol-1-yl]ethan-1-one
LV	H$_3$C–N(CH$_3$)– (4-(dimethylamino)phenyl)	-CH$_3$	2-chloro-1-{5-[4-(dimethylamino)phenyl]-3-(4-meth ylphenyl)-4,5-dihydro-1 H-pyrazol-1-yl}ethan-1-one
LVI	(E)-styryl	-CH$_3$	2-chloro-1-{3-(4-methyl phenyl)-5-[(E)-2-phenyleth enyl]-4,5-dihydro-1H-pyrazol-1-yl}ethan-1-one
LVII	furan-2-yl	-CH$_3$	2-chloro-1-[5-(furan-2-yl)-3-(4-methylphenyl)-4,5- dihydro-1H-pyrazol-1-yl]ethan-1-one

*XLI=1, XLII=2, XLIII=3, XLIV=4, XLV=5, XLVI=6, XLVII=10, XLVIII=11, XLIX=12, L=13, LI=14, LII=15, LIII=16, LIV=17, LV=18, LVI=19, LVII=20

Table (2.18): Chemical names of synthesized 1-[(aryl) amino acetyl] -

3,5-diaryl-2-pyrazoline derivatives (LVIII-LXXI)
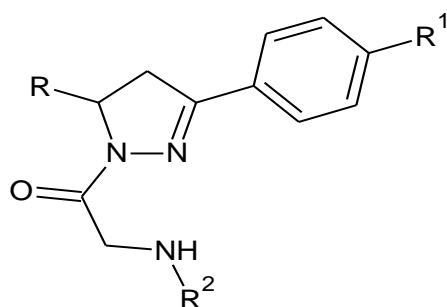
Comp-und No.*	R	R^1	R^2	Chemical name
LVIII		-H		4-((2-(3,5-diphenyl-4,5-di hydro-1H-pyrazol-1-yl)-2-oxoethyl) amino) benzene sulfonamide
LIX		-H		4-((2-(5-(4-chlorophenyl)-3-pheny l-4,5-dihydro-1H-pyrazol-1-yl)-2-oxo ethyl) amino) benzene sulfonamide
LX		-H		4-((2-(5-(4-(dimethylamin o)phenyl) -3-phenyl-4,5-dihydro-1H-pyrazol-1 -yl)-2-oxoethyl)amino)benzene sulfonamide
LXI		-H		(E)-4-((2-oxo-2-(3-phenyl-5-styryl-4,5-dihydro-1H-pyrazol-1-yl)ethyl)amino) benzene sulfonamide
LXII		-H		4-({2-[5-(furan-2-yl)-3-phenyl-4,5-dihydro-1*H*-pyrazol-1-yl]-2-oxoethyl} amino)benzene-1-sulfonamide
LXIII		-NO$_2$		4-((2-(5-(furan-2-yl)-3-(4-nitrophenyl)-4,5-dihydro-1H-pyrazol-1-yl)-2-oxoeth yl) amino)benzene sulfonamide
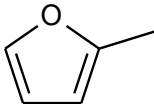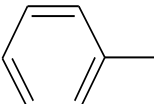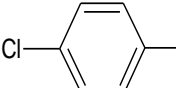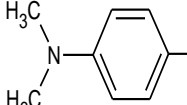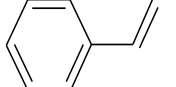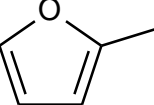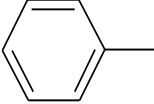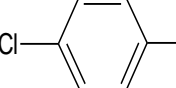
Table (2.18): continued				
LXIV		-CH$_3$		4-((2-oxo-2-(5-phenyl-3-(p-tolyl)-4,5-dihydro-1H-pyrazol-1-yl)ethyl)amino) benzene sulfonamide
LXV		-CH$_3$		4-((2-(5-(4-chlorophenyl)-3-(p-tolyl)-4,5-dihydro-1H-pyrazol-1-yl)-2-oxo ethyl) amino)benzene sulfonamide
LXVI		-CH$_3$		4-((2-(5-(4-(dimethyl ami no)phenyl)-3-(p-tolyl)-4,5-dihydro-1H-pyrazol-1-yl)-2-oxoethyl)amino)benzene sulfonamide
LXVII		-CH$_3$		4-((2-(5-(furan-2-yl)-3-(p-tolyl)-4,5-dihydro-1H-pyra zol-1-yl)-2-oxoethyl) amino)benzene sulfonamide
LXVIII		-H		4-((2-(5-(4-chlorophenyl)-3-phenyl-4,5-dihydro-1H-pyrazol-1-yl)-2-oxoethyl) amino)-N-(5,6-dimethoxy pyrimidin-4-yl)benzene sulfonamide
LXIX		-H		N-(5,6-dimethoxypyrimi d in-4-yl)-4-((2-(5-(4-(dime thylamino)phenyl)-3-phen yl-4,5-dihydro-1H-pyrazol -1-yl)-2-oxoethyl)amino) benzene sulfonamide
LXX		-CH$_3$		N-(5,6-dimethoxypyrimi din-4-yl)-4-((2-oxo-2-(5-phenyl-3-(p-tolyl)-4,5-dihydro-1H-pyrazol-1-yl)ethyl) amino) benzene sulfonamide
LXXI		-CH$_3$		N-(5,6-dimethoxypyrimid in-4-yl)-4-((2-(5-(4-(dime thylamino)phenyl)-3-(p-tol yl)-4,5-dihydro-1H-pyraz ol-1-yl)-2-oxoethyl) amino) benzene sulfonamide

*LVIII=21, LIX=22, LX=23, LXI=24, LXII=25, LXIII=35, LXIV=36, LXV=37, LXVI=38, LXVII=40, LXVIII=62, LXIX=63, LXX=76, LXXI=78

Table (2.19): Physiochemical data of synthesized α,β-unsaturated carbonyl derivatives (I-XX)
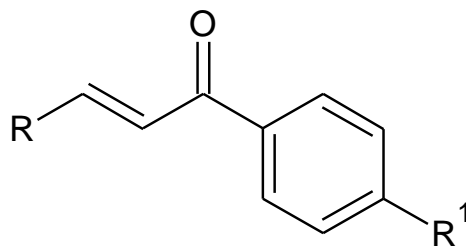
Compound No.	R	R^1	Color	MF	MW	m.p. (°C)	Yield (%)
I		-H	Pale yellow	$C_{15}H_{12}O$	208.25	48-50 (lit. 53-56, Osman *et al*, 2016)	91
II		-H	Light yellow	$C_{15}H_{11}ClO$	242.70	112-114 (lit. 115, Hadi, 2012)	78
III		-H	Orange	$C_{17}H_{17}NO$	251.32	106-108 (lit. 107-108, Elzupir *et al*, 2013)	92
IV		-H	Light yellow	$C_{17}H_{14}O$	234.29	96-98 (lit. 99-100, Sharma & Sharma, 2010)	89

V		-H	Brown	$C_{13}H_{10}O_2$	198.21	38-40 (lit. 37-40, Das *et al*, 2010)	51
VI		-Br	Light yellow	$C_{15}H_{11}BrO$	287.15	98-100 (lit. 91-92, Elzupir *et al*, 2013)	78
VII		-Br	Light yellow	$C_{15}H_{10}BrClO$	321.59	166-168	88
VIII		-Br	Yellow	$C_{17}H_{16}BrNO$	330.21	136-138 (lit. 139-142, Osman *et al*, 2016)	85
IX		-Br	Light yellow	$C_{17}H_{13}BrO$	313.18	148-150 (lit. 153-154, Elzupir *et al*, 2013)	94
X		-Br	Yellow	$C_{13}H_9BrO_2$	277.11	74-76 (lit. 66-68, Elzupir *et al*, 2013)	72
XI		-NO₂	Light brown	$C_{15}H_{11}NO_3$	253.25	130-132 (lit. 140-141, Ahmed *et al*, 2007)	64
XII		-NO₂	Cream	$C_{15}H_{10}ClNO_3$	287.69	164-166	84
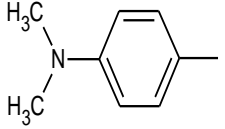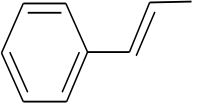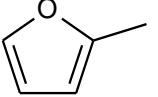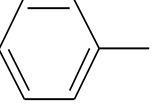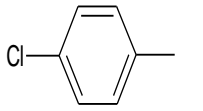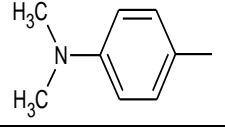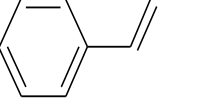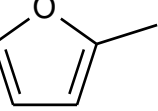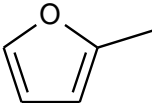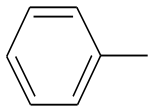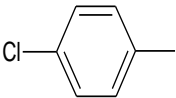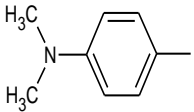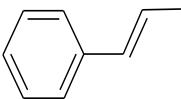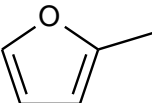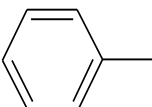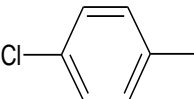
XIII		-NO$_2$	Blood red	C$_{17}$H$_{16}$N$_2$O$_3$	296.32	218-220	78
XIV		-NO$_2$	Yellow	C$_{17}$H$_{13}$NO$_3$	279.29	168-170 (lit. 173-174, Elzupir *et al*, 2013)	88
XV		-NO$_2$	Yellow	C$_{13}$H$_9$NO$_4$	243.21	142-144	78
XVI		-CH$_3$	Pale yellow	C$_{16}$H$_{14}$O	222.28	76-78 (lit. 70-72, Syam *et al*, 2012)	91
XVII		-CH$_3$	White	C$_{16}$H$_{13}$ClO	256.72	144-146	97
XVIII		-CH$_3$	Orange	C$_{18}$H$_{19}$NO	265.34	124-126 (lit. 124-125, Syam *et al*, 2012)	52
XIX		-CH$_3$	Yellow	C$_{18}$H$_{16}$O	248.31	94-96 (lit. 88-89, Sharma & Sharma, 2010)	76
XX		-CH$_3$	Cream	C$_{14}$H$_{12}$O$_2$	212.24	64-66	68

Table (2.20): Physiochemical data of synthesized 3,5-Diaryl-2-pyrazoline derivatives (XXI-XL)
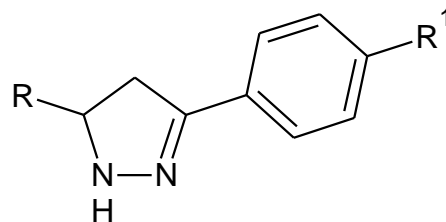
Compou-nd No.	R	R^1	Color	MF	MW	m.p.(˚C)	Yield (%)
XXI		-H	White	$C_{15}H_{14}N_2$	222.28	70-72	80
XXII		-H	White	$C_{15}H_{13}ClN_2$	256.73	72-74	83
XXIII		-H	Pale yellow	$C_{17}H_{19}N_3$	265.35	118-120	65
XXIV		-H	White	$C_{17}H_{16}N_2$	248.32	7 8-80	61

XXV		-H	Light brown	$C_{13}H_{12}N_2O$	212.24	60-62	58
XXVI		-Br	White	$C_{15}H_{13}BrN_2$	301.18	78-80	74
XXVII		-Br	Pale orange	$C_{15}H_{12}BrClN_2$	335.62	78-80	60
XXVIII		-Br	Light yellow	$C_{17}H_{18}BrN_3$	344.24	144-146	87
XXIX		-Br	Light orange	$C_{17}H_{15}BrN_2$	327.21	82-84	65
XXX		-Br	White	$C_{13}H_{11}BrN_2O$	291.14	90-92	67
XXXI		-NO$_2$	Yellow	$C_{15}H_{13}N_3O_2$	267.28	94-96	70
XXXII		-NO$_2$	Yellow	$C_{15}H_{12}ClN_3O_2$	301.72	130-132	75
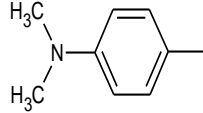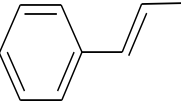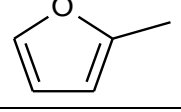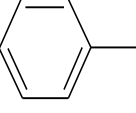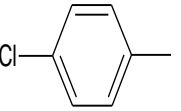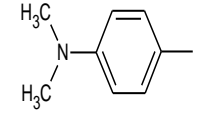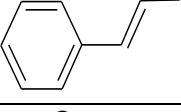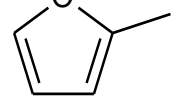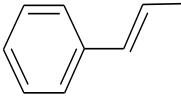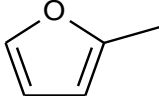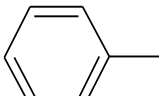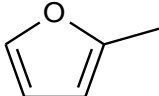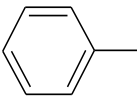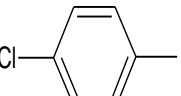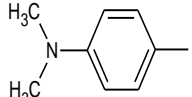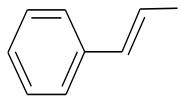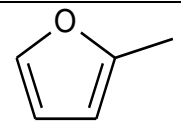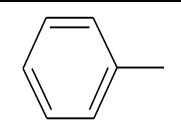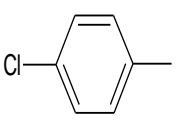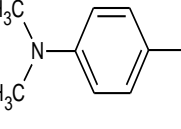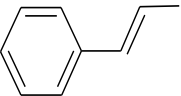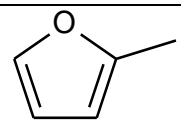
XXXIII	H_3C N H_3C (N,N-dimethylaniline)	$-NO_2$	Yellow	$C_{17}H_{18}N_4O_2$	310.35	150-152	81
XXXIV	(styryl benzene)	$-NO_2$	Pale orange	$C_{17}H_{15}N_3O_2$	293.31	110-112	78
XXXV	(furan)	$-NO_2$	Yellow	$C_{13}H_{11}N_3O_3$	257.24	98-100	84
XXXVI	(toluene)	$-CH_3$	White	$C_{16}H_{16}N_2$	236.31	60-62	83
XXXVII	Cl (chlorotoluene)	$-CH_3$	White	$C_{16}H_{15}ClN_2$	270.75	94-96	80
XXXVIII	H_3C N H_3C (N,N-dimethyl)	$-CH_3$	Pale yellow	$C_{18}H_{21}N_3$	279.37	120-122	60
XXXIX	(styryl benzene)	$-CH_3$	White	$C_{18}H_{18}N_2$	262.34	90-92	62
XL	(furan)	$-CH_3$	White	$C_{14}H_{14}N_2O$	226.27	78-80	71

Table (2.21): Physiochemical data of synthesized 1-(Chloroacetyl)-3,5-diaryl-2-pyrazoline derivatives (XLI-LVII)
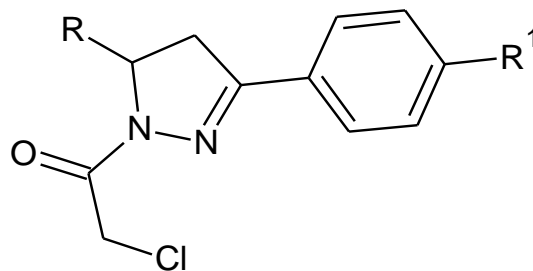
Compou-nd No.	R	R^1	color	MF	MW	m.p. (°C)	Yield (%)	R_f value*
XLI	(phenyl)	-H	Pale yellow	$C_{17}H_{15}ClN_2O$	298.76	130-132 (lit. 133, Turan-Zitouni *et al*, 2006)	46	0.75
XLII	(4-chlorophenyl)	-H	Light yellow	$C_{17}H_{14}Cl_2N_2O$	333.21	128-130	48	0.72
XLIII	(4-dimethylaminophenyl)	-H	Yellow	$C_{19}H_{20}ClN_3O$	341.83	130-132	64	0.53

XLIV		-H	Pale yellow	$C_{19}H_{17}ClN_2O$	324.80	136-138	49	0.70
XLV		-H	Light brown	$C_{15}H_{13}ClN_2O_2$	288.72	136-138	51	0.69
XLVI		-Br	Pale yellow	$C_{17}H_{14}BrClN_2O$	377.66	122-124	54	0.29
XLVII		-Br	White	$C_{15}H_{12}BrClN_2O_2$	367.62	128-130	50	0.31
XLVIII		-NO$_2$	Yellow	$C_{17}H_{14}ClN_3O_3$	343.76	136-138 (lit. 144-146, Abdel-Sayed *et al*, 2016)	65	0.43
XLIX		-NO$_2$	Pale yellow	$C_{17}H_{13}Cl_2N_3O_3$	378.20	160-162	61	0.30
L		-NO$_2$	Red	$C_{19}H_{19}ClN_4O_3$	386.83	196-198	52	0.50

	Structure		Color	Formula		Melting point		
LI	(styryl/phenyl vinyl)	-NO$_2$	Yellow	C$_{19}$H$_{16}$ClN$_3$O$_3$	369.80	142-144	71	0.42
LII	(2-methylfuran)	-NO$_2$	Yellow	C$_{15}$H$_{12}$ClN$_3$O$_4$	333.72	162-164	72	0.18
LIII	(methylphenyl)	-CH$_3$	Pale yellow	C$_{18}$H$_{17}$ClN$_2$O	312.79	118-120	64	0.60
LIV	(4-chloro-methylphenyl)	-CH$_3$	Light yellow	C$_{18}$H$_{16}$Cl$_2$N$_2$O	347.23	138-140	62	0.56
LV	(4-dimethylamino-methylphenyl)	-CH$_3$	Light brown	C$_{20}$H$_{22}$ClN$_3$O	355.86	134-136	46	0.47
LVI	(styryl/phenyl vinyl)	-CH$_3$	Pale yellow	C$_{20}$H$_{19}$ClN$_2$O	338.83	108-110	65	0.62
LVII	(2-methylfuran)	-CH$_3$	Pale yellow	C$_{16}$H$_{15}$ClN$_2$O$_2$	302.75	124-126	56	0.64

*Eluting solvent: hexane:ethyleacetate (8:2 v/v)

Table (2.22): Physiochemical data of synthesized 1-[(aryl) amino acetyl] -3,5-diaryl-2-pyrazoline derivatives (LVIII-LXXI)
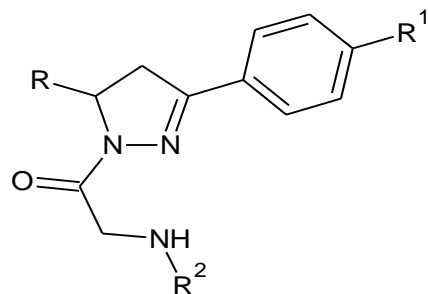
Compound No.	R	R^1	R^2	Color	MF	MW	m.p. (˚C)	Yield (%)	R_f value*
LVIII	(phenyl)	-H	(4-sulfamoylphenyl)	Wight powder	$C_{23}H_{22}N_4O_3S$	434.51	200-202	70	0.62
LIX	(4-chlorophenyl)	-H	(4-sulfamoylphenyl)	Wight powder	$C_{23}H_{21}ClN_4O_3S$	468.95	198-200	75	0.55
LX	(4-dimethylaminophenyl)	-H	(4-sulfamoylphenyl)	Pale yellow powder	$C_{25}H_{27}N_5O_3S$	477.57	110-112	57	0.71
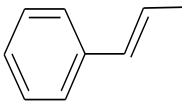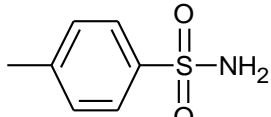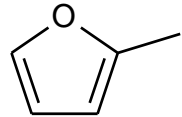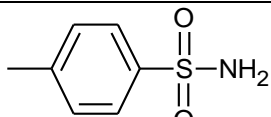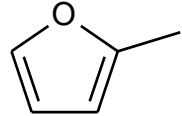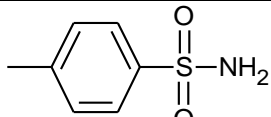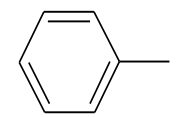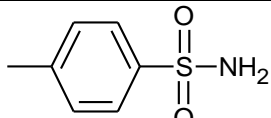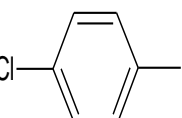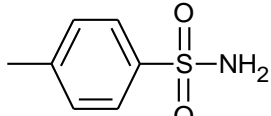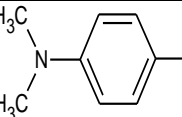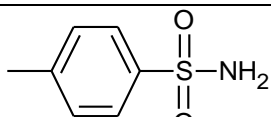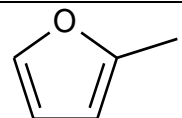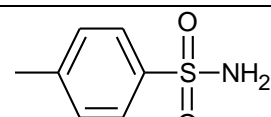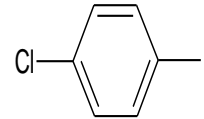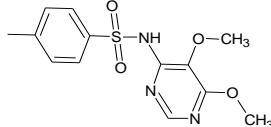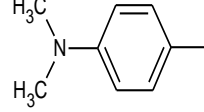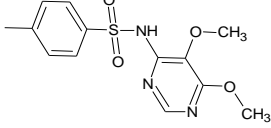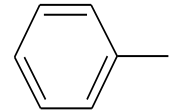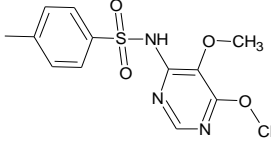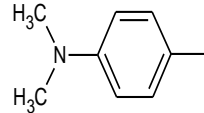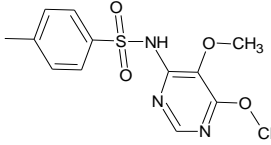
Table (2.22): continued									
LXI	(styryl-benzene structure)	-H	(benzenesulfonamide structure)	Yellow powder	$C_{25}H_{24}N_4O_3S$	460.54	140-142	42	0.68
LXII	(furan structure)	-H	(benzenesulfonamide structure)	Yellow powder	$C_{21}H_{20}N_4O_4S$	424.47	184-186	40	0.55
LXIII	(furan structure)	-NO$_2$	(benzenesulfonamide structure)	Yellow powder	$C_{21}H_{19}N_5O_6S$	469.47	190-192	45	0.58
LXIV	(benzene structure)	-CH$_3$	(benzenesulfonamide structure)	Wight powder	$C_{24}H_{24}N_4O_3S$	448.53	210-212	59	0.59
LXV	(Cl-benzene structure)	-CH$_3$	(benzenesulfonamide structure)	Yellow powder	$C_{24}H_{23}ClN_4O_3S$	482.98	216-218	48	0.45
LXVI	(dimethylamino-benzene structure)	-CH$_3$	(benzenesulfonamide structure)	Yellow powder	$C_{26}H_{29}N_5O_3S$	491.60	118-120	39	0.72
LXVII	(furan structure)	-CH$_3$	(benzenesulfonamide structure)	Yellow powder	$C_{22}H_{22}N_4O_4S$	438.49	202-204	51	0.72

84

Table (2.22): continued									
LXVIII	(4-Cl-phenyl)	-H	(sulfonyl-pyrimidine structure)	Pale yellow powder	$C_{29}H_{27}ClN_6O_5S$	607.07	138-140	59	0.44
LXIX	$(H_3C)_2N$-phenyl	-H	(sulfonyl-pyrimidine structure)	Yellow powder	$C_{31}H_{33}N_7O_5S$	615.70	168-170	50	0.67
LXX	(phenyl)	-CH$_3$	(sulfonyl-pyrimidine structure)	Yellow powder	$C_{30}H_{30}N_6O_5S$	586.66	192-194	47	0.32
LXXI	$(H_3C)_2N$-phenyl	-CH$_3$	(sulfonyl-pyrimidine structure)	Yellow powder	$C_{32}H_{35}N_7O_5S$	629.72	184-186	40	0.61

*Eluting solvent: hexane:ethyleacetate (4:6 v/v)

Table (2.23): Infra-red spectral data (KBr) cm^{-1} of synthesized α,β-unsaturated carbonyl derivatives

(I-XX)
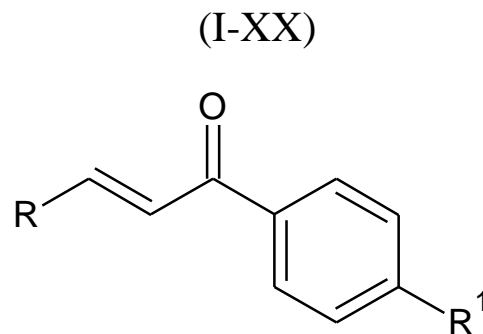
Compound No.	R	R^1	ArC-H st.vib.	C=O st.vib. in conjugation with C=C	C=C st.vib. in conjugation with C=O	Ar-C=C st.vib.	Other groups
I	(phenyl)	-H	3054	1659	1600	1492	
II	(Cl-phenyl)	-H	3055	1656	1592	1484	775 (R-Cl)
III	(H$_3$C)$_2$N-phenyl	-H	3089	1646	1562	1527	1374(-N(CH$_3$)$_2$)
IV	(styryl)	-H	3060	1650	1584	1443	1500 (aliphatic C=C st.vib.)
V	(furyl)	-H	3060	1659	1598	1548	1223(C-O-C st.vib.)

Table (2.23): continued							
VI	(phenyl)	-Br	3056	1657	1599	1482	684 (R-Br)
VII	(Cl-phenyl)	-Br	3085	1655	1591	1486	663 (R-Br), 739 (R-Cl)
VIII	(H_3C, H_3C)N-phenyl	-Br	2905	1646	1581	1529	663 (R-Br), 1374 (-N(CH$_3$)$_2$)
IX	(styryl)	-Br	3061	1649	1584	1447	685 (R-Br), 1482 (aliphatic C=C st.vib.)
X	(furyl)	-Br	3131	1654	1592	1471	667 (R-Br), 1222 (C-O-C st.vib.)
XI	(phenyl)	-NO$_2$	3067	1659	1594	1448	1518 (asym.-NO$_2$)-1334 (sym. -NO$_2$)
XII	(Cl-phenyl)	-NO$_2$	3104	1665	1592	1407	1520 (asym.-NO$_2$)-1334 (sym. -NO$_2$), 760 (R-Cl)
XIII	(H_3C, H_3C)N-phenyl	-NO$_2$	3102	1646	1565	1436	1519 (asym.-NO$_2$)-1335 (sym. -NO$_2$), 1369 (-N(CH$_3$)$_2$)
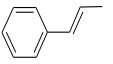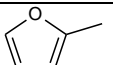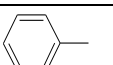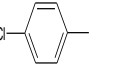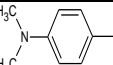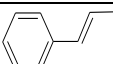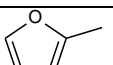
Table (2.23): continued							
XIV	(styrene structure)	-NO₂	3028	1655	1572	1445	1521 (asym.-NO₂)-1343 (sym. -NO₂)
XV	(furan structure)	-NO₂	3118	1658	1590	1448	1523 (asym.-NO₂)-1327 (sym. -NO₂), 1227 (C-O-C st.vib.)
XVI	(phenyl structure)	-CH₃	3057	1654	1606	1594	2915 (-CH₃)
XVII	(Cl-phenyl structure)	-CH₃	3026	1655	1602	1563	2914 (-CH₃), 760 (R-Cl)
XVIII	(N(CH₃)₂-phenyl structure)	-CH₃	3034	1644	1608	1573	2907 (-CH₃), 1369 (-N(CH₃)₂)
XIX	(styrene structure)	-CH₃	3046	1650	1604	1494	3024 (-CH₃), 1577 (aliphatic C=C st.vib.)
XX	(furan structure)	-CH₃	3051	1652	1597	1549	2913 (-CH₃), 1227(C-O-C st.vib.)

Table (2.24): Infra-red spectral data (KBr) cm^{-1} of synthesized 3,5-Diaryl-2-pyrazoline derivatives

(XXI-XL)
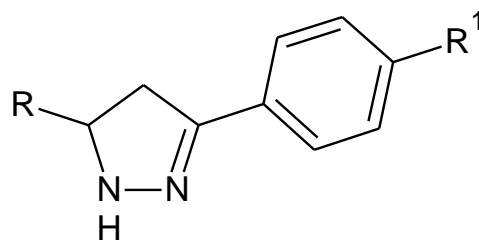
Comp-ound No.	R	R^1	ArC-H st.vib.	Pyrazo-line –NH st.vib.	-C=N str.vib	Ar-C=C st.vib.	C-N st.vib.	Ar-N-N str.vib	Other groups
XXI		-H	3063	3351	1633	1585	1161	1061	
XXII		-H	3046	3332	1651	1588	1168	1087	768 (R-Cl)
XXIII		-H	3071	3333	1609	1517	1165	1058	1349 (-N(CH$_3$)$_2$)
XXIV		-H	3037	3421	1613	1490	1240	1081	1575 (aliphatic C=C st.vib.)
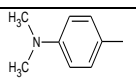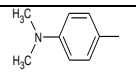
	Structure								
Table (2.24): continued									
XXV	(furan-methyl)	-H	3064	3249	1588	1564	1153	1052	1229 (C-O-C str.vib).
XXVI	(phenyl-methyl)	-Br	3057	3421	1664	1581	1178	1069	698 (R-Br)
XXVII	(Cl-phenyl-methyl)	-Br	3048	3338	1652	1588	1170	1088	629 (R-Br), 766 (R-Cl)
XXVIII	(H_3C, H_3C)N-phenyl-methyl	-Br	3074	3336	1650	1606	1166	1060	687 (R-Br), 1346 (-N(CH$_3$)$_2$)
XXIX	(styryl)	-Br	3025	3337	1677	1486	1175	1067	692 (R-Br), 1582 (aliphatic C=C st.vib.)
XXX	(furan-methyl)	-Br	3052	3350	1588	1477	1144	1070	665 (R-Br), 1245(C-O-C str.vib.)
XXXI	(phenyl)	-NO$_2$	3073	3350	1594	1557	1174	1068	1506 (asym.-NO$_2$)-1340 (sym. -NO$_2$)
XXXII	(Cl-phenyl-methyl)	-NO$_2$	2894	3337	1594	1562	1171	1090	1506 (asym.-NO$_2$)-1340 (sym. -NO$_2$), 761 (R-Cl)
XXXIII	(H_3C, H_3C)N-phenyl-methyl	-NO$_2$	3001	3332	1603	1556	1171	1060	1513 (asym.-NO$_2$)-1336 (sym. -NO$_2$), 1336 (-N(CH$_3$)$_2$)
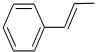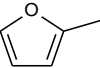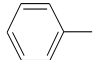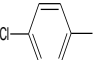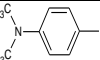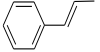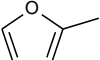
Table (2.24): continued								
XXXIV	(styrene structure)	$-NO_2$	3027	3250	1640	1559	1175	1053	1594 (aliphatic C=C st.vib.), 1503 (asym.-NO_2)-1335 (sym. -NO_2)
XXXV	(furan structure)	$-NO_2$	2884	3334	1681	1592	1180	1073	1506 (asym.-NO_2)-1339 (sym. -NO_2), 1236 (C-O-C st.vib.)
XXXVI	(benzene structure)	$-CH_3$	3026	3284	1671	1602	1178	1047	2911 (-CH_3)
XXXVII	(Cl-benzene structure)	$-CH_3$	3029	3338	1665	1597	1176	1055	2965 (-CH_3), 764(R-Cl)
XXXVIII	(H_3C–N(H_3C)–benzene structure)	$-CH_3$	3027	3333	1656	1613	1163	1056	2945 (-CH_3), 1344 (-N(CH_3)$_2$)
XXXIX	(styrene structure)	$-CH_3$	3024	3320	1671	1493	1181	1111	1598 (aliphatic C=C st.vib.), 2911 (-CH_3)
XL	(furan structure)	$-CH_3$	3029	3256	1668	1590	1150	1074	2961 (-CH_3), 1246(C-O-C st.vib.)

Table (2.25) Infra-red spectral data (KBr) cm^{-1} of synthesized 1-(Chloroacetyl)-3,5-diaryl-2-pyrazoline derivatives (XLI-LVII)
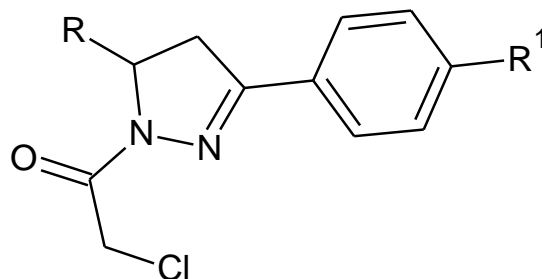
Compound No.	R	R^1	Ar-C-H st.vib.	C=O st.vib.	Ar-C=N st.vib.	Ar-C=C st.vib.	C-N st.vib.	Ar-N-N st.vib.	Other groups
XLI		-H	3028	1665	1570	1443	1197	1077	
XLII		-H	3026	1668	1599	1573	1174	1091	758(R-Cl)
XLIII		-H	3056	1664	1612	1565	1157	1035	1339 (-N(CH$_3$)$_2$)
XLIV		-H	3025	1666	1599	1434	1145	1076	1489 (aliphatic C=C st.vib.)
XLV		-H	3052	1669	1599	1501	1139	1074	1241 (C-O-C st.vib.)
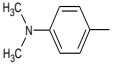
Table (2.25): continued									
XLVI		-Br	3034	1683	1589	1490	1140	1067	623 (R-Br)
XLVII		-Br	3059	1678	1589	1500	1134	1068	659 (R-Br), 1238(C-O-C st.vib.)
XLVIII		$-NO_2$	3030	1672	1577	1437	1144	1035	1515 (asym.-NO_2)-1341 (sym. -NO_2)
XLIX		$-NO_2$	3070	1667	1598	1445	1140	1044	1513 (asym.-NO_2)-1344(sym. -NO_2), 752 (R-Cl)
L		$-NO_2$	3076	1673	1608	1566	1173	1037	1517 (asym.-NO_2)-1338 (sym. -NO_2), 1336 (-$N(CH_3)_2$)
LI		$-NO_2$	3077	1684	1585	1430	1144	1032	1573 (aliphatic C=C st.vib.), 1510 (asym.-NO_2)-1339 (sym. -NO_2)
LII		$-NO_2$	3077	1667	1597	1573	1137	1040	1517 (asym.-NO_2)-1347 (sym. -NO_2), 1248(C-O-C st.vib.)
LIII		$-CH_3$	3031	1664	1522	1442	1138	1035	2949 (-CH_3)

93
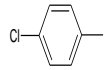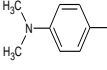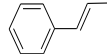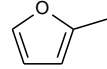
Table (2.25): continued								
LIV		-CH$_3$	3030	1684	1667	1603	1135	1041	2922 (-CH$_3$), 780(R-Cl)
LV		-CH$_3$	2908	1673	1613	1524	1140	1035	2799 (-CH$_3$), 1337 (-N(CH$_3$)$_2$)
LVI		-CH$_3$	3021	1671	1608	1433	1136	1034	2953 (-CH$_3$), 1486 (aliphatic C=C st.vib.)
LVII		-CH$_3$	3018	1683	1604	1563	1148	1036	2958 (-CH$_3$), 1240(C-O-C st.vib.)

94

Table (2.26): Infra-red spectral data (KBr) cm^{-1} of synthesized 1-[(aryl) amino acetyl] -3,5-diaryl-2-pyrazoline derivatives (LVIII-LXXI)
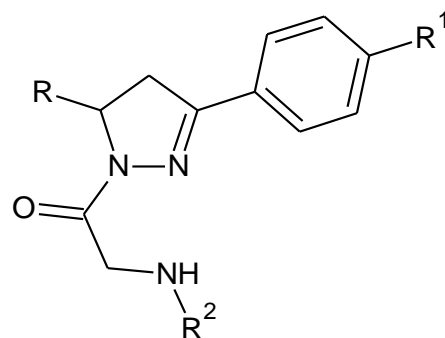
Compound No.	R	R^1	R^2	NH$_2$ st.vib.	NH st.vib.	C=O st.vib.	C=N st.vib.	Ar-C=C st.vib.	SO$_2$ st.vib.	Other groups
LVIII	(phenyl)	-H	(benzenesulfonamide)	3482(asym. NH$_2$) -3392(sym. NH$_2$)	3232	1660	1625	1594	1395(asym.-SO$_2$)- 1155(sym.-SO$_2$)	
LIX	(4-Cl-phenyl)	-H	(benzenesulfonamide)	3479(asym. NH$_2$) -3375(sym. NH$_2$)	3224	1651	1593	1500	1396(asym.-SO$_2$)- 1153(sym.-SO$_2$)	725(R-Cl)
LX	(4-N(CH$_3$)$_2$-phenyl)	-H	(benzenesulfonamide)	3441(asym. NH$_2$) -3363(sym. NH$_2$)	3228	1651	1600	1523	1392(asym.-SO$_2$)- 1153(sym.-SO$_2$)	1342 (-N(CH$_3$)$_2$)

95
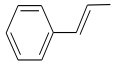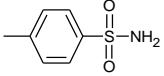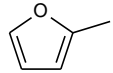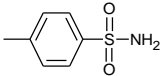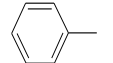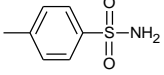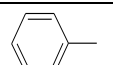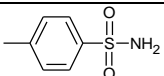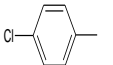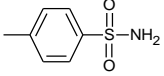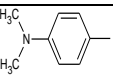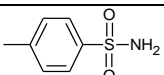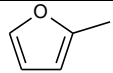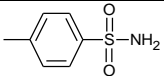
Table (2.26): continued										
LXI	(styrene structure)	-H	(benzenesulfonamide structure)	3464(asym. NH$_2$) -3360(sym. NH$_2$)	3236	1654	1597	1438	1388(asym.-SO$_2$)- 1149(sym.-SO$_2$)	1504 (aliphatic C=C st.vib.)
LXII	(furan structure)	-H	(benzenesulfonamide structure)	3471(asym. NH$_2$) -3371(sym. NH$_2$)	3224	1658	1597	1507	1311(asym.-SO$_2$)- 1153(sym.-SO$_2$)	
LXIII	(phenyl structure)	-NO$_2$	(benzenesulfonamide structure)	3448(asym. NH$_2$) -3383(sym. NH$_2$)	3240	1670	1631	1597	1342(asym.-SO$_2$)- 1153(sym.-SO$_2$)	1516 (asym.-NO$_2$) - 1315 (sym. -NO$_2$)
LXIV	(phenyl structure)	-CH$_3$	(benzenesulfonamide structure)	3448(asym. NH$_2$) -3356(sym. NH$_2$)	3217	1670	1635	1597	1311(asym.-SO$_2$)- 1153(sym.-SO$_2$)	2985 (-CH$_3$)
LXV	(4-chlorophenyl structure)	-CH$_3$	(benzenesulfonamide structure)	3448(asym. NH$_2$) -3367(sym. NH$_2$)	3251	1662	1597	1492	1319(asym.-SO$_2$)- 1149(sym.-SO$_2$)	2920 (-CH$_3$), 721 (R-Cl)
LXVI	(dimethylaminophenyl structure)	-CH$_3$	(benzenesulfonamide structure)	3452(asym. NH$_2$) -3363(sym. NH$_2$)	3213	1651	1597	1519	1311(asym.-SO$_2$)- 1153(sym.-SO$_2$)	2958 (-CH$_3$), 1342 (-N(CH$_3$)$_2$)
LXVII	(furan structure)	-CH$_3$	(benzenesulfonamide structure)	3444(asym. NH$_2$) -3356(sym. NH$_2$)	3213	1654	1597	1504	1315(asym.-SO$_2$)- 1153(sym.-SO$_2$)	2920 (-CH$_3$), 1261(C-O-C st.vib.)

96
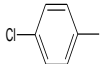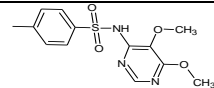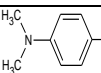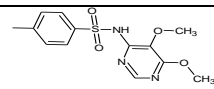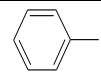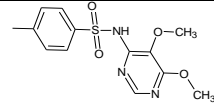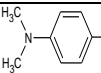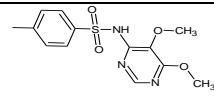
Table (2.26): continued										
LXVIII		-H			3402	1658	1597	1577	1323(asym.-SO_2)-1130(sym.-SO_2)	759(R-Cl)
LXIX		-H			3398	1662	1597	1523	1338(asym.-SO_2)-1157(sym.-SO_2)	
LXX		-CH_3			3425	1658	1600	1519	1330(asym.-SO_2)-1118(sym.-SO_2)	2940 (-CH_3)
LXXI		-CH_3			3394	1658	1612	1597	1330(asym.-SO_2)-1157(sym.-SO_2)	2920 (-CH_3)

97

Table (2.27): UV spectral data of synthesized 1-(Chloroacetyl)-3,5-diaryl-2-pyrazoline derivatives (XLI-LVII)
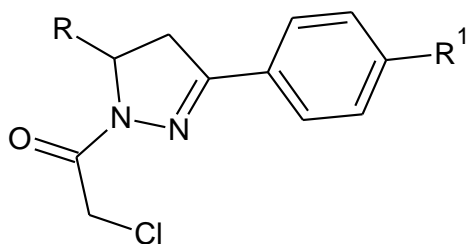
Compound No.	R	R^1	λ_{max} (DMSO)
XLI		-H	300.80, 293.20
XLII		-H	349.60
XLIII		-H	350.20, 265.60
XLIV		-H	351.40
XLV		-H	347.60
XLVI		-Br	299.40, 293.00
XLVII		-Br	300.00, 255.00
XLVIII		-NO$_2$	350.00
XLIX		-NO$_2$	300.00
L		-NO$_2$	301.60, 265.60
LI		-NO$_2$	295.00, 255.80
LII		-NO$_2$	294.40, 254.40
LIII		-CH$_3$	300.00
LIV		-CH$_3$	298.40, 266.80
LV		-CH$_3$	295.80, 255.80
LVI		-CH$_3$	296.40
LVII		-CH$_3$	300.00

Table (2.28): UV spectral data of synthesized 1-[(aryl) amino acetyl] -
3,5-diaryl-2-pyrazoline derivatives (LVIII-LXXI)
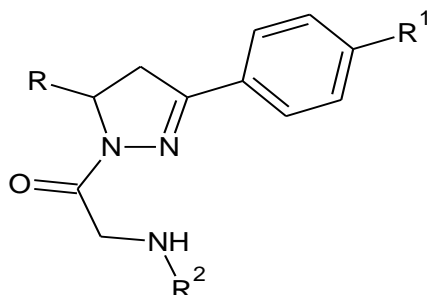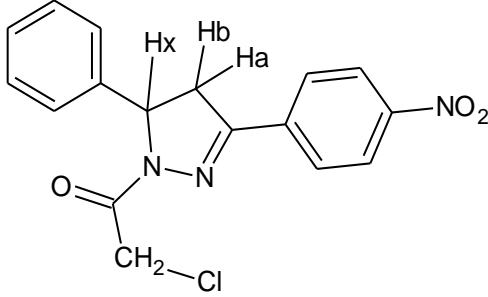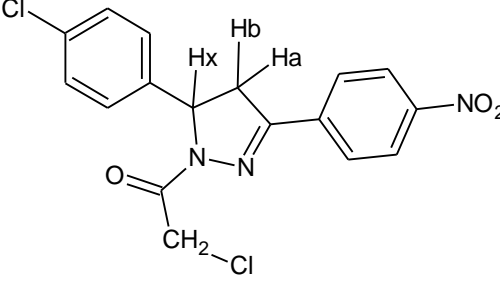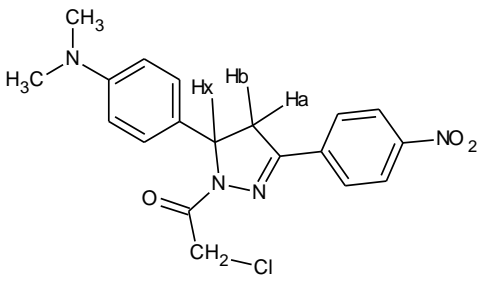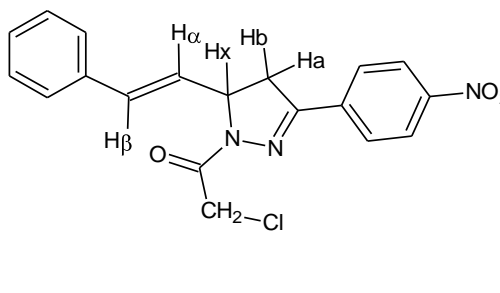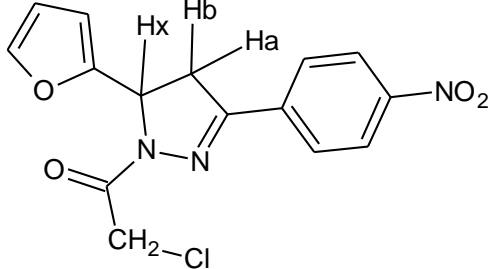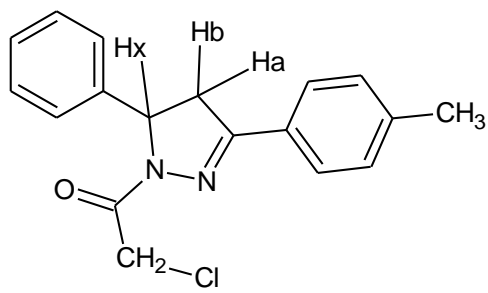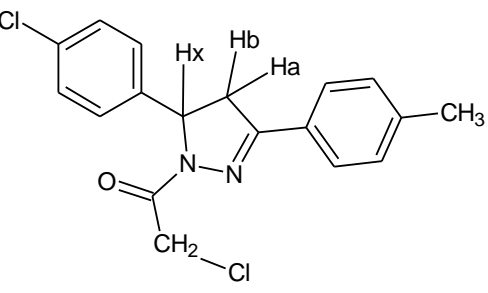
Compound No.	R	R_1	R_2	λ_{max} (DMSO)
LVIII		-H		291.60, 276.80
LIX		-H		286.80, 271.60
LX		-H		292.00, 267.40
LXI		-H		293.40
LXII		-H		349.00, 287.60
LXIII		-NO$_2$		288.60, 279.60
LXIV		-CH$_3$		294.20
LXV		-CH$_3$		293.60, 291.40, 276.40
LXVI		-CH$_3$		294.60, 267.20
LXVII		-CH$_3$		280.60, 276.60
LXVIII		-H		290.40
LXIX		-H		294.60, 265.40
LXX		-CH$_3$		294.00
LXXI		-CH$_3$		295.20, 265.40

Table (2.29):^{1}H NMR Data of synthesized 1-(Chloroacetyl)-3,5-diaryl-2-pyrazoline derivatives (XLI-LVII)

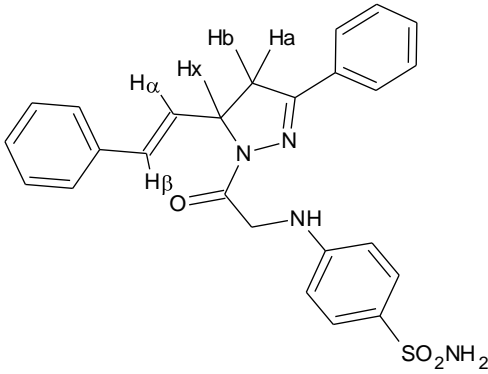| Compound No.	Structure of compound	Chemical shift (ppm)
XLI		3.17 ppm (dd, 1H, $J_{Ha,Hb}$= 18.2 Hz, $J_{Ha,Hx}$= 4.72 Hz, Ha) 3.87 ppm (dd, 1H, $J_{Hb,Ha}$= 18.2 Hz, $J_{Hb,Hx}$= 11.72 Hz, Hb) 4.68 ppm (d,1H, J= 13.8 Hz, CO-C<u>H</u>) 4.77 ppm (d, 1H, J= 13.8 Hz, CO-C<u>H</u>) 5.57 ppm (dd, 1H, $J_{Hb,Hx}$= 11.72 Hz, $J_{Ha,Hx}$= 4.64 Hz, Hx) 7.22-7.84 ppm (m, 10H, Ar-H).
XLII		3.19 ppm (dd, 1H, $J_{Ha,Hb}$= 18.24 Hz, $J_{Ha,Hx}$ = 4.88 Hz, Ha) 3.87 ppm (dd, 1H, $J_{Hb,Ha}$= 18.28 Hz, $J_{Hb,Hx}$= 11.76 Hz, Hb) 4.67 ppm (d, 1H, J= 13.84 Hz, CO-C<u>H</u>) 4.77 ppm (d, 1H, J= 13.84 Hz, CO-C<u>H</u>) 5.58 ppm (dd, 1H, $J_{Hb,Hx}$= 11.76 Hz, $J_{Ha,Hx}$= 4.84 Hz, Hx) 7.26-7.83 ppm (m, 9H, Ar-H)
XLIII		2.85 ppm (s, 6H, CH_3-N) 3.14 ppm (dd, 1H, $J_{Ha,Hb}$ = 18.16 Hz, $J_{Ha,Hx}$ = 4.44 Hz, Ha) 3.80 ppm (dd, 1H, $J_{Hb,Ha}$= 18.16 Hz, $J_{Hb,Hx}$= 11.59 Hz, Hb) 4.64 ppm (d, 1H, J= 13.72 Hz, CO-C<u>H</u>) 4.72 ppm (d, 1H, J= 13.72 Hz, CO-C<u>H</u>) 5.45 ppm (dd, 1H, $J_{Hb,Hx}$ = 11.56 Hz, $J_{Ha,Hx}$ = 4.4 Hz, Hx) 6.66 ppm (d, 2H, J= 8.72 Hz, Ar-H) 7.03 ppm (d, 2H, J= 8.72 Hz, Ar-H) 7.48-7.83 ppm (m, 5H, Ar-H)
XLIV		3.25 ppm (dd, 1H, $J_{Ha,Hb}$ = 18 Hz, $J_{Ha,Hx}$ = 4.68 Hz, Ha) 3.65 ppm (dd, 1H, $J_{Hb,Ha}$ = 17.96Hz, $J_{Hb,Hx}$ = 11.32 Hz, Hb) 4.67 ppm (d, 1H, J= 13.84 Hz, CO-C<u>H</u>) 4.73 ppm (d, 1H, J= 13.72 Hz, CO-C<u>H</u>) 5.19-5.25 ppm (m, 1H, Hx)

		6.30 ppm (dd, 1H, $J_{\alpha\text{-H},\beta\text{-H}}$ = 15.88 Hz, $J_{\alpha\text{-H,Hx}}$ =7.08Hz, α-H) 6.57 ppm (d, 1H , J= 15.88 Hz, β-H) 7.32-7.83 ppm (m, 10H, Ar-H)
XLV		3.40 ppm (dd, 1H, $J_{Ha,Hb}$ = 18.04 Hz, $J_{Ha,Hx}$ = 4.72 Hz, Ha) 3.74 ppm (dd, 1H, $J_{Hb,Ha}$ = 18.04 Hz, $J_{Hb,Hx}$ = 11.8 Hz, Hb) 4.65 ppm (d, 1H, J= 14 Hz, CO-C<u>H</u>) 4.70 ppm (d, 1H, J= 14.04 Hz, CO-C<u>H</u>) 5.67 ppm (dd, 1H, $J_{Hb,Hx}$ = 11.76 Hz, $J_{Ha,Hx}$ = 4.72 Hz, Hx) 6.38-6.42 ppm (m, 2H, furan-H) 7.47-7.52 ppm (m, 3H, Ar-H) 7.58 ppm (d, 1H, J=1.60 Hz, furan-H) 7.82-7.85 ppm (m, 2H, Ar-H)
XLVI		3.17 ppm (dd, 1H, $J_{Ha,Hb}$ = 18.24 Hz, $J_{Ha,Hx}$ = 4.8 Hz, Ha) 3.86 ppm (dd, 1H, $J_{Hb,Ha}$ = 18.24 Hz, $J_{Hb,Hx}$ = 11.8 Hz, Hb) 4.67 ppm (d, 1H, J= 13.84 Hz, CO-C<u>H</u>) 4.77 ppm (d, 1H, J= 13.84 Hz, CO-C<u>H</u>) 5.57 ppm (dd, 1H, $J_{Hb,Hx}$ = 11.72 Hz, $J_{Ha,Hx}$ = 4.76 Hz, Hx) 7.22-7.37 ppm (m, 5H, Ar-H) 7.67 ppm (d, 2H, J=8.56 Hz, Ar-H) 7.75 ppm (d, 2H, J=8.56 Hz, Ar-H)
XLVII		3.39 ppm (dd, 1H, $J_{Ha,Hb}$ = 18.12 Hz, $J_{Ha,Hx}$ = 4.84 Hz, Ha) 3.73 ppm (dd, 1H, $J_{Hb,Ha}$ = 18.08 Hz, $J_{Hb,Hx}$ = 11.8 Hz, Hb) 4.65 ppm (d, 1H, J= 14.08 Hz, CO-C<u>H</u>) 4.70 ppm (d, 1H, J= 14.04 Hz, CO-C<u>H</u>) 5.68 ppm (dd, 1H, $J_{Hb,Hx}$ = 11.8 Hz, $J_{Ha,Hx}$ = 4.84Hz, Hx) 6.39-6.42 ppm (m, 2H, furan-H) 7.58 ppm (d, 1H, J=0.72 Hz, furan-H) 7.69 ppm (d, 2H, J=8.56 Hz, Ar-H) 7.76 ppm (d, 2H, J=8.52 Hz, Ar-H)

XLVIII		3.25 ppm (dd, 1H, $J_{Ha,Hb}$ = 18.36 Hz, $J_{Ha,Hx}$ = 4.96 Hz, Ha) 3.93 ppm (dd, 1H, $J_{Hb,Ha}$ = 18.32 Hz, $J_{Hb,Hx}$ = 11.92 Hz, Hb) 4.72 ppm (d, 1H, J= 13.96 Hz, CO-C<u>H</u>) 4.82 ppm (d, 1H, J= 14 Hz, CO-C<u>H</u>) 5.63 ppm (dd, 1H, $J_{Hb,Hx}$ = 11.88 Hz, $J_{Ha,Hx}$ = 4.96 Hz, H_{5a}) 7.24-7.38 ppm (m, 4H, Ar-H) 8.05 ppm (d, 2H, J= 8.88 Hz, Ar-H) 8.30 ppm (d, 2H, J= 8.88 Hz, Ar-H)
XLIX		3.27 ppm (dd, 1H, $J_{Ha,Hb}$ = 18.36 Hz, $J_{Ha,Hx}$ = 5.16 Hz, Ha) 3.92 ppm (dd, 1H, $J_{Hb,Ha}$ = 18.36Hz, $J_{Hb,Hx}$ = 11.99 Hz, Hb) 4.71 ppm (d, 1H, J= 14 Hz, CO-C<u>H</u>) 4.81 ppm (d, 1H, J= 14 Hz, CO-C<u>H</u>) 5.63 ppm (dd, 1H, $J_{Hb,Hx}$ = 11.92 Hz, $J_{Ha,Hx}$ = 5.2 Hz, Hx) 7.28 ppm (d, 2H, Ar-H) 7.40 ppm (d, 2H, Ar-H) 8.04 ppm (d, 2H, Ar-H) 8.30 ppm (d, 2H, Ar-H)
L		2.87 ppm (s, 6H, CH_3-N) 3.22 ppm (dd, 1H, $J_{Ha,Hb}$ = 18.28 Hz, $J_{Ha,Hx}$ = 4.76 Hz, Ha) 3.86 ppm (dd, 1H, $J_{Hb,Ha}$ = 18.24 Hz, $J_{Hb,Hx}$ = 11.8, Hz, Hb) 4.68 ppm (d, 1H, J= 13.88 Hz, CO-C<u>H</u>) 4.77 ppm (d, 1H, J= 13.88 Hz, CO-C<u>H</u>) 5.51 ppm (dd, 1H, $J_{Hb,Hx}$ = 11.68 Hz, $J_{Ha,Hx}$ = 4.68 Hz, Hx) 6.71-8.34 ppm (m, 8H, Ar-H)
LI		3.32 ppm (dd, 1H, $J_{Ha,Hb}$ = 18.04 Hz, $J_{Ha,Hx}$ = 4.96 Hz, Ha) 3.70 ppm (dd, 1H, $J_{Hb,Ha}$ = 18.08 Hz, $J_{Hb,Hx}$ = 11.44 Hz, Hb) 4.71 ppm (d, 1H, J= 14 Hz, CO-C<u>H</u>) 4.77 ppm (d, 1H, J= 14.04 Hz, CO-C<u>H</u>) 5.25-5.31 ppm (m, 1H, Hx) 6.32 ppm (dd, 1H, $J_{\alpha-H,\beta-H}$ = 15.88 Hz, $J_{\alpha-H,Hx}$ = 7.28 Hz, α-H) 6.60 ppm (d, 1H , J= 15.88 Hz, β-H)

		7.23-7.45 ppm (m, 5H, Ar-H) 8.05-8.34 ppm (m, 4H, Ar-H)
LII		3.48 ppm (dd, 1H, $J_{Ha,Hb}$ = 18.16 Hz, $J_{Ha,Hx}$ = 5.00 Hz, Ha) 3.80 ppm (dd, 1H, $J_{Hb,Ha}$ = 18.16 Hz, $J_{Hb,Hx}$ = 11.88 Hz, Hb) 4.69 ppm (d, 1H, J= 14.16 Hz, CO-C$\underline{H}$) 4.75 ppm (d, 1H, J= 14.16 Hz, CO-C$\underline{H}$) 5.74 ppm (dd, 1H, $J_{Hb,Hx}$ = 11.92 Hz, $J_{Ha,Hx}$ = 4.96 Hz, Hx) 6.42-6.43 ppm (m, 2H, J=1.24 Hz, furan-H) 7.59 ppm (d, 1H, J=0.72 Hz, furan-H) 8.07-8.33 ppm (m, 4H, Ar-H)
LIII		2.35 ppm (s, 3H, CH$_3$) 3.14 ppm (dd, 1H, $J_{Ha,Hb}$ = 18.16 Hz, $J_{Ha,Hx}$ = 4.64 Hz, Ha) 3.84 ppm (dd, 1H, $J_{Hb,Ha}$ = 18.2 Hz, $J_{Hb,Hx}$ = 11.76 Hz, Hb) 4.66 ppm (d, 1H, J= 13.76 Hz, CO-C$\underline{H}$) 4.76 ppm (d, 1H, J= 13.8 Hz, CO-C$\underline{H}$) 5.55 ppm (dd, 1H, $J_{Hb,Hx}$ = 11.68 Hz, $J_{Ha,Hx}$ = 4.6 Hz, Hx) 7.21-7.36 ppm (m,7H,Ar-H) 7.70 ppm (d, 2H, J= 8.16 Hz, Ar-H)
LIV		2.35 ppm (s, 3H, CH$_3$) 3.14 ppm (dd, 1H, $J_{Ha,Hb}$ = 18.24 Hz, $J_{Ha,Hx}$ = 4.8 Hz, Ha) 3.83 ppm (dd, 1H, $J_{Hb,Ha}$ = 18.2Hz, $J_{Hb,Hx}$ = 11.76 Hz, Hb) 4.65 ppm (d, 1H, J= 13.8 Hz, CO-C$\underline{H}$) 4.75 ppm (d, 1H, J= 13.8 Hz, CO-C$\underline{H}$) 5.55 ppm (dd, 1H, $J_{Hb,Hx}$ = 11.72 Hz, $J_{Ha,Hx}$ = 4.76 Hz, Hx) 7.24-7.30 ppm (m, 4H, Ar-H) 7.39 ppm (d, 2H, J= 8.44 Hz, Ar-H), 7.69 ppm (d, 2H, J= 8.12 Hz, Ar-H)
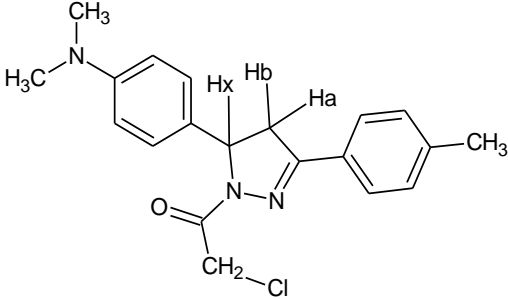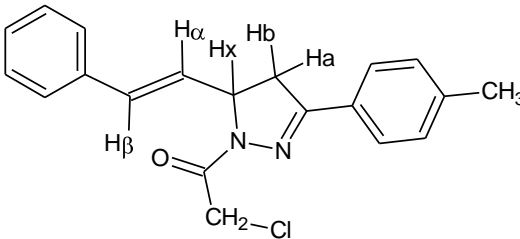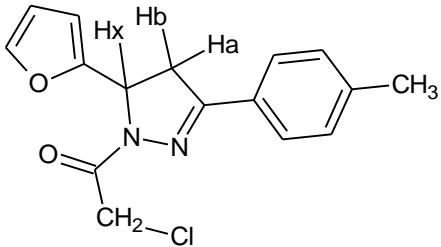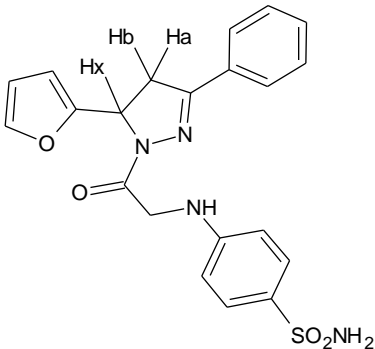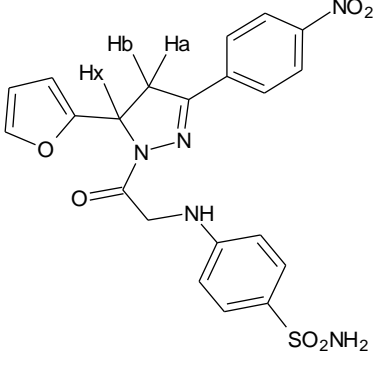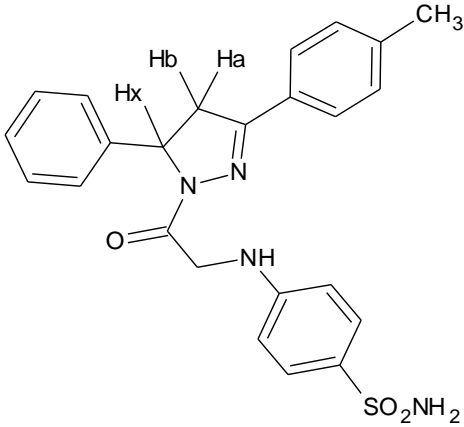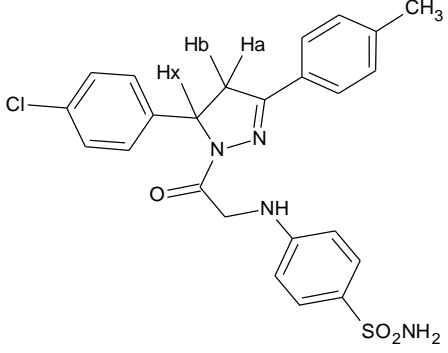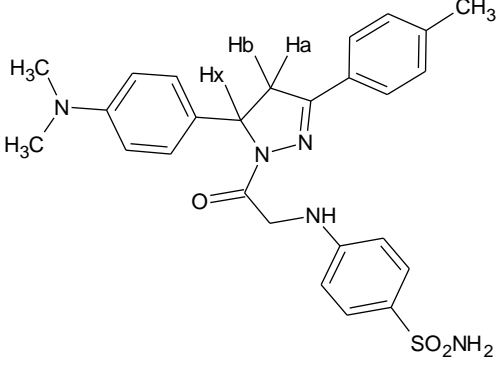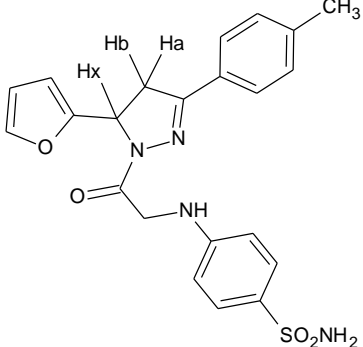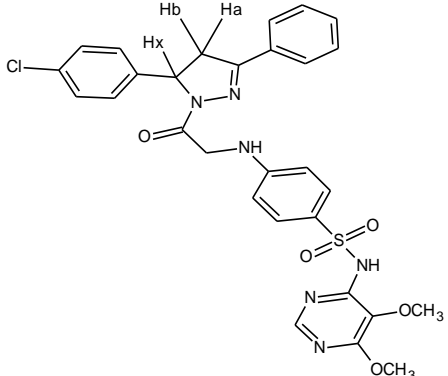
LV		2.36 ppm (s, 3H, CH₃) 2.85 ppm (s, 6H, CH₃-N) 3.11 ppm (dd, 1H, $J_{Ha,Hb}$ = 18.12 Hz, $J_{Ha,Hx}$ = 4.36 Hz, Ha) 3.76 ppm (dd, 1H, $J_{Hb,Ha}$ = 18.08 Hz, $J_{Hb,Hx}$ = 11.56 Hz, Hb) 4.62 ppm (d, 1H, J= 13.72 Hz, CO-CH̲) 4.70 ppm (d, 1H, J= 13.68 Hz, CO-CH̲) 5.43 ppm (dd, 1H, $J_{Hb,Hx}$ = 11.48 Hz, $J_{Ha,Hx}$ = 4.32 Hz, Hx) 6.65 ppm (d, 2H, J= 8.72 Hz, Ar-H), 7.01 ppm (d, 2H, J= 8.72 Hz, Ar-H), 7.28 ppm (d, 2H, J= 8.00 Hz, Ar-H), 7.70 ppm (d, 2H, J= 8.12 Hz, Ar-H),).
LVI		2.35 ppm (s, 3H, CH₃) 3.20 ppm (dd, 1H, $J_{Ha,Hb}$ = 18.00 Hz, $J_{Ha,Hx}$ = 4.72 Hz, Ha) 3.59 ppm (dd, 1H, $J_{Hb,Ha}$ = 17.96Hz, $J_{Hb,Hx}$ = 11.28 Hz, Hb) 4.65 ppm (d, 1H, J= 13.80 Hz, CO-CH̲) 4.71 ppm (d, 1H, J= 13.84 Hz, CO-CH̲) 5.16-5.22 ppm (m, 1H, Hx) 6.28 ppm (dd, 1H, $J_{\alpha-H,\beta-H}$= 15.88 Hz, $J_{\alpha-H,Hx}$ =7.08 Hz, α-H) 6.57 ppm (d, 1H , J= 15.88 Hz, β-H) 7.22-7.34 ppm (m, 5H, Ar-H) 7.42 ppm (d, 2H, J=7.40 Hz, Ar-H) 7.69 ppm (d, 2H, J=8.08 Hz, Ar-H)
LVII		2.36 ppm (s, 3H, CH₃) 3.36 ppm (dd, 1H, $J_{Ha,Hb}$ = 18.04Hz, $J_{Ha,Hx}$ = 4.72 Hz, Ha) 3.71 ppm (dd, 1H, $J_{Hb,Ha}$ = 18.00 Hz, $J_{Hb,Hx}$ = 11.76 Hz, Hb) 4.63 ppm (d, 1H, J= 14.00 Hz, CO-CH̲) 4.68 ppm (d, 1H, J= 13.96 Hz, CO-CH̲) 5.65 ppm (dd, 1H, $J_{Hb,Hx}$ = 11.68 Hz, $J_{Ha,Hx}$ = 4.72 Hz, Hx) 6.37-6.42 ppm (m, 2H, furan-H) 7.29 ppm (d, 2H, J= 8.00 Hz, Ar-H), 7.57 ppm (d, 1H, J= 0.84 Hz, furan-H), 7.71 ppm (d, 2H, J= 8.12 Hz, Ar-H).

Table (2.30): ^{1}H NMR Data of synthesized 1-[(aryl) amino acetyl] -3,5-diaryl-2-pyrazoline derivatives (LVIII-LXXI)

Compound No.	Structure of compound	Chemical shift (ppm)
LVIII		3.10 ppm (dd, 1H, $J_{Ha,Hb}$ = 18.12 Hz, $J_{Ha,Hx}$ = 4.72 Hz, Ha) 3.80 ppm (dd, 1H, $J_{Hb,Ha}$ = 18.16 Hz, $J_{Hb,Hx}$ = 11.80 Hz, Hb) 4.02 ppm (d, 2H, J= 6.00 Hz, CO-C$\underline{H}_2$) 5.44 ppm (dd, 1H, $J_{Hb,Hx}$ = 11.76 Hz, $J_{Ha,Hx}$ = 4.64 Hz, Hx) 5.95 ppm (s, 2H, NH_2-1˚amino group) 6.58 ppm (d, 2H, J= 8.68 Hz, Ar-H) 7.13 ppm (d, 2H, J= 7.16 Hz, Ar-H) 7.24 ppm (t, 1H, NH-2˚amino group) 7.32-7.78 ppm (m, 10H, Ar-H)
LIX		3.11 ppm (dd, 1H, $J_{Ha,Hb}$ = 18.24 Hz, $J_{Ha,Hx}$ = 4.72 Hz, Ha) 3.80 ppm (dd, 1H, $J_{Hb,Ha}$ = 18.20 Hz, $J_{Hb,Hx}$ = 11.80 Hz, Hb) 4.01 ppm (d, 2H, J= 5.72 Hz, CO-C$\underline{H}_2$) 5.44 ppm (dd, 1H, $J_{Hb,Hx}$ =11.72 Hz, $J_{Ha,Hx}$ = 4.54 Hz, Hx) 5.95 ppm (s, 2H, NH_2-1˚amino group) 6.58 ppm (d, 2H, J= 8.48 Hz, Ar-H), 7.16 ppm (d, 2H, J= 8.24 Hz, Ar-H), 7.31 ppm (t, 1H, NH, 2˚amino group) 7.36-7.77 ppm (m, 9H, Ar-H
LX		2.84 ppm (s, 6H, CH_3-N) 3.07 ppm (dd, 1H, $J_{Ha,Hb}$ = 18.12 Hz, $J_{Ha,Hx}$ = 4.36 Hz, Ha) 3.73 ppm (dd, 1H, $J_{Hb,Ha}$ = 18.08 Hz, $J_{Hb,Hx}$ = 11.60 Hz, Hb) 3.92-4.04 ppm (m, 2H, CO-C$\underline{H}_2$) 5.33 ppm (dd, 1H, $J_{Hb,Hx}$ = 11.52 Hz, $J_{Ha,Hx}$ = 4.32 Hz, Hx) 5.95 ppm (s, 2H, NH_2-1˚amino group) 6.59 ppm (dd, 2H, J= 8.60 Hz, Ar-H) 6.94 ppm (d, 2H, J= 8.60 Hz, Ar-H) 7.25 ppm (t, 1H, NH, 2˚amino group) 7.45-7.77 ppm (m, 9H, Ar-H)

LXI	 Hb Ha Hx Hα Hβ O NH SO₂NH₂	3.17 ppm (dd, 1H, $J_{Ha,Hb}$ = 17.84 Hz, $J_{Ha,Hx}$ = 4.56 Hz, Ha) 3.98-3.99ppm (m, 1H, Hb) 4.62 ppm (m, 2H, CO-C$\underline{H}_2$) 5.11-5.15 ppm (m, 1H, Hx) 5.94ppm (s, 1H, NH₂-1°amino group) 6.29 ppm (m, 2H, α-H & β-H) 6.44-7.76 ppm (m, 14H, Ar-H) 7.25 ppm (s, 1H, NH -2°amino group)
LXII	Hb Ha Hx O O NH SO₂NH₂	3.67-3.71 ppm (m, 1H, Ha) 3.93-3.98 ppm (m, 1H, Hb) 4.54 ppm (m, 2H, CO-C$\underline{H}_2$) 5.54-5.56 ppm (m, 1H, Hx) 5.94 ppm (s, 2H, NH₂-1°amino group) 6.28-7.79 ppm (m, 12H, Ar-H) 7.35 ppm (s, 1H, NH -2°amino group)
LXIII	NO₂ Hb Ha Hx O O NH SO₂NH₂	3.10-3.17 ppm (m, 1H, Ha) 3.72 ppm (dd, 1H, $J_{Hb,Ha}$ = 18.12 Hz, $J_{Hb,Hx}$ = 11.84 Hz, Hb) 3.97-4.01 ppm (m, 2H, CO-C$\underline{H}_2$) 5.59 ppm (dd, 1H, $J_{Hb,Hx}$ = 11.8 Hz, $J_{Ha,Hx}$ = 4.72 Hz, Hx) 5.94 ppm (s, 2H, NH₂-1°amino group) 6.32-8.33 ppm (m, 11H, Ar-H) 7.21 ppm (s, 1H, NH-2°amino group)
LXIV	CH₃ Hb Ha Hx O NH SO₂NH₂	2.35 ppm (s, 3H, -CH₃) 3.06 ppm (dd, 1H, $J_{Ha,Hb}$ = 18.16 Hz, $J_{Ha,Hx}$ = 4.64 Hz, Ha) 3.77 ppm (dd, 1H, $J_{Hb,Ha}$ = 18.12 Hz, $J_{Hb,Hx}$ = 11.76 Hz, Hb) 4.00 ppm (d, 2H, J= 6.00 Hz, CO-C$\underline{H}_2$) 5.42 ppm (dd, 1H, $J_{Hb,Hx}$ = 11.68 Hz, $J_{Ha,Hx}$ = 4.64 Hz, Hx) 5.94 ppm (s, 2H, NH₂-1°amino group) 6.57 ppm (d, 2H, J= 8.68 Hz, Ar-H) 7.12 ppm (d, 2H, J= 7.12Hz, Ar-H) 7.28 ppm (t, 1H, NH-2° amino group) 7.30-7.67 ppm (m, 9H, Ar-H)

LXV		2.34 ppm (s, 3H, -CH$_3$) 3.10-3.13 ppm (m, 1H, Ha) 3.76-3.87 ppm (m, 1H, Hb) 4.00 ppm (d, 2H, CO-C$\underline{H}_2$) 5.42-5.58 ppm (m, 1H, Hx) 5.95 ppm (s, 2H, NH$_2$-1˚amino group) 6.59-7.95 ppm (m, 12H, Ar-H) 7.35 ppm (t, 1H, J=16.6 Hz, NH- 2˚ amino group).
LXVI		2.35 ppm (s, 3H, CH$_3$) 2.84 ppm (s, 6H, CH$_3$-N) 3.04-3.08 ppm (m, 1H, Ha) 3.69 ppm (dd, 1H, $J_{Hb,Ha}$ = 18.00 Hz, $J_{Hb,Hx}$ = 11.52 Hz, Hb) 3.95 ppm (m, 2H, CO-C$\underline{H}_2$) 5.31 ppm (dd, 1H, $J_{Hb,Hx}$ = 11.44 Hz, $J_{Ha,Hx}$ = 4.20 Hz, Hx) 5.94ppm (s, 2H, NH$_2$-1˚amino group) 6.59 ppm (dd, 4H, J= 8.64, 15.96 Hz, Ar-H) 6.93 ppm (d, 2H, J= 8.640 Hz, Ar-H) 7.23 ppm (t, 1H, NH-2˚amino group) 7.26-7.29 ppm (m, 2H, Ar-H) 7.44 ppm (d, 2H, J= 8.60 Hz, Ar-H) 7.64 ppm (d, 2H, J= 8.00 Hz, Ar-H)
LXVII		2.36 ppm (s, 3H, CH$_3$) 3.40 ppm (m, 1H, Ha) 3.89 ppm (m, 1H, Hb) 4.62 ppm (s, 2H, CO-C$\underline{H}_2$) 5.19 ppm (m, 1H, Hx) 5.95 ppm (s, 2H, NH$_2$-1˚amino group) 6.27-7.68 ppm (m, 11H, Ar-H) 7.29 ppm (t, 1H, NH-2˚amino group)
LXVIII		3.07-3.09 ppm (m, 1H, Ha) 3.62 ppm (s, 3H, -OCH$_3$) 3.81 ppm (m, 1H, Hb) 3.83 ppm (s, 3H, -OCH$_3$) 4.40-4.60 ppm (m, 2H, CO-C$\underline{H}_2$) 4.80 ppm (t, 1H, NH bend to CH$_2$) 5.45-5.65 ppm (m, 1H, Hx) 6.60-7.88 ppm (m, 14H, Ar-H)
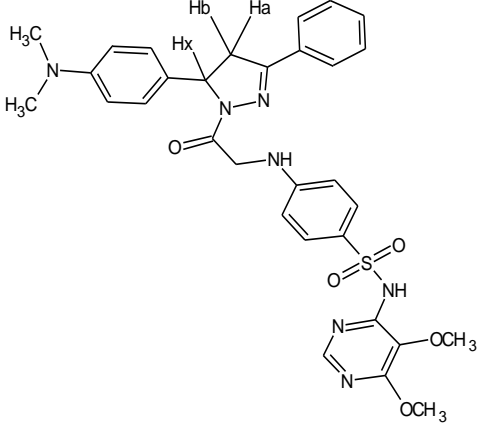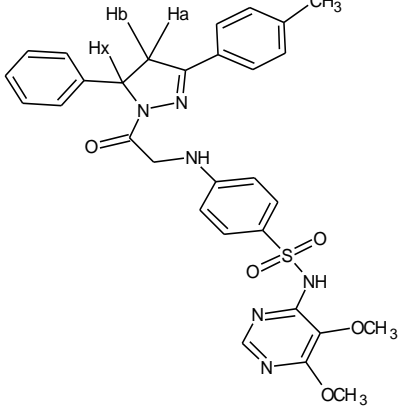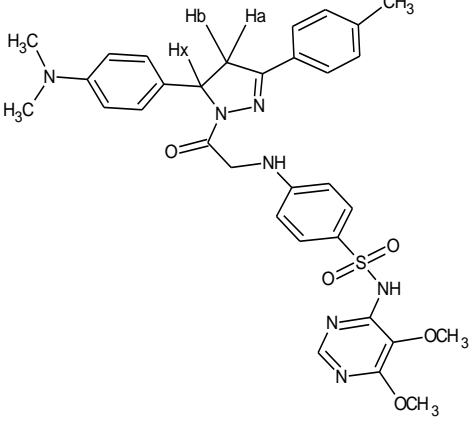
LXIX		2.85 ppm (s, 6H, CH$_3$-N) 3.66 ppm (s, 3H, -OCH$_3$) 3.13 ppm (dd, 1H, $J_{Ha,Hb}$ = 17.88 Hz, $J_{Ha,Hx}$ = 4.36 Hz, Ha) 3.82-3.87 ppm (m, 1H, Hb) 4.00 ppm (s, 3H, -OCH$_3$) 4.33-4.44 ppm (m, 2H, CO-C<u>H$_2$</u>) 4.76-4.78 ppm (t, 1H, NH bend to CH$_2$) 5.44-5.47 ppm (m, 1H, Hx) 6.63-7.87 ppm (m, 14H, Ar-H)
LXX		2.34 ppm (s, 3H, -CH$_3$) 3.62 ppm (s, 3H, -OCH$_3$) 3.13-3.15 ppm (m, 1H, Ha) 3.78-3.80 ppm (m, 1H, Hb) 3.85 ppm (s, 3H, -OCH$_3$) 4.42-4.49 ppm (m, 2H, CO-C<u>H$_2$</u>) 4.83 ppm (t, 1H, NH bend to CH$_2$) 5.52-5.59 ppm (m, 1H, Hx) 6.27-7.95 ppm (m, 14H, Ar-H)
LXXI		2.35 ppm (s, 3H, CH$_3$) 2.84 ppm (s, 6H, CH$_3$-N) 3.01-3.05 ppm (m, 1H, Ha) 3.65-3.66 ppm (m, 1H, Hb) 3.83 ppm (s, 3H, -OCH$_3$) 4.00 ppm (s, 3H, -OCH$_3$) 4.39-4.42 ppm (m, 2H, CO-C<u>H$_2$</u>) 4.73 ppm (t, 1H, NH bend to CH$_2$) 5.41-5.45 ppm (m, 1H, Hx) 6.64-7.68 ppm (m, 14H, Ar-H)

Table (2.31): Mass spectral data of of synthesized 1-(Chloroacetyl)-3,5-diaryl-2-pyrazoline derivatives (XLI-LVII)
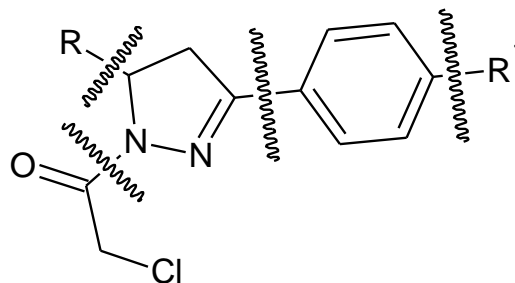
Compound No.	R	R^1	MW (calculated)	MW(M$^+$) (found)	M+1	M+2	M+4	Other peaks
XLI	(phenyl)	-H	298.76	298.05 (100)	299 (22.08)	300 (34.72)	-	222(62.79), 145(44.27), 115(18.70), 104(27.34), 91(26.92), 77(41.06)
XLII	Cl-(phenyl)	-H	333.21	332 (86.9)	333 (19.99)	334 (58.16)	336 (10.34)	256(100), 221(14.68), 145(69.75), 119 (23.24), 104(47.02), 91(23.81), 77(68.89)
XLIII	H$_3$C,H$_3$C-N-(phenyl)	-H	341.83	341.15 (61.12)	342 (15.72)	343 (21.37)	-	264(17.67), 189(100), 147(43.90), 118 (7.80), 104(7.88), 91(10.43), 77 (20.45)

Table (2.31): continued
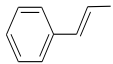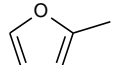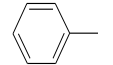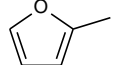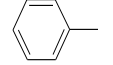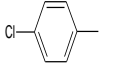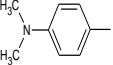
	Structure	R						Fragments
XLIV		-H	324.80	324.10 (54.66)	325 (16.56)	326 (18.50)	-	247(100), 186(20.48), 144(41.89), 129 (71.58), 115(75.89), 104(40.61), 91(86.60), 77(78.18)
XLV		-H	288.72	288.30 (93.41)	289 (18.55)	290 (32.18)	-	211(50.84), 185(45.66), 150(56.53),136 (16.54), 115(22.45), 103(24.76), 94(47.27), 77(100)
XLVI		-Br	377.66	376.30 (75.18)	377 (19.62)	378 (100)	380 (26.44)	300(75.81), 223(33.26), 181(3.54), 145(1.91), 102(15.89), 91(22.99), 72(86.33)
XLVII		-Br	367.62	366.25 (74.80)	367 (16.41)	368 (100)	370 (25.16)	291(46.99), 185(59.48), 150(88.49), 136(23.89), 94(72.88), 77(47.20)
XLVIII		-NO$_2$	343.76	343 (56.93)	344 (13.08)	345 (20.00)	-	267(100), 190(28.19), 144(10.40), 115(7.85), 104(16.49), 91(14.59), 77(22.39)
XLIX		-NO$_2$	378.20	377 (61.92)	378 (17.02)	379 (42.13)	381 (7.62)	301(100), 266(22.55), 190(35.42), 144(12.91), 115(5.74), 103(10.48), 89(19.77), 77(29.53)
L		-NO$_2$	386.83	386.10 (55.15)	387 (14.01)	388 (19.52)	-	309(10.15), 263(4.51), 189(100), 147(37.12), 103(4.01), 91(4.81), 77(11.99)
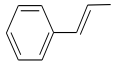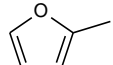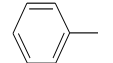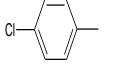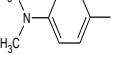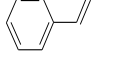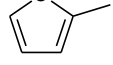
Table (2.31): continued								
LI	(styryl/phenyl-vinyl)	-NO$_2$	369.80	369.45 (32.40)	370 (12.21)	371 (11.96)	-	292(59.86), 246(19.88),186(19.63), 144(25.81), 129 (67.79),115(51.00), 104(29.02), 91(100), 77(39.64)
LII	(furyl-methyl)	-NO$_2$	333.72	333.35 (79.03)	334 (16.63)	335 (27.08)	-	256(75.83), 228(52.06), 185(88.18), 150(72.61), 136(28.88), 94(100), 77(58.52)
LIII	(tolyl/methylphenyl)	-CH$_3$	312.79	312.05 (100)	313 (23.62)	314 (34.43)	-	236(62.23), 159(30.93), 115(17.47), 104(7.98), 91(25.98), 77(17.06)
LIV	(Cl-phenyl-methyl)	-CH$_3$	347.23	346.05 (100)	347 (24.60)	348 (66.08)	350 (12.05)	270(95.17), 159(36.28), 118(24.71), 104(2.28), 91(23.37), 77(19.35)
LV	(H$_3$C)$_2$N-phenyl-methyl	-CH$_3$	355.86	355.15 (74.63)	356 (20.41)	357 (26.21)	-	278(22.75), 189(100), 147(45.83), 117 (12.11), 105(5.78), 91(11.13), 77(13.59)
LVI	(styryl/phenyl-vinyl)	-CH$_3$	338.83	338.40 (75.88)	339 (21.60)	340 (27.17)	-	261(100), 246(30.15), 186 (17.51), 171 (13.86), 158 (12.46) 144(18.17), 129(48.08) 115(46.53), 91 (61.13) , 77(30.89)
LVII	(furyl-methyl)	-CH$_3$	302.75	302 (100)	303 (20.13)	304 (33.66)	-	225(65.27), 185(32.19), 150(50.15) 115 (34.59), 94(56.20), 77(35.67)

Table (2.32): Mass spectral data of of synthesized 1-[(aryl) amino acetyl] -3,5-diaryl-2-pyrazoline derivatives (LVIII-LXXI)
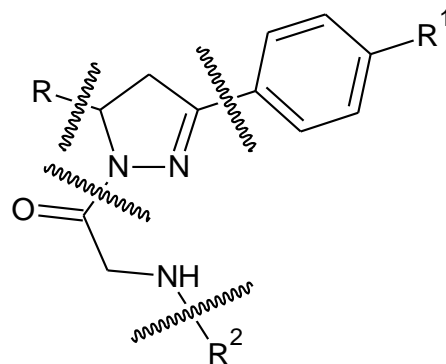
Compo-und No.	R	R^1	R^2	MW (calculated)	MW (found)(M$^+$)	M+1	M+2	Other peaks
LVIII	(phenyl)	-H	(4-sulfonamidophenyl)	434.51	434 (15.49)	435 (5.11)	-	278(12.72), 222(100), 156 (19.83), 145 (38.35), 119(16.69), 104(19.70), 92(31.42), 77(19.02)
LIX	(4-chlorophenyl)	-H	(4-sulfonamidophenyl)	468.95	468 (16.81)	469 (5.44)	470 (7.17)	312(13.65), 256(100), 156(28.12),145(26.13), 119(13.21), 104(17.86), 92(38.12), 77(15.31)
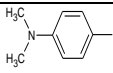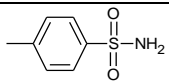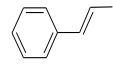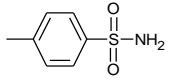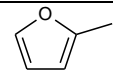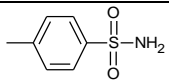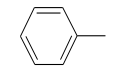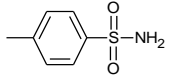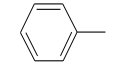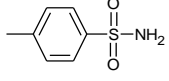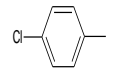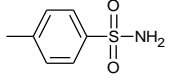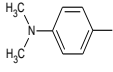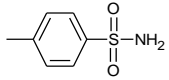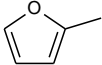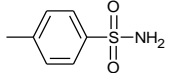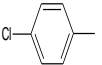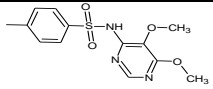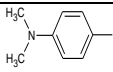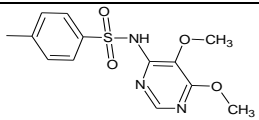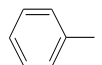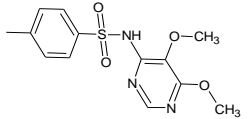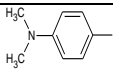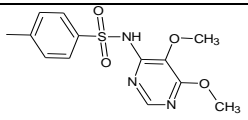
		R		MW	M⁺	M+1	M+2	Fragment ions (m/z, %)
LX	(structure: (CH₃)₂N-phenyl)	-H	(structure: benzenesulfonamide)	477.57	477 (100)	478 (29.89)	-	292(35.04), 264(75.51), 218(77.33), 189 (32.91) ,156(18.73), 147(52.71), 92(38.21), 77(19.21)
LXI	(structure: styryl)	-H	(structure: benzenesulfonamide)	460.54	460 (6.88)	461 (2.50)	-	304(21.28), 248(100), 156(32.70),145(49.87), 129 (20.36), 116(49.46), 104(39.30), 92 (64.71) , 77 (55.20)
LXII	(structure: furyl)	-H	(structure: benzenesulfonamide)	424.47	424 (15.17)	425 (4.57)	-	268(8.55), 212(100), 156(20.89), 145(5.99), 108(13.82), 92(28.40), 77(14.63)
LXIII	(structure: phenyl)	-NO₂	(structure: benzenesulfonamide)	469.47	469 (4.70)	470 (1.41)	-	313(7.14), 257(86.37), 156(59.25), 115(27.23), 108(60.77), 92(100), 77(29.47)
LXIV	(structure: phenyl)	-CH₃	(structure: benzenesulfonamide)	448.53	448 (19.49)	449 (6.04)	-	292(10.19), 236(100), 159(27.36), 118(14.09), 108(11.80), 92(24.42), 77(6.97)
LXV	(structure: 4-Cl-phenyl)	-CH₃	(structure: benzenesulfonamide)	482.98	482 (16.39)	483 (5.04)	484 (7.06)	467(1.08), 270(100), 159(33.46), 118(44.62), 108(16.24), 91(47.25), 77(16.83)
LXVI	(structure: (CH₃)₂N-phenyl)	-CH₃	(structure: benzenesulfonamide)	491.60	491 (100)	492 (32.77)	-	278(80.20), 218(78.92), 189(36.02), 156 (15.04), 147 (45.27), 118(11.64), 108(16.30), 92(26.24), 77(6.83)

Table (2.32): continued								
LXVII		-CH₃		438.49	438 (11.41)	439 (3.53)	-	282(6.75), 226(100), 156(15.45), 145(2.30), 92(34.55), 77(7.73)
LXVIII		-H		607.07	607 (1.46)	608 (0.74)	-	592(8.73), 309(35.05), 256(100), 145(70.54), 139(26.23), 105(77.62), 91(45.27), 77(78.33)
LXIX		-H		615.70	615 (4.75)	616 (1.33)	-	292(40.02), 264(100), 189(27.34), 146(80.96), 118(31.36), 104(40.30), 91(34.97), 77(57.35)
LXX		-CH₃		586.66	583 (8.70)	584 (4.40)	-	447(3.38), 293(19.84), 263(10.76), 236(100), 159 (36.28), 119(44.88), 104(20.95), 91(60.77), 77(25.68)
LXXI		-CH₃		629.72	629 (5.36)	630 (1.89)	-	306(49.54), 278(100), 189(23.38), 159(42.50), 146(59.69), 105(22.95), 91(37.06), 77(20.67)

2.4. Docking study

Molecular docking of the drug molecule with the receptor (target) gives important information about drug receptor interactions and is commonly used to find out the binding orientation of drug candidates to their protein targets in order to predict the affinity and activity (Bano *et al.*, 2015). Molecular docking softwares are mainly used in drug development. The most important application of docking software is virtual screening. In virtual screening the most interesting and promising molecules are selected from existing database for further research (Mukesh & Rakesh, 2011).

2.4.1. Major steps in molecular docking

Step I –*Building the Receptor*

- Downloaded PDB structure of the receptor.
- Removal of the water molecules from the cavity, stabilizing charges, filling in the missing residues, generation the side chains.

Step II –*Identification of the Active Site*

- After the receptor is built, the active site within the receptor should be identified.
- The receptor may have many active sites but the one of the interest should be selected

Step III –*Ligand Preparation*

- Ligands can be obtained from various databases like ZINC, PubChem or can be sketched using tools like Chemsketch.
- While selecting the ligand, the LIPINSKY'S RULE OF 5 should be applied.

Step IV-*Docking*

This is the last step, where the ligand is docked onto the receptor and the interactions are checked. The scoring function generates scores depending on which the ligand with the best fit is selected (Jade, 2016).

All synthesized trisubstituted pyrazoline derivatives were subjected to docking study to investigate their binding mechanism with 1JD0 protein, which was downloaded from protein data bank (PDB). Compounds (LXVIII, LXIX, LXX and LXXI) were excluded from study, because their molecular weight over 500 (Lipinsky's rule of 5).
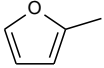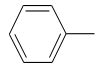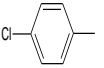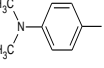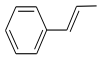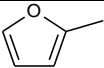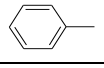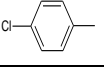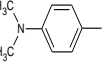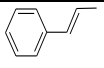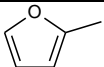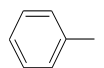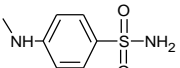
Carbonic anhydrase inhibitor acetazolamide (AZA) was used as the reference drug, molecular docking of standard acetazolamide was carried out and corresponding docking score which was obtained, set as a standard in table (2.33).
Synthesized α,β-unsaturated carbonyl derivatives were also subjected to docking study, the protein file (PDB ID: 3DKC) selected for this purpose and the result was tabulated in table (2.34)

Table 2.33: Docking results of the synthesized trisubstituted pyrazoline derivatives (XLI-LXVII) with 1JD0 using MOE software version 10.2008
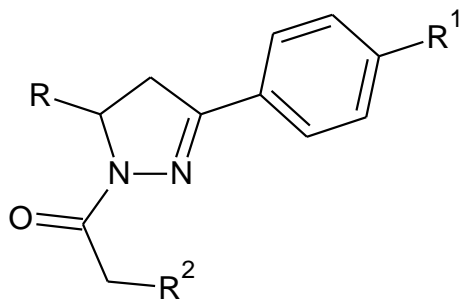
Compo-und No.	R	R^1	R^2	S (kcal/mol)	Amino acids	Interacting groups	Type of interaction	Length (A˚)
XLI	*phenyl*	-H	-Cl	-14.2976	Thr200	N-pyrazoline	H-bond (acceptor)	2.44
XLII	*Cl-phenyl*	-H	-Cl	-18.1364	His64	Phenyl	π-cation	-
XLIII	*H3C-N-H3C-phenyl*	-H	-Cl	No interaction				
XLIV	*styryl*	-H	-Cl	-18.1048	His64	Phenyl	π-cation	-
XLV	*furan*	-H	-Cl	No interaction				
XLVI	*phenyl*	-Br	-Cl	-15.1608	His64	Phenyl	π-cation	-

XLVII	furan-CH	-Br	-Cl	-14.6619	Asn62 Lys67	C=O C=O	H-bond (acceptor) H-bond (acceptor)	2.23 2.06
XLVIII	phenyl	-NO₂	-Cl	-15.8963	His64	Phenyl	π-cation	-
XLIX	Cl-phenyl	-NO₂	-Cl	No interaction				
L	(H₃C)₂N-phenyl	-NO₂	-Cl	No interaction				
LI	styryl	-NO₂	-Cl	-15.6714	Lys67	Phenyl	π-cation	-
LII	furan-CH	-NO₂	-Cl	-15.0406	His64	furfuryl	π-cation	-
LIII	phenyl	-CH₃	-Cl	-17.9555	His64	Phenyl	π-cation	-
LIV	Cl-phenyl	-CH₃	-Cl	-18.0680	His64	Phenyl	π-cation	-
LV	(H₃C)₂N-phenyl	-CH₃	-Cl	-18.9400	His64	Phenyl	π-cation	-
LVI	styryl	-CH₃	-Cl	-17.5249	His64	Phenyl	π-cation	-
LVII	furan-CH	-CH₃	-Cl	-17.0885	His64	Furfuryl	π-cation	-
LVIII	phenyl	-H	NH-phenyl-SO₂NH₂	-21.9174	Lys67 Lys67 Thr200 His94	Phenyl C=O SO₂ Phenyl	π-cation H-bond (acceptor) H-bond (acceptor) π-π	- 1.96 2.60 -
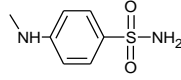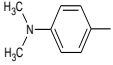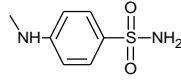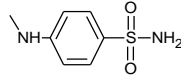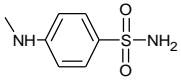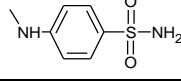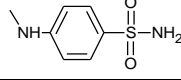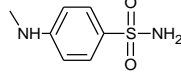
					His94	SO$_2$NH$_2$	Metal complex(Zn)	2.06
					His119	SO$_2$NH$_2$	Metal complex(Zn)	2.04
					His96	SO$_2$NH$_2$	Metal complex(Zn)	2.03
LIX		-H		-20.1280	Asn62	SO$_2$	H-bond (acceptor)	2.15
LX		-H		-20.5811	Thr200	SO$_2$	H-bond (acceptor)	3.07
LXI		-H		-20.3494	Asn62	SO$_2$	H-bond (acceptor)	2.04
					His94	Phenyl	π-π	
LXII		-H		-22.2056	His64	Phenyl	π-cation	-
					Lys67	C=O	H-bond (acceptor)	1.89
					Thr200	SO$_2$	H-bond (acceptor)	2.56
					His94	Phenyl	π-π	-
					His94	SO$_2$NH$_2$	Metal complex(Zn)	2.06
					His119	SO$_2$NH$_2$	Metal complex(Zn)	2.04
					His96	SO$_2$NH$_2$	Metal complex(Zn)	2.03
LXIII		-NO$_2$		No interaction				
LXIV		-CH$_3$		-20.3157	Asn62	SO$_2$	H-bond (acceptor)	2.17
LXV		-CH$_3$		-21.0321	Asn62	SO$_2$	H-bond (acceptor)	2.16

119
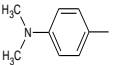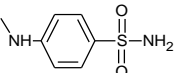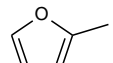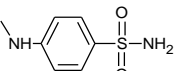
Table (2.33): continued								
LXVI		-CH$_3$		-22.0545	Lys67	Phenyl	π-cation	-
					Lys67	C=O	H-bond (acceptor)	1.96
					Asn62	C=O	H-bond (acceptor)	2.12
					Thr200	SO$_2$	H-bond (acceptor)	2.54
					His94	SO$_2$NH$_2$	Metal complex(Zn)	2.06
					His119	SO$_2$NH$_2$	Metal complex(Zn)	2.04
					His96	SO$_2$NH$_2$	Metal complex(Zn)	2.03
LXVII		-CH$_3$		-21.2136	His94	Phenyl	π- π	-
					Thr200	SO$_2$	H-bond (acceptor)	2.91
					His94	SO$_2$NH$_2$	Metal complex(Zn)	2.06
					His119	SO$_2$NH$_2$	Metal complex(Zn)	2.04
					His96	SO$_2$NH$_2$	Metal complex(Zn)	2.03
AZA	-	-	-	-21.0578	Thr199	SO$_2$	H-bond (acceptor)	2.00
					Thr199	SO$_2$	H-bond (acceptor)	3.02
					Thr200	N-thiadiazole	H-bond (acceptor)	2.14
					His94	SO$_2$NH$_2$	Metal complex(Zn)	2.06
					His119	SO$_2$NH$_2$	Metal complex(Zn)	2.04
					His96	SO$_2$NH$_2$	Metal complex(Zn)	2.03

Table 2.34: Docking results of the synthesized α,β-unsaturated carbonyl derivatives with 3DKC using MOE software version 10.2008
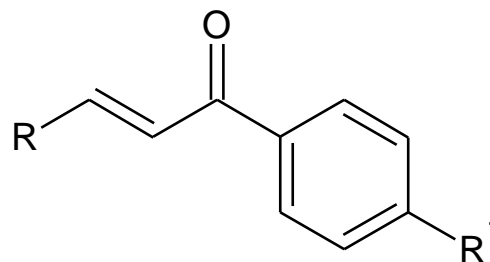
Compound No.	R	R^1	S (Kcal/mol)	Amino acids	Interacting groups	Type of interaction	Length (A˚)
II		-H	-21.356	Asp1222	C=O	Metal complex (Mg)	2.10
				Asn1209	C=O	Metal complex (Mg)	2.03
IV		-H	-21.1818	Asp1222	C=O	Metal complex (Mg)	2.10
				Asn1209	C=O	Metal complex (Mg)	2.03
V		-H	-16.1714	Asp1222	C=O	Metal complex (Mg)	2.10
				Asn1209	C=O	Metal complex (Mg)	2.03
VI		-Br	-22.9170	Asp1222	C=O	Metal complex (Mg)	2.10
				Asn1209	C=O	Metal complex (Mg)	2.03

121
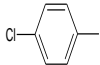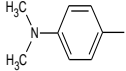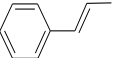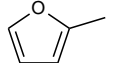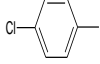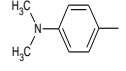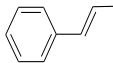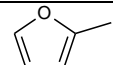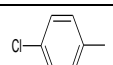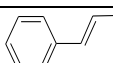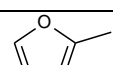
Table (2.34): continued							
VII	(4-chlorophenyl structure)	-Br	-20.5912	Asp1222	C=O	Metal complex (Mg)	2.10
				Asn1209	C=O	Metal complex (Mg)	2.03
VIII	(N,N-dimethylaminophenyl structure)	-Br	-22.5738	Asp1222	C=O	Metal complex (Mg)	2.10
				Asn1209	C=O	Metal complex (Mg)	2.03
				Arg1208	Phenyl	π-cation	-
IX	(styryl structure)	-Br	-20.6469	Asp1222	C=O	Metal complex (Mg)	2.10
				Asn1209	C=O	Metal complex (Mg)	2.03
X	(furyl structure)	-Br	-22.0121	Asp1222	C=O	Metal complex (Mg)	2.10
				Asn1209	C=O	Metal complex (Mg)	2.03
XI	(phenyl structure)	-NO$_2$	-23.2468	Asp1222	C=O	Metal complex (Mg)	2.10
				Asn1209	C=O	Metal complex (Mg)	2.03
XII	(4-chlorophenyl structure)	-NO$_2$	-20.7988	Asp1222	C=O	Metal complex (Mg)	2.10
				Asn1209	C=O	Metal complex (Mg)	2.03
XIII	(N,N-dimethylaminophenyl structure)	-NO$_2$	-23.4193	Asp1222	C=O	Metal complex (Mg)	2.10
				Asn1209	C=O	Metal complex (Mg)	2.03

Table (2.234): continued							
XIV	(styrene structure)	$-NO_2$	-22.4421	Asp1222	C=O	Metal complex (Mg)	2.10
				Asn1209	C=O	Metal complex (Mg)	2.03
XV	(furan structure)	$-NO_2$	-21.7925	Asp1222	C=O	Metal complex (Mg)	2.10
				Asn1209	C=O	Metal complex (Mg)	2.03
XVII	(chlorophenyl structure)	$-CH_3$	-20.3991	Asp1222	C=O	Metal complex (Mg)	2.10
				Asn1209	C=O	Metal complex (Mg)	2.03
XIX	(styrene structure)	$-CH_3$	-20.5758	Asp1222	C=O	Metal complex (Mg)	2.10
				Asn1209	C=O	Metal complex (Mg)	2.03
XX	(furan structure)	$-CH_3$	-22.5230	Asp1222	C=O	Metal complex (Mg)	2.10
				Asn1209	C=O	Metal complex (Mg)	2.03

3. Discussion

3.1. QSAR study

Cancer has been prevailing as most serious disease and its incidence is rising day-to-day in the world. Cancer treatment usually falls into the category of surgery, radiation and chemotherapy. Despite of all these treatments, cancer is still continuing as uncontrollable disease and exploring for new approaches in anticancer therapy. Chemotherapy is generally used to treat cancer that has spread or metastasized because the medicines travel throughout the entire body (Reddy *et al*., 2016).

The worldwide cancer burden is expected to increase by as much as 15 million new cancer cases per year by 2020, according to the World Health Organization, unless further preventive measures are put into practice. Generally, cancers of the breast, lung, colorectal, and prostate are the most frequent types in developed countries while those of the stomach, liver, oral cavity, and cervix, in developing countries, although this pattern seems to be evolving, especially due to population aging and life style changes (George *et al*., 2016).

In a recent report of the American Cancer Society breast cancer was classified as the most frequently diagnosed cancer and the leading cause of cancer death among females. Although there are many therapeutic strategies, more than one million new cases of breast cancer are diagnosed every year. Some of the main problems in the treatment of cancer are high cytotoxicity and drug resistance, and no clinically active substances are known to act selectively on tumour cells. Scientists put great effort in finding new therapeutic targets for cancer and to the development of new selective drugs (Dimic *et al*., 2015). New, effective cytotoxic agents with novel mechanisms of action are therefore urgently

needed for the treatment of women with metastatic breast cancer (Yahya *et al.*, 2014).

Pyrazoline derivatives have attracting continuing attention over the years because of their broad spectrum biological activities and strong efficacy. Some representative of this heterocyclic exhibit anti-proliferative, anti-inflammatory, anti-infective carrying the biologically active sulfonamide moieties. Among the wide range of compounds tested as potential anticancer agents, derivatives comprising the sulphonamide. Recently three sulphonamides derivatives have been reported as potent antitumor agents and are in advanced clinical trials (Rathore *et al.*, 2014).

If we can understand how a molecular structure brings about a particular effect in a biological system, we have a key to unlocking the relationship and using that information to our advantage. Formal development of these relationships on this premise has proved to be the foundation for the development of predictive models. If we take a series of chemicals and attempt to form a quantitative relationship between the biological effects (i.e. the activity) and the chemistry (i.e. the structure) of each of the chemicals, then we are able to form a quantitative structure–activity relationship or QSAR (Cronin, 2010).

In-silico modeling methodologies such as QSAR prove to be a key for the analysis of bio-chemo-physical property and activity. QSAR is a broadly used tool for developing relationships between the effects of a series of molecules with their structural properties (Mishra *et al.*, 2017). It is used in many areas of science to reduce the excessive number of experiments, sometimes long, expensive and harmful for environment protection (N'guessan *et al.*, 2017).

Structural properties expressed in terms of descriptors. Molecular descriptors play a fundamental role in developing models for chemistry.

Molecular descriptors can be calculated from the chemical formula (1D descriptors), the 2D structure (2D descriptors), and the 3D conformation (3D descriptors) using a large number of methods based on atom types, molecular fragments, and the three dimensional structure, respectively (Bajot, 2010).

In this work, QSAR study was carried out for two groups, trisubstituted pyrazoline derivatives (group I) and α,β-unsaturated carbonyl derivatives (group II). Data set in each group collected from literature (Qin *et al*, 2015 and Syam *et al*, 2012) consists of **18** compounds, table (2.1) and (2.2), which was then divided into two sub sets: training data set containing **15** compounds and test set of three compounds.

Total of 11 molecular descriptors namely, molecular weight (MW), molar refractivity (MR), molar volume (MV), refractive index (RI), density (D), surface tension (ST), logarithm of the Partition coefficient Log P (octanol/water) (Log P(o/w)), heat of formation (HF), ionization potential (IP), dipole moment (dipole) and potential energy (E) were calculated for training set in group (I) table (2.4).

Only 8 molecular descriptors (MW, MV, ST, MR, E, RI, D and Log P(o/w)) were calculated for each compound in training set in group (II) table (2.5). All descriptors were calculated by using MOE and ACD/lab programmes.

For a statistically reliable model, the number of compounds and number of descriptors should bear a ratio of at least 5:1. Thus, only three descriptors are required for **15** compounds in training set to develop statistically reliable QSAR model in each group. Selection of a set of appropriate descriptors from a large number of them requires a method, which is able to discriminate between the parameters. Pearson's correlation matrix has been performed for all selected descriptors by using MOE Software fig (2.1) and (2.2) in order to select appropriate sub

set descriptors. The analysis of these matrixes revealed appropriate eight descriptors in group (I) and five in group (II).

Multiple Linear Regression (MLR) is a commonly used method in QSAR due to its simplicity, transparency, reproducibility, and easy interpretability (Roy *et al*., 2015). 46 QSAR models were devolved during MLR analysis in group (I) with three descriptors and the best equation (No. 28) which showed high squared correlation coefficient (r^2) and low root mean square error (RMSE), was considered as the best model with D, logP(o/w) and IP descriptors.

Pc= 23.8154+14.28884x D- 2.47851x log P(o/w)- 2.85524xIP…model (I)

The developed QSAR model equation (model I) shows a relationship between *in vitro* biological activity and correlated three chemical descriptors (D, logP(o/w) and IP). It is evident from the model equation that the molecular descriptors, namely log P(o/w) partition coefficient and ionization potential are negatively correlated. On the other hand, density shows positive correlation.

In group II, about 20 QSAR models were devolved during MLR analysis, and the best equation (No. 19) with high r^2 and low RMSE was considered as the best model.

Pc= 4.3730- 0.04322 x E+ 1.59035 x D+ 0.31076x logP(o/w*)…*model (II)

The model (II) equation shows that there is positive correlation between the biological activity, density and Log P(o/w) partition coefficient, and negative correlation with potential energy.

Validation is a crucial aspect of any QSAR analysis, this step achieved by internal validation by training set compounds (cross validation) and external validation by test set compounds. The statistical fit of a QSAR

can be assessed in many easily available statistical terms. The statistical quality of the resulting models, as depicted in table (2.8), is determined by r, r^2, Q^2, RMSE, S, F and *P* value

The correlation coefficient, r is a measure of the degree of linearity of the relationship. It signifies the quality of fit of the model and quantifies the variance in the data. In an ideal situation the correlation coefficient must be equal to or approach **1** (Verma *et al*, 2010).

The squared correlation coefficient, r² which gives an evaluation of the dispersion of theoretical values around the experimental data. The quality of the model is improved when the points are close to the fitting line. The adjustment of the points to this line can be evaluated by the correlation coefficient (N'guessan *et al*, 2017), that means if **r^2** value closes to **1** the theoretical and experimental values will be assumed to correlate.

Cross-validation Q² is one of the most extensively employed methods for the internal validation of a statistical model. In cross-validation, the predictive ability of a model is estimated using a reduced set of structural data. Usually, one element of the set is extracted each time, and a new model is derived based on the reduced dataset, which is then employed to predict the activity of the excluded molecule. The procedure is repeated ***n*** number of times until all compounds have been excluded and predicted once. This is the so-called leave-one-out (*LOO*) method. The outcome of *LOO* procedure is a cross- validated correlation coefficient (Q^2, q^2 or CV) which is a criterion of both robustness and predictive ability of the mode. It has been established that, in cases where test sets with known values of biological activities were available for prediction, there existed no correlation between the Q^2 and r^2. Q^2 should be regarded as a measure of internal consistency of the derived model rather than as a true indicator of

the predictability. It should be noted that, since it is easier to fit the experimental data than to predict them from the QSAR model, r^2 of the model is always higher than Q^2 (Verma *et al*, 2010). For a satisfactory model $\mathbf{Q^2 > 0.5}$ and for an excellent model $\mathbf{Q^2 > 0.9}$. So, for a given training set, a model will be performance if the acceptance criterion $\mathbf{r^2\text{-} Q^2 < 0.3}$ is respected (N'guessan *et al*, 2017).

The Fischer statistic (F value) parameter is one of the several variance related parameters that can be used as a measure of the level of statistical significance of the regression model. A higher F value implies that a more significant correlation has been reached (Verma *et al*, 2010).

Root mean square error (RMSE), has been used as a standard statistical metric to measure model performance in meteorology, air quality, and climate research studies (Chai & Draxler, 2014). The lower its value the better the model.

Standard error of estimate (s), for a good model, the standard error of estimate of Y should be low, it measures the dispersion of the observed values about the regression line. The smaller the value of s means higher reliability of the prediction (Roy *et al.*, 2015)

P value is defined as the probability under null distributions of the sample outcome equal to or more extreme than that observed (Gibbons & Pratt, 1975).

The QSAR models present robustness, with good internal and external predictive capabilities and these models are acceptable because all the values of statistical measures are found to be in the acceptable range,

in group (I):

r= 0.8720 r^2= 0.7603   RMSE= 0.33535 Q^2= 0.5348

s= 0.56   F= 34.05   P= 0.133

in group (II):

r= 0.9202 r^2= 0.84684   RMSE= 0.14550 Q^2= 0.7621

s= 0.38484   F= 101.434   P= 0.010

One of the most important characteristics of a QSAR model is its predictive power, i.e., the ability of a model to predict accurately the biological activity of compounds that were not used for model development (external validation). While the internal validation techniques described above can be used to establish model robustness, they do not directly assess model predictivity. In principle, external validation is the only way to "determine" the true predictive power of a QSAR model. This type of assessment requires the use of an external test set, i.e., compounds not used for the model development.

The predictivity of a regression models were estimated by comparing the predicted and observed values of pIC_{50} against breast cancer of training set and cross validation in each group, the residual values were calculated and are tabulated in table (2.9) and (2.11).

The values of biological activity of a test set compounds in group (I) and (II) were calculated with the derived models (I) and (II), respectively. These data are compared with experimentally obtained values as shown in table (2.10) and (2.12).

Data presented in table (2.9) and (2.11), show the agreement between experimental and predicted pIC_{50} values in each group. The residual

values shown are small, indicating the good predictability of the established models (Kuzmanovic *et al.*, 2009).

Figures (3.1), (3.2) and (3.3) show the plots of linear regression predicted versus experimental values of the biological activity of training set, cross validation and test set compounds in group (I) against human breast cancer MCF-7, respectively. The plots for QSAR model show good fit with $r^2 = 0.7603$; r= 0.8720 for training set, $r^2= 0.5348$; r= 0.7313 for cross validation and very good fit with $r^2= 0.8593$; r= 0.9270 for test set.
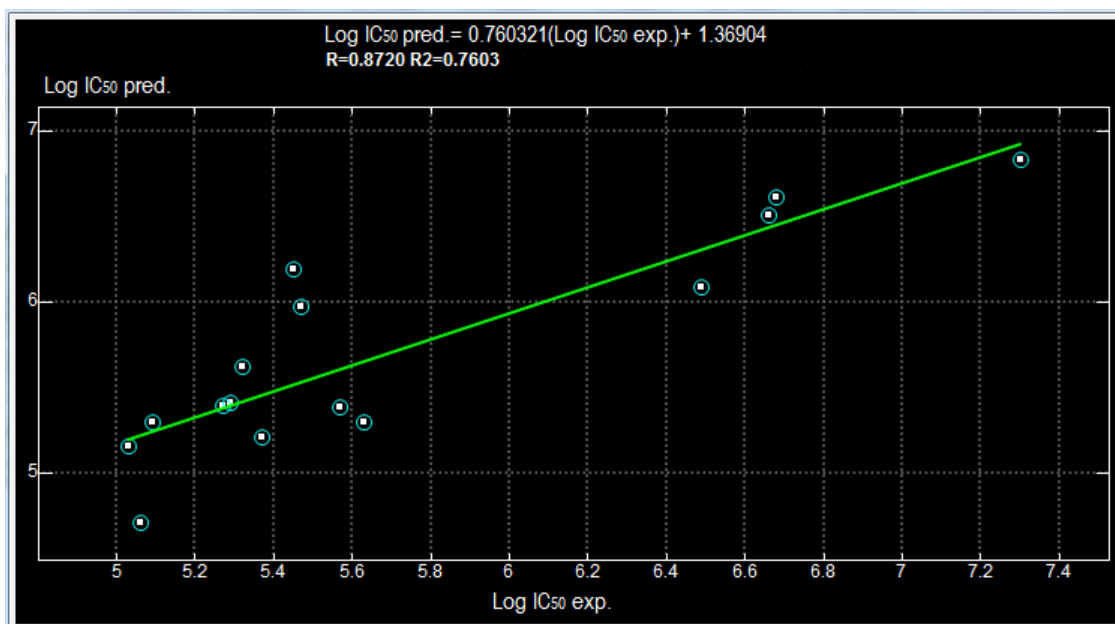
Figure (3.1): Plots of predicted versus experimentally observed log IC_{50} of training set compounds (group I) against human breast cancer MCF-7
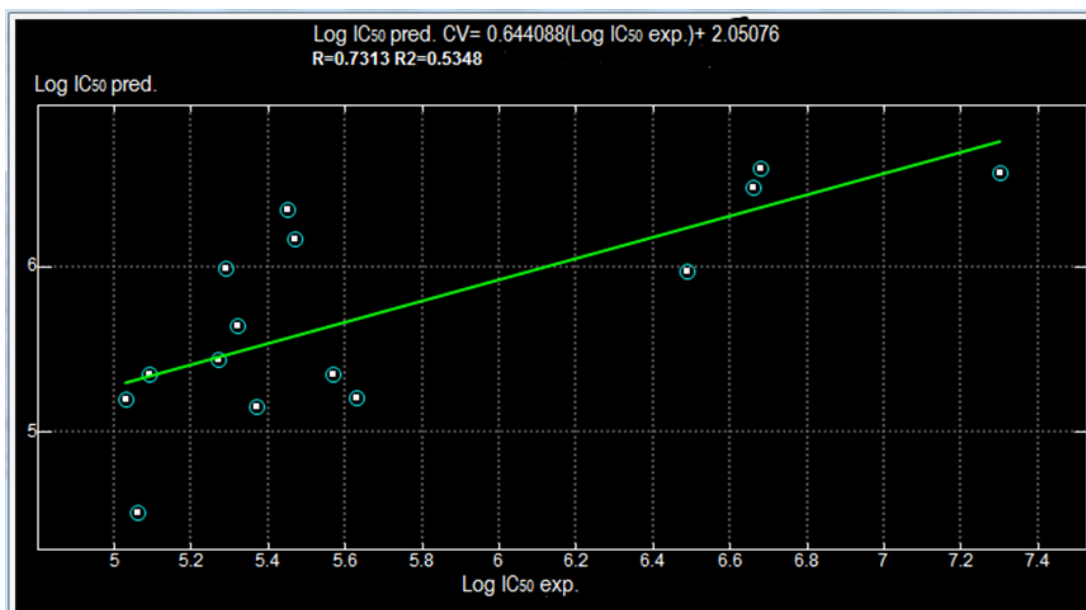
Figure (3.2): Plots of predicted versus experimentally observed log IC_{50} of cross validation (group I) against human breast cancer MCF-7
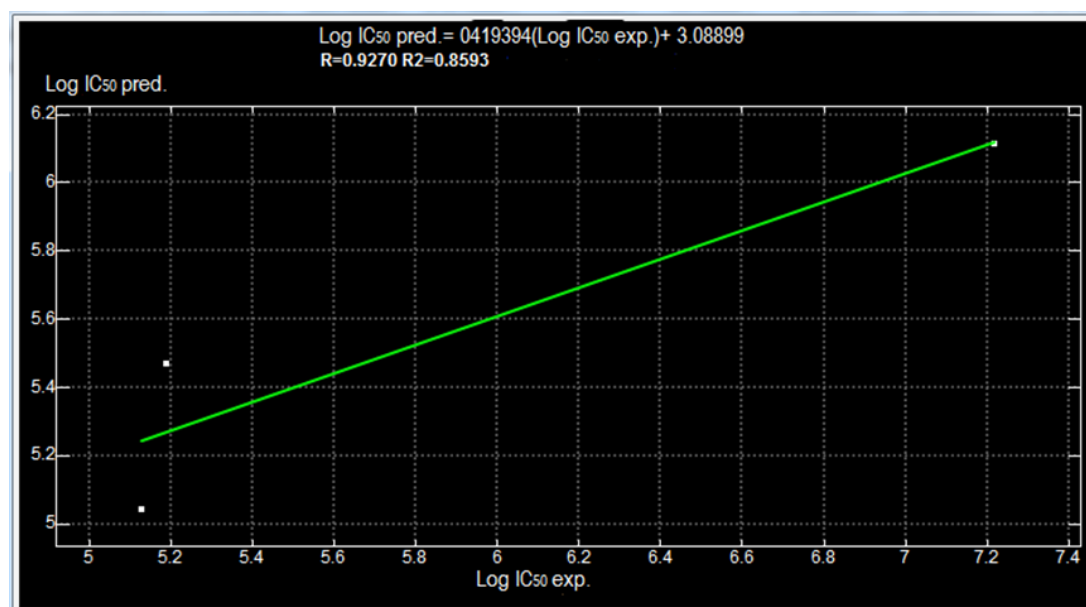
Figure (3.3): Plots of predicted versus experimentally observed log IC_{50} of test set compounds (group I) against human breast cancer MCF-7

Figures (3.4), (3.5) and (3.6) show the plots of linear regression predicted versus experimental values of the biological activity of training set, cross validation and test set compounds, in group (II), against human breast cancer MCF-7, respectively. The plots for QSAR model show very good

fit with $r^2 = 0.8468$; r= 0.9202 for training set, $r^2 = 0.7621$; r= 0.8730 for cross validation and excellent fit with $r^2 = 0.9430$; r= 0.9711 for test set.
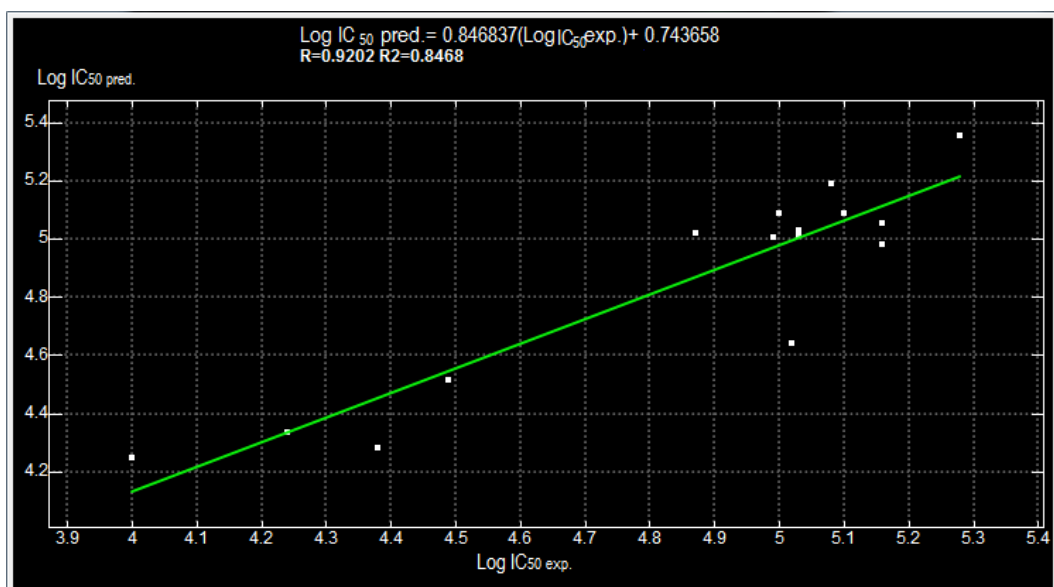
Figure (3.4): Plots of predicted versus experimentally observed log IC_{50} of training set compounds (group II) against human breast cancer MCF-7
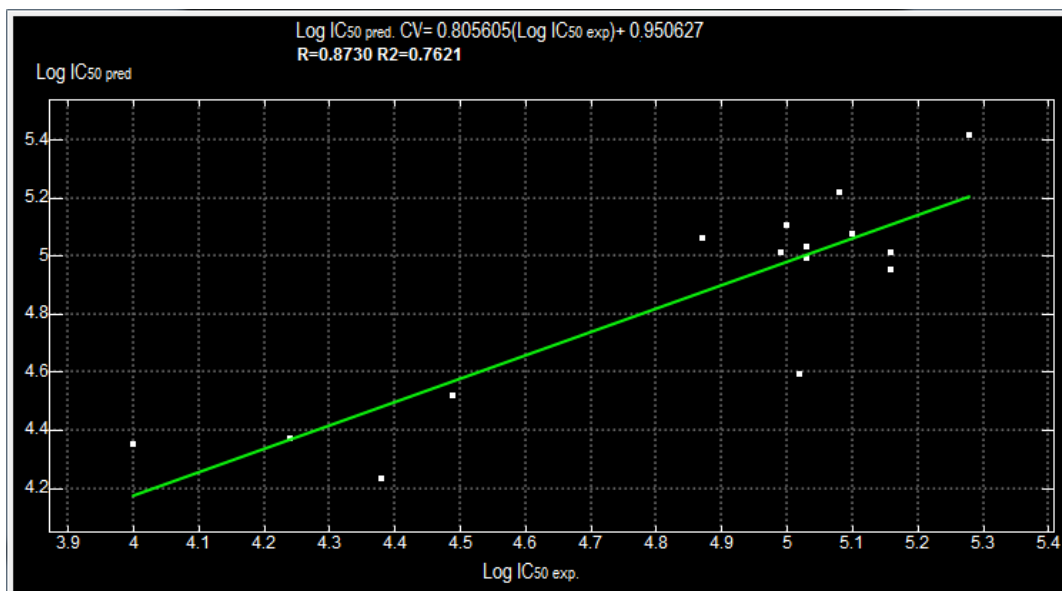
Figure (3.5): Plots of predicted versus experimentally observed log IC_{50} of cross validation (group II) against human breast cancer MCF-7
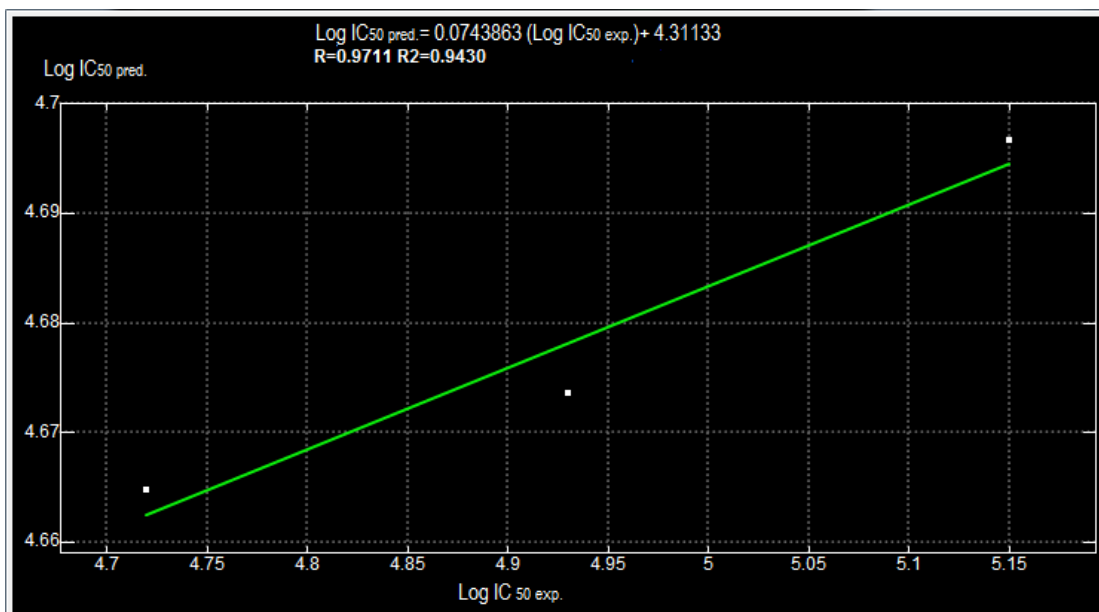
Figure (3.6): Plots of predicted versus experimentally observed log IC_{50} of test set compounds (group II) against human breast cancer MCF-7

3.1.1. Designing of compounds

3.1.1.1. Designing of trisubstituted pyrazoline derivatives

Pyrazoline derivatives have attracted attention of medicinal chemists in both heterocyclic chemistry and in pharmacological activities associated with them. In order to synthesize pyrazoline derivatives expecting to possess biological activity against breast cancer about 120 compounds were designed as anti-breast cancer and their structures are illustrated in appendix (A)

The proposed model (I) has all conditions to be considered as predictive model. It has correlation coefficient of cross validation (Q^2) larger than 0.5, prediction (r^2) higher than 0.6 and very good prediction in external validation ($r^2 = 0.85$). Thus, this model was used to predict the *in-vitro* biological activity of designed pyrazoline derivatives (1-120) against human breast cancer cell line MCF-7, predicted biological activity of

134

these compounds along with predicted chemical descriptors are listed in appendix (A).

To select compounds for synthesis from designed one, the drugability of these compounds were evaluated through Lipinski's parameters "rule of five" which proposes that molecules with poor permeation and oral absorption have logP >5, molecular weight >500, more than 5 hydrogen-bond donor and more than 10 acceptor groups.

The hydrogen bond donor and acceptor groups correlate to the capacity of intermolecular interactions, mainly with water molecules. The passage through cellular membrane becomes thermodynamically unfavorable with the increase of hydrogen bond count groups because desolvatation is needed to enter in the lipidic environment (Gimenez *et al,* 2010). All designed pyrazoline derivatives have acceptable number of hydrogen bond donor and acceptor groups shown in Appendix (A).

The logP value is one of the most important descriptors to evaluate oral bioavailability because it indicates the lipophilicity and hydrosolubility of a compound . As many lipophilic is the compound, as better is the capacity to cross the lipidic-bilayer of the cellular membrane, and consequently, as high will be the bioavailability. The problem is that compounds, excessively lipophilic, have difficulty to dissolve in the water of the organism, and then, they will not be absorbed (Gimenez *et al,* 2010).

The compounds that overcame the logP threshold value were 7, 8, 9, 19, 65, 67, 68, 69, 70, 73, 75, 80, 88, 90, 102, 103, 104, 105, 107-115 and117-120.

The molecular weight describes the molecular size. Big molecules will have difficulty to be absorbed, because the passage through biological

membranes is unfavorable (Gimenez *et al,* 2010). The compounds that not passed in this criterion were 26, 27, 28, 29, 30, 32, 33, 34 and 41-120. Compounds 1-6 (XLI-XLVI), 10-25 (XLVII-LXI), 31 (LXII) and 35-40 (LXIII-LXVII) fit in the rule of five and can be classified as drug-like compounds, these compounds were selected for synthesis. Compounds 62 (LXVIII), 63 (LXIX), 76 (LXX) and 78 (LXXI) were randomly selected for synthesis as shown in Table (2.13).

Combretastatin A-4 (CA-4) is a potent anticancer and antiangiogenesis natural substance isolated from *Combretum caffrum* (Shan *et al*, 2011); it is used as standard drug for designed pyrazoline derivatives in Table (2.13).

Selected compunds XLI, XLII, XLIV, XLIX, LI, LIII, LIV and LVI showed low predicted pIC_{50} ranging from 2.64 to 6.45 M in comparison with CA-4 (pIC_{50}= 6.51 M). The rest of selected compounds showed high predicted pIC_{50} (6.72-14.88 M) when compared with CA-4.

3.1.1.2. Designing of α,β-unsaturated carbonyl derivatives

Substituted α,β-unsaturated carbonyl derivatives have been reported to possess some interesting biological properties (Das *et al*, 2010). Twenty α,β-unsaturated carbonyl derivatives were designed as anticancer agent against breast cancer. Their biological activity were predicted by using obtained predictive QSAR model (II) (r^2= 0.84684), the results were compared with the anticancer drug tamoxifen (Dorchies *et al*., 2013), and listed in Table (2.14). All designed compounds gave biological activity (pIC_{50}) ranging from 3.74 to 6.24 M less than that of the standard drug (pIC_{50}= 7.39 M). The drugability of designed α,β-unsaturated carbonyl derivatives were also evaluated through Lipinski's parameters and all were within acceptable ranges of parameters as shown in Table (2.14)

3.2. Organic synthesis

3.2.1. Synthetic Design

The synthetic design of the compounds selected in this part is based mainly upon retrosynthetic analysis of the target pyrazolines. Standard C-X and C-C disconnection was followed, bearing in mind the concepts of regio and chemoselectivity, Figure (3.7).
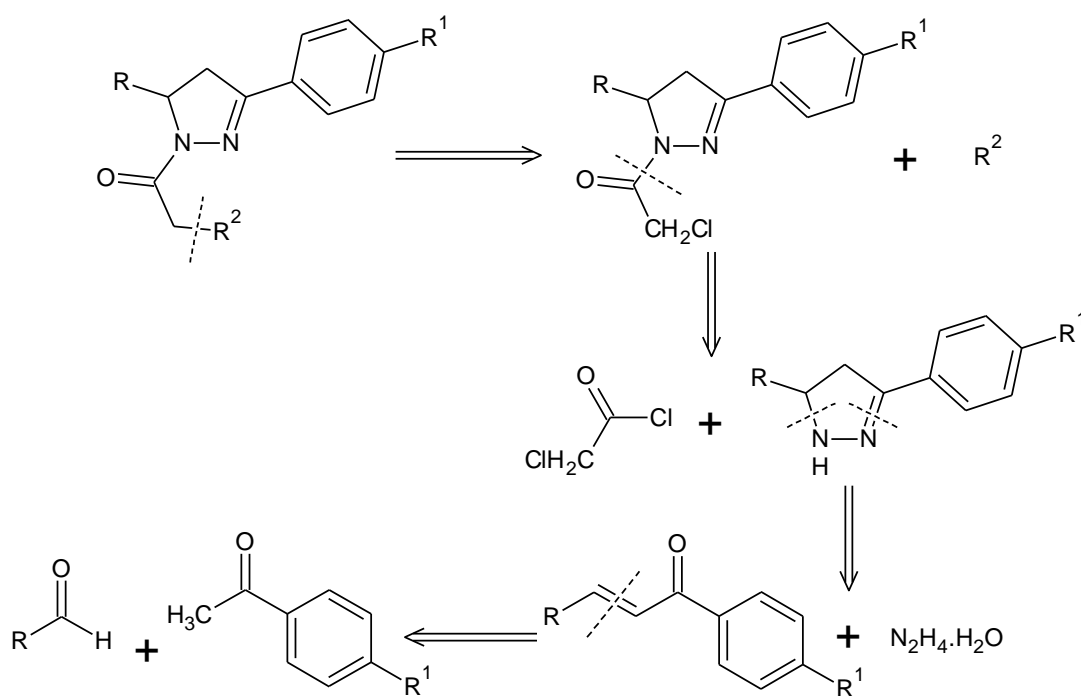
Figure (3.7): Retrosynthetic analysis of target compounds

3.2.2. First step: Synthesis of α,β-unsaturated carbonyl derivatives (I-XX)

α,β-unsaturated carbonyl derivatives are 1,3-diaryl-2-propene-1-one, in which two aromatic rings are linked by a three carbon with α, β-unsaturated carbonyl system (Balaji *et al*., 2010). They possess conjugated double bonds and a completely delocalized π-electron system on both aryl rings. Molecules possessing such system have relatively low redox potentials and have a greater probability of undergoing electron

transfer reactions (Patil *et al*., 2009). α,β-unsaturated carbonyl derivatives are useful intermediates in the synthesis of various heterocyclic compounds such as pyrzolines, isoxazolines pyrimidines, flavones, flavonols and quinoxalines (Kaithwal *et al*., 2009).

In the present work twenty α,β-unsaturated carbonyl derivatives (I-XX) were synthesised via Claisen- Schmidt reaction by treating benzaldehyde, 4-Chloro-benzaldehyde, 4-Dimethylamino benzaldehyde, Cinnamaldehyde and Furfural with acetophenones like 4-Nitroacetophenone , 4-Bromoacetophenone, 4-Methylacetophenone and acetophenone in presence of NaOH. The suggested mechanism for this reactions is illustrated in scheme (3.1).
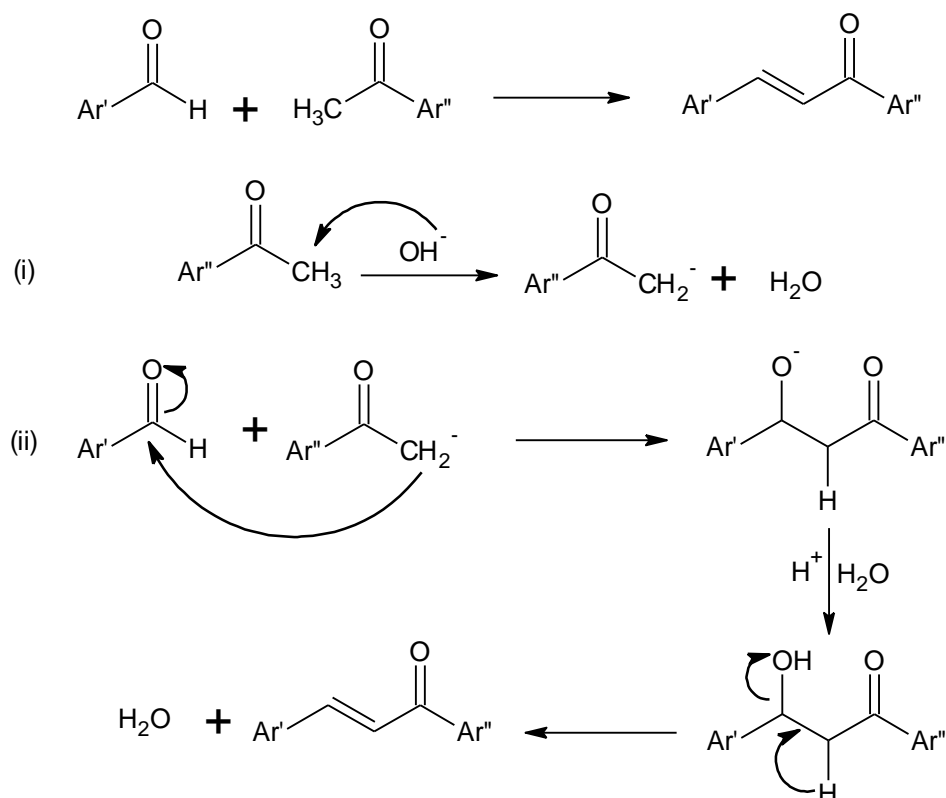
Scheme (3.1.): Proposed mechanism for Claisen- Schmidt condensation of acetophenone and benzaldehyde

3.2.3. Second step: Synthesis of 3,5-Diaryl-2-pyrazolines (XXI-XL)

Twenty 3,5-Diaryl-2-pyrazoline derivatives (XXI-XL) were synthesized by cyclization of α,β-unsaturated carbonyl derivatives (I-XX). This step was achieved via heating under reflux of α,β-unsaturated carbonyl derivatives with excess of hydrazine monohydrate in absolute ethanol to give the cyclized 3,5-Diaryl-2-pyrazoline derivatives (XXI-XL). This reaction appears to involve the subsequent addition of **N-H** across the carbon-carbon double bond. Scheme (3.2) shows the mechanism of this reaction.
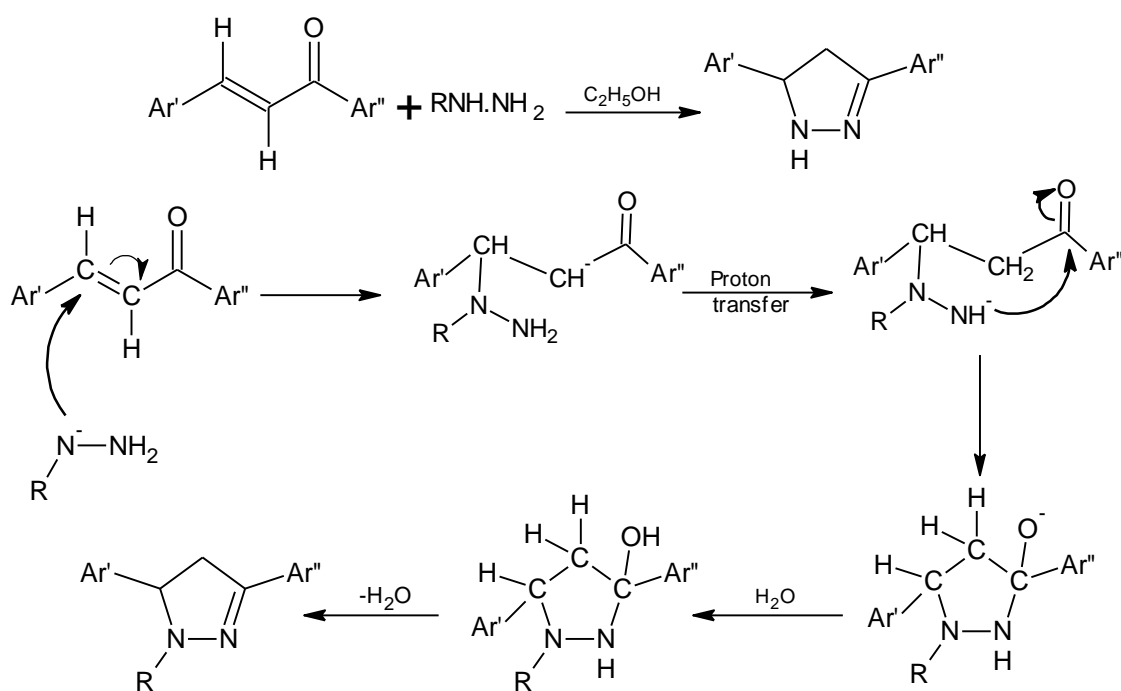
Scheme (3.2): Proposed mechanism for the formation of 3,5-Diaryl-2-pyrazoline derivatives

The reaction proceeds by Michael addition which involves nucleophilic attack by hydrazine nucleophile (**R-N⁻NH₂**) at the β-carbon of the α,β-unsaturated compound (1,4-addition) followed by proton transfer from nitrogen to oxygen leading ultimately to amine, then cyclization via

Claisen addition, and hydrolysis. The later with a hydroxy group and amino group on the carbon loses water molecule to yield the pyrazolines (dehydration).

3.2.4. Third step: Synthesis of 1-(Chloroacetyl)-3,5-diaryl-2-pyrazoline derivatives (XLI-LVII)

1-(Chloroacetyl)-3,5-diaryl-2-pyrazolines (XLI-LVII) were synthesized by treatment of 3,5-Diaryl-2-pyrazoline derivatives (XXI-XL) with chloroacetylchloride in the presence of triethylamine in dry toluene at 0˚C. Seventeen 1-(Chloroacetyl)-3,5-diaryl-2-pyrazoline derivatives were synthesized and characterized by physiochemical properties, IR, UV, ^{1}HNMR and MS. This reaction is summarized in scheme (3.3).
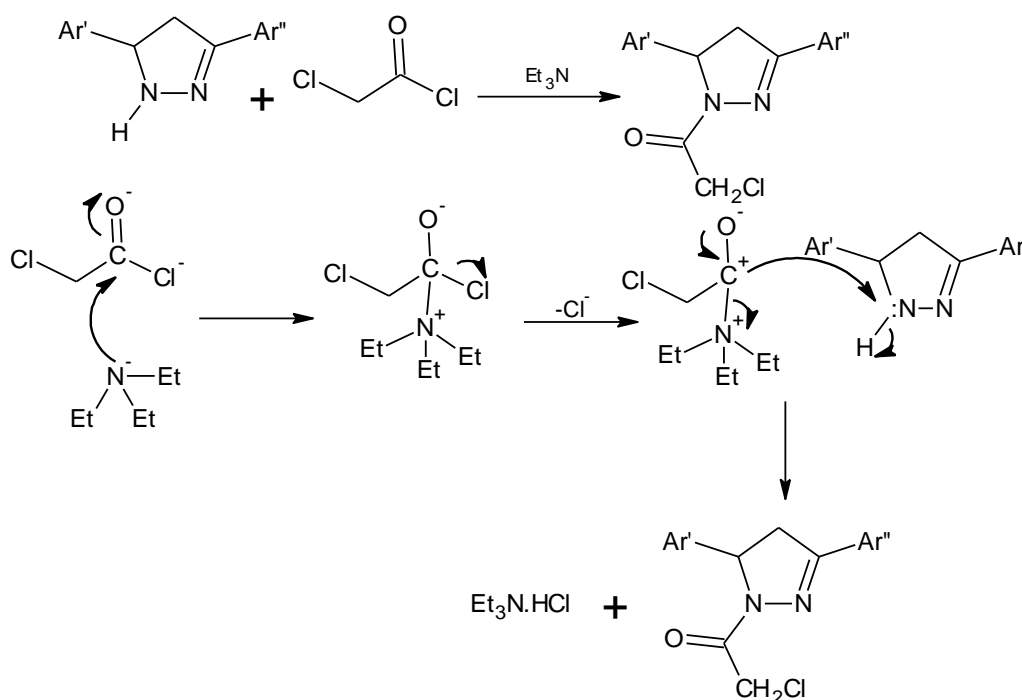
Scheme (3.3): Proposed mechanism for preparation of 1-(Chloroacetyl)-3,5-diaryl-2-pyrazoline derivatives

Acylation with chloroacetyl chloride leads to the amide (Lednicer & Mitscher, 2008). This reaction achieved via nucleophilic addition to the

carbonyl group in chloroacetyl chloride (triethylamine acts as the nucleophile) followed by elimination of chloride ion and formation of carbocation, which is then attacked N-pyrazoline (electrophilic substitution) to form 1-(Chloroacetyl)-3,5-diaryl-2-pyrazolines. By the end of this reaction the precipitate triethylamine hydrochloride is obtained as by product, it dissolves in water and melts at 260°C.

3.2.5. Forth step: Synthesis of 1-[(aryl) amino acetyl] -3,5-diaryl-2-pyrazoline derivatives (LVIII-LXXI)

Appropriate 1-(Chloroacetyl)-3,5-diaryl-2-pyrazolines were tested as alkylating agents in the reaction with sulfanilamide and sulfadoxine in dry DMF and unhydrous K_2CO_3 with stirring under reflux. Thus the corresponding 1-[(aryl) amino oacetyl] -3,5-diaryl-2-pyrazoline derivatives (LVIII-LXXI) have been obtained as shown in scheme (3.4).
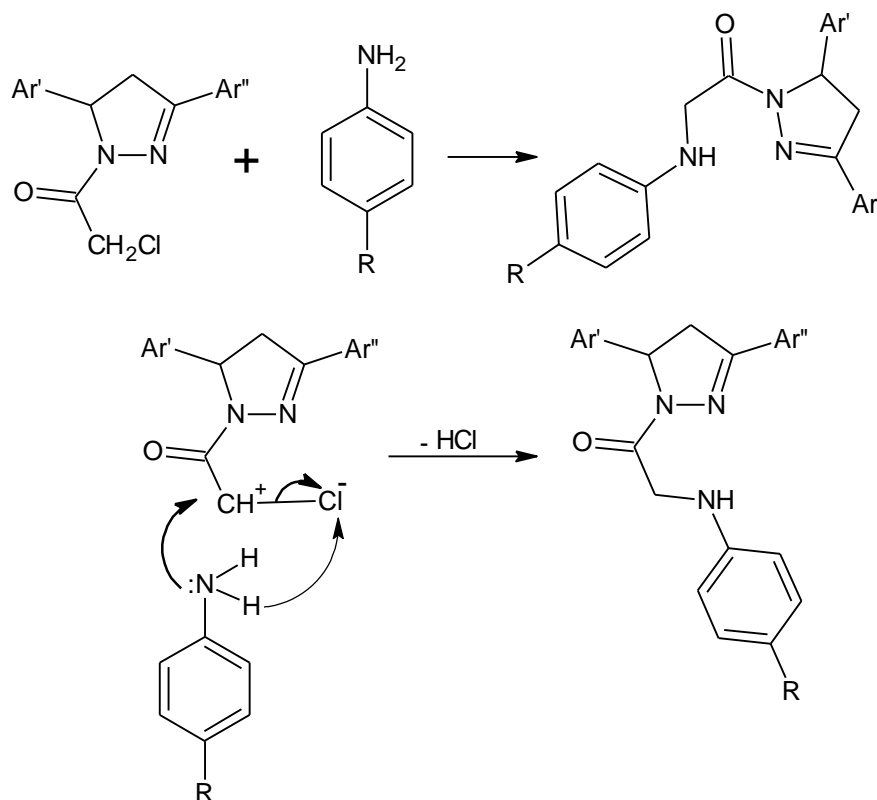
Scheme (3.4): Proposed mechanism for the formation of 1-[(aryl) amino acetyl] -3,5-diaryl-2-pyrazoline derivatives

In this proposed nucleophilic substitution reaction mechanism (whether it is S_N1 or S_N2), the **N** in secondary amino group of sulfanilamide or sulfadoxine functions as the nucleophile and attacks the electrophilic **C** of the 1-(Chloroacetyl)-3,5-diaryl-2-pyrazoline displacing good the leaving group (chloride ion) and creating the new **C-N** bond. Fourteen of the desired derivatives were synthesized and characterized by physiochemical properties, IR, UV, H[1]NMR and MS.

All the synthesized compounds were isolated in satisfactory yield, α,β-unsaturated derivatives (I- XX) ranges of 52-97%, 60-87% 3,5-Diaryl-2-pyrazoline derivatives (XXI - XL), 46-72% 1-(Chloroacetyl)-3,5-diaryl-2-pyrazoline derivatives (XLI - LVII) and 39-75% 1-[(aryl)amino acetyl]-3,5-diaryl-2-pyrazoline derivatives (LVIII-LXXI).

3.3. Spectroscopic Analysis

3.3.1. Fourier infra-red Spectroscopic analysis (FT-IR)

Almost any compound having covalent bonds, whether organic or inorganic, absorbs frequencies of electromagnetic radiation in the infrared region of the electromagnetic spectrum. The region lies at wavelengths longer than those associated with visible light and shorter than that associated with microwaves. For chemical purposes, scientists interested in the vibrational portion of the infrared region. The instrument that determines the absorption for a compound is called an infrared spectrometer or, more precisely, a spectrophotometer. Two types of infrared spectrometers are in common use in organic laboratory: dispersive and fourier transform (FT) instruments. Both of these types of instruments provide spectra of compounds in the common range of 4000 to 400 cm^{-1}. Although the two provide nearly identical spectra for a given

compound, FT infrared spectrometers provide the infrared spectrum much rapidly than the dispersive instruments (Pavia *et al*., 2013).

3.3.1.1. Synthesized α,β-unsaturated carbonyl compounds (I-XX)

These compounds showed several characteristic sharp bands in the IR region, where the bands in the range between 1644-1665 cm^{-1} indicated the appearance of the carbonyl C=O st.vib group of the formed ketone, which was conjugated to both the aromatic and the alkene systems. The absorption bands for C=C st.vib of the α,β-unsaturated carbonyl system and C=C st.vib of aromatic rings appeared at 1562-1608 cm^{-1} and 1407-1594 cm^{-1}, respectively.

Absorption bands at 1365-1374 cm^{-1} in compounds III, VIII, XIII and XVIII indicated the presence of $N(CH_3)_2$ st.vib group.

Compounds V, X, XV and XX showed C-O-C stretching at 1222-1227 cm^{-1} referring to furfural ring.

Compounds XI-XV showed two absorption bands at 1407-1448 cm^{-1} and 1334-1343 cm^{-1} due to asymmetry and symmetry stretching NO_2. Compounds contain CH_3 group (XVI-XX) absorption bands at 2907-3024 cm^{-1} were observed. Aromatic C-H stretch also observed at 2095-3131 cm^{-1} in all derivatives.

3.3.1.2. Synthesized 3,5-Diaryl-2-pyrazoline derivatives (XXI-XL)

The IR spectra of these compounds show the disappearance of conjugated system (-C=C-C=O) of α,β-unsaturated carbonyl derivatives (I-XX), and appearance of strong band at 3249-3421 cm^{-1} due to closure of ring and formation of –NH st.vib group. C=C stretching band of aromatic rings appeared at 1477-1613 cm^{-1}. The absorption bands at 1588-1681 cm^{-1}, 1144-1240 cm^{-1} and 1047-1111 cm^{-1} were attributed to the (C=N), (C-N)

and (N-N) stretching vibrations, these confirms the formation of the pyrazoline ring in all the compounds (XXI-XL).

3.3.1.3. Synthesized of 1-(Chloroacetyl)-3,5-diaryl-2-pyrazoline derivatives (XLI-LVII)

These compounds showed a strong band at 1664–1757cm^{-1} due to the presence of carbonyl group(C=O st.vib) and disappearance of -NH stretching. Some significant stretching bands due to C=N and aromatic C=C stretching bands appeared in the region of 1573–1671 cm^{-1} and 1442–1608 cm^{-1}, respectively.

3.3.1.4. Synthesized of 1-[(aryl) amino acetyl] -3,5-diaryl-2-pyrazoline derivatives (LVIII-LXXI)

All these derivatives have a strong characteristic band in the region 3213–3425 cm^{-1} due to the formation of amide N-H, amide C=O stretching vibration appeared at 1651-1670 cm^{-1} , also IR spectrum exhibited two asymmetric and symmetric stretching bands in all derivatives at 1311–1396 cm^{-1} and 1118–1157 cm^{-1} due to SO$_2$ st.vib group.

Compounds LVIII-LXVII which contain NH$_2$ group show two stretching vibration absorption bands at range 3482-3441 cm^{-1} and 3392-3356 cm^{-1}.

C=N st.vib group showed absorption at 1593–1635 cm^{-1} confirmation of pyrazoline ring, while aromatic C=C st.vib showed peak at 1492–1597 cm^{-1}.

3.3.2. Ultra violet Spectroscopic Analysis (UV)

Most organic molecules and functional groups are transparent in the portions of the electromagnetic spectrum which we call the ultraviolet (UV) and visible (VIS) regions that is, the regions where wavelengths range from 190 nm to 800 nm. Consequently, absorption spectroscopy is of limited utility in this range of wavelengths. However, in some cases we

can derive useful information from these regions of the spectrum. That information, when combined with the detail provide by infrared and nuclear magnetic resonance, can led to valuable structural proposals (Pavia *et al*., 2013). Pyrazolines absorb light in the range 300–400 nm and emit blue fluorescence because the heterocyclic ring contains two nitrogen atoms (Pant *et al*., 2011).

3.3.2.1. Synthesized 1-(Chloroacetyl)-3,5-diaryl-2-pyrazoline derivatives (XLI-LVII)

The UV-Vis spectra of 1-(Chloroacetyl)-3,5-diaryl-2-pyrazolines (XLI-LVII) recorded in DMSO exhibit an intense absorption band which is attributed to the $\pi - \pi^*$ transition of the conjugated system in pyrazoline moiety ($-N^1-N^2=C^3-$). The absorption maxima (λmax) wavelength was observed in the range of 294.40−351.40 nm Table (2.21).

3.2.2.2. Synthesized 1-[(aryl) amino acetyl] -3,5-diaryl-2-pyrazoline derivatives (LVIII-LXXI)

The electronic spectra of the 1-[(aryl)amino acetyl] -3,5-diaryl-2-pyrazoline (LVIII-LXXI) recorded in DMSO. The λmax values are summarized in Table (2.22).The absorption band positions broadly lie between 280.60-349 nm assignable to π-π^* transitions due to the conjugation in pyrazoline ring.

The absorption spectra of the compounds XLI-LVII and LVIII-LXXI show that the spectral shapes are very similar in two groups of the compounds because all these compounds possess the same 2-pyrazoline central nucleus. The difference of absorption wavelengths is due to the effect of substituents in the position 3 and 5 of pyrazoline moiety in case of compounds XLI-LVII, in addition of that the substitution in methylene ($-CH_2$) attached to carbonyl group in case of the derivatives LVIII-LXXI .

3.3.3. Nuclear Magnetic Resonance Spectroscopic Analysis (^{1}HNMR)

Nuclear magnetic resonance (NMR) is a spectroscopic method that is even more important to the organic chemist than infrared spectroscopy. Whereas infrared spectroscopy reveals the types of functional groups present in a molecule, NMR gives information about the number of magnetically distinct atoms of the type being studied. The combination of IR and NMR data is often sufficient to determine completely the structure of an unknown molecule (Pavia *et al*., 2013).

3.3.3.1. Synthesized of 1-(Chloroacetyl)-3,5-diaryl-2-pyrazoline derivatives (XLI-LVII)

In the ^{1}H-NMR spectra all the three protons in pyrazoline ring of 1-(Chloroacetyl)-3,5-diaryl-2-pyrazoline derivatives (XLI-LVII), HA, HB and HX attached to the C-4 and C-5 carbon atoms gave an ABX spin system fig (3.8).
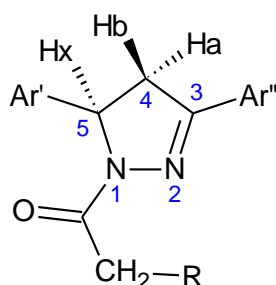
Figure (3.8): ABX spin system of pyrazoline ring

In all compounds the CH_2 protons of the pyrazoline ring resonated as a doublets of doublets (dd) at δ 3.11–3.48 ppm proton (C4-Ha), 3.59–3.93 ppm proton (C4-Hb). The CH proton (C5-Hx, except for XLIV, LI and LVI) also appeared as a doublet of doublets at δ 5.43–5.74 ppm due to the vicinal coupling with two magnetically nonequivalent protons of the

methylene group at position four of the pyrazoline ring ($J_{Ha,Hb}$ = 18.00–18.36 Hz, $J_{Ha,Hx}$ = 4.44–5.16 Hz, $J_{Hb,Hx}$ = 11.28–11.99 Hz).

The CH_2 protons of the acetyl group at position 1 of the all pyrazolines ring were observed as two doublets at δ 4.62–4.72 ppm (J = 13.72–14.16 Hz) and at δ 4.68–4.82 ppm (J = 13.96–14.16 Hz). This geminal coupling resulted from the steric structure of the compound. These geminal protons were observed as a doublet due to two different possible conformations since rigid protons occurred fig (3.5).

The CH proton (C5-Hx) in XLIV, LI and LVI compounds appeared as multiplets (5.16-5.31ppm) due to the vicinal coupling with two methylene protons (Ha, Hb) and α-proton (Hα) fig (3.9).
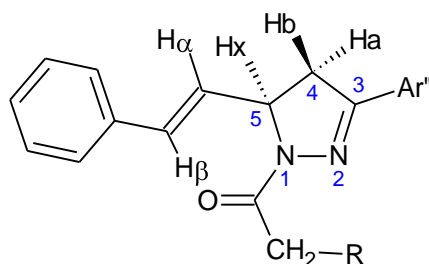
Figure (3.9): α-proton in XLIV, LI and LVI compounds

Also these compounds contain a pair of trans-olefinic proton, Hα appeared as a doublet of doublets at δ 6.28–6.32 ppm ($J_{α-H,β-H}$= 15.88 Hz, $J_{α-H,Hx}$ =7.08 Hz) because of the vicinal coupling with two protons Hx and Hβ which are magnetically not equivalent. Hβ appeared as doublet δ 6.57–6.60 ppm (J= 15.88 Hz) fig (3.9).

Compounds XLIII, L and LV showed singlet signal at δ (2.85-2.87 ppm) which indicated the six protons of -N(CH$_3$)$_2$.

Compounds LIII-LVII showed (s, 3H) at δ 2.35–2.36 ppm indicated a three protons of methyl group (-CH$_3$).

Furan protons in compounds XLV, XLVII, LII and LVII appeared as multiplet 2H at δ 6.37-6.43ppm and duplet 1H at δ 7.57-7.60 ppm with small coupling constant (J= 0.72-2.32 Hz)

All the other aromatic protons were observed at expected regions and the results are tabulated in table (2.16).

3.3.3.2. Synthesized of 1-[(aryl) amino acetyl] -3,5-diaryl-2-pyrazoline derivatives (LVIII-LXXI)

All these derivatives also showed ABX spin system of pyrazoline ring, Ha appeared as two doublets (δ 3.06-3.17 ppm) or multiplet (δ 3.04-3.71 ppm). Hb also appeared as doublet of doublet or multiplet at δ 3.69-3.80 ppm and δ 3.76-3.99 ppm respectively. Another doublet of doublet at δ 5.31-5.59 ppm or multiplet at δ 5.11-5.65 ppm region due to the methine proton (Hx) which was coupled with the magnetically nonequivalent methylene protons of pyrazoline ring ($J_{Ha,Hb}$ = 17.84–18.24 Hz, $J_{Ha,Hx}$ = 4.20–4.72 Hz, $J_{Hb,Hx}$ = 11.52–11.84 Hz).

Two protons of methylene group attached to carbonyl group (CO$\underline{CH}_2$) observed in all derivatives as doublet (δ 4.00-4.02 ppm, J= 5.52-6.00 Hz) or multiplet at δ 3.92-4.62 ppm.

LVIII-LXVII compounds exhibits a single peak in the region δ 5.94-5.95 ppm characteristic of NH$_2$ protons (1°amino group SO$_2$$\underline{NH}_2$). Another signal for proton attached with nitrogen in COCH$_2$$\underline{NH}$ system (2°amino group) appeared as triplet or distorted triplet at between δ 7.21 and 7.35 ppm.

LXVIII-LXXI compounds exhibits two single peak at δ 3.62-3.83 ppm and δ 3.85-4.00 ppm characteristic of methoxy group (-OCH$_3$) which is located far and near the nitrogen atom of eterocyclic ring.

Compounds LX and LXIX showed single peak at δ 2.84-2.85 ppm indicated six protons of two methyl groups which linked with nitrogen atom (-N(CH$_3$)$_2$).

Olefinic proton in compound LXI (Hα and Hβ) appeared as multiplet at δ 6.29-6.46 ppm.

Three protons of methyle group (-CH$_3$) attached to LXIV, LXV, LXVII and LXX observed as single peak at δ 2.34-2.36 ppm.

Compounds LXVI and LXXI showed two single peaks, first one at δ 2.35 ppm indicated the protons of methyle group, and second peak at δ 2.84 ppm indicated six protons of methyl groups attached to nitrogen atom.

3.3.4. Mass Spectroscopic Analysis (MS)

In its simplest form, the mass Spectrometer performs three essential functions:

a) Molecules are subjected to bombardment by stream of high energy electrons, converting some of the molecules to ions, which are accelerated in an electric field.

b) The accelerated ions are separated according to their mass-to-charge rations in a magnetic or electric field.

c) The ions that have a particular mass-to-charge ratio are detected by a device which can count the number of ions striking it. The detector's output is amplified and fed to a recorder (Pavia *et al*., 2013).

Mass Spectrometry (MS) was used to determine the molecular weights of synthesized compounds (XLI-LXXI). A molecular ion peak (M$^+$) was observed for all trisubstituted pyrazoline (XLI-LXXI), in their respective mass spectra.

3.3.4.1. Synthesized 1-(Chloroacetyl)-3,5-diaryl-2-pyrazoline derivatives (XLI-LVII)

The mass spectrum of the compounds **(XLI-LVII)** shows a molecular ion peaks (M$^+$) at m/z 298.05 (100%), 332 (86.9%), 341.15 (61.12%), 324.10 (54.66%), 288.30 (93.415), 376.30 (75.18%), 366.25 (74.80%), 343 (56.93%), 377 (61.92%), 386.10 (55.1%5), 369.45 (32.40%), 333.35 (79.03%), 312.05 (100%), 346.05 (100%), 355.15 (74.63%), 338.40 (75.88%), 302 (100%) corresponding to the molecular formulas that consistent with their structures.

Compounds XLI, LIII, LIV and LVII showed a molecular ion peak (M$^+$) as base peak.

The M+1 and M+2 isotope peaks was also observed in all derivatives. M+1 occur due to the presence of isotopes ^{2}H or ^{13}C observed with a relative abundance ranging from 12-24%. M+2 the isotope peak of halogen atom appears due to the presence of (COCH$_2$Cl) group in all derivatives with a relative abundance between 11-100%. Compounds XLII, XLVI, XLVII, XLIX and LIV exhibit peaks at 336(10.34%), 380(26.44%), 370(25.16%), 381(7.62%) and 350(12.05%) respectively due to M+4 characteristic of compounds contain two halogen atom (Cl or Br). XLII, XLIX and LIV contain 2Cl atoms, XLVI and XLVII contain one Cl and one Br atoms. The fragmentation pattern of the synthesized compounds exemplified by that of compounds XLI, XLV and LVI in schemes (3.5), (3.6) and (3.7), respectively**.** The common fragmentation pattern involves some rearrangement with the removal of simple and smaller molecules.
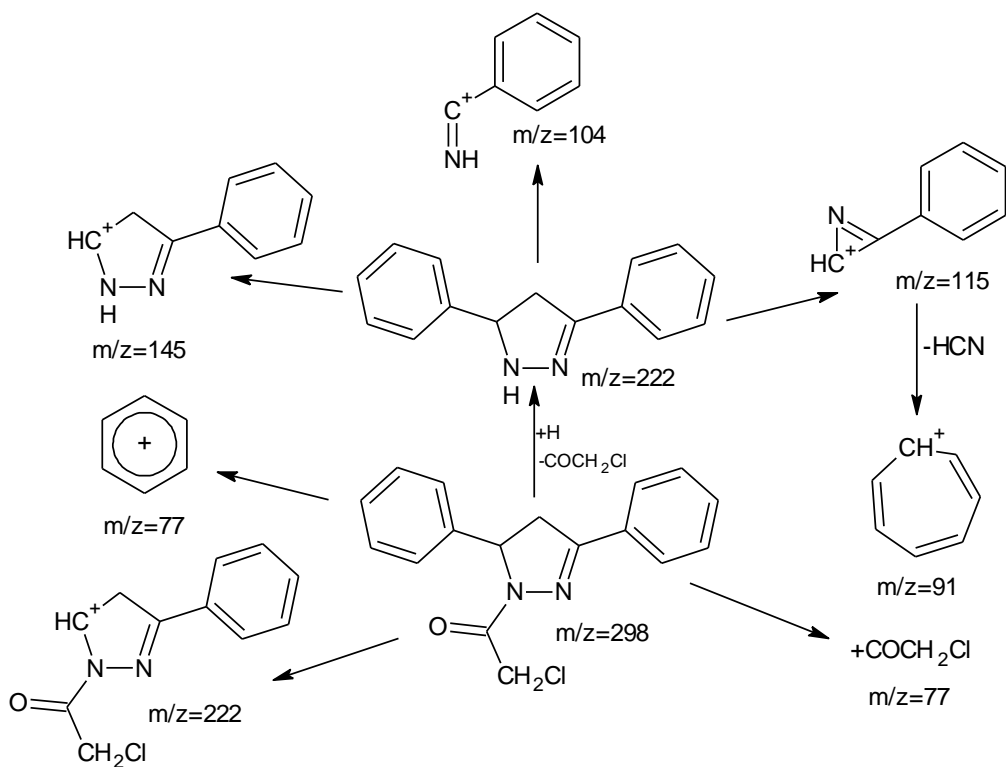
Scheme (3.5): Mass fragmentation of XLI
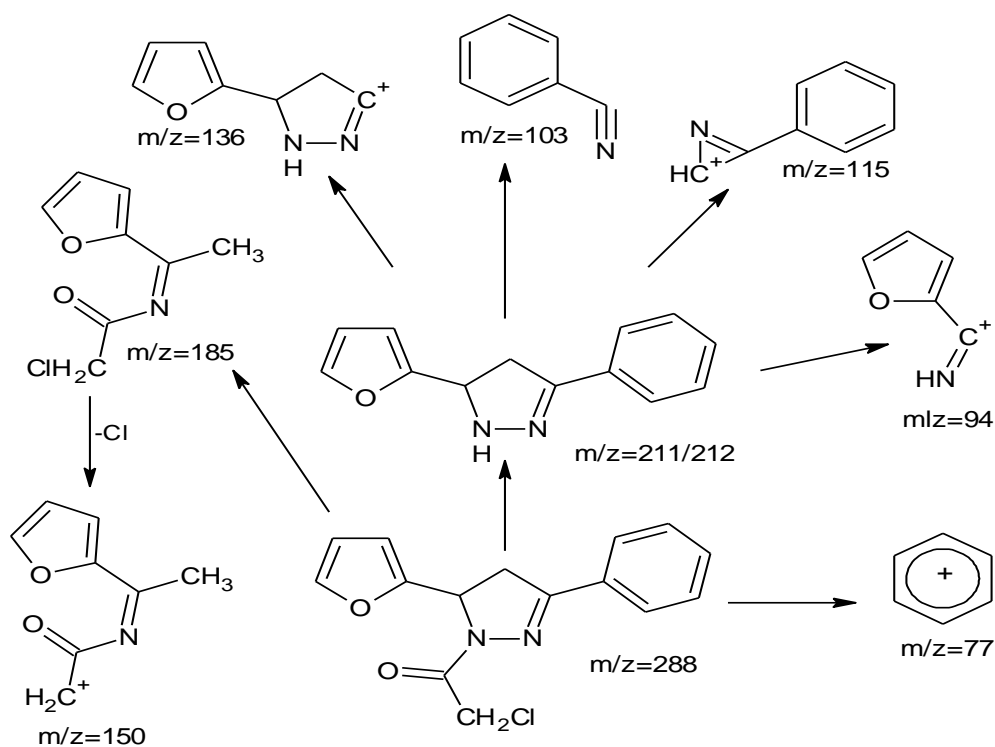
Scheme (3.6): Mass fragmentation of XLV
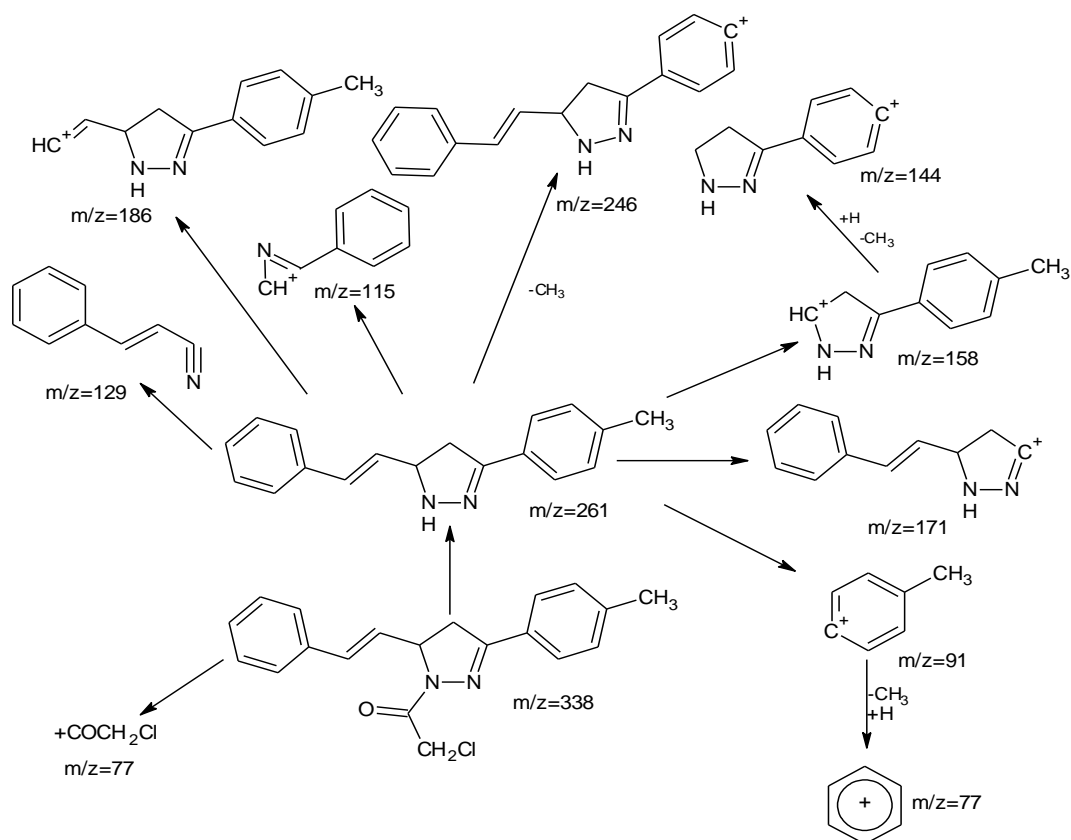
Scheme (3.7): Mass fragmentation of LVI

3.3.4.2. Synthesized 1-[(aryl) amino acetyl] -3,5-diaryl-2-pyrazoline derivatives (LVIII-LXXI)

All the synthesized new compounds (LVIII-LXXI) gave significantly stable molecular ion peaks with a relative abundance ranging from 4.70-100%. Compounds LX and LXVI showed a molecular ion peak (M$^+$) as base peak. M+1 isotope peaks was observed in all derivatives with a relative abundance 0.74-32.77%.

Compounds LIX and LXV showed isotope peak of halogen atom (M+2) due to presence of Cl atom at position 5 of pyrazoline ring (Ph-Cl). The other peaks are due to fragments exemplified by the fragmentation of compound LVIII shown in scheme (3.8).
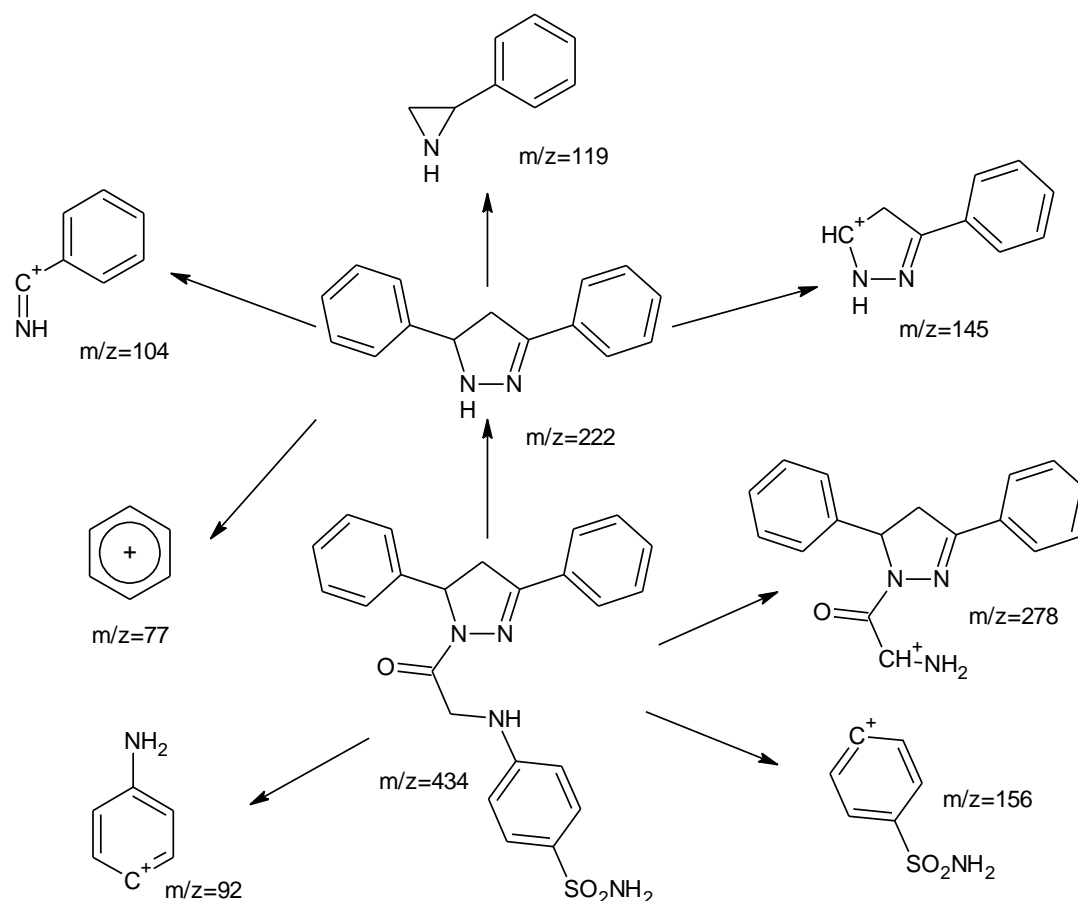
Scheme (3.8): Mass fragmentation of LVIII

3.4. Docking study

Docking of molecules is not an easy task. The difficulties are mainly associated with the choice of the crystallographic structure of a target protein. Some molecules may have a specific mechanism of chemical behaviour associated with their unique binding properties. For instance, some molecules may have multiple binding modes resulting in higher overall interaction energies in comparison with molecules with a single binding mode. Such a molecule can be attractive as a potential drug. Alkylating agents have been found no doubt as potent anticancer agents (Gowramma *et al.*, 2009). Sulfonamides have been reported for potent antitumor activity *in vitro* and *in vivo* against numerous types of cancers. A number of mechanisms of action were reported to be associated with

the anticancer ability of sulfonamides, the most prominent being their power to act as carbonic anhydrase inhibitors (CAIs). Carbonic anhydrases are a group of metalloenzymes that catalyze the hydration of carbon dioxide (cellular waste product) to bicarbonate and a proton (Ghorab *et al*., 2014). Human carbonic anhydrase XII (hCAXII) is expressed in a variety of normal human tissues and becomes stronger or more widespread in tumors compared to the corresponding normal tissues. This characteristic of CAXII can act as potential target for anticancer studies. The catalytic activity of CAXII has been demonstrated to facilitate tumor metabolism and thus to trigger tumor growth. Inhibition of hCAXII can be used as a novel means of targeting cancer (Barua *et al*., 2017).

Most of synthesized trisubstituted pyrazoline derivatives listed in table (2.13) revealed promising biological activity against human breast cancer MCF-7. Thus, it was interesting to perform molecular docking to study the differences in docking patterns and amino acid interactions for the newly synthesized trisubstituted pyrazoline derivatives.

Acetazolamide was reported as a strong inhibitor of several carbonic anhydrase isozymes. It acts as a potential modulator of anticancer therapies in combination with different cytotoxic agents (alkylating agents, nuclueoside analogs, etc.) (Ghorab *et al*, 2014), it was used as reference drug.

The protein CAXII had the PDB ID: 1JD0 which was used to download the protein structure. The file contains hCAXII co-crystallized with acetazolamide. All docking procedures were achieved by MOE (Molecular Operating Environment) software, the docking protocol was verified by re-docking of the co-crystallized ligand (acetazolamide) in the vicinity of the active site of the enzyme with energy score (S) = -21.0578

kcal/mol. Figure (3.10) shows structure of CAXII that was imported from PDB using ID 1JD0, figure (3.11) shows structure of CAXII after protein preparation and 2D interaction of AZA inside the active site of hCAXII.
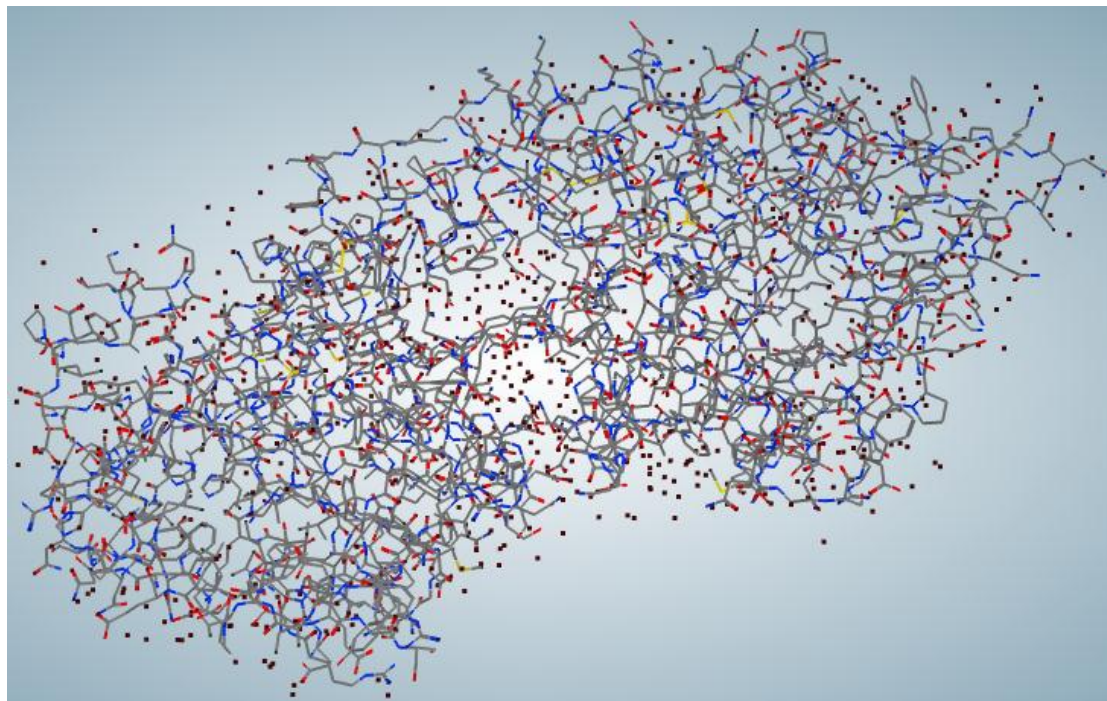
Figure (3.10): Structure of CAXII that was imported from PDB using ID 1JD0
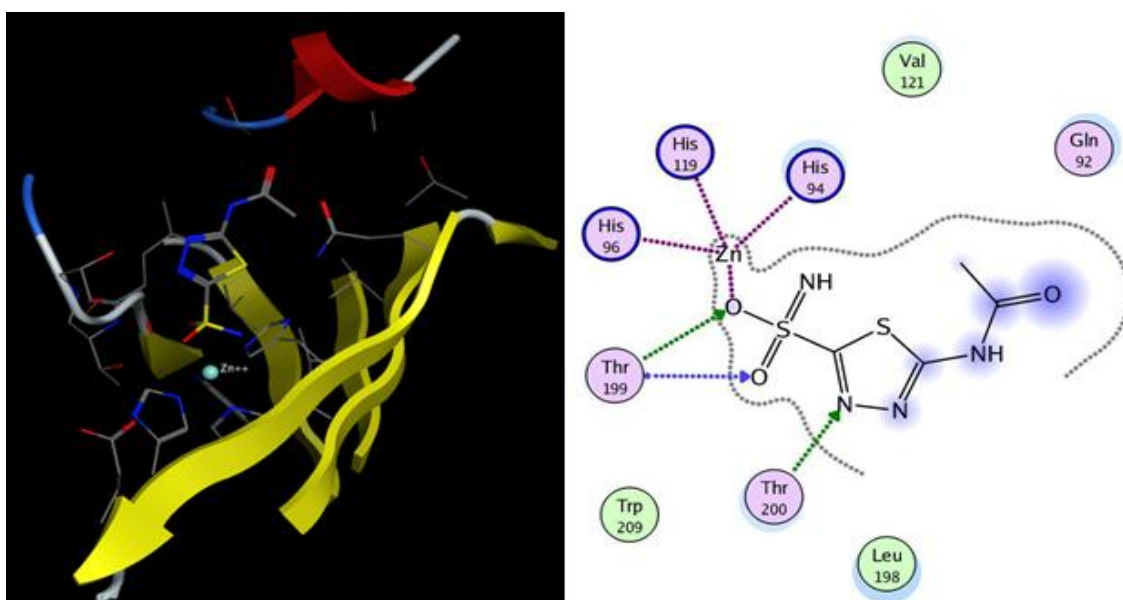
Figure (3.11): Structure of CAXII after protein preparation and 2D binding interaction of AZA inside the active site of CAXII

155

Docking on the active site of hCAXII was performed for all synthesized trisubstituted pyrazolines (XLI-LXVII) except XLVIII, LXIX, LXX and LXXI because they did not fit in rule of five, the results were tabulated in table (2.33).

Acetazolamide interacted with the active site of hCAXII by: two hydrogen bonds between Thr 199 and the SO_2 group, one hydrogen bond between Thr 200 and N3 of the thidiazole ring, and finally metal complex between the Zn(II) ion, His94, His96 and His119 and the SO_2NH_2 group of AZA as shown in Figure (3.11).

Compounds XLI-LVII showed low docking scores ranging from -14.29 to -18.94 kcal/mol comparing with AZA (-21.0578 kcal/mol) and with compounds that carrying sulfanilamide moiety (LVIII-LXVII), which showed proper fitting to the active site of hCAXII with high energy scores ranging from -20.12 to -22.20 kcal/mol, supporting the observation of these sulfonamides as hCAXII inhibitors. The best docking score was assigned to compound LXII (-22.2056 kcal/mol).

XLIII, XLV, XLIX and L failed to show interaction with the amino acid in the docking study.

In a further look to the docking results side by side to QSAR results when predicted the pIC_{50} for this newly synthesized compounds, we can observe that the more active compounds LVIII, LXII, LXVI and LXVII (pIC_{50}= 9.17, 13.40, 9.5 and 12.39 M respectively) have shown excellent docking scores (-21.9174, -22.2056, -22.0545 and -21.2136 respectively), also these compounds were capable of forming a metal complex with the Zn ion through His 94, His 96 and His 119 in a similar manner to the co-crystallized ligand (AZA). Amino acid interactions of the most active compounds (LVIII, LXII, LXVI and LXVII) towards hCAXII are illustrated in figures (3.12), (3.13), (3.14) and (3.15), the rest of figures

can be found in the appendix C. These results merit further investigation of these new sulfonamides as potential antitumor agents.
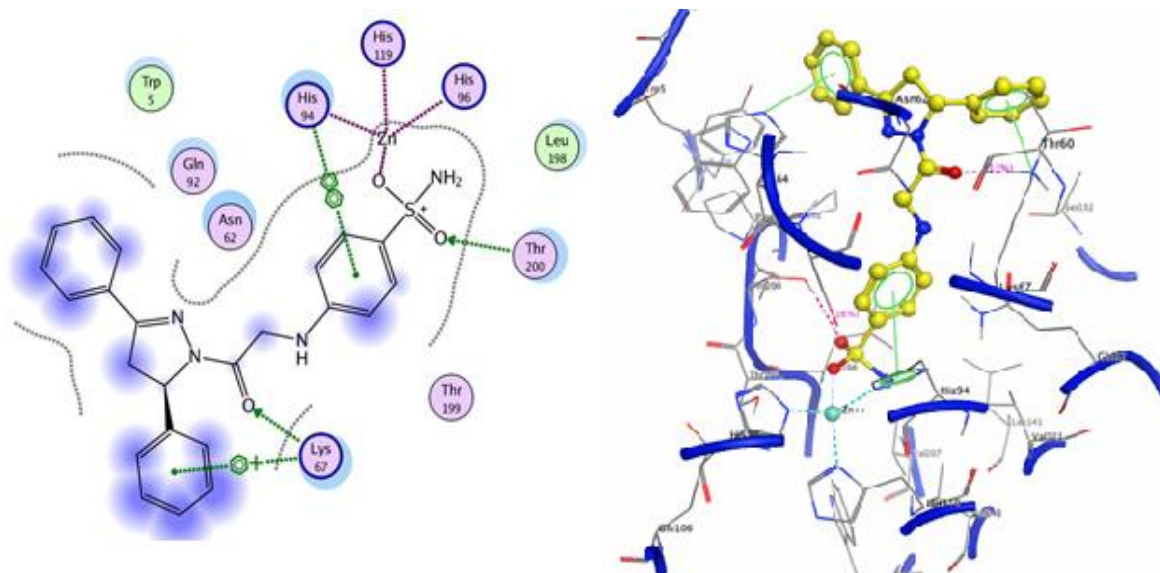
Figure (3.12): 2D Binding interaction and 3D structure of LVIII inside the active site of hCAXII
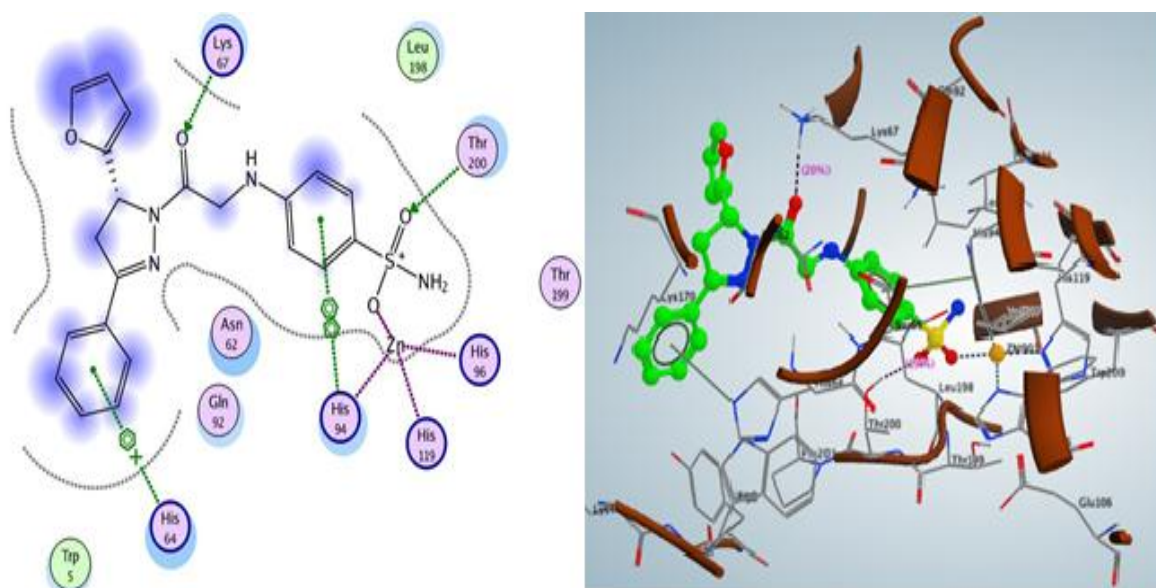
Figure (3.13): 2D Binding interaction and 3D structure of LXII inside the active site of hCAXII
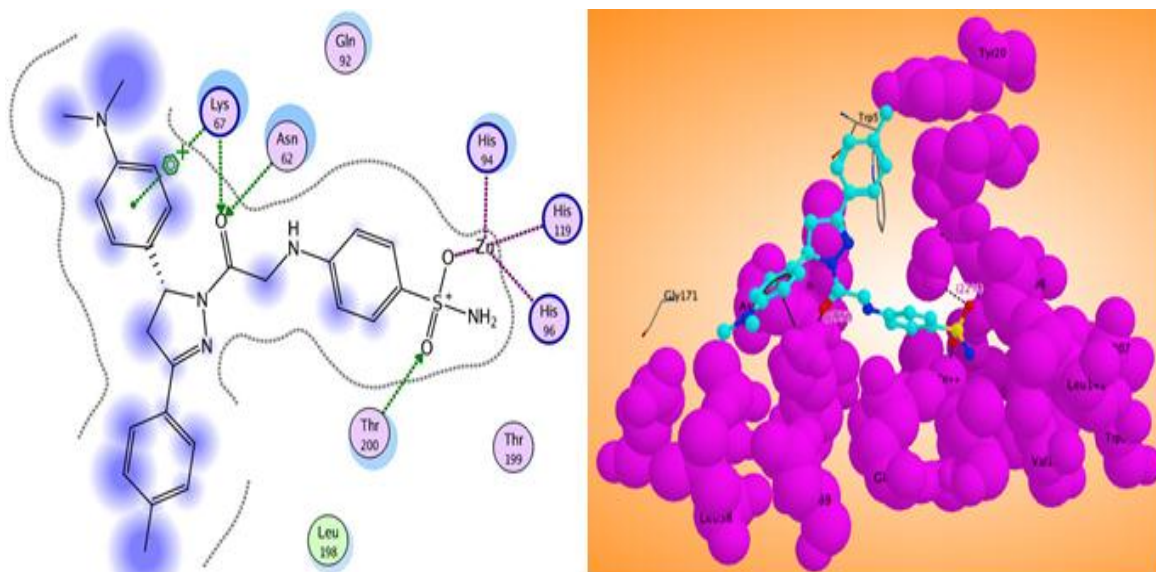
Figure (3.14): 2D Binding interaction and 3D structure of LXVI inside the active site of hCAXII
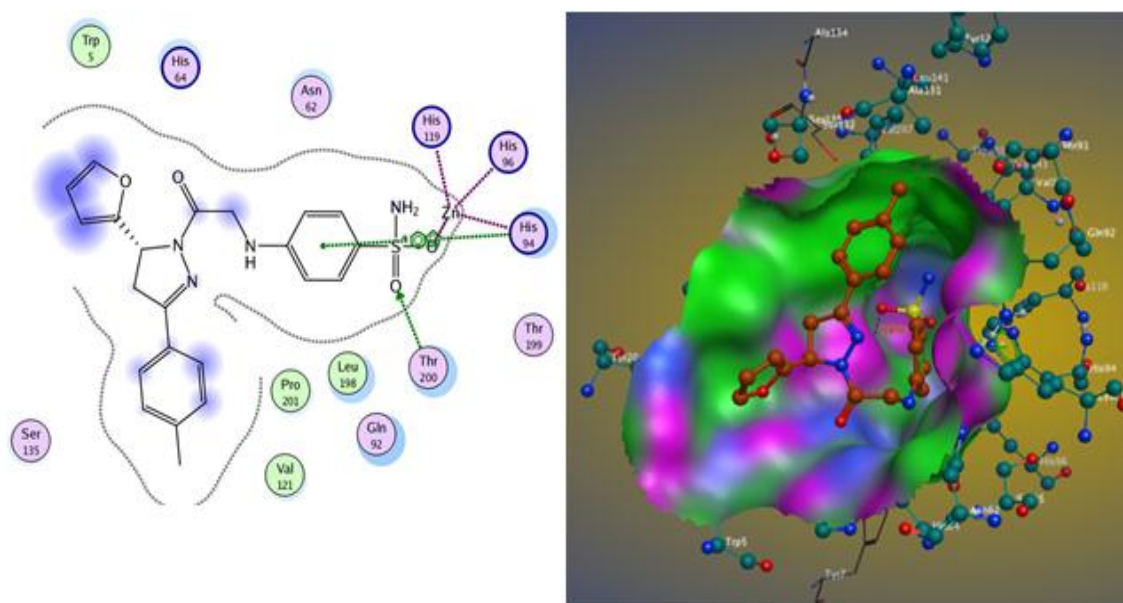
Figure (3.15): 2D Binding interaction and 3D structure of LXVII inside the active site of hCAXII

A number of human malignancies exhibit sustained stimulation, mutation or gene amplification of the receptor tyrosine kinase human mesenchymal-epithelial transition factor (c-Met) (Eathiraj *et al*., 2011).

The over expression and mutations of c-Met and its natural ligand, hepatocyte growth factor (HGF), have been found in different types of tumors including breast, ovarian, colorectal, lung, gastric, pancreatic, melanoma, prostate, head and neck, glioma, hepatocellular, renal and a number of sarcomas. The protein 3DKC is the crystal structure of c-Met kinase in complex with ATP which is widely used in docking study (Ye *et al*., 2017).

Synthesized α,β-unsaturated carbonyl derivatives were selected to predict their binding interaction on c-Met kinase. Figure (3.16) shows structure of c-Met kinase that was imported from PDB using ID 3DKC, and the structure of it after protein preparation.
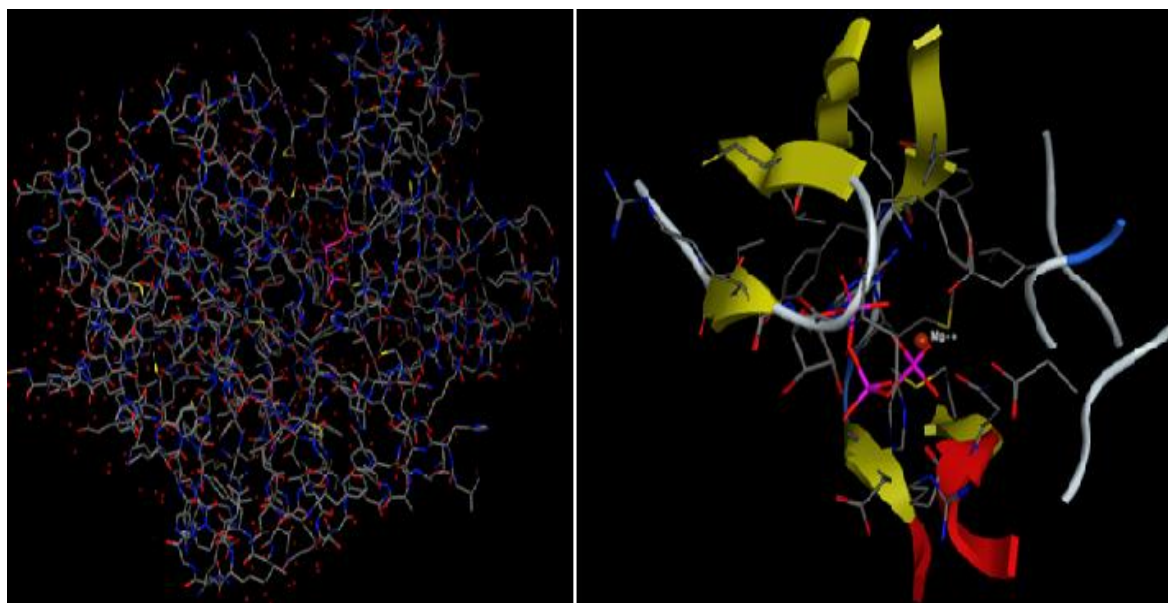
Figure (3.16): Structure of c-Met kinase that was imported from PDB using ID 3DKC before and after preparation

α,β-unsaturated carbonyl derivatives were docked on the active site of 3DKC. The result suggested that all compounds were capable of forming a metal complex with the Mg ion through Asp1222 (bond length 2.10 Å) and Asn1209 (bond length 2.03 Å). Compound VIII showed three

interactions, beside two interactions mentioned above, one π-cation interaction was revealed between Arg1208 residue with phenyl ring of 4-bromo benzoyl moiety figure (3.17) and all other figures can be found in the appendix C. Docking score of these compounds ranging between -22.9170 to -16.1714 kcal/mol. The energy score (S) of the complexes between each α,β-unsaturated carbonyl derivatives and the active site of the 3DKC as well as amino acid interacted are listed in table (2.33).
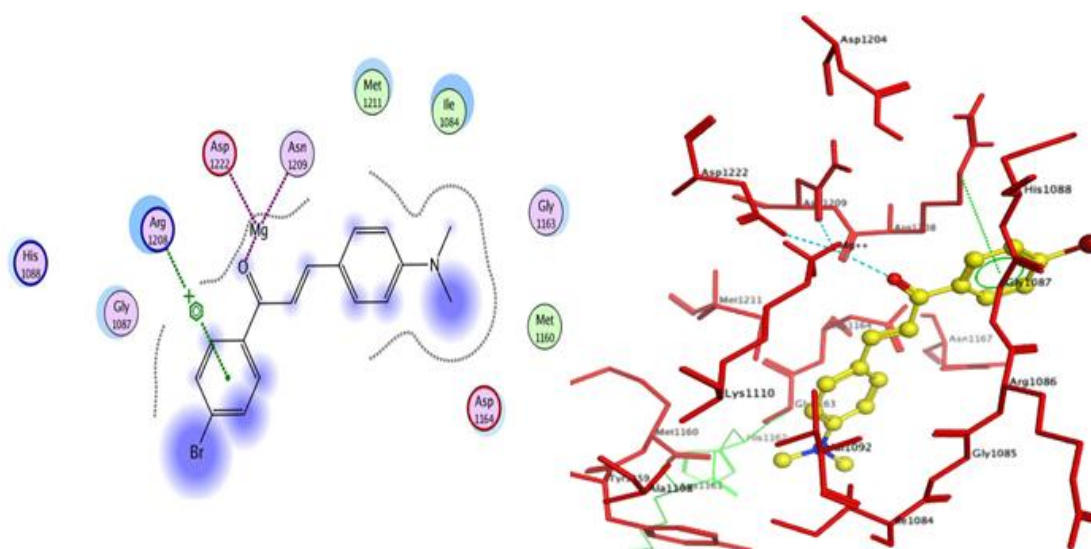
Figure (3.17): 2D Binding interaction and 3D structure of VIII inside the active site of 3DKC

4. Conclusion and Recommendation

In summary, the following points can be concluded according to this study:

- Two QSAR models were developed, and they were statistically significant and predictive, and could be used for the design and synthesis of new anti-cancer molecules against breast cancer MCF-7.
- First model showed that the anti-cancer activity was positively correlated with density and negatively correlated with log P(o/w) partition coefficient and ionization potential. This model was used to predict the anti-cancer activity of designed 120 pyrazoline derivatives
- Second model showed that there was positive correlation between the anti-cancer activity, density and log P(o/w) partition coefficient, and negative correlation with potential energy. Developed model was used to predict the activity of designed 16 α-β unsaturated carbonyl derivatives.
- 33 out of 120 designed pyrazoline derivatives and all α-β unsaturated carbonyl derivatives were selected for synthesis according to Lipinski's "rule of five".
- Total of 71 compounds were synthesized in synthetic part, including the intermediates.
- The reactions of synthesized trisubstituted pyrazoline derivatives were followed by TLC, and their structures were characterized using spectroscopic analysis such as IR, UV, GC-MS and ^{1}H-NMR.
- Molecular docking studies were carried out to investigate the interaction between the cancer proteins and synthesized

trisubstituted pyrazoline derivatives, α-β unsaturated carbonyl derivatives.

- There was a good correlation between QSAR and docking results.

- Further research can be carried out on synthesized compounds (LVIII, LXII, LXVI and LXVII) to investigate their *in vitro* anticancer activity against breast cancer MCF-7.

4. References

➤ Abdel-Sayed, M. A,; Bayomi, S. M.; El-Sherbeny, M. A.; Abdel-Aziz, N. I.; Eltahir, K. E. H.; Shehatou, G. S. G. & Abdel-Aziz, A. A. M. (2016); Synthesis, Anti-inflammatory, Analgesic, COX-1/2 Inhibition Activities and Molecular Docking Study of Pyrazoline Derivatives; *Bioorganic and Medicinal Chemistry*, 24(9), 2032–2042.

➤ Aboul-Enein, M. N.; El-Azzouny1, A. A.; Amin, K. M.; Maklad, Y. A.; Attia, M. I. & El-Behairy, M. F. (2014); Pyrazolines with Anticonvulsant and MAO Inhibitory Activities; *Journal of Pharmaceutical Sciences*, 49, 242-252.

➤ Acharya, B. N.; Saraswat, D.; Tiwari, M.; Shrivastava, A. K.; Ghorpadea, R.; Bapnab, S. & Kaushik, M. P. (2010); Synthesis and Antimalarial Evaluation of 1, 3, 5-trisubstituted Pyrazolines; *European Journal of Medicinal Chemistry*, 45(2), 430–438.

➤ Ahmed, M. G.; Romman, U. K. R.; Ahmed, S. M.; Akhter, K. & Halima, M. E. (2007); Synthesis and Correlation of Spectral Properties of Some Substituted 1,3-Diphenyl-2-Propen-1-Ones; *Bangladesh Journal of Scientific and Industrial Research*, 42(1), 45-52.

➤ Alam, M. J.; Alam, O.; Alam, P. & Naim, M. J. (2015); A Review on Pyrazole Chemical Entity and Biological Activity; *International Journal of Pharma Sciences and Research*, 6(12), 1433-1442.

➤ Ali, M. A.; Shaharyar, M. & Siddiqui, A. A. (2007); Synthesis, Structural Activity Relationship and Anti-tubercular Activity of

Novel Pyrazoline Derivatives; *European Journal of Medicinal Chemistry*, 42(2), 268-275.

➤ Alvarez-Builla, J. & Barluenga, J. (2011); Modern Heterocyclic Chemistry; 1st Edition; Wiley-VCH Verlag GmbH & Co. KGaA.

➤ Avupati, V. R. & Yejella, R. P. (2014); Bioactive Pyrazolines: An Update; *World Journal of Pharmaceutical Research*, 3(8), 1181-1215.

➤ Azarifar, D; Khosravi, K. & Veisi, R. (2010); An Efficient Oxidation of 2-pyrazolines and Isoxazolines by Bisbromine-1,4-diazabicyclo[2.2.2]octane Complex (DABCO-Br2); *Archive for Organic Chemistry*, 9, 178-184.

➤ Bai, G.; Li, J.; Li, D.; Dong, C.; Han, X. & Lin, P. (2007); Synthesis and Spectrum Characteristic of Four New Organic Fluorescent Dyes of Pyrazoline Compounds; *Dyes and Pigments*, 75, 93-98.

➤ Bajot, F. (2010); The Use of QSAR and Computational Methods in Drug Design; 8th edition, New York, Springer Science & Business Media B.V.

➤ Balaji. P. N.; Sreevani, M. S.; Harini, P.; Rani, P. J.; Prathusha, K. & Chandu. T. J. (2010); Antimicrobial Activity of Some Novel Synthesized Heterocyclic Compounds From Substituted Chalcones; *Journal of Chemical and Pharmaceutical Research*, 2(4),754-758.

➤ Bano, S.; Alam, M. S.; Javed, K.; Dudeja, M.; Das, A. K. & Dhulap, A. (2015); Synthesis, Biological Evaluation and Molecular Docking of Some Substituted Pyrazolines and Isoxazolines as

Potential Antimicrobial Agents; *European Journal of Medicinal Chemistry*, 95, 96-103.

➤ Barua, H.; Bhagat, N. & Toraskar, M. P. (2017); Study of Binding Interactions of Human Carbonic Anhydrase XII; International *Journal of Current Pharmaceutical Research*, 9(1), 118-125.

➤ Basaif, S. A.; Faidallah, H. M. & Hassan, S. Y. (1997); Synthesis and Biological Activity of New Pyrazoline and Pyrazole Derivatives; *Journal of King Abduaziz University*, 9, 83-90.

➤ Blair, M. & Sperry, J. (2013); Natural Products Containing a Nitrogen−Nitrogen Bond Lachlan; *Journal of Natural Products*, 76, 794-821.

➤ Boudiar, T.; Hichem, L.; Khalfallah, A.; Kabouche, A., Kabouche, Z.; Brouard, I.; Bermejo, J. & Bruneau, C. (2010); A New Alkaloid and Flavonoids From The Aerial Parts of Euphorbia Guyoniana; *Natural Product Communications*, 5(1), 35-37.

➤ Bush, J. W. M. (2011); Surface Tension Module, Research Gate.

➤ Chai, T. & Draxler, R. R. (2014); Root Mean Square Error (RMSE) or Mean Absolute Error (MAE) - Arguments Against Avoiding in The Literature; Geoscientific Model Development, 7, 1247-1250.

➤ Chimenti, F.; Fioravanti, R.; Bolasco, A.; Manna, F.; Chimenti, P.; Secci, D.; Rossi, F.; Turini, P.; Ortuso, F.; Alcaro, S. & Cardia, M. C. (2008); Synthesis, Molecular Modeling Studies and Selective Inhibitory Activity Against MAO of N1-propanoyl-3,5-diphenyl-4, 5-dihydro-(1H)-pyrazole Derivatives; *European Journal of Medicinal Chemistry*, 43(10), 2262-2267.

➢ Consonni, V. & Todeschini, R. (2010); Recent Advances in QSAR Studies; 8th edition, New York, Springer Science & Business Media B.V.

➢ Cronin, M. T. D. (2010); Quantitative Structure Activity Relationships (QSARs) – Applications and Methodology; 8th edition, New York, Springer Science & Business Media B.V.

➢ Danishuddin & Khan, A. U. (2016); Descriptors and Their Selection Methods in QSAR Analysis: Paradigm for Drug Design; *Drug Discovery Today*, 1-12.

➢ Das, B. C.; Bhowmik, D.; Bhattacharjee, C. & Mariappan, G. (2010); Synthesis and Biological Evaluation of Some Pyrazolines Derivatives; *Journal of Pharmacy Research*, 3(6), 1345-1348.

➢ Das, B. C.; Mariappan, G.; Saha, S. & Bhowmik, D. (2010); Anthelmintic and Anti-microbial Activity of Some Novel Chalcone Derivatives; *Journal of Chemical and Pharmaceutical Research*, 2(1), 113-120.

➢ Dimic, D.; Mercader, A. G. & Castro, E. A. (2015); Chalcone Derivative Cytotoxicity Activity Against MCF-7 Human Breast Cancer Cell QSAR Study; *Chemometrics and Intelligent Laboratory Systems*, 146, 378–384.

➢ Dorchies, O. M.; Reutenauer-Patte, J.; Dahmane, E.; Ismail, H. M.; Petermann, O.; Patthey-Vuadens, O.; Comyn, S. A.; Gayi, E.; Piacenza,T.; Handa, R. J.; Decosterd, L. A. & Ruegg, U. T. (2013); The Anticancer Drug Tamoxifen Counteracts the Pathology in a Mouse Model of Duchenne Muscular Dystrophy; *The American Journal of Pathology*, 182(2), 485-504.

➢ Eathiraj, S.; Palma, R.; Volckova, E.; Hirschi, M.; France, D. S.; Ashwell, M. A. &Chan, T. C. K. (2011); Discovery Of A novel Mode Of Protein Kinase Inhibition Characterized By The Mechanism Of Inhibition Of Human Mesenchymal-epithelial Transition Factor (c-Met) Protein Autophosphorylation By ARQ 197 ; *Journal of Biological Chemistry*, 23, 20666-20676.

➢ Eicher, T. & Hauptmann, S.; Speicher, A. (2003); The Chemistry of Heterocycles - Structures, Reactions, Synthesis, and Applications, 3rd edition. New York: John Wiley & Sons.

➢ Eisinger, J.; Boens, N. & Flores, J. (1981); Fluorescence Polarization Study of Human Erythrocyte Membranes with 1-phenyl-3-(2-naphthyl)-2- pyrazoline as Orientational Probe; *Biochimica et Biophysica Acta*, 646, 334-343.

➢ Elzupir, A. O.; Saeed, A. E. M.; Barakat, I. E. & Westhuizen, J. H. V. (2013); Ultrasound Irradiation Promoted Synthesis of Chalcones, Analogues, Homologues and Related Furanyl Containing Compounds and Their Antibacterial Activity; *International Journal of Current Pharmaceutical Research*, 5(4), 23–25.

➢ Evans, N. A.; Rivett, D. E. & Wilshire, J. F. K. (1974); The Chemical and Photochemical Properties of Some 1,3-Diphenyl-2-pyrazolines, *Australian Journal of Chemistry*, 27, 2267-74.

➢ George, R. F.; Fouad, M. A. & Gomaa, I. E. O. (2016); Synthesis and Cytotoxic Activities of Some Pyrazoline Derivatives Bearing Phenyl Pyridazine Core as New Apoptosis Inducers; *European Journal of Medicinal Chemistry*, 112, 48-59.

➢ Ghorab, M. M.; Ceruso, M.; Alsaid, M. S.; Yassin M. Nissan, Y. M.; Arafa, R. K. & Supuran, C. T. (2014); Novel Sulfonamides Bearing Pyrrole and Pyrrolopyrimidine Moieties as Carbonic Anhydrase Inhibitors: Synthesis, Cytotoxic Activity and Molecular Modeling; *European Journal of Medicinal Chemistry*, 87, 186-196.

➢ Gibbons, J. D. & Pratt, J. W. (1975); P-values: Interpretation and Methodology; *The American Statistician*, 29(1).

➢ Gimenez, B. G.; Santos, M. S.; Ferrarini, M. & Fernandes, J. P. S. (2010); Evaluation of blockbuster drugs under the Rule-of-five, Research Gate.

➢ Gowramma, B.; Jubie, S.; Kalirajan, R.; Gomathy, S. & Elango, K. (2009); Synthesis, Anticancer Activity of Some 1- (Bis N, N-(ChloroEthyl) - Amino Acetyl)-3, 5- Disubstituted 1, 2-Pyrazolines; *International Journal of PharmTech Research*, 1(2), 347-352.

➢ Guedes, I. A.; Magalhaes, C. S. & Dardenne, L. E. (2014); Receptor– Ligand Molecular Docking; Research Gate.

➢ Gupta, R.; Gupta, N. & Jaina, A. (2010); Improved Synthesis of Chalcones and Pyrazolines under Ultrasonic Irradiation*; Indian Journal of Chemistry*, 49B, 351-355.

➢ Hadi, A. A. (2012); Synthesis and Microbail Studies of Pyrazoline and its Derivatives; M.Sc. Thesis, Fergusson College, Pune University, India.

➢ Hansch, C.; Leo, A. & Hoekman, D. (1995); Exploring QSAR, Fundamentals and Application in Chemistry and Biology, American Chemical Society, Washington, DC, USA.

- Hidnert, P. & Peffer, E. L. (1950); Density of Solids and Liquids; *National Bureau of Standards Circular*, 1-28.

- Hirata, K.; Takashina, J.; Nakagami, H.; Ueyama, S.; Murakami, K.; Kanamori, T. & Miyamoto, K. (1996); Growth Inhibition of Various Organisms by a Violet Pigment, Nostocine A, Produced by Nostoc Spongiaeforme; *Bioscience Biotechnology and Biochemistry*, 60 (11), 1905-1906.

- Imai, T. (2007); Molecular Theory of Partial Molar Volume and Its Applications to Biomolecular Systems; *Condensed Matter Physics*, 10(3), 343–361.

- Jade, D. D. (2016); Introduction to Methods for Molecular Docking and HT Virtual Screening; *Research Gate*.

- Jadhav, S. A.; Kulkarni, K. M.; Patil, P. B.; Dhole, V. R. & Patil, S. S. (2016); Design, Synthesis and Biological Evaluation of Some Novel Pyrazoline Derivatives; *Der Pharma Chemica*, 8(3), 38-45.

- Jagadish, P. C.; Soni, N. & Verma, A. (2013); Design , Synthesis , and In Vitro Antioxidant Activity of 1 , 3 , 5-Trisubstituted-2-pyrazolines Derivatives, *Journal of Chemistry,* 1-6.

- Jayaprakash, V.; Barij N. Sinha, B. N.; Ucar, G. & Ercan, A. (2008); Pyrazoline-based Mycobactin Analogues as MAO-Inhibitors; *Bioorganic & Medicinal Chemistry Letters*, 18(24), 6362–6368.

- Joshi, V. D.; Kshirsagar, M. D. & Singhal, S. (2012); Synthesis and Antimicrobial Activities of Various Pyrazolines From Chalcones; *International Journal of ChemTech Research*, 4(3), 971-975.

➢ Kaithwal, M. K.; Garg, P. & Ahmad, S. (2009); Synthesis and Antimicrobial Activity of Some Novel Chalcones and Their Related Compounds; *Oriental Journal of Chemistry*, 25(4), 935-943.

➢ Kandeel, M. M.; Abbady, M. S. & Youssef, M. S. K. (2002); Some Reactions of 3-Methyl-5-oxo-1-phenyl-Δ2 -pyrazoline-4-thiocarbohydrazide; *Bulletin of the Korean Chemical Society*, 23(1), 41-47.

➢ Kaplancikli, Z. A.; Turan-Zitouni, G.; Ozdemir, A.; Can, O. D. & Chevallet, P. (2009); Synthesis and Antinociceptive Activities of Some Pyrazoline Derivatives; *European Journal of Medicinal Chemistry*, 44(6), 2606–2610.

➢ Karuppasamy, M.; Mahapatra, M.; Yabanoglu, S.; Ucar, G.; Sinha, B. N.; Basu, A.; Mishra, N.; Ashoke Sharon, A.; Kulandaivelu, U. & Jayaprakash, V. (2010); Development of Selective and Reversible Pyrazoline Based MAO-A Inhibitors: Synthesis, Biological Evaluation and Docking Studies; *Bioorganic & medicinal chemistry*, 18(5), 1875–1881.

➢ Kelekci, N.; Koyunoglu, S; Yabanoglu, S; Yelekci, K; Ozgene, O; Ucar, G; Erol, K; Kendi, E. & Yesilada, A. (2009); New Pyrazoline Bearing 4(3H)-quinazolinone Inhibitors of Monoamine Oxidase: Synthesis, Biological Evaluation, and Structural Determinants of MAO-A and MAO-B Selectivity; *Bioorganic & Medicinal Chemistry*, 17, 675–689.

➢ Krishna, P. R. & Sekhar, E. R. (2008); Lewis Acid and/or Lewis Base catalyzed [3+2] cycloaddition reaction: Synthesis of

Pyrazoles and Pyrazolines; *Tetrahedron Letters*, 49(48), 6768-6772.

➤ Kumar, K. A. & Govindaraju, M. (2015); Pyrazolines: Versatile Molecules of Synthetic and Pharmaceutical Applications-A Review; *International Journal of ChemTech Research*, 8(1), 313-322.

➤ Kumar, K. A. & Jayaroopa, P. (2013); Pyrazoles: Synthetic Strategies and Their Pharmaceutical Applications- An Overview; *International Journal of PharmTech Research*, 5(4), 1473-1486.

➤ Kuzmanovic, S. O. P.; Cvetkovic, D. D. & Barna, D. J. (2009); QSAR Analysis of 2-Amino or 2-Methyl-1-Substituted Benzimidazoles Against Pseudomonas aeruginosa; *International Journal Molecular Sciences*, 10, 1670-1682.

➤ Leach, A. R.; Gillet, V.J. (2007); An Introduction to Chemoinformatics; The Netherlands, Springer.

➤ Lednicer, D. & Mitscher, L. (2008); The Organic Chemistry of Drug Synthesis; John Wiley & Sons, Inc., Hoboken, New Jersey.

➤ Li, J. F.; Guan, B.; Li, D. X. & Dong, C. (2007); Study on The Fluorescence Properties of a New Intramolecular Charge Transfer Compound 1,5-diphenyl-3-(N-ethylcarbazole-3-yl)-2-pyrazoline; *Spectrochimica Acta Part A*, 68(2), 404–408.

➤ Li, J. T.; Zhang, X. H. & Lin, Z. P. (2007); An improved synthesis of 1, 3, 5-triaryl- 2-pyrazolines in acetic acid aqueous solution under ultrasound irradiation; *Beilstein Journal of Organic Chemistry*., 3, 1860-5397.

➢ Loh, W.; Quah, C. K.; Chia, T. S.; Fun, H.; Sapnakumari, M.; Badiadka Narayana, B. & Sarojini, B. K. (2013); Synthesis and Crystal Structures of N-Substituted Pyrazolines; *Molecules*, 18(2), 2386-2396.

➢ Lu, Z.; Jiang, Q.; Zhu, W.; Xie, M.; Hou, Y.; Chen, X. & Wang, Z. (2000); Novel Pyrazoline Derivative Used as Light Emitter in Blue Organic Electroluminescent Devices; *Synthetic Metals*, 111, 465–468.

➢ Marsili, L. (2013); Development of New Synthetic Methodologies Aimed to Poly-functionalize Heterocyclic Compounds having Biological Activity; PhD thesis, school of advanced studies, Universita di Camerino.

➢ Meng, X.; Zhang, H.; Mezei, M. & Cui, M. (2011); Molecular Docking: A Powerful Approach for Structure-Based Drug Discovery; *Current Computer-Aided Drug Design*, 7(2).

➢ Mishra, G.; Sehgal, D. & Valadi, J. K. (2017); Quantitative Structure Activity Relationship Study of the Anti-Hepatitis Peptides Employing Random Forests and Extra-trees regressors; *Bioinformation*, 13(3), 60-62.

➢ Mishra, S. K.; Sahoo, S.; Panda, P. K.; Mishra, S. R.; Mohanta, R. K.; Ellaiah, P. & Panda, C. S. (2007); Synthesis and Antimicrobial Activity of Some 1-(2,4-dinitrophenyl)-3-(3-nitrophenyl)-5-(4-substituted phenyl)-4-bromo-2- Pyrazolines and 1-(2,4-dinitrophenyl)-3-(3-nitrophenyl)-5-(4- substituted phenyl)-2-pyrazolin-4-ones; *Acta Poloniae Pharmaceutica* - Drug Research, 64(4), 359-364.

➢ Mukesh, B. & Rakesh, K. (2011); Molecular Docking: A review; *International Journal of Research in Ayurveda & Pharmacy*, 2(6), 1746-1751.

➢ Nantasenamat, C.; Ayudhya, C. I.; Naenna, T. & Prachayasittikul, V. (2009); Review Article: A practical Overview of Quantitative Structure Activity Relationship; *EXCLI Journal*, 8, 74-88.

➢ N'guessan, K. N.; Koné, M. G.; Bamba, K.; Patrice, O. W. & Ziao, N. (2017); Quantitative Structure Anti-Cancer Activity Relationship (QSAR) of a Series of Ruthenium Complex Azopyridine by the Density Functional Theory (DFT) Method, Computational, *Molecular Bioscience*, 7, 19-31.

➢ Nikitin, K. V. & Andryukhova, N. P. (1954); Chemistry of Heterocyclic Compounds; *Nature*, 174(5), 241-257.

➢ Osman, A. M.; Nour, A. H.; Ali, D. M. H.; Osman, H. A. & Saeed, A. E. M. (2016); Design and synthesis of 2-pyrazoline derivatives; *Der Pharmacia Lettre*, 8(1), 8-11.

➢ Pacak, P. (1989); Molar Refractivity and Interactions in Solutions I. Molar Refractivity of Some Monovalent Ions in Aqueous and Mimethyl Sulfoxide Solutions; *Chemical Papers*, 43(4), 489-500.

➢ Pallicer, J. M.; Roses, M; Rafols, C.; Bosch, E.; Pascual, R. & Port, A. (2014); Evaluation of log Po/w values of drugs from some molecular structure calculation software; *ADMET & DMPK*, 2(2), 107-114.

➢ Pant, G. J. N.; Singha, P.; Rawatb, B. S.; Rawata, M. S. M. & Joshib, G. C. (2011); Synthesis, Characterization and Fluorescence Studies of 3,5-diaryl Substituted 2-pyrazolines; Spectrochimica

Acta - Part A: *Molecular and Biomolecular Spectroscopy*, 78(3), 1075–1079.

➢ Patil, C. B.; Mahajan, S. K. & Suvarna A. Katti, S. A. (2009); Chalcone: A Versatile Molecule; *Journal of Pharmaceutical Science and Research*, 1(3), 11-22.

➢ Patel, H. M.; Noolvi, M. N.; Sharma, P.; Jaiswal, V.; Bansal, S.; Lohan, S.; Kumar, S. S.; Abbot, V.; Dhiman, S. & Bhardwaj, V. (2014); Quantitative Structure Activity Relationship (QSAR) Studies as Strategic Approach in Drug Discovery, *Medicinal Chemistry Research*, 23, 4991–5007.

➢ Pavia, D. L.; Lampman, G. M. & Kriz, G. S. (2001); Introduction to Spectroscopy- A Gide for Students of Organic Chemistry, 3rd edition, Thomson Learning, Inc.

➢ Pitucha, M.; Pachuta-Stec, A. & Kaczor, A. A. (2013); New Five-Membered Ring Heterocyclic Compounds With Antibacterial and Antifungal Activity, *Formatex*, 562-573

➢ Qin, Y.; Li, Y.; Jiang, A.; Yang, M.; Zhu, Q.; Dong, H. & Zhu, H. (2015); Design, Synthesis and Biological Evaluation of Novel Pyrazoline- Containing Derivatives as Potential Tubulin Assembling Inhibitors; *European Journal of Medicinal Chemistry*, 94, 447-457.

➢ Rahman, M. A. & Siddiqui, A. A. (2010); Pyrazoline Derivatives: A Worthy Insight into the Recent Advances and Potential Pharmacological Activities; *International Journal of Pharmaceutical Sciences and Drug Research*, 2(3), 165-175.

➢ Rathore, P.; Yaseen, S.; Ovais, S.; Bashir, R.; Yaseen, R.; Hameed, A. D.; Samim, M.; Gupta, R.; Hussain, F. & Javed, K. (2014); Synthesis and Evaluation of Some New Pyrazoline Substituted Benzenesulfonylureas as Potential Antiproliferative Agents; *Bioorganic & Medicinal Chemistry Letters*, 24(7), 1685–1691.

➢ Reddy, L. S. S.; Raju, M. B. & Sridhar, C. (2016); Novel Pyrazolines: Synthesis and Evaluation of Their Derivatives with Anticancer and Anti-inflammatory Activities*; International Journal of Pharmacy and Pharmaceutical Sciences*, 8(1), 247-254.

➢ Roy, K.; Kar, S. & Das, R. N. (2015); Statistical methods in QSAR/QSPR; SpringerBriefs in Molecular Science.

➢ Sahoo, A.; Parida, M.; Sinha, B. N. & Venkatesan, J. (2011); Antimicrobial Studies of Some New Novel Pyrazolne Derivatives; *International Journal of Research in Pharmacy and Chemistry*, 1(3), 458-464.

➢ Samuels, R. J. (1981); Application of Refractive Index Measurements to Polymer Analysis; *Journal of Applied Polymer Science*, 26, 1383-1412.

➢ Sauzem, P. D.; Machado, P.; Rubin, M. A.; Sant'Anna, G. S.; Faber, H. B.; Souza, A. H.; Mello, C. F.; Beck, P.; Burrow, R. A.; Bonacorso, H. G.; Zanatta, N. & Martins, M. A. P. (2008); Design and Microwave-assisted Synthesis of 5-trifluoromethyl-4,5-dihydro-1H-pyrazoles: Novel Agents with Analgesic and Anti-inflammatory Properties, *European Journal of Medicinal Chemistry*, 43(6), 1237-1247.

➢ Shahlaei, M. (2013); Descriptor Selection Methods in Quantitative Structure Activity Relationship Studies: Areview study, *Chemical Reviews*, 113(10), 8093–8103.

➢ Shan, Y.; Zhang, J.; Liu, Z.; Wang, M. & Dong, Y. (2011); Developments of Combretastatin A-4 Derivatives as Anticancer Agents, *Current Medicinal Chemistry*, 18, 523-538

➢ Sharma, S.; Kaurt, S.; Bansal, T. & Gaba, J. (2014); Review on Synthesis of Bioactive Pyrazoline Derivatives; *Chemical Science Transactions*, 3(3), 861-875.

➢ Sharma, V. & Sharma K. V. (2009); Synthesis and Biological Activity of Some 3, 5-Diarylisoxazoline Derivatives: Reaction of Substituted Chalcones with Hydroxylamine Hydrochloride; *E-Journal of Chemistry*, 6(2), 348-356.

➢ Shinde, S.; Jadhav, W.; Pawarb, R. & Bhusare, S. (2004); Synthesis and Antibacterial Activity of Some 3,5-Diphenyl and 1,3,5-Triphenyl-2-pyrazolines; *Journal of the Chinese Chemical Society*, 51, 775-778.

➢ Shinkar, S. A.; Shetty, V. J. & Jagdale, D. M. (2015); A review on Synthetic Approaches of Pyrazoline Derivatives*; World Journal of Pharmacy and Pharmaceutical Science*, 4(11), 505-514.

➢ Shomana, M. E.; Abdel-Aziz, M.; Alya, O. M.; Farag, H. H. & Morsy, M. A. (2009); Synthesis and Investigation of Anti-inflammatory Activity and Gastric Ulcerogenicity of Novel Nitric oxide-donating Pyrazoline Derivatives; *European Journal of Medicinal Chemistry*, 44(7), 3068–3076.

➢ Shukla, R. K.; Misra, P.; Sharma, S.; Tomar, N. & Jain, P. (2012); Refractive Index and Molar Refractivity of Benzonitrile, Chlorobenzene, Benzyl Chloride and Benzyl Alcohol with Benzene at T = 298.15, 303.15, 308.15 and 313.15 K; *Journal of the Iranian Chemical Society*, Research Gate.

➢ Sid, A.; Lamara, K.; Mokhtari, M.; Ziani, N. & Mosset, P. (2011); Synthesis and Characterization of 1-formyl-3-phenyl-5-aryl-2-pyrazolines; *European Journal of Chemistry*, 2(3), 311-313.

➢ Singh, S. K. (2009); Absolute potential energy; Open Stax CNX, 2-6.

➢ Smirnov, V. V.; Kiprianova E. A.; Garagulya A. D.; Esipov S. E. & Dovjenko, A. D. (1997); Fluviols, bicyclic nitrogen-rich antibiotics produced by Pseudomonas fluorescens*; Federation of European Micropiology Letters*, 153, 357-361.

➢ Sridhar, S. & Rajendraprasad, Y. (2012); Synthesis and Analgesic Studies of Some New 2- pyrazolines; *E-Journal of Chemistry*, 9(4), 1810-1815.

➢ Supriya, T.; Shankar, M.; Lalitha, S. K.; J. Dastgiri, J. & Babu, M. N. (2016); An Over View on Molecular Docking; *American Journal of Biological and Pharmaceutical Research*, 3(2), 83-89.

➢ Suri, M.; Jousseaume,T.; Neumann, J. J. & Glorius, F. (2012); An Efficient Copper-Catalyzed Formation of Highly Substituted Pyrazoles Using Molecular Oxygen as the Oxidant; *Green Chemistry*, 4(8), 166-1169.

➢ Syam, S; Abdelwahab, S. I.; Mohammed Ali Al-Mamary, M. A. & Mohan, S. (2012); Synthesis of Chalcones with Anticancer Activities; *Molecules*, 17, 6179-6195.

➢ Tripathi, A. & Misra, K. (2017); Molecular Docking: A Structure-Based Drug Designing Approach; *JSM Chemistry,* 5(2), 1042-1047

➢ Turan-Zitouni, G.; Ozdemir, A. & Zafer Asım Kaplancikli, Z. A. (2006); Synthesis and Antimicrobial Activities of Some 1-[(N,N-Disubstitutedthiocarbamoylthio)acetyl]-3,5-   diaryl-2-pyrazolines; *Phosphorus, Sulfur, and Silicon and the Related Elements*, 180(12), 2717-2724.

➢ Vaidya, S. S.; Vinaya, H. & Mahajan, S. S. (2012); Microwave-assisted Synthesis, Pharmacological Evaluation, and QSAR Studies of 1,3-diaryl-2-propen-1-ones; *Medicinal Chemistry Research*, Springer Science & Business Media, LLC.

➢ Verma, J.; Khedkar, V. M. & Coutinho, E. C. (2010); 3D-QSAR in Drug Design - A Review; *Current Topics in Medicinal Chemistry*, 10, 95-115.

➢ Venkataraman, S.; Jain, S.; Shah, K. & Upmanyu, N. (2010); Synthesis and Biological Activity of Some Novel Pyrazolines; *Acta Poloniae Pharmaceutica - Drug Research*, 67(4), 361-366.

➢ Winkler, D. A. (2001); The Role of Quantitative Structure Activity Relationships (QSAR) in Biomolecular Discovery; *Briefings in Bioinformatics*, 3(1), 73-86.

➢ Yadav, D. K.; Ahmad, I.; Shukla, A.; Khan, F.; Negi, A. S. & Gupta, A. (2014); QSAR and Docking Studies on Chalcone

Derivatives for Antitubercular Activity Against M. tuberculosis $H_{37}Rv$; *Journal of Chemometrics*, 28(6), 499–507.
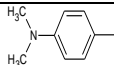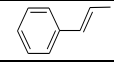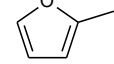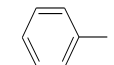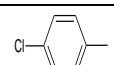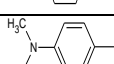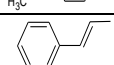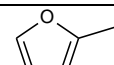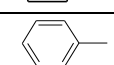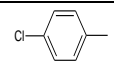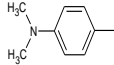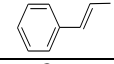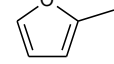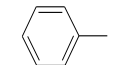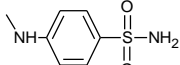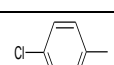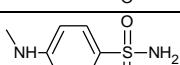
➢ Yadav, D. K.; Kumar, S.; Saloni, ; Singh, H.; Kim, M.; Sharma, P.; Misra, S. & Khan, F. (2017); Molecular Docking, QSAR and ADMET Studies of Withanolide Analogs Against Breast Cancer; Drug Design, *Development and Therapy*, 11, 1859–1870.

➢ Yahya, T. A. A.; Abdullaha, J. H.; Al-Ghorafib, M. A. & Yassin, S. H. (2014); Synthesis and Evaluation of Some Pyrazoline Derivatives as Anticancer Agents; *Journal of Chemical and Pharmaceutical Research*, 6(11), 234-238.

➢ Yakovleva, K. V.; Petrova, D. V.; Dokicheva, V. A. & Tomilovb, Y.V. (2009); Synthesis of 3-Substituted Pyrazoles by Oxidative Dehydrogenation of 4,5-Dihydro-3H-pyrazoles; *Russian Journal of Organic Chemistry*, 45, 950–952.

➢ Ye, L.; Wu, J.; Chen, W.; Feng, Y. & Shen, Z. (2017); Novel Anti-cancer Agents Based on Germacrone: Design, Synthesis, Biological Activity, Docking Studies and MD Simulations; *Royal Society of Chemistry Advances*, 7, 3760-3767.

➢ Yusuf, M. & Jain, P. (2014); Synthetic and biological studies of pyrazolines and related heterocyclic compounds; *Arabian Journal of Chemistry*, 7, 553–596.
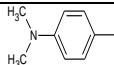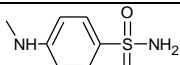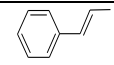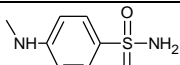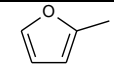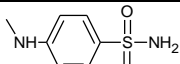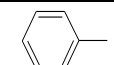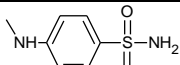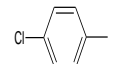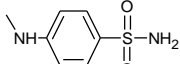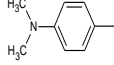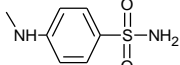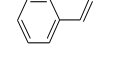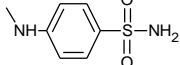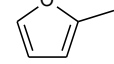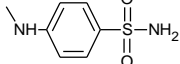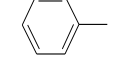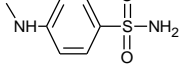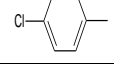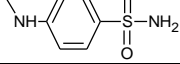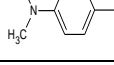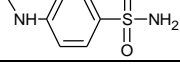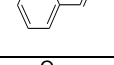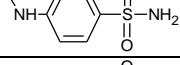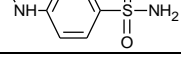
5. APPENDIX
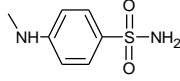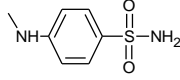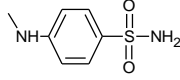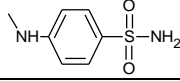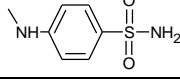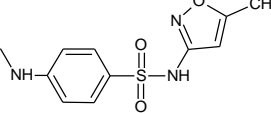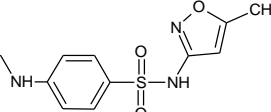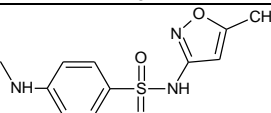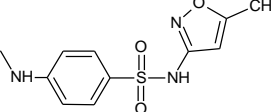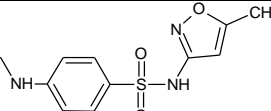
5.1. Appendix A: Designed trisubstituted 2-pyrazoline derivatives
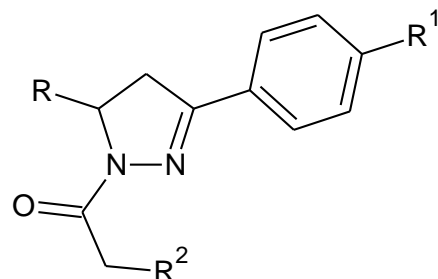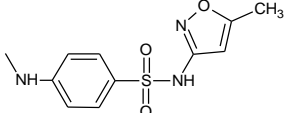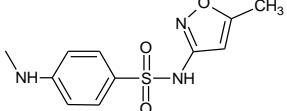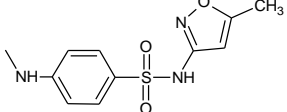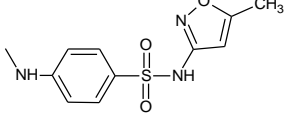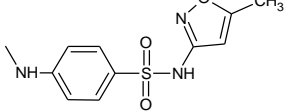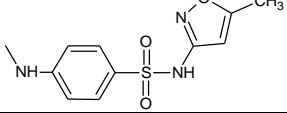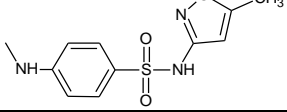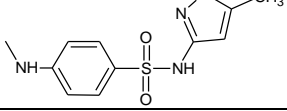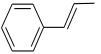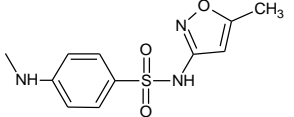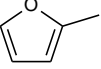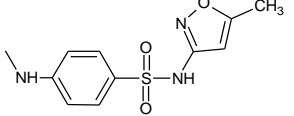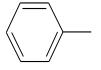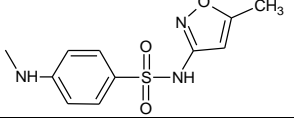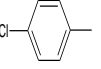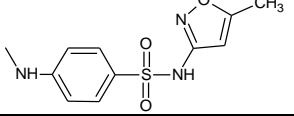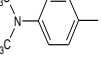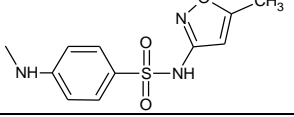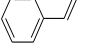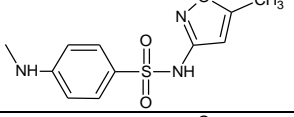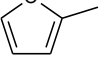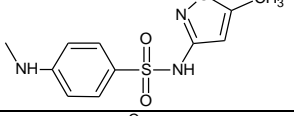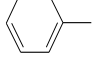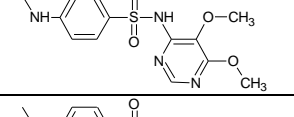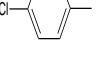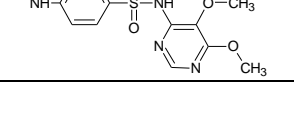
Compound No	R	R^1	R^2	MW	D	logP(o/w)	IP	Number of hydrogen bond donors	Number of hydrogen bond acceptors	Predicted pIC_{50}
1		-H	-Cl	298.76	1.23	4.100	8.972	0	2	5.60
2		-H	-Cl	333.21	1.32	4.692	9.064	0	2	5.16
3		-H	-Cl	341.83	1.20	4.015	8.319	0	2	7.25
4		-H	-Cl	324.80	1.18	4.744	8.964	0	2	3.32
5		-H	-Cl	288.72	1.32	2.816	8.984	0	2	10.04
6		-Br	-Cl	377.66	1.47	4.899	9.066	0	2	6.79
7		-Br	-Cl	412.11	1.55	5.094	9.067	0	2	6.94
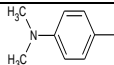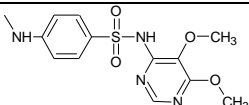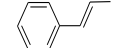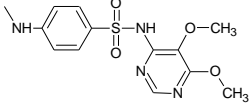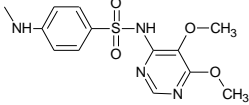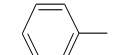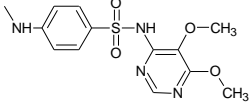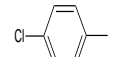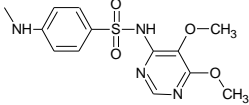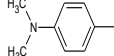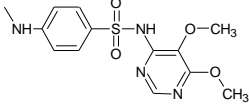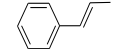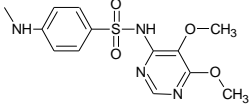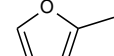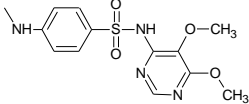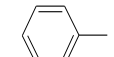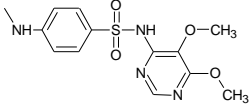
8	(structure)	-Br	-Cl	420.73	1.41	5.491	9.105	0	2	6.42
9	(structure)	-Br	-Cl	403.70	1.40	5.065	8.37	0	2	7.84
10	(structure)	-Br	-Cl	367.62	1.60	3.614	9.075	0	2	11.80
11	(structure)	-NO$_2$	-Cl	343.76	1.38	4.035	9.482	2	4	6.45
12	(structure)	-NO$_2$	-Cl	378.20	1.46	4.627	9.591	2	7	5.82
13	(structure)	-NO$_2$	-Cl	386.83	1.33	3.951	8.500	2	7	8.75
14	(structure)	-NO$_2$	-Cl	369.80	1.31	4.679	9.226	2	7	4.58
15	(structure)	-NO$_2$	-Cl	333.72	1.49	2.750	9.497	2	7	11.17
16	(structure)	-CH$_3$	-Cl	312.79	1.21	4.399	8.841	2	7	4.95
17	(structure)	-CH$_3$	-Cl	347.23	1.29	4.991	8.937	2	7	4.35
18	(structure)	-CH$_3$	-Cl	355.86	1.18	4.314	8.311	2	7	6.25
19	(structure)	-CH$_3$	-Cl	338.83	1.16	5.023	8.842	2	7	2.64
20	(structure)	-CH$_3$	-Cl	302.75	1.30	3.114	8.909	2	7	9.23
21	(structure)	-H	(structure)	434.51	1.34	3.237	9.022	0	2	9.17
22	(structure)	-H	(structure)	468.95	1.41	3.829	9.073	2	7	8.56
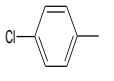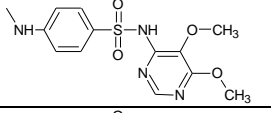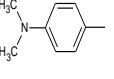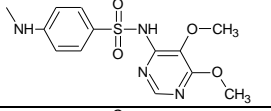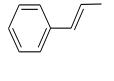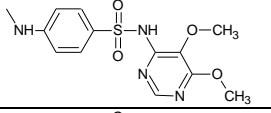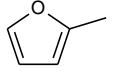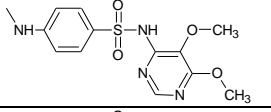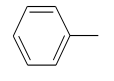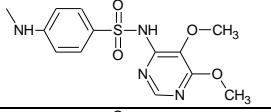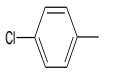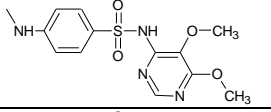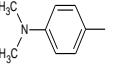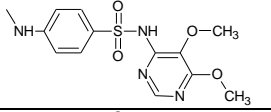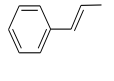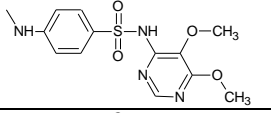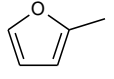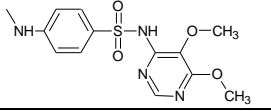
#	Structure	R	Structure						
23	(N,N-dimethylaminophenyl)	-H	(sulfonamide)	477.57	1.31	3.153	8.405	2	7	10.71
24	(styryl)	-H	(sulfonamide)	460.54	1.29	3.882	9.070	2	7	6.72
25	(furyl)	-H	(sulfonamide)	424.47	1.42	1.952	9.056	2	7	13.40
26	(phenyl)	-Br	(sulfonamide)	513.41	1.52	4.599	8.789	2	7	8.99
27	(chlorophenyl)	-Br	(sulfonamide)	547.85	1.58	2.670	8.830	2	7	14.69
28	(N,N-dimethylaminophenyl)	-Br	(sulfonamide)	556.47	1.47	4.318	8.610	2	7	9.42
29	(styryl)	-Br	(sulfonamide)	539.44	1.46	4.910	8.616	2	7	7.74
30	(furyl)	-Br	(sulfonamide)	503.36	1.62	4.233	8.330	2	7	12.29
31	(phenyl)	-NO$_2$	(sulfonamide)	479.50	1.46	4.664	8.613	2	7	8.38
32	(chlorophenyl)	-NO$_2$	(sulfonamide)	513.95	1.52	4.628	9.591	0	2	7.19
33	(N,N-dimethylaminophenyl)	-NO$_2$	(sulfonamide)	522.58	1.41	3.033	8.575	2	7	11.99
34	(styryl)	-NO$_2$	(sulfonamide)	505.55	1.40	3.951	8.501	0	2	9.65
35	(furyl)	-NO$_2$	(sulfonamide)	469.47	1.55	4.68	9.234	0	2	8.24
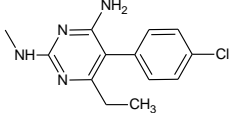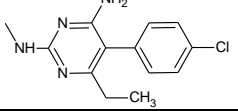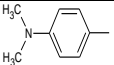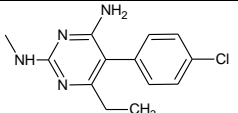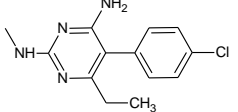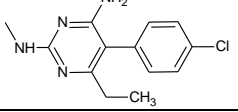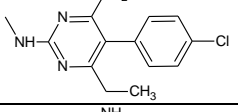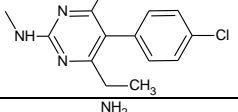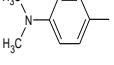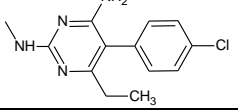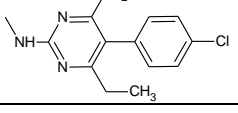
36		-CH$_3$		448.53	1.32	3.536	9.032	0	2	8.12
37		-CH$_3$		482.98	1.38	4.127	9.084	0	2	7.36
38		-CH$_3$		491.60	1.29	3.451	8.439	0	2	9.59
39		-CH$_3$		474.57	1.28	4.314	8.309	0	2	7.48
40		-CH$_3$		438.49	1.40	2.250	9.052	0	2	12.39
41		-H		515.58	1.36	3.114	8.912	0	2	10.38
42		-H		550.02	1.42	3.238	9.027	2	4	10.63
43		-H		558.65	1.33	3.83	9.069	2	4	7.78
44		-H		541.62	1.32	3.153	8.424	2	4	10.78
45		-H		505.55	1.43	3.882	9.072	2	4	9.01
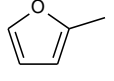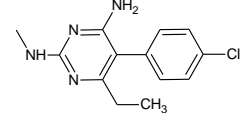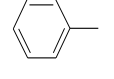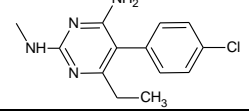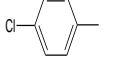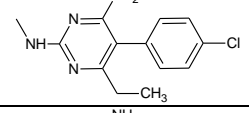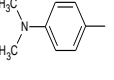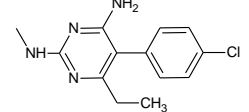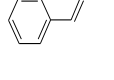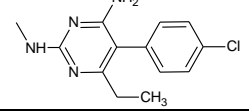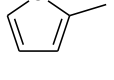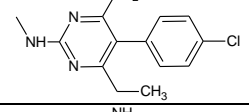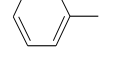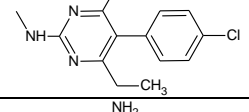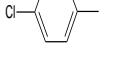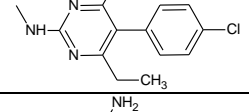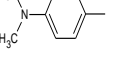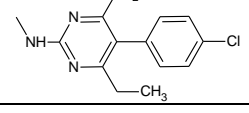
#										
46	[structure]	-Br	[structure]	594.48	1.52	1.953	9.054	2	4	15.25
47	[structure]	-Br	[structure]	628.92	1.57	4.036	9.053	2	4	10.56
48	[structure]	-Br	[structure]	637.55	1.48	4.628	9.127	2	4	7.65
49	[structure]	-Br	[structure]	620.52	1.47	3.951	8.478	2	4	10.65
50	[structure]	-Br	[structure]	584.44	1.60	4.68	9.110	2	4	9.19
51	[structure]	$-NO_2$	[structure]	560.58	1.46	2.751	9.135	2	4	12.20
52	[structure]	$-NO_2$	[structure]	595.03	1.52	3.173	9.223	2	4	11.74
53	[structure]	$-NO_2$	[structure]	603.65	1.42	3.765	9.285	2	4	8.72
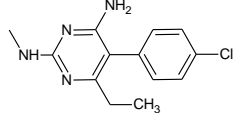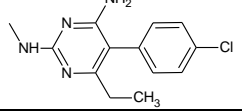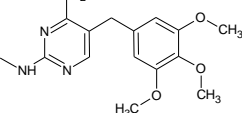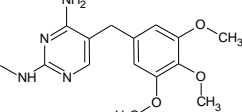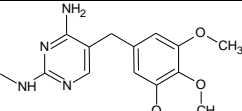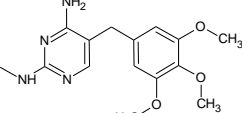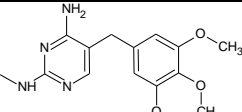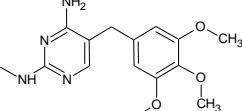
54		-NO$_2$		586.62	1.41	3.088	8.877	2	4	11.20
55		-NO$_2$		550.54	1.54	3.817	9.227	2	4	10.35
56		-CH$_3$		529.61	1.35	1.888	9.355	2	4	12.46
57		-CH$_3$		564.06	1.40	3.536	9.037	2	4	9.57
58		-CH$_3$		572.68	1.32	4.128	9.079	2	4	6.86
59		-CH$_3$		555.65	1.31	3.451	8.421	2	4	9.88
60		-CH$_3$		519.57	1.41	4.18	8.869	2	4	8.40
61		-H		572.63	1.36	2.251	9.049	2	4	12.31
62		-H		607.07	1.41	4.244	9.083	2	5	7.50
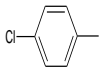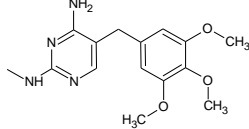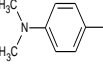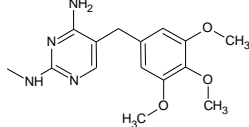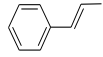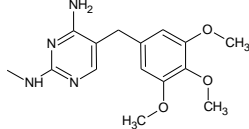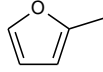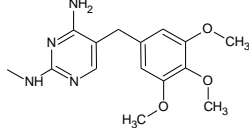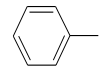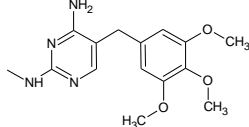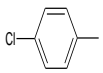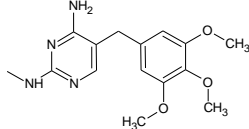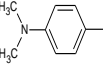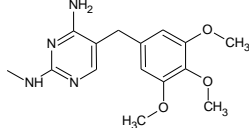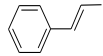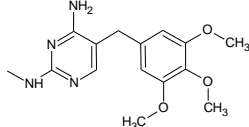
#	R₁	R₂	Structure							
63	(structure)	-H	(structure)	615.70	1.33	3.567	8.394	2	5	10.00
64	(structure)	-H	(structure)	598.67	1.32	4.422	8.409	2	5	7.54
65	(structure)	-H	(structure)	562.60	1.42	5.151	9.054	2	5	5.64
66	(structure)	-Br	(structure)	651.53	1.50	3.222	9.063	2	5	11.69
67	(structure)	-Br	(structure)	685.98	1.55	5.305	9.08	2	5	6.98
68	(structure)	-Br	(structure)	694.60	1.46	5.897	9.106	2	5	4.15
69	(structure)	-Br	(structure)	677.57	1.46	5.22	8.481	2	5	7.23
70	(structure)	-Br	(structure)	641.49	1.57	5.949	9.097	2	5	5.53
71	(structure)	-NO₂	(structure)	617.63	1.45	4.02	9.089	2	5	8.89
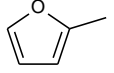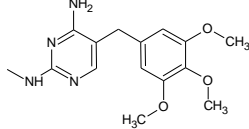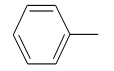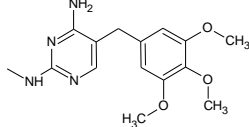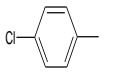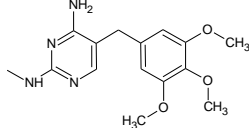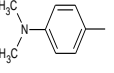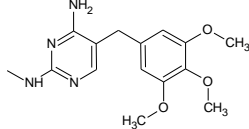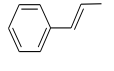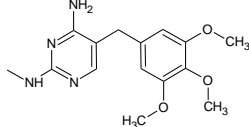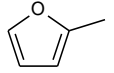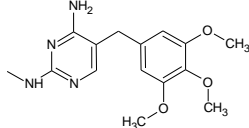
No.	Structure	R	Structure	MW						
72		-NO$_2$		652.08	1.50	4.442	9.221	2	5	8.19
73		-NO$_2$		660.70	1.41	5.034	9.263	2	5	5.35
74		-NO$_2$		643.67	1.41	4.357	8.567	2	5	8.59
75		-NO$_2$		607.59	1.52	5.086	9.256	2	5	6.74
76		-CH$_3$		586.66	1.35	3.950	8.948	2	5	7.76
77		-CH$_3$		621.11	1.40	4.805	9.0143	2	5	6.34
78		-CH$_3$		629.72	1.32	3.865	8.413	2	5	9.07
79		-CH$_3$		612.70	1.31	4.72	8.409	2	5	6.63
80		-CH$_3$		576.62	1.41	5.449	9.023	2	5	4.79

81		-H		511.02	1.31	3.52	9.057	2	5	8.34
82		-H		545.46	1.37	3.652	8.852	2	7	9.25
83		-H		554.09	1.29	4.245	9.088	2	7	6.13
84		-H		537.05	1.27	3.568	8.444	2	7	8.98
85		-H		500.97	1.38	4.297	8.961	2	7	7.49
86		-Br		589.91	1.47	2.368	8.910	2	7	13.81
87		-Br		624.36	1.51	4.451	9.043	2	7	8.69
88		-Br		632.98	1.43	5.043	9.067	2	7	6.024
89		-Br		615.95	1.42	4.366	8.655	2	7	8.52

90	(furan)	-Br	(structure)	579.88	1.54	5.095	8.868	2	7	7.82
91	(phenyl)	-NO$_2$	(structure)	556.01	1.41	3.165	8.989	2	7	10.76
92	(chlorophenyl)	-NO$_2$	(structure)	590.46	1.46	3.588	9.273	2	7	9.75
93	(dimethylaminophenyl)	-NO$_2$	(structure)	599.08	1.37	4.179	9.437	2	7	6.64
94	(styryl)	-NO$_2$	(structure)	582.05	1.36	3.503	8.728	2	7	9.77
95	(furan)	-NO$_2$	(structure)	545.98	1.48	4.232	9.341	2	7	8.21
96	(phenyl)	-CH$_3$	(structure)	525.04	1.30	2.303	9.285	2	7	10.85
97	(chlorophenyl)	-CH$_3$	(structure)	559.49	1.35	3.951	8.933	2	7	8.04
98	(dimethylaminophenyl)	-CH$_3$	(structure)	568.11	1.27	4.543	8.793	2	7	5.72

189

99		-CH₃		551.08	1.26	3.866	8.394	2	7	8.19
100		-CH₃		515.01	1.36	4.595	8.592	2	7	7.24
101		-H		552.62	1.28	2.666	8.734	2	7	10.83
102		-H		587.07	1.34	5.816	8.607	2	4	3.79
103		-H		595.69	1.26	6.408	8.633	2	4	1.11
104		-H		578.66	1.25	5.731	8.336	2	4	3.36
105		-H		542.59	1.34	6.46	8.698	2	4	1.93
106		-Br		631.52	1.43	4.531	8.637	2	4	8.27

107		-Br		665.96	1.47	6.614	8.722	2	4	3.26
108		-Br		674.59	1.39	7.206	8.757	2	4	0.56
109		-Br		657.56	1.38	6.529	8.392	2	4	2.96
110		-Br		621.48	1.49	7.258	8.699	2	4	1.92
111		-NO$_2$		597.62	1.37	5.329	8.753	2	4	5.14
112		-NO$_2$		632.07	1.42	5.751	8.818	2	4	4.59
113		-NO$_2$		640.69	1.34	6.343	8.842	2	4	1.92
114		-NO$_2$		623.66	1.33	5.666	8.494	2	4	4.28

115		-NO$_2$		587.58	1.43	6.395	8.807	2	4	3.09
116		-CH$_3$		566.65	1.27	4.466	8.773	2	4	5.96
117		-CH$_3$		601.09	1.32	6.114	8.649	2	4	2.65
118		-CH$_3$		609.72	1.25	6.706	8.605	2	4	0.27
119		-CH$_3$		592.69	1.24	6.029	8.274	2	4	2.59
120		-CH$_3$		556.61	1.33	6.758	8.596	2	4	1.24

5.2. Appendix B: Spectroscopic analysis figures
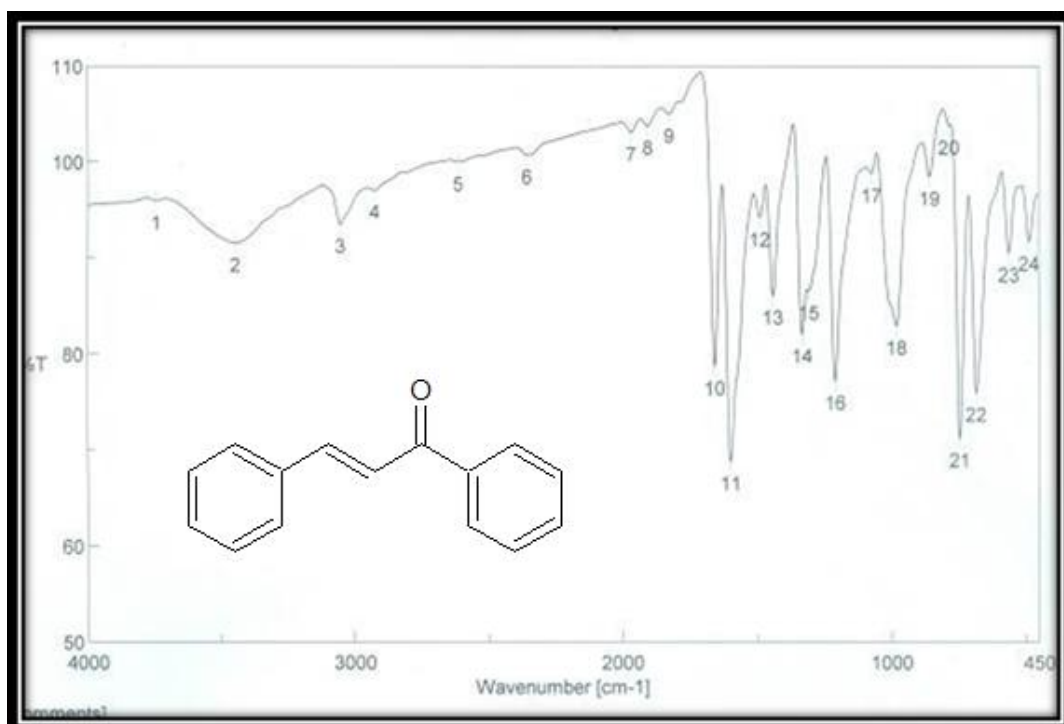
Figure (4.1): IR Spectrum of (2*E*)-1,3-diphenyl prop-2-en-1-one (**I**)
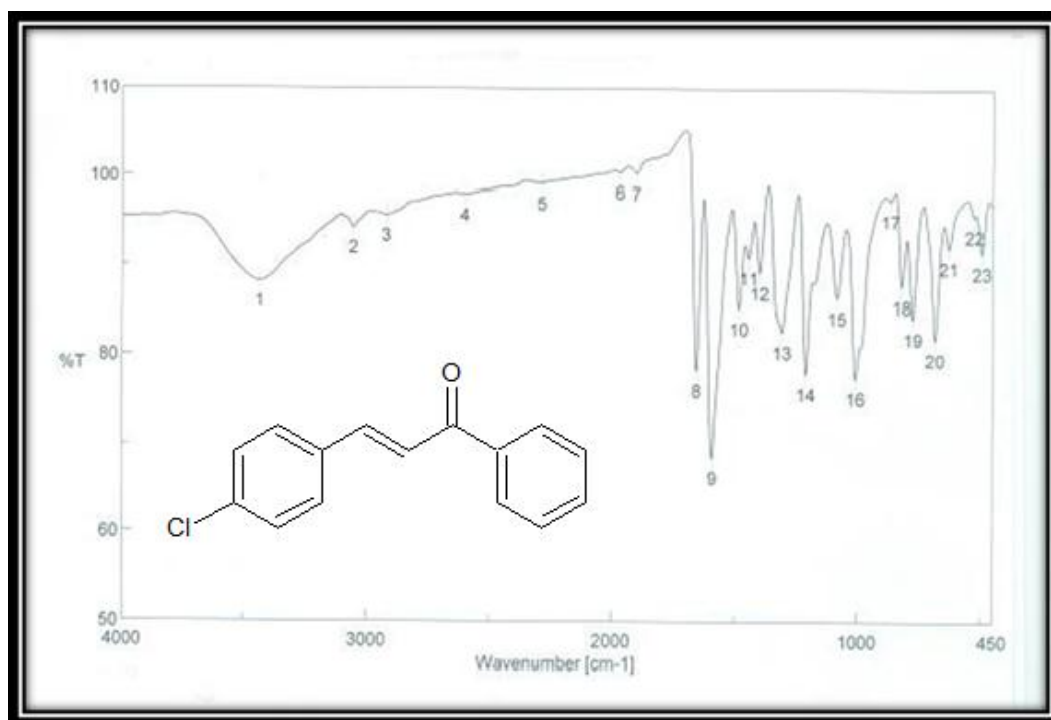
Figure (4.2): IR Spectrum of (2*E*)-3-(4-chloro phenyl)-1-phenyl prop-2-en-1-one (**II**)
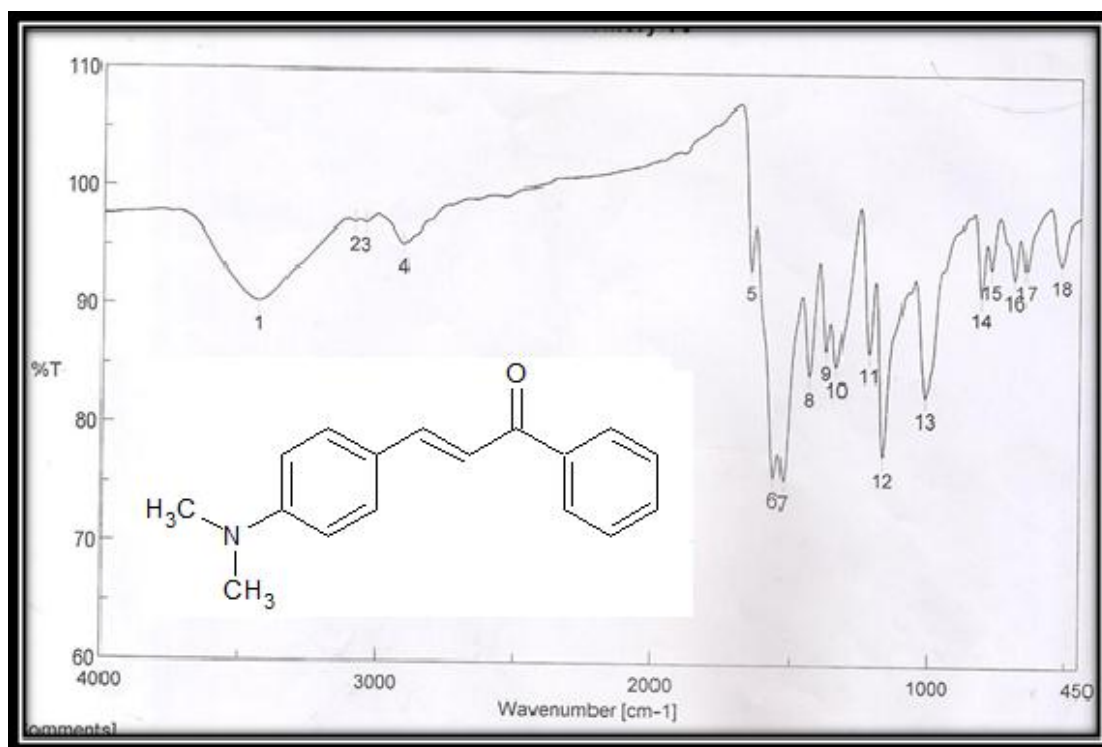
Figure (4.3): IR Spectrum of (2*E*)-3-[4-(dimethylamino)phenyl]-1-phenyl prop-2-en-1-one (**III**)
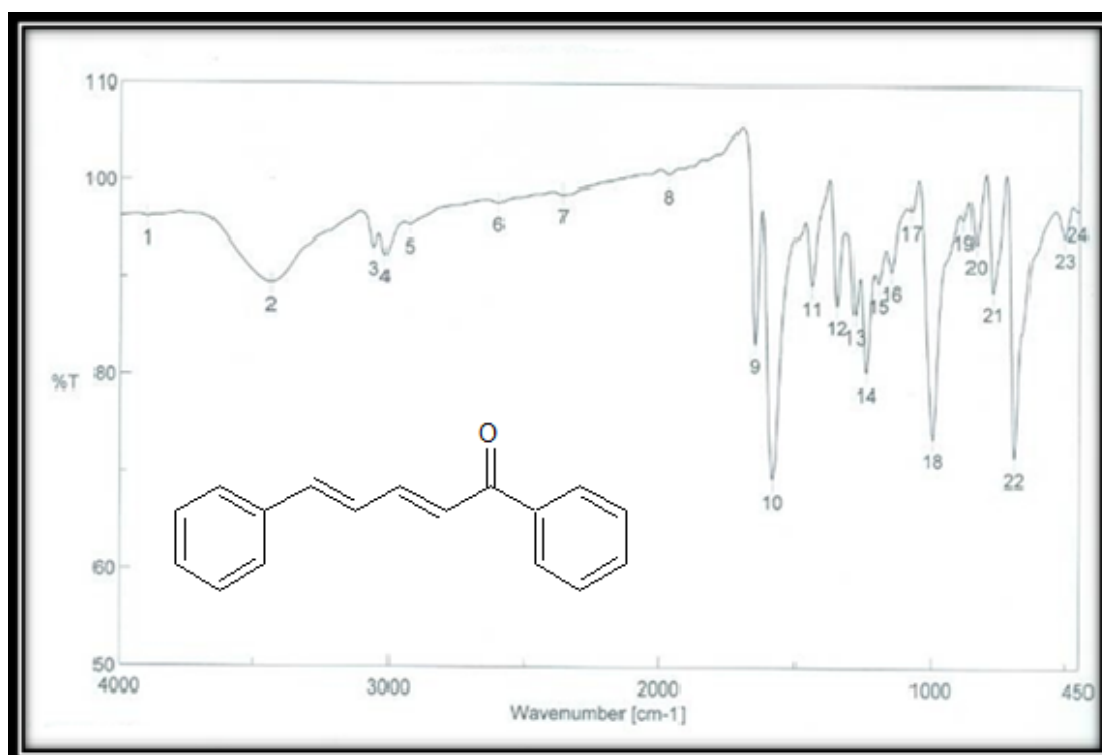
Figure (4.4): IR Spectrum of (2*E*,4*E*)-1,5-diphenylpenta-2,4-dien-1-one (**IV**)

194
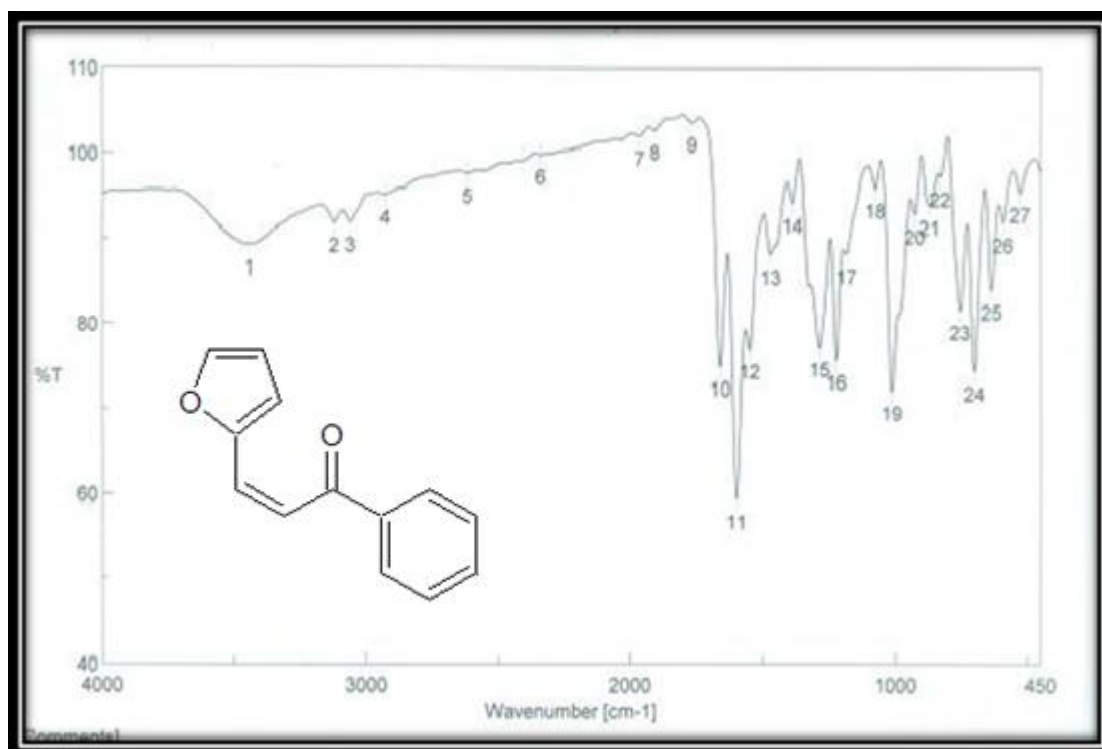
Figure (4.5): IR Spectrum of (2*Z*)-3-(furan-2-yl)-1-phenylprop-2-en-1-one (**V**)
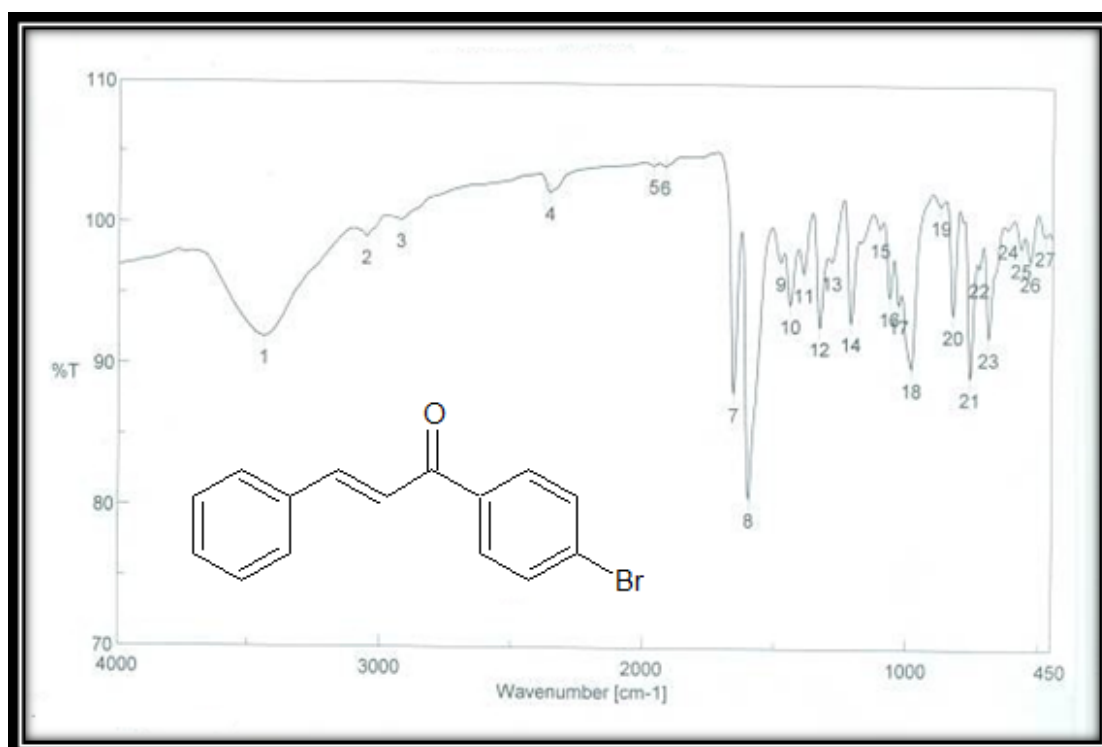
Figure (4.6): IR Spectrum of (2*E*)-1-(4-bromo phenyl)-3-phenyl prop-2-en-1-one (**VI**)
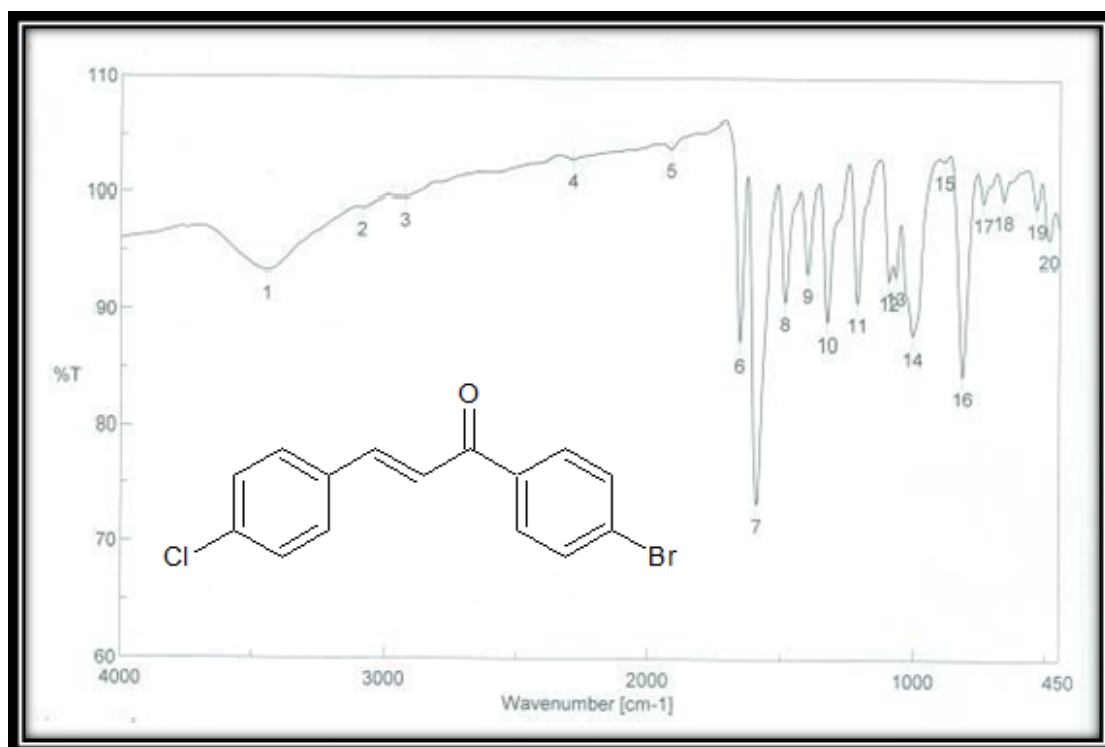
Figure (4.7): IR Spectrum of (2*E*)-1-(4-bromo phenyl-3-(4-chlorophenyl) prop-2-en-1-one (**VII**)
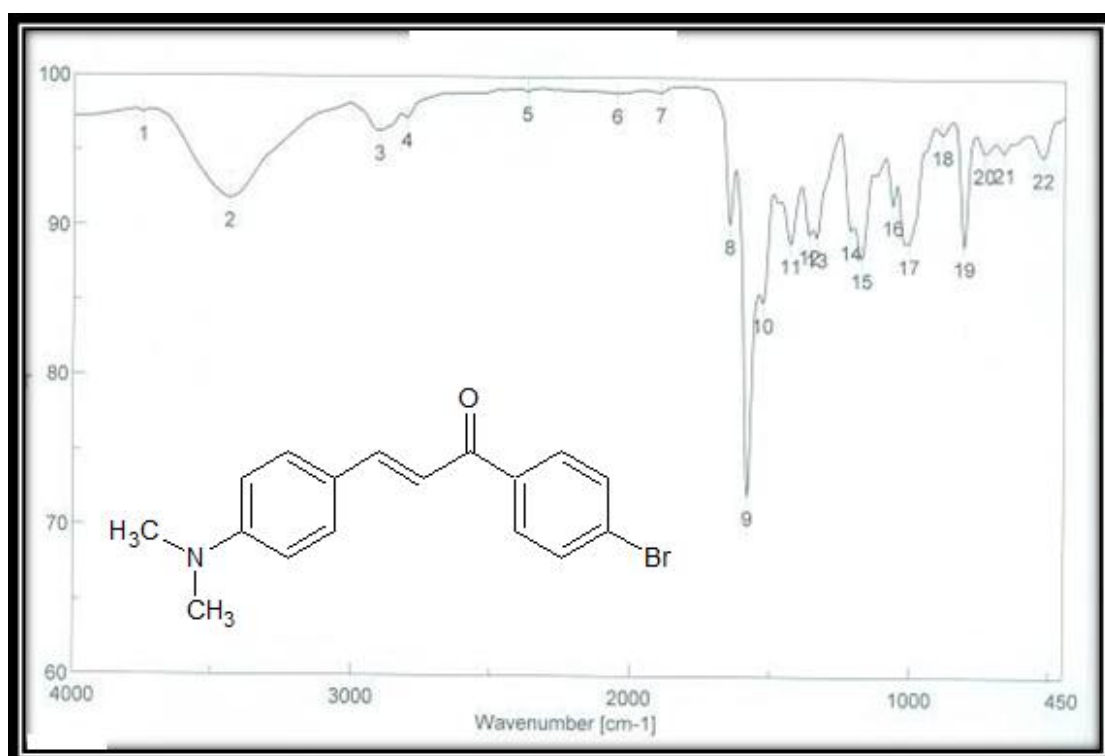
Figure (4.8): IR Spectrum of (2*E*)-1-(4-bromophenyl)-3-[4-(dimethylamino) phenyl]prop-2-en-1-one (**VIII**)
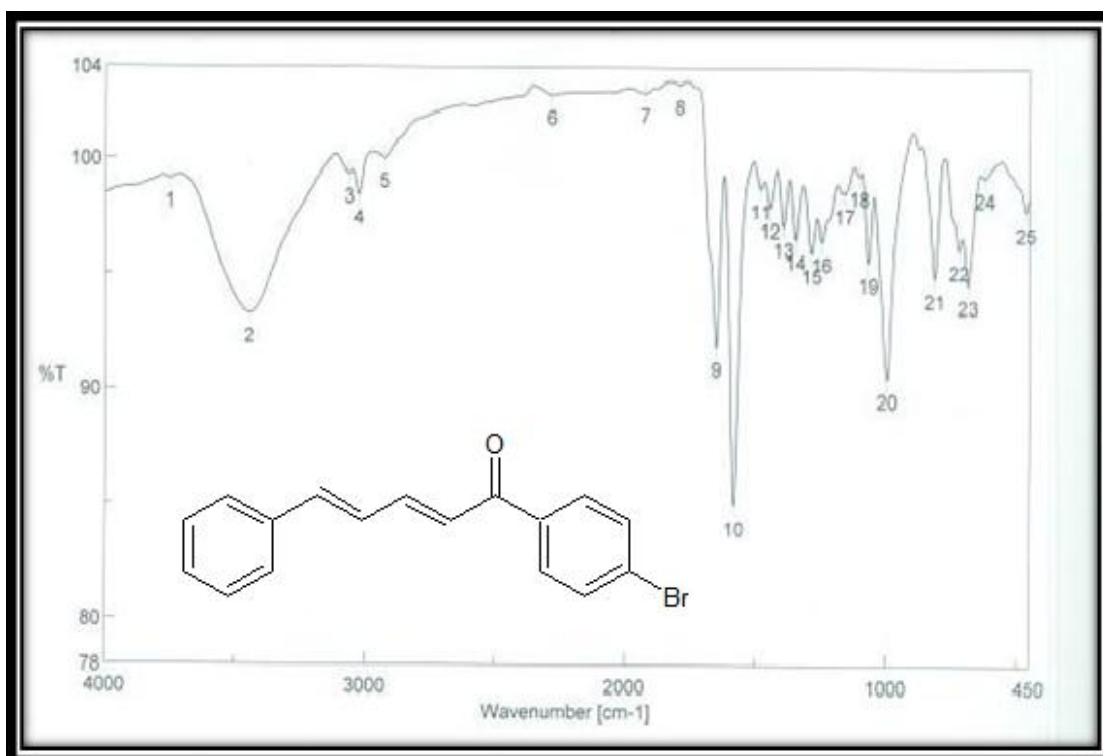
Figure (4.9): IR Spectrum of (2*E*,4*E*)-1-(4-bromo phenyl)-5-phenylpenta-2,4-dien-1-one (**IX**)
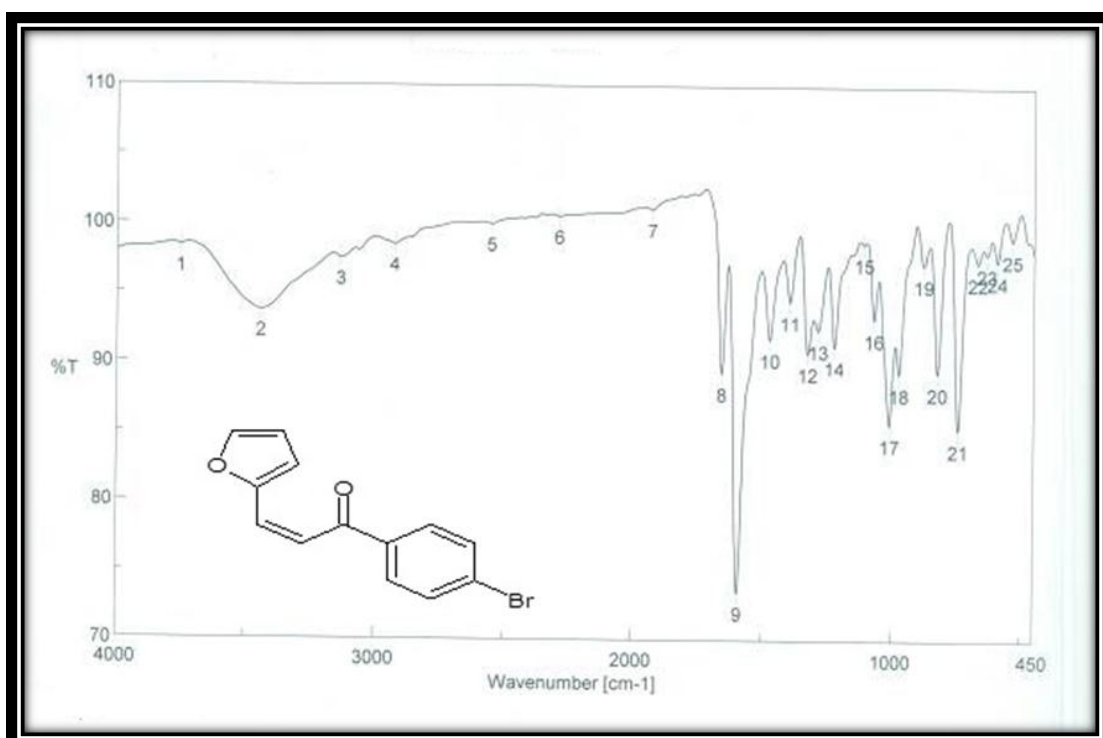
Figure (4.10): IR Spectrum of (2*Z*)-1-(4-bromo phenyl)-3-(furan-2-yl)prop-2-en-1-one (**X**)

197
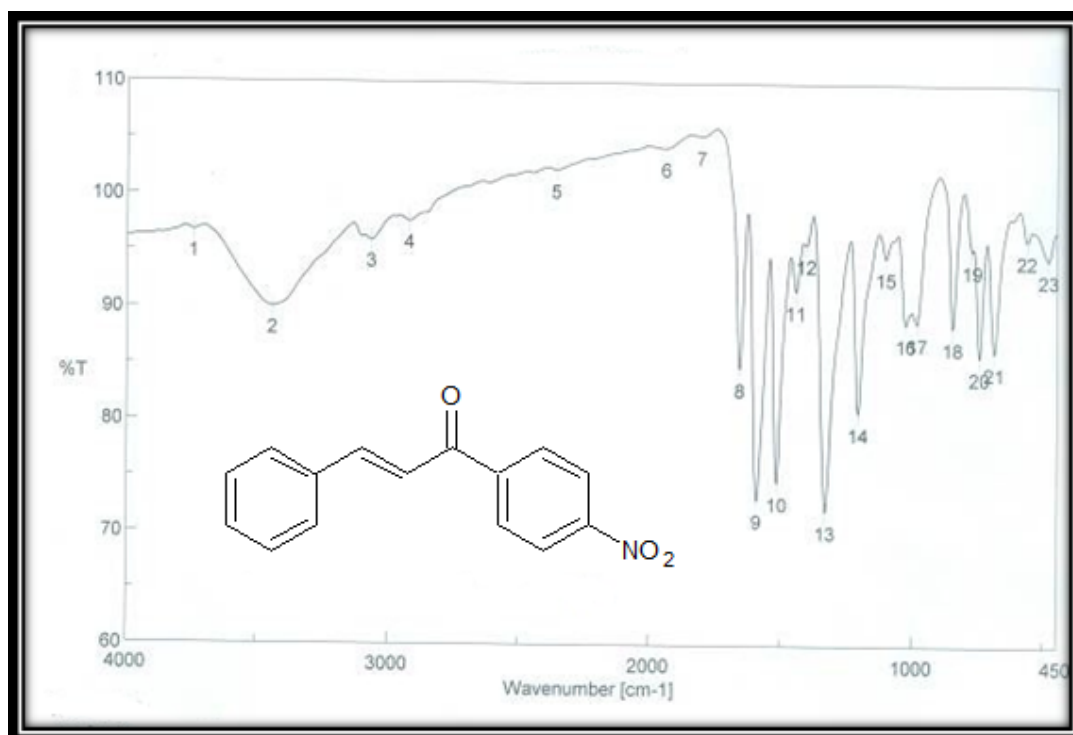
Figure (4.11): IR Spectrum of (2*E*)-1-(4-nitro phenyl)-3-phenyl prop-2-en-1-one (**XI**)
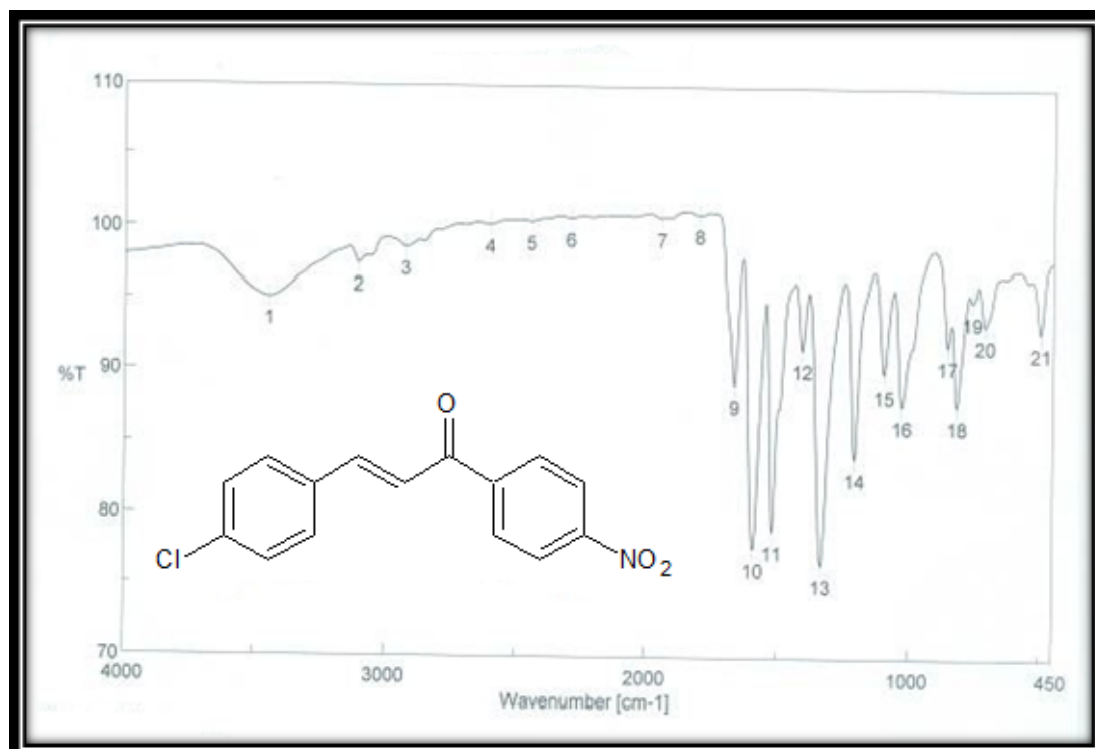
Figure (4.12): IR Spectrum of (2*E*)-3-(4-chloro phe nyl)-1-(4-nitrophenyl) prop-2-en-1-one (**XII**)
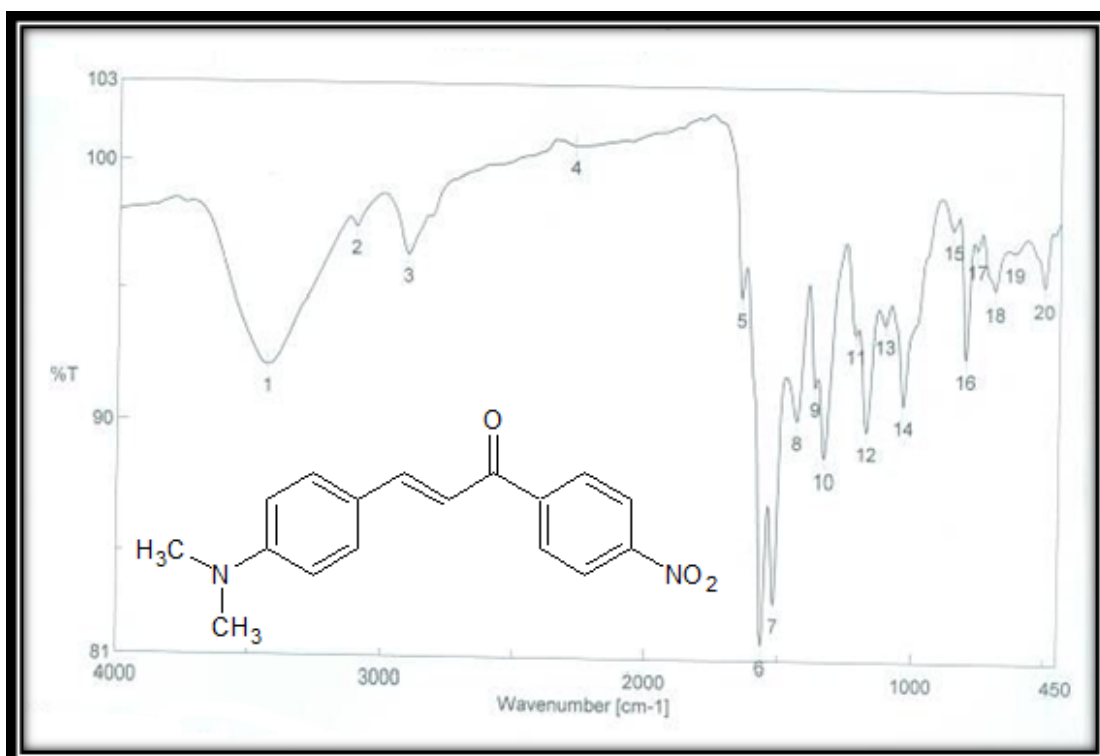
Figure (4.13): IR Spectrum of (2*E*)-3-[4-(dimethylami- no)phenyl]-1-(4-nitrophenyl) prop-2-en-1-one (**XIII**)
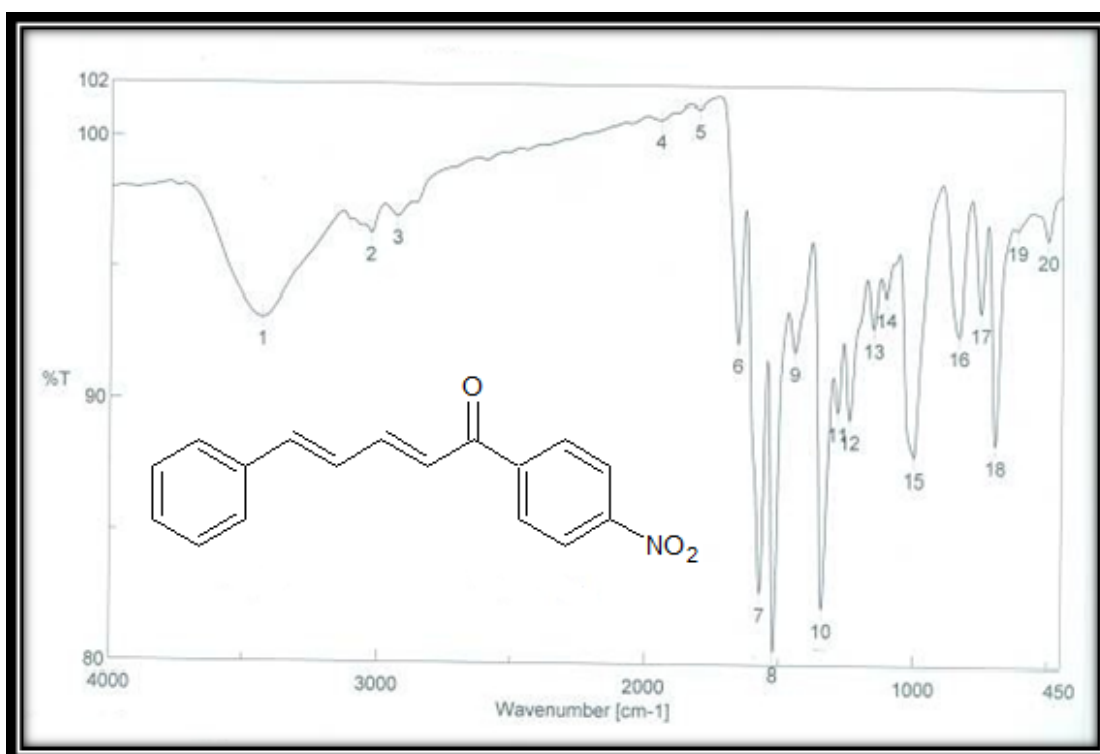
Figure (4.14): IR Spectrum of (2*E*,4*E*)-1-(4-nitro phe nyl)-5-phenylpenta-2,4-dien-1-one (**XIV**)
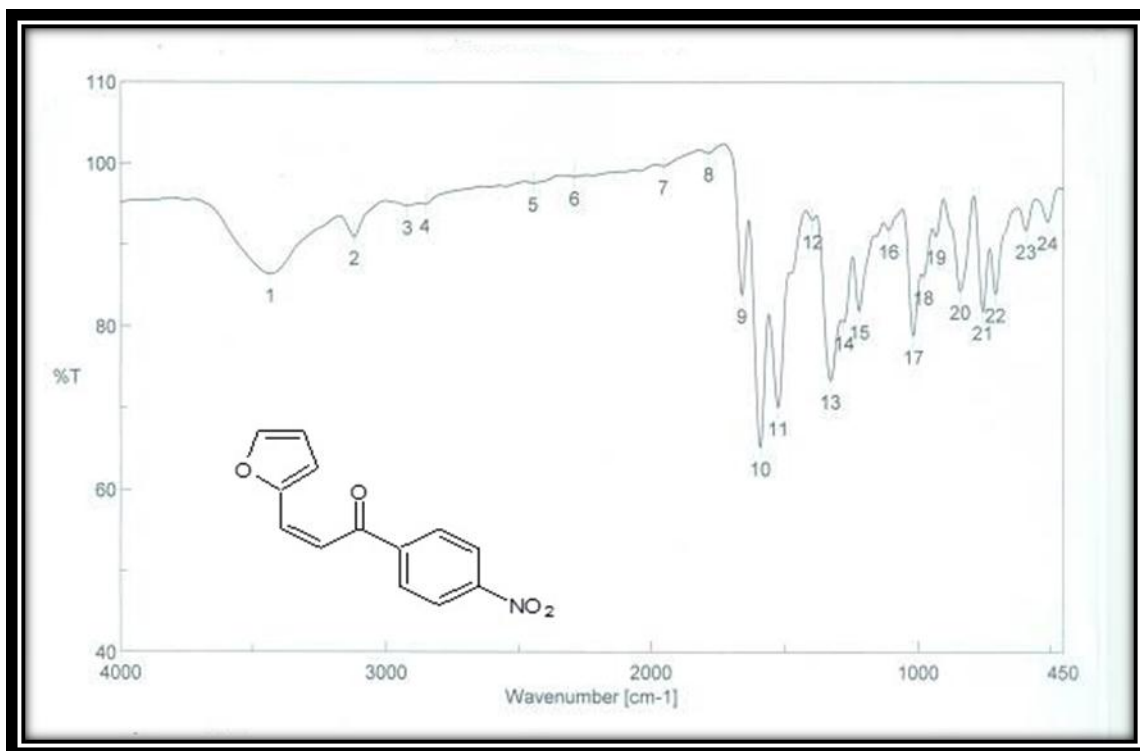
Figure (4.15): IR Spectrum of (2*Z*)-3-(furan-2-yl)-1-(4-nitrophenyl) prop-2-en-1-one (**XV**)
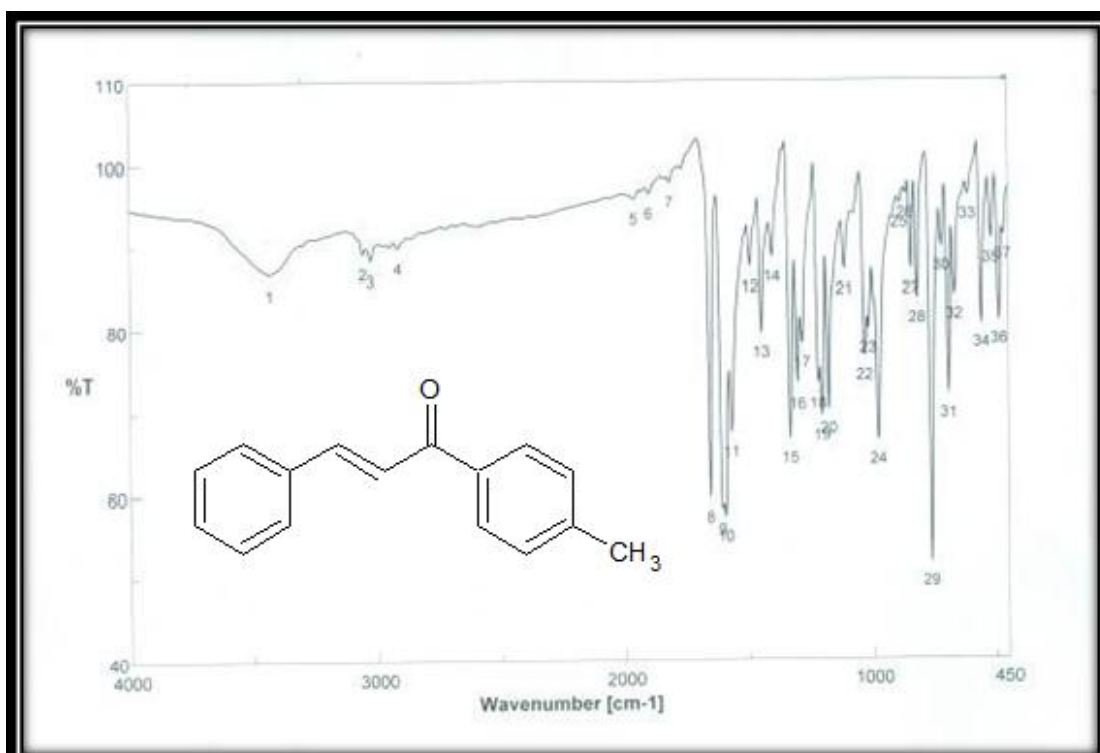
Figure (4.16): IR Spectrum of (2*E*)-1-(4-methyl phenyl)-3-phenyl prop-2-en-1-one (**XVI**)
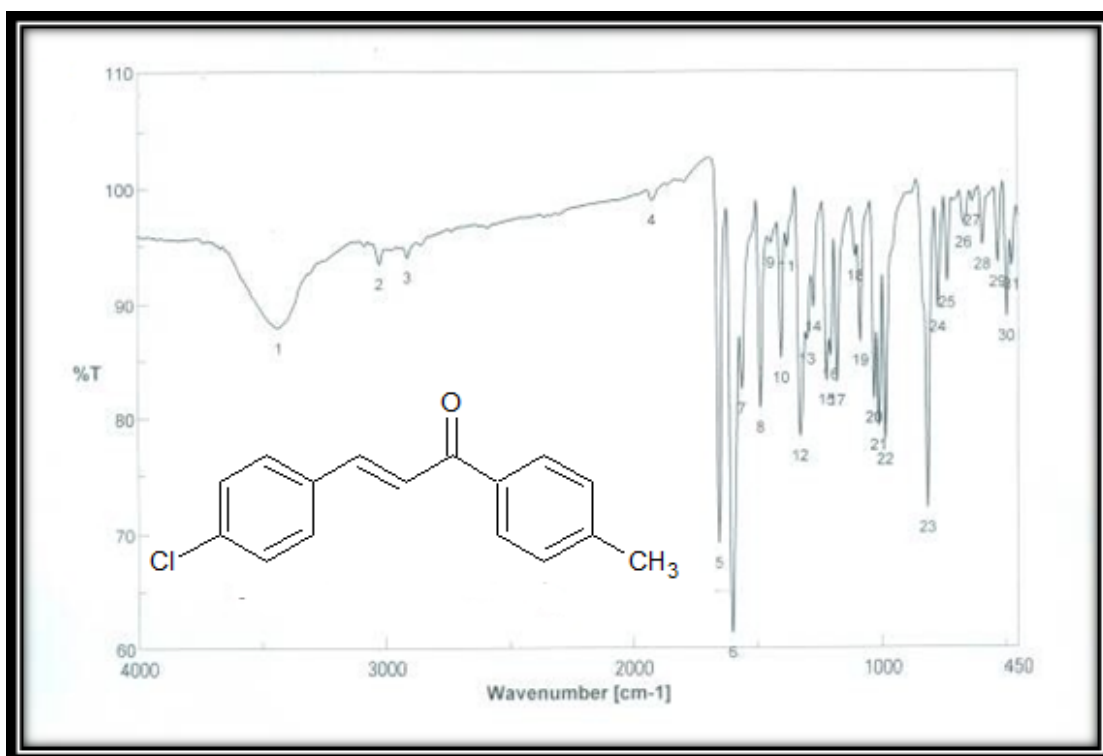
Figure (4.17): IR Spectrum of (2*E*)-3-(4-chloro phenyl)-1-(4-methyl phenyl)prop-2-en-1-one (**XVII**)
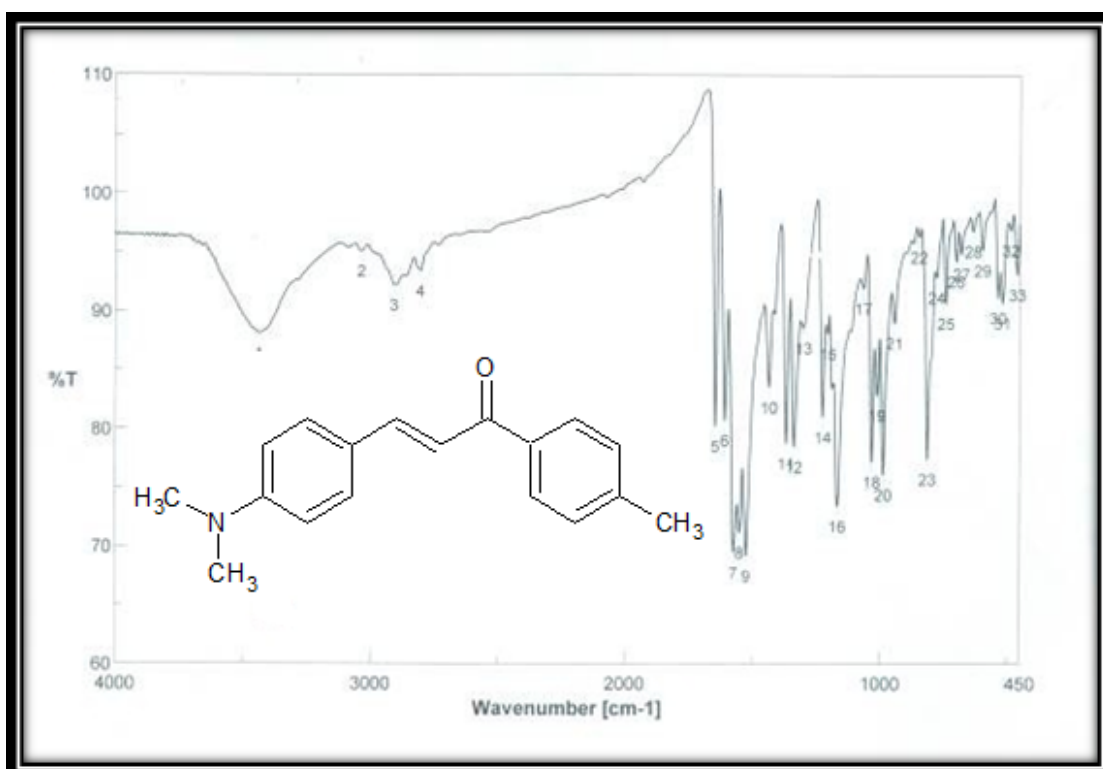
Figure (4.18): IR Spectrum of (2*E*)-3-[4-(dimethylamino)phenyl]-1-(4-methyl phenyl) prop-2-en-1-one (**XVIII**)
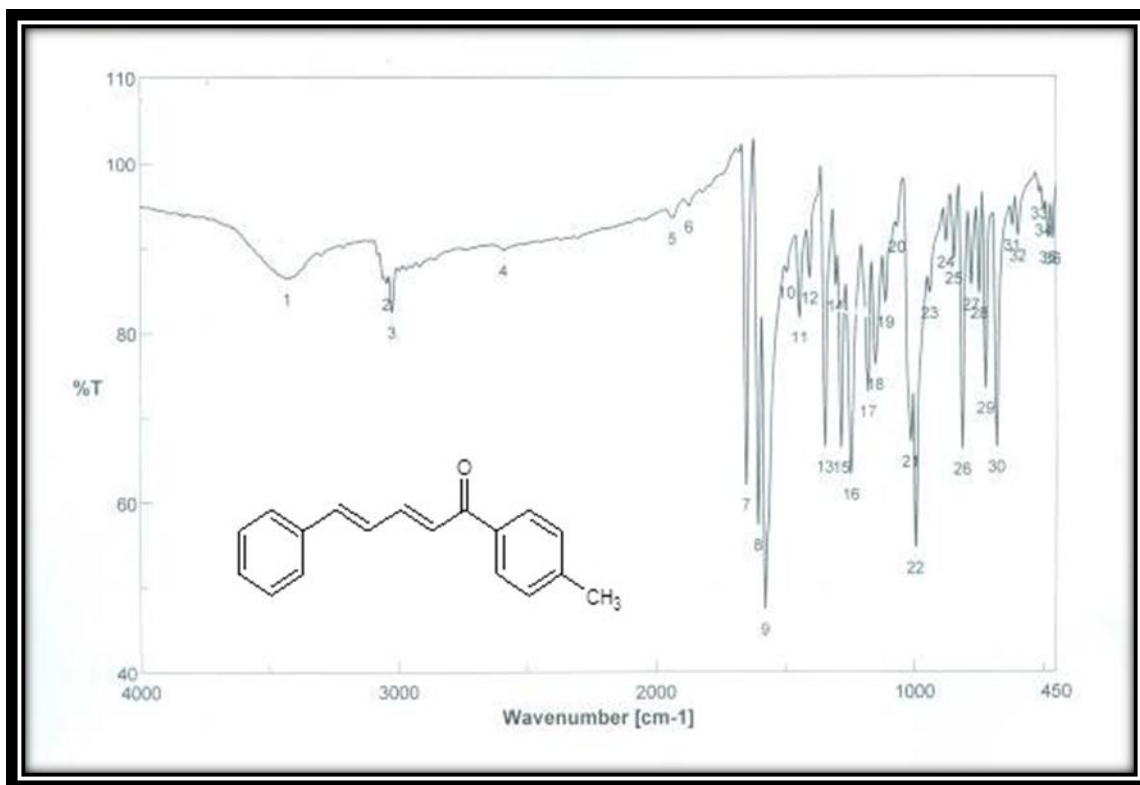
Figure (4.19): IR Spectrum of (2*E*,4*E*)-1-(4-methyl phenyl)-5-phenylpenta-2,4-dien-1-one (**XIX**)
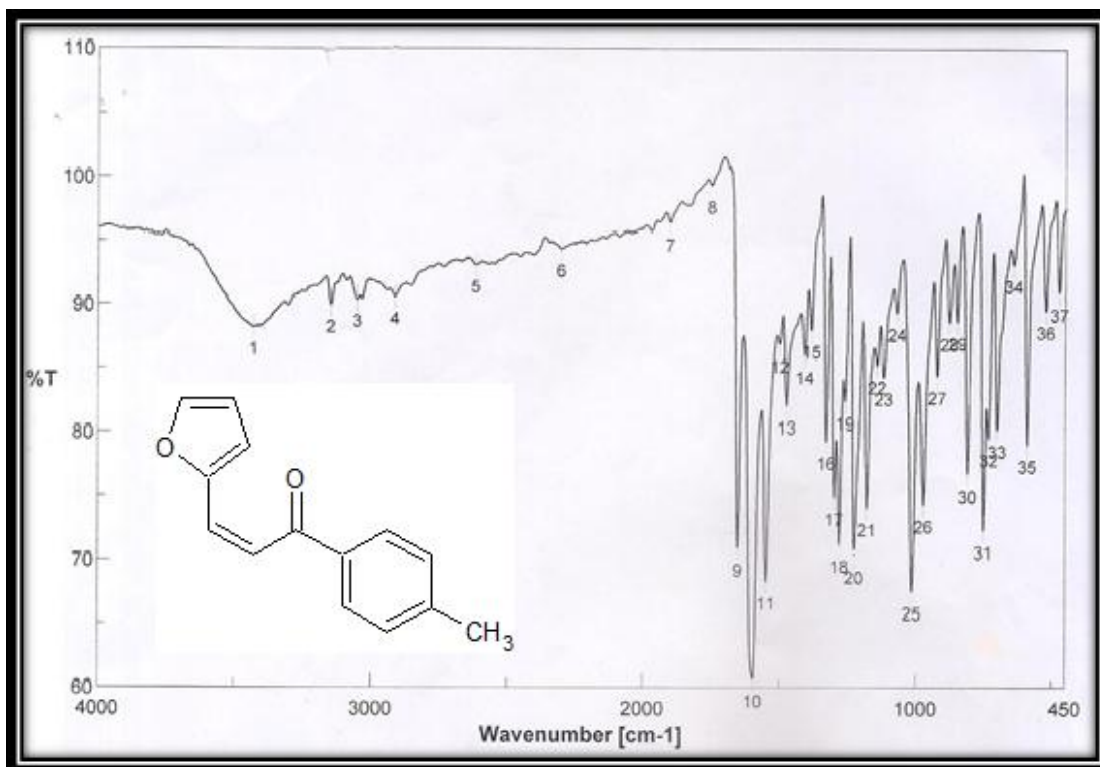
Figure (4.20): IR Spectrum of (2*Z*)-3-(furan-2-yl)-1-(4-methyl phenyl) prop-2-en-1-one (**XX**)
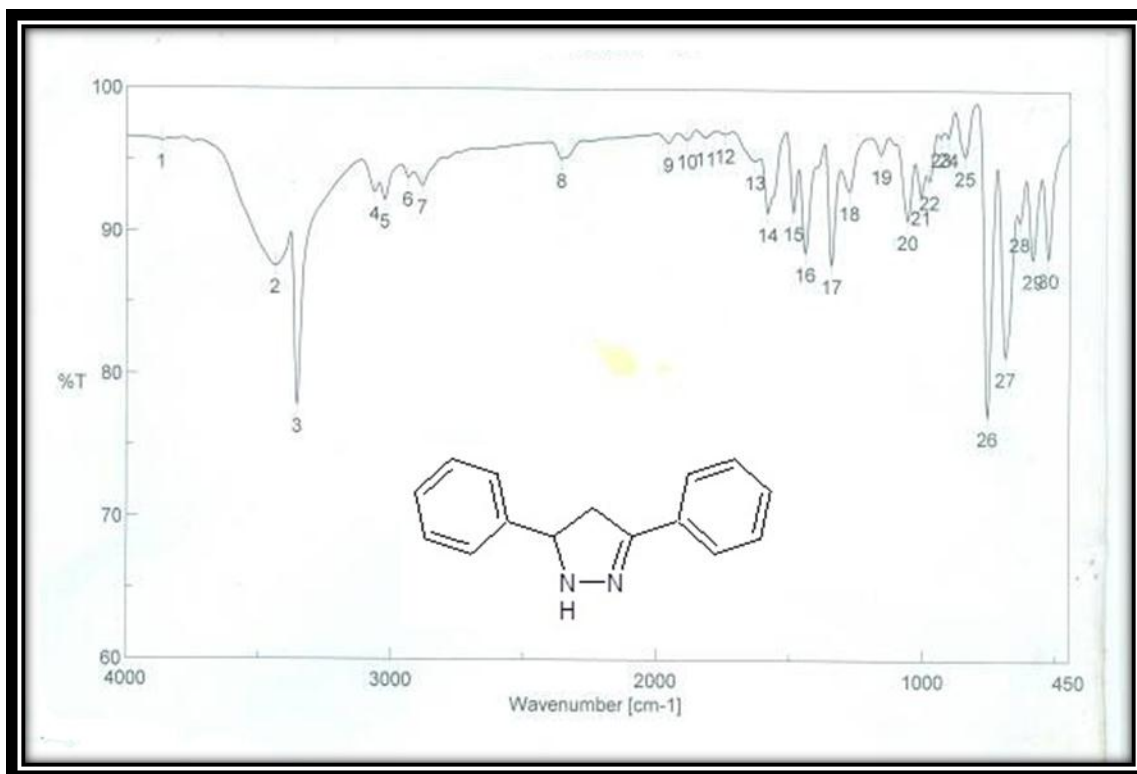
Figure (4.21): IR Spectrum of 3,5-diphenyl-4,5-dihydro-1H-pyrazole (**XXI**)
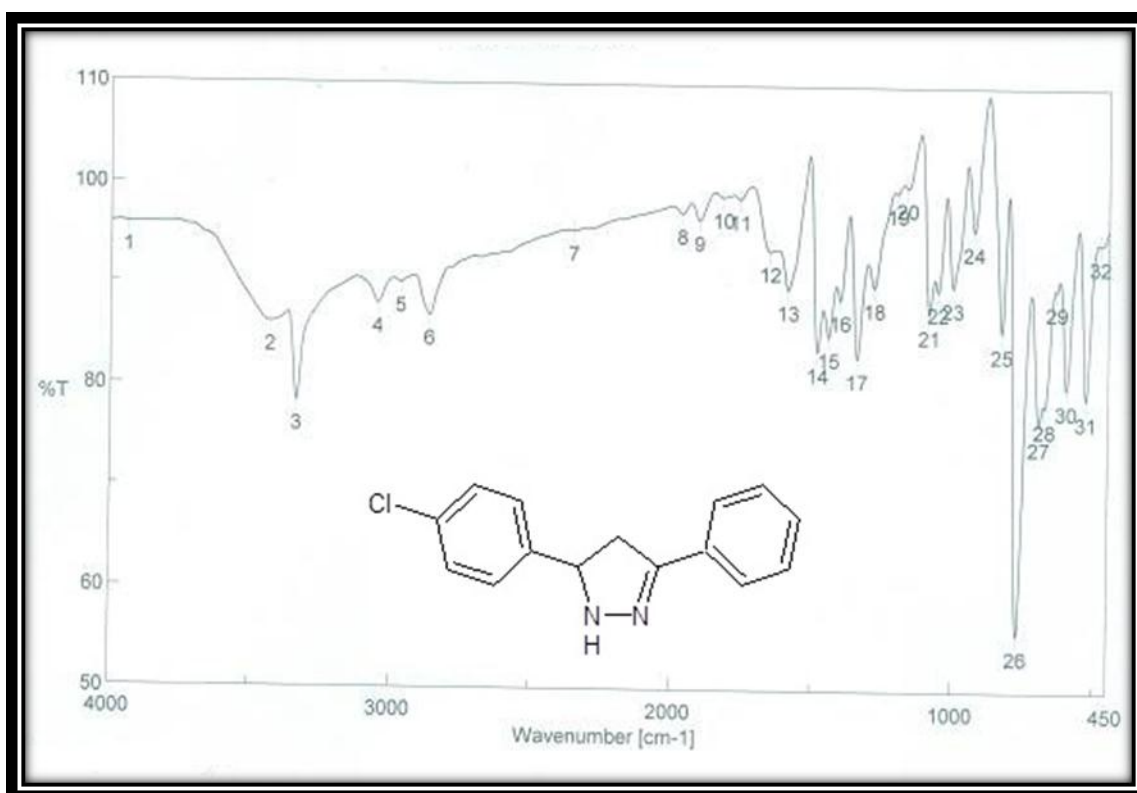
Figure (4.22): IR Spectrum of 5-(4-chlorophe nyl)-3-phenyl-4,5-dihydro-1H-pyrazole (**XXII**)
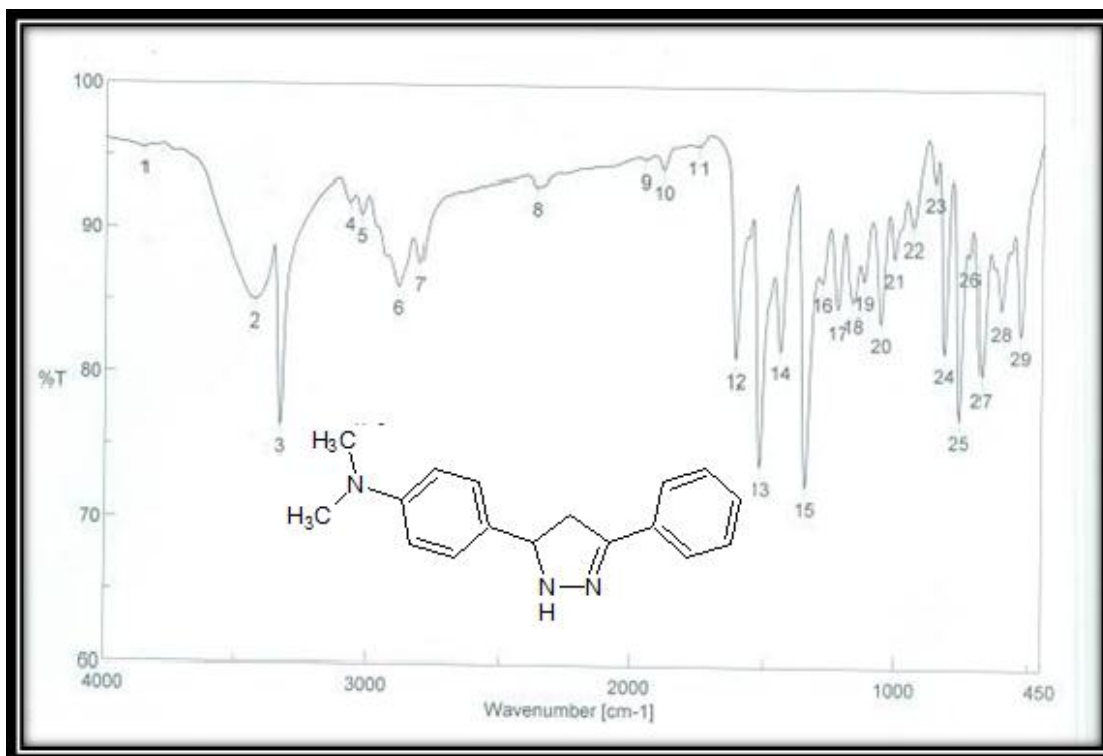
Figure (4.23): IR Spectrum of N,N-dimethyl-4-(3-phenyl-4,5-di hydro-1H-pyra zol-5-yl) aniline (**XXIII**)
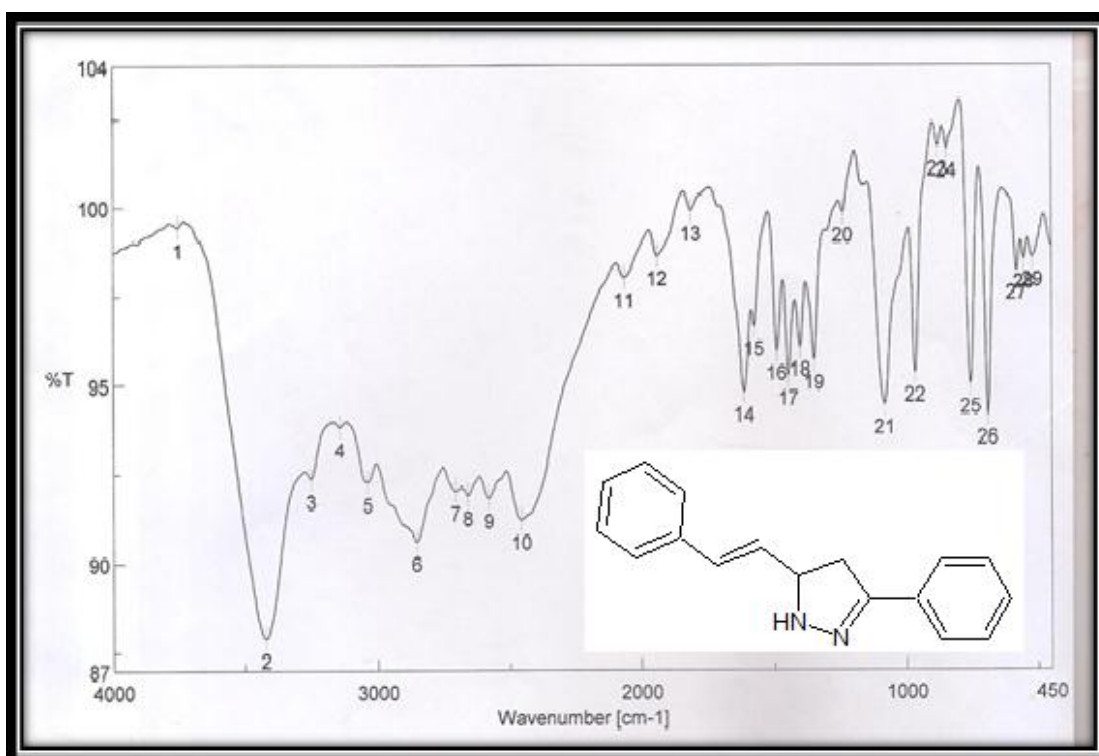
Figure (4.24): IR Spectrum of 3-phenyl-5-[(E)-2-phenyl ethen yl]-4,5-dihydro-1H-pyrazole (**XXIV**)
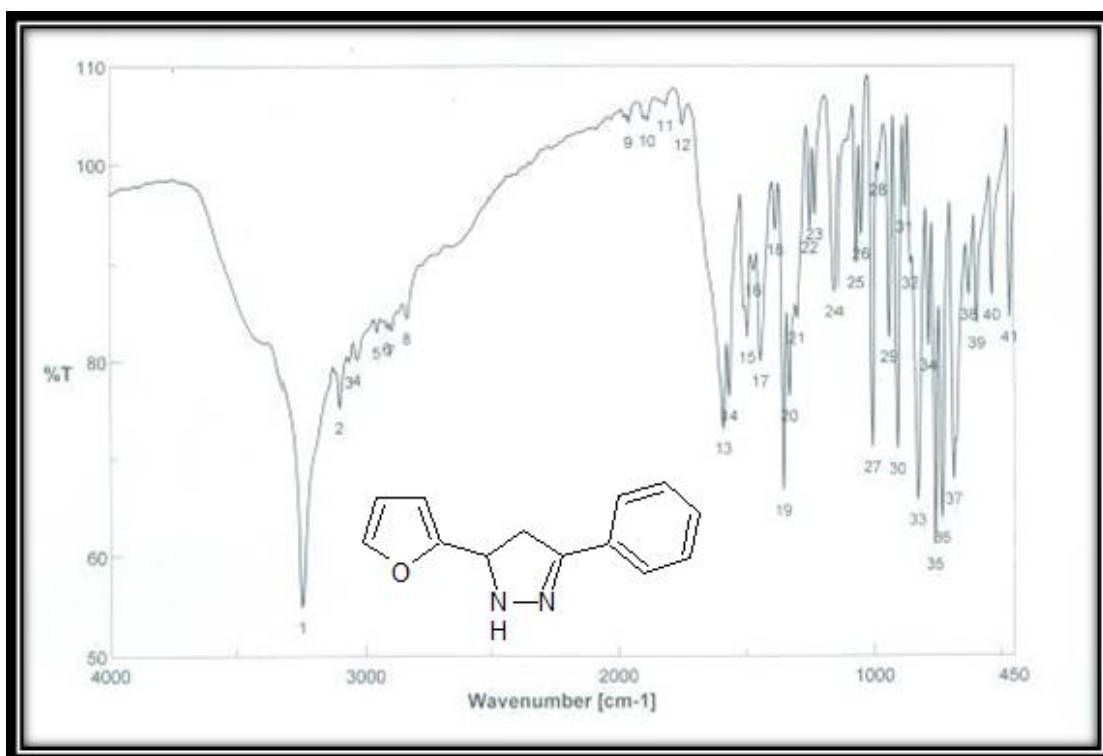
Figure (4.25): IR Spectrum of 5-(furan-2-yl)-3-phenyl-4,5-dihydro-1H-pyrazole **(XXV)**
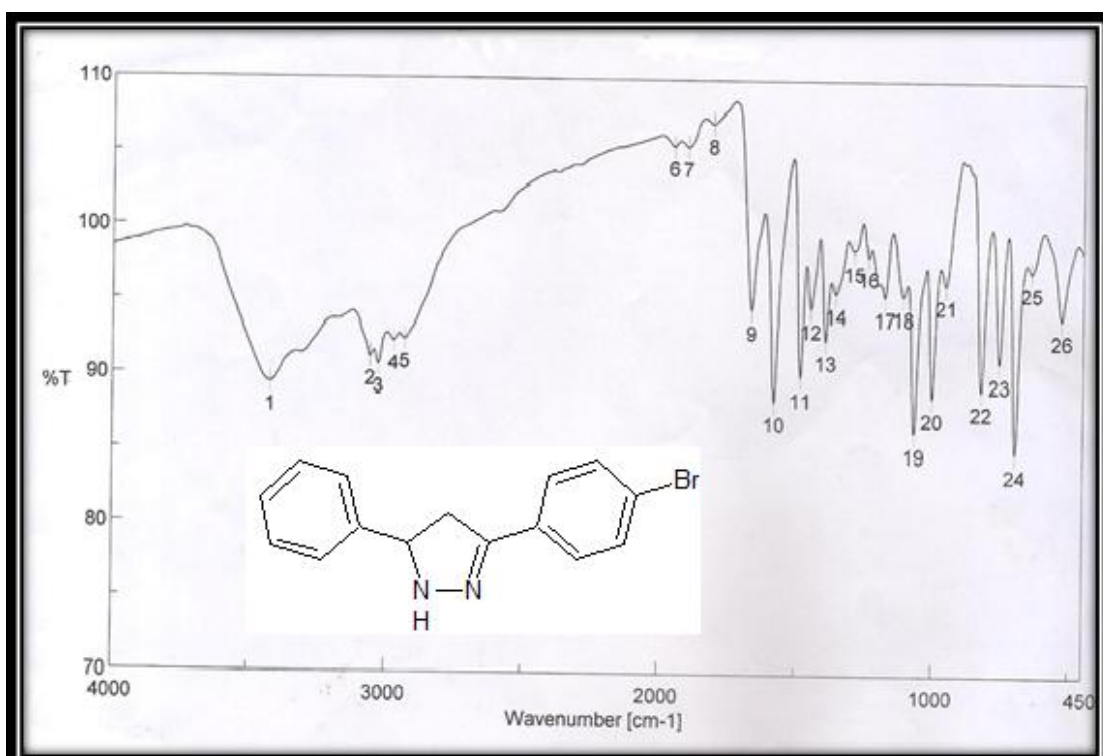
Figure (4.26): IR Spectrum of 3-(4-bromophenyl)-5-phenyl-4,5-dihydro-1H-pyrazole **(XXVI)**
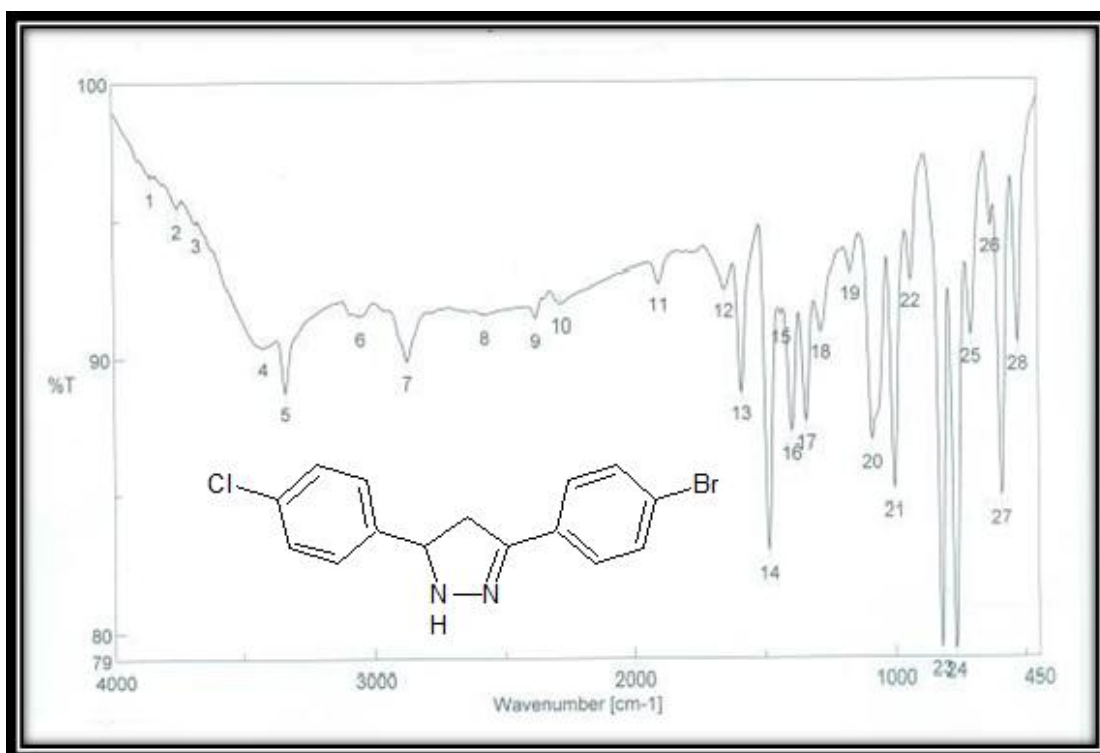
Figure (4.27): IR Spectrum of 3-(4-bromophenyl)-5 -(4-chlorophenyl)-4, 5- dihydro-1H-pyrazole **(XXVII)**
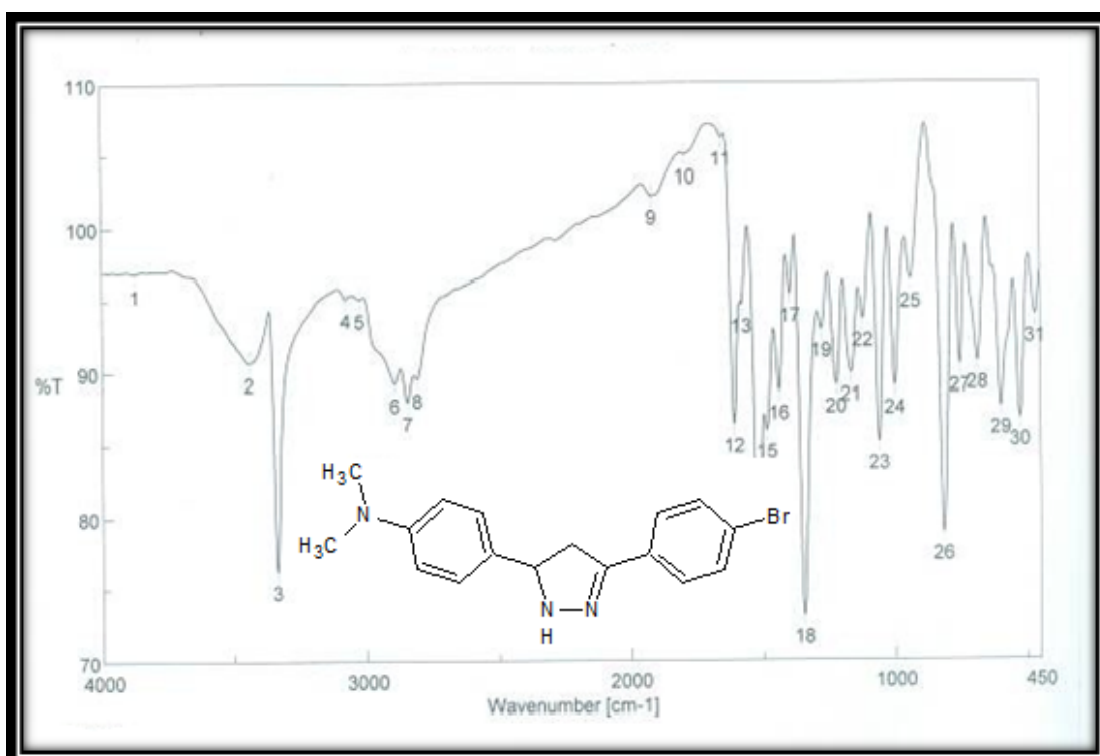
Figure (4.28): IR Spectrum of 4-[3-(4-bromophenyl)-4,5-dihydro-1H-pyrazol-5-yl]-N,N-dimethylaniline **(XXVIII)**
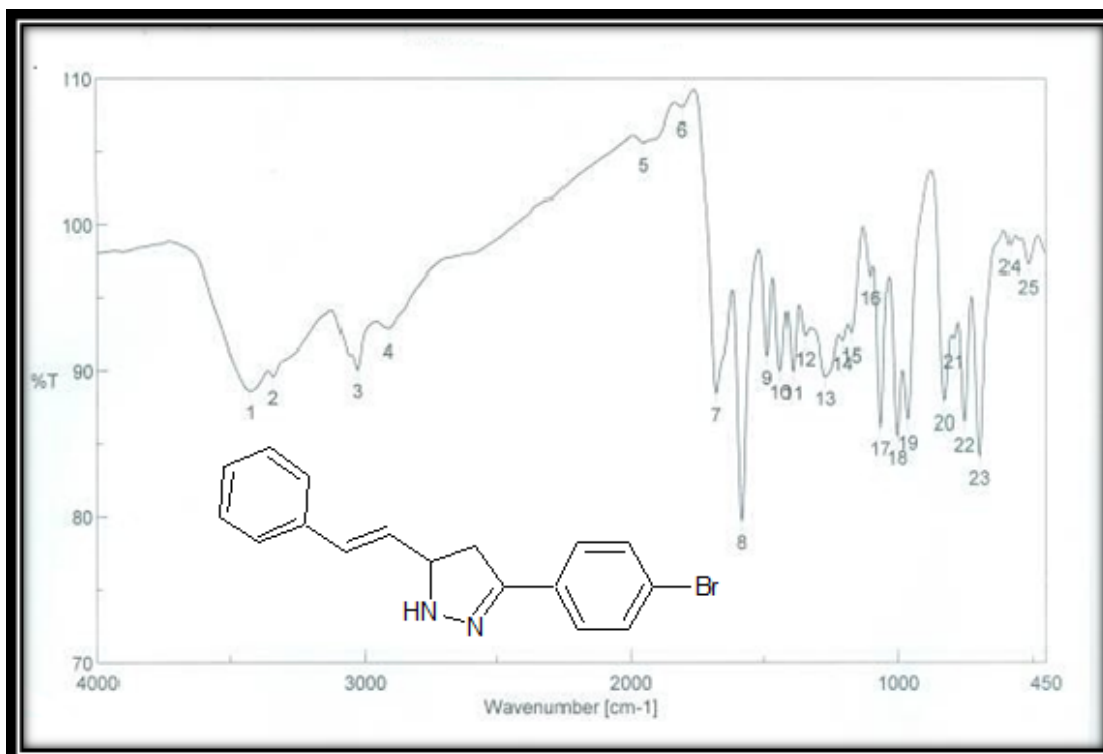
Figure (4.29): IR Spectrum of 3-(4-bromophenyl)-5-[(E)-2-phenylethenyl]-4,5-dihydro-1H-pyrazole (**XXIX**)
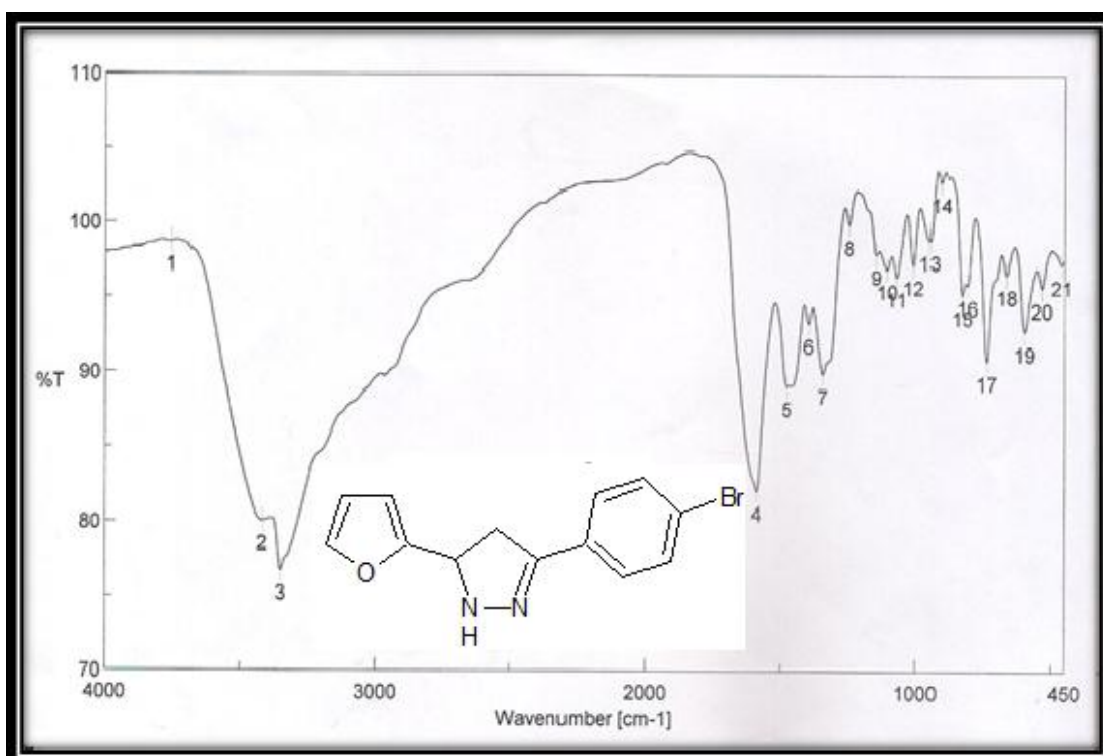
Figure (4.30): IR Spectrum of 3-(4-bromophenyl)-5-(furan-2-yl)-4,5-dihydro-1H-pyrazole (**XXX**)

207
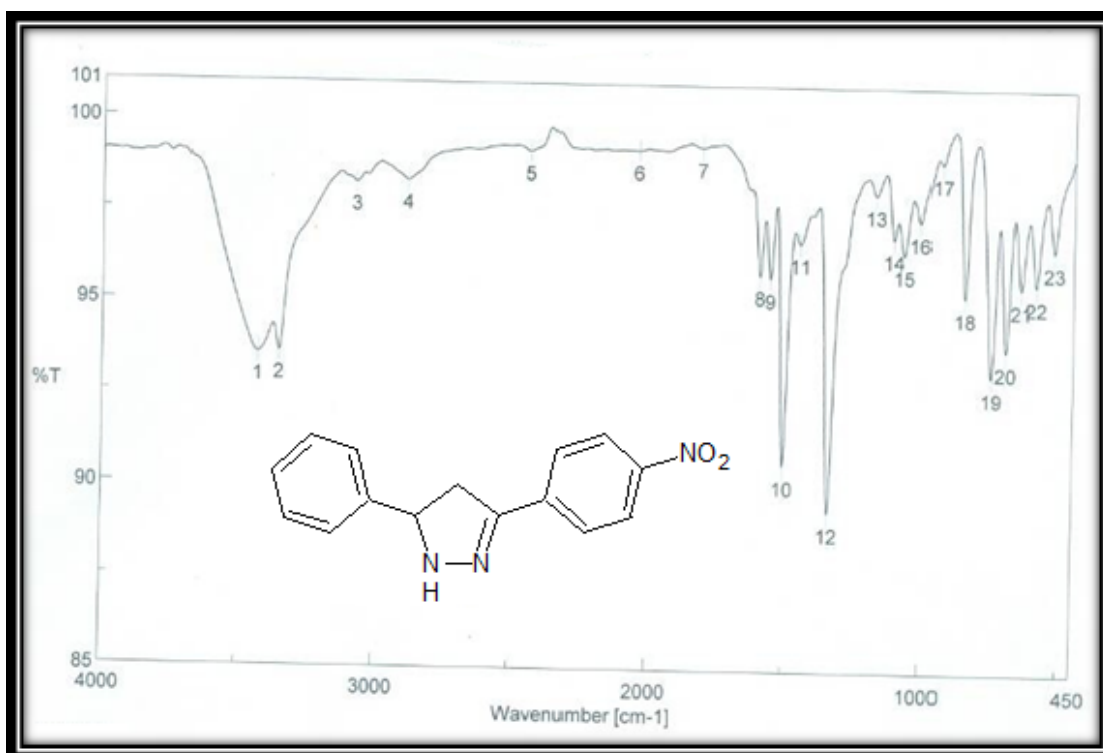
Figure (4.31): IR Spectrum of 3-(4-nitrophenyl)-5-phenyl-4,5-dihydro-1H-pyrazole **(XXXI)**
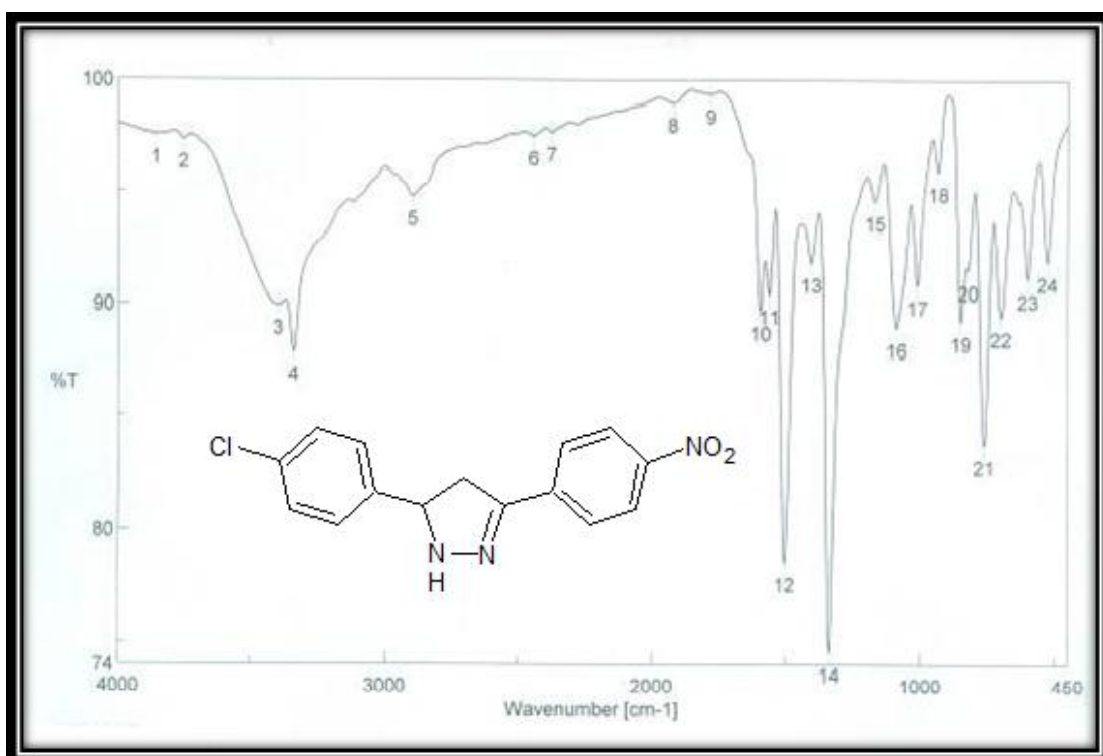
Figure (4.32): IR Spectrum of 5-(4-chlorophenyl)-3-(4-nitrophenyl)-4,5-dihydro-1H-pyrazole **(XXXII)**

208
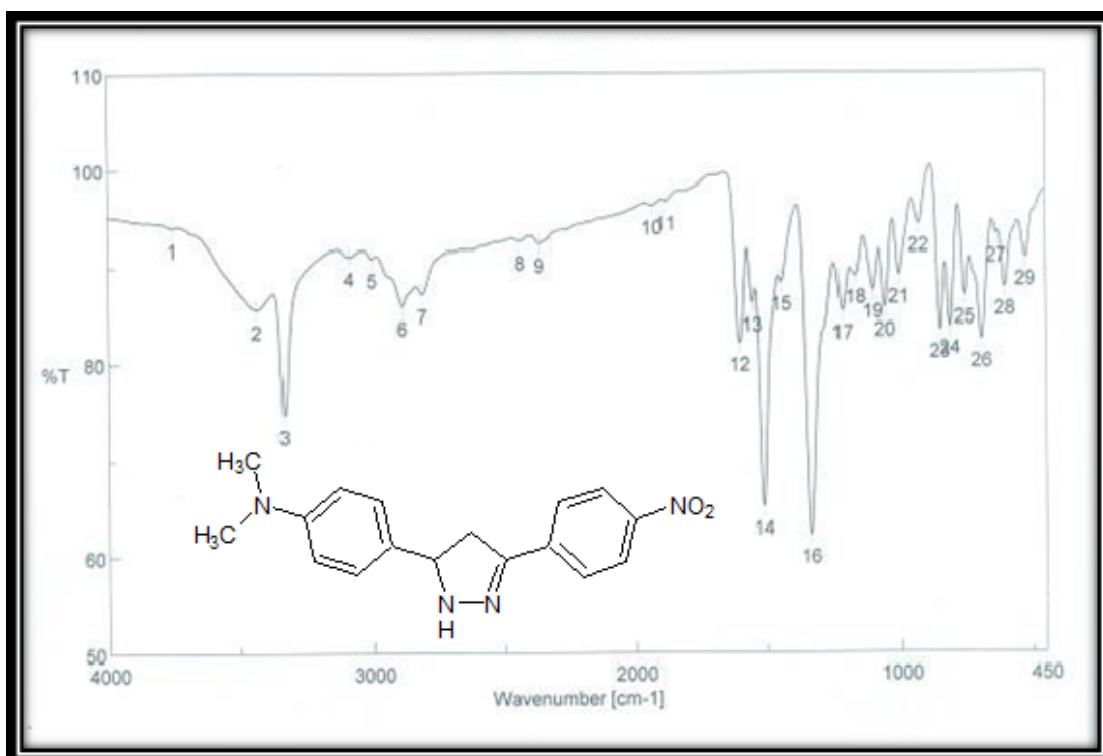
Figure (4.33): IR Spectrum of N,N-dimethyl-4-[3-(4-nitrophen yl)-4,5-dihy dro-1H-pyrazol-5-yl]aniline **(XXXIII)**
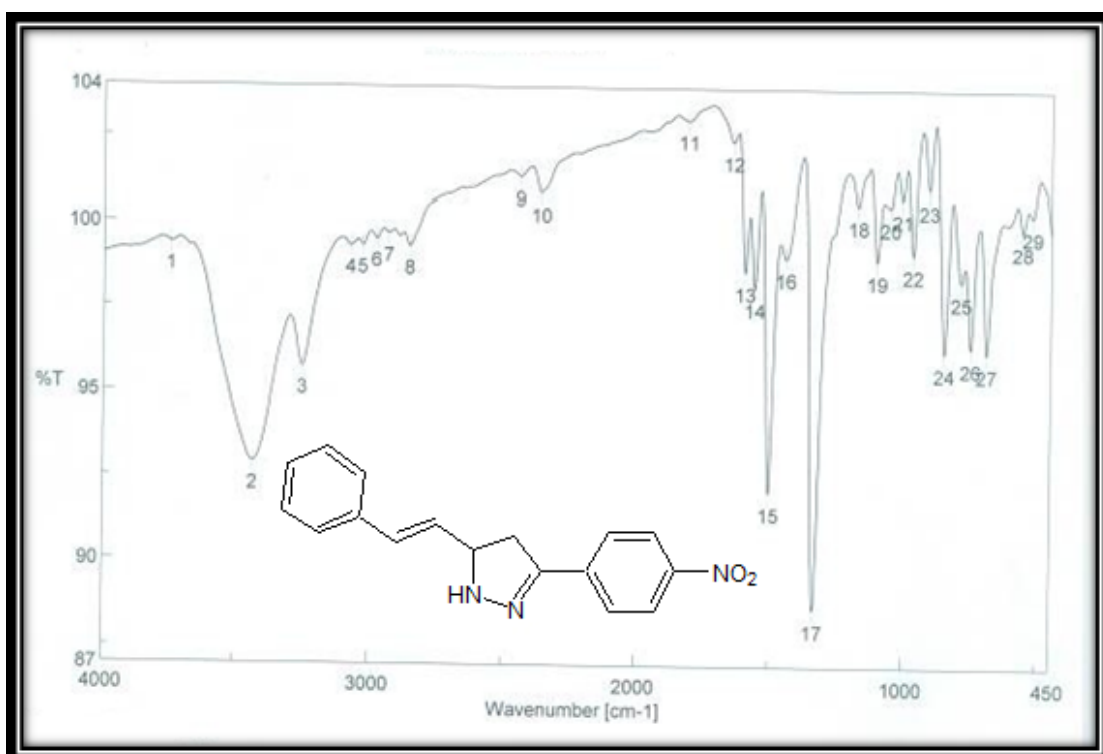
Figure (4.34): IR Spectrum of 3-(4-nitrophenyl)-5-[(E)-2-phenylethenyl]-4,5-dihydro-1H-pyrazole **(XXXIV)**

209
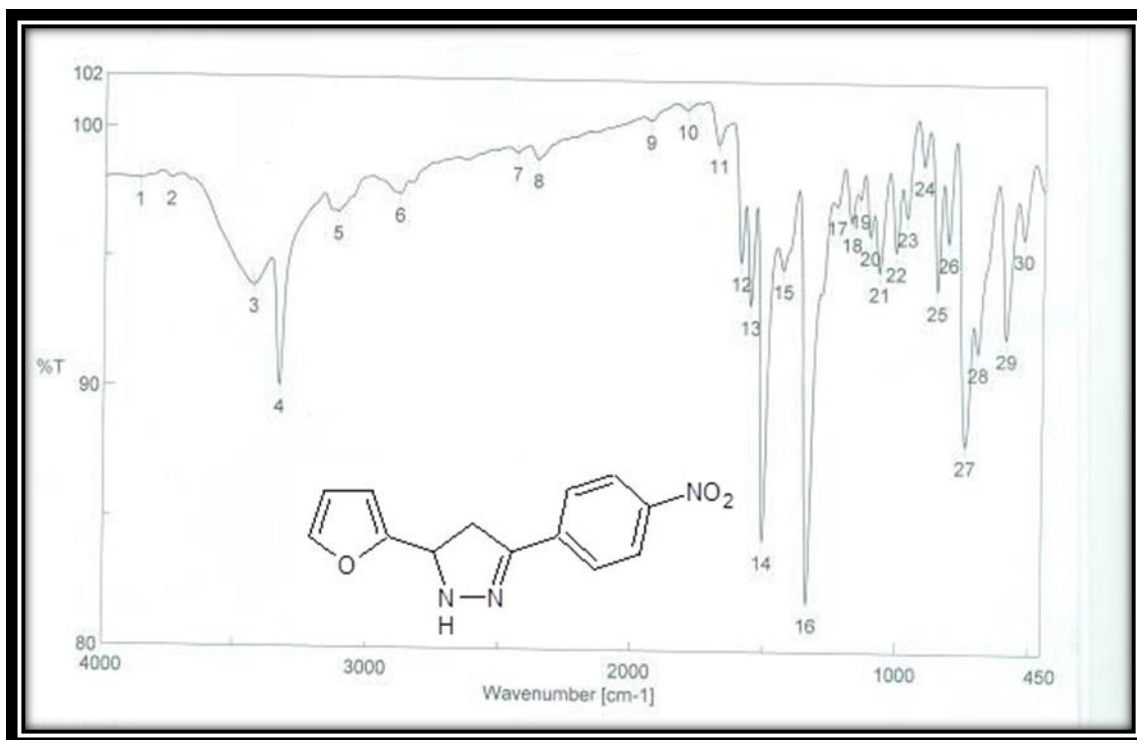
Figure (4.35): IR Spectrum of 5-(furan-2-yl)-3-(4-nitrophenyl)-4,5-dihydro-1H-pyrazole **(XXXV)**
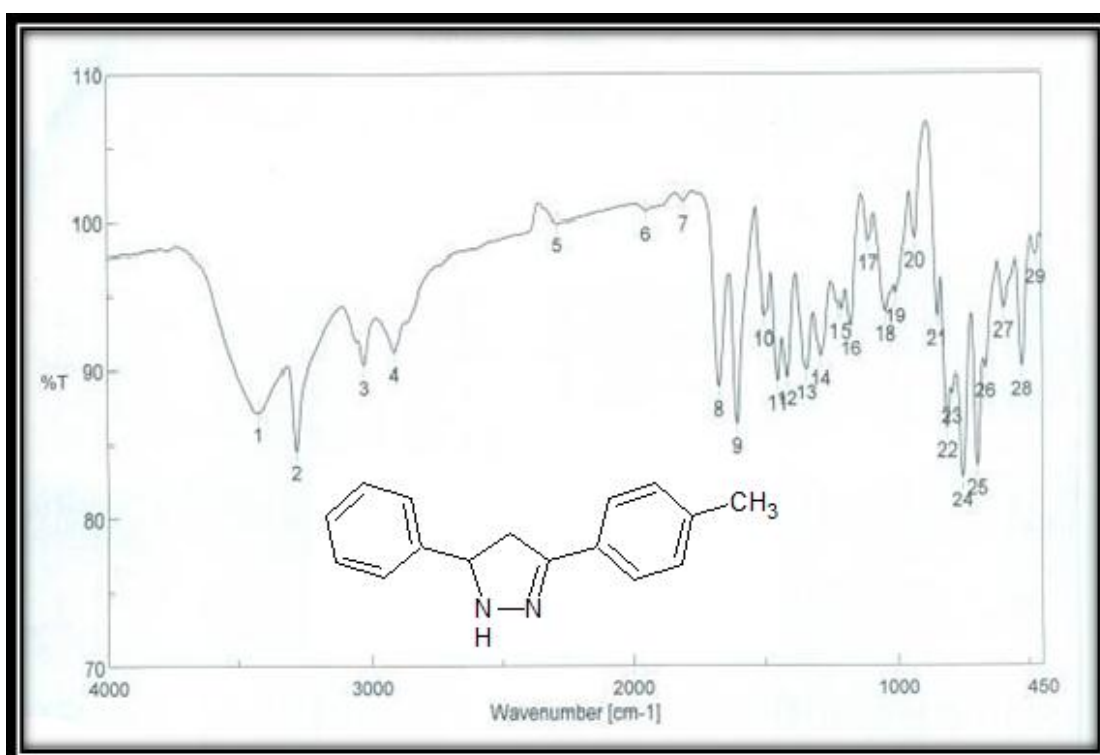
Figure (4.36): IR Spectrum of 3-(4-methylphenyl)-5-phenyl-4,5-dihydro-1H-pyrazole **(XXXVI)**
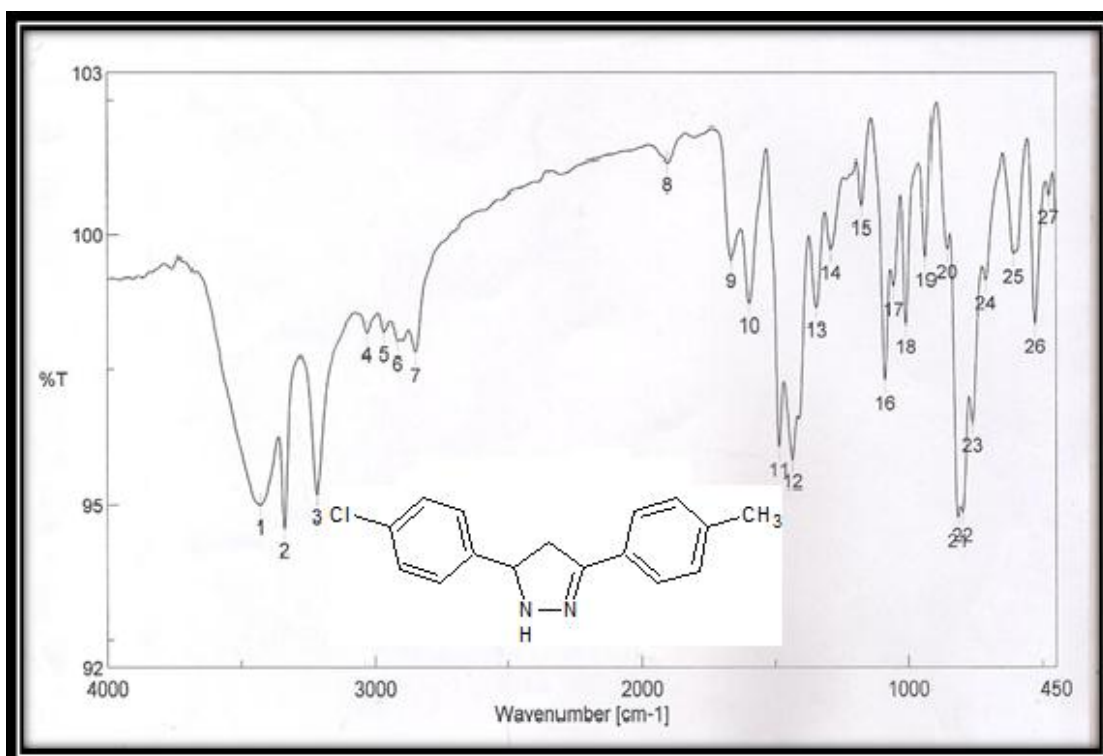
Figure (4.37): IR Spectrum of 5-(4-chlorophenyl)-3-(4-methyl phenyl)-4,5-dihydro-1H-pyrazole **(XXXVII)**
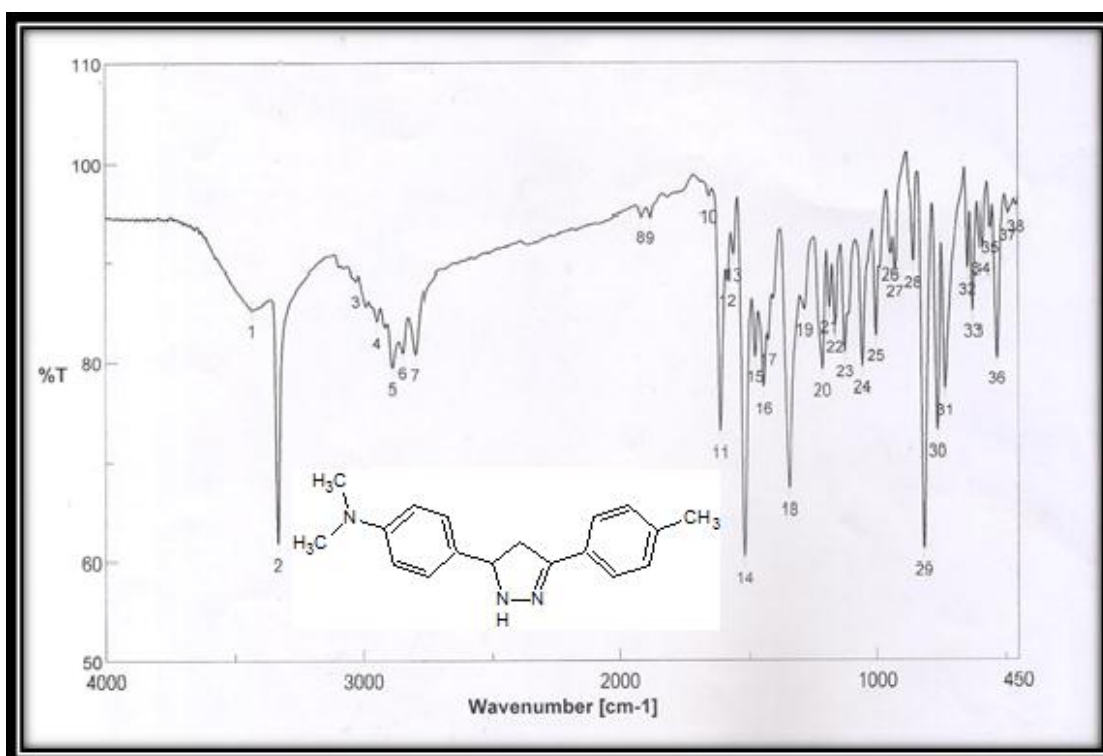
Figure (4.38): IR Spectrum of N,N-dimethyl-4-[3-(4-methylphenyl)-4,5-dihydro-1H-pyrazol-5-yl]aniline **(XXXVIII)**
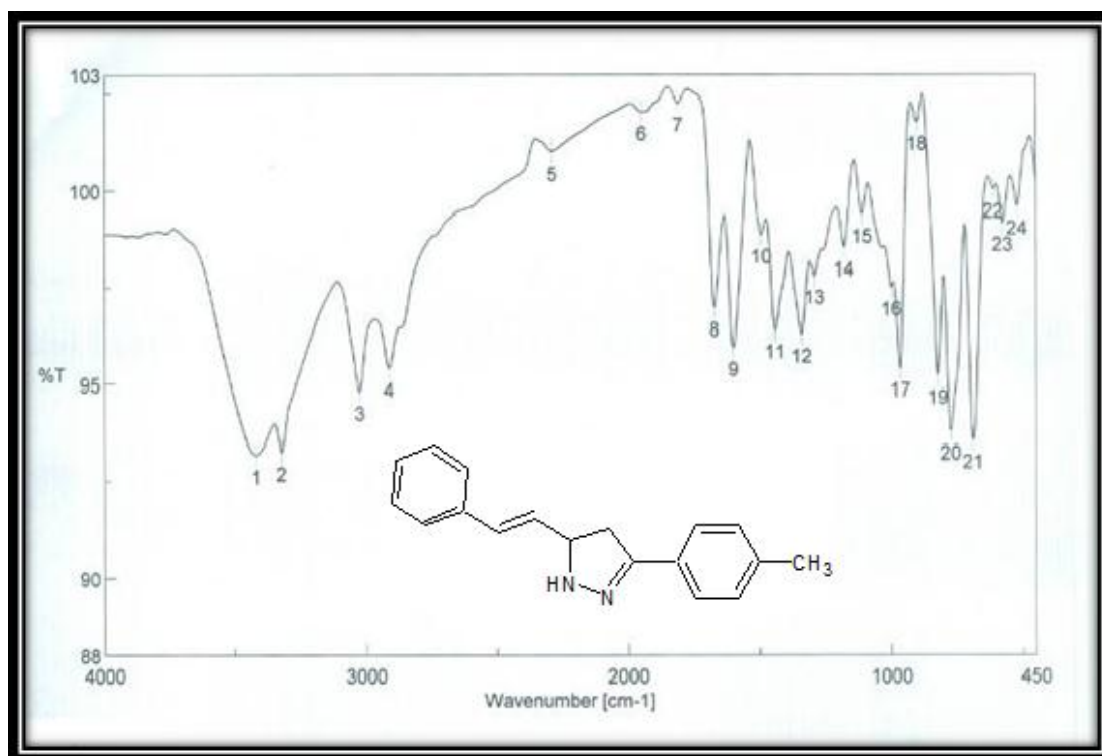
Figure (4.39): IR Spectrum of 3-(4-methylphen yl)-5-[(*E*)-2-phenylethenyl]-4,5-dihydro-1*H*-pyrazole **(XXXIX)**
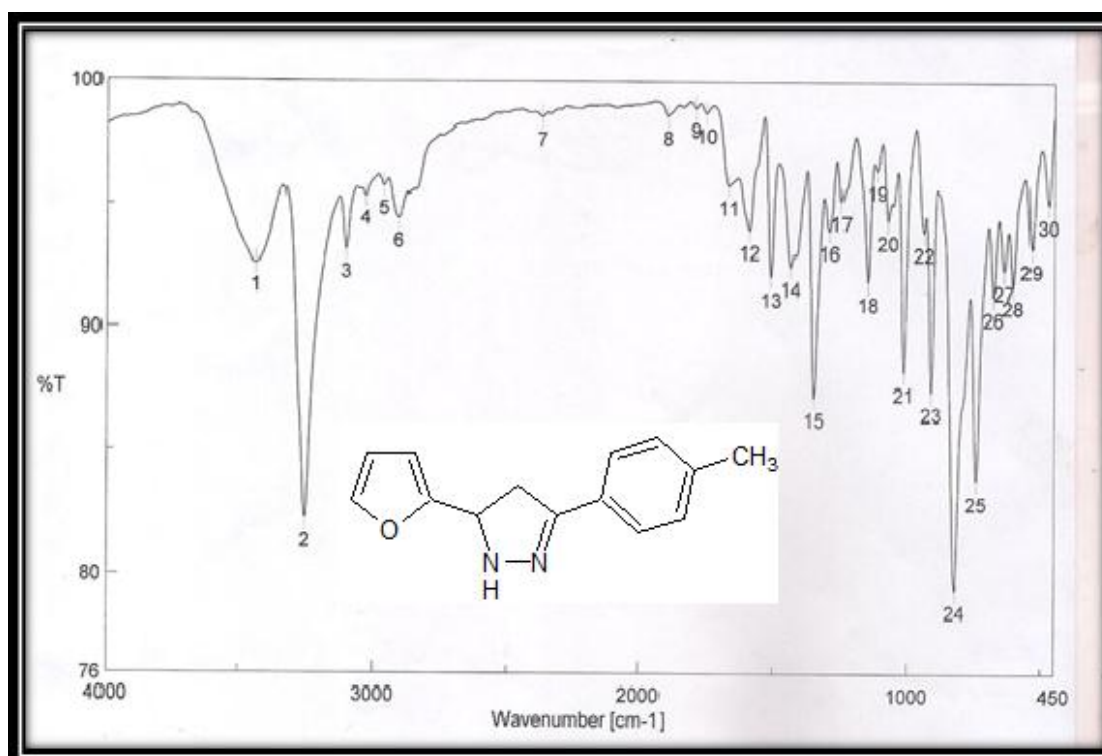
Figure (4.40): IR Spectrum of 5-(furan-2-yl)-3-(4-methylphen yl)-4,5-dihydro-1H-pyrazole **(XL)**
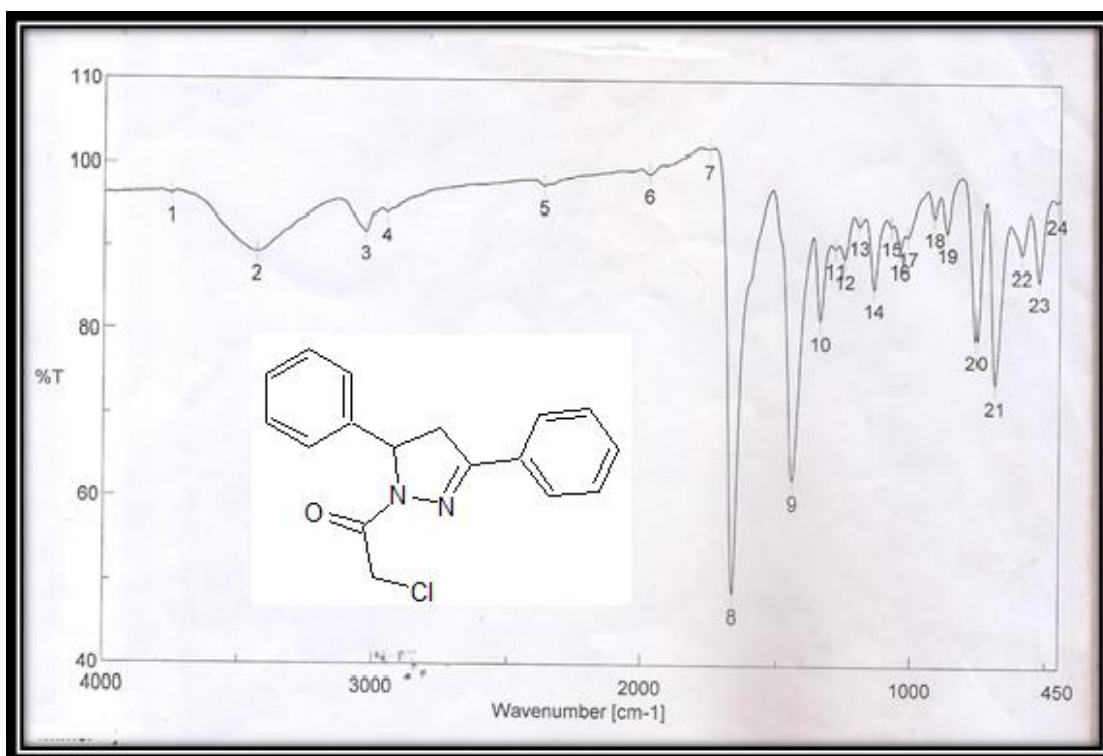
Figure (4.41): IR Spectrum of 2-chloro-1-(3,5-diphe nyl-4,5-dih ydro-1*H*-py razol-1-yl) ethan-1-one **(XLI)**
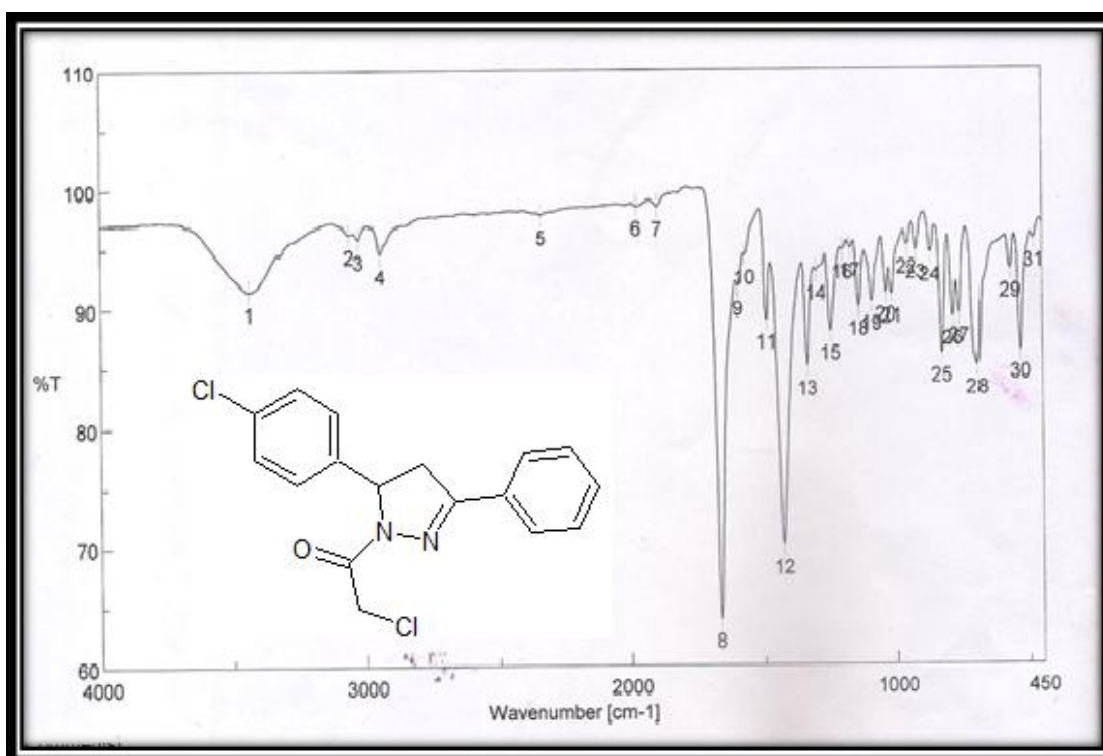
Figure (4.42): IR Spectrum of 2-chloro-1-[5-(4-chlorophenyl)-3-phenyl-4,5-dihydro-1*H*-pyrazol-1-yl] ethan-1-one **(XLII)**
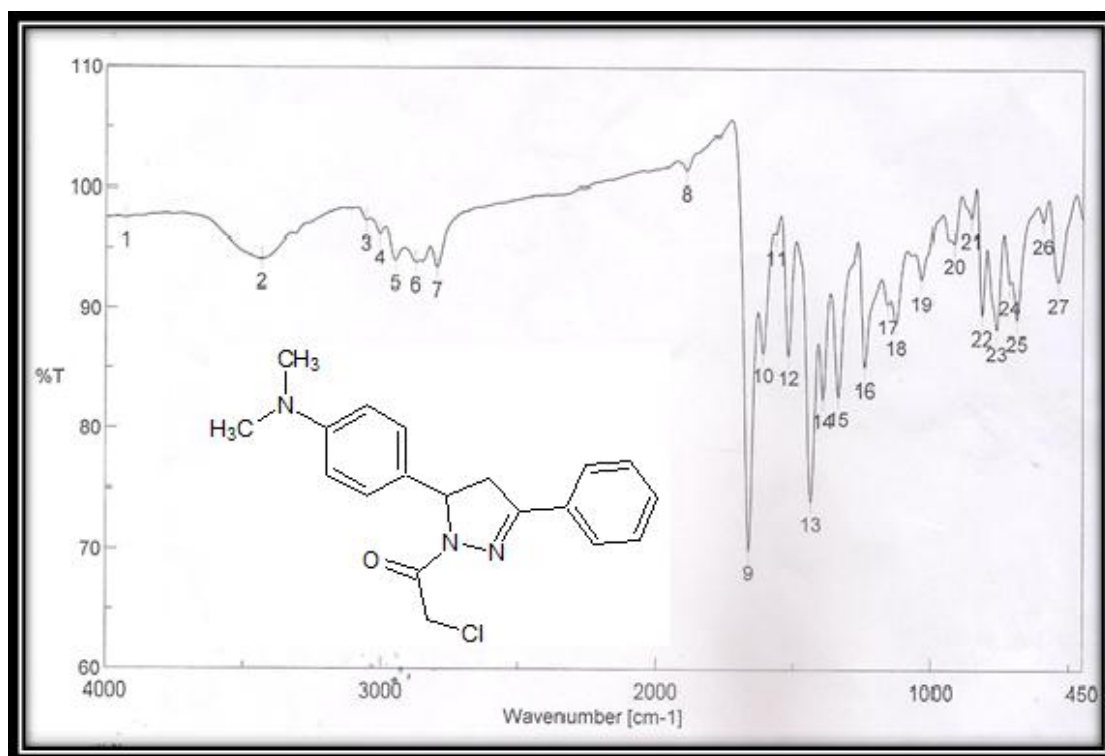
Figure (4.43): IR Spectrum of 2-chloro-1-{5-[4-(dime thylamino) phenyl]-3-phenyl-4,5-dihydro-1*H*-pyrazol-1-yl} ethan-1-one **(XLIII)**
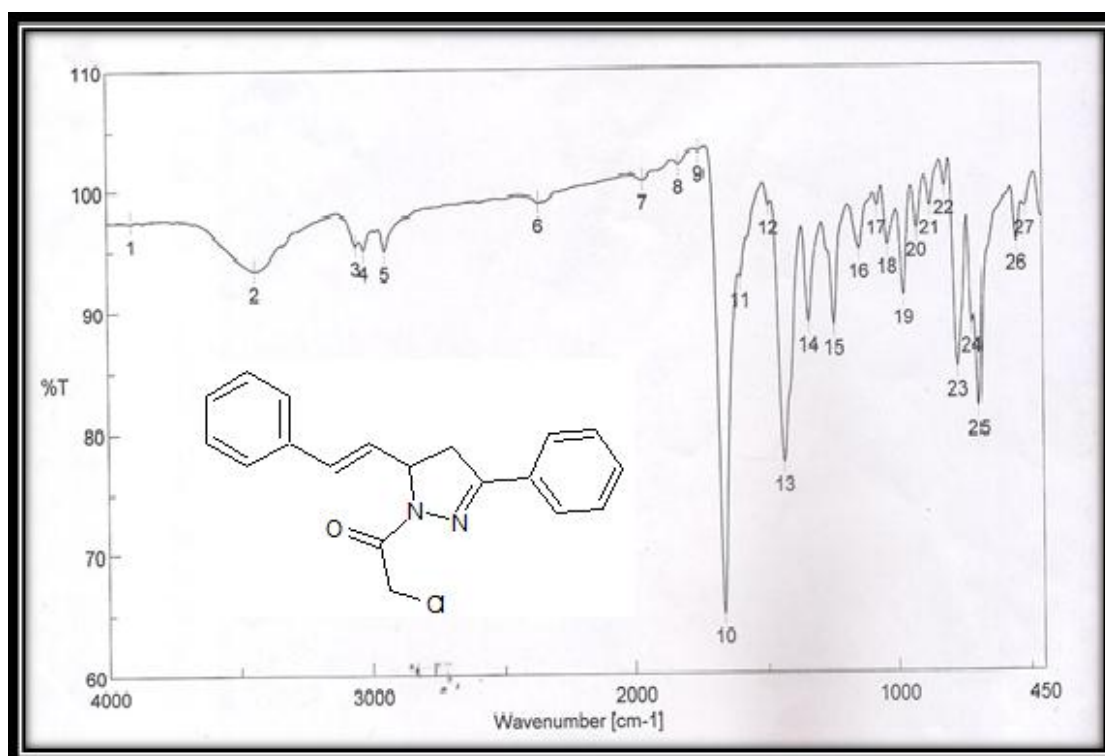
Figure (4.44): IR Spectrum of 2-chloro-1-{3-phenyl-5-[(*E*)-2-phenylethenyl]-4,5-dihydro-1*H*-pyrazol-1-yl}ethan-1-one **(XLIV)**
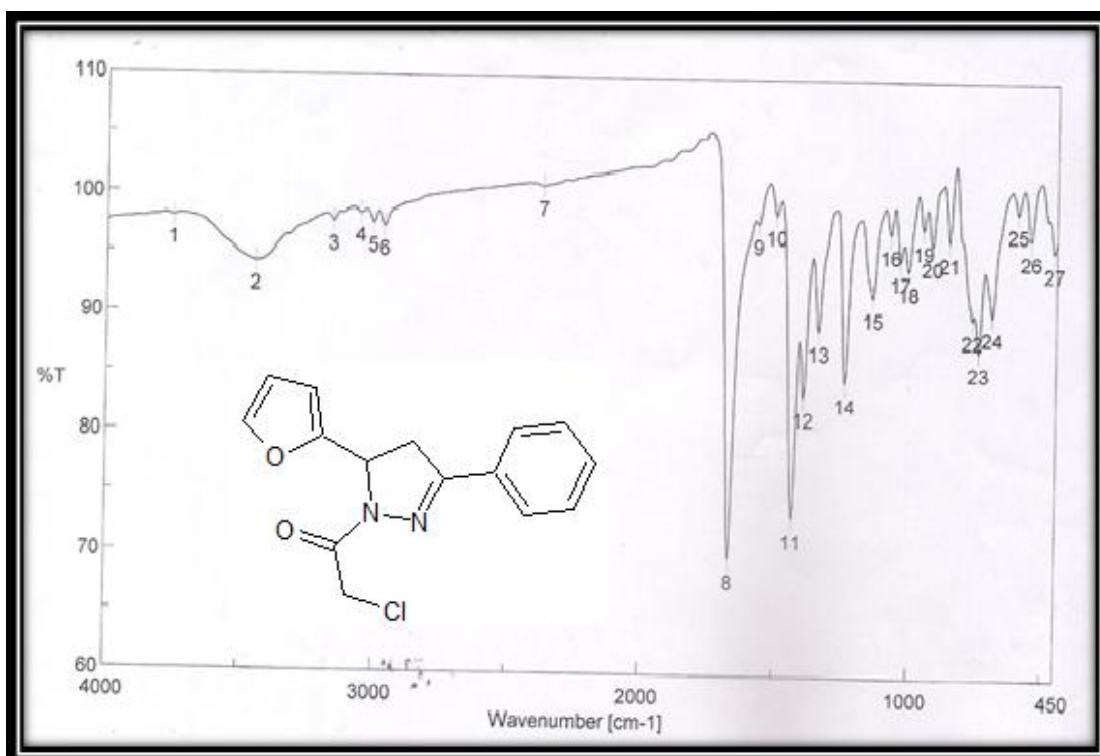
Figure (4.45): IR Spectrum of 2-chloro-1-[5-(fura n-2-yl)-3-phenyl-4,5-dihydro-1H-pyrazol-1-yl]ethan-1-one **(XLV)**
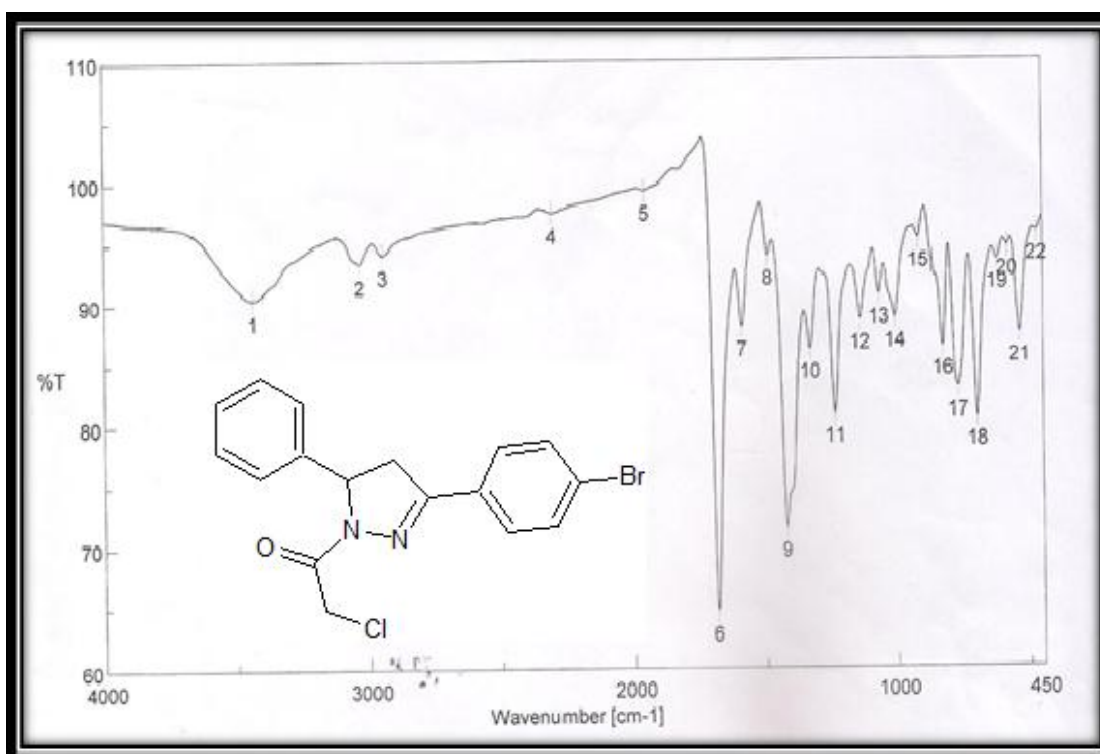
Figure (4.46): IR Spectrum of 1-[3-(4-bromophenyl)-5-phenyl-4,5-dihydro-1*H*-pyrazol-1-yl]-2-chloroethan-1-one **(XLVI)**

215
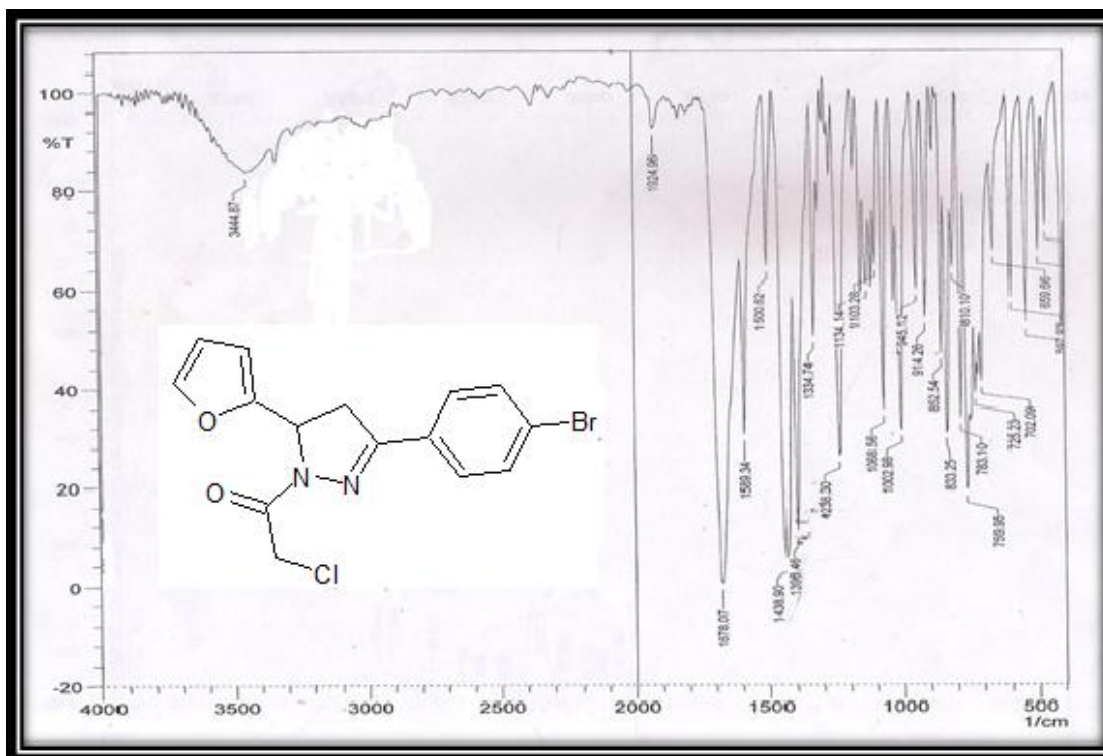
Figure (4.47): IR Spectrum of 1-[3-(4-bromophenyl)-5-(furan-2-yl)-4,5-dihydro-1*H*-pyrazol-1-yl]-2-chloroethan-1-one **(XLVII)**
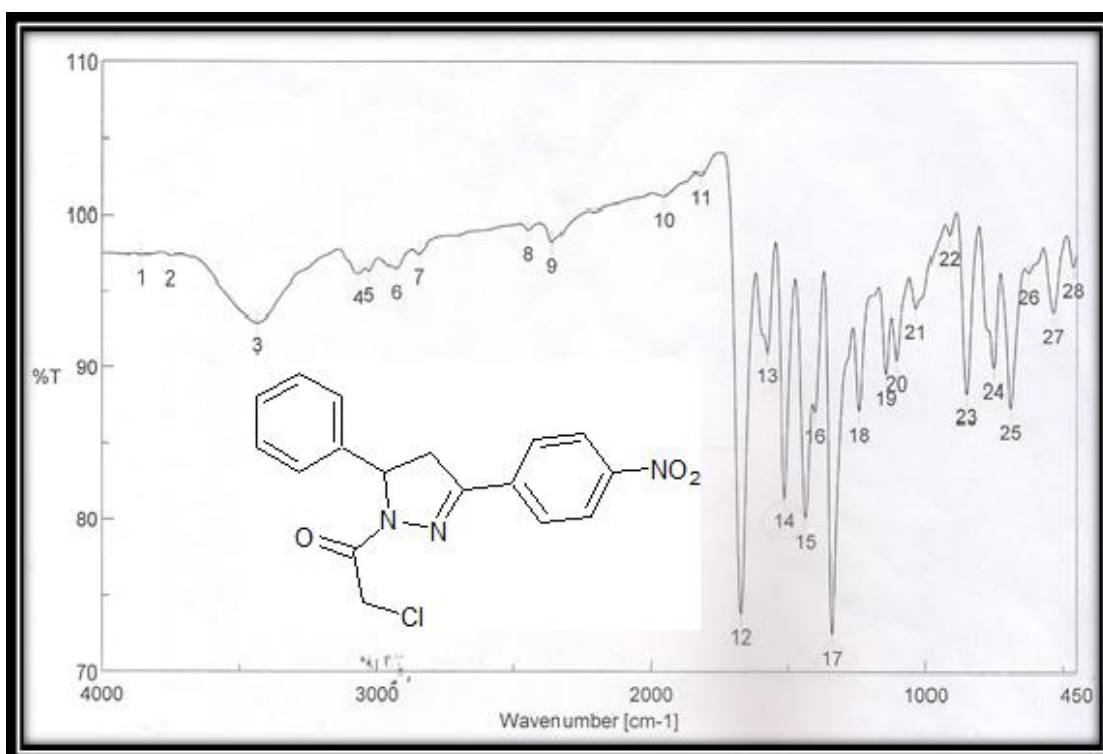
Figure (4.48): IR Spectrum of 2-chloro-1-[3- (4-nitro phenyl)-5-phenyl-4,5-dihydro-1*H*-pyrazol-1-yl] ethan-1-one **(XLVIII)**

216
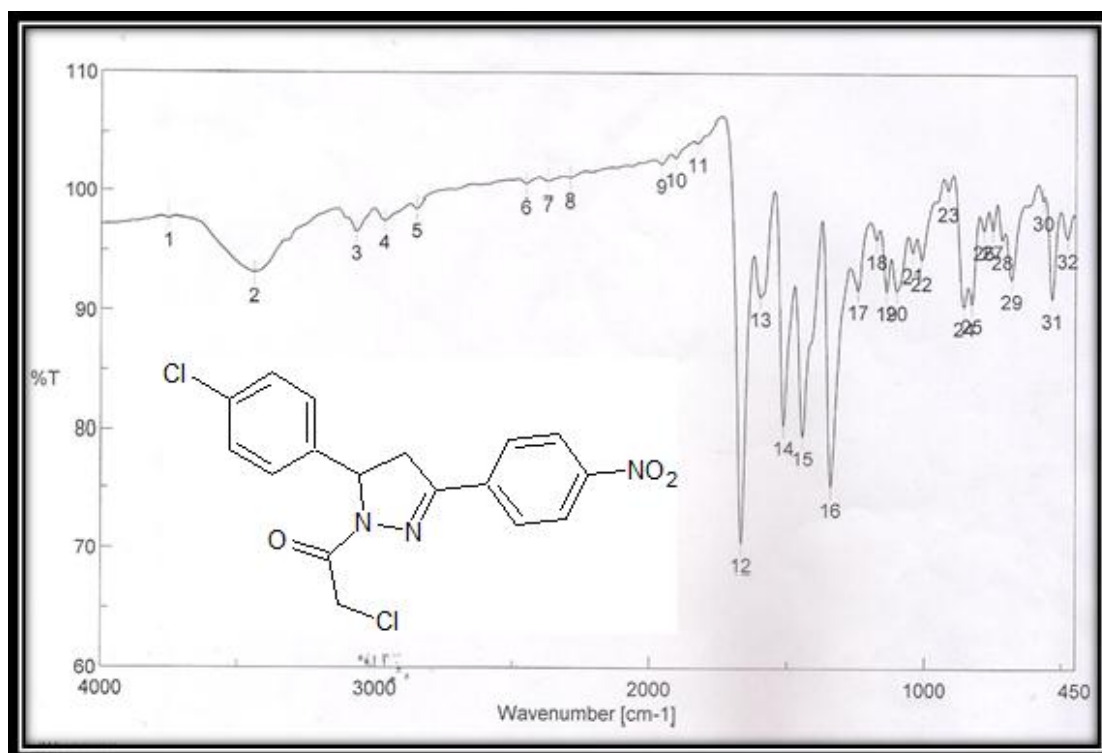
Figure (4.49): IR Spectrum of 2-chloro-1-[5-(4-chloro phenyl)-3-(4-nitro phenyl)-4,5-dihydro-1*H*-pyrazol-1-yl]ethan-1-one **(XLIX)**
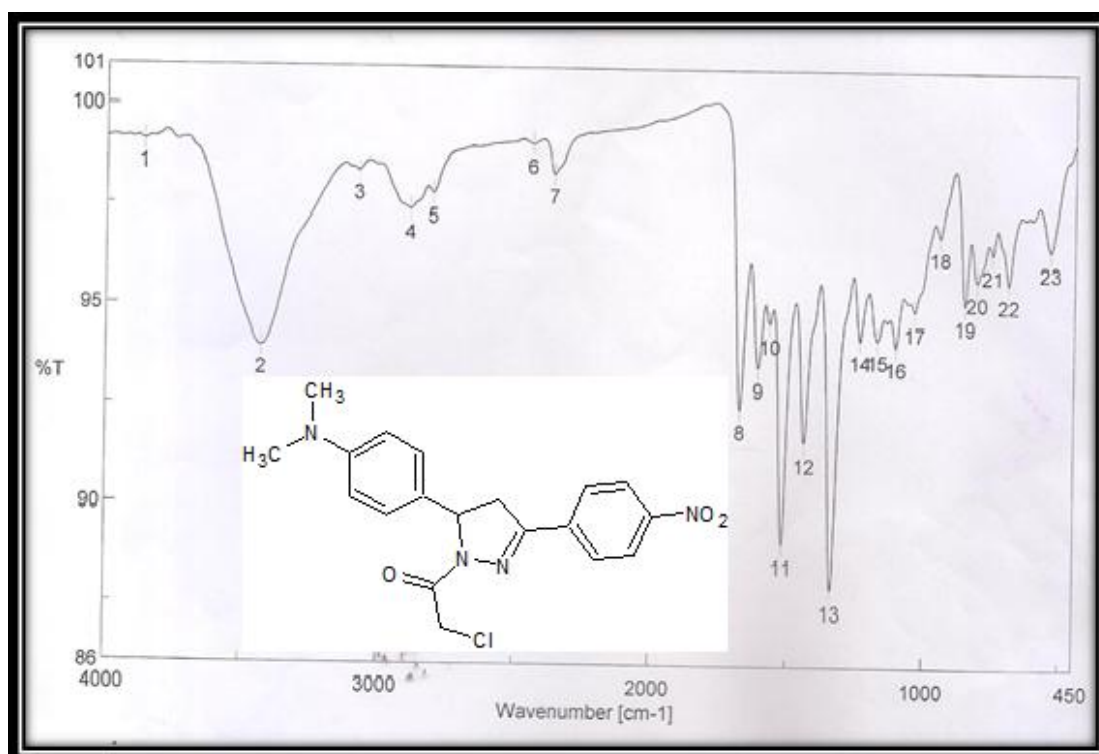
Figure (4.50): IR Spectrum of 2-chloro-1-{5-[4-(dimethylamino)phenyl]-3-(4-nitrophenyl)-4,5-dihydro-1 *H*-pyrazol-1-yl} ethan-1-one **(L)**

217
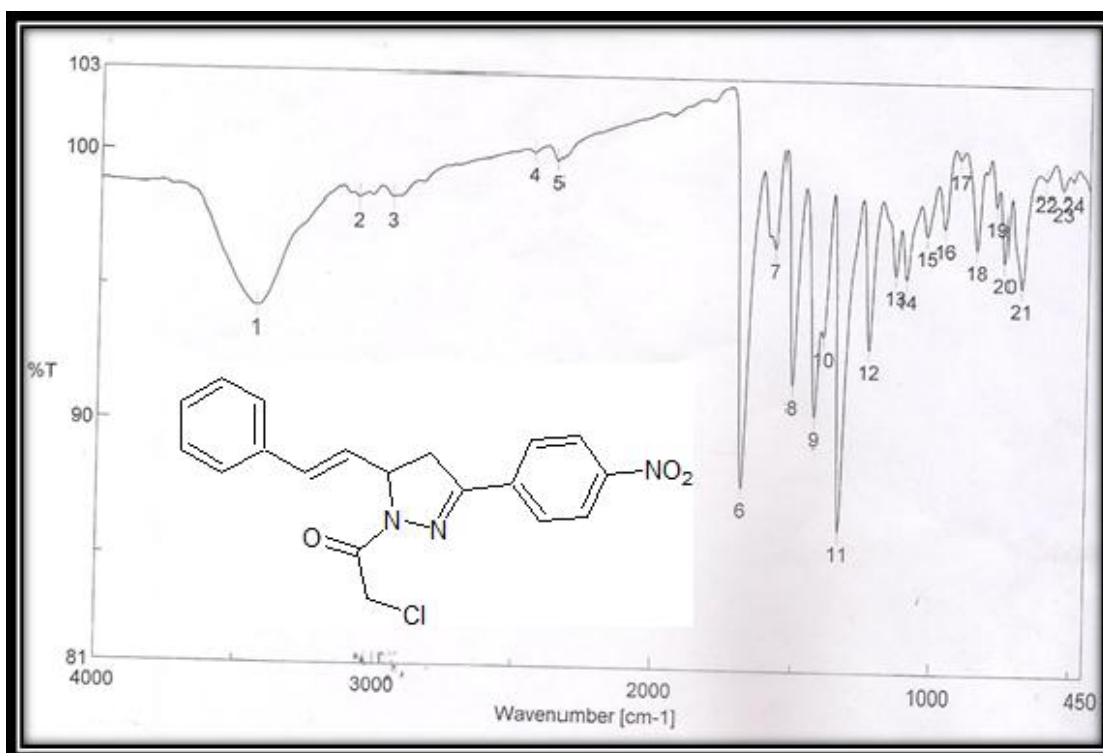
Figure (4.51): IR Spectrum of 2-chloro-1-{3-(4-nitrophenyl)-5-[(*E*)-2-phenylethenyl]-4,5-dihydro-1*H*-pyrazol-1-yl}ethan-1-one **(LI)**
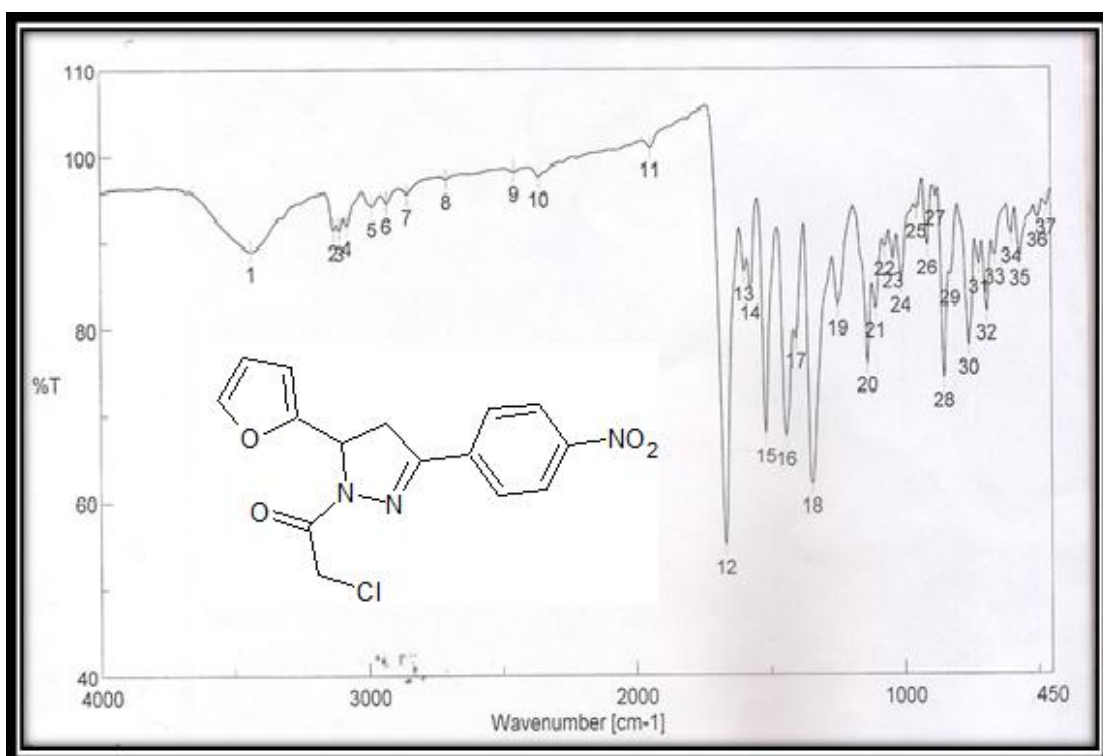
Figure (4.52): IR Spectrum of 2-chloro-1-[5-(furan-2-yl)-3-(4-nitrophenyl)-4,5-dihydro-1*H*-pyrazol-1-yl]ethan-1-one **(LII)**

218
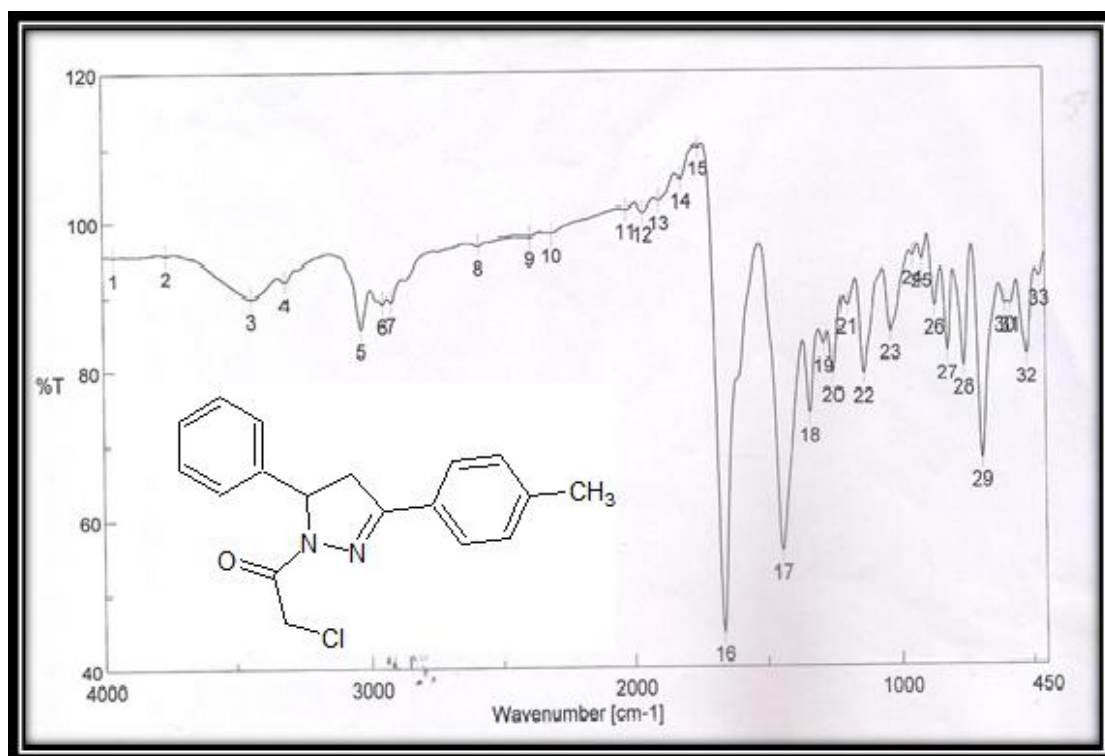
Figure (4.53): IR Spectrum of 2-chloro-1-[3-(4-methylphenyl)-5-phenyl-4,5-dihydro-1*H*-pyrazol-1-yl] ethan-1-one **(LIII)**
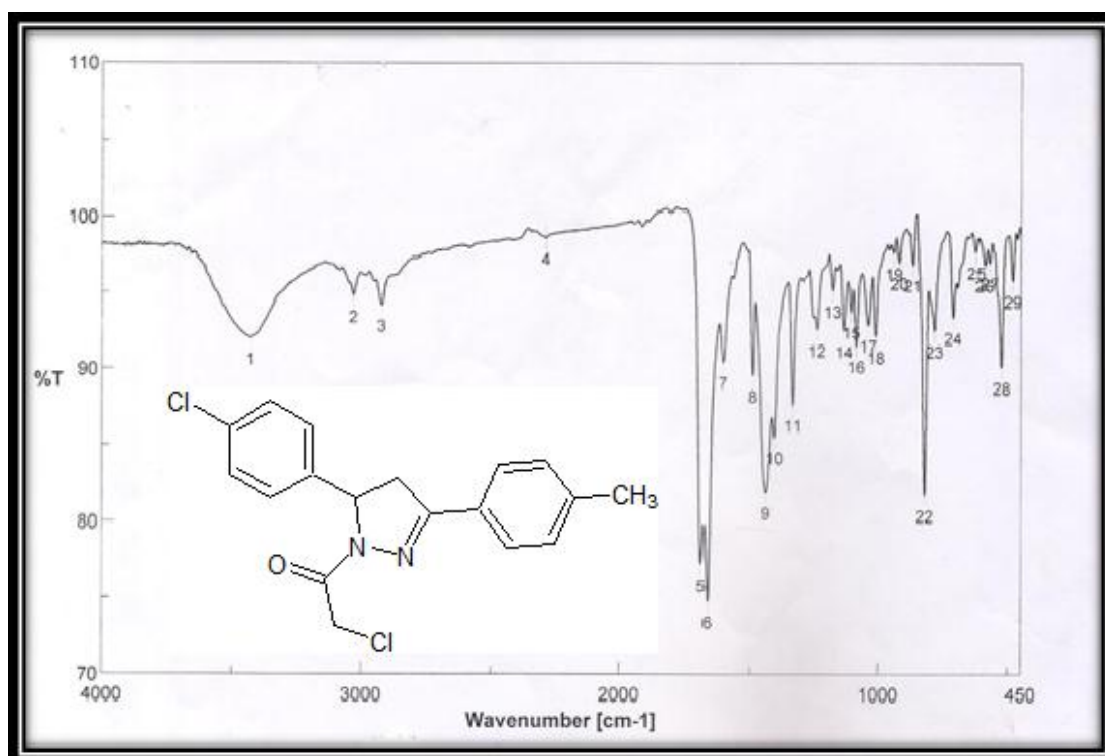
Figure (4.54): IR Spectrum of 2-chloro-1-[5-(4-chloro p henyl)-3-(4-methylphenyl)-4,5-dihydro-1H-pyrazol-1-yl]ethan-1-one **(LIV)**
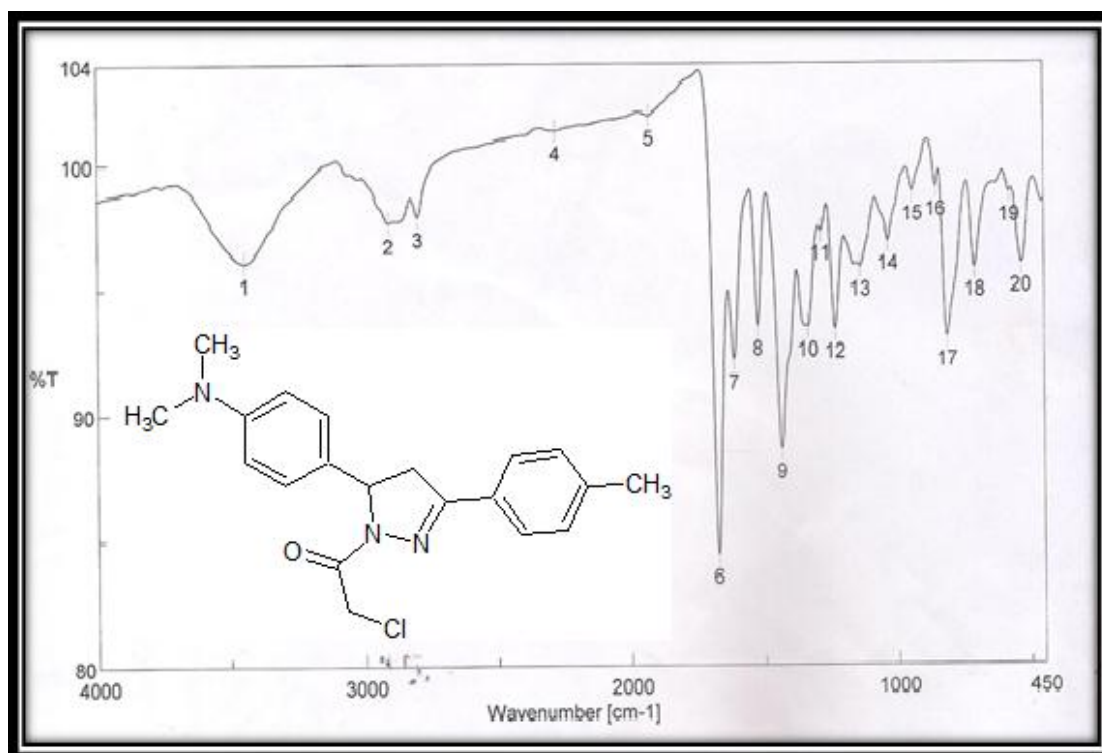
Figure (4.55): IR Spectrum of 2-chloro-1-{5-[4-(dimethylamino) phenyl]-3-(4-methylphenyl)-4,5-dihydro-1 H-pyrazol-1-yl}ethan-1-one **(LV)**
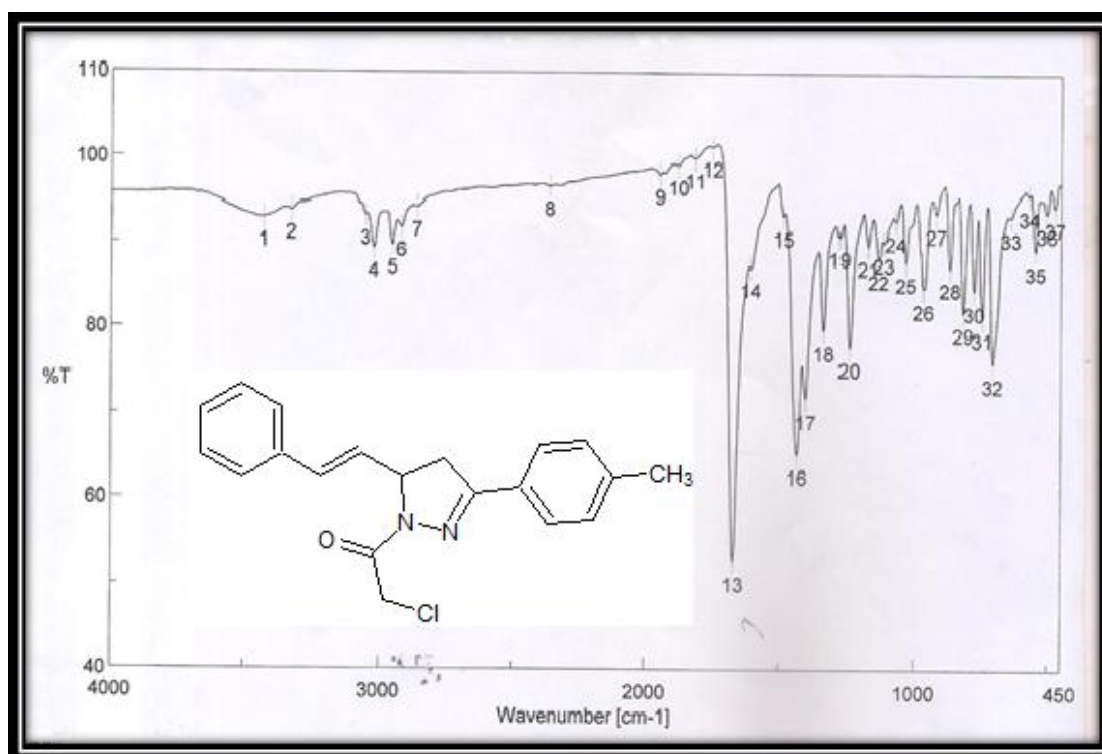
Figure (4.56): IR Spectrum of 2-chloro-1-{3-(4-methyl phenyl)-5-[(E)-2-phenylethenyl]-4,5-dihydro-1H-pyrazol-1-yl}ethan-1-one **(LVI)**
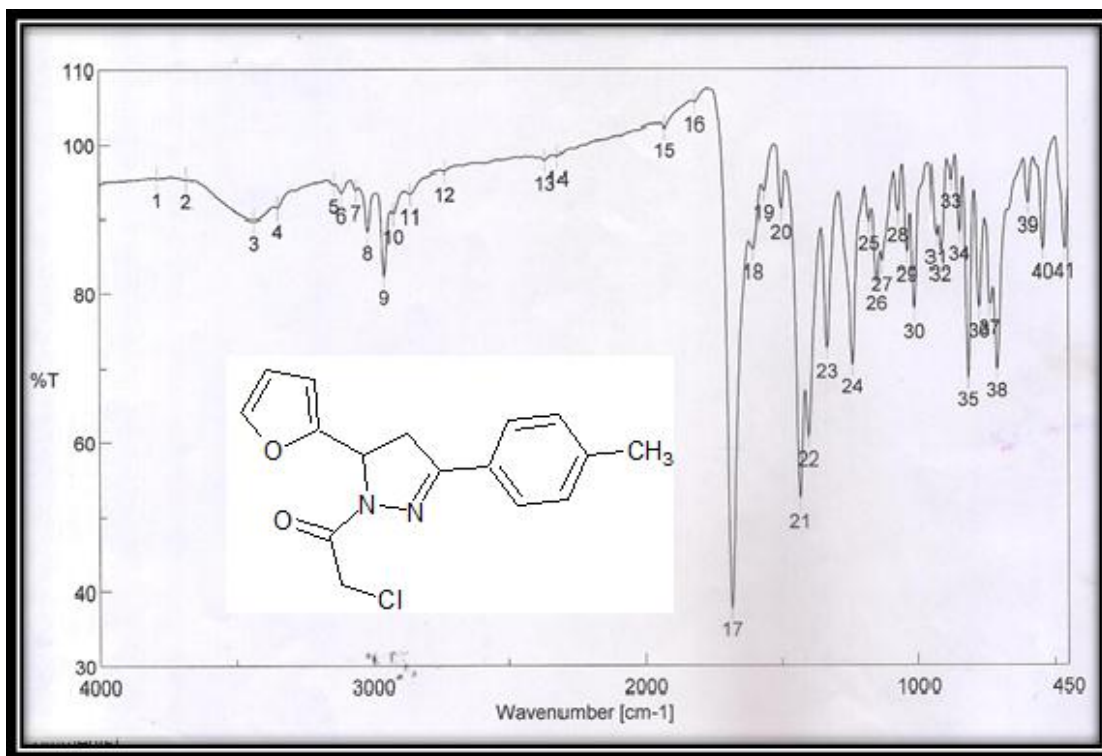
Figure (4.57): IR Spectrum of 2-chloro-1-[5-(furan-2-yl)-3-(4-methylphenyl)-4,5-dihydro-1*H*-pyrazol-1-yl]ethan-1-one (**LVII**)
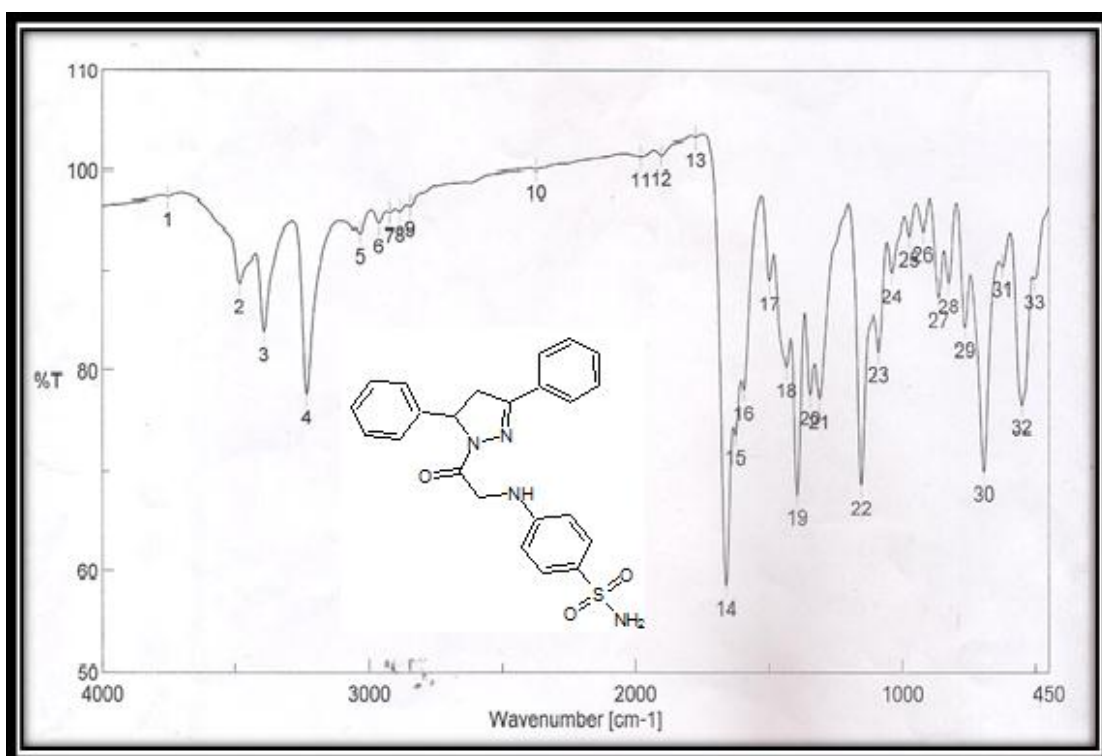
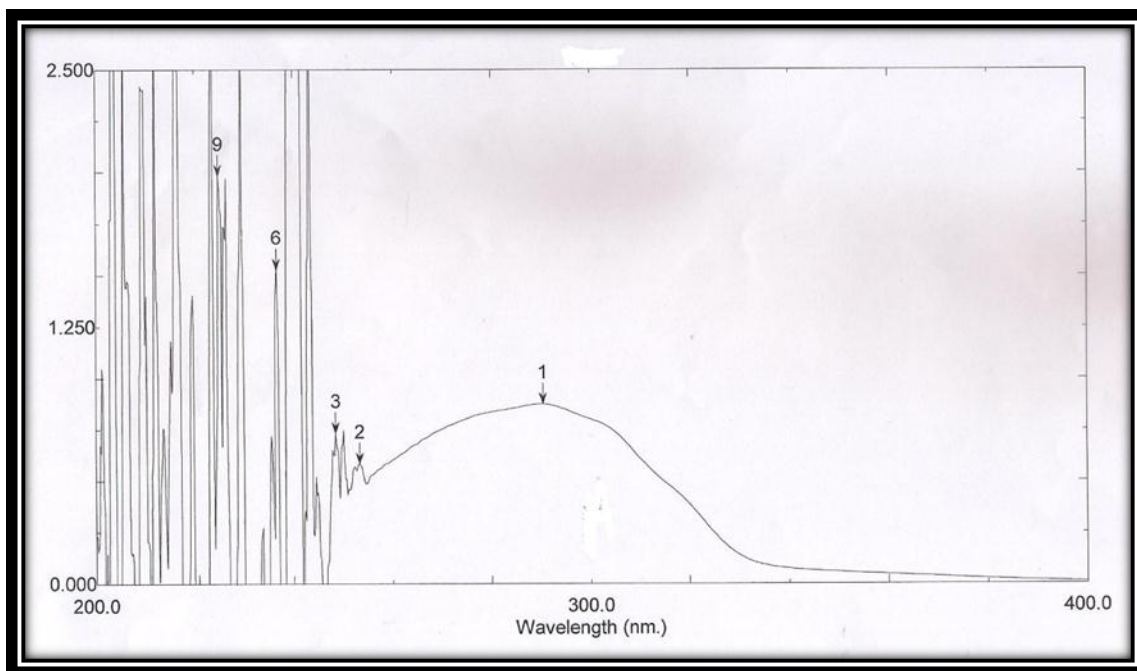**Figure (4.58):** IR Spectrum of 4-((2-(3,5-diphenyl-4,5-di hydro-1H-pyrazol-1-yl)-2-oxoethyl)amino)benzene sulfonamide **(LVIII)**
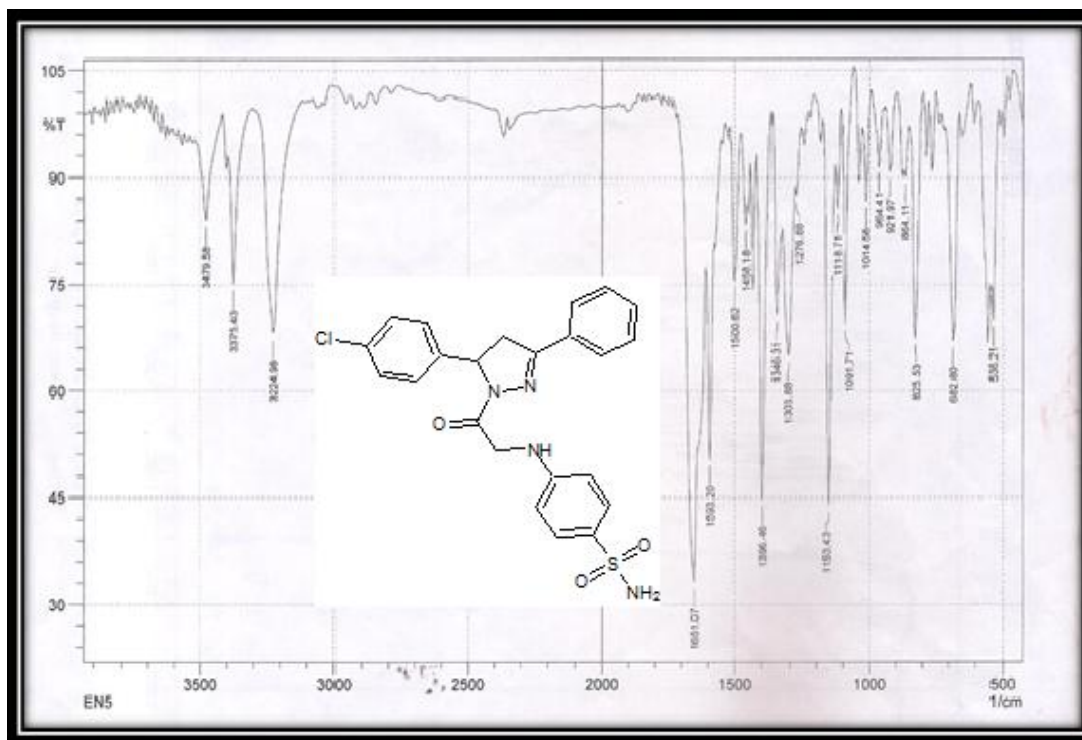
Figure (4.59): IR Spectrum of 4-((2-(5-(4-chlorophenyl)-3-phenyl-4,5-dihydro-1H-pyrazol-1-yl)-2-oxoethyl) amino) benzene sulfonamide **(LIX)**
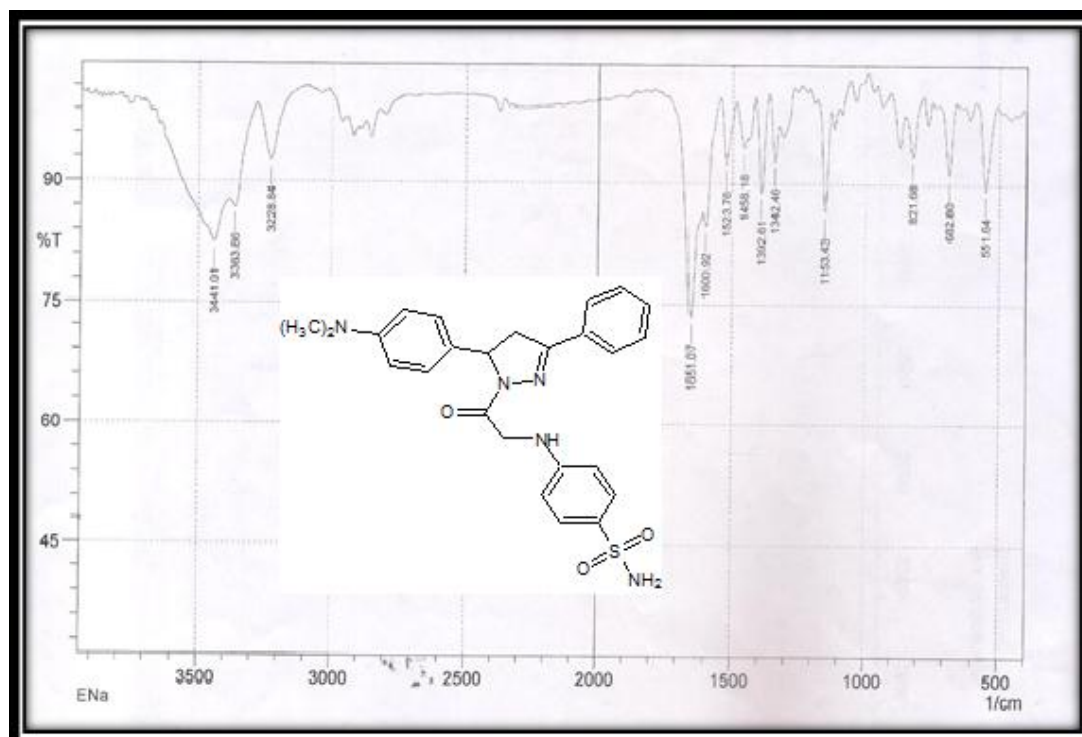
Figure (4.60): IR Spectrum of 4-((2-(5-(4-(dimethylamin o)phenyl)-3-phenyl-4,5-di hydro-1H-pyrazol-1-yl)-2-oxoethyl)amino)benzene sulfonamide **(LX)**
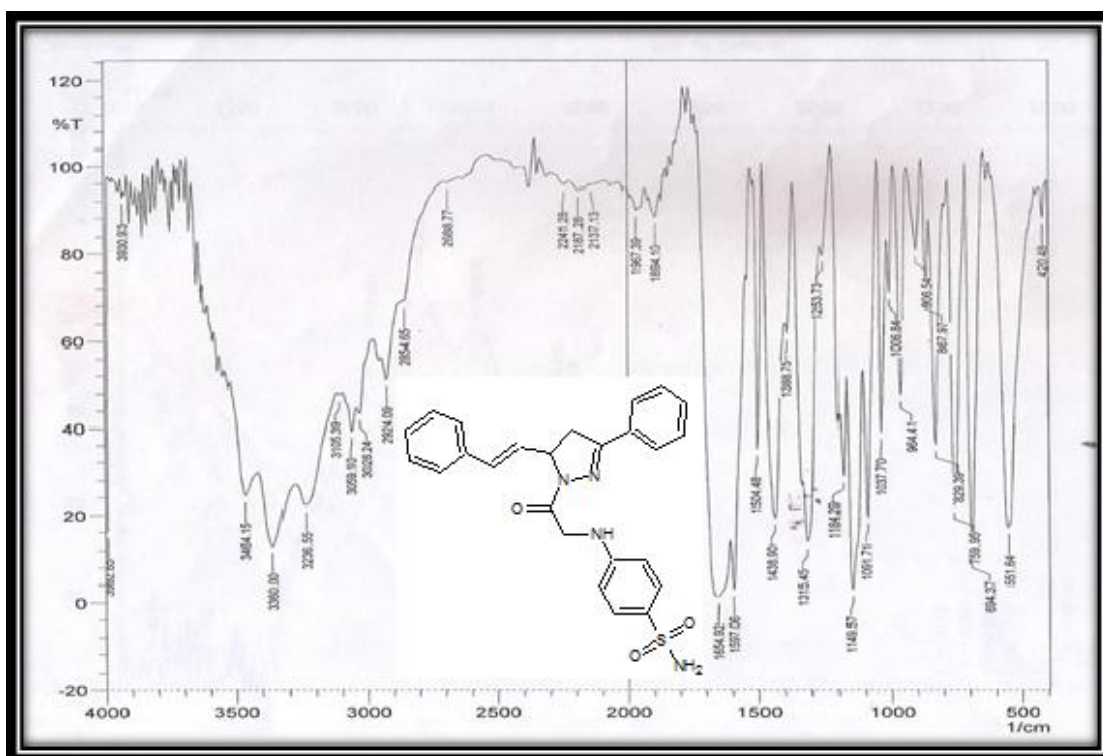
**Figure (4.61):** IR Spectrum of (E)-4-((2-oxo-2-(3-phenyl-5-styryl-4,5-dihydro-1H-pyrazol-1-yl)ethyl)amino) benzenesulfonamide **(LXI)**
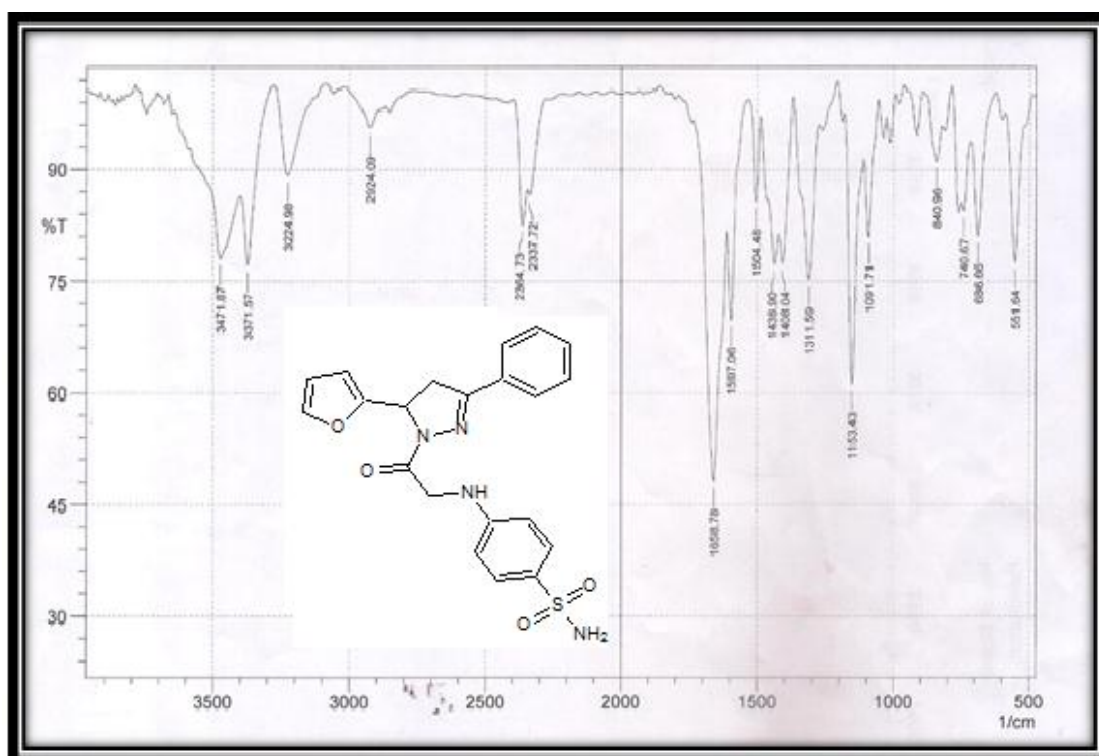
Figure (4.62): IR Spectrum of 4-({2-[5-(furan-2-yl)-3-phenyl-4,5-dihydro-1*H*-pyrazol-1-yl]-2-oxoethyl}amino)benzene-1-sulfonamide **(LXII)**
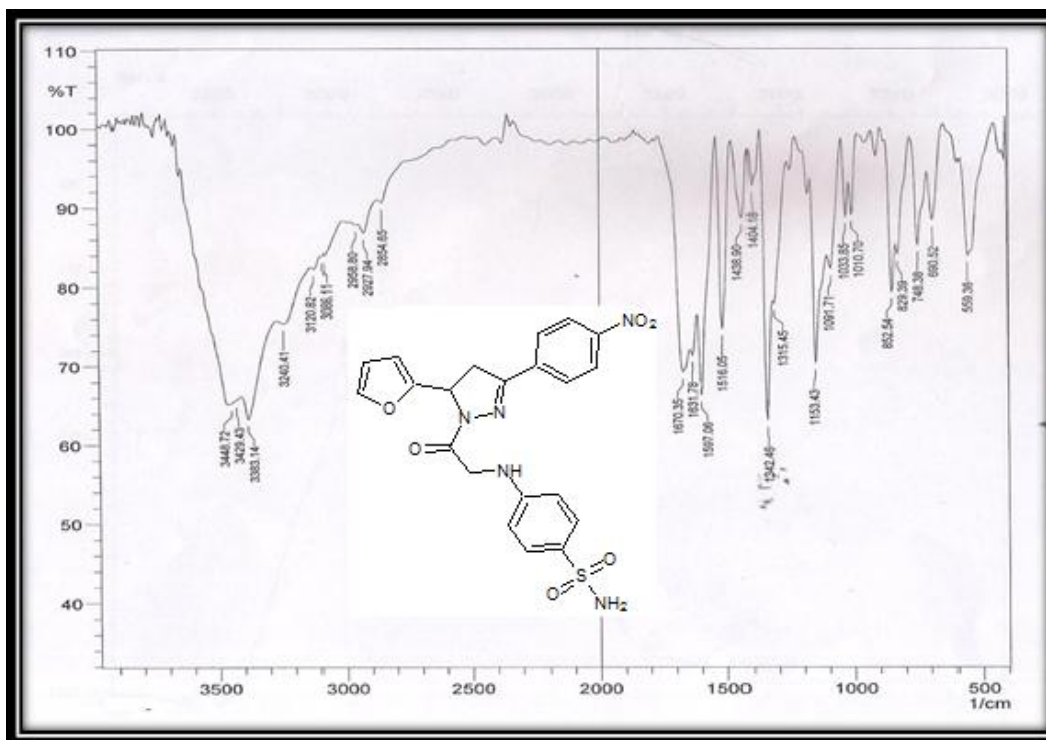
Figure (4.63): IR Spectrum of 4-((2-(5-(furan-2-yl)-3-(4-nitrophenyl)-4,5-dihydro-1H-pyrazol-1-yl)-2-oxoeth yl) amino)benzene sulfonamide **(LXIII)**
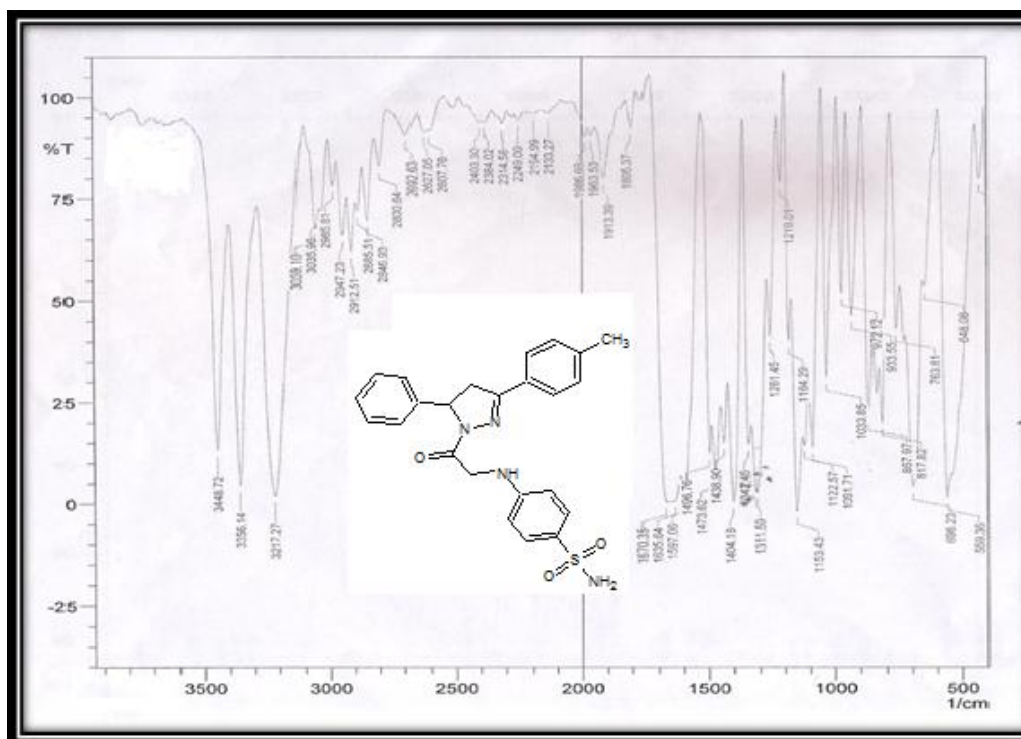
Figure (4.64): IR Spectrum of 4-((2-oxo-2-(5-phenyl-3-(p-tolyl)-4,5-dihydro-1H-pyrazol-1-yl)ethyl)amino) benzenesulfonamide **(LXIV)**
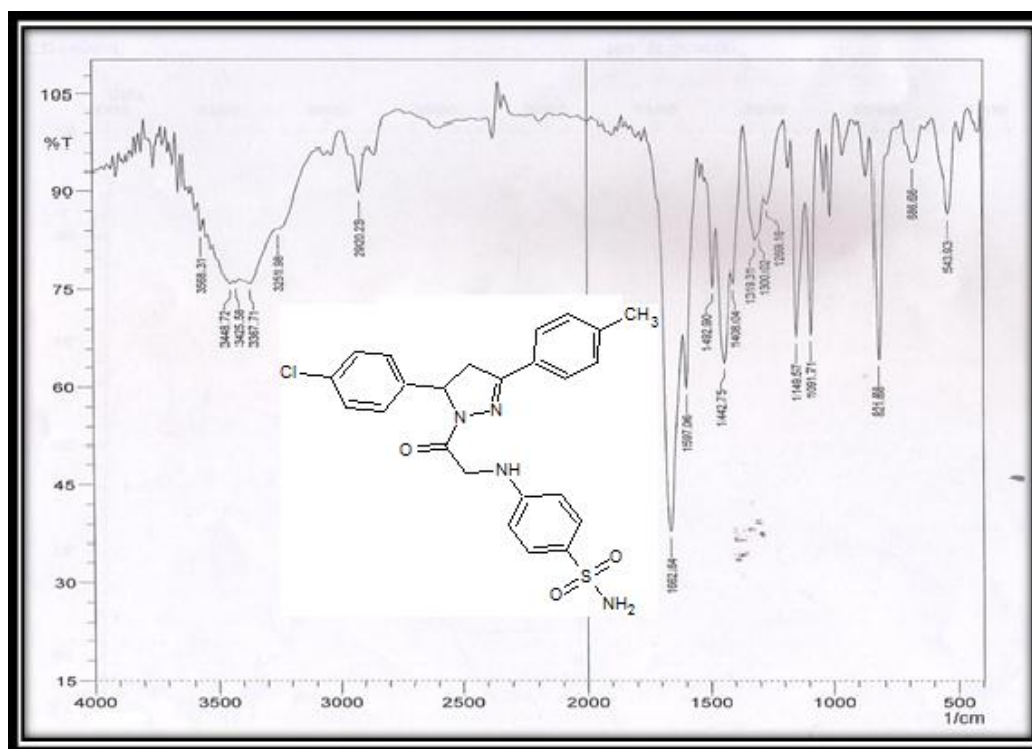
Figure (4.65): IR Spectrum of 4-((2-(5-(4-chlorophenyl)-3-(p-tolyl)-4,5-dihydro-1H-pyrazol-1-yl)-2-oxoethyl)amino)benzene sulfonamide **(LXV)**
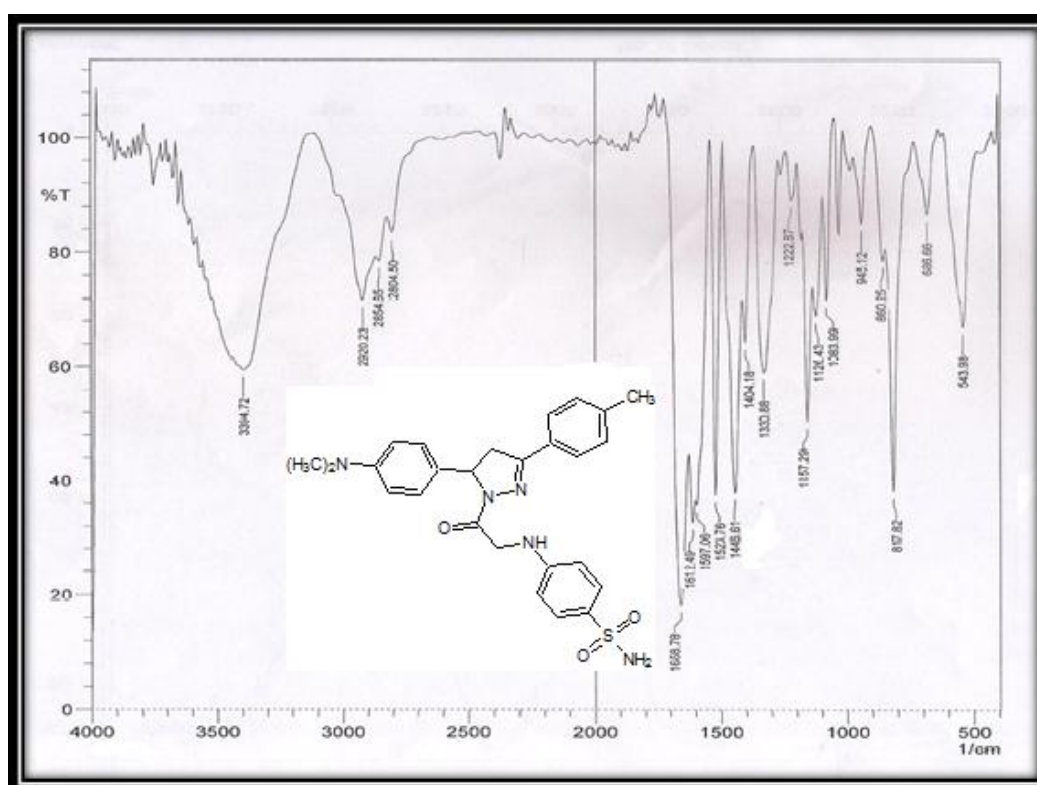
Figure (4.66): IR Spectrum of 4-((2-(5-(4-(dimethyl amino)phenyl)-3-(p-tolyl)-4,5-dihydro-1H-pyrazol-1-yl)-2-oxoethyl)amino)benzene sulfonamide **(LXVI)**
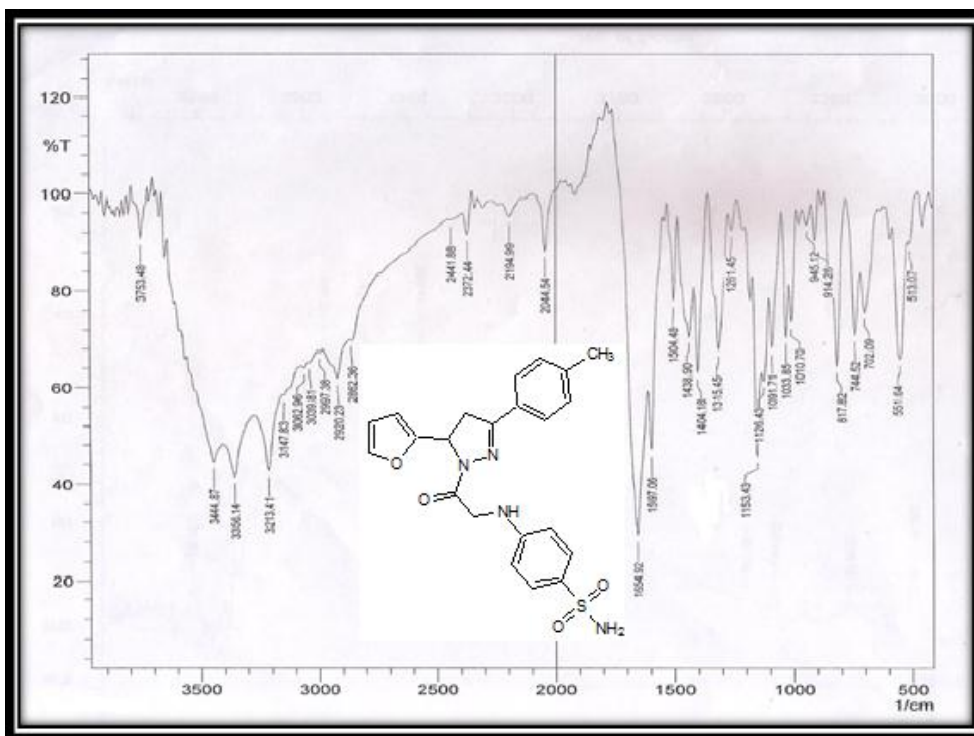
Figure (4.67): IR Spectrum of 4-((2-(5-(furan-2-yl)-3-(p-tolyl)-4,5-dihydro-1H-pyrazol-1-yl)-2-oxoethyl)amino)benzene sulfonamide **(LXVII)**
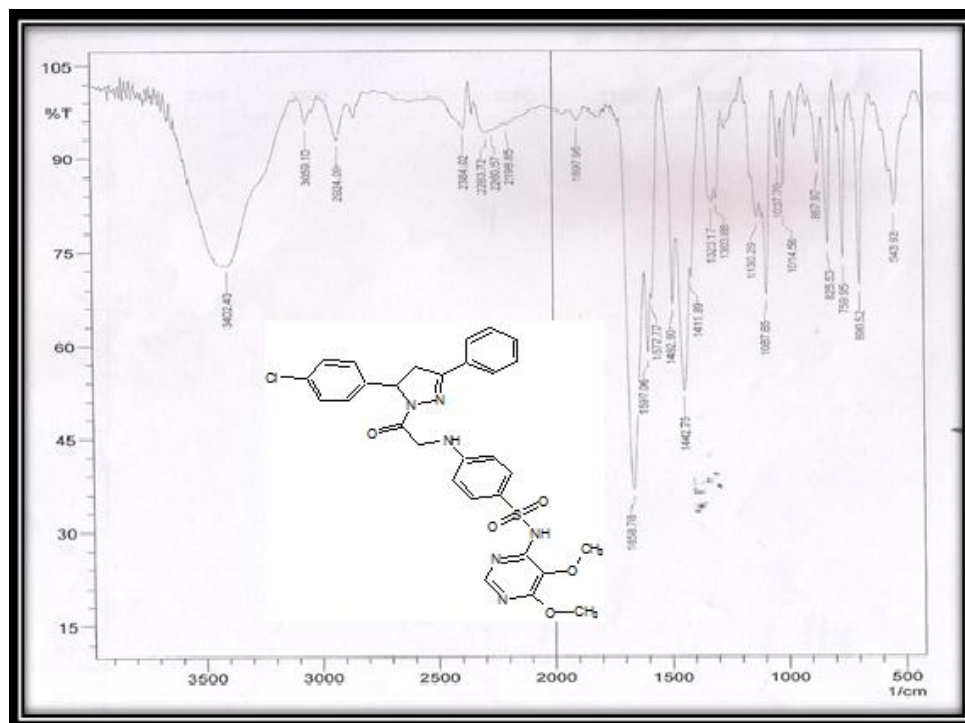
Figure (4.68): IR Spectrum of 4-((2-(5-(4-chlorophenyl)-3-phenyl-4,5-dihydro-1H-pyrazol-1-yl)-2-oxoethyl) amino)-N-(5,6-dimethoxy pyrimidin-4-yl)benzene sulfonamide **(LXVIII)**

226
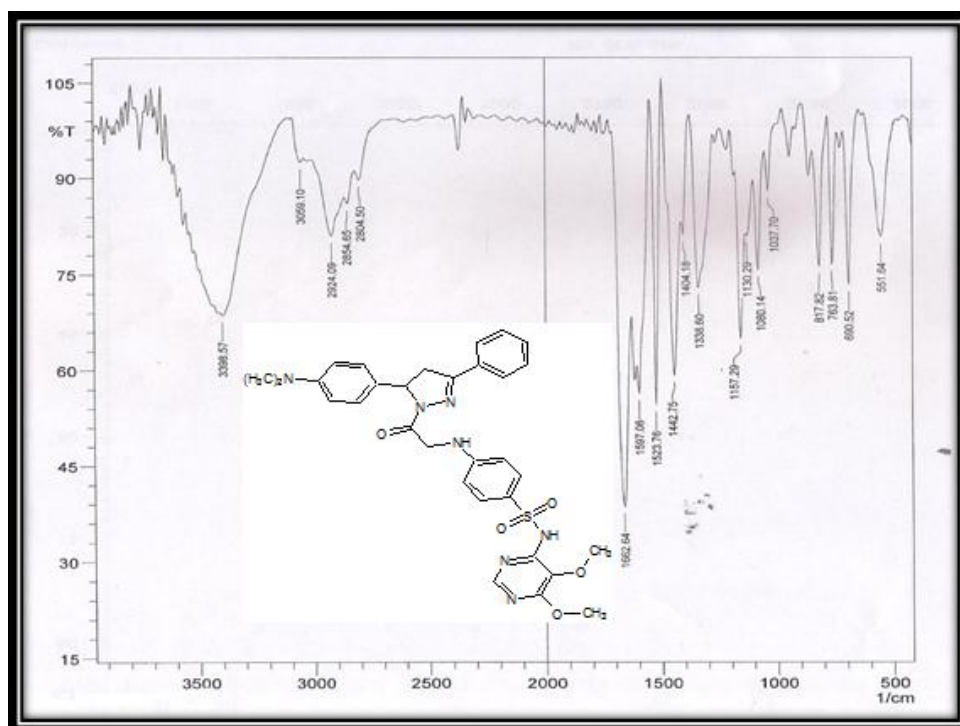
Figure (4.69): IR Spectrum of N-(5,6-dimethoxypyrimi d in-4-yl)-4-((2-(5-(4-(dime thylamino)phenyl)-3-phen yl-4,5-dihydro-1H-pyrazol -1-yl)-2-oxoethyl)amino) benzenesulfonamide **(LXIX)**
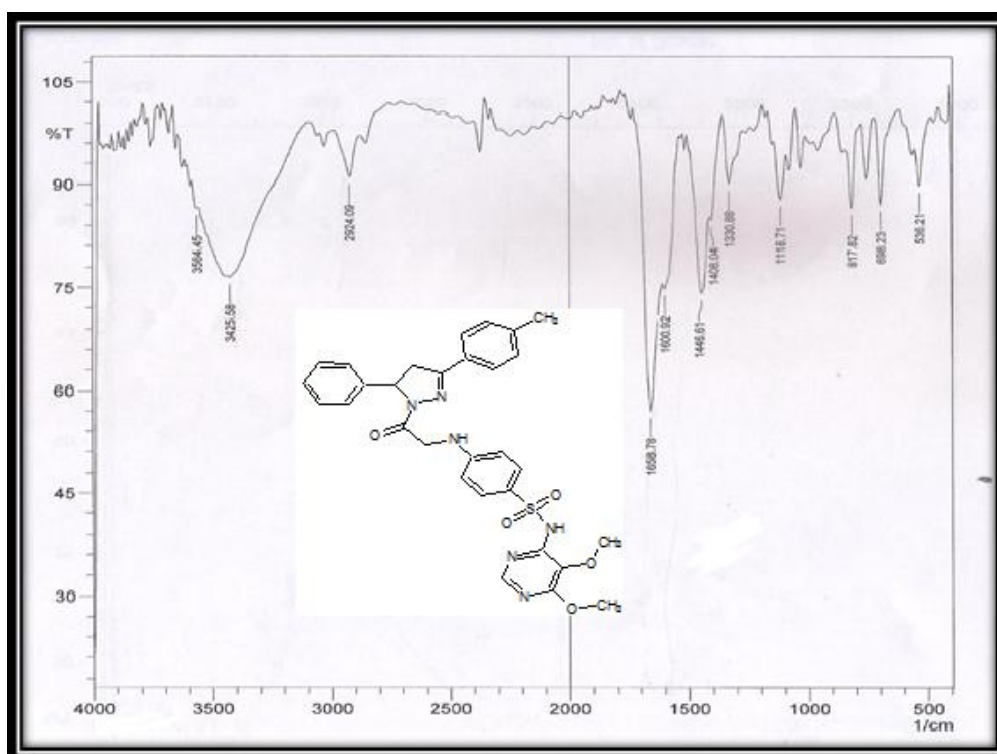
Figure (4.70): IR Spectrum of N-(5,6-dimethoxypyrimidin-4-yl)-4-((2-oxo-2-(5-phenyl-3-(p-tolyl)-4,5-dihydro-1H-pyrazol-1-yl)ethyl)amino)benzenesulfonamide **(LXX)**
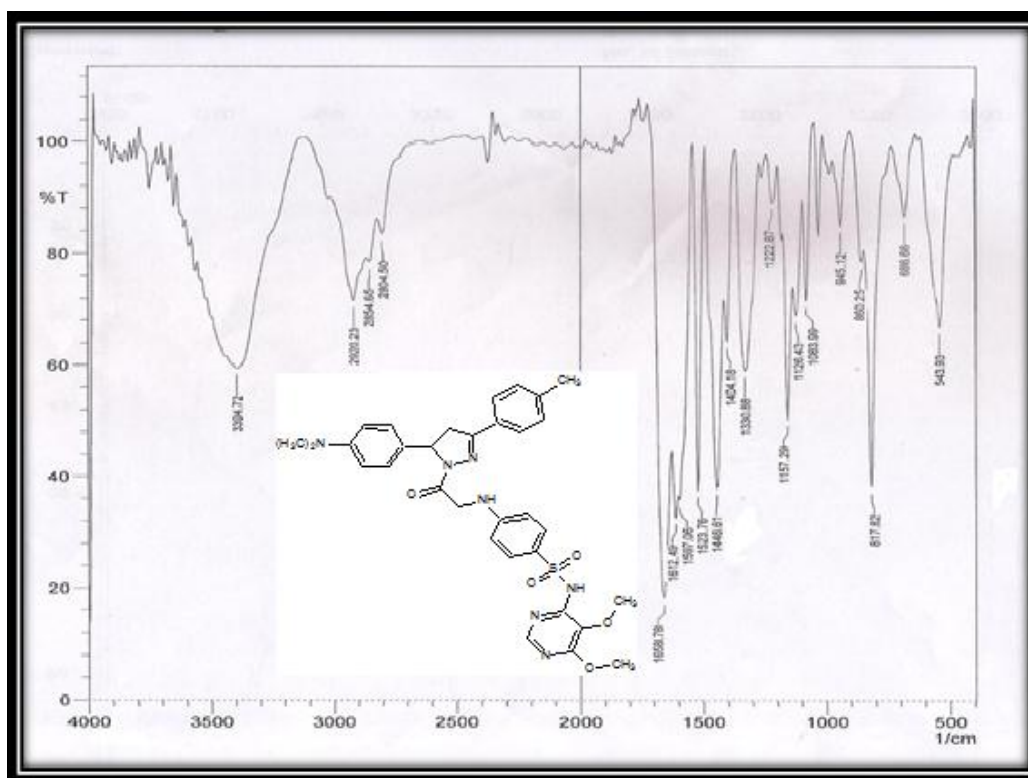
Figure (4.71): IR Spectrum of N-(5,6-dimethoxypyrimid in-4-yl)-4-((2-(5-(4-(dime thylamino)phenyl)-3-(p-tol yl)-4,5-dihydro-1H-pyraz ol-1-yl)-2-oxoethyl)amino)benzene sulfonamide **(LXXI)**
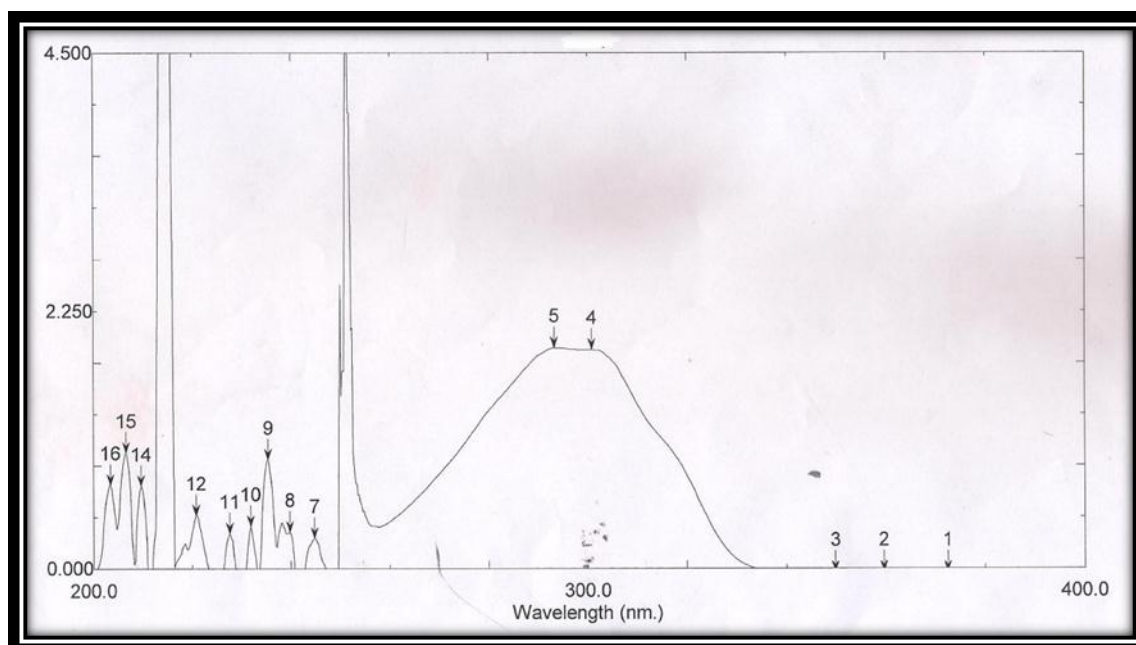
Figure (4.72): UV Spectrum of 2-chloro-1-(3,5-diphe nyl-4,5-dih ydro-1*H*-py razol-1-yl) ethan-1-one **(XLI)**
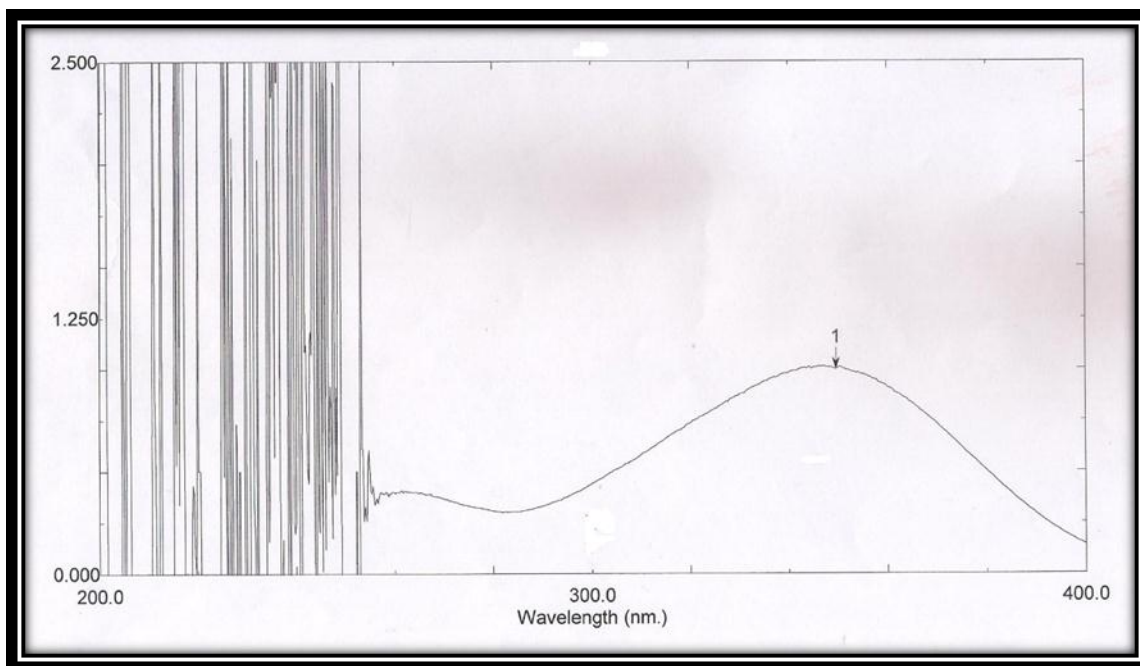
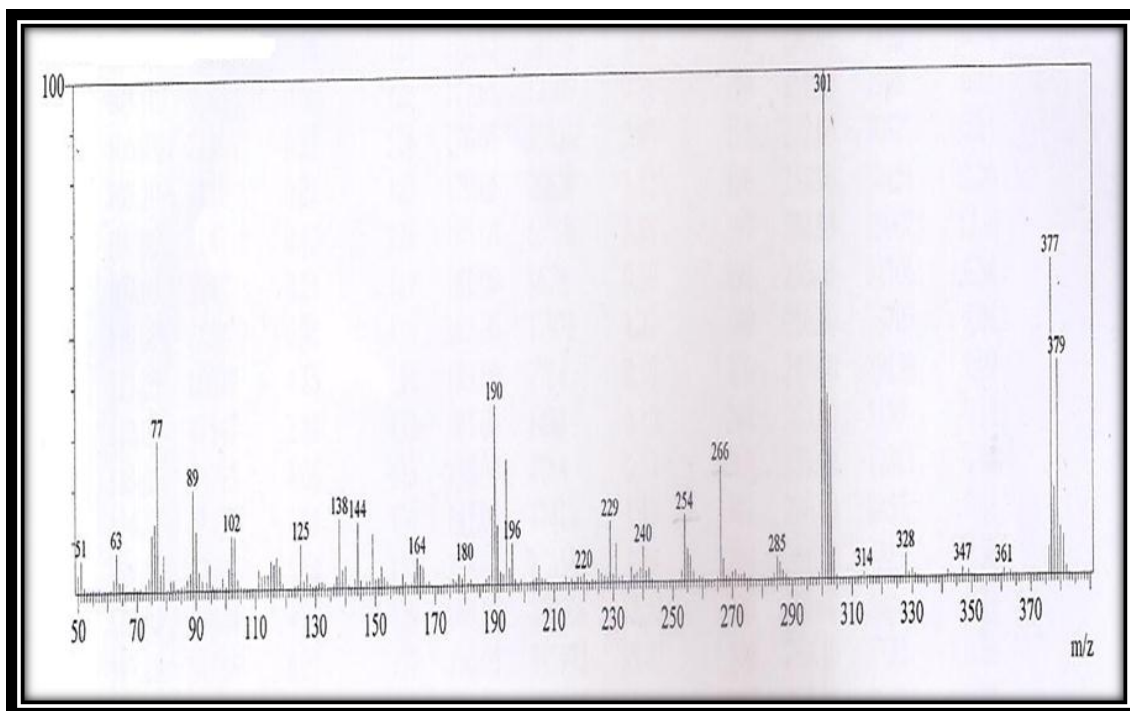**Figure (4.73):** UV Spectrum of 2-chloro-1-[5-(4-chlorophenyl)-3-phenyl-4,5-dihydro-1*H*-pyrazol-1-yl] ethan-1-one **(XLII)**
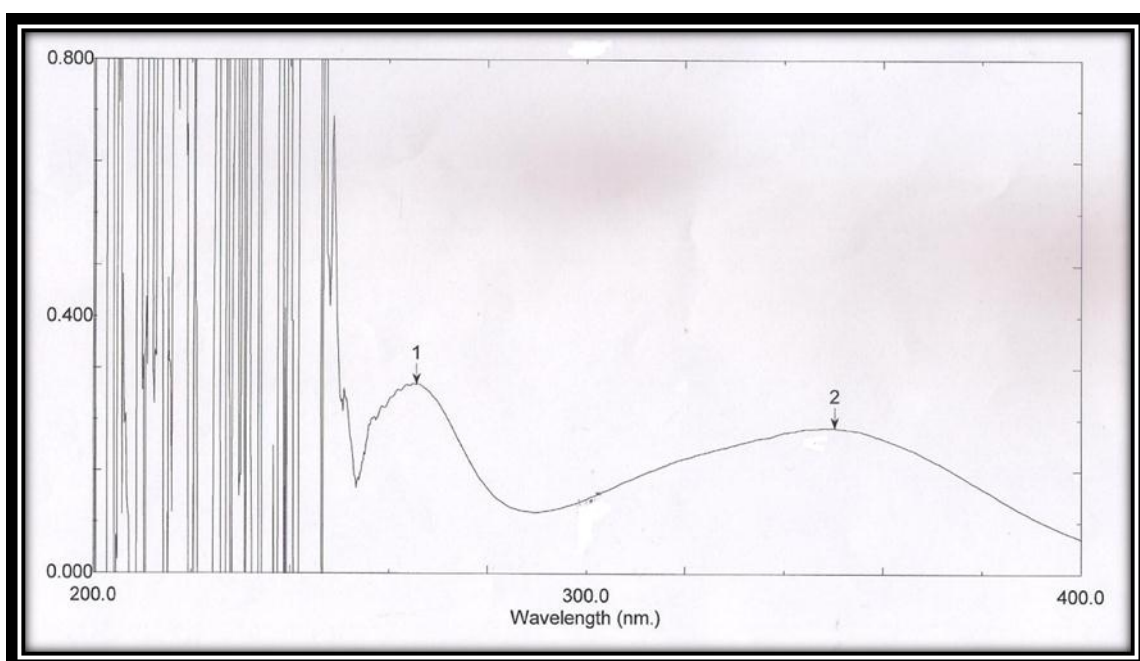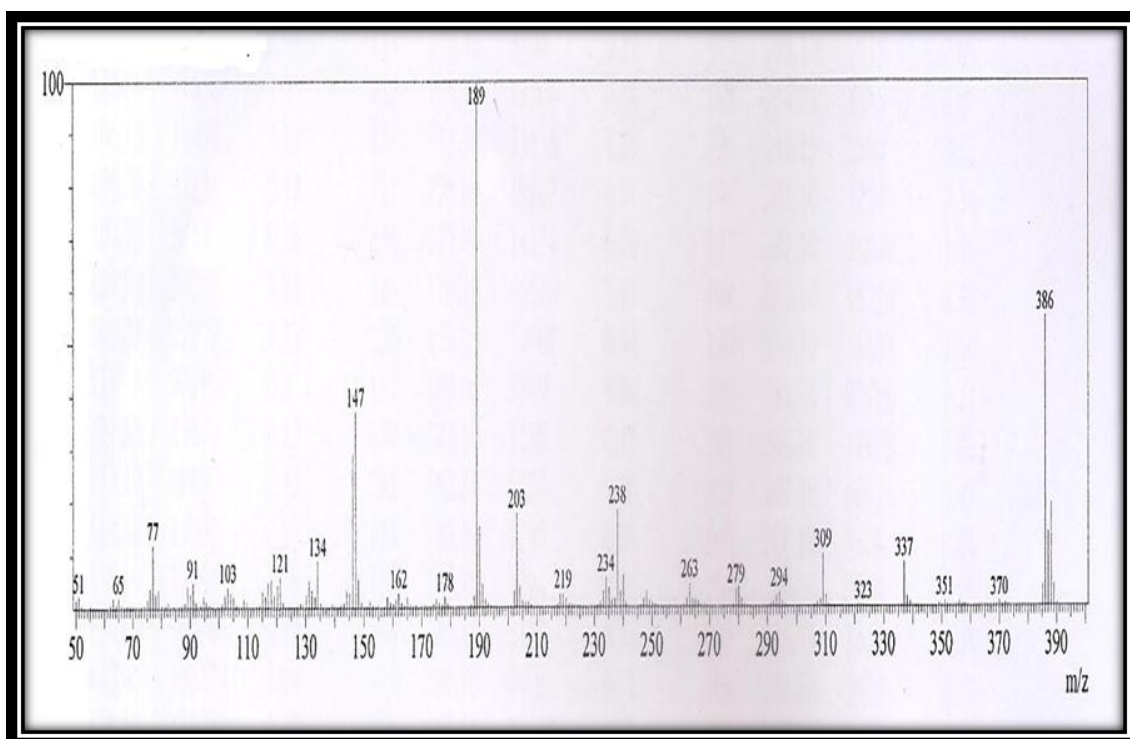

Figure (4.74): UV Spectrum of 2-chloro-1-{5-[4-(dimethylamino) phenyl]-3-phenyl-4,5-dihydro-1*H*-pyrazol-1-yl} ethan-1-one **(XLIII)**
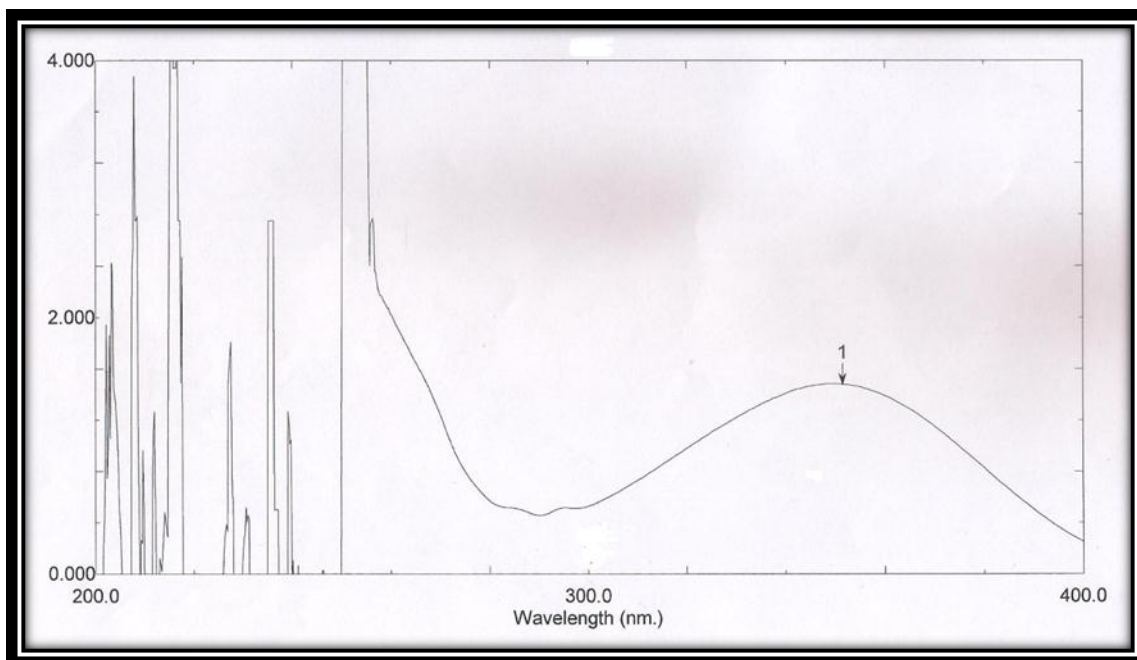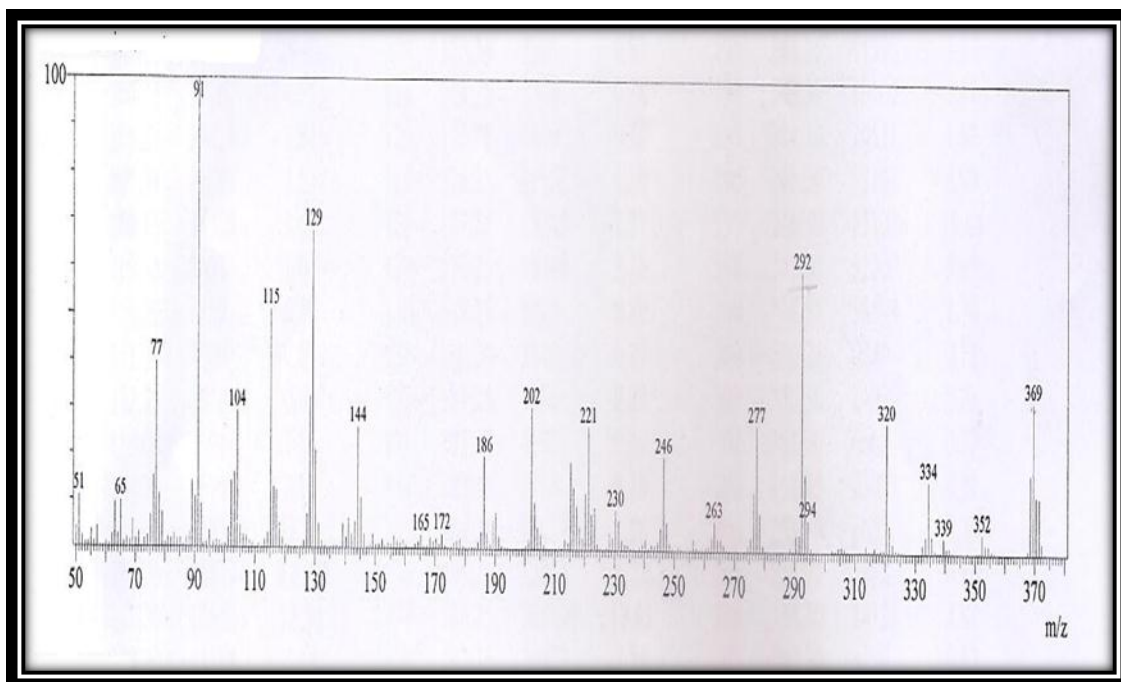
Figure (4.75): UV Spectrum of 2-chloro-1-{3-phenyl-5-[(*E*)-2-phenylethenyl]-4,5-dihydro-1*H*-pyrazol-1-yl}ethan-1-one **(XLIV)**
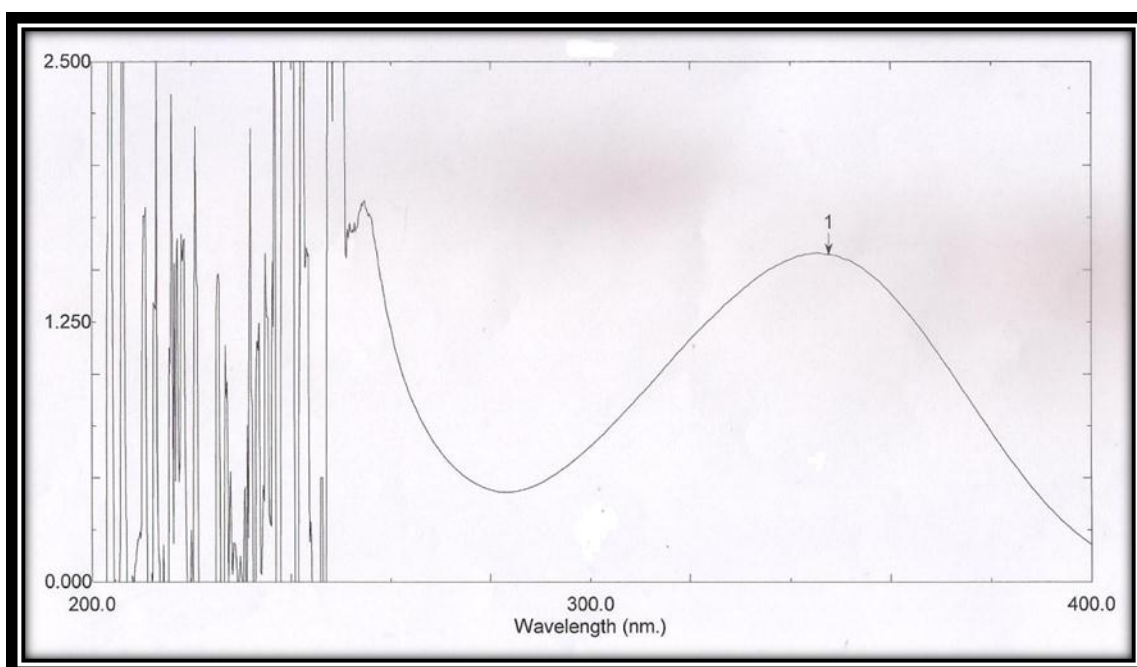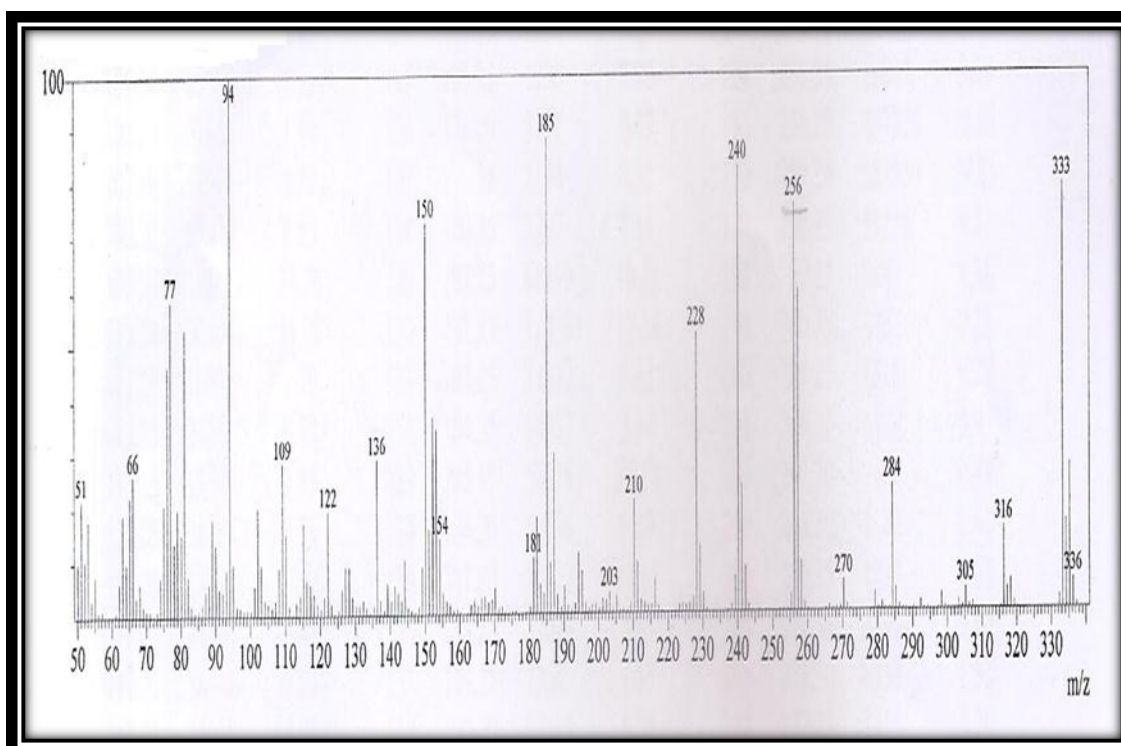

Figure (4.76): UV Spectrum of 2-chloro-1-[5-(fura n-2-yl)-3-phenyl-4,5-dihydro-1H-pyrazol-1-yl]ethan-1-one **(XLV)**
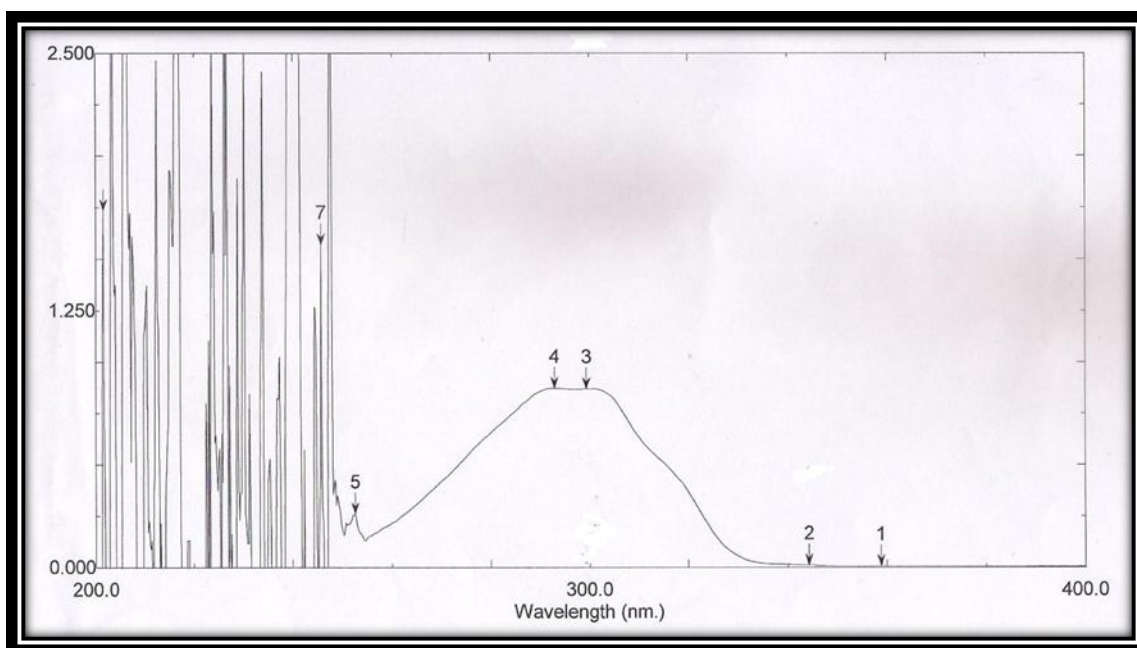
Figure (4.77): UV Spectrum of 1-[3-(4-bromophenyl)-5-phenyl-4,5-dihydro-1*H*-pyrazol-1-yl]-2-chloroethan-1-one (**XLVI**)
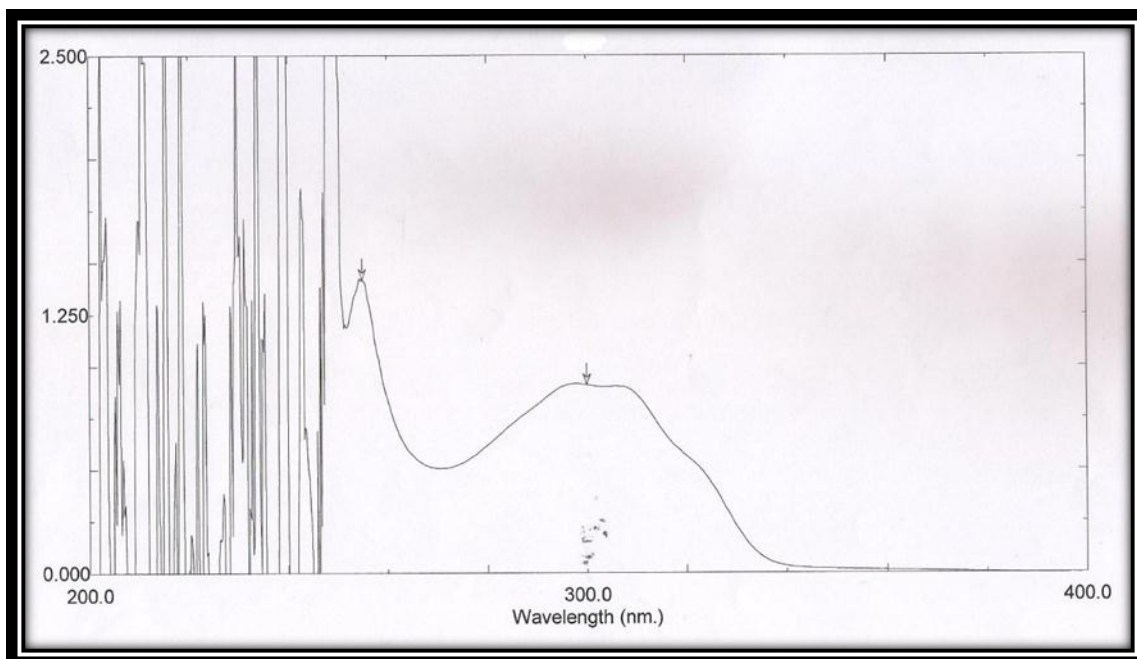
Figure (4.78): UV Spectrum of 1-[3-(4-bromophenyl)-5-(furan-2-yl)-4,5-dihydro-1*H*-pyrazol-1-yl]-2-chloroethan-1-one (**XLVII**)
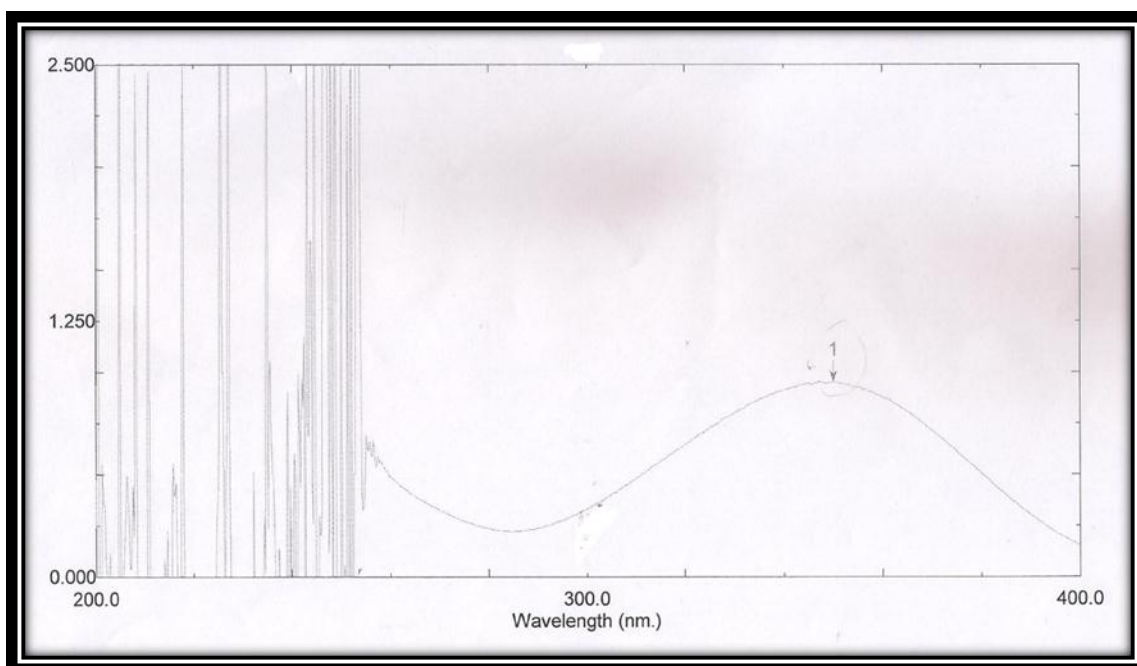
Figure (4.79): UV Spectrum of 2-chloro-1-[3- (4-nitro phenyl)-5-phenyl-4,5-dihydro-1*H*-pyrazol-1-yl] ethan-1-one **(XLVIII)**
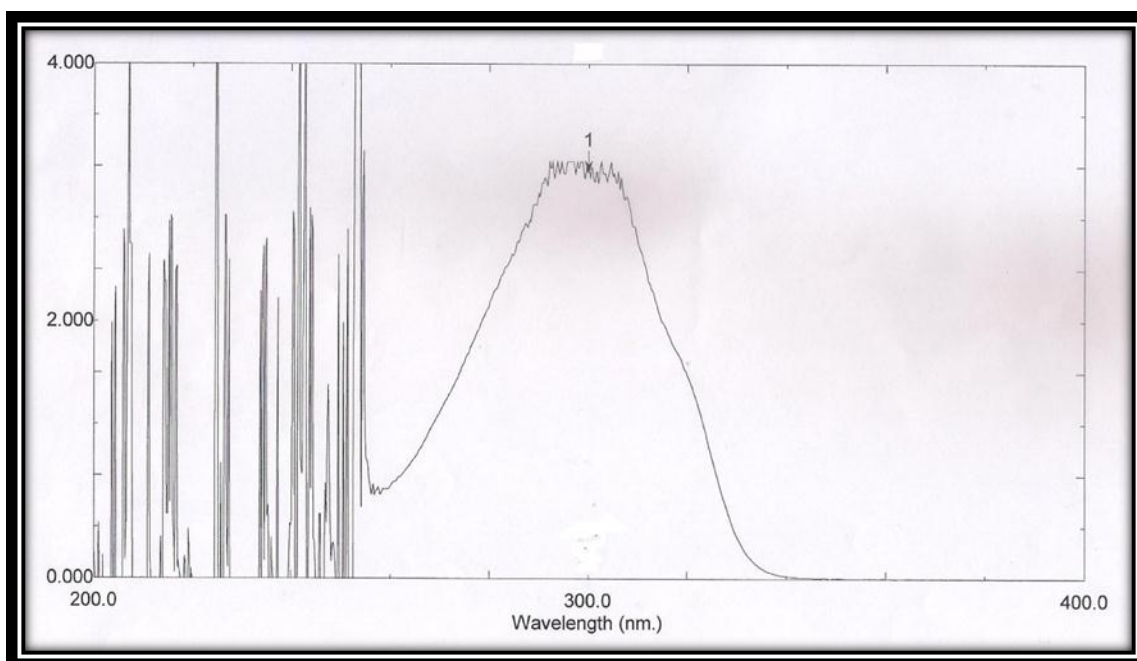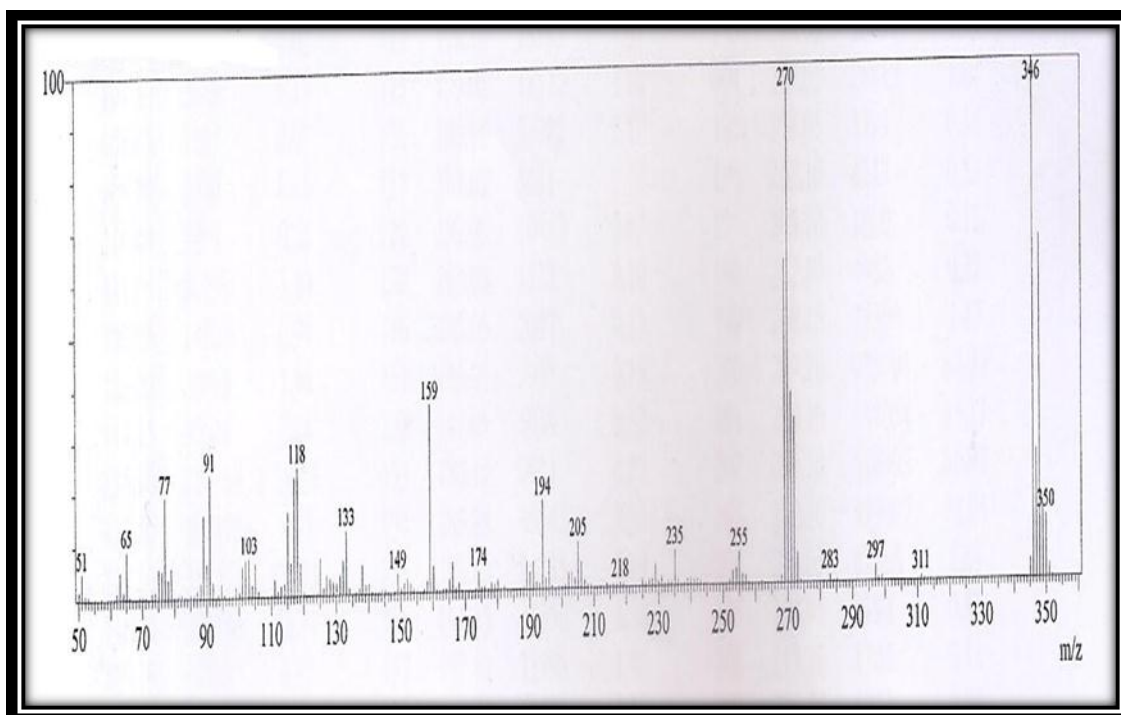

Figure (4.80): UV Spectrum of 2-chloro-1-[5-(4-chloro phenyl)-3-(4-nitro phenyl)-4,5-dihydro-1*H*-pyrazol-1-yl]ethan-1-one **(XLIX)**
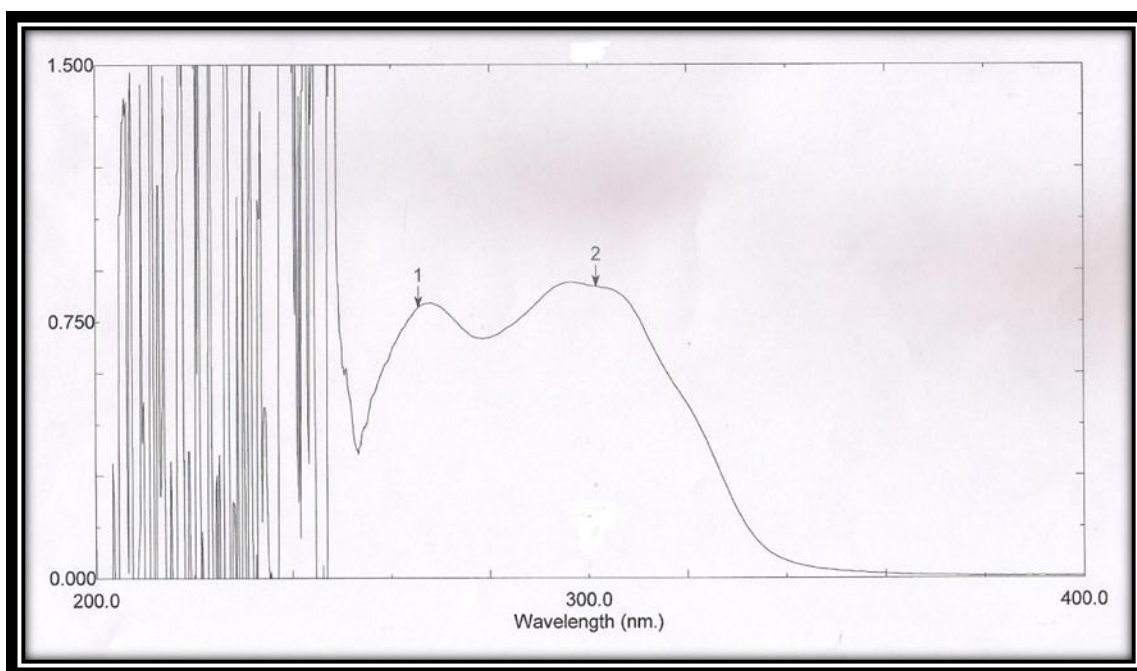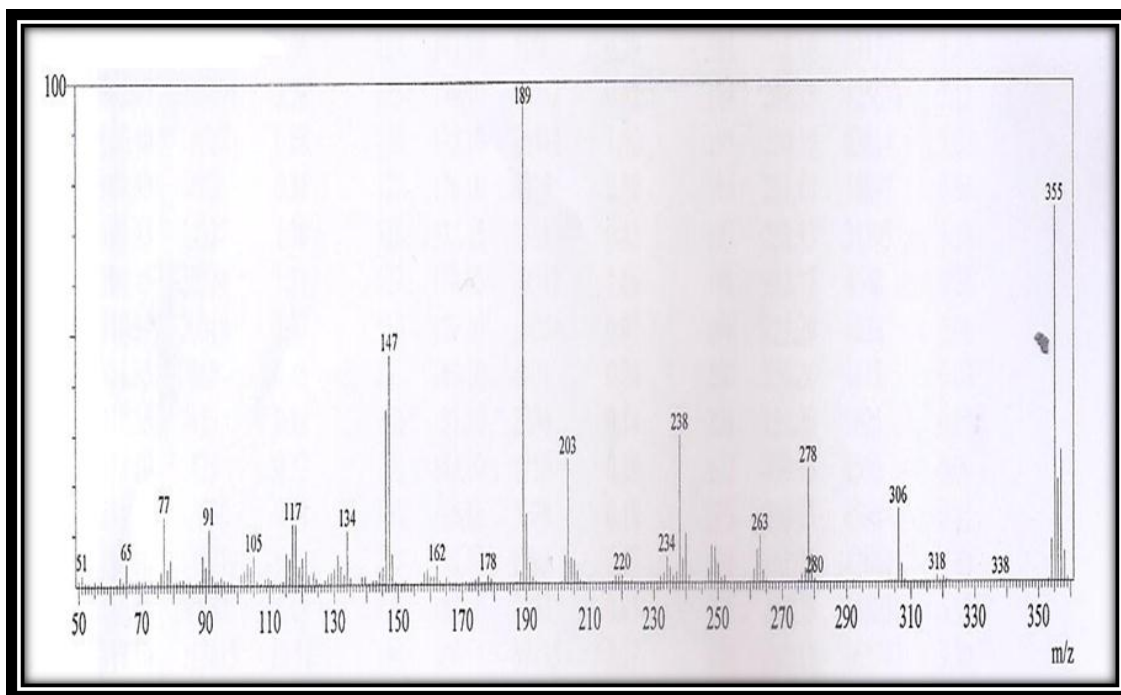
Figure (4.81): UV Spectrum of 2-chloro-1-{5-[4-(dimethylamino)phenyl]-3-(4-nitrophenyl)-4,5-dihydro-1 *H*-pyrazol-1-yl} ethan-1-one **(L)**
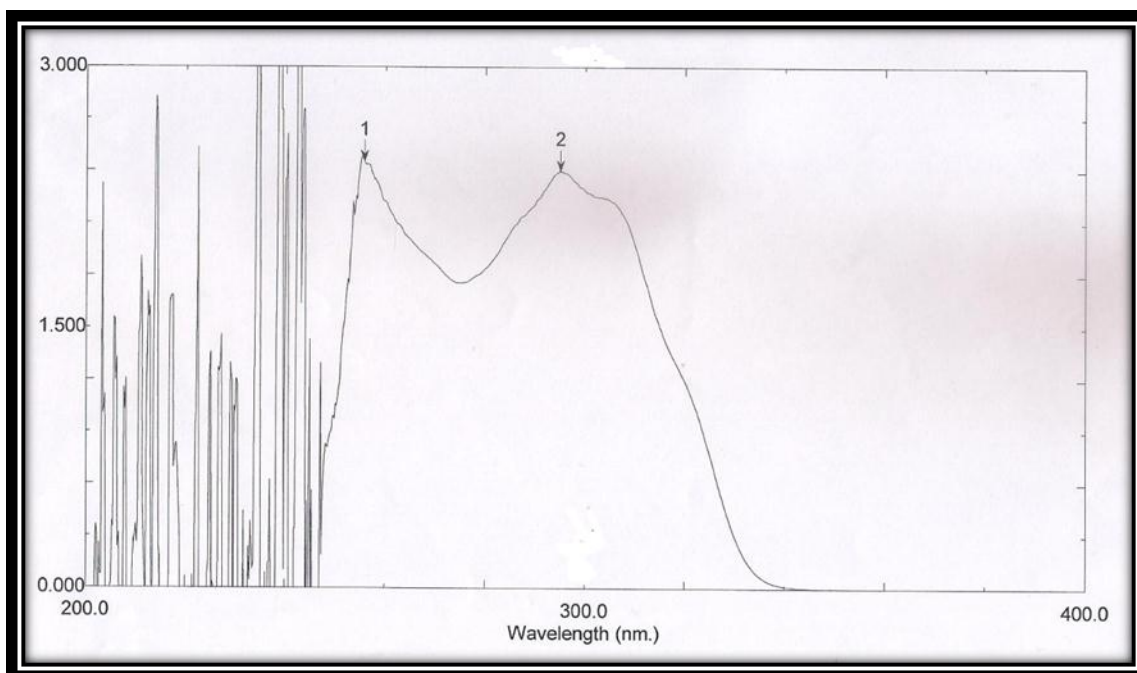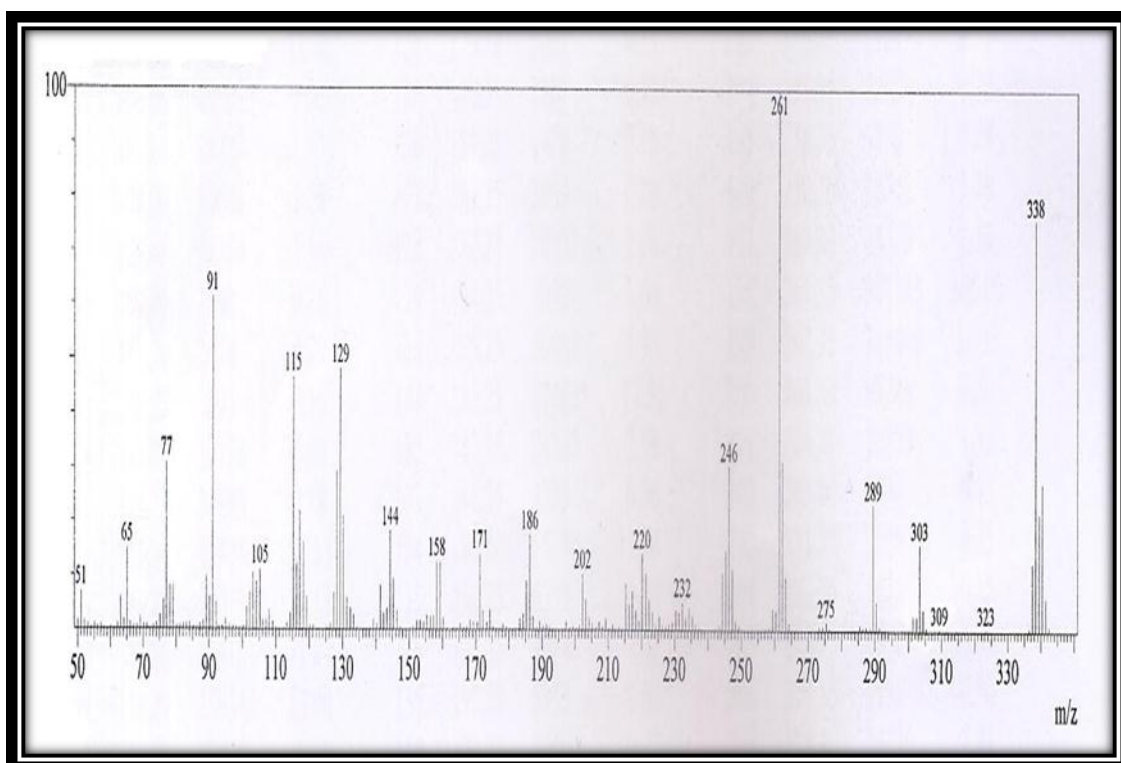

Figure (4.82): UV Spectrum of 2-chloro-1-{3-(4-nitrophenyl)-5-[(*E*)-2-phenylethenyl]-4,5-dihydro-1*H*-pyrazol-1-yl}ethan-1-one **(LI)**
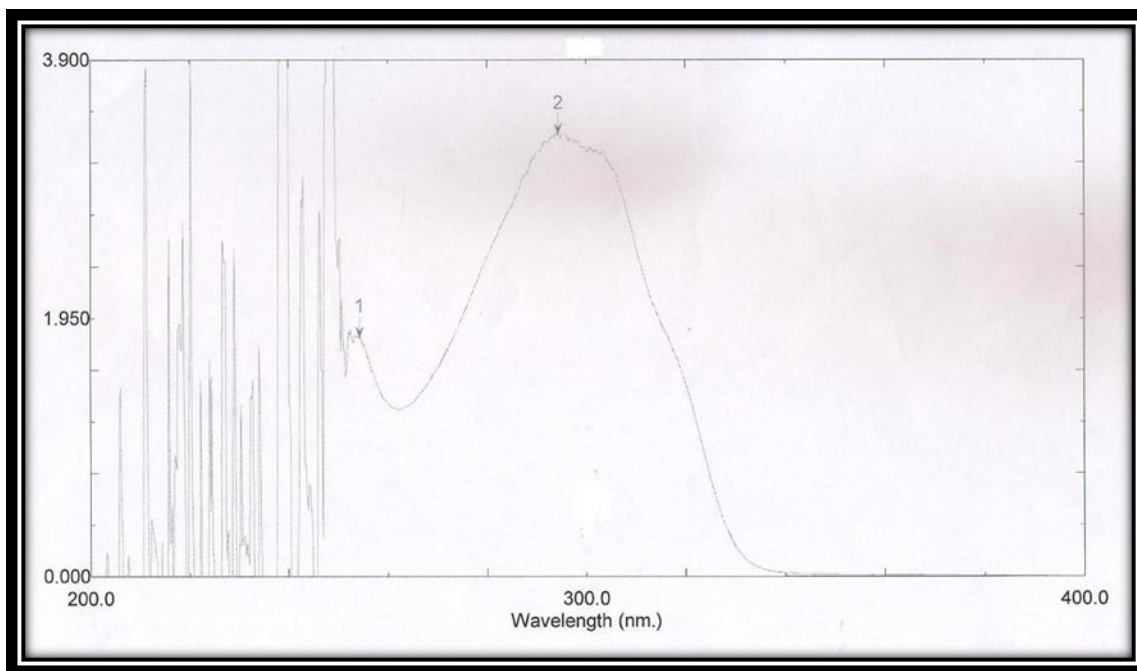
Figure (4.83): UV Spectrum of 2-chloro-1-[5-(furan-2-yl)-3-(4-nitrophenyl)-4,5-dihydro-1*H*-pyrazol-1-yl]ethan-1-one **(LII)**
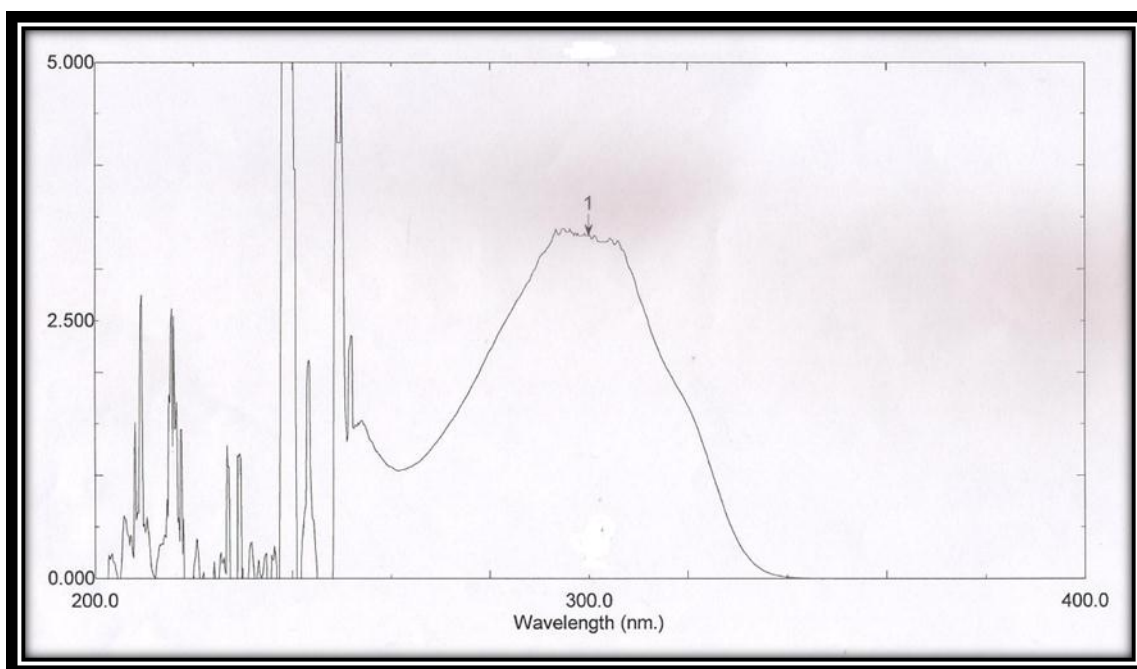

Figure (4.84): UV Spectrum of 2-chloro-1-[3-(4-methylphenyl)-5-phenyl-4,5-dihydro-1*H*-pyrazol-1-yl]ethan-1-one **(LIII)**
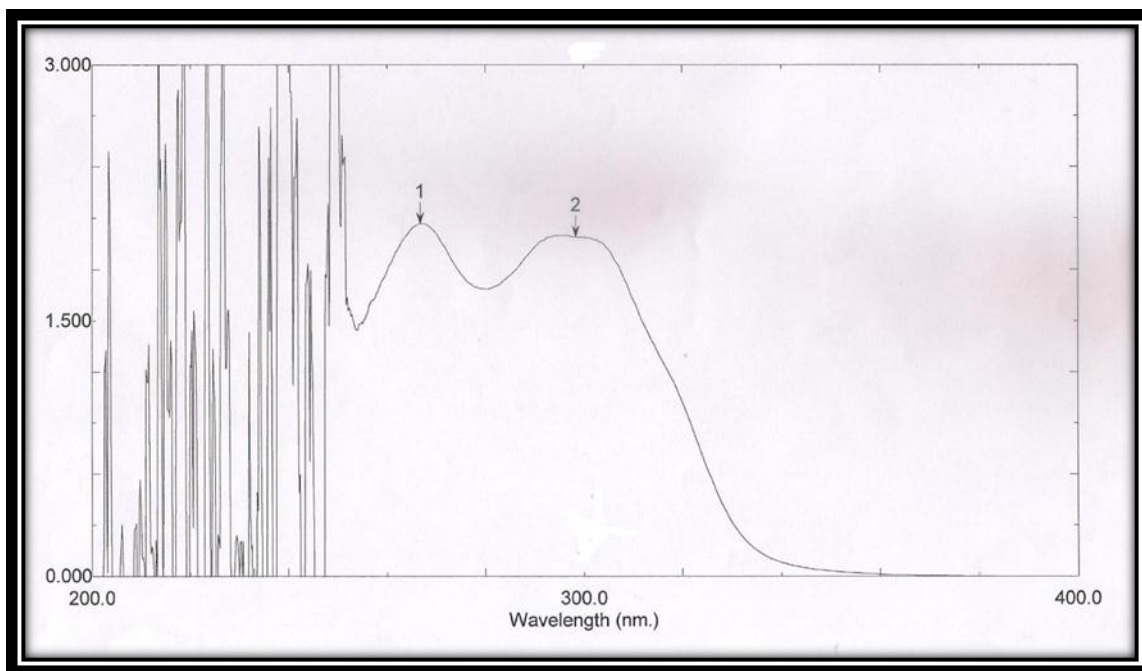
Figure (4.85): UV Spectrum of 2-chloro-1-[5-(4-chlorophenyl)-3-(4-methylphenyl)-4,5-dihydro-1H-pyrazol-1-yl]ethan-1-one **(LIV)**
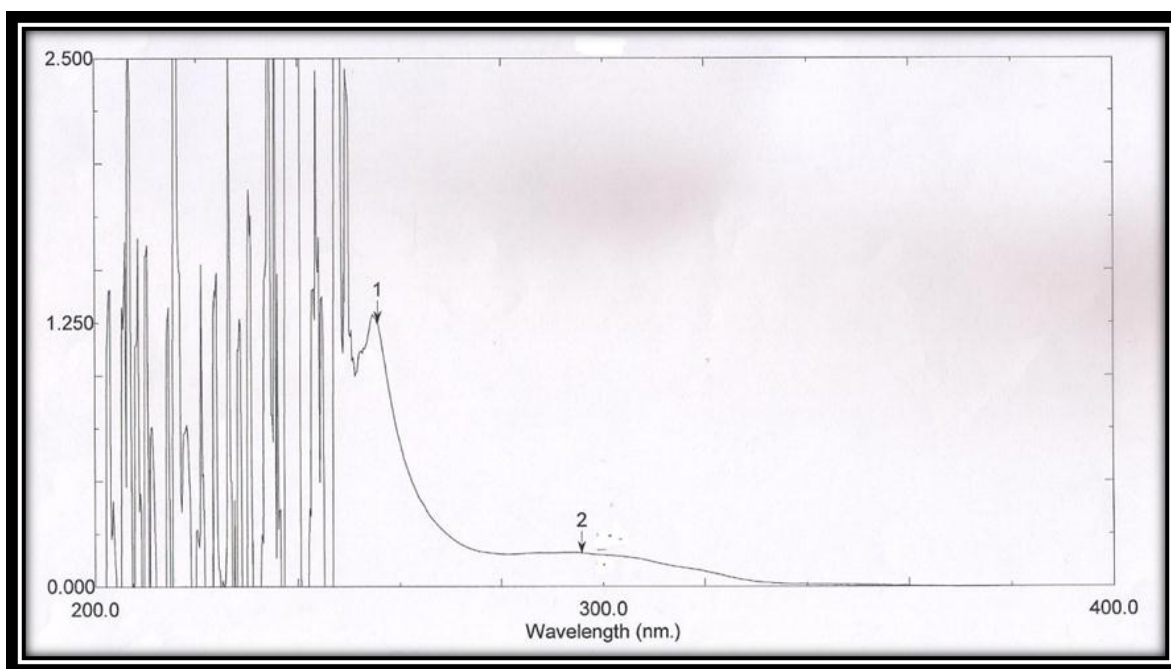
Figure (4.86): UV Spectrum of 2-chloro-1-{5-[4-(dimethylamino) phenyl]-3-(4-methylphenyl)-4,5-dihydro-1 H-pyrazol-1-yl}ethan-1-one **(LV)**

235
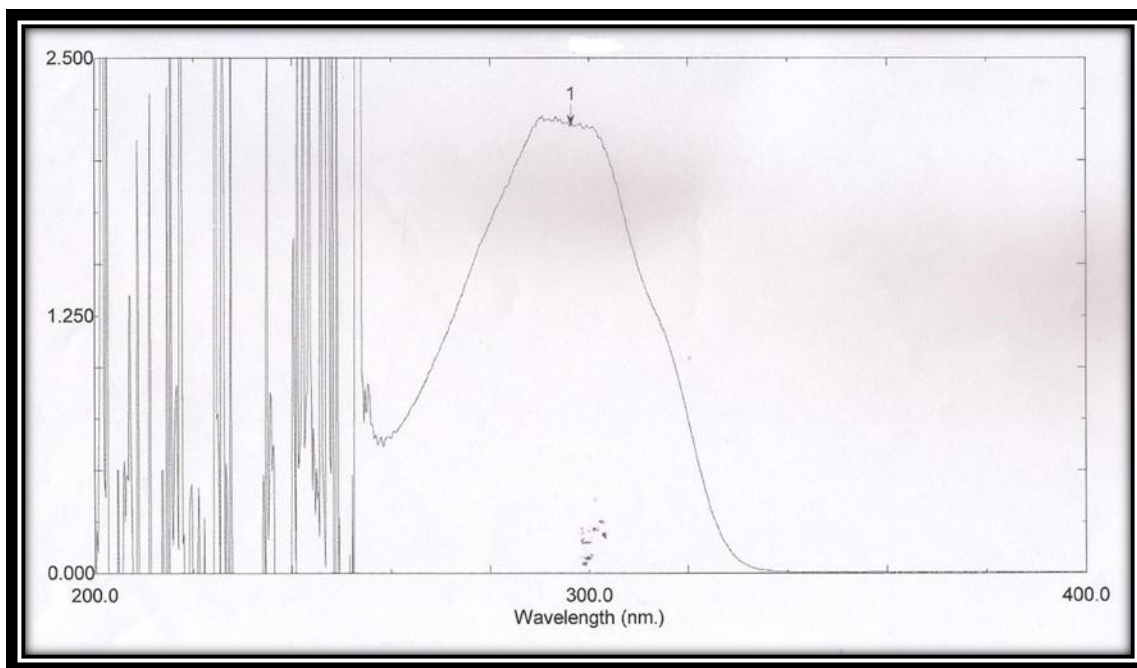
Figure (4.87): UV Spectrum of 2-chloro-1-{3-(4-methyl phenyl)-5-[(E)-2-phenylethenyl]-4,5-dihydro-1H-pyrazol-1-yl}ethan-1-one **(LVI)**
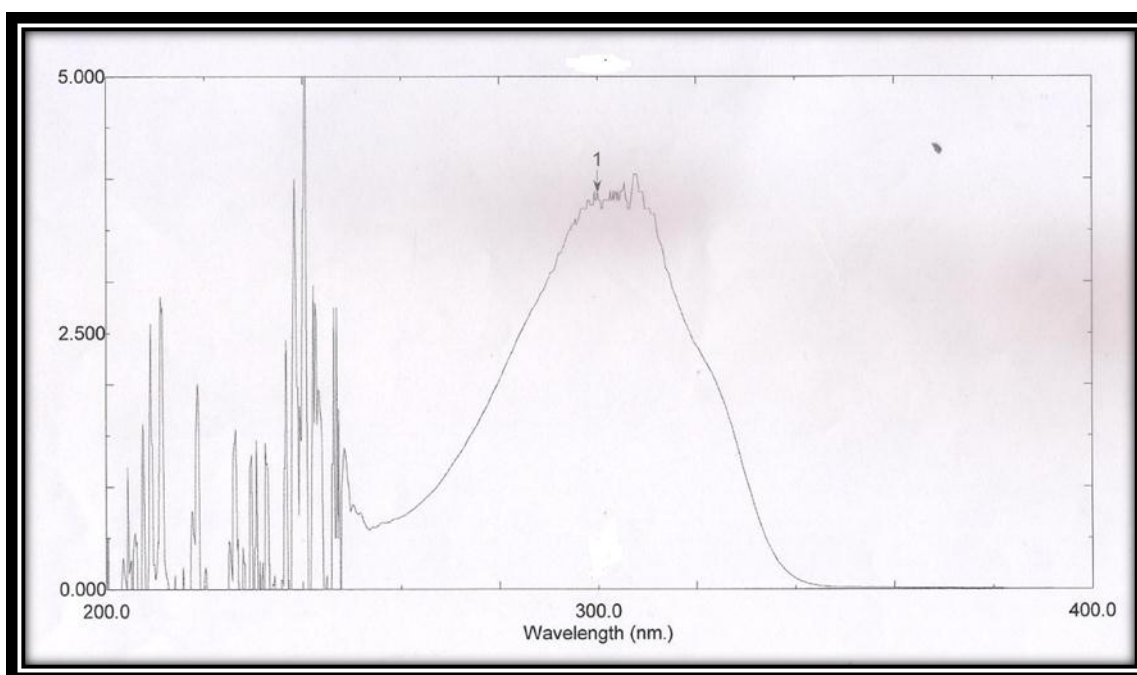
Figure (4.88): UV Spectrum of 2-chloro-1-[5-(furan-2-yl)-3-(4-methylphenyl)-4,5-dihydro-1*H*-pyrazol-1-yl]ethan-1-one **(LVII)**
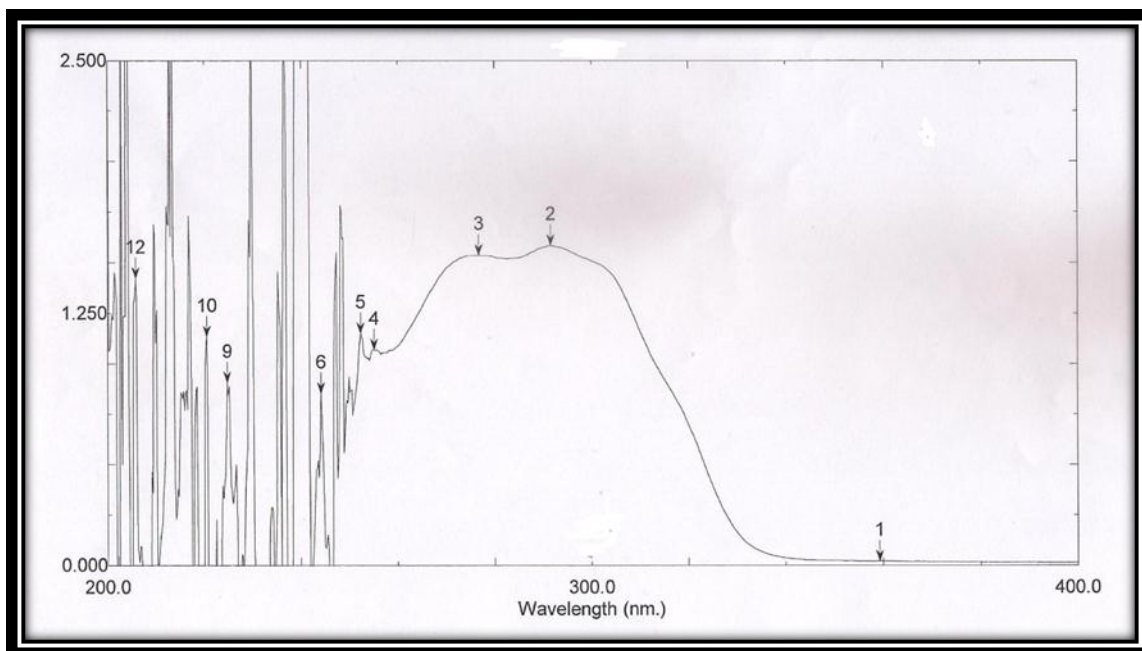
Figure (4.89): UV Spectrum of 4-((2-(3,5-diphenyl-4,5-di hydro-1H-pyrazol-1-yl)-2-oxoethyl)amino)benzene sulfonamide **(LVIII)**
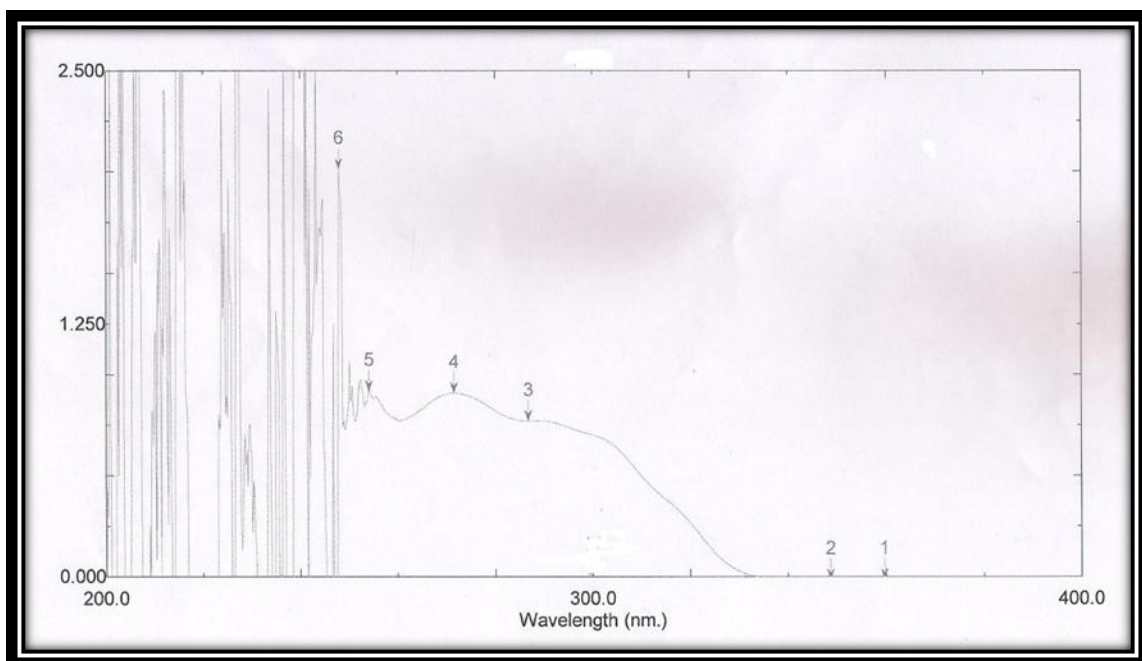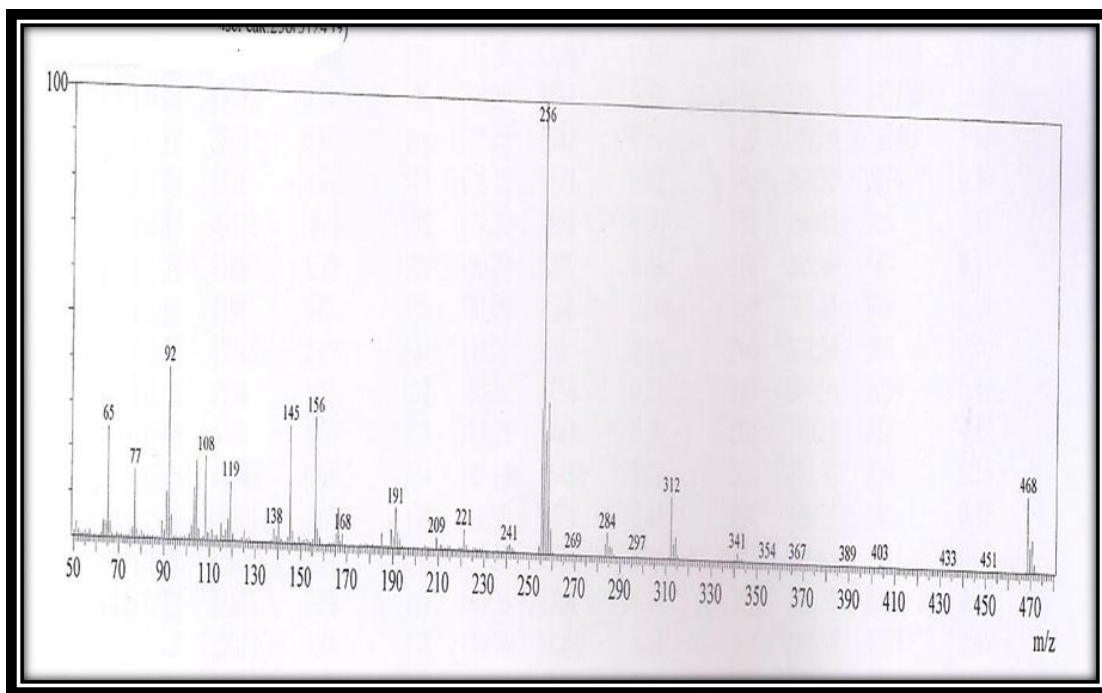

Figure (4.90): UV Spectrum of 4-((2-(5-(4-chlorophenyl)-3-phenyl-4,5-dihydro-1H-pyrazol-1-yl)-2-oxoethyl) amino) benzene sulfonamide **(LIX)**
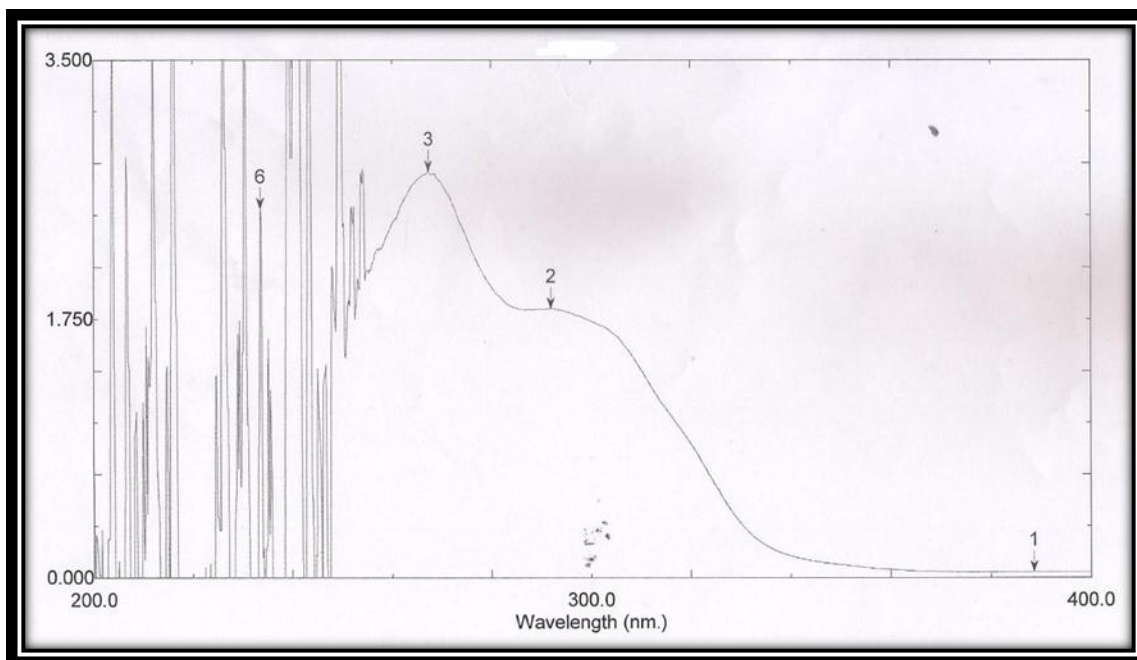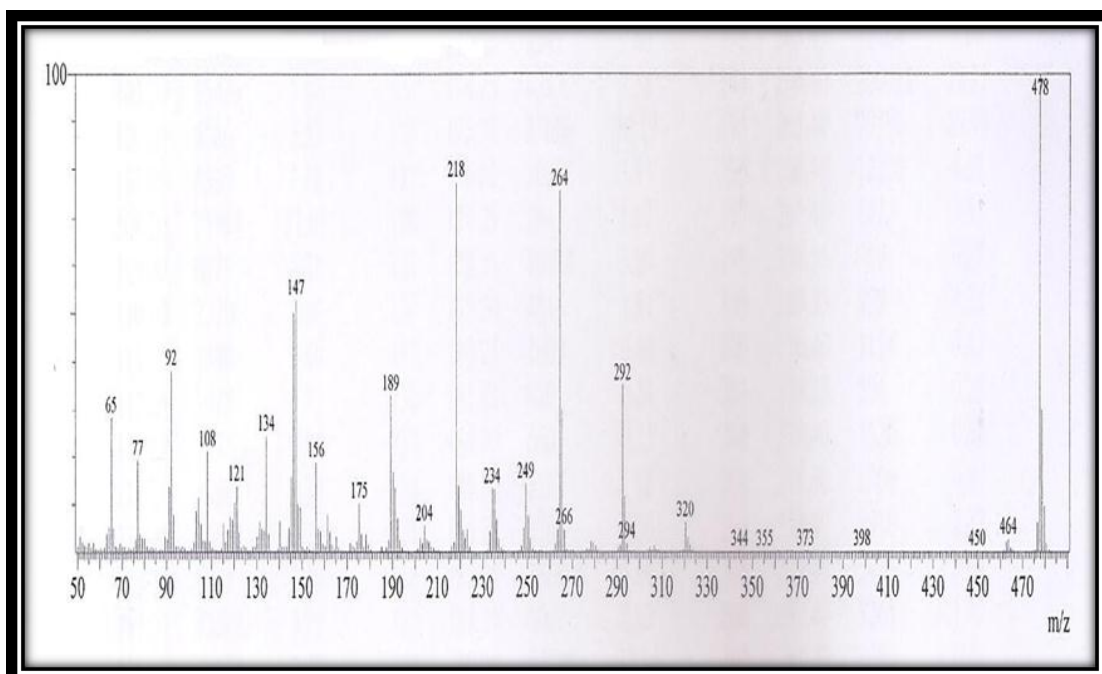
Figure (4.91): UV Spectrum of 4-((2-(5-(4-(dimethylamino)phenyl)-3-phenyl-4,5-di hydro-1H-pyrazol-1-yl)-2-oxoethyl)amino)benzene sulfonamide **(LX)**
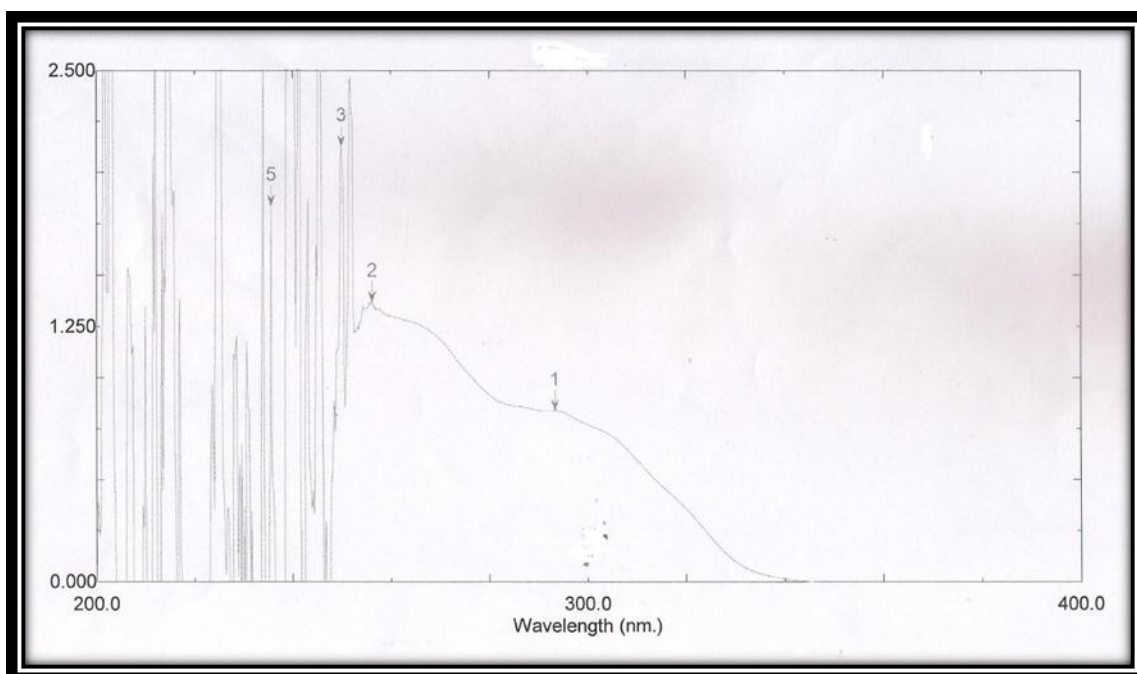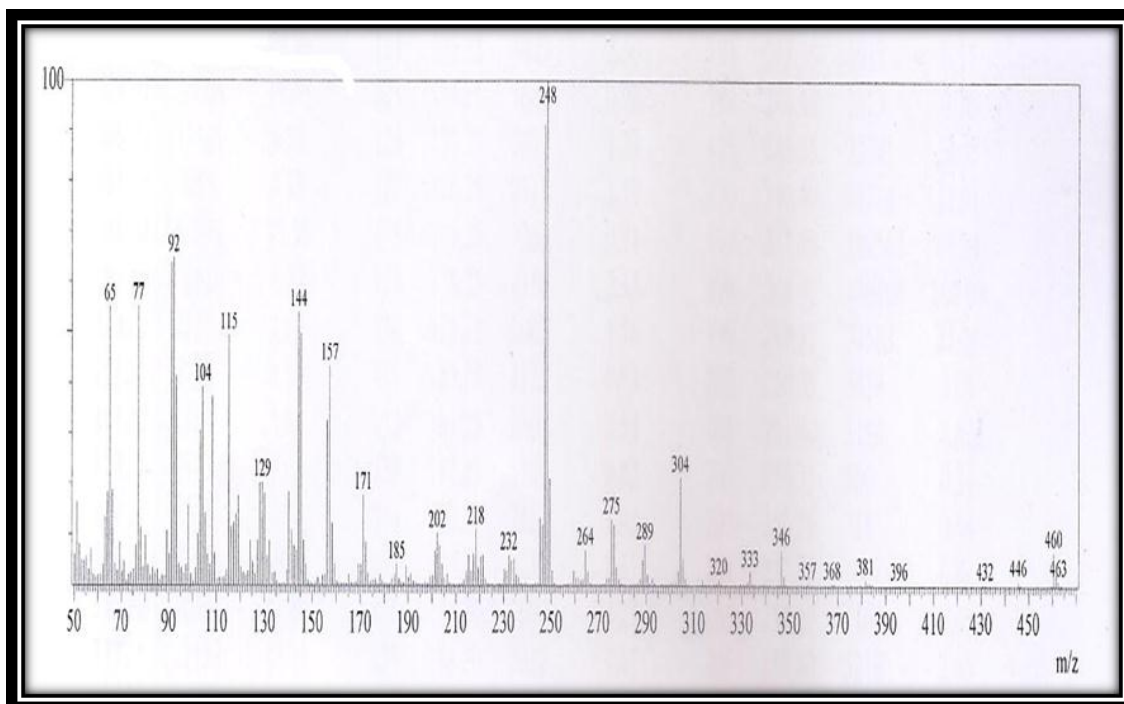

Figure (4.92): UV Spectrum of (E)-4-((2-oxo-2-(3-phenyl-5-styryl-4,5-dihydro-1H-pyrazol-1-yl)ethyl)amino) benzenesulfonamide **(LXI)**
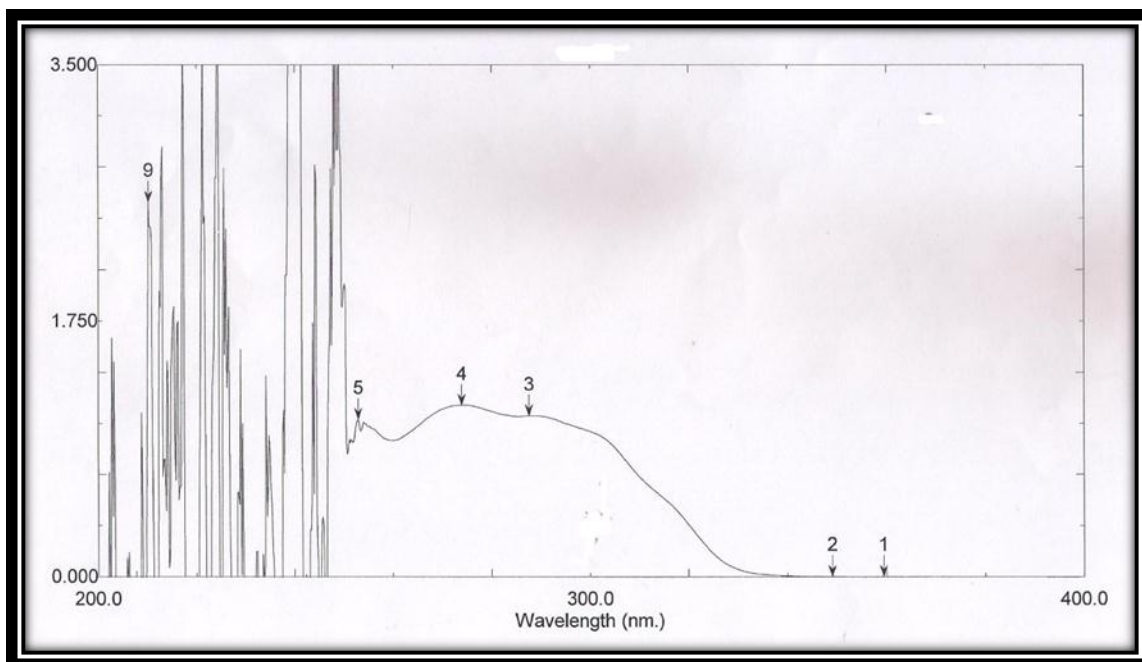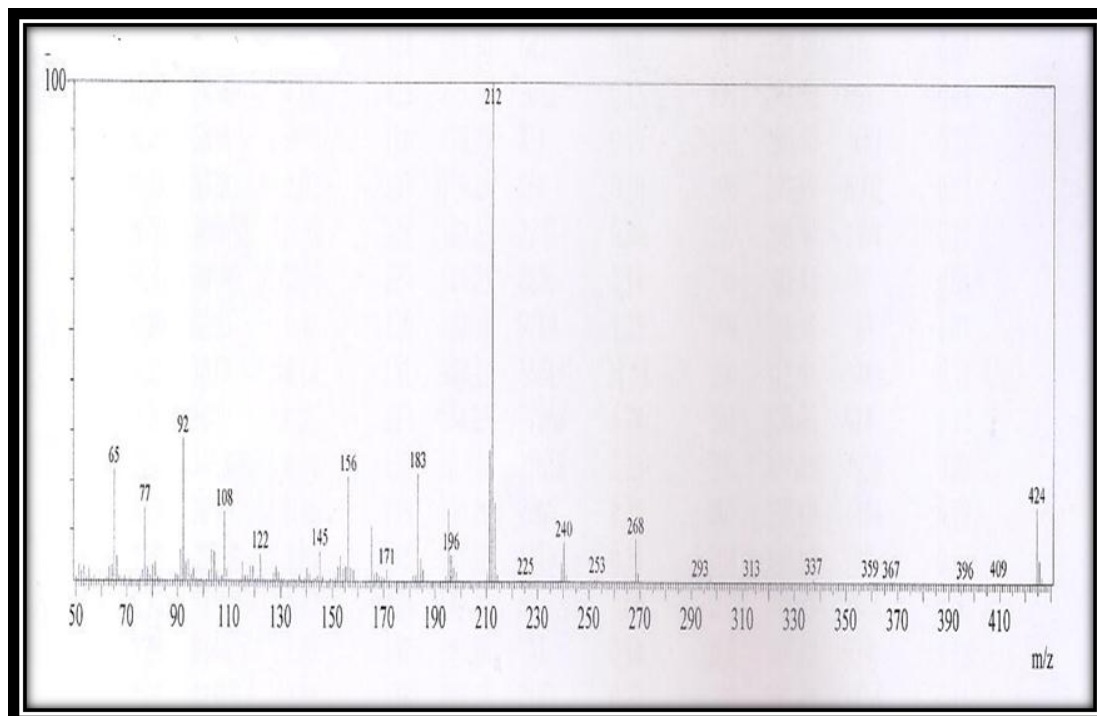
Figure (4.93): UV Spectrum of 4-({2-[5-(furan-2-yl)-3-phenyl-4,5-dihydro-1*H*-pyrazol-1-yl]-2-oxoethyl}amino)benzene-1-sulfonamide
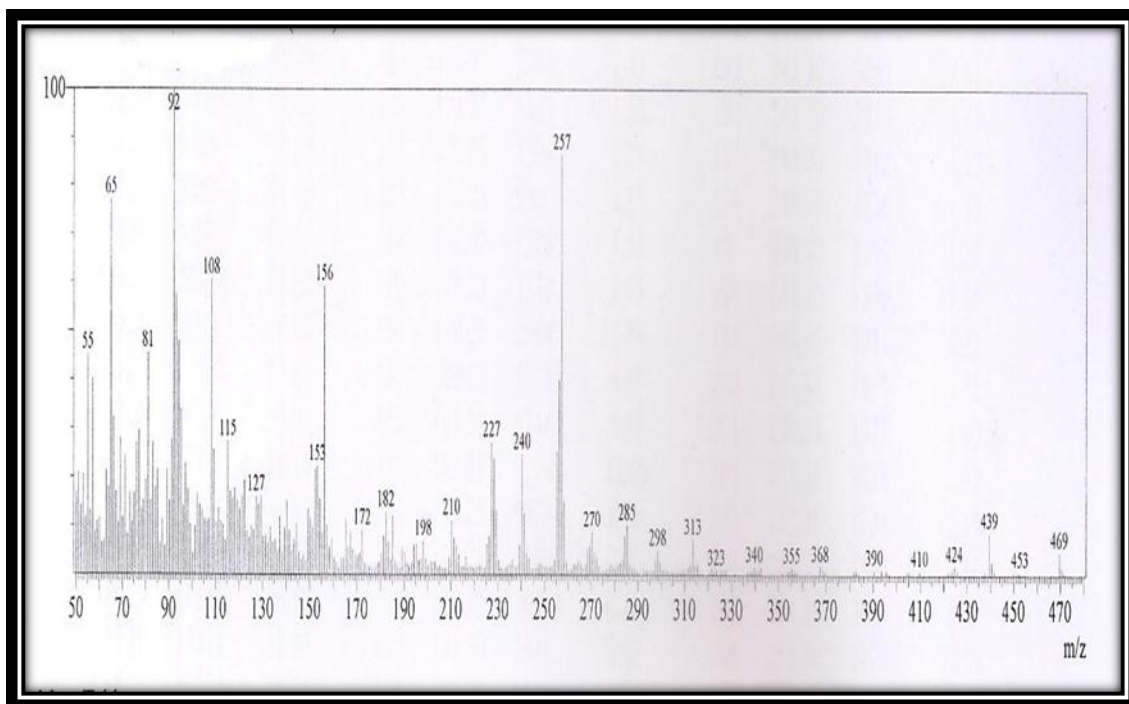**(LXII)**
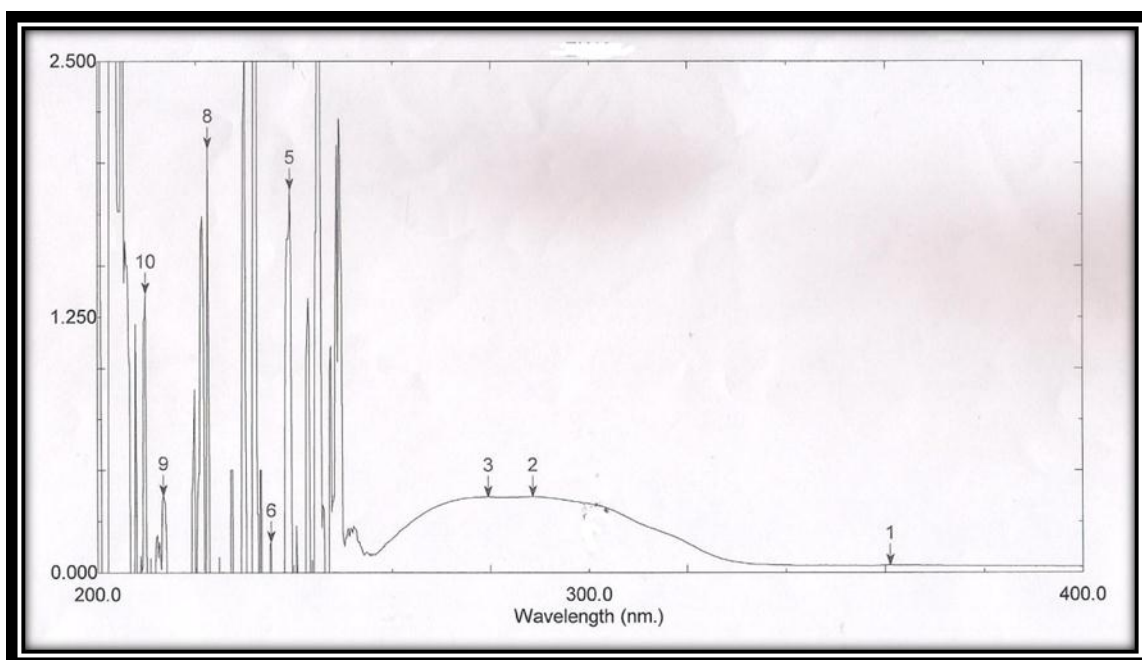
Figure (4.94): UV Spectrum of 4-((2-(5-(furan-2-yl)-3-(4-nitrophenyl)-4,5-dihydro-1H-pyrazol-1-yl)-2-oxoeth yl) amino)benzene sulfonamide
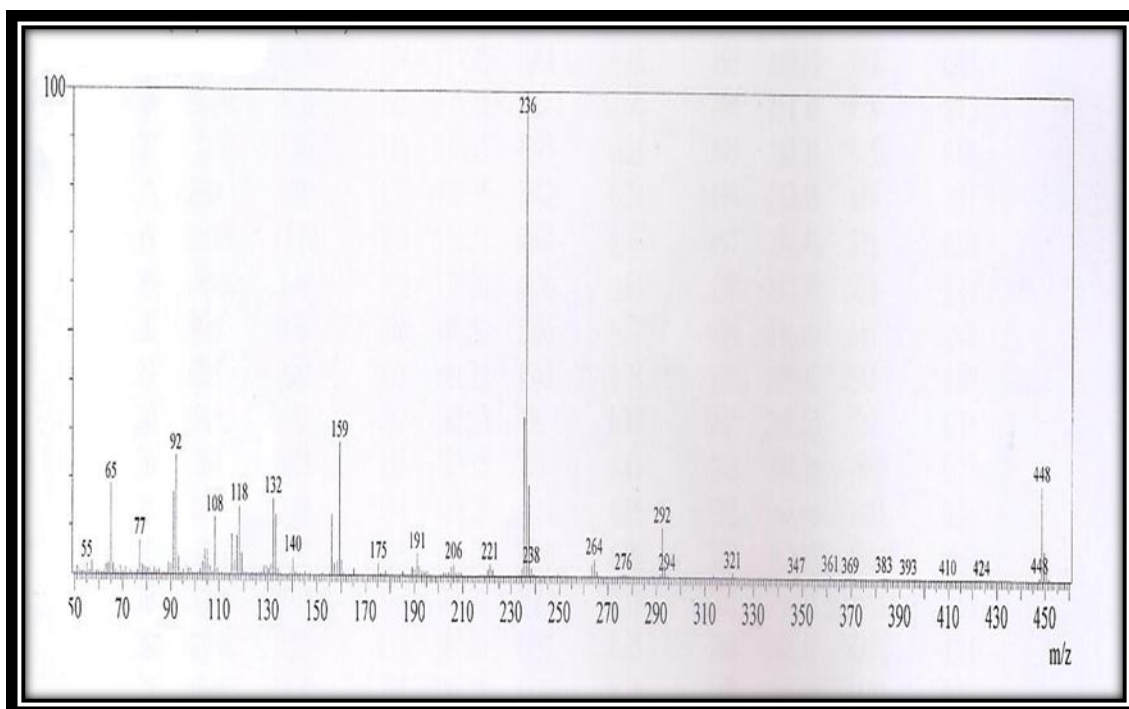**(LXIII)**
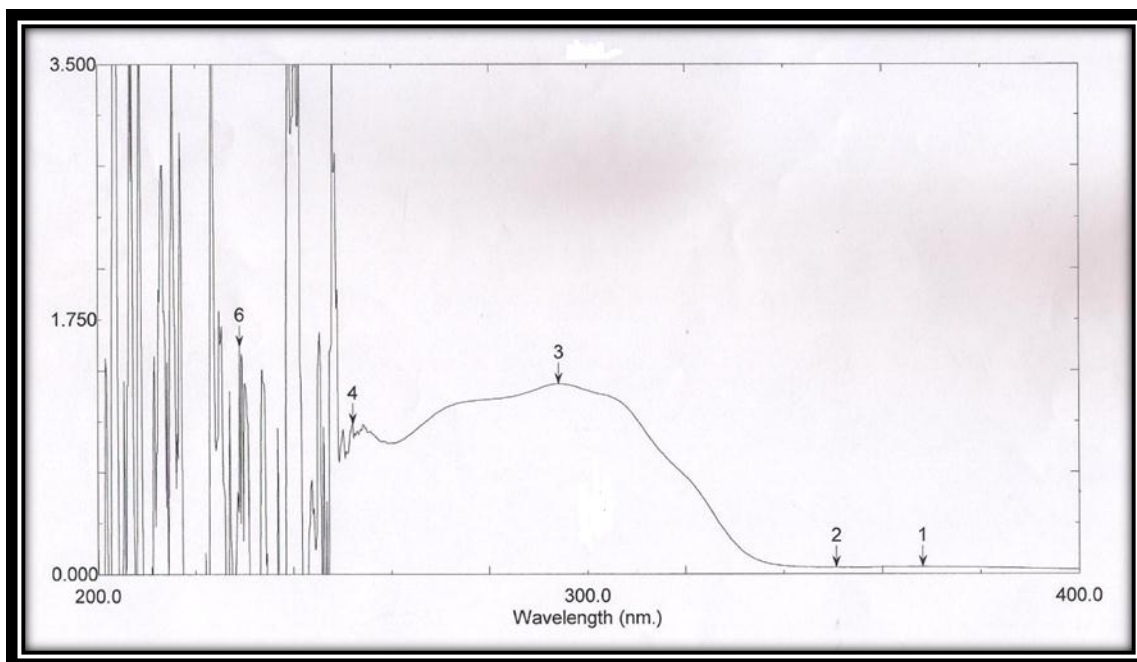
Figure (4.95): UV Spectrum of 4-((2-oxo-2-(5-phenyl-3-(p-tolyl)-4,5-dihydro-1H-pyrazol-1-yl)ethyl)amino) benzenesulfonamide **(LXIV)**
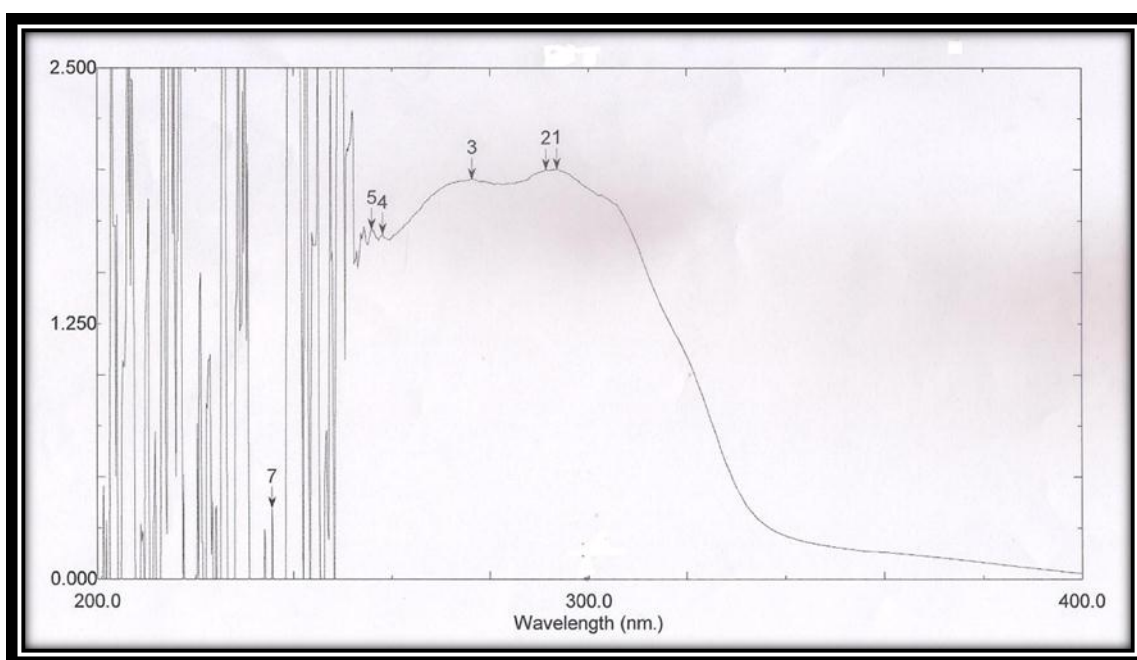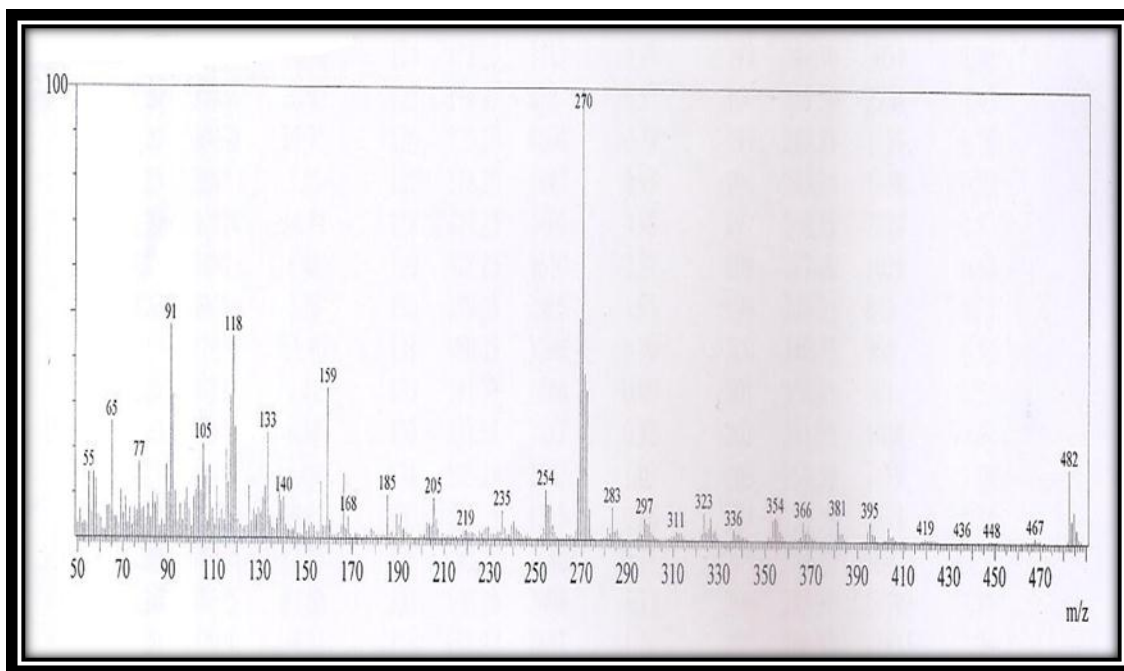

Figure (4.96): UV Spectrum of 4-((2-(5-(4-chlorophenyl)-3-(p-tolyl)-4,5-dihydro-1H-pyrazol-1-yl)-2-oxoethyl)amino)benzene sulfonamide **(LXV)**
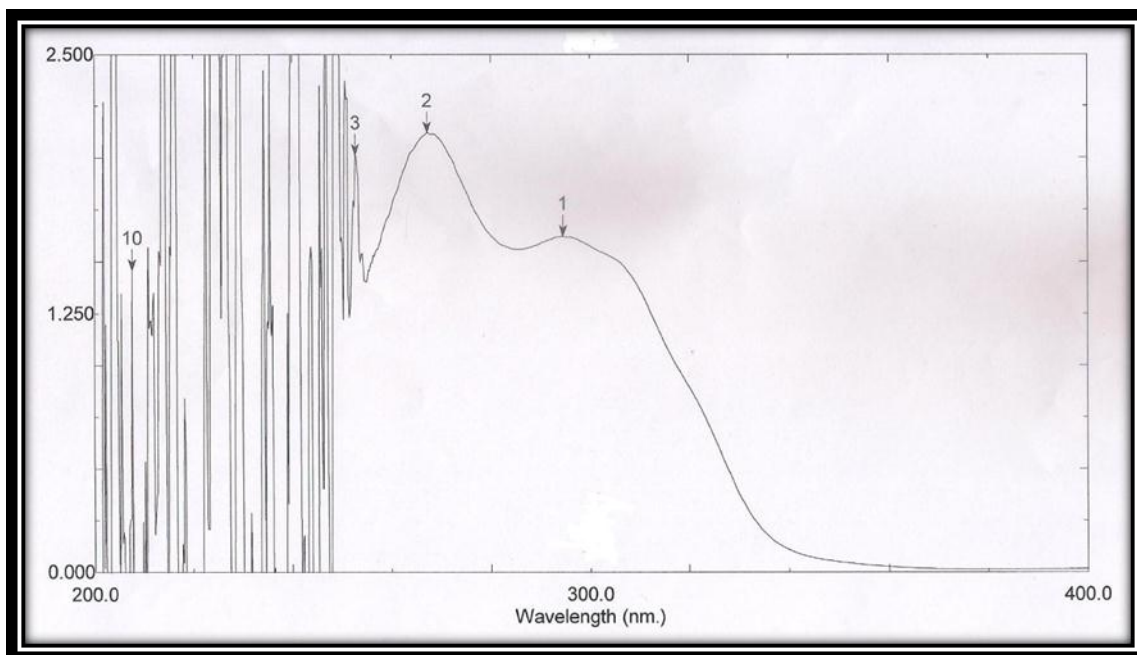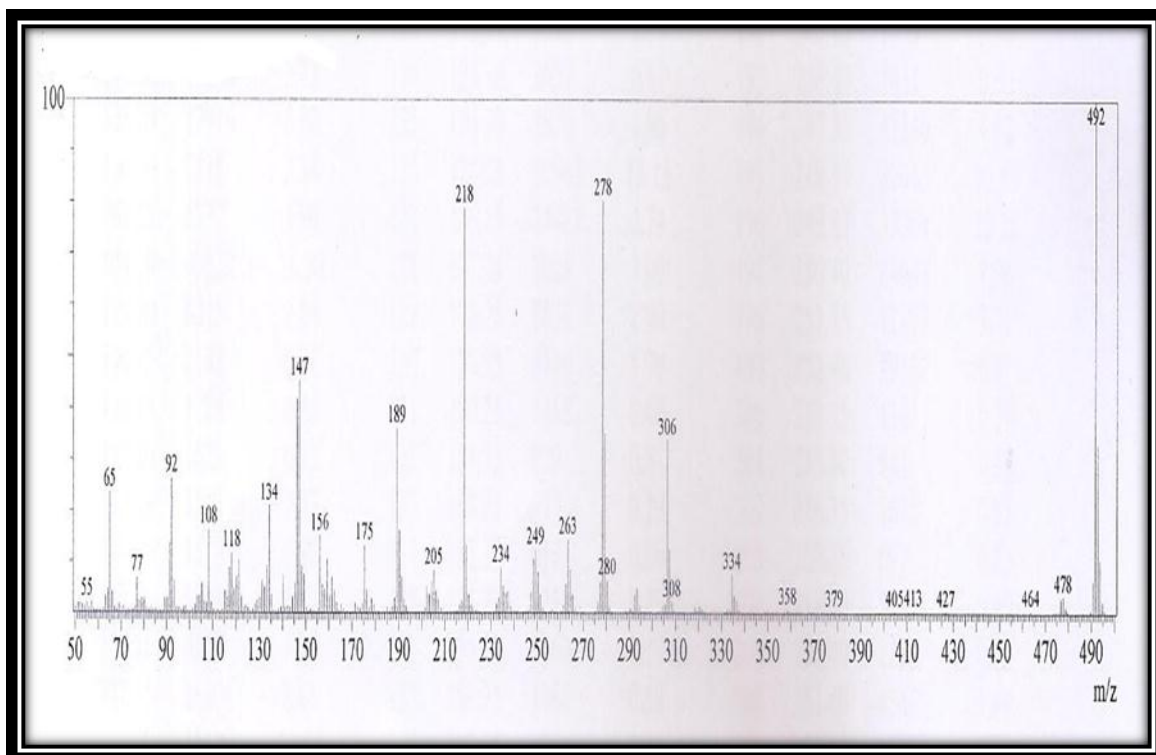
Figure (4.97): UV Spectrum of 4-((2-(5-(4-(dimethyl amino)phenyl)-3-(p-tolyl)-4,5-dihydro-1H-pyrazol-1-yl)-2-oxoethyl)amino)benzene sulfonamide (**LXVI**)
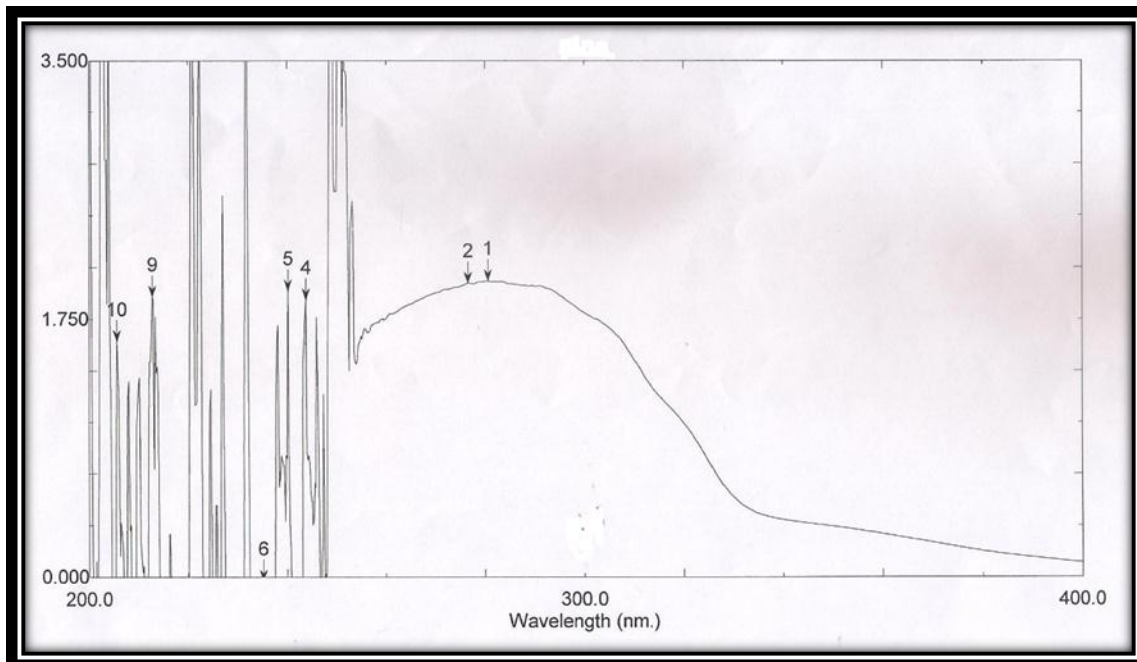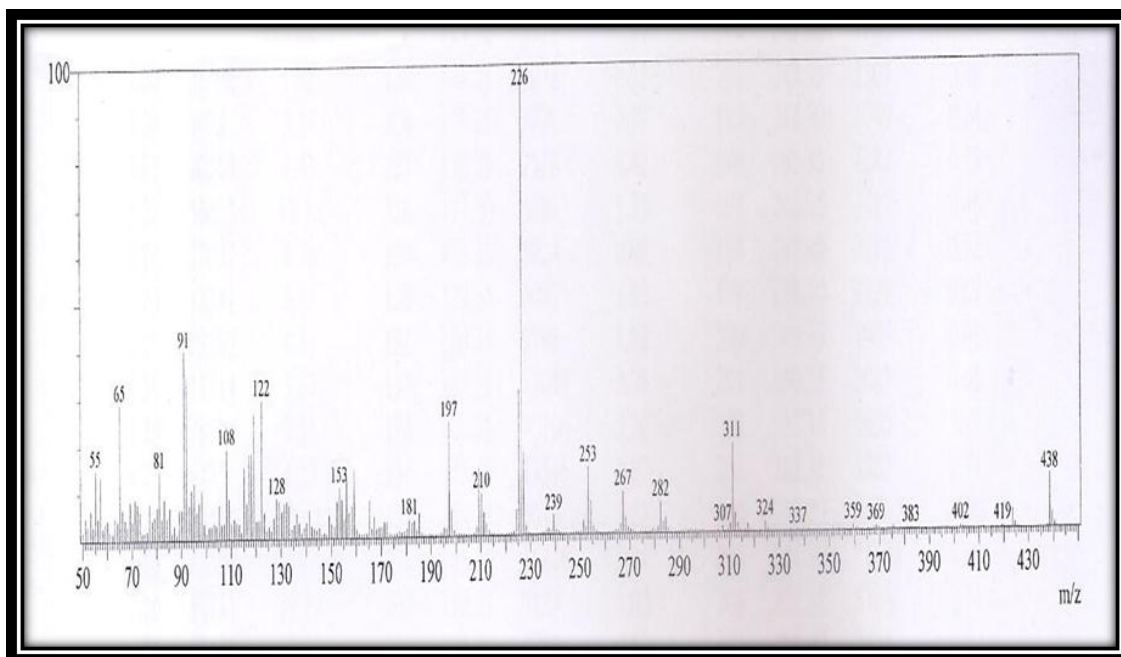

Figure (4.98): UV Spectrum of 4-((2-(5-(furan-2-yl)-3-(p-tolyl)-4,5-dihydro-1H-pyrazol-1-yl)-2-oxoethyl)amino)benzene sulfonamide (**LXVII**)
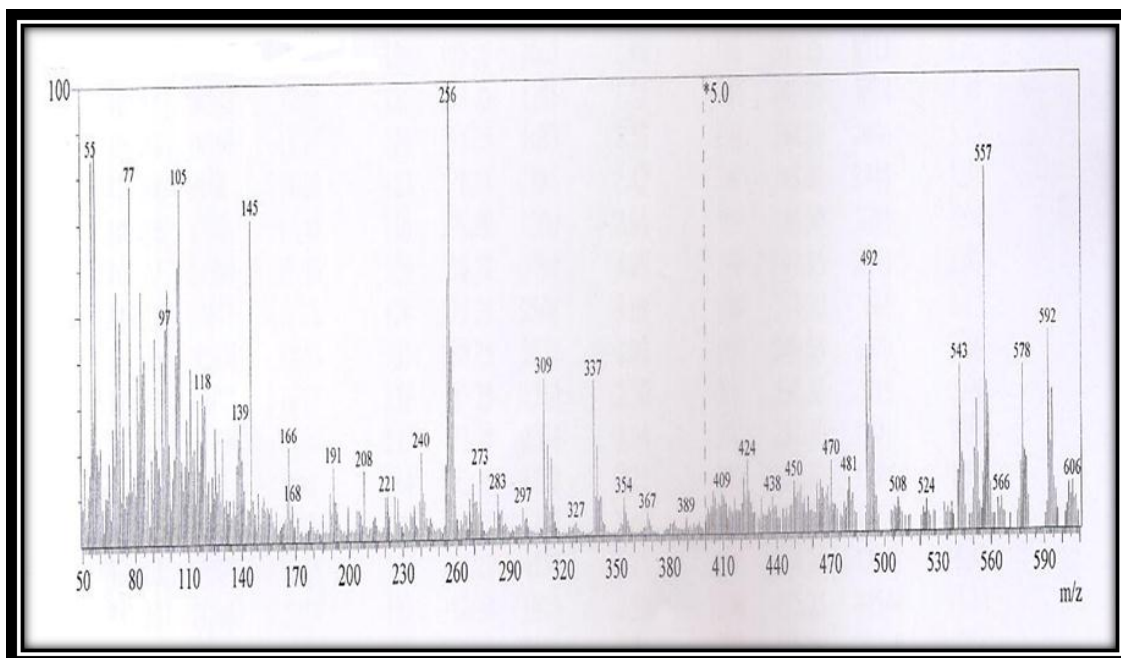
241

Figure (4.99): UV Spectrum of 4-((2-(5-(4-chlorophenyl)-3-phenyl-4,5-dihydro-1H-pyrazol-1-yl)-2-oxoethyl) amino)-N-(5,6-dimethoxy pyrimidin-4-yl)benzene sulfonamide **(LXVIII)**
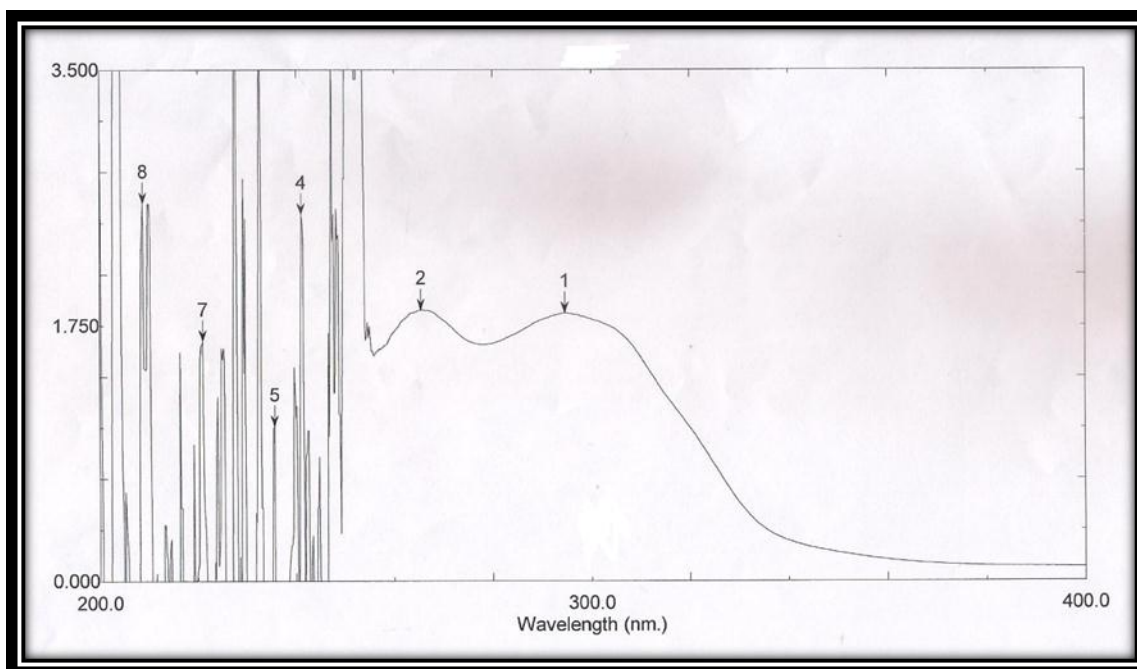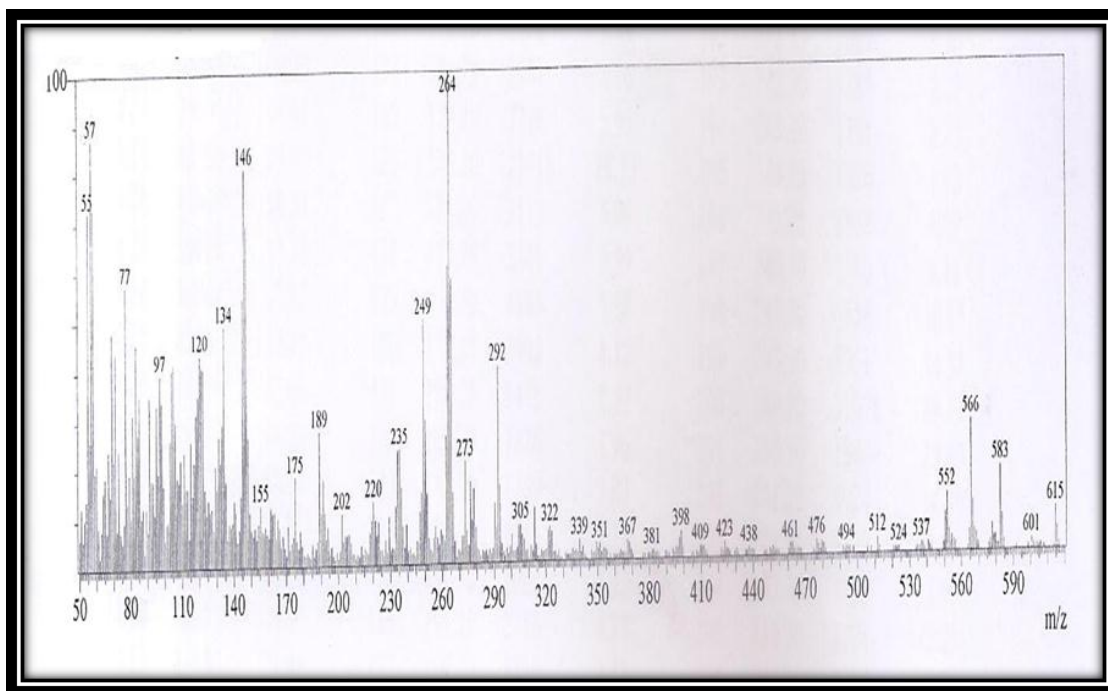

Figure (4.100): UV Spectrum of N-(5,6-dimethoxypyrimidin-4-yl)-4-((2-(5-(4-(dimethylamino)phenyl)-3-phenyl-4,5-dihydro-1H-pyrazol-1-yl)-2-oxoethyl)amino)benzenesulfonamide **(LXIX)**
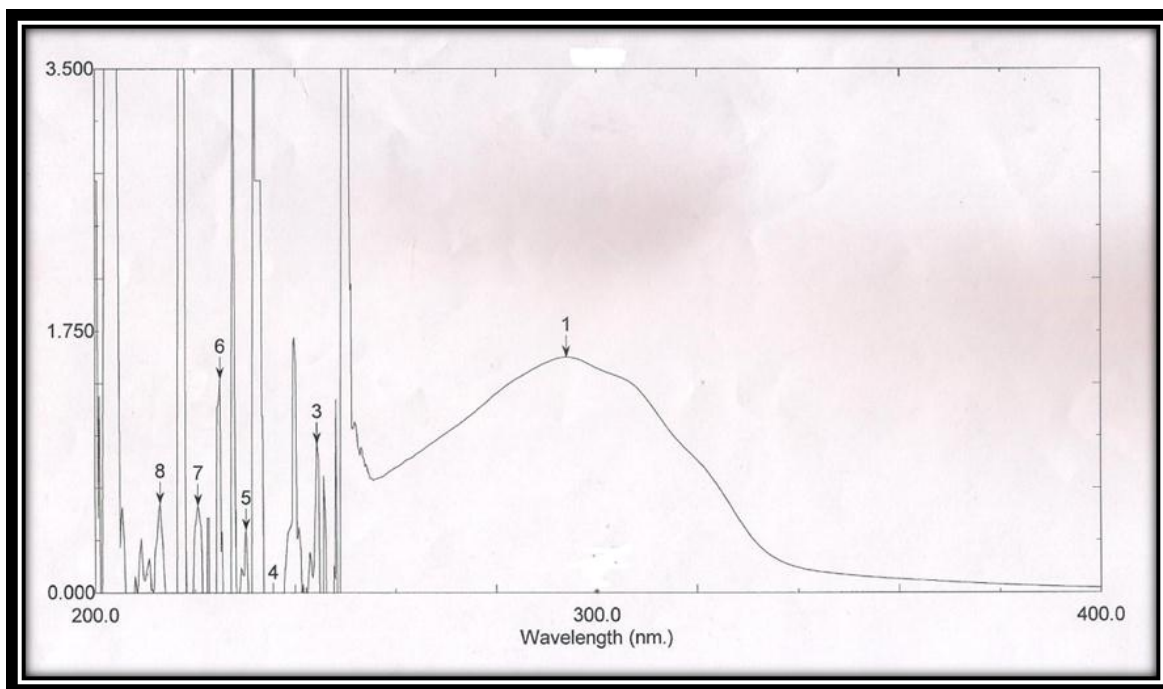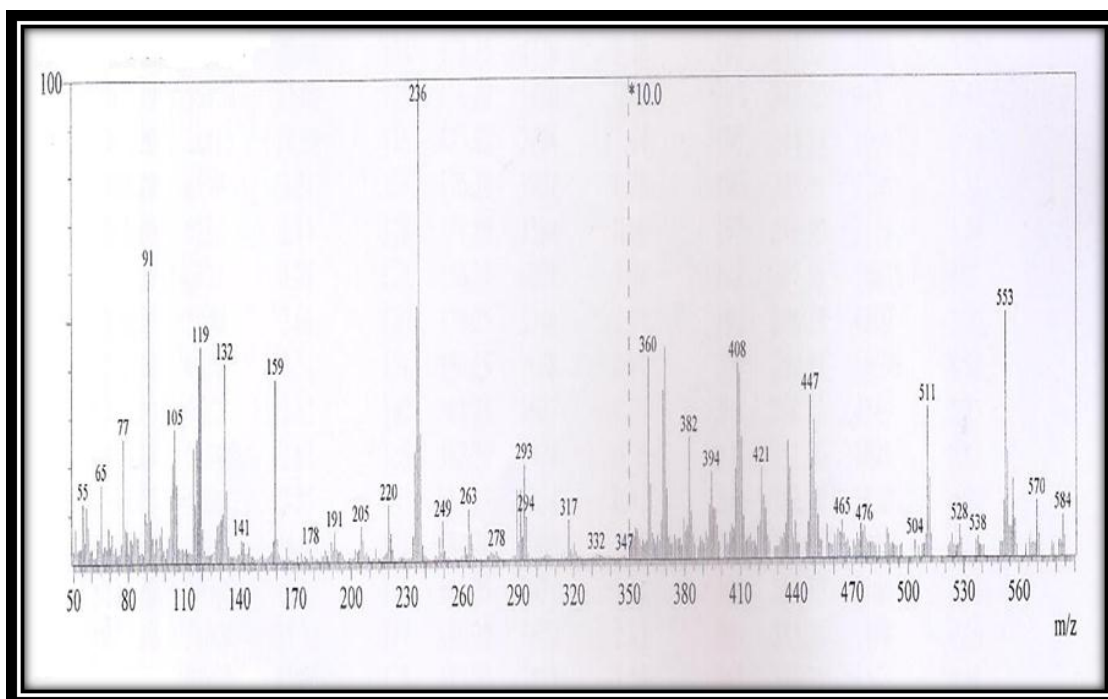
Figure (4.101): UV Spectrum of N-(5,6-dimethoxypyrimidin-4-yl)-4-((2-oxo-2-(5-phenyl-3-(p-tolyl)-4,5-dihydro-1H-pyrazol-1-yl)ethyl)amino)benzenesulfonamide **(LXX)**
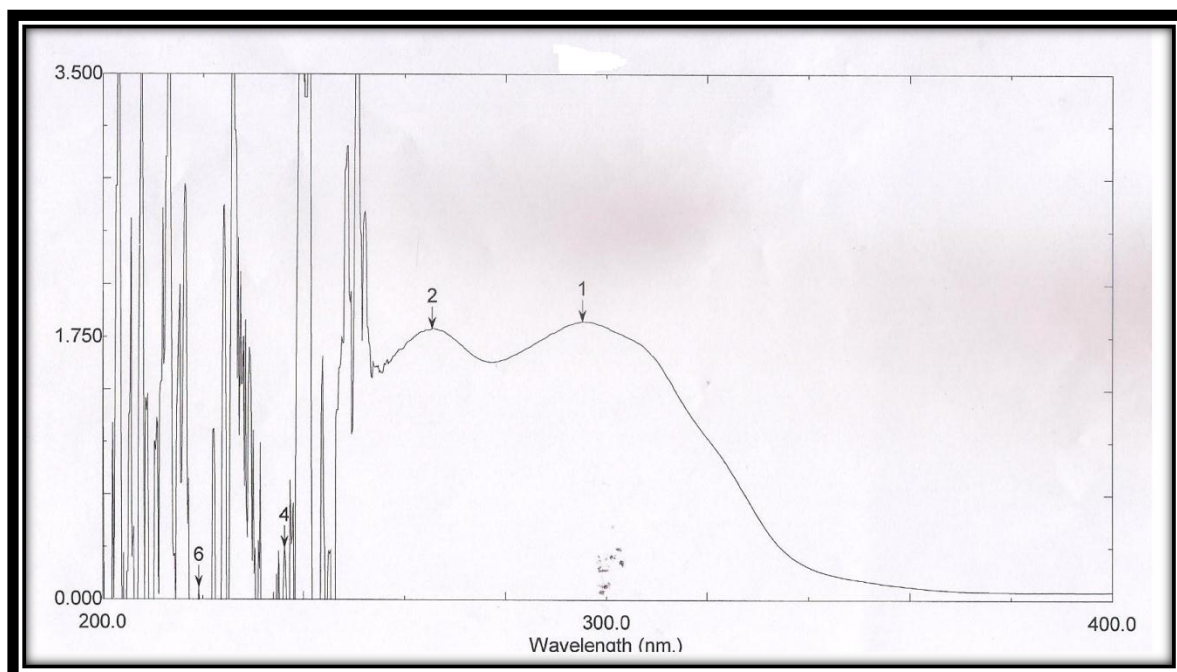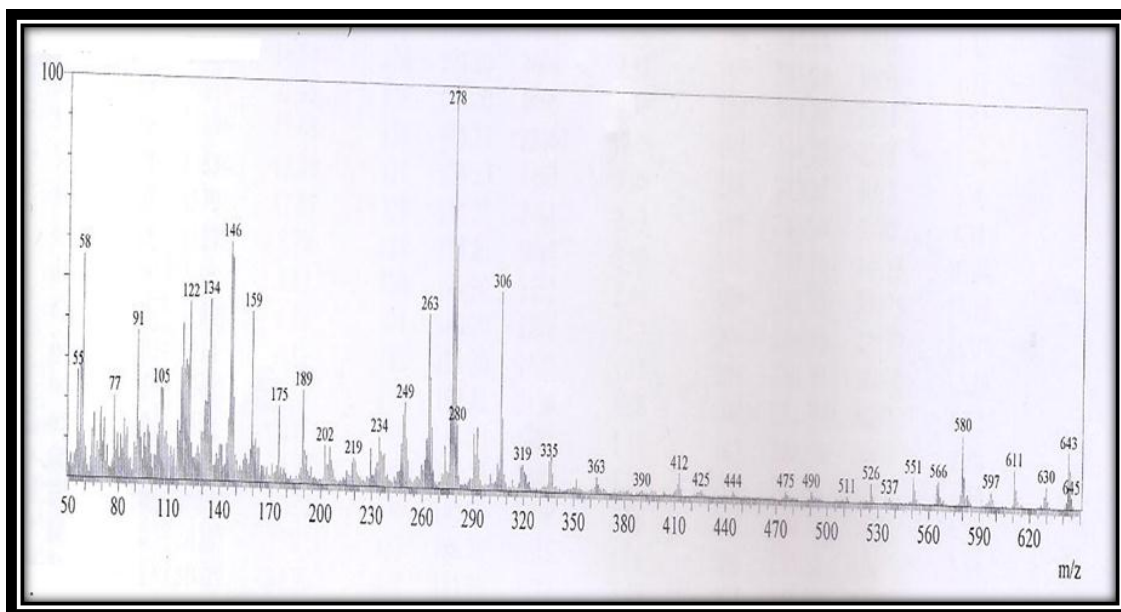

Figure (4.102): UV Spectrum of N-(5,6-dimethoxypyrimid in-4-yl)-4-((2-(5-(4-(dime thylamino)phenyl)-3-(p-tol yl)-4,5-dihydro-1H-pyraz ol-1-yl)-2-oxoethyl)amino)benzene sulfonamide **(LXXI)**
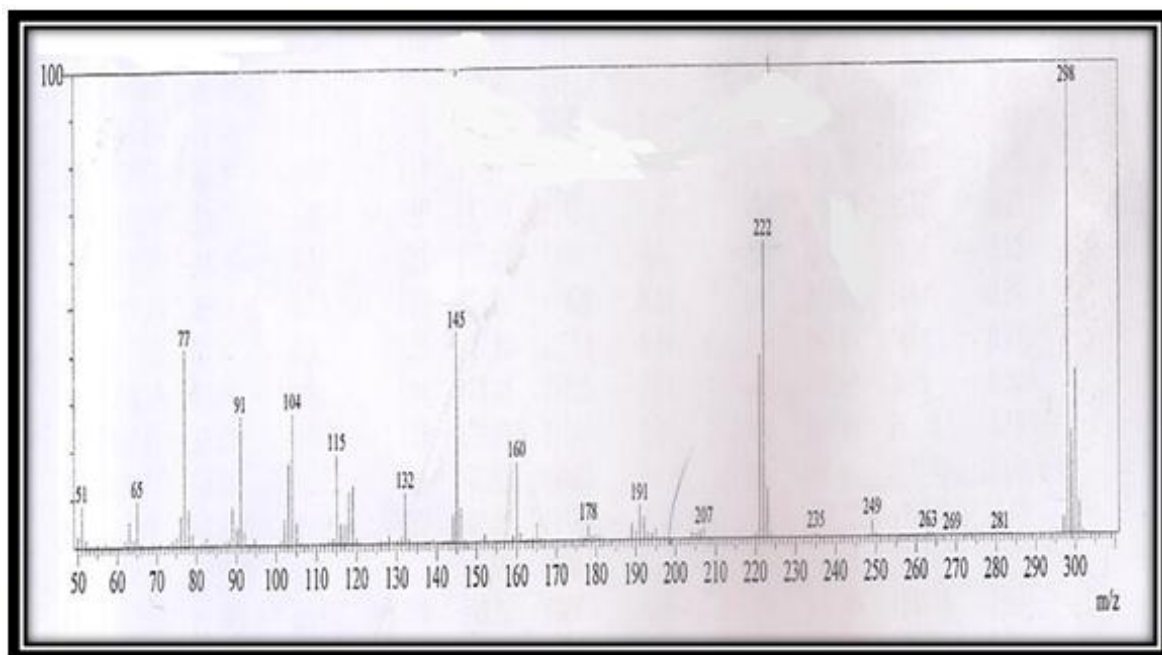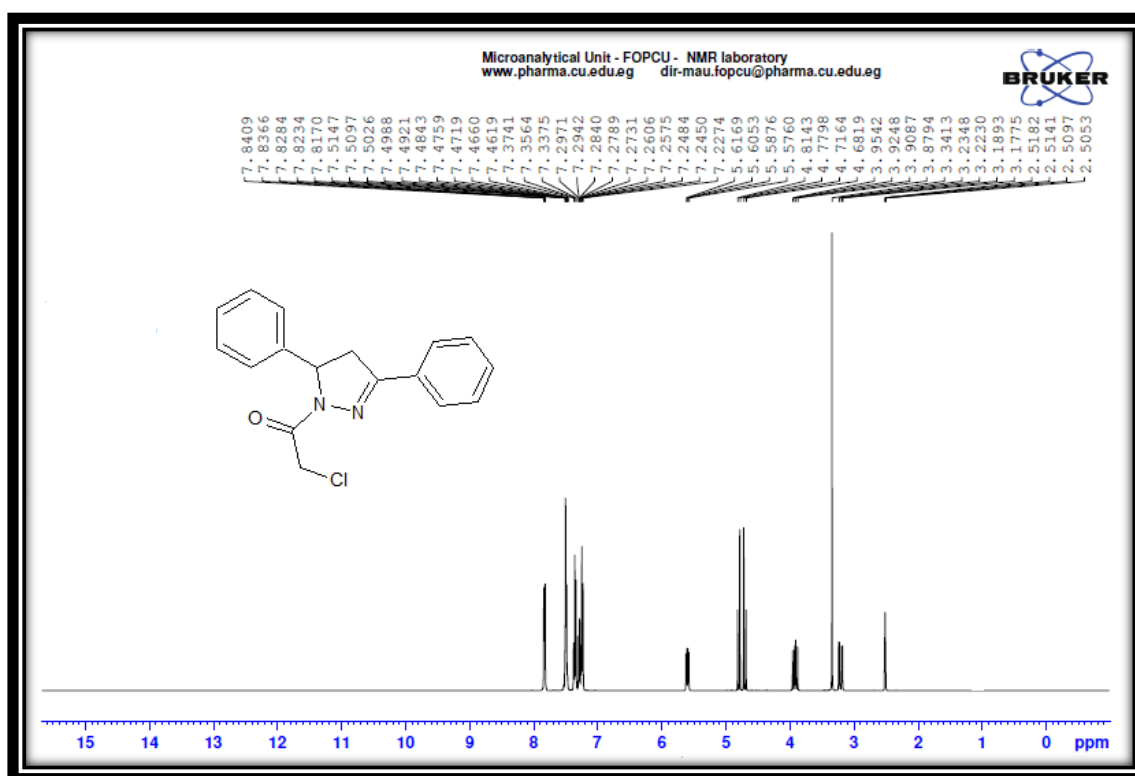
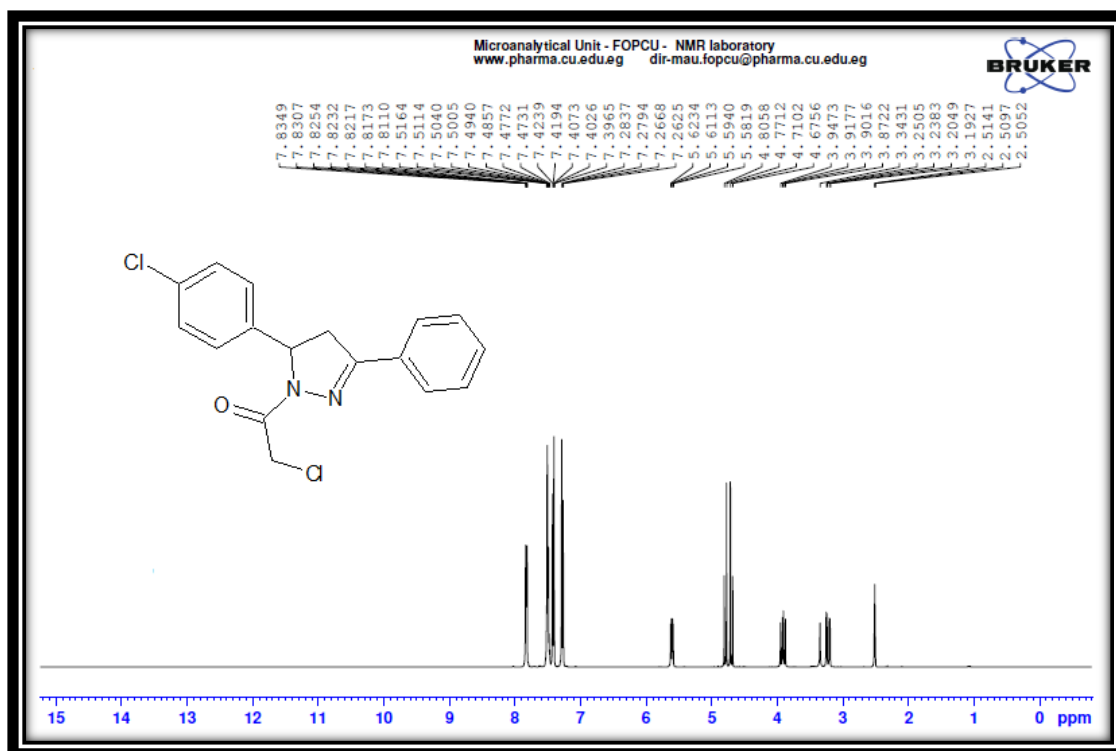**Figure (4.103):** MS Spectrum of 2-chloro-1-(3,5-diphe nyl-4,5-dih ydro-1*H*-py razol-1-yl) ethan-1-one **(XLI)**
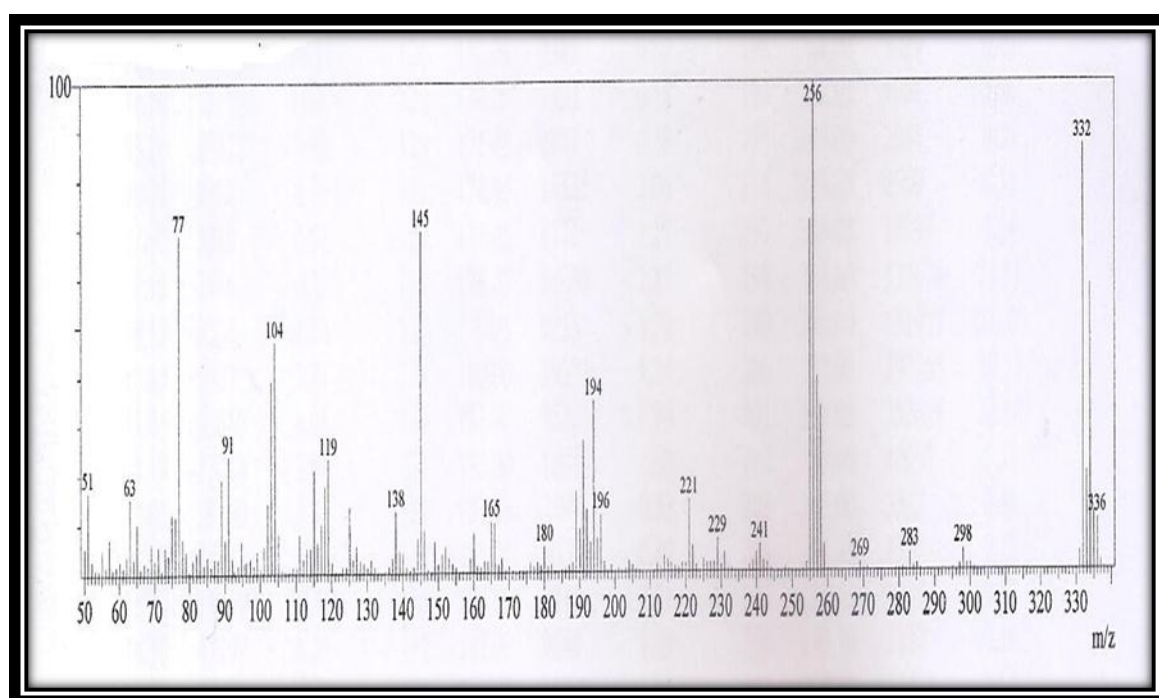
Figure (4.104): MS Spectrum of 2-chloro-1-[5-(4-chlorophenyl)-3-phenyl-4,5-dihydro-1*H*-pyrazol-1-yl] ethan-1-one **(XLII)**
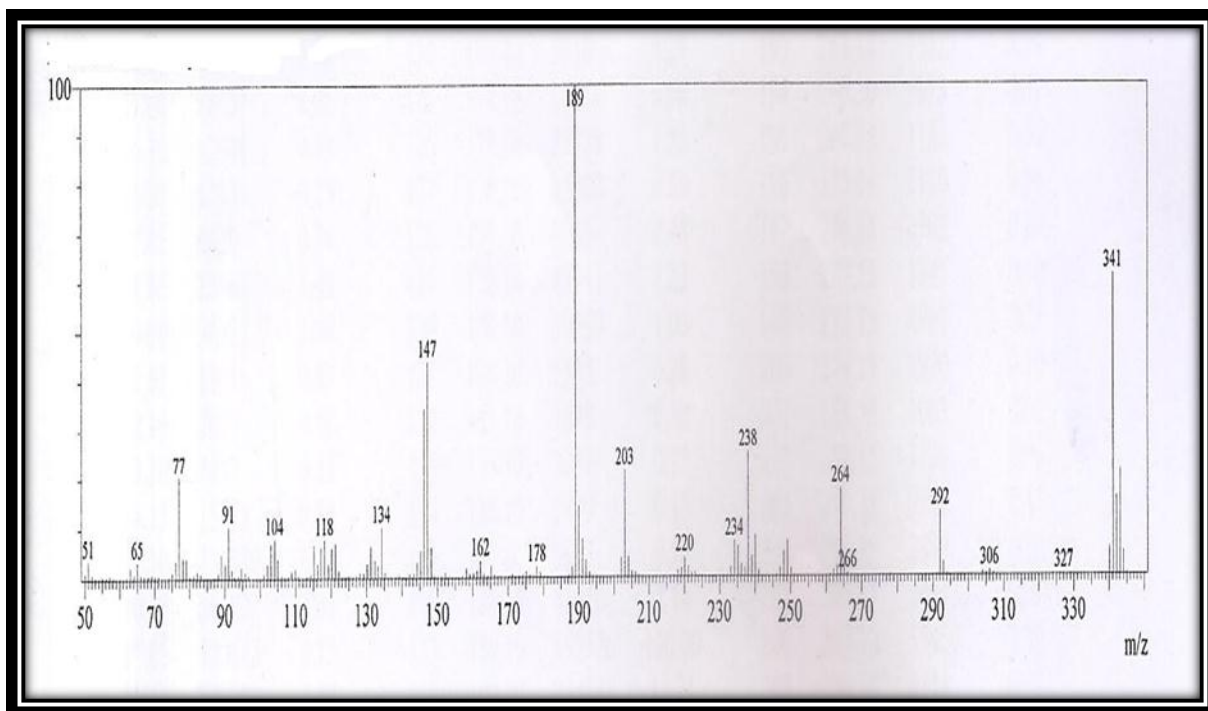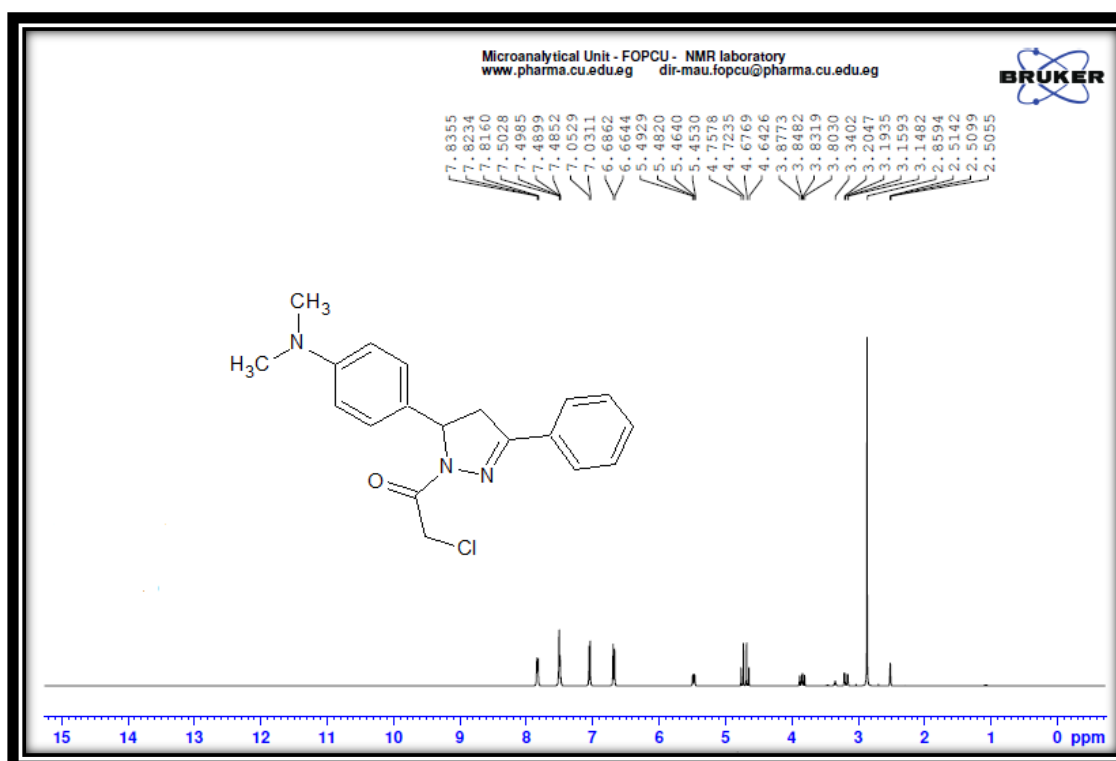
Figure (4.105): MS Spectrum of 2-chloro-1-{5-[4-(dimethylamino) phenyl]-3-phenyl-4,5-dihydro-1*H*-pyrazol-1-yl} ethan-1-one **(XLIII)**
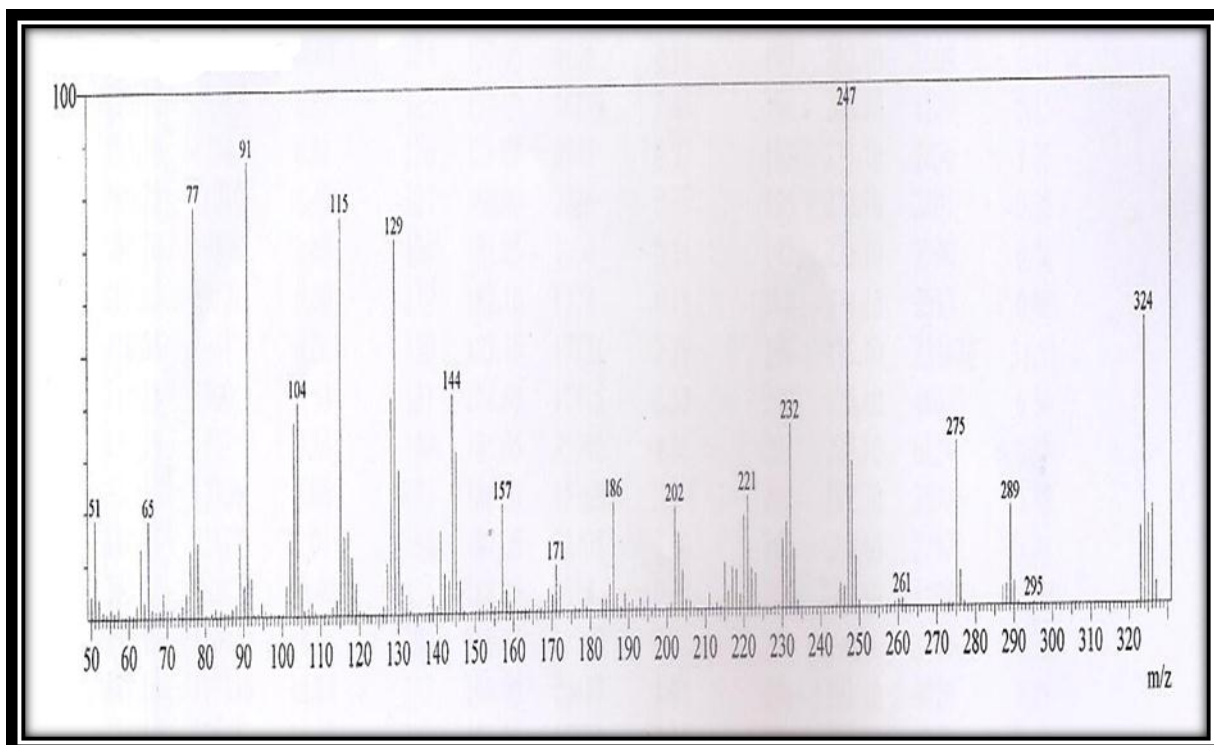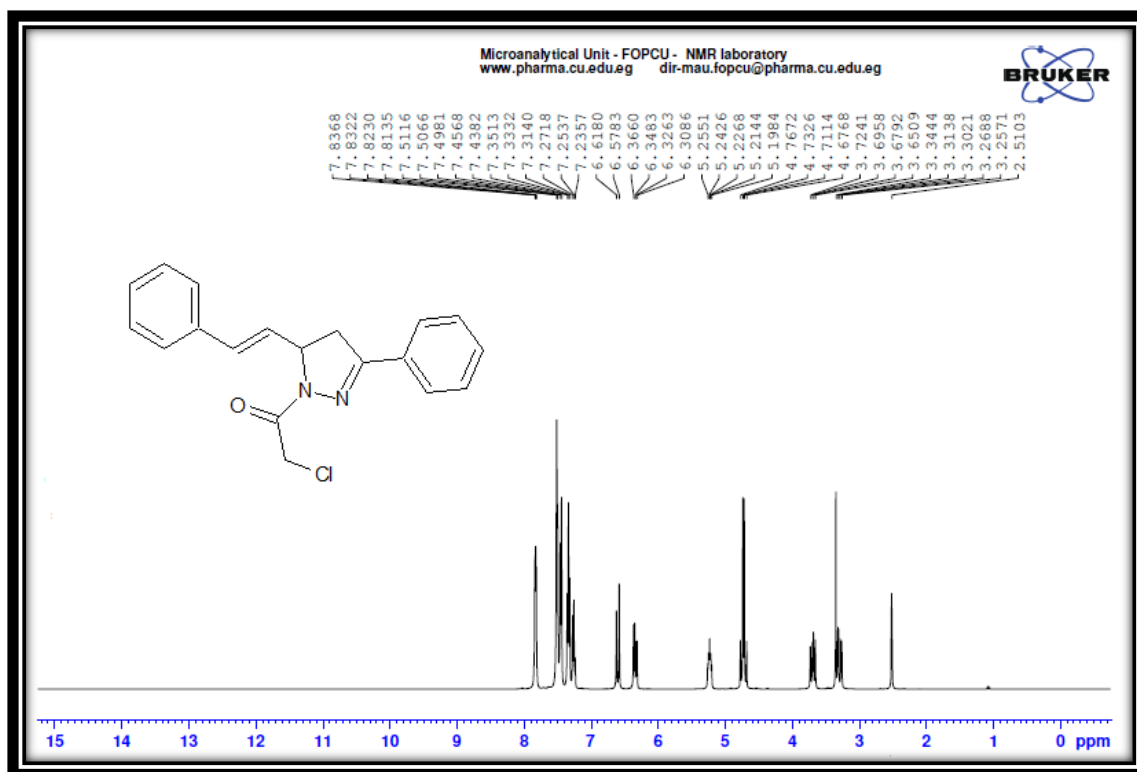

Figure (4.106): MS Spectrum of 2-chloro-1-{3-phenyl-5-[(*E*)-2-phenylethenyl]-4,5-dihydro-1*H*-pyrazol-1-yl}ethan-1-one **(XLIV)**
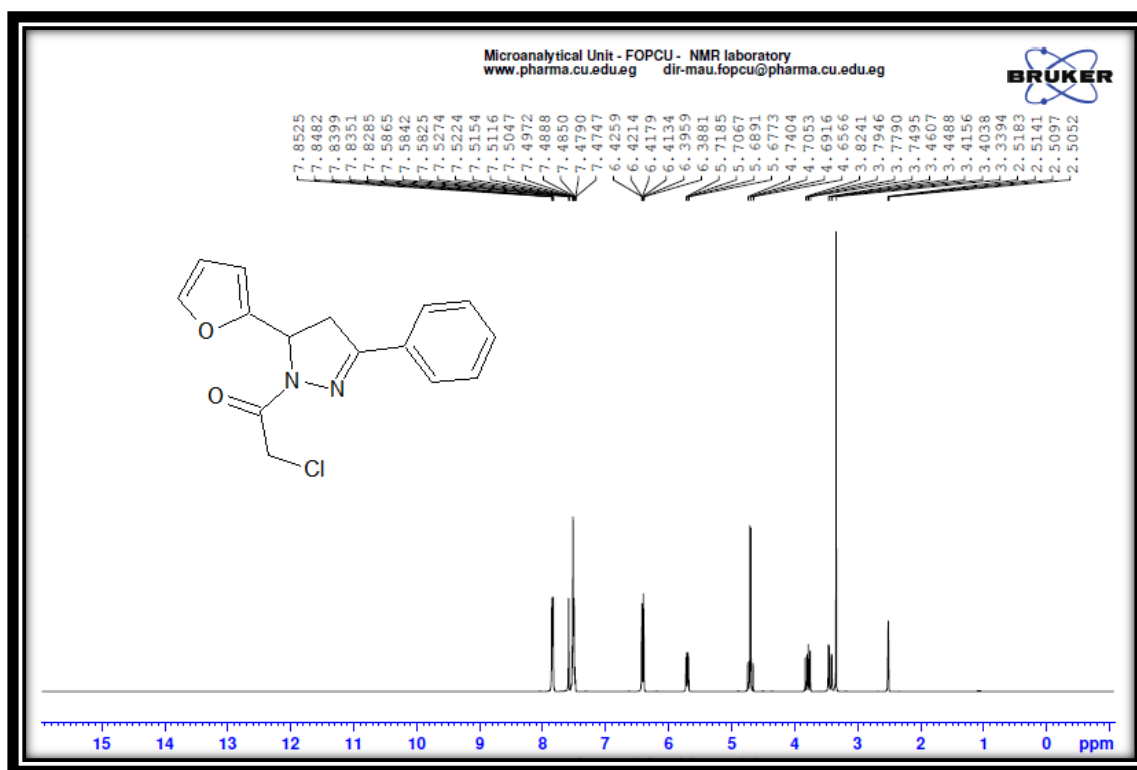
245
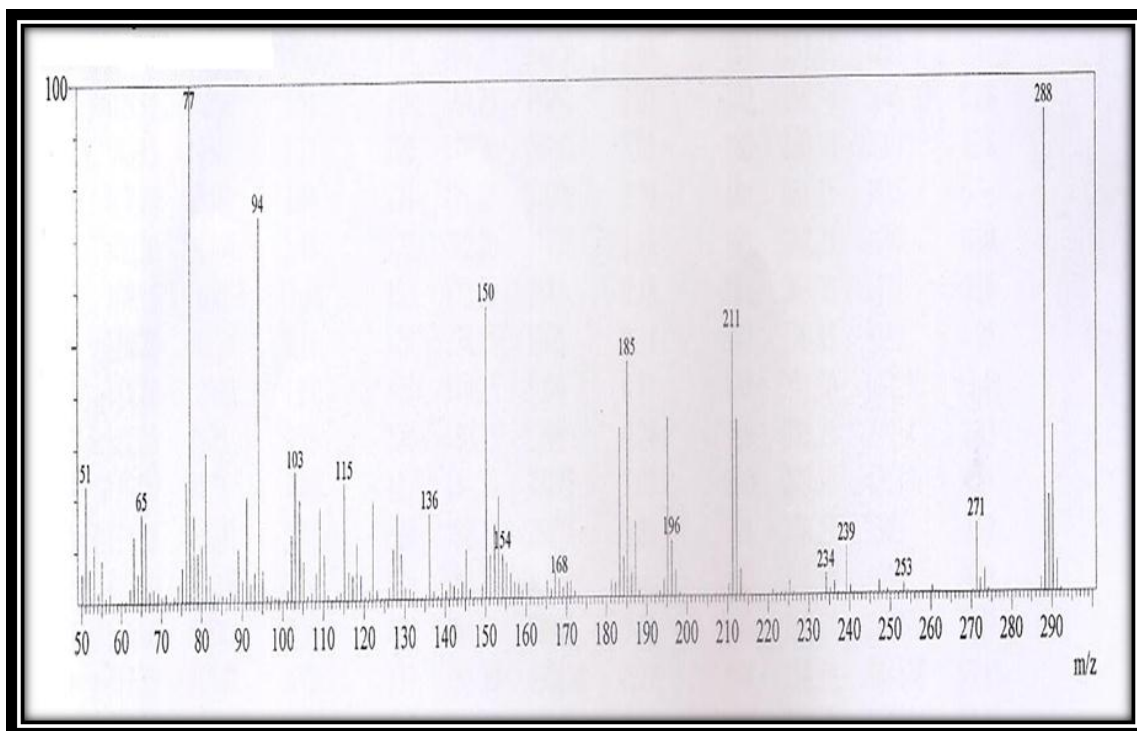
Figure (4.107): MS Spectrum of 2-chloro-1-[5-(fura n-2-yl)-3-phenyl-4,5-dihydro-1H-pyrazol-1-yl]ethan-1-one **(XLV)**
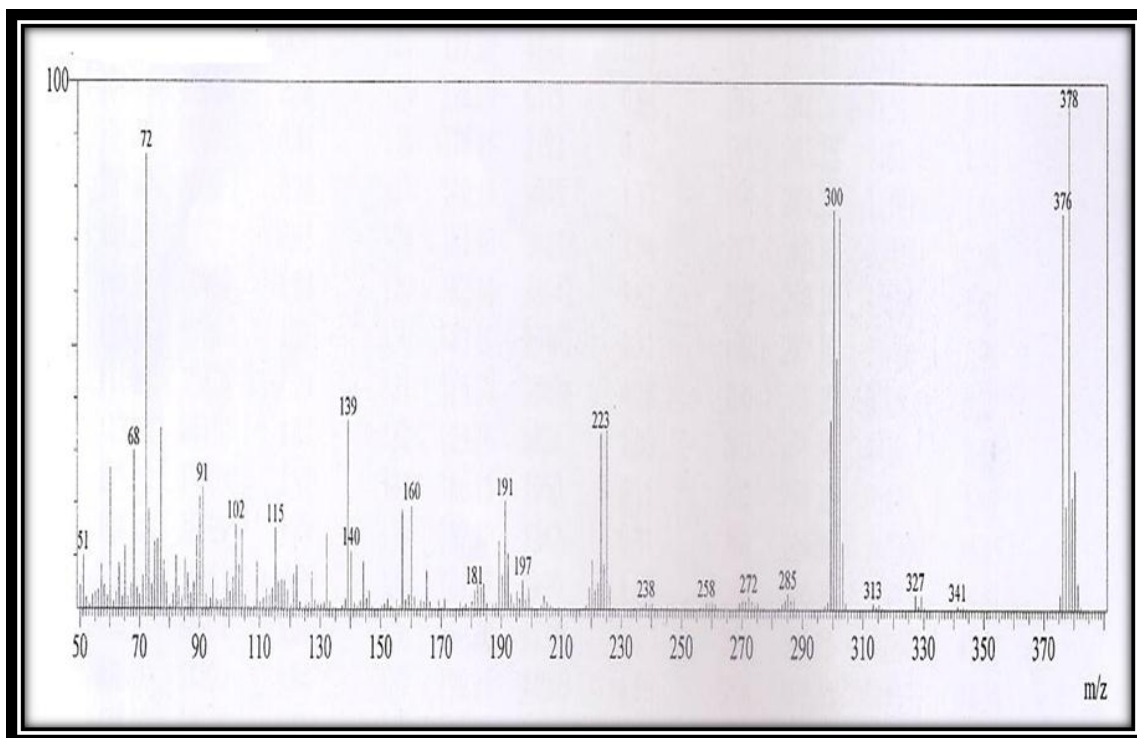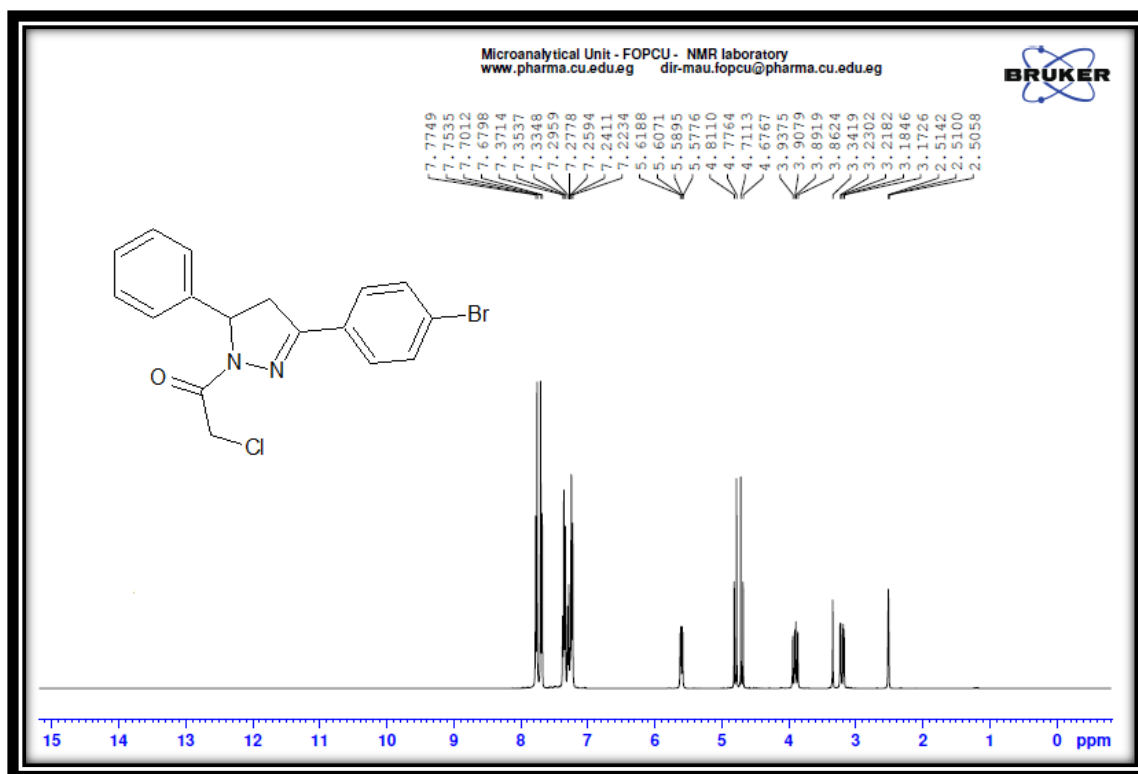

Figure (4.108): MS Spectrum of 1-[3-(4-bromophenyl)-5-phenyl-4,5-dihydro-1*H*-pyrazol-1-yl]-2-chloroethan-1-one **(XLVI)**
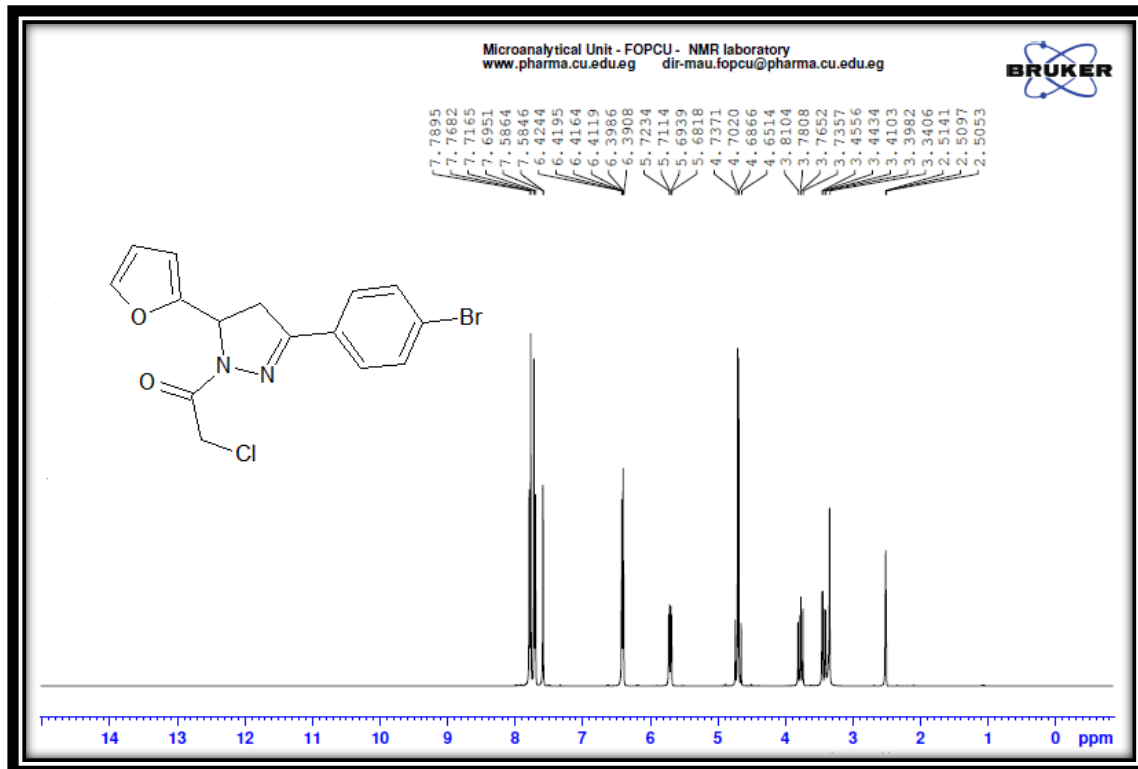
246
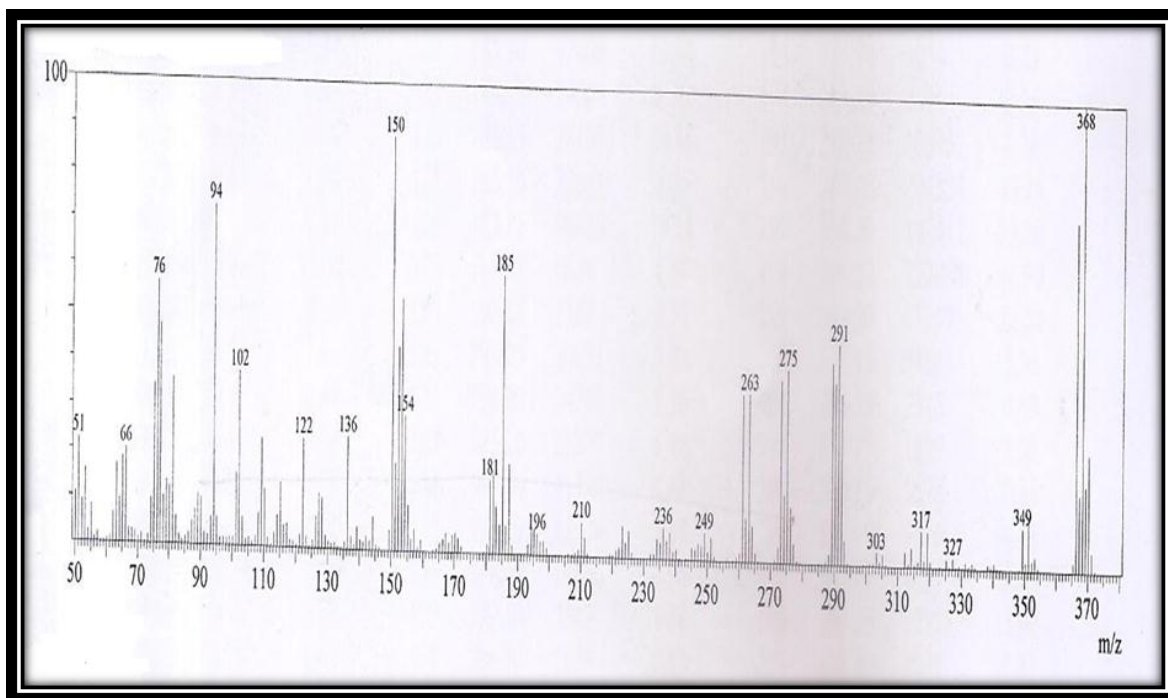
Figure (4.109): MS Spectrum of 1-[3-(4-bromophenyl)-5-(furan-2-yl)-4,5-dihydro-1*H*-pyrazol-1-yl]-2-chloroethan-1-one **(XLVII)**
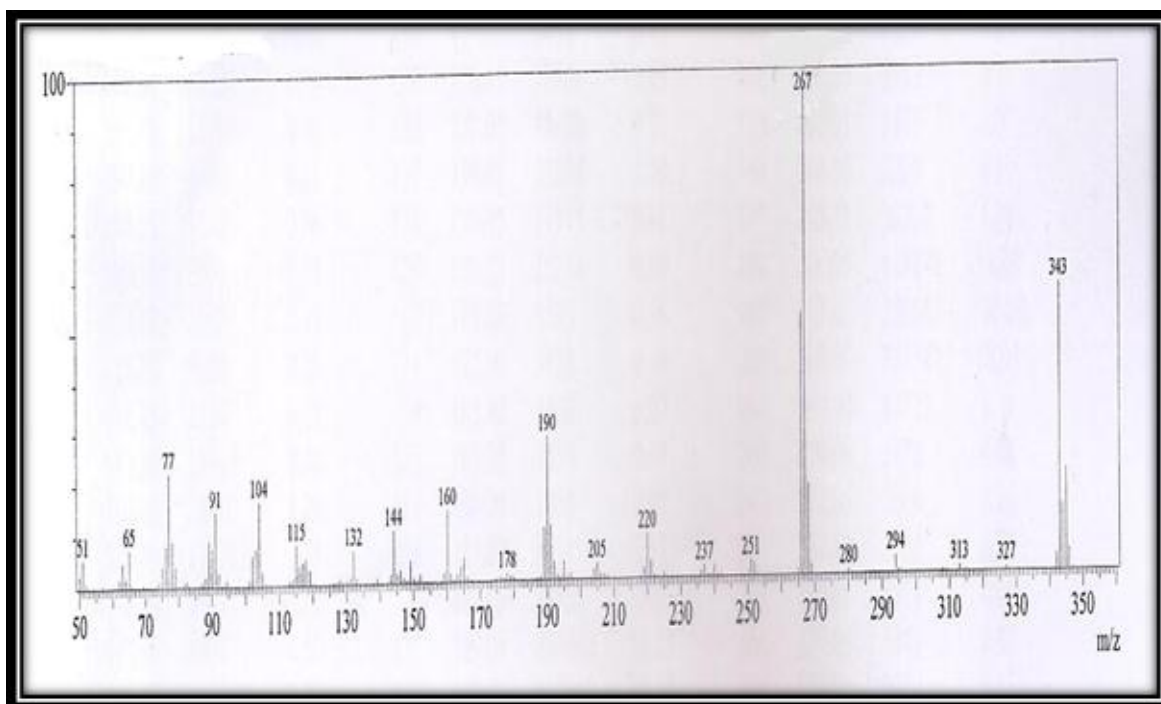
Figure (4.110): MS Spectrum of 2-chloro-1-[3- (4-nitro phenyl)-5-phenyl-4,5-dihydro-1*H*-pyrazol-1-yl] ethan-1-one **(XLVIII)**

Figure (4.111): MS Spectrum of 2-chloro-1-[5-(4-chloro phenyl)-3-(4-nitro phenyl)-4,5-dihydro-1*H*-pyrazol-1-yl]ethan-1-one **(XLIX)**

Figure (4.112): MS Spectrum of 2-chloro-1-{5-[4-(dimethylamino)phenyl]-3-(4-nitrophenyl)-4,5-dihydro-1 *H*-pyrazol-1-yl} ethan-1-one **(L)**

Figure (4.113): MS Spectrum of 2-chloro-1-{3-(4-nitrophenyl)-5-[(*E*)-2-phenylethenyl]-4,5-dihydro-1*H*-pyrazol-1-yl}ethan-1-one **(LI)**

Figure (4.114): MS Spectrum of 2-chloro-1-[5-(furan-2-yl)-3-(4-nitrophenyl)-4,5-dihydro-1*H*-pyrazol-1-yl]ethan-1-one **(LII)**
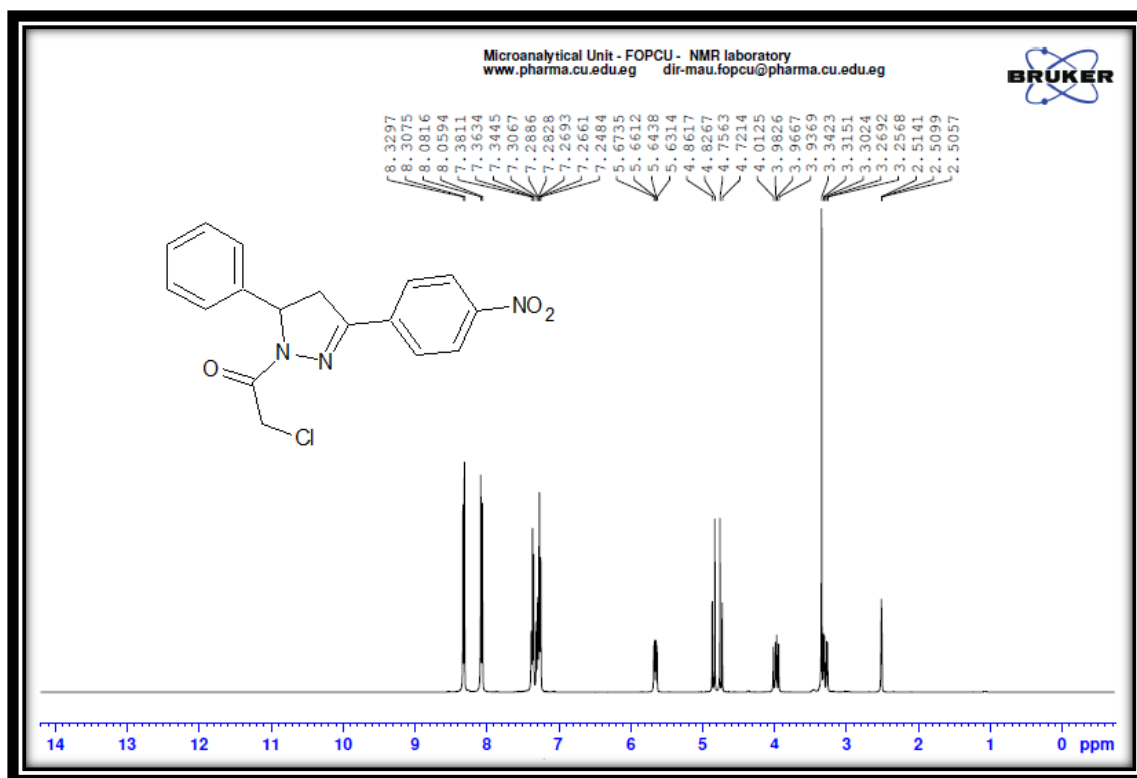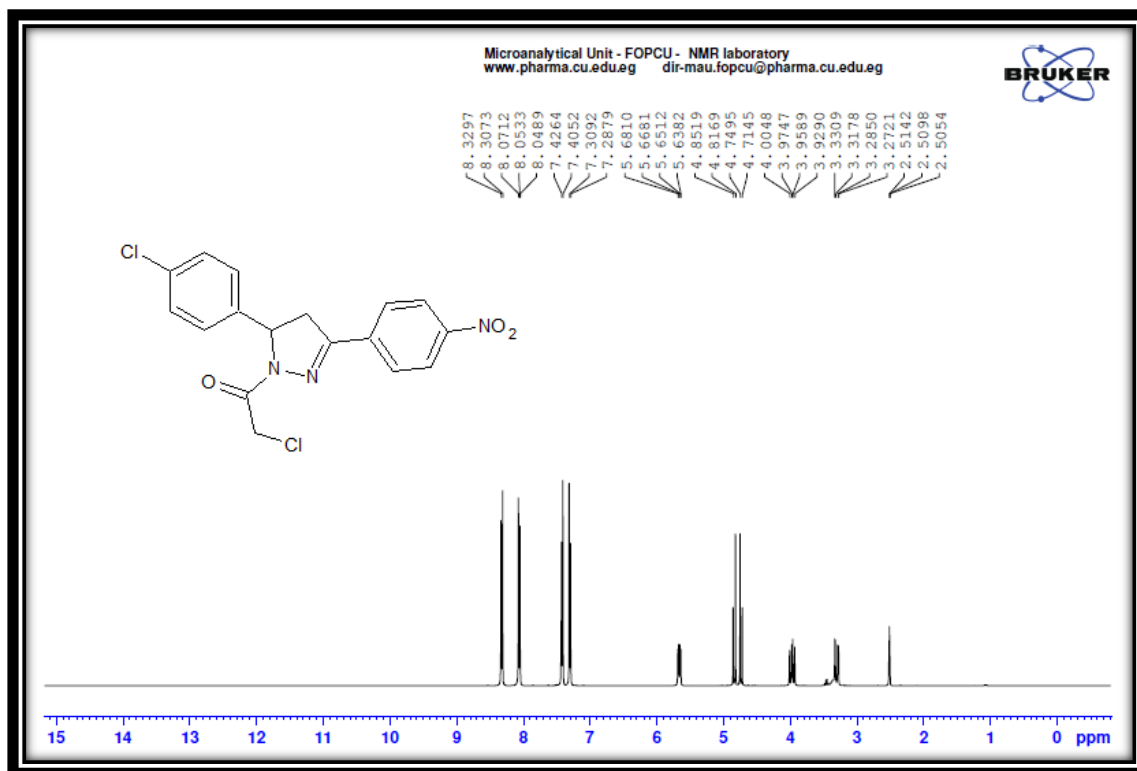
249
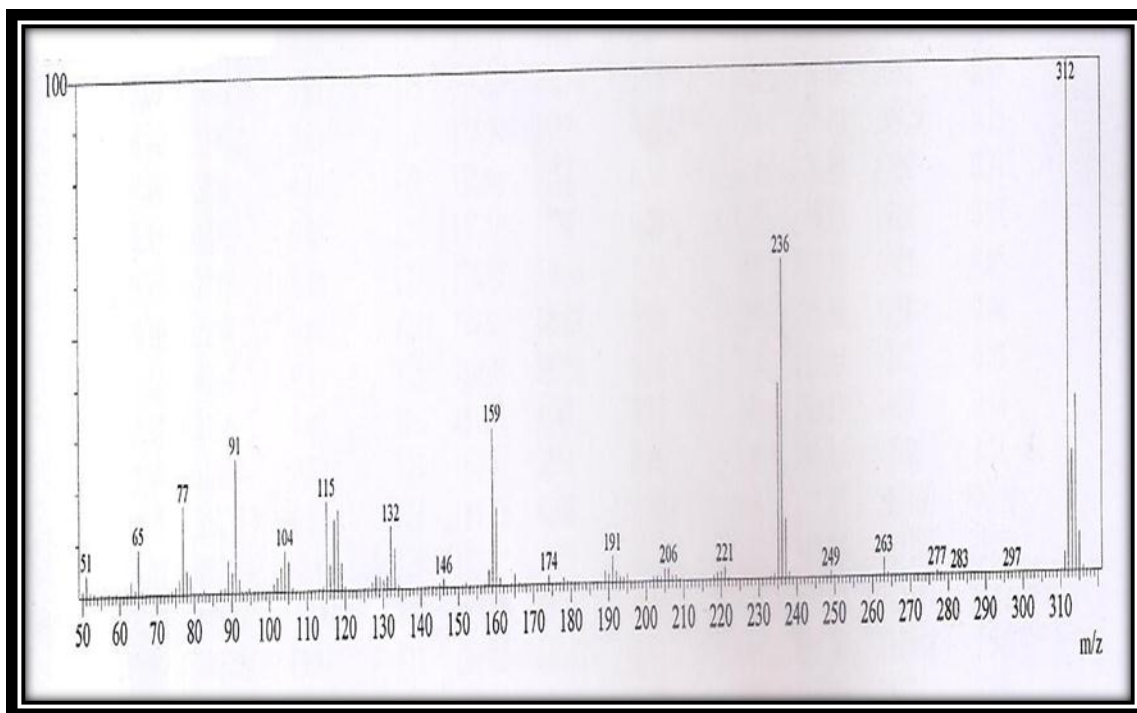
Figure (4.115): MS Spectrum of 2-chloro-1-[3-(4-methylphenyl)-5-phenyl-4,5-dihydro-1*H*-pyrazol-1-yl] ethan-1-one **(LIII)**

Figure (4.116): MS Spectrum of 2-chloro-1-[5-(4-chloro p henyl)-3-(4-methylphenyl)-4,5-dihydro-1H-pyrazol-1-yl]ethan-1-one **(LIV)**
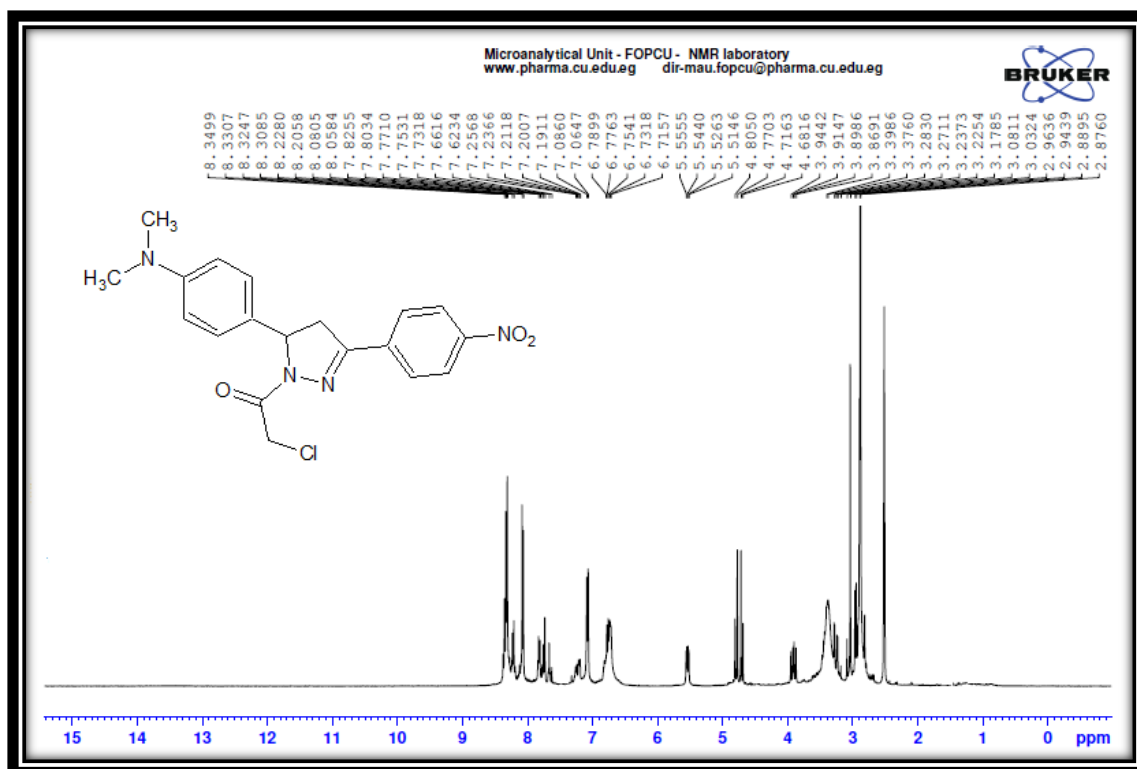
Figure (4.117): MS Spectrum of 2-chloro-1-{5-[4-(dimethylamino) phenyl]-3-(4-methylphenyl)-4,5-dihydro-1 H-pyrazol-1-yl}ethan-1-one **(LV)**
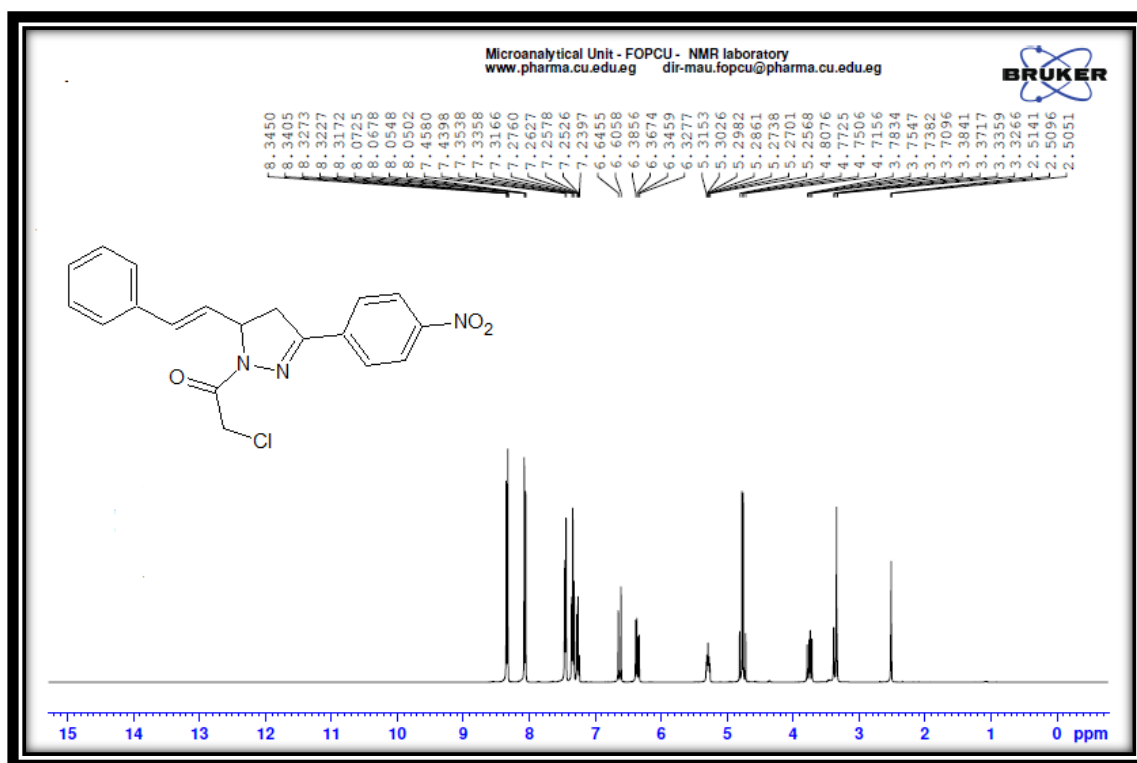

Figure (4.118): MS Spectrum of 2-chloro-1-{3-(4-methyl phenyl)-5-[(E)-2-phenylethenyl]-4,5-dihydro-1H-pyrazol-1-yl}ethan-1-one **(LVI)**
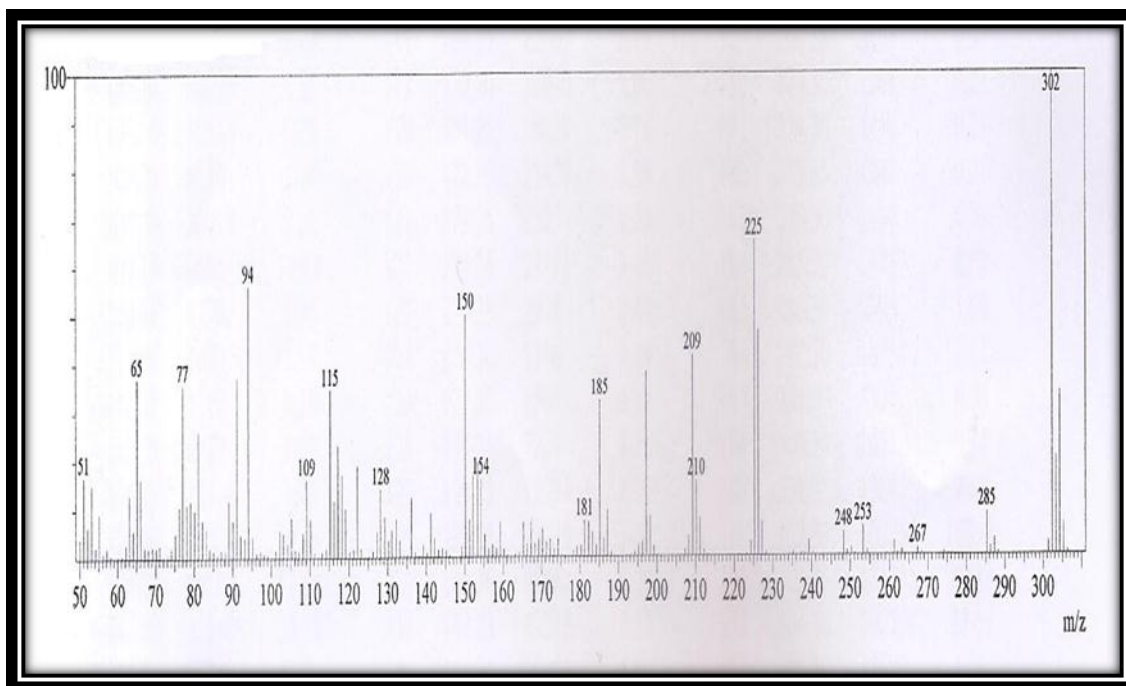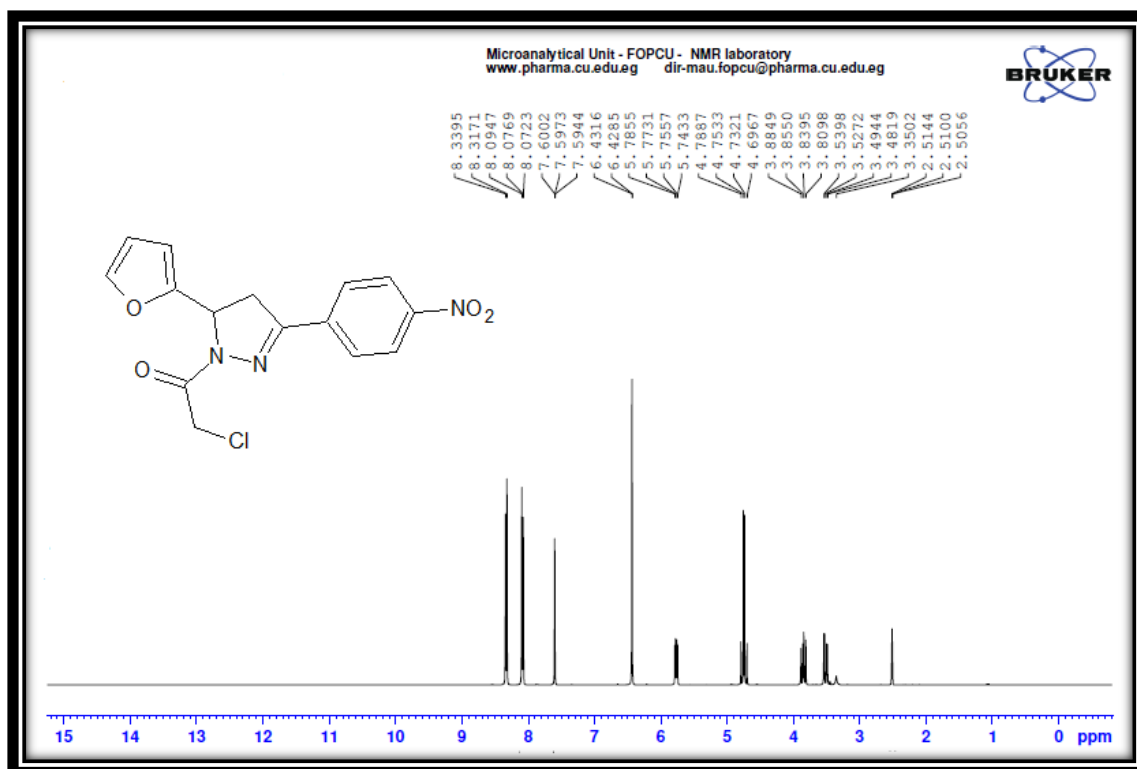
Figure (4.119): MS Spectrum of 2-chloro-1-[5-(furan-2-yl)-3-(4-methylphenyl)-4,5-dihydro-1*H*-pyrazol-1-yl]ethan-1-one **(LVII)**
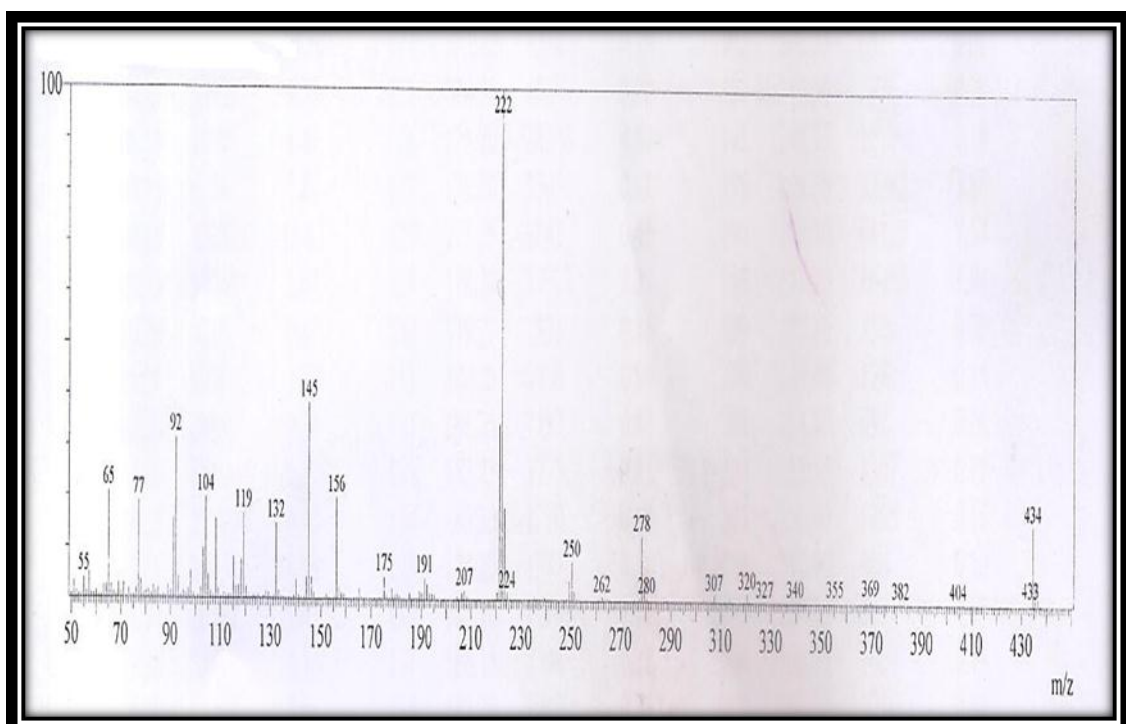

Figure (4.120): MS Spectrum of 4-((2-(3,5-diphenyl-4,5-di hydro-1H-pyrazol-1-yl)-2-oxoethyl)amino)benzene sulfonamide **(LVIII)**

Figure (4.121): MS Spectrum of 4-((2-(5-(4-chlorophenyl)-3-phenyl-4,5-dihydro-1H-pyrazol-1-yl)-2-oxoethyl) amino) benzene sulfonamide **(LIX)**

Figure (4.122): MS Spectrum of 4-((2-(5-(4-(dimethylamin o)phenyl)-3-phenyl-4,5-di hydro-1H-pyrazol-1-yl)-2-oxoethyl)amino)benzene sulfonamide **(LX)**

Figure (4.123): MS Spectrum of (E)-4-((2-oxo-2-(3-phenyl-5-styryl-4,5-dihydro-1H-pyrazol-1-yl)ethyl)amino) benzenesulfonamide **(LXI)**

Figure (4.124): MS Spectrum of 4-({2-[5-(furan-2-yl)-3-phenyl-4,5-dihydro-1*H*-pyrazol-1-yl]-2-oxoethyl}amino)benzene-1-sulfonamide **(LXII)**

Figure (4.125): MS Spectrum of 4-((2-(5-(furan-2-yl)-3-(4-nitrophenyl)-
4,5-dihydro-1H-pyrazol-1-yl)-2-oxoeth yl) amino)benzene sulfonamide
(LXIII)

Figure (4.126): MS Spectrum of 4-((2-oxo-2-(5-phenyl-3-(p-tolyl)-4,5-
dihydro-1H-pyrazol-1-yl)ethyl) amino) benzene sulfonamide **(LXIV)**
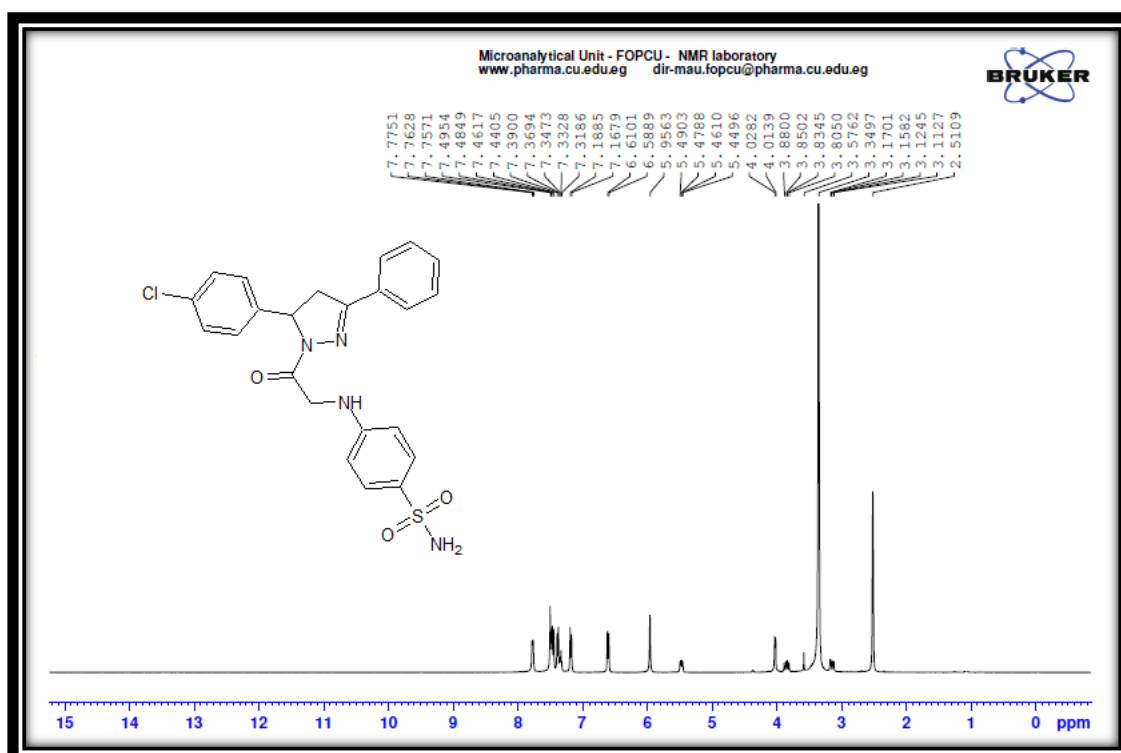
255

Figure (4.127): MS Spectrum of 4-((2-(5-(4-chlorophenyl)-3-(p-tolyl)-4,5-dihydro-1H-pyrazol-1-yl)-2-oxoethyl)amino)benzene sulfonamide **(LXV)**
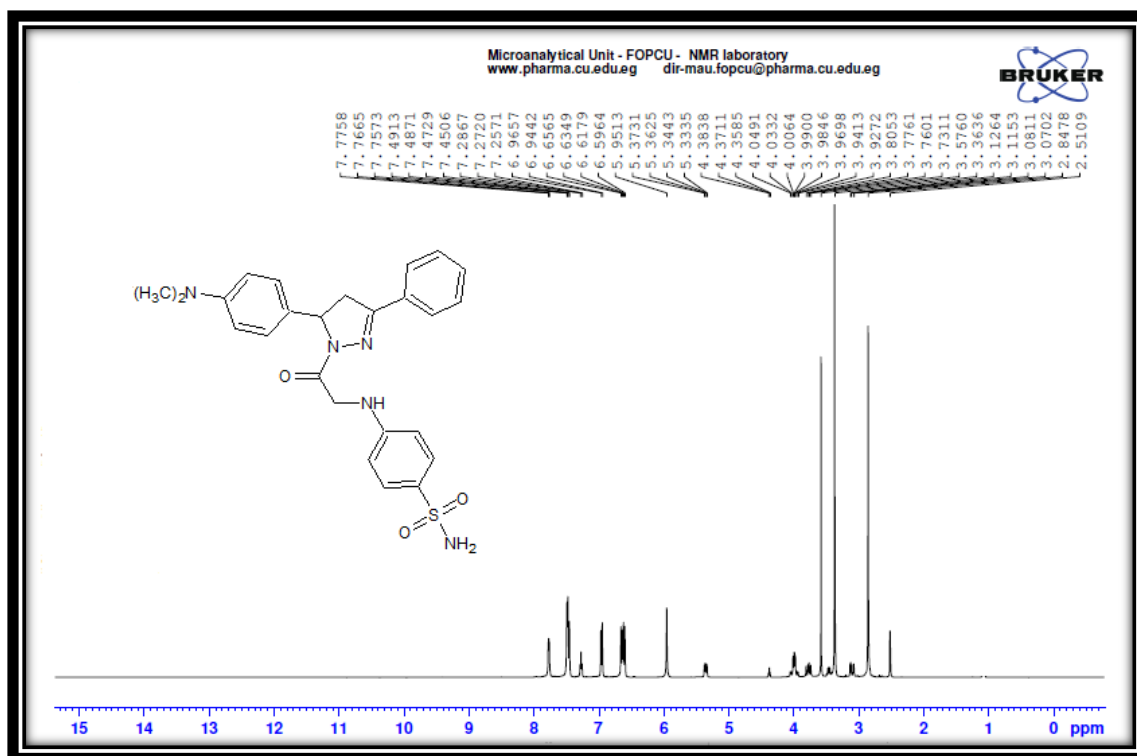

Figure (4.128): MS Spectrum of 4-((2-(5-(4-(dimethyl amino)phenyl)-3-(p-tolyl)-4,5-dihydro-1H-pyrazol-1-yl)-2-oxoethyl)amino)benzene sulfonamide **(LXVI)**

Figure (4.129): MS Spectrum of 4-((2-(5-(furan-2-yl)-3-(p-tolyl)-4,5-dihydro-1H-pyrazol-1-yl)-2-oxoethyl)amino)benzene sulfonamide **(LXVII)**

Figure (4.130): MS Spectrum of 4-((2-(5-(4-chlorophenyl)-3-phenyl-4,5-dihydro-1H-pyrazol-1-yl)-2-oxoethyl) amino)-N-(5,6-dimethoxy pyrimidin-4-yl)benzene sulfonamide **(LXVIII)**

257

Figure (4.131): MS Spectrum of N-(5,6-dimethoxypyrimidin-4-yl)-4-((2-(5-(4-(dimethylamino)phenyl)-3-phenyl-4,5-dihydro-1H-pyrazol-1-yl)-2-oxoethyl)amino)benzenesulfonamide **(LXIX)**

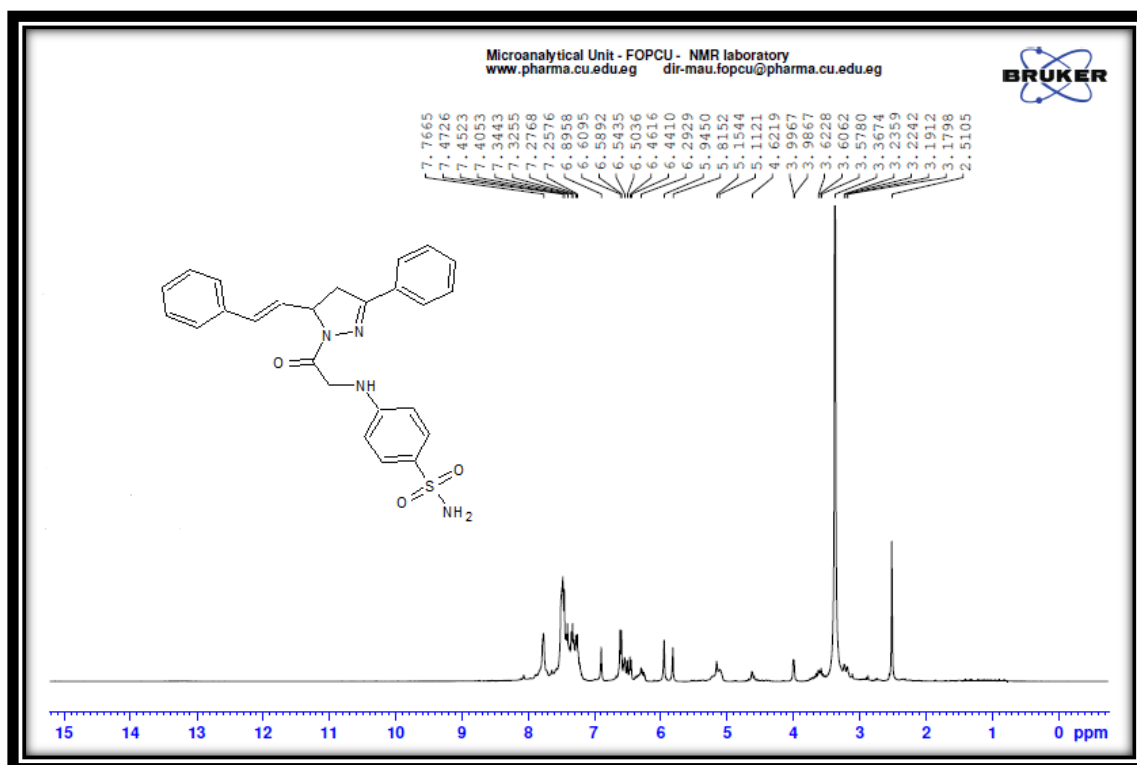**Figure (4.132):** MS Spectrum of N-(5,6-dimethoxypyrimidin-4-yl)-4-((2-oxo-2-(5-phenyl-3-(p-tolyl)-4,5-dihydro-1H-pyrazol-1-yl)ethyl)amino)benzenesulfonamide **(LXX)**

Figure (4.133): MS Spectrum of N-(5,6-dimethoxypyrimid in-4-yl)-4-
((2-(5-(4-(dime thylamino)phenyl)-3-(p-tol yl)-4,5-dihydro-1H-pyraz ol-
1-yl)-2-oxoethyl)amino)benzene sulfonamide **(LXXI)**

Figure (4.134): ^{1}HNMR Spectrum of 2-chloro-1-(3,5-diphe nyl-4,5-
dihydro-1*H*-pyrazol-1-yl) ethan-1-one **(XLI)**

259

Figure (4.135): ¹HNMR Spectrum of 2-chloro-1-[5-(4-chlorophenyl)-3-phenyl-4,5-dihydro-1*H*-pyrazol-1-yl] ethan-1-one **(XLII)**

Figure (4.136): ¹HNMR Spectrum of 2-chloro-1-{5-[4-(dimethylamino) phenyl]-3-phe n yl-4,5-dihydro-1*H*-pyrazol-1-yl} ethan-1-one **(XLIII)**

Figure (4.137): ^{1}HNMR Spectrum of 2-chloro-1-{3-phenyl-5-[(*E*)-2-phenylethenyl]-4,5-dihydro-1*H*-pyrazol-1-yl}ethan-1-one **(XLIV)**

Figure (4.138): ^{1}HNMR Spectrum of 2-chloro-1-[5-(fura n-2-yl)-3-phenyl-4,5-dihydro-1H-pyrazol-1-yl]ethan-1-one **(XLV)**

Figure (4.139): ^{1}HNMR Spectrum of 1-[3-(4-bromophenyl)-5-phenyl-4,5-dihydro-1*H*-pyrazol-1-yl]-2-chloroethan-1-one **(XLVI)**

Figure (4.140): ^{1}HNMR Spectrum of 1-[3-(4-bromophenyl)-5-(furan-2-yl)-4,5-dihydro-1*H*-pyrazol-1-yl]-2-chloroethan-1-one **(XLVII)**

Figure (4.141): ^{1}HNMR Spectrum of 2-chloro-1-[3- (4-nitro phenyl)-5-phenyl-4,5-dihydro-1*H*-pyrazol-1-yl] ethan-1-one **(XLVIII)**

Figure (4.142): ^{1}HNMR Spectrum of 2-chloro-1-[5-(4-chloro phenyl)-3-(4-nitro phenyl)-4,5-dihydro-1*H*-pyrazol-1-yl]ethan-1-one **(XLIX)**

Figure (4.143): ¹HNMR Spectrum of 2-chloro-1-{5-[4-(dimethylamino) phenyl]-3-(4-nitrophenyl)-4,5-dihydro-1 *H*-pyrazol-1-yl} ethan-1-one **(L)**

Figure (4.144): ¹HNMR Spectrum of 2-chloro-1-{3-(4-nitrophenyl)-5-[(*E*)-2-phenylethenyl]-4,5-dihydro-1*H*-pyrazol-1-yl}ethan-1-one **(LI)**

Figure (4.145): ^{1}HNMR Spectrum of 2-chloro-1-[5-(furan-2-yl)-3-(4-nitrophenyl)-4,5-dihydro-1*H*-pyrazol-1-yl]ethan-1-one **(LII)**
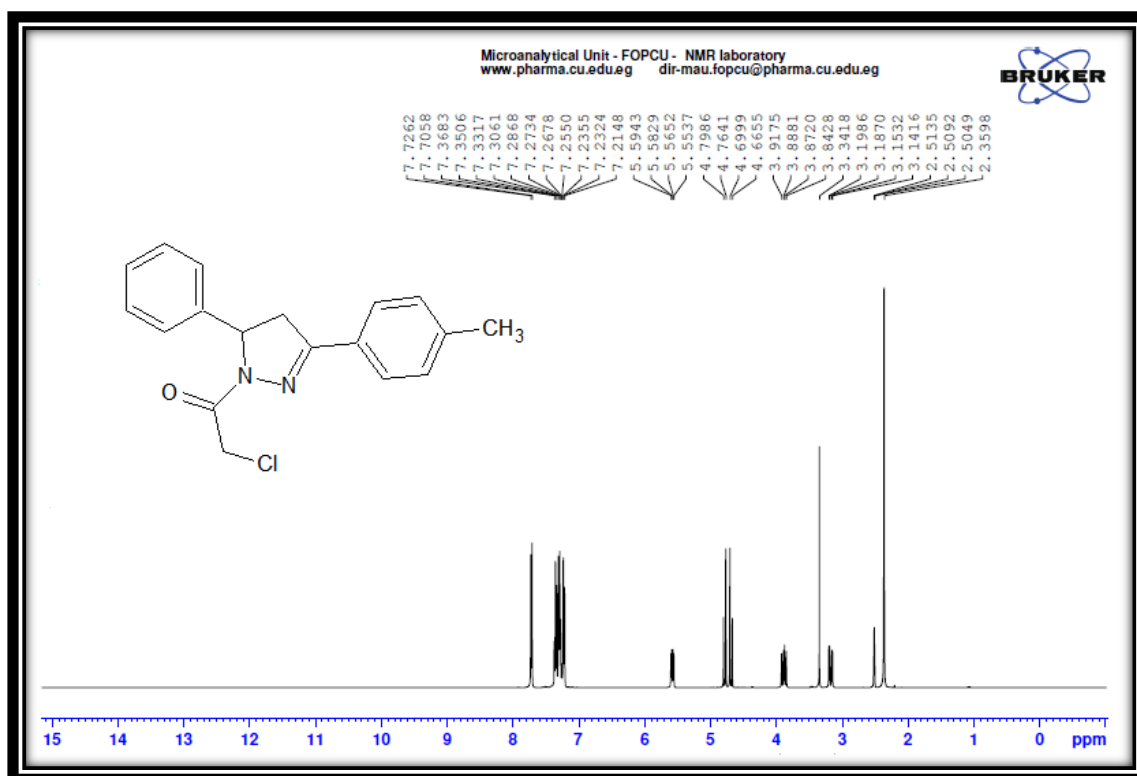
Figure (4.146): ^{1}HNMR Spectrum of 2-chloro-1-[3-(4-methylphenyl)-5-ph enyl-4,5-dihydro-1*H*-pyrazol-1-yl] ethan-1-one **(LIII)**
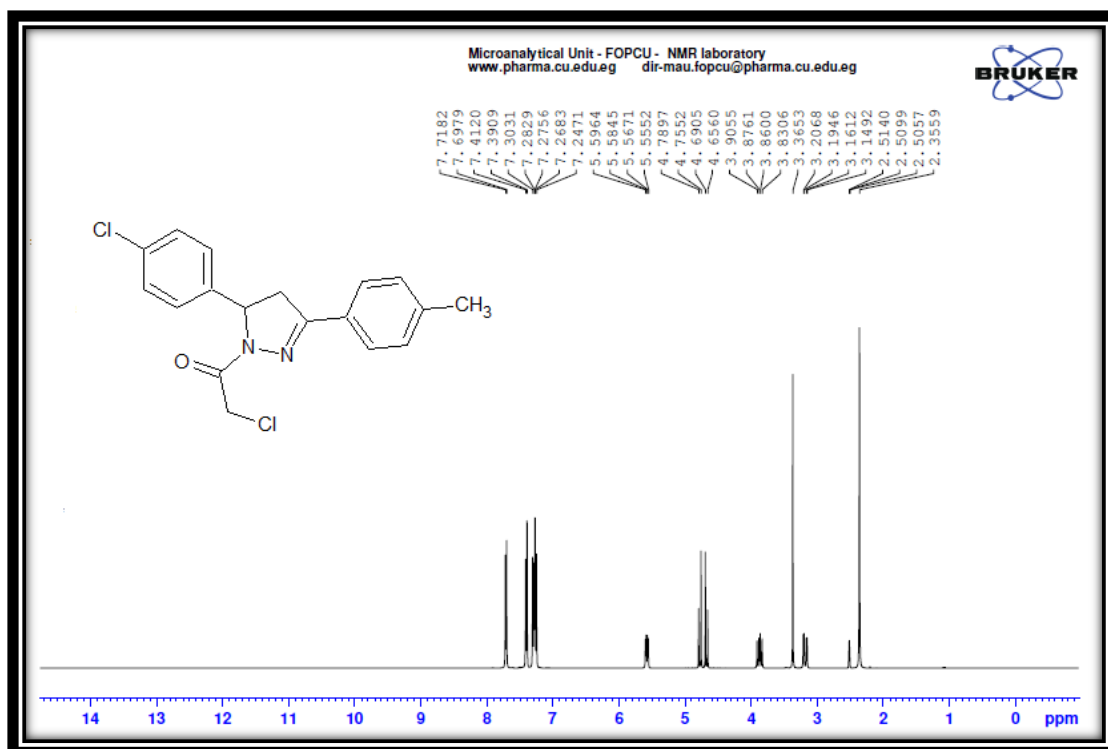
Figure (4.147): ^{1}HNMR Spectrum of 2-chloro-1-[5-(4-chlorophenyl)-3-(4-methylphenyl)-4,5-dihydro-1H-pyrazol-1-yl]ethan-1-one **(LIV)**
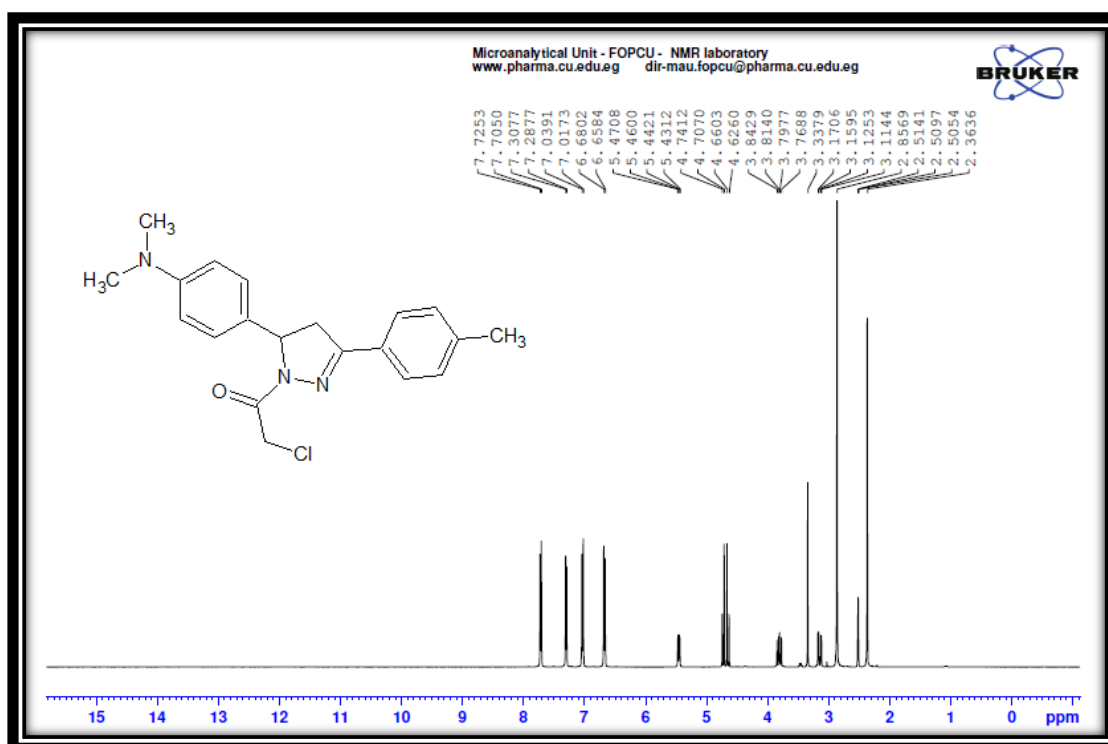
Figure (4.148): ^{1}HNMR Spectrum of 2-chloro-1-{5-[4-(dimethylamino) phenyl]-3-(4-methylphenyl)-4,5-dihydro-1 H-pyrazol-1-yl}ethan-1-one **(LV)**
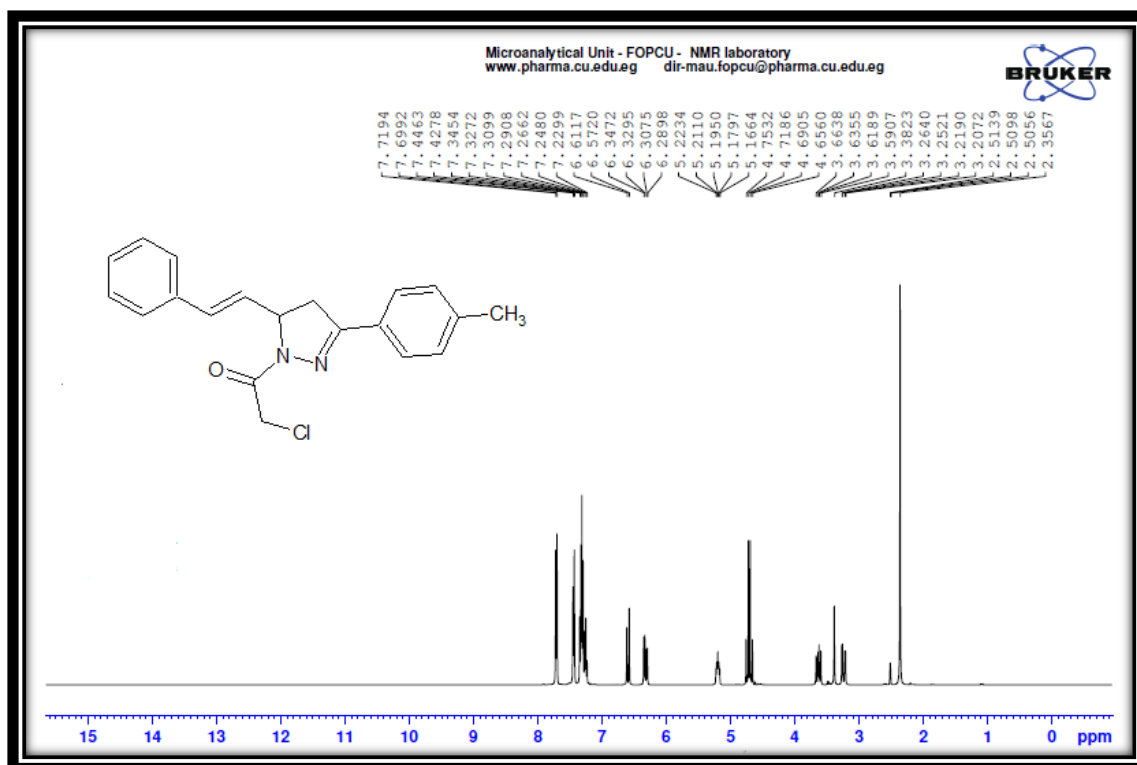
Figure (4.149): ^{1}HNMR Spectrum of 2-chloro-1-{3-(4-methyl phenyl)-5-[(E)-2-phenylethenyl]-4,5-dihydro-1H-pyrazol-1-yl}ethan-1-one **(LVI)**
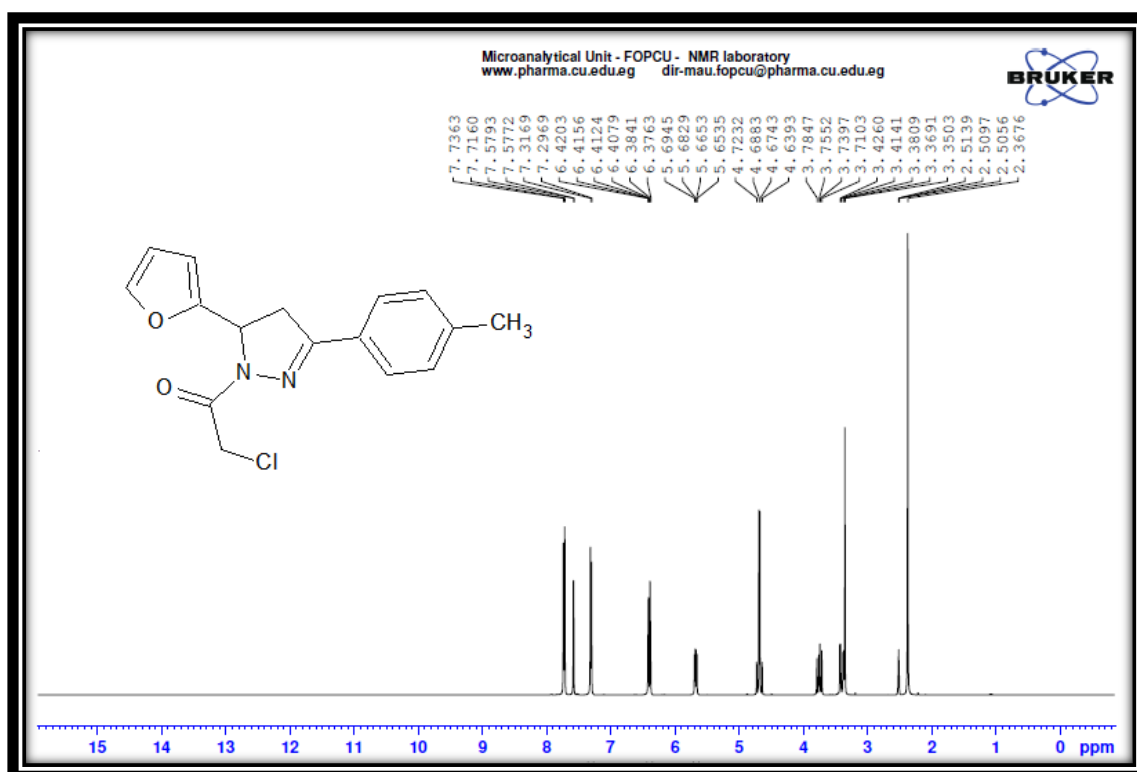
Figure (4.150): ^{1}HNMR Spectrum of 2-chloro-1-[5-(furan-2-yl)-3-(4-methylphenyl)-4,5-dihydro-1*H*-pyrazol-1-yl]ethan-1-one **(LVII)**
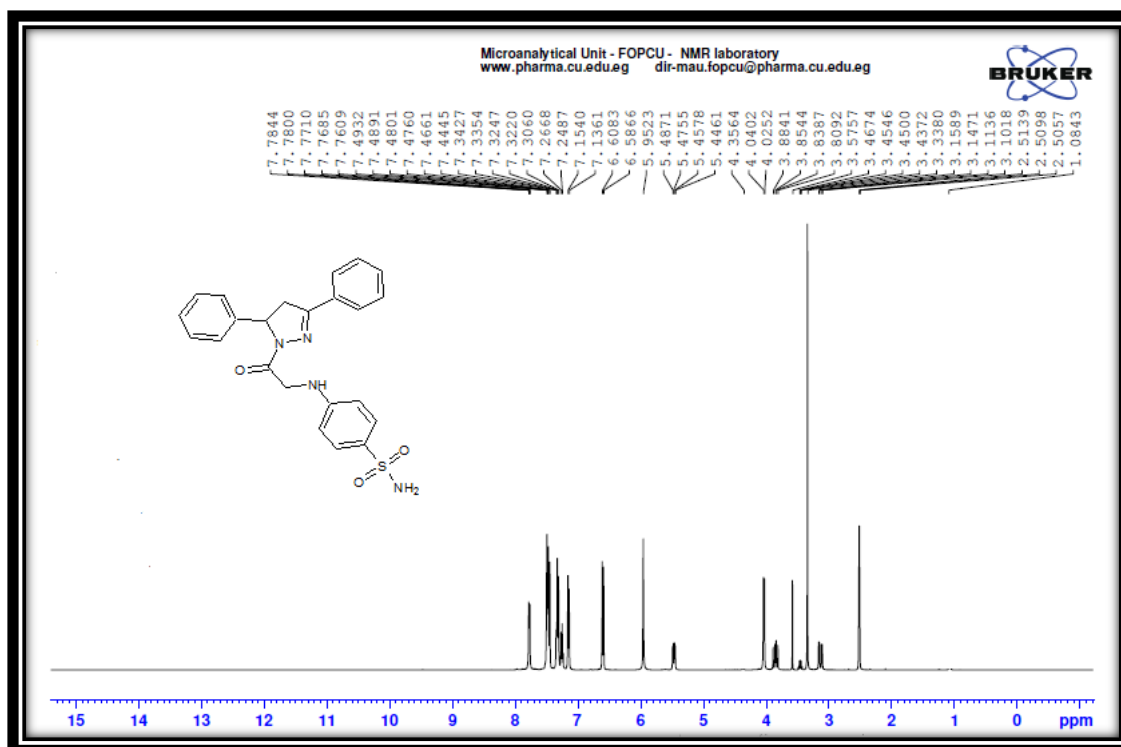
Figure (4.151): ^{1}HNMR Spectrum of 4-((2-(3,5-diphenyl-4,5-di hydro-1H-pyrazol-1-yl)-2-oxoethyl)amino)benzene sulfonamide **(LVIII)**

Figure (4.152): ^{1}HNMR Spectrum of 4-((2-(5-(4-chlorophenyl)-3-phenyl-4,5-dihydro-1H-pyrazol-1-yl)-2-oxoethyl) amino) benzene sulfonamide **(LIX)**

Figure (4.153): ^{1}HNMR Spectrum of 4-((2-(5-(4-(dimethylamin o)phenyl)-3-phenyl-4,5-di hydro-1H-pyrazol-1-yl)-2-oxoethyl)amino)benzene sulfonamide **(LX)**

Figure (4.154): ^{1}HNMR Spectrum of (E)-4-((2-oxo-2-(3-phenyl-5-styryl-4,5-dihydro-1H-pyrazol-1-yl)ethyl)amino) benzenesulfonamide **(LXI)**
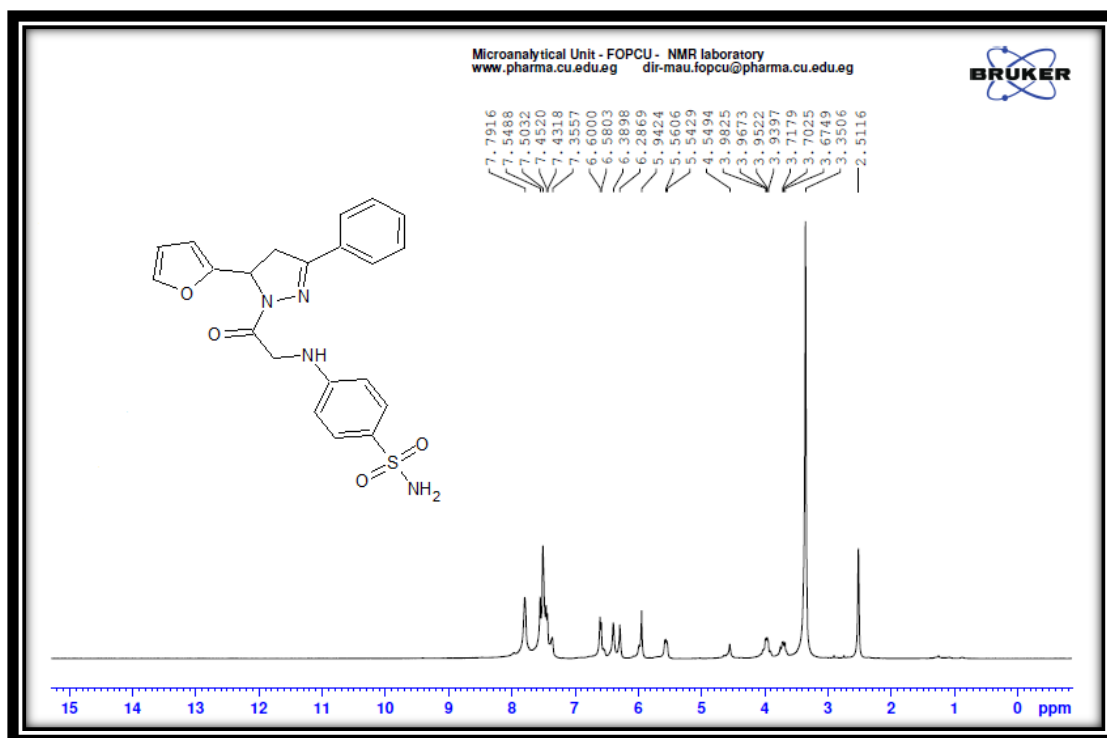
Figure (4.155): ^{1}HNMR Spectrum of 4-({2-[5-(furan-2-yl)-3-phenyl-4,5-dihydro-1*H*-pyrazol-1-yl]-2-oxoethyl}amino)benzene-1-sulfonamide **(LXII)**
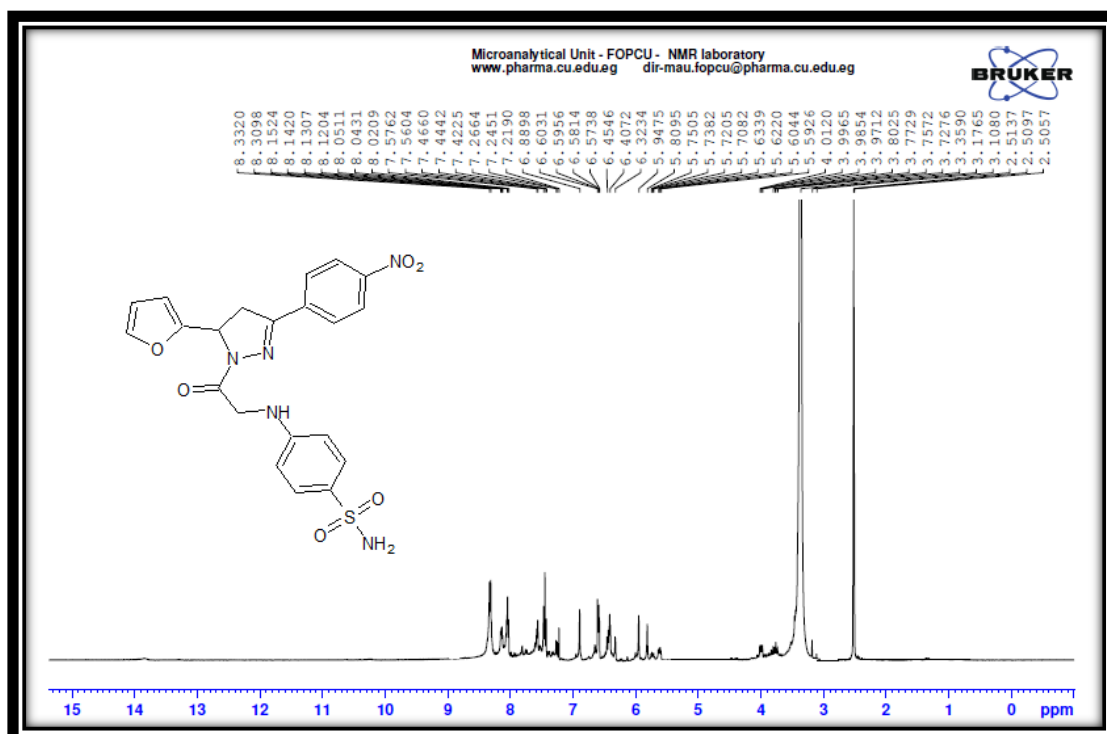
Figure (4.156): ^{1}HNMR Spectrum of 4-((2-(5-(furan-2-yl)-3-(4-nitrophenyl)-4,5-dihydro-1H-pyrazol-1-yl)-2-oxoeth yl) amino)benzene sulfonamide **(LXIII)**
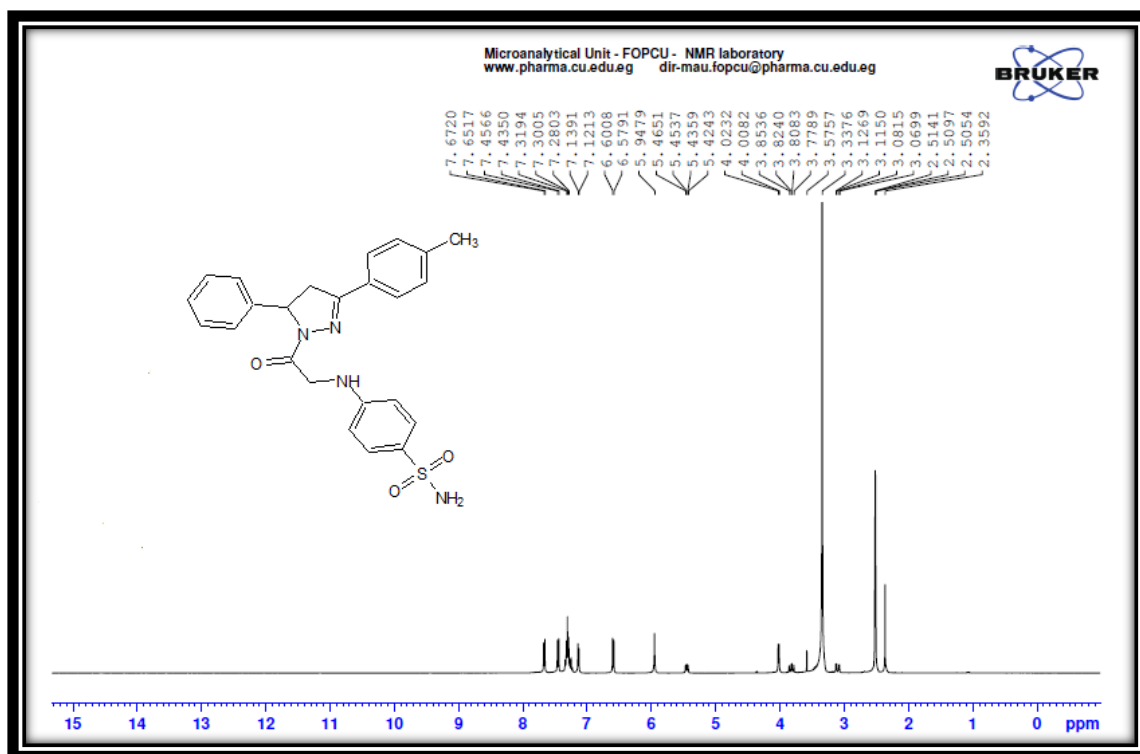
Figure (4.157): ^{1}HNMR Spectrum of 4-((2-oxo-2-(5-phenyl-3-(p-tolyl)-4,5-dihydro-1H-pyrazol-1-yl)ethyl)amino) benzene sulfonamide **(LXIV)**
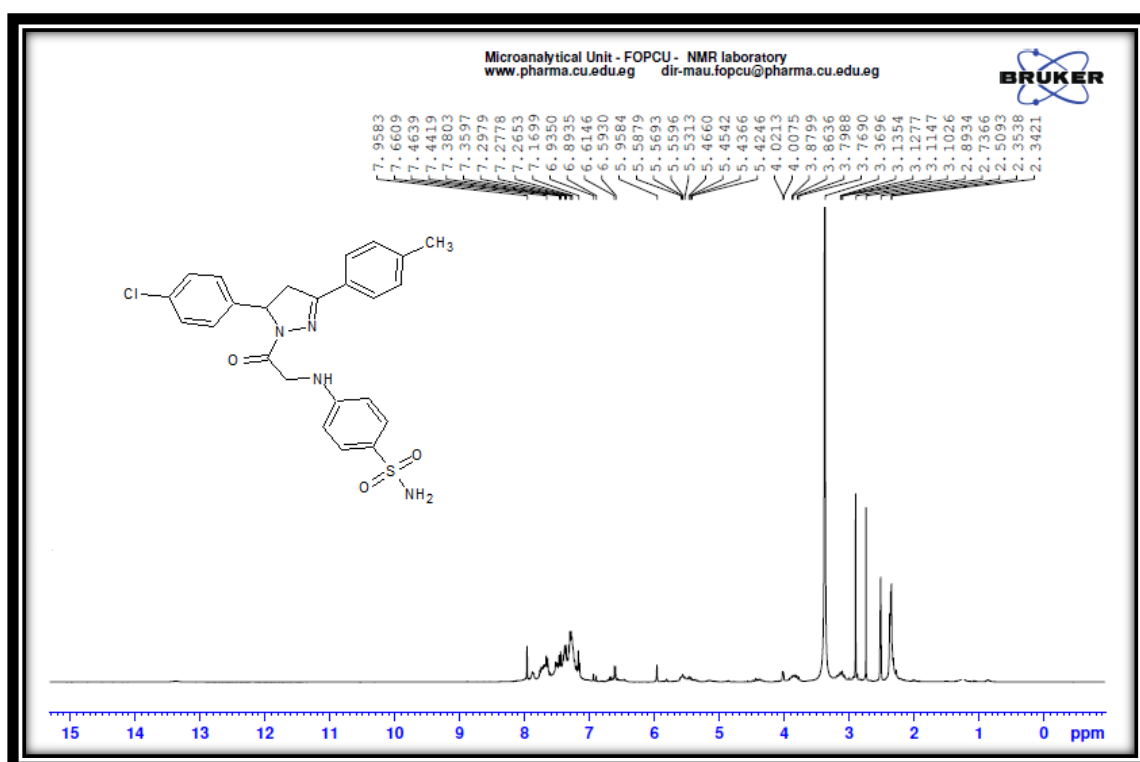
Figure (4.158): ^{1}HNMR Spectrum of 4-((2-(5-(4-chlorophenyl)-3-(p-tolyl)-4,5-dihydro-1H-pyrazol-1-yl)-2-oxoethyl)amino)benzene sulfonamide **(LXV)**
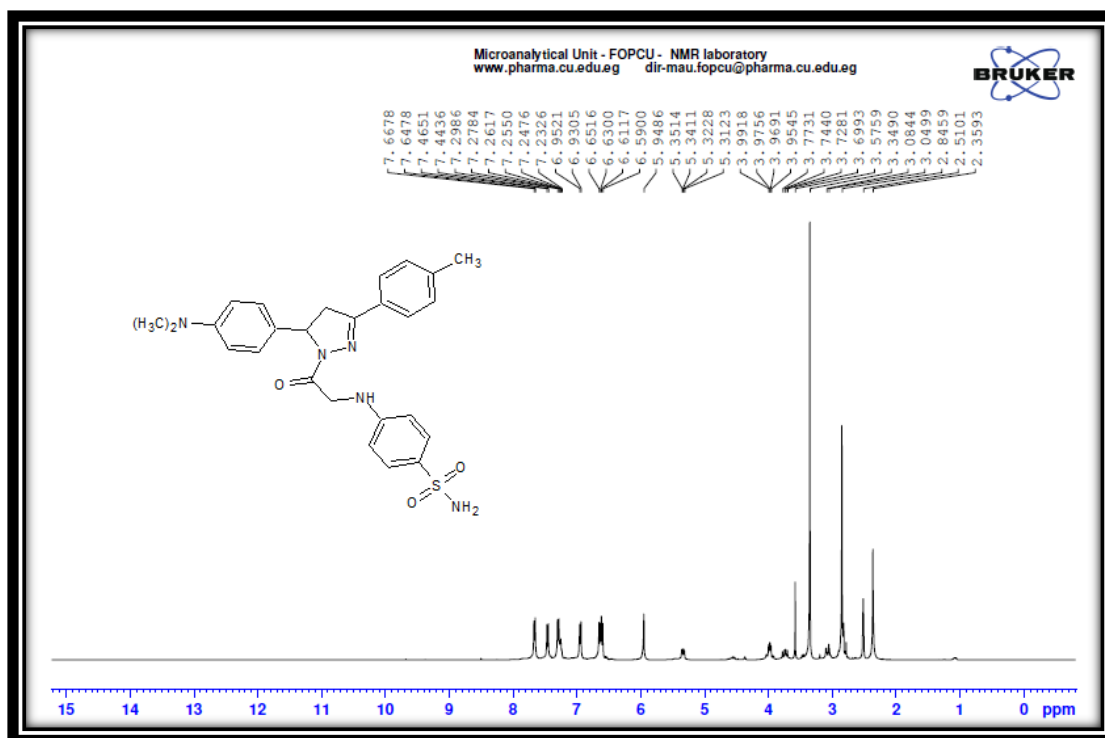
Figure (4.159): ^{1}HNMR Spectrum of 4-((2-(5-(4-(dimethyl amino)phenyl)-3-(p-tolyl)-4,5-dihydro-1H-pyrazol-1-yl)-2-oxoethyl)amino)benzene sulfonamide **(LXVI)**
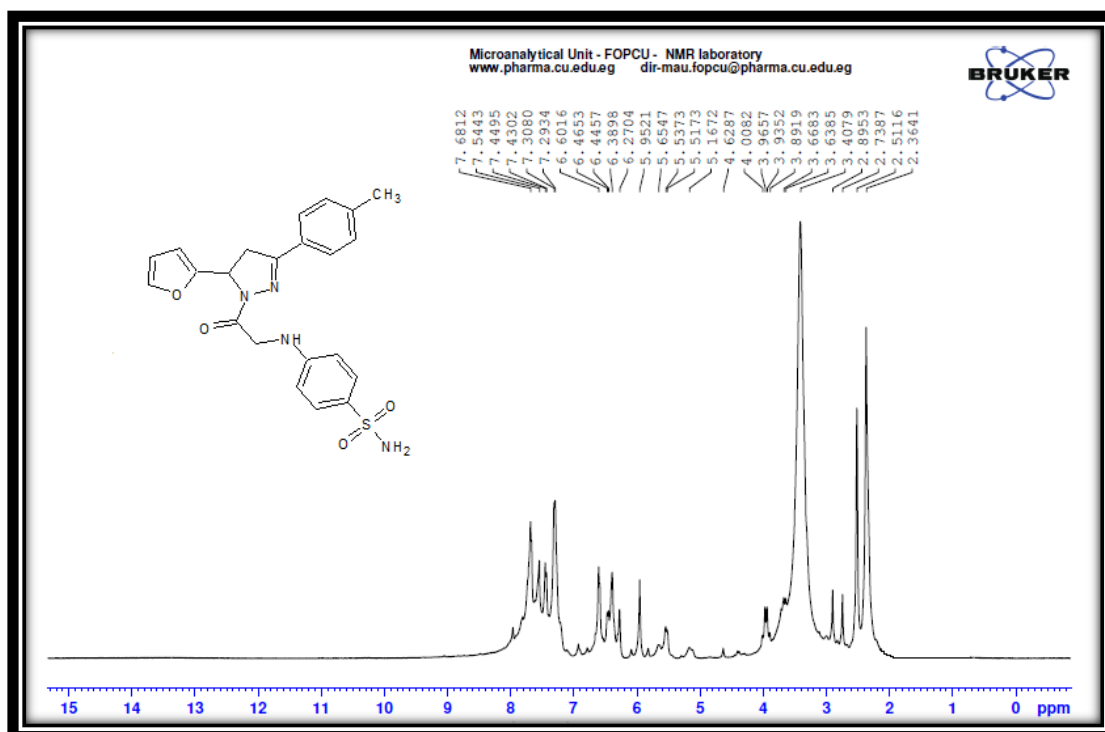
Figure (4.160): ^{1}HNMR Spectrum of 4-((2-(5-(furan-2-yl)-3-(p-tolyl)-4,5-dihydro-1H-pyrazol-1-yl)-2-oxoethyl)amino)benzene sulfonamide **(LXVII)**
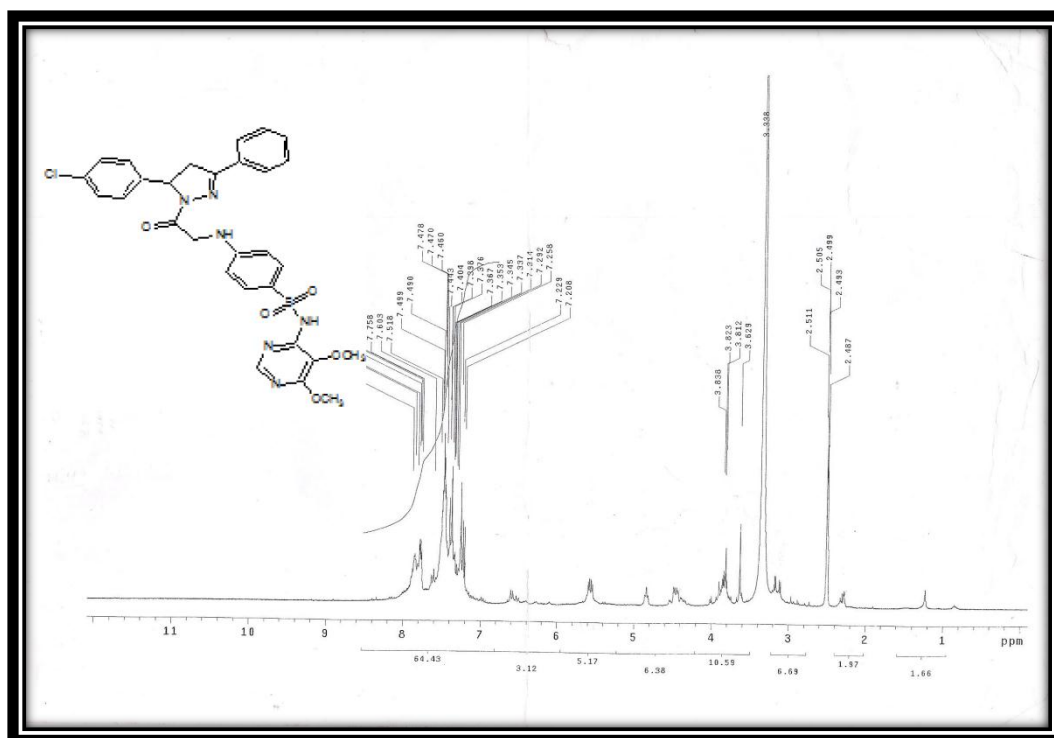
Figure (4.161): ^{1}HNMR Spectrum of 4-((2-(5-(4-chlorophenyl)-3-phenyl-4,5-dihydro-1H-pyrazol-1-yl)-2-oxoethyl) amino)-N-(5,6-dimethoxy pyrimidin-4-yl)benzene sulfonamide **(LXVIII)**
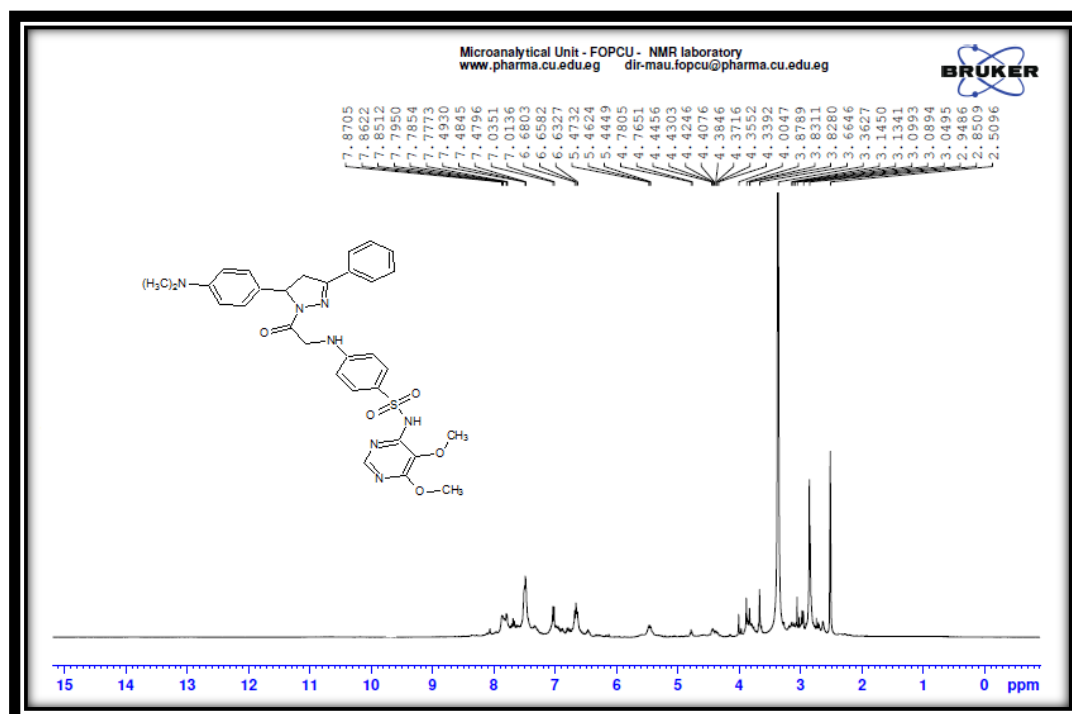
Figure (4.162): ^{1}HNMR Spectrum of N-(5,6-dimethoxypyrimidin-4-yl)-4-((2-(5-(4-(dimethylamino)phenyl)-3-phenyl-4,5-dihydro-1H-pyrazol-1-yl)-2-oxoethyl)amino)benzene sulfonamide **(LXIX)**
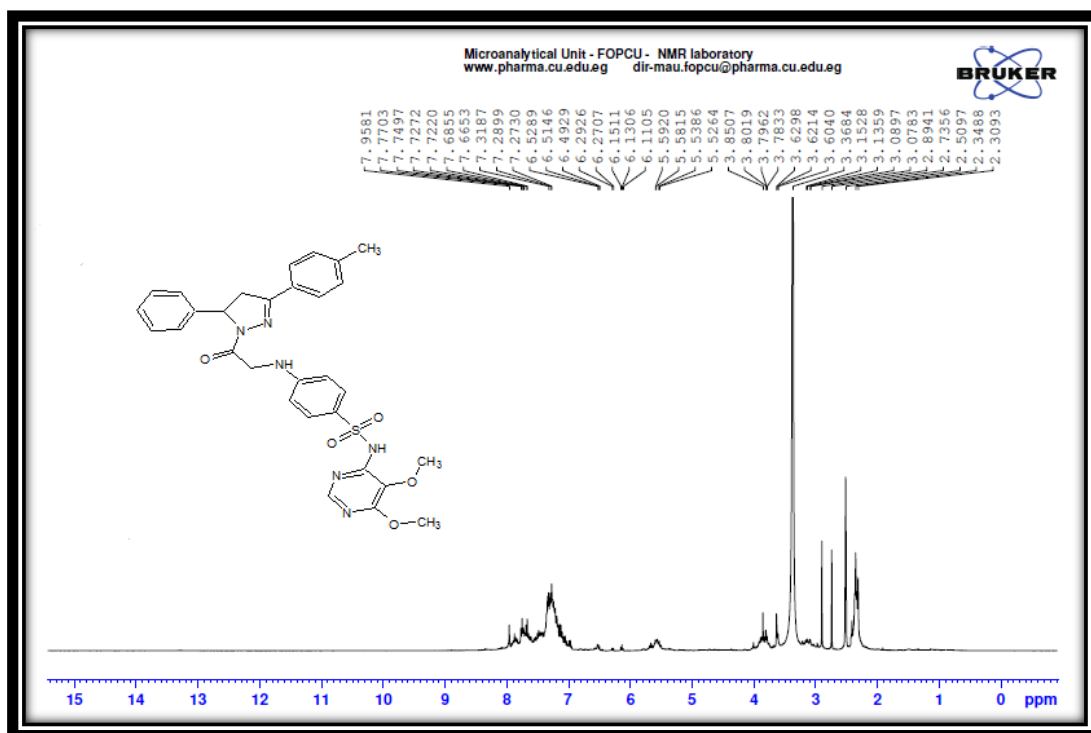
Figure (4.163): ^{1}HNMR Spectrum of N-(5,6-dimethoxypyrimidin-4-yl)-4-((2-oxo-2-(5-phenyl-3-(p-tolyl)-4,5-dihydro-1H-pyrazol-1-yl)ethyl)amino)benzene sulfonamide **(LXX)**
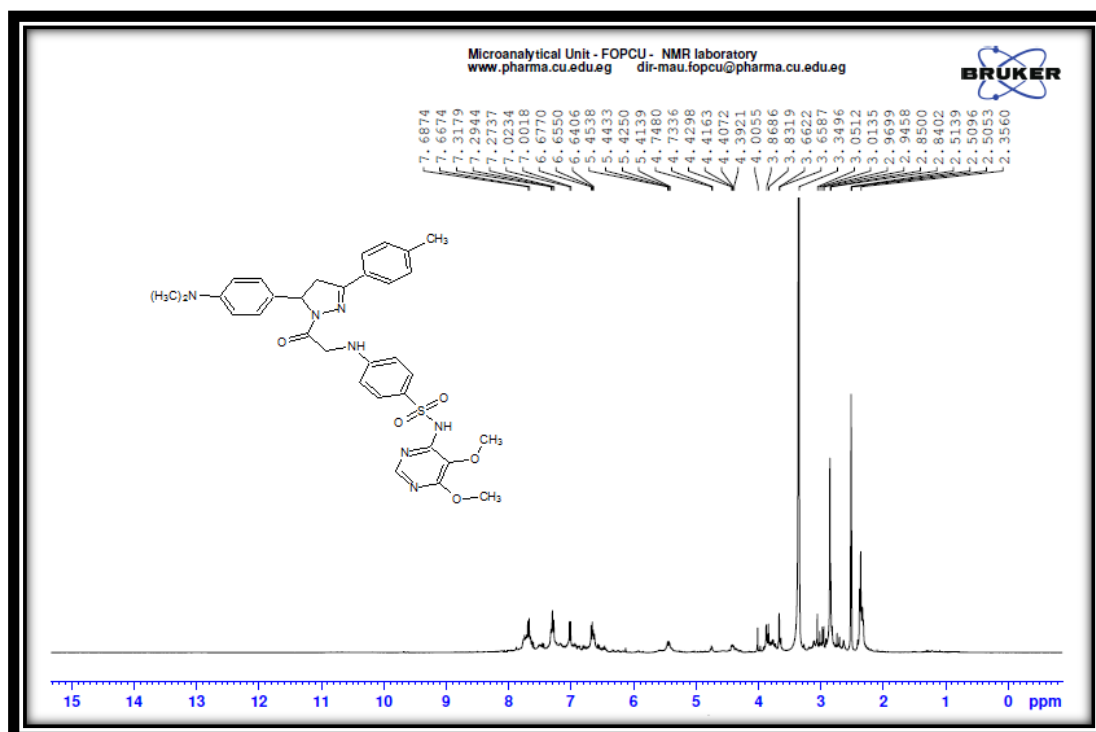
Figure (4.164): ^{1}HNMR Spectrum of N-(5,6-dimethoxypyrimid in-4-yl)-4-((2-(5-(4-(dime thylamino)phenyl)-3-(p-tol yl)-4,5-dihydro-1H-pyraz ol-1-yl)-2-oxoethyl)amino)benzene sulfonamide **(LXXI)**

5.3.Appendix C: Docking figures
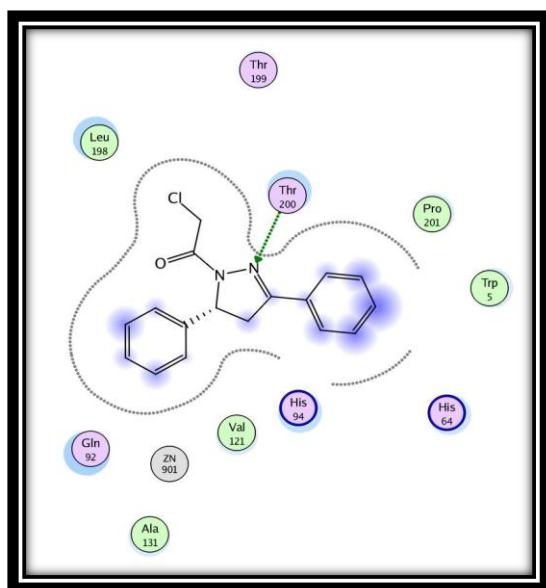
Figure (4.165): 2D interaction of compound **XLI** with the active site amino acid of hCAXII
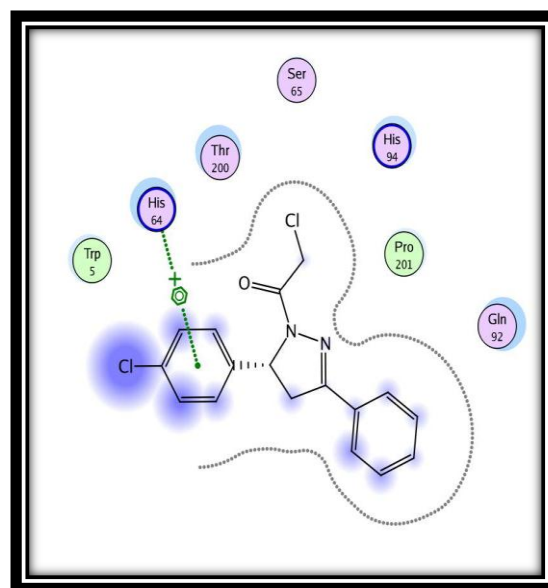
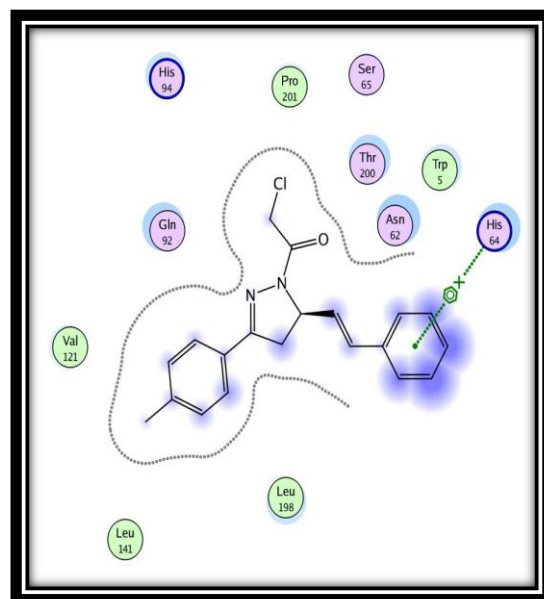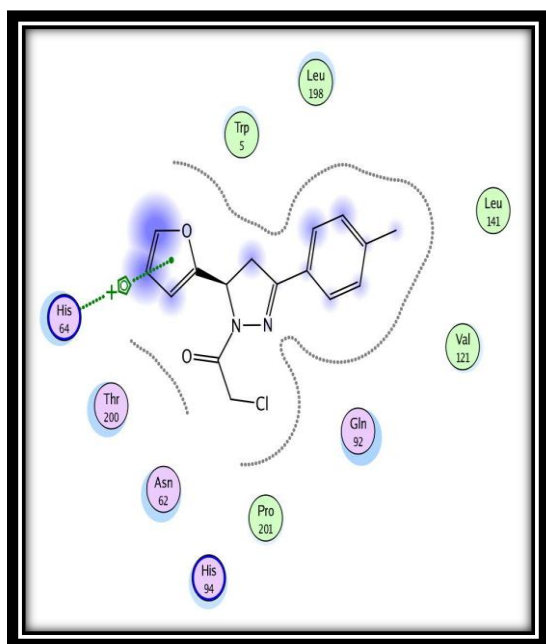**Figure (4.166):** 2D interaction of compound **XLII** with the active site amino acid of hCAXII
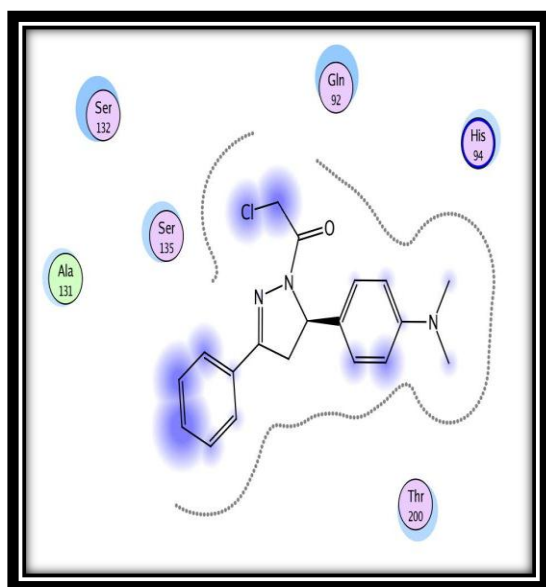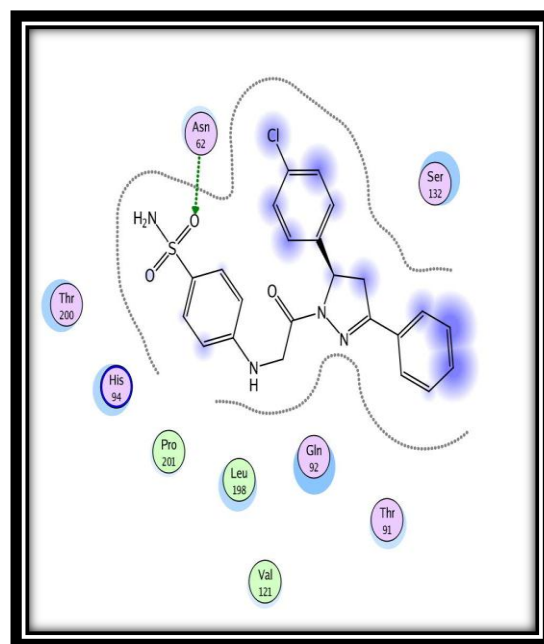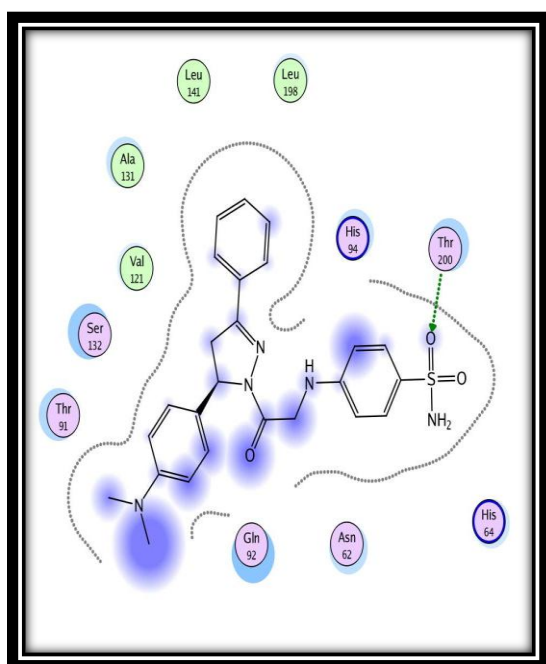

Figure (4.167): Compound **XLIII** showed no interaction with the active site amino acid of hCAXII
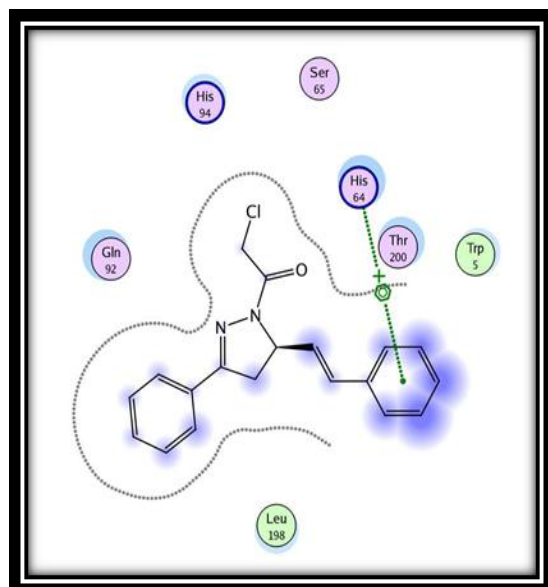
Figure (4.168): 2D interaction of compound **XLIV** with the active site amino acid of hCAXII
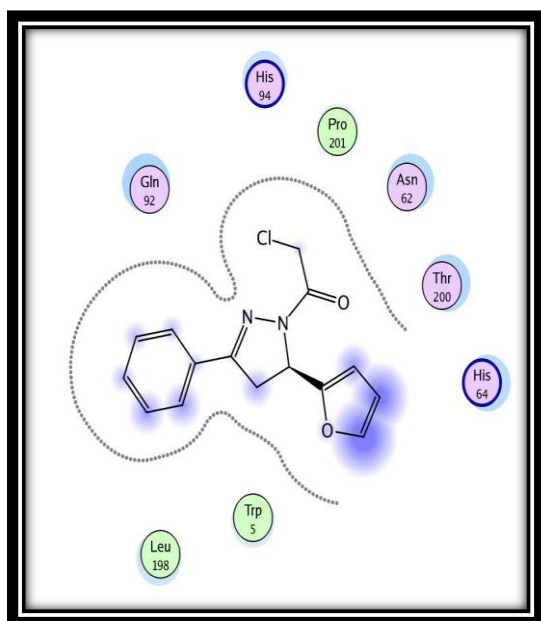
Figure (4.169): Compound **XLV** showed no interaction with the active site amino acid of hCAXII
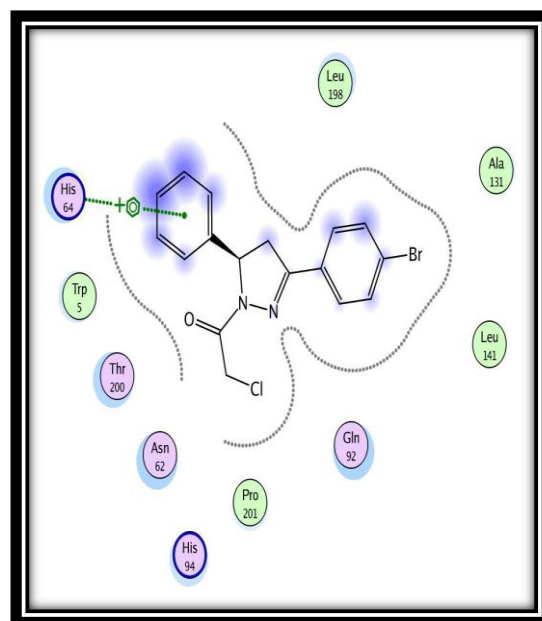
Figure (4.170): 2D interaction of compound **XLVI** with the active site amino acid of hCAXII
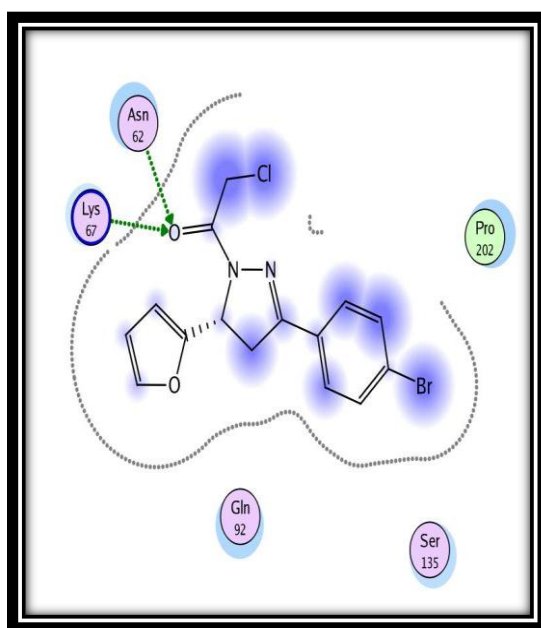
Figure (4.171): 2D interaction of compound **XLVII** with the active site amino acid of hCAXII
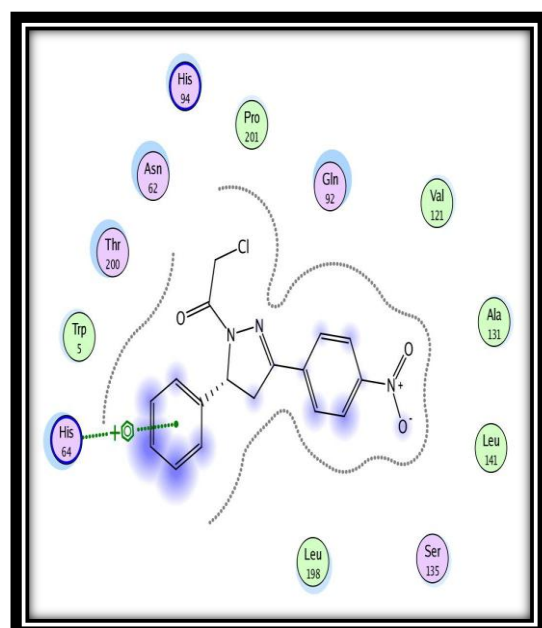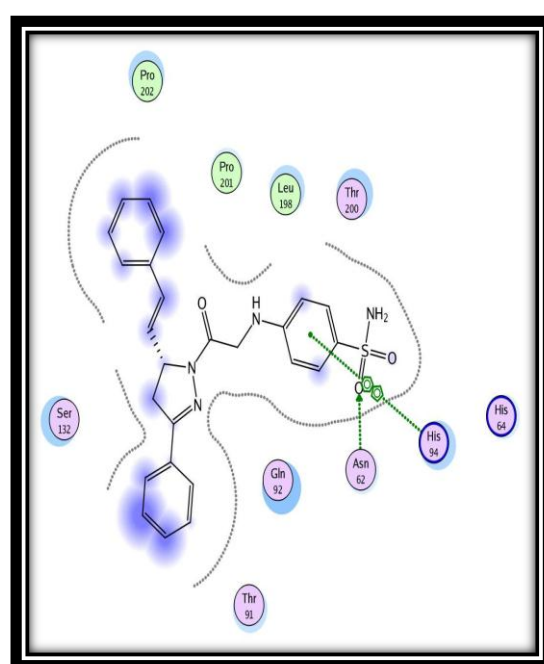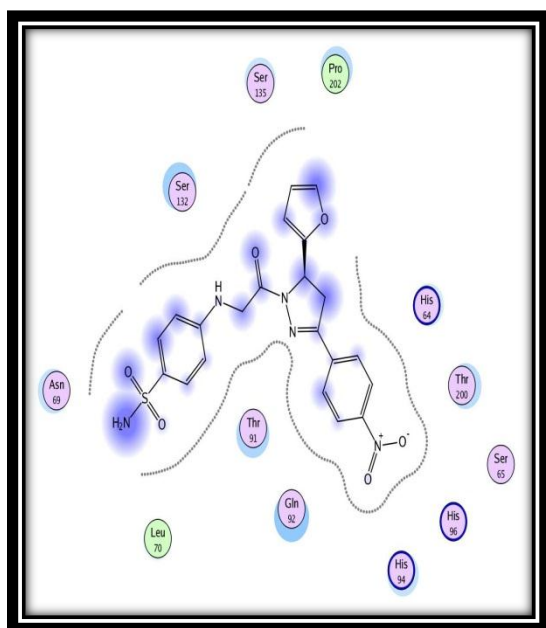

Figure (4.172): 2D interaction of compound **XLVIII** with the active site amino acid of hCAXII
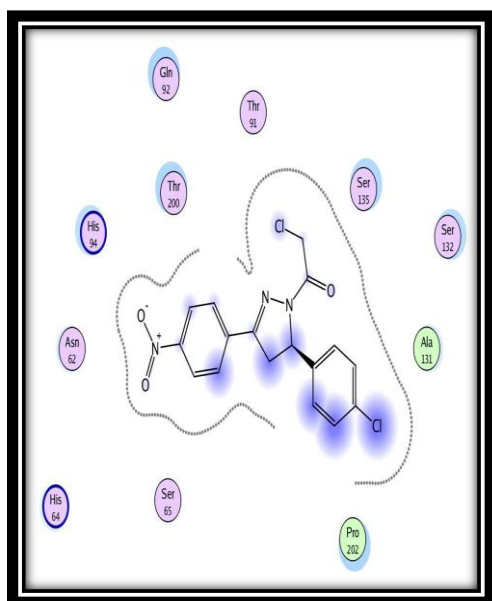
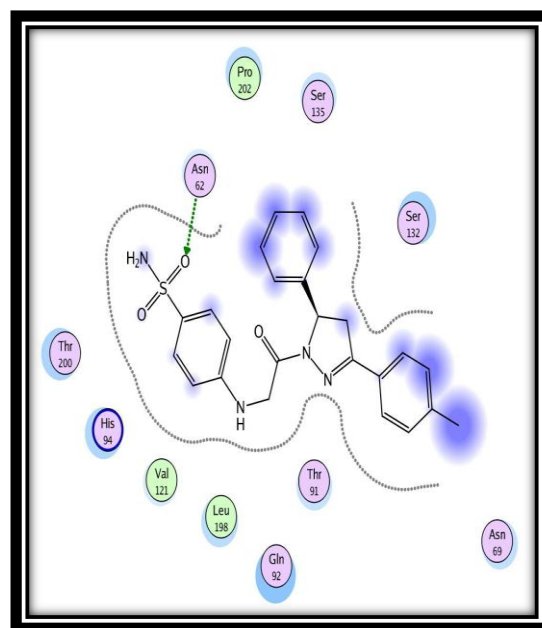**Figure (4.173):** Compound **XLIX** showed no interaction with the active site amino acid of hCAXII
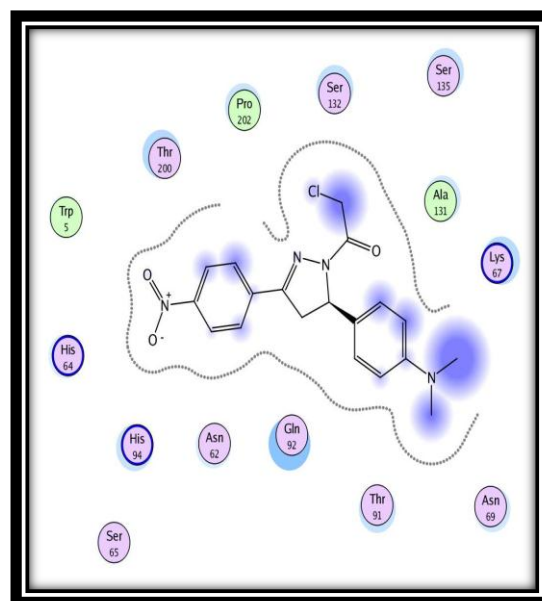
Figure (4.174): Compound **L** showed no interaction with the active site amino acid of hCAXII
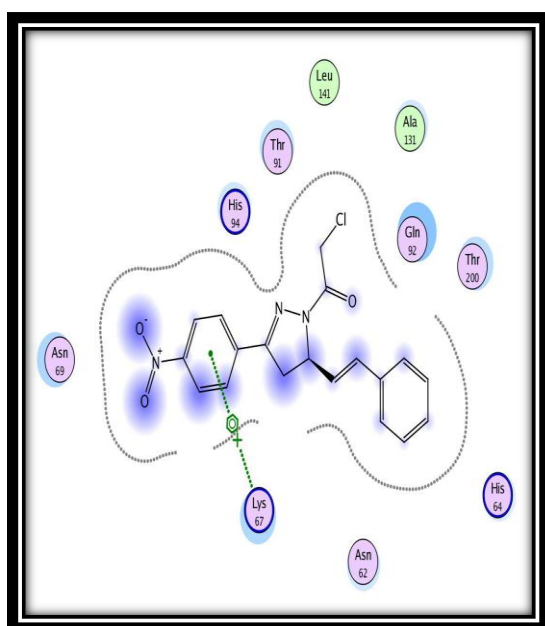
Figure (4.175): 2D interaction of compound **LI** with the active site amino acid of hCAXII
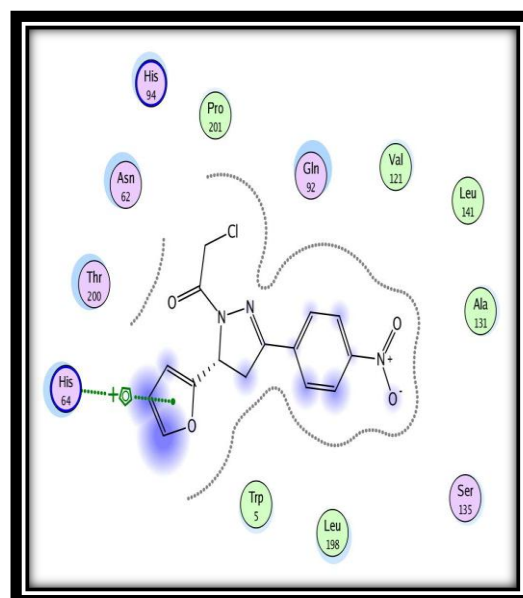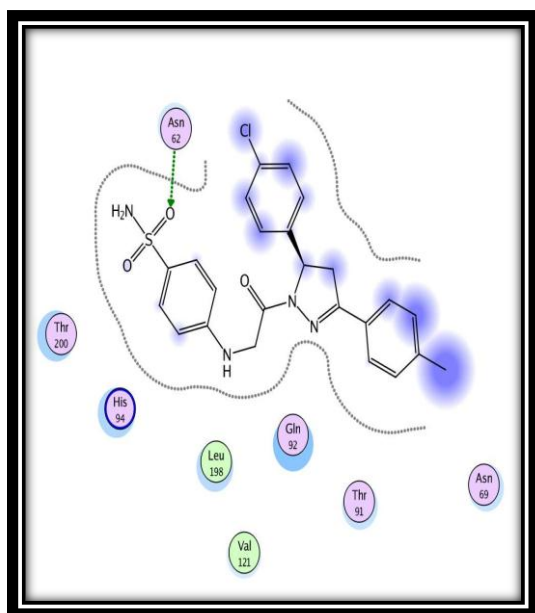

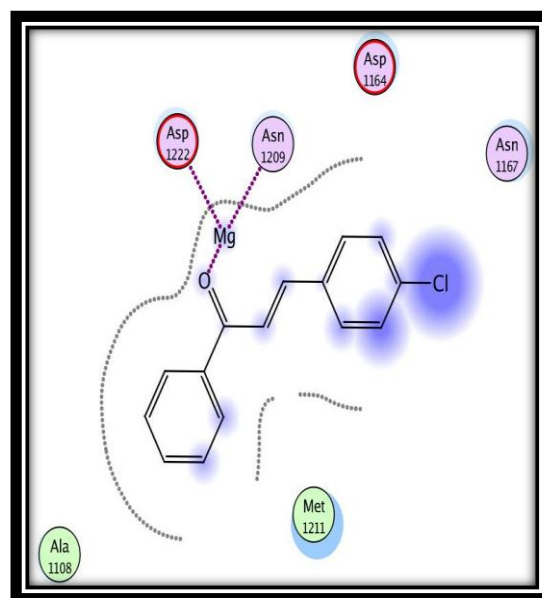**Figure (4.176):** 2D interaction of compound **LII** with the active site amino acid of hCAXII
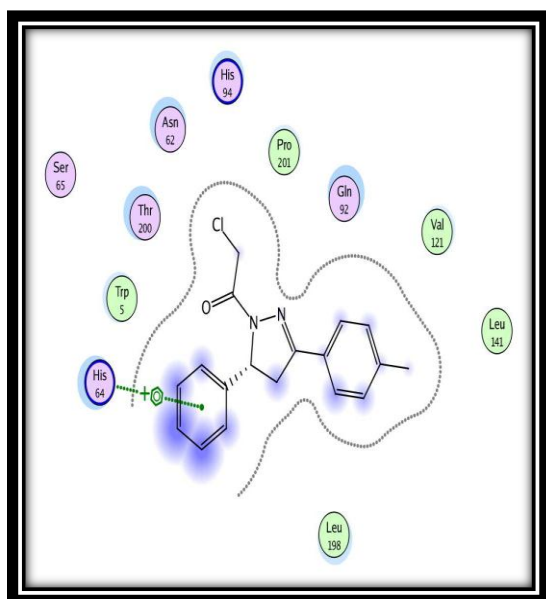
Figure (4.177): 2D interaction of compound **LIII** with the active site amino acid of hCAXII
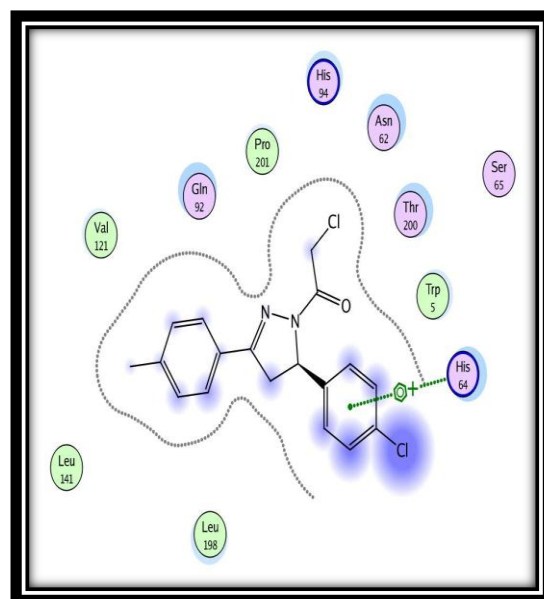
Figure (4.178): 2D interaction of compound **LIV** with the active site amino acid of hCAXII
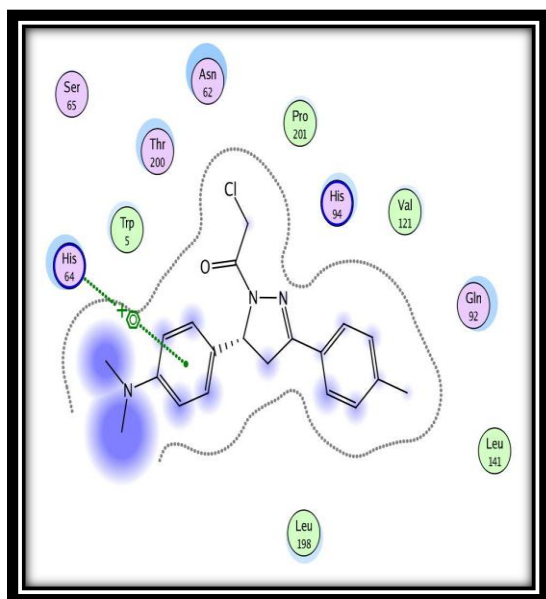
Figure (4.179): 2D interaction of compound **LV** with the active site amino acid of hCAXII

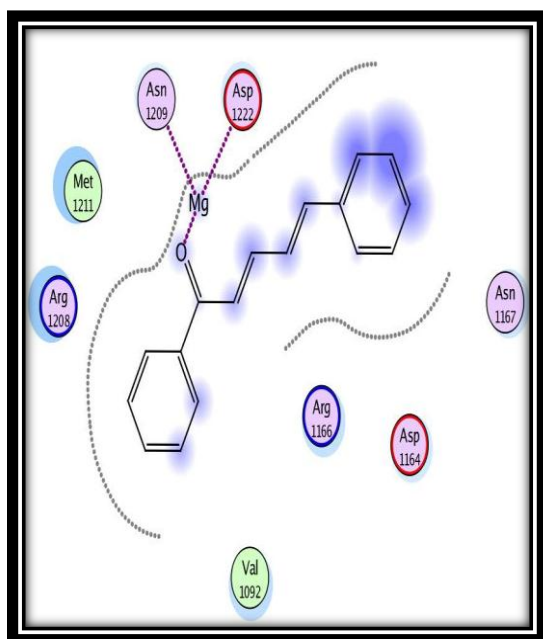**Figure (4.180):** 2D interaction of compound **LVI** with the active site amino acid of hCAXII

Figure (4.181): 2D interaction of compound **LVII** with the active site amino acid of hCAXII

Figure (4.182): 2D interaction of compound **LIX** with the active site amino acid of hCAXII

Figure (4.183): 2D interaction of compound **LX** with the active site amino acid of hCAXII

Figure (4.184): 2D interaction of compound **LXI** with the active site amino acid of hCAXII

Figure (4.185): Compound **LXIII** showed no interaction with the active site amino acid of hCAXII

Figure (4.186): 2D interaction of compound **LXIV** with the active site amino acid of hCAXII

Figure (4.187): 2D interaction of compound **LXV** with the active site amino acid of hCAXII

Figure (4.188): 2D interaction of compound **II** in the active site of 3DKC

Figure (4.189): 2D interaction of compound **IV** in the active site of 3DKC
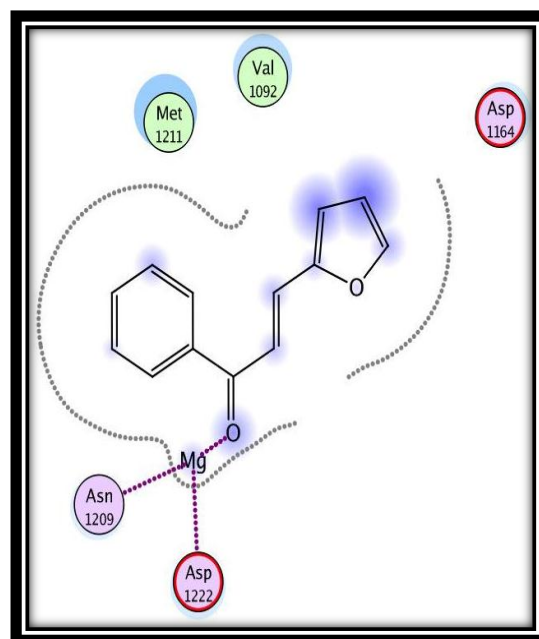
Figure (4.190): 2D interaction of compound **V** in the active site of 3DKC
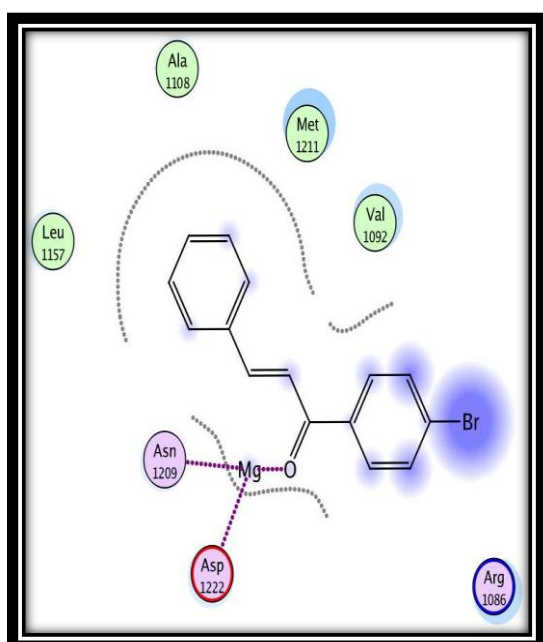
Figure (4.191): 2D interaction of compound **VI** in the active site of 3DKC
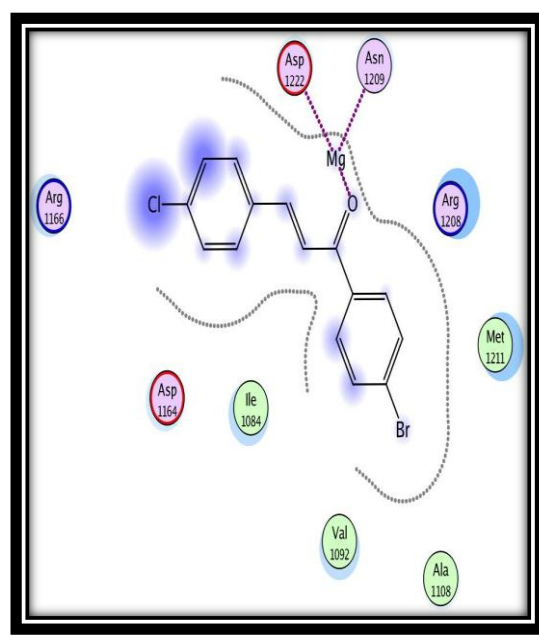
Figure (4.192): 2D interaction of compound **VII** in the active site of 3DKC
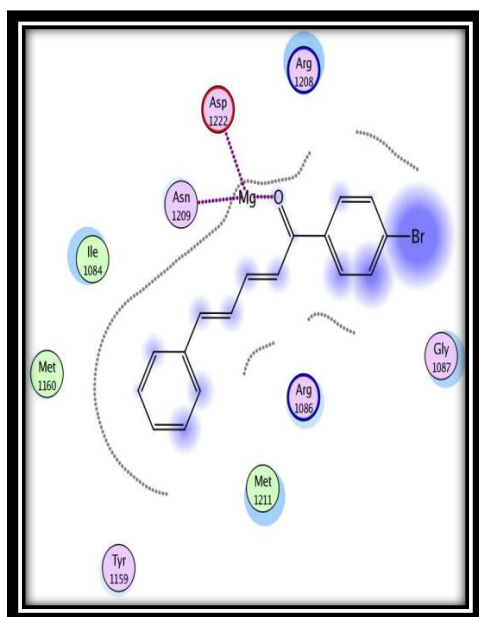
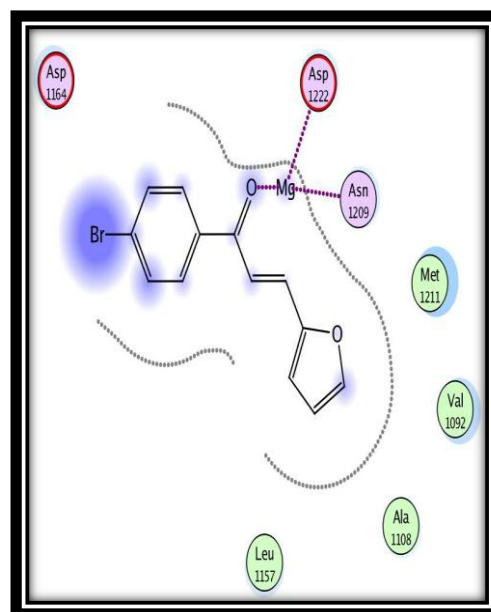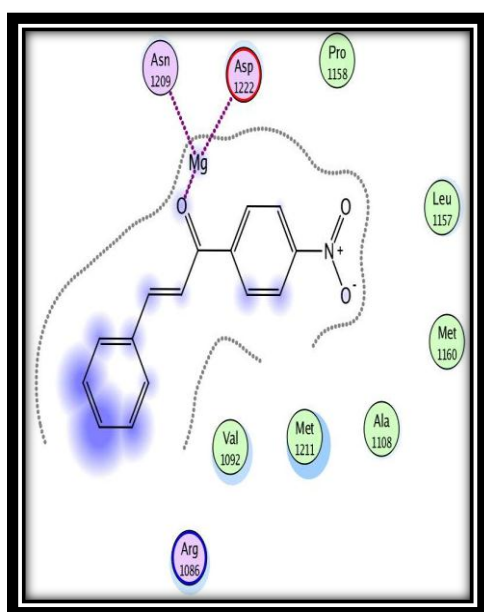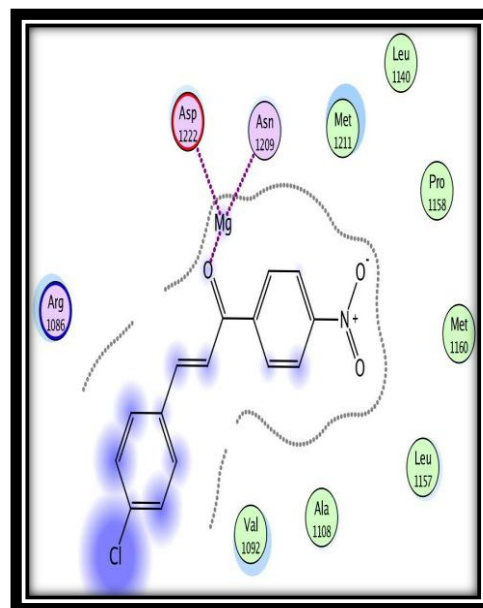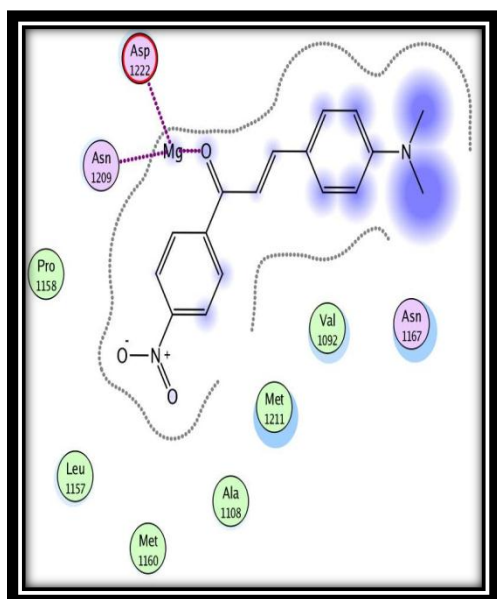**Figure (4.193):** 2D interaction of compound **IX** in the active site of 3DKC

Figure (4.194): 2D interaction of compound **X** in the active site of 3DKC

Figure (4.195): 2D interaction of compound **XI** in the active site of 3DKC

Figure (4.196): 2D interaction of compound **XII** in the active site of 3DKC

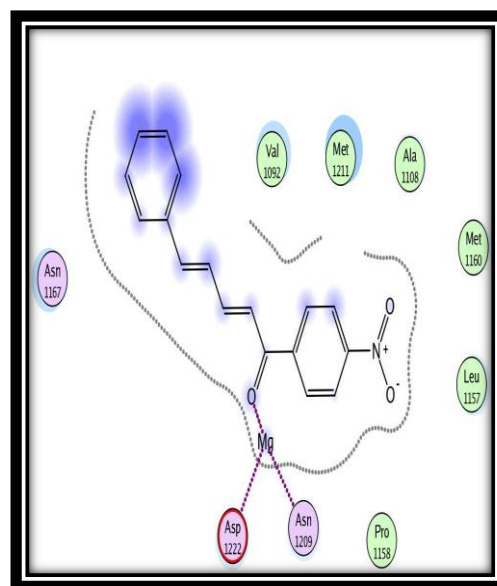**Figure (4.197):** 2D interaction of compound **XIII** in the active site of 3DKC

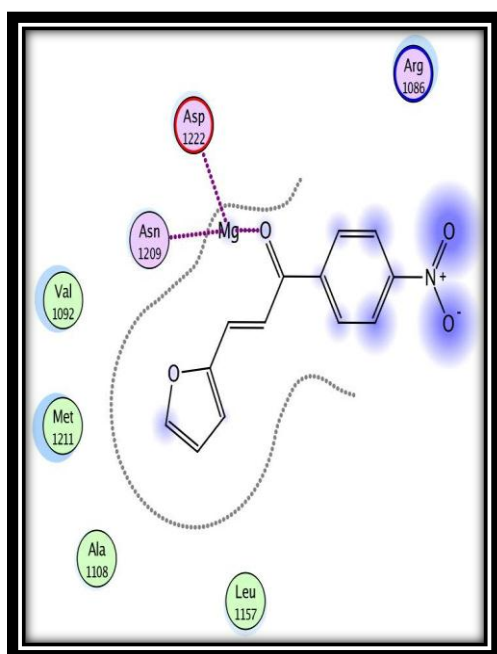**Figure (4.198):** 2D interaction of compound **XIV** in the active site of 3DKC

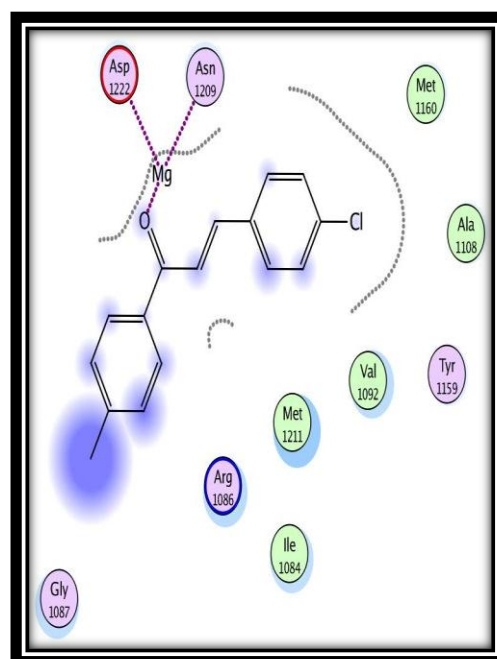**Figure (4.199):** 2D interaction of compound **XV** in the active site of 3DKC

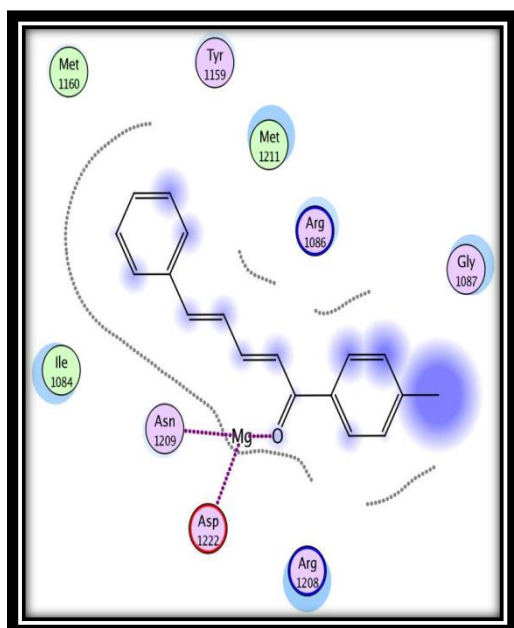**Figure (4.200):** 2D interaction of compound **XVII** in the active site of 3DKC

257

Figure (4.201): 2D interaction of compound **XIX** in the active site of 3DKC
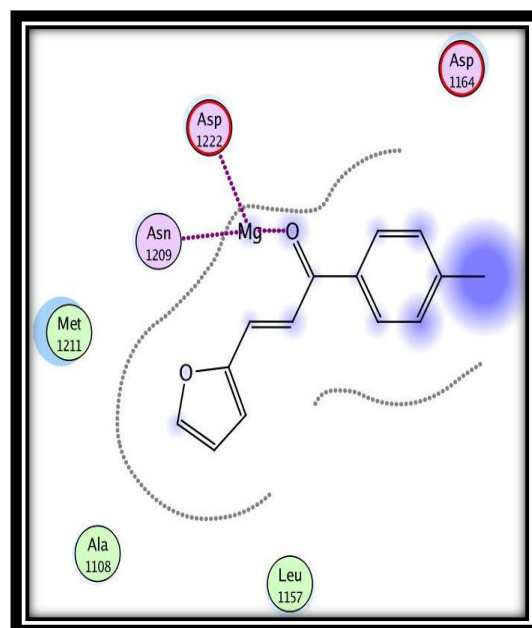

Figure (4.202): 2D interaction of compound **XX** in the active site of 3DKC